

University of Reading



**Evolution of Swimming Motility in Aflagellate Strains of
Pseudomonas fluorescens SBW25**

Astrid Eleanor Altamirano Junqueira

A dissertation submitted to the School of Biological Sciences in partial fulfilment of
the requirements for the degree of Doctor of Philosophy

27th June 2019

Reading, United Kingdom

Authorship Declaration

This thesis is my own work and any figures taken from publications and references cited had been appropriately acknowledged.

Date: 27th June 2019

Astrid Eleānor Altamirano Junqueira

Publications

This work had been published in part in a peer reviewed journal in the following paper:

Alsohim Abdullah S, Taylor Tiffany B, Barrett Glyn A, Gallie J, Zhang Xue-Xian, Altamirano-Junqueira Astrid E, Johnson Louise J, Rainey Paul B, Jackson Robert W. (2014). The biosurfactant viscosin produced by *Pseudomonas fluorescens* SBW25 aids spreading motility and plant growth promotion. *Environ Microbiol* [Internet]. Available from: <http://www.ncbi.nlm.nih.gov/pubmed/24684210>.

This work had been presented at the following meetings:

Altamirano-Junqueira Astrid E. (2018). Microbial strategies for survival: nitrogen starvation and aflagellate strains. Presented in: Antimicrobial resistance looking beyond the microbiological: Conference proceedings (14th November 2018: Society for Applied Microbiology, London), p. 2.

Altamirano-Junqueira Astrid E. (2016). Aflagellate *Pseudomonas fluorescens* SBW25 KO FleQ re-express flagella under starving conditions. Presented in: Bio imaging from cells to molecules: Conference proceedings (14-15 June 2016: Cambridge, UK.)

Altamirano-Junqueira Astrid E, Mulley Geraldine, Andrews Simon C. (2015). The evolutionary cost of re-evolving motility in *Pseudomonas fluorescens* $\Delta fleQ$ mutants. Presented in: The 4th Midlands Molecular Microbiology Meeting: Conference proceedings (14th September 2015: University of Nottingham), p. 66.

Altamirano-Junqueira Astrid E, Jackson Robert W. (2015). Understanding how *Pseudomonas fluorescens* evolves motility re-wiring of its regulatory networks. Presented in: Molecular Biology of Plant Pathogens Annual Conference: Conference proceedings (8th April 2015: University of the West of England, Bristol), p.36.

Abstract

Background: Swimming motility, an important trait for successful root colonization, by *Pseudomonas fluorescens* SBW25 requires flagella, expression of which is activated in a hierarchical manner by the master regulator FleQ. A non-motile, aflagellate strain, AR2 $\Delta fleQ\Delta viscB$ had been shown to reacquire flagella driven motility through 2 step mutation of a related two-component regulator, the NtrBC nitrogen sensor:regulator. Overexpressed NtrC-P is assumed to activate flagella expression. NtrBC responds to nitrogen limitation by upregulating expression of operons involved in nitrogen assimilation, including *glnAntrBC* [encoding: glutamine synthetase (GS), NtrBC] and *glnKamtB* (encoding PII and AmtB ammonium channel).

Aims: To investigate the influence of different nitrogen sources and different motility phenotypes on the evolution pathway and probability/frequency of re-establishment of swimming motility in aflagellate *P. fluorescens* SBW25 $\Delta fleQ$ strains.

Research hypothesis: The physiological status of NtrBC under nitrogen limitation will increase the probability of identification of evolved swimming isolates of *P. fluorescens* SBW25 $\Delta fleQ$ strains carrying mutations in *ntrBC*. Also, as mutation of *ntrBC* has global effects and impact on cell fitness, it was hypothesized that other enhancer binding proteins (EBP) might rescue loss of *fleQ*, particularly in nitrogen replete conditions.

Methods: Evolution of swimming motility in the aflagellate strains, SBW25 $\Delta fleQ$ (*Fla*⁻, *Visc*⁺), AR1 (*Fla*⁻, *Visc*⁻), and AR2 (*Fla*⁻, *Visc*⁻) was performed in 0.25 % M9 –glucose agar medium with glutamine, glutamate (nitrogen limiting) or ammonium (nitrogen replete) as nitrogen source. Colony spreading phenotypes of evolved isolates on minimal and rich media were monitored and quantitated by time-lapse photography. Mutations were identified by targeted sequencing of segments of *ntrB*, *ntrC* and the entire *glnK* gene or by whole genome sequencing (WGS).

Results: As predicted, swimming motility of the sessile strains, AR1 and AR2, evolved later with ammonium as N-source (mean = 5.53 days, *SD* = 0.61 days, *n* = 19) compared to glutamine (mean = 2.88 days, *SD* = 0.89 days, *n* = 17) or glutamate (mean = 2.94 days, *SD* = 0.80 days, *n* = 17). Notably, SBW25 $\Delta fleQ$ which spreads with spidery-like tendrils over the surface of the agar also evolved swimming motility thus enhancing migration within the liquid phase and access to nutrients within the agar. Irrespective of parent strain or N-source all evolved mutants had acquired a mutation in NtrB, primarily T97P within the PAS domain, or a D228A/N mutation known to interfere with PII interaction, thus increasing NtrC-P levels by decreasing phosphatase activity. Despite impaired growth in ammonium, none of the evolved mutants possessed anticipated secondary mutations in the Helix-turn-Helix (HTH) domain of NtrC that might moderate the unregulated Ntr response. Mutation in AlgP histone-like protein may have been selected in response to a different stress, but could be an indication of involvement of an alternate EBP. Possession of an unrelated mutation in a predicted ammonium transporter PFLU_RS08590, correlated with improved growth on ammonium and deserves further investigation.

Conclusions: Mutation in NtrB is the primary evolutionary pathway for re-establishment of swimming motility in *P. fluorescens* $\Delta fleQ$ strains irrespective of nitrogen status. Delayed recovery of these mutants from ammonium/glucose plates may be due to a combination of low transcription of *ntrBC* and uncontrolled assimilation of ammonia due to dysregulation of the Ntr regulon. Details of the mechanism by which mutated NtrBC compensates for loss of the FleQ regulator remain to be fully elucidated and will provide a fuller picture of the evolution pathway. Understanding details of crosstalk between these critical regulons, flagella regulon, and the Ntr system are likely to enhance understanding of the ecology of this important rhizosphere associated bacterium and may have downstream implications in the application of *P. fluorescens* as biopesticide or biofertiliser.

Dedicated to my dear parents:
Astrid F. Junqueira de Barros and Carlos A. Altamirano Silva

Acknowledgements

I am extremely grateful to my parents for all their support throughout my career. Similarly, I am thankful to all my professors who taught me and for their valuable contribution towards my professional development. I also appreciate the important role of all the educational institutions, for the opportunity they gave me to attend their sessions/labs/etc. due to which I was able to successfully complete my studies.

I am grateful to Dr. Sheila MacIntyre and Dr. Geraldine Mulley at Reading University for their helpful comments and suggestions to improve this thesis, and their guidance during research done in their lab. I also acknowledge provision of strains and guidance in initial techniques provided by Professor Rob Jackson's laboratory in the early stages of my project.

Table of Contents

Authorship Declaration.....	i
Publications.....	ii
Abstract.....	iii
Acknowledgements.....	v
List of Figures	xiii
List of Tables	xxi
List of Abbreviations.....	xxiv
1 Introduction	1
1.1 The Importance of Plant Growth Promoting Bacteria in Agriculture and the Environment.....	1
1.2 Characteristics and Ecological Importance of <i>Pseudomonas</i>	3
1.3 <i>Pseudomonas fluorescens</i> Complex Group.....	4
1.4 Viscosin Is a Biosurfactant Involved in Swarming Motility	15
1.4.1 <i>Classes of cyclic lipopeptides produced by Pseudomonas</i>	16
1.4.2 <i>Viscosin: properties and ecological importance</i>	16
1.4.3 <i>Viscosin biosynthesis in P. fluorescens SBW25</i>	16
1.4.4 <i>Quorum sensing</i>	18
1.5 The Importance of Flagella in Bacterial Ecology	19
1.6 Overview of Bacterial Motility and Chemotaxis	20
1.6.1 <i>Flagella movement: swimming and tumbling</i>	23
1.6.2 <i>Classic experiments in bacterial chemotaxis</i>	24
1.7 <i>Pseudomonas fluorescens</i> SBW25 Movement Is Versatile	28
1.7.1 <i>Flagella driven swimming motility and chemotaxis</i>	29
1.7.2 <i>Flagella and swimming pattern of P. fluorescens SBW25</i>	30
1.7.3 <i>Regulation of flagella biosynthesis in Pseudomonas</i>	32
1.8 FleQ Is the Master Regulator of Flagella Expression.....	36
1.8.1 <i>Structure and function of FleQ</i>	37
1.8.2 <i>The second messenger c-di-GMP binds and regulates FleQ</i>	41
1.8.2.1 <i>Diguanylate cyclases and phosphodiesterases regulate the intracellular c-di-GMP levels in P. fluorescens</i>	42
1.8.3 <i>Enhancers and regulation of the σ^{54} promoters of flagella genes in Pseudomonas</i>	43

1.8.4	<i>Cryptic flagella operons are absent in P. fluorescens SBW25</i>	44
1.9	Bacterial Evolution and Adaptation to an Ever Changing Environment.....	45
1.9.1	<i>Mutational models</i>	48
1.9.1.1	Cairnsian mutational model: stress induced mutations.....	50
1.9.1.2	Adaptive mutations	51
1.9.1.3	Amplification mutagenesis: stress does not alter mutation rate ...	52
1.9.2	<i>Rewiring of the nitrogen pathway to restore flagella in sessile mutants</i> 54	
1.10	Bacterial Regulators and Signalling	57
1.11	Nitrogen metabolism, regulation and types of nitrogen sources.....	62
1.11.1	<i>Transport of ammonia/ammonium (NH₃/NH₄⁺) and amino acids glutamate and glutamine</i>	62
1.11.2	<i>Overview of nitrogen assimilation</i>	66
1.11.3	<i>Function of regulatory protein PII (GlnK)</i>	70
1.11.4	<i>Nitrogen regulation: sensor histidine kinase (GlnL or NtrB)</i>	71
1.11.5	<i>Nitrogen metabolism: NtrC and regulation at the genetic level</i>	75
1.11.6	<i>Nitrogen regulation at the enzymatic level</i>	81
1.12	Carbon and Nitrogen Metabolism in <i>Pseudomonas</i>	84
1.12.1	<i>Roles of glutamine and glutamate in bacterial metabolism</i>	92
1.12.2	<i>Nitrogen Limitation in Pseudomonas</i>	94
1.13	General Aims and Research Hypothesis	98
2	General Methods	101
2.1	Strain History	101
2.2	Evolved Strains.....	103
2.3	Culture of <i>P. fluorescens</i> Strains.....	104
2.3.1.1	Luria-Bertani Agar (LA).....	105
2.3.1.2	Luria-Bertani Broth (LB).....	105
2.3.1.3	Minimal medium M9 based agar 0.25 % w/v (200 mL) for evolution experiment	105
2.3.2	<i>Growth curves</i>	106
2.4	Assessment of Colony Expansion.....	107
2.4.1	<i>Preparation of motility plates</i>	107
2.4.2	<i>Low strength nutrient plates to confirm swimming motility</i>	107
2.4.3	<i>Recording colony expansion</i>	108

2.4.3.1	Hand-Drawn method.....	108
2.4.3.2	Time-Lapse photography.....	109
2.5	Quantitation and Classification of Colony Expansion Rate	110
2.5.1	<i>Swimming and swarming rates of wild type and parent strains</i>	111
2.5.2	<i>Sliding and spidery-spreading for individual plates</i>	111
2.6	Experimental Evolution Assay.....	112
2.6.1	<i>Isolation and testing of evolved mutants</i>	113
2.7	Agarose Gel Electrophoresis	114
2.8	Plasmid Isolation from <i>Escherichia coli</i> DH5 α	114
2.8.1	<i>Plasmid purification</i>	114
2.8.2	<i>Electroporation of Pseudomonas strains</i>	115
2.9	DNA Amplification and Sequencing of Target Regions of <i>ntrB</i> , <i>ntrC</i> and <i>glnK</i> 115	
2.10	Analysis of Single Colony	116
2.11	Concurrent Assessment of Colony Expansion of Multiple Colonies on the Same Plate	117
2.12	Whole Genomic DNA Extraction, Sequencing and Concurrent Assessment of Colony Expansion of Multiple Colonies on a Single Plate	118
2.12.1	<i>From an overnight broth culture</i>	118
2.12.2	<i>From an overnight agar culture</i>	119
2.12.3	<i>Illumina technique for whole genome sequencing</i>	120
2.13	Observation of Swimming via Light Microscopy.....	121
2.14	Observation of Flagella via Transmission Electron Microscopy	121
2.15	Bacterial Staining with Fluorescent NanoOrange Dye	121
2.16	Multivariate Analysis of the Strains: Discriminant.....	122
2.17	Databases.....	122
3	Active and Passive Movements	125
3.1	Introduction	125
3.2	Complementation of SBW25 Δ <i>fleQ</i> with plasmid (<i>pfleQ</i>)	129
3.3	Active Movements in the <i>P. fluorescens</i> strains.....	134
3.3.1	<i>Swimming and swarming motilities of the wild type strain SBW25</i> ...	134
3.3.1.1	Swimming and swarming motilities in swarming medium	134
3.3.1.2	The flagellated but non-viscosin producing strain, SBW25C swims but does not swarm	142

3.3.1.3	Comparison of the evolved strains AR2S and AR2SF (Taylor et al. ¹⁰⁸)	144
3.4	Passive Movements in the <i>P. fluorescens</i> Strains	145
3.4.1	<i>Spidery-Spreading movement of strain SBW25ΔfleQ relies on viscosin and cell division to expand the sliding colony</i>	145
3.4.2	<i>Overproduction of the biosurfactant viscosin hinders spidery-spreading movement in strain AR9</i>	154
3.4.3	<i>Sessile strains AR1 and AR2 exhibit cumulative growth on the surface of agar</i>	158
3.5	Growth Curves and Phenotype	165
3.5.1	<i>Rich medium LB</i>	166
3.5.2	<i>M9 medium containing ammonium and glucose</i>	167
3.5.3	<i>Glutamine/Glucose M9 treatment</i>	167
3.5.4	<i>Glutamate/Glucose M9 treatment</i>	168
3.6	Multivariate analysis: Discriminant	172
3.7	Summary of the Characteristics of the Strains Studied	173
4	Evolution of Swimming Motility under Different Nitrogen Sources in the Aflagellate Strain SBW25ΔfleQ	180
4.1	Introduction	180
4.2	Initial Spidery-Spreading Motility of SBW25ΔfleQ with Different Nitrogen and Carbon Sources	181
4.2.1	<i>Comparison of colony expansion between SBW25ΔfleQ and SBW25:</i>	186
4.2.2	<i>Glutamine as the Sole Carbon and Nitrogen Source for P. fluorescens</i>	188
4.3	Nitrogen Limitation and Evolution of Swimming Motility	189
4.3.1	<i>Evolution of swimming motility in aflagellate SBW25ΔfleQ on a poor carbon source</i>	193
4.4	Purification of Individual Evolved Mutants of SBW25ΔfleQ	197
4.5	Swimming and Swarming Phenotypes of Evolved FleQS Strains	198
4.5.1	<i>Classification of evolved FleQS strains based on rate of colony expansion</i>	204

4.6	Mutational Changes in the Nitrogen Regulation Pathway (NtrBC) and Evolution of Swimming Motility.....	207
4.7	Growth Comparison of Evolved FleQS Mutants in M9 Liquid Medium for Different Nitrogen Sources and Rich LB Medium.....	208
4.7.1	<i>Growth in rich medium LB:.....</i>	210
4.7.2	<i>Growth in ammonium/glucose M9 medium.....</i>	212
4.7.3	<i>Growth in glutamine/glucose M9 medium.....</i>	213
4.7.4	<i>Growth in glutamate/glucose M9 medium.....</i>	213
4.8	FleQS Strains Produce Flagella.....	216
4.9	Multivariate Analysis: Discriminant.....	219
5	Evolution of Swimming Motility in Sessile Strains AR1 and AR2 under different Nitrogen and Carbon sources	222
5.1	Introduction	222
5.2	Evolution of Swimming Motility in Strain AR1 with Different Nitrogen Sources in a Rich Energy Environment.....	224
5.2.1	<i>Colony expansion curves of evolved replicates under different nitrogen treatments using glucose as carbon source.....</i>	228
5.3	Evolution of Swimming Motility for Different Nitrogen Sources and a Poor Carbon Source.....	231
5.3.1	<i>Colony spreading of evolved sessile strain AR1 for different nitrogen sources and a poor carbon source</i>	233
5.4	Testing Isolates Picked from Evolved AR1 Colonies for Swimming Motility	235
5.5	Swimming Motility Phenotypes	236
5.5.1	<i>Spurs and spur-swarming.....</i>	236
5.5.2	<i>Differences in colony expansion rate.....</i>	237
5.6	Mutations in the Nitrogen Metabolism Pathway in Strain AR1S.....	240
5.7	Evolution of Swimming Motility in Strain AR2 for Different Nitrogen Sources in a Rich Energy Environment.....	242
5.7.1	<i>Colony expansion of evolved AR2 colonies for different nitrogen sources in a rich energy environment.....</i>	246
5.8	Evolution of Swimming Motility in AR2 for Different Nitrogen sources in a Poor Energy Environment.....	249
5.9	Evolved AR2 Colonies from Different Nitrogen and Carbon Sources	253

5.10	The Evolved AR2S Strains Possess Mutations in the NtrBC system.....	256
5.11	Motility Phenotypes of Evolved Strains AR2S.....	258
5.11.1	<i>Rate of colony expansion changes in evolved AR2S strains</i>	266
5.11.2	<i>Types of swarming observed in evolved strains FleQS, AR1S and AR2S</i>	267
5.11.3	<i>Strains isolated from blebs</i>	269
5.12	Study of Single Colonies of Strain AR2S15	272
5.13	Summary of Evolution of Swimming Motility in Sessile Strains AR1 and AR2	278
6	Whole Genome Sequencing of Evolved Strains FleQS and AR2S	281
6.1	Introduction	281
6.2	Whole Genome Sequencing Results	282
6.2.1	<i>Parent strains AR2 and SBW25ΔfleQ</i>	282
6.2.2	<i>Evolved strains FleQS and AR2S: nitrogen related mutations</i>	283
6.2.3	<i>Other mutations, unrelated to nitrogen assimilation pathway</i>	290
a)	Putative ammonia channel (PFLU_RS08590, old locus tag PFLU_1747)	291
b)	Oxidoreductase or short chain dehydrogenase (PFLU_RS16245; old locus tag PFLU_3332).....	293
c)	Fusidic acid resistance (PFLU_RS27180; old locus tag PFLU_5530)	294
d)	Putative filamentous adhesin gene (PFLU_RS20605; old locus tag PFLU_4201)	294
e)	Transcriptional regulatory protein AlgP1 (PFLU_RS31200; old locus tag PFLU_5927).....	294
f)	Hypothetical putative membrane protein (PFLU_RS14795; old locus tag PFLU_3035)	297
7	Concluding Remarks	298
7.1	Dominance of T97P NtrB Mutation in Evolutionary Pathway for Restoration of Swimming Motility	298
7.2	Reduced Recovery of Evolved Mutants with Ammonium As Nitrogen Source.....	300
7.3	Mutation of the Sensor Might Be a More Effective Pathway to Replacement of FleQ	304
7.4	Poor Growth in Ammonia Is the Biochemical Impact of a Mutated NtrBC System	306
7.5	Swarming Types of the Evolved Strains FleQS, AR1S/AR2S.....	307
7.6	FleQ is the Sole Master Regulator of Flagella Expression in <i>P. fluorescens</i> KO FleQ.....	308
7.7	Active and Passive Motilities.....	309
7.8	Sources of Variation in Motility Plates.....	311

7.8.1	<i>Water content in the motility plates</i>	311
7.8.2	<i>Physical factors that affect swarming motility</i>	312
7.8.3	<i>Changes in pH and temperature affect bacterial growth</i>	312
7.9	Experimental Evolution Shows that Nitrogen Limitation Is the Evolutive Force for NtrB Re-Wiring to Flagella Restoration in KO <i>fleQ</i> Strains	314
7.9.1	<i>Absolute and relative fitness of the evolved swimming phenotype</i> ...	315
7.10	Significance.....	316
7.11	Further Research	318
8	Bibliography	320

List of Figures

Figure 1-1 Phylogenetic classification of <i>Proteobacteria</i>	3
Figure 1-2 Phylogenetic relationships within the <i>Pseudomonas</i> strictu sensu group as well as other <i>Gammaproteobacteria</i> based on 16S rRNA hypervariable regions..	6
Figure 1-3 Phylogenetic intrageneric relationships of species from the <i>Pseudomonas</i> genus based on <i>gyrB</i> and <i>rpoD</i> gene	9
Figure 1-4 Number of shared conserved protein-coding genes within different <i>Pseudomonas</i> species and with different <i>P. fluorescens</i> strains.....	11
Figure 1-5 Presence of selected biosynthetic/catabolic genes or gene clusters in ten different strains.....	13
Figure 1-6 Structural comparison of the flagella and injectisome	15
Figure 1-7 Viscosin operon and structure.....	17
Figure 1-8 Viscosin is important for swarming and biofilm formation	18
Figure 1-9 Bacterial motility in response to chemical gradients: chemotaxis.....	21
Figure 1-10 Model of chemotaxis signalling and structure of MCP	22
Figure 1-11 Structure of the flagella motor - rotor and stator.....	23
Figure 1-12 Swimming and tumbling in peritrichous <i>E. coli</i>	24
Figure 1-13 Chemotaxis assay methods	28
Figure 1-14 Chemotaxis pathway in <i>P. fluorescens</i> SBW25	29
Figure 1-15 Che cluster genes present in the genome of <i>P. fluorescens</i> F113.....	30
Figure 1-16 The free-swimming behaviour of <i>P. fluorescens</i> SBW25	31
Figure 1-17 Flagella biosynthesis gene clusters in <i>P. fluorescens</i> SBW25.....	32
Figure 1-18 Flagella assembly in <i>P. fluorescens</i> SBW25.....	33
Figure 1-19 Flagella synthesis cascade for polar flagella in <i>P. aeruginosa</i>	35
Figure 1-20 FleQ binding sites in promoters of flagella regulon in <i>P. aeruginosa</i> ...	37
Figure 1-21 FleQ from <i>P. aeruginosa</i> PAO1	38
Figure 1-22 Inhibition of FleQ activity via the sequestration by FleN.....	40
Figure 1-23 C-di-GMP model for FleQ regulation in <i>P. aeruginosa</i>	42
Figure 1-24 Regulation of the σ^{54} promoters of flagella genes in <i>P. aeruginosa</i>	44
Figure 1-25 Mutagenesis is the source of variability for natural selection	47
Figure 1-26 Amplification mutagenesis is temporal.....	53
Figure 1-27 Amplification mutagenesis and evolution of leaky <i>lac</i> mutant	54

Figure 1-28 Motility phenotype of sessile parent and evolved strains in swarming medium	55
Figure 1-29 Star phylogenies showing a comparison of the full length protein sequences that are homologous to FleQ.....	56
Figure 1-30 The different types of signalling transduction systems in prokaryotes .	58
Figure 1-31 A one component system (OCS)	59
Figure 1-32 Isomerisation of transcription bubble:RNAP- σ^{54} holoenzymes	60
Figure 1-33 Chemotaxis alters the direction of flagella rotation and changes the swimming direction.....	61
Figure 1-34 Mechanisms of transport for ammonia/ammonium ($\text{NH}_3/\text{NH}_4^+$) in <i>E. coli</i>	64
Figure 1-35 Ammonium channel (AmtB) is regulated by sensor protein GlnK	65
Figure 1-36 Ammonia assimilation pathways	67
Figure 1-37 Nitrogen regulation of the glutamine synthetase (GS) pathway	68
Figure 1-38 Carbon and nitrogen metabolism are interconnected by 2-OG	68
Figure 1-39 Conformational state of PII regulates nitrogen metabolism.....	69
Figure 1-40 Ribbon diagram illustrating the structure of PII in <i>E. coli</i>	71
Figure 1-41 Structure of NtrB of <i>P. fluorescens</i> SBW25.....	71
Figure 1-42 NtrB sequence features and transcript unit in <i>P. fluorescens</i> SBW25 ..	73
Figure 1-43 Diagram of NtrB dimers, PII binding site and localisation of mutations that dampen phosphatase activity in <i>E. coli</i>	74
Figure 1-44 DNA looping due to NtrC dimers binding to boxes around the <i>gdhA</i> promoter.....	76
Figure 1-45 Nitrogen regulation in <i>E. coli</i> under nitrogen limitation conditions.....	77
Figure 1-46 Promoters of <i>glnALG</i> operon are regulated by the nitrogen status	78
Figure 1-47 NtrC domain structure in <i>E. coli</i>	79
Figure 1-48 NtrC sequence features in <i>P. fluorescens</i> SBW25.....	79
Figure 1-49 Molecular regulation: <i>glnALG</i> operon transcription by NtrC in <i>E. coli</i> ...	80
Figure 1-50 Closed complex isomerisation of the promoter for <i>glnALG</i> operon expression.....	81
Figure 1-51 Cumulative feedback inhibition of GS	83
Figure 1-52 The repression of carbon catabolite in <i>Pseudomonas</i>	85
Figure 1-53 Enzymes pertaining to glucose and fructose utilisation in <i>Pseudomonas fluorescens</i>	87

Figure 1-54 Assimilation of ammonium and the synthesis of other metabolites	89
Figure 1-55 Ammonium assimilation, synthesis of glutamine and glutamate, and their control	91
Figure 1-56 Specific activities of important enzymes of nitrogen metabolism within <i>P. fluorescens</i> ATCC 13525	91
Figure 1-57 Glutamine and glutamate synthesis pathways: GS-GOGAT and GDH.	92
Figure 1-58 Localisation of loci <i>amtB</i> , <i>glnA</i> , <i>glnK</i> , <i>ntrB</i> and <i>ntrC</i> in the genome of <i>P. fluorescens</i> SBW25	96
Figure 1-59 Proposed Ntr driven pathways of evolution of swimming motility in $\Delta fleQ$ strains	100
Figure 2-1 Hand-Drawn method to assess colony expansion	109
Figure 2-2 Isolation of evolved strain and preparation of glycerol stock	113
Figure 2-3 Study of single colony of <i>Pseudomonas</i> strain	117
Figure 2-4 Concurrent assessment of colony expansion for multiple colonies on the same plate	118
Figure 2-5 Assessment of colony expansion for multiple colonies on the same plate from an overnight broth culture	119
Figure 3-1 Illustration of the mechanism for sliding motility in aflagellate strains ...	125
Figure 3-2 Sliding colony phenotypes classed based on the type of chemical released	126
Figure 3-3 Colony phenotype of strains in swimming	130
Figure 3-4 Colony expansion curve of wild type strain SBW25	130
Figure 3-5 Phenotype of <i>P. fluorescens</i> strains at 22 h	132
Figure 3-6 Colony expansion of <i>P. fluorescens</i> strains	133
Figure 3-7 TEM image of wild type strain SBW25 and aflagellate strains SBW25 $\Delta fleQ$ and AR2	134
Figure 3-8 Swimming and swarming of the wild type strain SBW25	135
Figure 3-9 Colony expansion curves of strain SBW25 on swarming medium	135
Figure 3-10 Colony expansion curves for strain SBW25 on swarming medium	136
Figure 3-11 Swimming and swarming of the wild type strain SBW25	137
Figure 3-12 Box plot: The swarming time of the wild type strain SBW25	138
Figure 3-13 Box plot: Swimming and swarming mean rates for individual plates ...	141
Figure 3-14 Swimming, non-swarming motility of SBW25C	143
Figure 3-15 Colony expansion curve of strain SBW25C	143

Figure 3-16 Colony expansion of flagellated, non-viscosin producer strains.....	144
Figure 3-17 Spidery-Spreading growth of strain SBW25 Δ <i>fleQ</i>	145
Figure 3-18 Spread of aflagellate strain SBW25 Δ <i>fleQ</i>	148
Figure 3-19 Spread of individual replicates of SBW25 Δ <i>fleQ</i>	148
Figure 3-20 Development of spidery-spreading phenotype of strain SBW25 Δ <i>fleQ</i>	149
Figure 3-21 Box plot: Rates of colony expansion before and after the spidery- phenotype developed in SBW25 Δ <i>fleQ</i>	152
Figure 3-22 Box plot: Appearance of the spidery phenotype in aflagellate strains with different levels of viscosin production	156
Figure 3-23 Colony expansion curves of strain AR9 in swarming medium with and without kanamycin supplementation	157
Figure 3-24 Spidery phenotype of aflagellate strains AR9 and SBW25 Δ <i>fleQ</i>	158
Figure 3-25 Box plot: Comparison of colony's area from both sessile strains AR1/AR2 at 24 h	160
Figure 3-26 Phenotypes of sessile strains AR1, AR2 and the spidery-spreading strain SBW25 Δ <i>fleQ</i>	161
Figure 3-27 Cumulative growth curve of strain AR1	162
Figure 3-28 Cumulative growth curve of strain AR2	162
Figure 3-29 Box plot: Cumulative growth rates for sessile strains AR1/AR2	163
Figure 3-30 Box plot: Mean rates of cumulative growth during the slow and fast phases for both sessile strains AR1/AR2	164
Figure 3-31 Comparison of growth of wild type strain SBW25 in LB or M9 medium (broth) supplemented with different nitrogen sources.....	166
Figure 3-32 Growth curves in rich medium LB and medium M9.....	169
Figure 3-33 Box plot: Comparison of sessile and non-sessile strains growth in rich medium LB at 10 h	170
Figure 3-34 Box plot: Comparison of sessile and non-sessile strains growth in nitrogen/glucose M9 medium at 10 h	171
Figure 3-35 Average of colony's spreading area in 24 h	178
Figure 4-1 Colony expansion of <i>P. fluorescens</i> SBW25 Δ <i>fleQ</i> on M9 glucose plus glutamine.....	183
Figure 4-2 Colony expansion of <i>P. fluorescens</i> SBW25 Δ <i>fleQ</i> on M9 glucose plus glutamate	184

Figure 4-3 Colony expansion of <i>P. fluorescens</i> SBW25 Δ <i>fleQ</i> on M9 glucose plus ammonium	185
Figure 4-4 Box plots: Comparison of colony expansion area (mm ²) between SBW25 and SBW25 Δ <i>fleQ</i> under different nitrogen treatments.....	187
Figure 4-5 Comparison of colony expansion between SBW25 and SBW25 Δ <i>fleQ</i> for different nitrogen sources with glucose as the carbon source.....	188
Figure 4-6 Colony expansion of a sliding spidery colony of SBW25 Δ <i>fleQ</i> grown on glutamine and sucrose	189
Figure 4-7 Evolution of swimming motility of the aflagellate strain SBW25 Δ <i>fleQ</i> with ammonium as the nitrogen source and glucose as the carbon source.....	191
Figure 4-8 Evolution of swimming motility of spidery-spreading strain SBW25 Δ <i>fleQ</i>	192
Figure 4-9 Box plot: Comparison of days to evolve swimming motility between different sugars and glutamine	195
Figure 4-10 Colony expansion of evolved SBW25 Δ <i>fleQ</i> swimming colonies grown on ammonium and sucrose	196
Figure 4-11 Swimming motility of wild type strain SBW25 colonies grown on ammonium and sucrose	197
Figure 4-12 Spidery-Swarming of evolved strain FleQS3.....	200
Figure 4-13 Swimming and wild-swarming of strain FleQS6	201
Figure 4-14 Colony expansion of the evolved strain FleQS5	202
Figure 4-15 Colony phenotype of strain FleQS9	203
Figure 4-16 Colony phenotype of evolved strain FleQS9	204
Figure 4-17 Colony expansion curves of the evolved FleQS strains compared to SBW25 and SBW25 Δ <i>fleQ</i>	206
Figure 4-18 Colony expansion curves of evolved strain FleQS6.....	207
Figure 4-19 Growth curves of FleQS strains in LB and liquid medium M9-glucose	210
Figure 4-20 Box plot: Growth comparison between parent strain SBW25 Δ <i>fleQ</i> and evolved FleQS strains in rich medium LB.....	211
Figure 4-21 Box plot: Growth comparison between parent strain SBW25 Δ <i>fleQ</i> and evolved FleQS strains in nitrogen/glucose minimal medium M9	215
Figure 4-22 Box plot: Comparison of cell lengths (μ m) among FleQS strains, parent (SBW25 Δ <i>fleQ</i>) and wild type strain SBW25	217

Figure 4-23 TEM of evolved strains FleQS7 and FleQS5	218
Figure 4-24 Box plot: Comparison of the cell size (μm) of strain SBW25 determined in this research with the reported value of Ping et al. ²⁴	218
Figure 5-1 Cumulative growth and presumably twitching of sessile strain AR1	225
Figure 5-2 Chi-Square test for association	226
Figure 5-3 Blebbing of evolved colonies grown on poor nitrogen sources	227
Figure 5-4 Evolution of swimming motility in sessile strain AR1 with ammonium as the nitrogen source.....	227
Figure 5-5 Evolution of swimming motility in sessile strain AR1 with glutamine as the nitrogen source	228
Figure 5-6 Evolution of swimming motility in sessile strain AR1 in with glutamate as the nitrogen source.....	228
Figure 5-7 Box plot: Comparison of colony's spreading area of evolved colonies..	229
Figure 5-8 Colony expansion curves of evolved swimming AR1 colonies.....	230
Figure 5-9 Box plot: Evolved swimming motility when sucrose was the carbon source and different nitrogen sources.....	232
Figure 5-10 Box plot: Comparison of the evolution of swimming motility in sessile strain AR1 for different carbon and nitrogen sources	233
Figure 5-11 Colony expansion curve of evolved sessile strain AR1	234
Figure 5-12 Box plot: Days to observe evolution of swimming motility under different carbon sources and glutamine as nitrogen source	235
Figure 5-13 Phenotypic comparison of AR1S8, FleQS5 and SBW25	237
Figure 5-14 Colony expansion of the AR1S5	239
Figure 5-15 Colony expansion of the AR1S6	239
Figure 5-16 Colony expansion curves of all evolved strains AR1S	241
Figure 5-17 Evolution of swimming motility in sessile strain AR2 with ammonium as the nitrogen source and glucose as the carbon source	244
Figure 5-18 Evolution of swimming motility in sessile strain AR2 with glutamine as the nitrogen source and glucose as the carbon source	244
Figure 5-19 Evolution of swimming motility of sessile transposon mutants AR1 and AR2 with different nitrogen sources and glucose as the carbon source.....	245
Figure 5-20 Chi-Square test for association	246

Figure 5-21 Colony expansion curves for evolved colonies from parent strain AR2	248
Figure 5-22 Box plot: Comparison of colony's spreading of evolved colonies	249
Figure 5-23 Box plot: Evolution of swimming motility in strain AR2 for different nitrogen and carbon sources	251
Figure 5-24 Colony expansion curve of evolved AR2 colonies	251
Figure 5-25 Swimming motility in evolved strain AR2.....	252
Figure 5-26 Swimming motility in evolved strain AR2.....	252
Figure 5-27 Box plot: Comparison of evolution of swimming motility under different carbon sources and glutamine as nitrogen source	253
Figure 5-28 Colony expansion curves of all the evolved AR2S strains	261
Figure 5-29 Colony expansion curves of all the replicates of strain AR2S19	262
Figure 5-30 Spur and spur-swarming in strain AR2S7	263
Figure 5-31 Example of a skew experimental population: evolved strain AR2S19.	264
Figure 5-32 Comparison between swarming and non-swarming strains after 6 days	265
Figure 5-33 Swarming types in evolved strains.....	268
Figure 5-34 Types of blebs observed.....	270
Figure 5-35 Comparison of colony spreading curves of strains isolated from blebs from an evolved parent colony	271
Figure 5-36 Colony expansion curve of strain AR2S15.....	272
Figure 5-37 Colony expansion curve in swarming medium	273
Figure 5-38 Colony expansion curves of two different single AR2S15 colonies: A and B.....	274
Figure 5-39 Box plot: Comparison of colony spreading area between single colonies A and B	275
Figure 5-40 Comparison of rate of colony expansion changes in single colonies of AR2S15 with the rate of colony expansion changes of strain AR2S15	276
Figure 5-41 Comparison of acceleration changes in single colonies of AR2S15 with acceleration changes of strain AR2S15	276
Figure 5-42 Single AR2S15 colony A at different time points.....	277
Figure 6-1 Strain SBW25 Δ <i>fleQ</i> and AR2 grown on swarming medium.....	283
Figure 6-2 Origin of strains FleQSD and FleQS7W.....	286
Figure 6-3 Ammonium channel PFLU_RS08590	292

Figure 6-4 Model for ammonium channel.....	293
Figure 6-5 KEGG genome map: PFLU_RS31200 (gene <i>algP1</i>)	296
Figure 6-6 AlgP1 is a regulatory transcription factor rich in proline	297
Figure 7-1 Summary of nitrogen regulation and evolution of swimming motility.....	302

List of Tables

Table 1-1 Cluster characteristics based on phylogenetic relationships for <i>gyrB</i> and <i>rpoD</i> (Yamamoto et al. ³⁴)	7
Table 1-2 Characteristics of <i>P. fluorescens</i> complex	8
Table 1-3 Architecture of the <i>P. fluorescens</i> SBW25 genome	12
Table 1-4 Structure of viscosin-group of cyclic lipopeptides.....	16
Table 1-5 Flagellar genes regulated by FleQ in <i>P. aeruginosa</i>	39
Table 1-6 NtrB point mutations and their effects	74
Table 1-7 Growth of <i>Pseudomonas</i> strains on amino acids	90
Table 2-1 Properties of <i>P. fluorescens</i> strains.....	101
Table 2-2 Properties of evolved strains	103
Table 2-3 Stock solutions and preparation of 200 mL semi-solid medium M9	105
Table 2-4 Recipe for 50x TAE buffer.....	114
Table 2-5 Primer sequences for the nitrogen regulation genes ¹⁰⁸	116
Table 2-6 Region of the genes amplified by PCR	116
Table 2-7 Gene symbol, description and locus tags.....	123
Table 3-1 Swimming and swarming dependant rates of colony expansion for individual replicates of SBW25.....	140
Table 3-2 One-way ANOVA: Initiation of spidery phenotype time (h) versus plate diameter	147
Table 3-3 Colony expansion rates per plate before and after the spidery phenotype developed.....	150
Table 3-4 Discriminant analysis	173
Table 3-5 Summary of the characteristics of the studied strains	176
Table 3-6 Descriptive statistics of colony's area (mm ²) at 24 h in swarming medium	177
Table 3-7 Summary of results	179
Table 4-1 Evolution of swimming motility under different nitrogen/glucose treatments	193
Table 4-2 Number of evolved and non-evolved replicates	196
Table 4-3 Frequency of recovery of motility mutants.....	198
Table 4-4 Swimming phenotype of FleQS strains	198
Table 4-5 Swarming phenotype of FleQS strains.....	199

Table 4-6 Mutations in <i>ntrB</i> and the associated amino acid position changes	208
Table 4-7 Growth in ammonium/glucose minimal medium M9 after 10 h and the motility phenotype of FleQS strains.....	214
Table 4-8 Strains SBW25 Δ <i>fleQ</i> and SBW25 responded equally to rich and poor nitrogen sources.....	214
Table 4-9 Discriminant analysis	220
Table 4-10 Summary of results	221
Table 5-1 Mean number of days for the evolution of swimming motility for different nitrogen sources with glucose as carbon source.....	225
Table 5-2 Range of days and the number of blebs after the evolution of swimming motility for different nitrogen sources.....	227
Table 5-3 Average number of days for the evolution of swimming motility for different carbon sources when glutamine was the nitrogen source.....	231
Table 5-4 Frequency of recovery of evolved AR1 isolates	236
Table 5-5 Origin of evolved isolates and motility phenotype	238
Table 5-6 Time of spur appearance and motility phenotype.....	238
Table 5-7 Genotype and phenotype of the evolved strains	241
Table 5-8 Days to evolve swimming motility in sessile strains in different nitrogen sources.....	243
Table 5-9 Range of days and number of blebs that appeared after swimming commenced for different nitrogen and carbon sources	245
Table 5-10 Descriptive statistics.....	250
Table 5-11 Testing isolates for swimming phenotype.....	254
Table 5-12 List of evolved AR2S strains:phenotype and origin	255
Table 5-13 Blebs obtained from the same evolved swimming colony in treatment glutamine/glucose	256
Table 5-14 Mutations in the genes studied for all evolved strains AR2S.....	257
Table 5-15 Motility phenotypes and spur formation time of the evolved AR2S strains	260
Table 5-16 ANOVA for Sessile Strains: Days to evolve swimming motility with different nitrogen/glucose sources	279
Table 5-17 ANOVA for Sessile Strains: Days to evolve swimming motility with poor nitrogen sources and glucose as carbon source	280

Table 5-18 ANOVA for Sessile Strains: Days to evolve swimming motility with different carbon sources	280
Table 6-1 Phenotype and history of the strains	288
Table 6-2 Whole genome sequencing results for evolved strains and their parent strains.....	289
Table 6-3 Whole genome sequencing results for selected evolved strains	290

List of Abbreviations

2-OG	2-Oxoglutarate
AAA+	<u>A</u> TPase <u>A</u> ssociated with diverse cellular <u>A</u> ctivities
ACC	1-Aminocyclopropane-1-carboxylate
ATase	Adenylyltransferase
bEBP	<u>B</u> acterial <u>E</u> nhancer- <u>B</u> inding <u>P</u> rotein
CCW	<u>C</u> ounter <u>c</u> lock <u>w</u> ise
c-di-GMP	Cyclic-diguanosine-monophosphate
CW	<u>C</u> lock <u>w</u> ise
FVG	4-Formylaminoxyvinylglycine
Gm	Gentamycin
GOGAT	<u>G</u> lutamine <u>o</u> xoglutarate <u>a</u> minotransferase or Glutamate synthase
GS	<u>G</u> lutamine <u>s</u> ynthetase
HK	<u>H</u> istidine <u>k</u> inase
IHF	<u>I</u> ntegrated <u>H</u> ost <u>F</u> actor
ISR	<u>I</u> nduced <u>S</u> ystemic <u>R</u> esistance
Km	Kanamycin
KO	Knockout
LA	Luria-Bertani agar
LB	Luria-Bertani broth
MCP	<u>M</u> ethyl- <u>A</u> ccepting <u>C</u> hemotaxis <u>P</u> roteins
N-P-K	Nitrogen-Phosphorus-Potassium
NRPS	<u>N</u> on- <u>r</u> ibosomal <u>p</u> eptide <u>s</u> ynthetase
OCS	<u>O</u> ne- <u>C</u> omponent <u>S</u> ystem
PCA	Phenazine-1-carboxylic acid
PGPB	<u>P</u> lant <u>G</u> rowth- <u>P</u> romoting <u>B</u> acteria
PMF	<u>P</u> roton <u>M</u> otive <u>F</u> orce
RNAP	RNA polymerase
ROS	<u>R</u> eactive <u>O</u> xygen <u>S</u> pecies
RR	Response Regulator
rt	Room temperature
TAE	Tris-acetate-EDTA
TCS	<u>T</u> wo <u>C</u> omponent <u>S</u> ystem
T3SS	Type III Protein Secretion System
T4P	Type IV Pili
UTase/UR	Uridyltransferase/uridylyl-removing enzyme
WGS	<u>W</u> hole <u>G</u> enome <u>S</u> equencing

1 Introduction

1.1 The Importance of Plant Growth Promoting Bacteria in Agriculture and the Environment

Plant growth-promoting bacteria (PGPB) can be free-living bacteria or endophytic bacteria that live within plant tissue. They may dwell within the phyllosphere (above the ground) or live in the rhizosphere (within the soil zone) where they are influenced by plant roots¹⁻⁴ and can establish symbiotic associations⁴. These soil bacteria are able to promote growth and protect plants from pathogens⁵. There are many genera known to contain PGPB, including *Pseudomonas*, *Enterobacter*, *Bacillus*, *Variovorax*, *Klebsiella*, *Burkholderia*, *Azospirillum*, *Serratia* and *Azotobacter*⁶. These PGPB also decrease the detrimental effects of stress caused by biotic factors, for example viruses, other bacteria, fungi, nematodes and insects^{3,6}, and abiotic factors, for example salinity, flooding, drought, temperature, heavy metals, gases and imbalanced levels of nutrients^{6,7}. The concomitant inoculation of *Pseudomonas mendocina* and the arbuscular mycorrhizal fungus *Glomus intraradices* in lettuce (*Lactuca sativa* L.) has been shown to lead to a decrease in drought stress induced reactive oxygen species (ROS)³. ROS, which is derived from the reduction of molecular oxygen (O₂), causes both oxidative damage to cells (e.g. fatty acid desaturation in leaves) and DNA damage resulting in cell death. The inoculation of these rhizotrophs into *Lactuca sativa* L. triggers expression of antioxidant enzymes such as peroxidase, catalase, and phosphatase in the plant host; these enzymes scavenge the ROS species released as result of the higher salt content in the soil. Examples of ROS species are H₂O₂, hydroxyl radicals (·OH), singlet oxygen (¹O₂), and superoxide (O₂⁻). Furthermore, it is known that PGPB release secondary metabolites, such as phytohormones, which are also plant produced compounds that regulate their growth and development and are involved in stress responses. Another secondary metabolite, produced by *Pseudomonas* spp, is 1-aminocyclopropane-1-carboxylate (ACC) deaminase. ACC is able to negate the deleterious effects of drought and salinity on plant growth and crop yields⁶ through the inhibition of overproduction of ethylene (C₂H₄), which causes the inhibition of root elongation, lateral root growth and root hair formation⁸.

In addition, PGPB have multiple applications as biofertilisers, in biocontrol and bioremediation, and as sources of novel secondary metabolites⁹. Biofertilisers, or live mixtures of soil microorganisms, are capable of supplying nutrients or enhancing their availability to plants^{7,10}. Their use can diminish nutrient loss associated with nitrogen-phosphorus-potassium (N-P-K) fertilisers and formation of non-soluble compounds^{3,11}. Consequently, the application of PGPB facilitates the use of less chemical fertilisers while retaining comparable crop yields³. PGPB also induce an increased plant root mass and length, as well as root tip growth, and these morphological changes make a plant more competent to efficiently absorb nitrates and phosphates³. This in turn decreases fertiliser run-off into rivers and the plethora of deleterious effects to the environment³.

There are a few well-known mechanisms used by PGPB to protect plants from pathogens¹². PGPB compete for the same ecological niche and substrates. They also antagonise pathogens using allelochemicals or inhibitory compounds, e.g. siderophores, antibiotics and biocidal volatiles¹², and trigger an induced systemic resistance (ISR) in their plant host¹². Due to these mechanisms PGPB are marketed as biopesticides, which prevent infections in crop plants¹³. Cedomon® is a commercial preparation consisting of live *Pseudomonas chlororaphis*, strain MA342, which is intended to protect cereal seeds, such as oat and barley, from fungal diseases like net blotch, which is caused by *Pyrenophora teres* Drechs¹⁴.

PGPB have been shown to be useful in bioremediation processes for the recovery of eroded and polluted soils¹, for instance PGPB play an important role in the recovery of mine tailings^{1,7,13,15}. This phytoremediation is due to their ability to enhance tolerance in plants to heavy metal stress, increase nutrient availability (e.g. soluble Fe²⁺) and the uptake of insoluble minerals (e.g. P, Ca, Mg, K, S), thereby improving plant productivity⁸. Consequently, the spread of toxic metals decreases in the environment, and therefore wildlife is protected¹⁵. In addition, PGPB facilitate the re-vegetation of native plants in degraded soils¹⁵. Therefore, PGPB are useful in decreasing the utilisation of agrochemicals in agriculture, horticulture and silviculture¹⁶, and to restore degraded arid areas at a lower cost¹⁵. However, enhanced commercialisation of PGPB strains requires improvement to their application in the field or greenhouse, and the determination of the most useful biological characteristics for specific environmental conditions¹⁶. Consequently, a good understanding of the

interactions of PGPB between their plant-host and the indigenous microbiota within the rhizosphere is necessary in order to increase the use of PGPB strains within agriculture¹⁶.

1.2 Characteristics and Ecological Importance of *Pseudomonas*

The phylum *Proteobacteria* is divided into five classes: *Alphaproteobacteria*, *Betaproteobacteria*, *Gammaproteobacteria*, *Deltaproteobacteria* and *Epsilonproteobacteria*^{18,19}. The class *Gammaproteobacteria* contains the order *Pseudomonadales*, the family *Pseudomonadaceae*, and genus *Pseudomonas* (Figure 1-1)¹⁸.

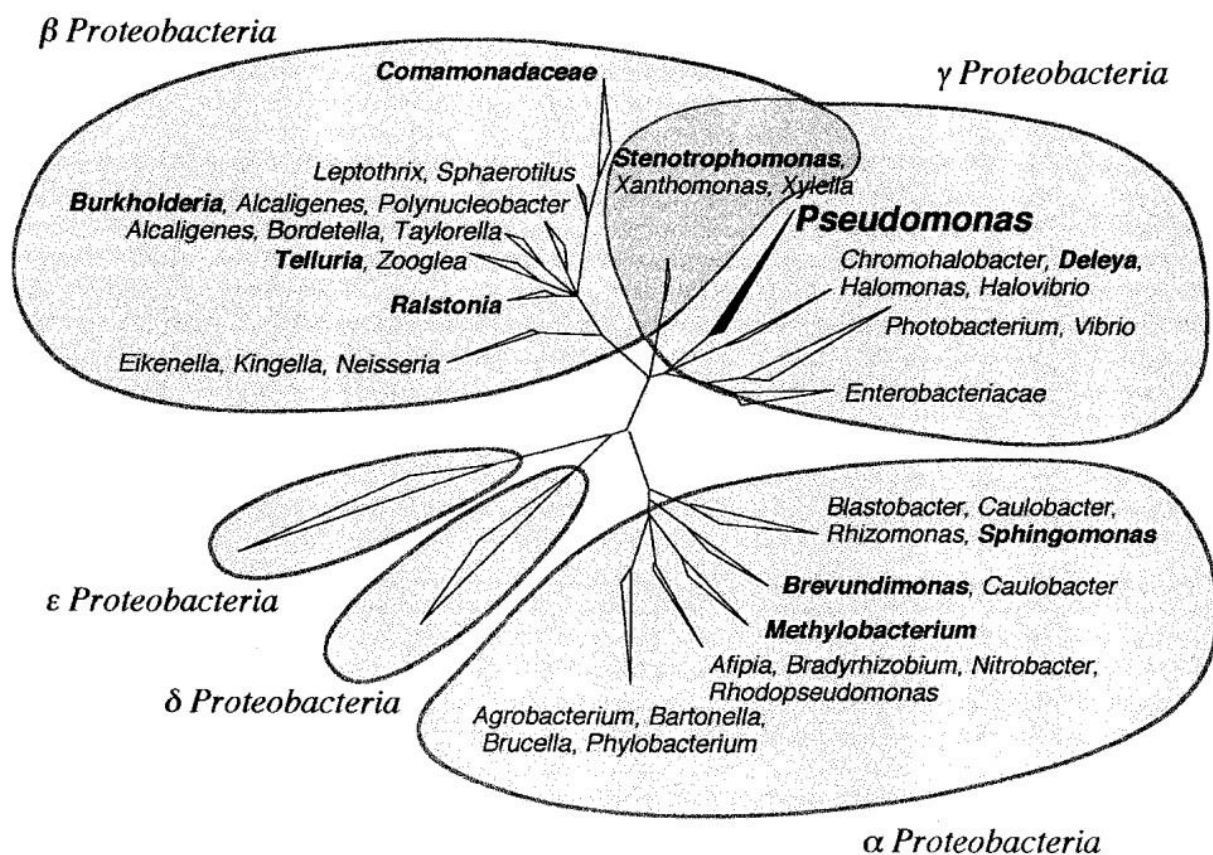


Figure 1-1 Phylogenetic classification of *Proteobacteria*

The phylum *Proteobacteria* is divided into five classes: *Alpha* (α), *Beta* (β), *Gamma* (γ), *Epsilon* (ϵ) and *Delta* (δ), based on DNA:DNA homologies, rRNA similarities and multilocus sequence analysis (MLSA). (Source: 19, p.53).

Pseudomonas are environmentally ubiquitous²⁰, and play a key role in the carbon cycle due to their metabolic versatility²¹, which permits them to degrade a plethora of simple and complex low molecular weight organic substances²², aromatics, halogenated derivatives, and recalcitrant organic residues²¹. This genus includes

plant, animal and human pathogens²², and individual species can be used as biocontrol agents for minor and major pathogens²⁰. *P. fluorescens* is not an animal and human pathogen like *P. aeruginosa*, but is associated with many of the plant and environment associated applications.

The genus *Pseudomonas* contains motile, catalase positive, aerobic, chemoorganotrophs, Gram-negative, non-sporulated and rod-shaped (straight or slightly curved) bacteria with a maximum length of $\sim 4 \mu\text{m}$ ^{18,23}. *P. fluorescens* SBW25 is $3.1 \pm 0.8 \mu\text{m}$ by $0.9 \pm 0.1 \mu\text{m}$ ²⁴. *Pseudomonas* have polar flagella, occasionally sub-polar, and in some instances lateral flagella in swarming cells. The *Pseudomonas* genome is 4.6 to 7.1 Mb with a GC content of 58 % - 69 %¹⁸, and encodes 4237 to 6396 predicted gene products²⁵. This genus possesses the TCA cycle, glyoxylate shunt, pentose phosphate pathway, and Entner–Doudoroff pathway²³. *Pseudomonas* preferentially use amino acids as carbon and nitrogen source^{23,26}, and also utilise substrates in a sequential manner (catabolite repression). This catabolite repression or diauxie permits *Pseudomonas* to utilise selected amino acids over glucose by preventing the expression of genes for glucose metabolism²³, a strategy which optimises metabolism, energy utilisation and improves the growth rate^{26,27}.

In addition, this genus produces multiple secondary metabolites²⁸ with diverse functions, including protection from competitors or predators, conferring virulence and facilitating nutrient uptake²⁵. *Pseudomonas* characteristically use a range of organic compounds as energy and carbon sources²⁹, and this metabolic versatility, together with their environmental ubiquity²⁸, fast growth rate and chemotactic responses,³⁰ has led to interest in using bacteria from this genus in agriculture as bioremediation and biological control agents²⁸.

1.3 *Pseudomonas fluorescens* Complex Group

In 1894 the botanist Walter Emil Friedrich August Migula proposed and described the genus *Pseudomonas* based on morphology. Later, physiological characteristics were introduced by Orla-Jensen in 1909 as the main criteria for bacterial taxonomy^{31,32} and subsequently interactions with higher organisms (e.g. pathogenicity) were included as taxonomic characteristics³¹. By 1970 there were 800 species assigned to this genus³⁵ when the first tentative attempt at a molecular based classification was undertaken³⁵. The initial approach determined the degree of relatedness via rRNA-DNA

hybridisations among all known species included under the generic name *Pseudomonas* (*Pseudomonas sensu lato*)³⁵. Thereafter, the *Pseudomonas sensu lato* group was divided into five rRNA subgroups (or Palleroni RNA groups), and only those assigned to group I remained in the genus *Pseudomonas*, defined as *Pseudomonas strictu sensu*^{31,35}. The *Pseudomonas strictu sensu* group is comprised of *P. aeruginosa*, all fluorescent species (*P. fluorescens*, *P. putida*, and *P. syringae*), and some non-fluorescent species (*P. stutzeri*, *P. alcaligenes*, *P. pseudoalcaligenes*, and *P. mendocina*)³⁵. From the 1990s onwards, Palleroni's RNA groups were reclassified according to sequence similarity of the 16S rRNA gene³¹, which is routinely used to determine phylogenetic relationships³². This study of sequence similarities of hotspot regions of the 16S rRNA gene of the genus *Pseudomonas strictu sensu* (species related to type species *P. aeruginosa*, and those assigned to rRNA group I)²¹ led to the identification of two intrageneric clusters, named: *Pseudomonas aeruginosa* and *Pseudomonas fluorescens*²² (Figure 1-2). Within each cluster, groups of closely related species (lineages) were also identified. It is difficult to distinguish between each lineage using shared metabolic or phenotypic characteristics, as can be used to differentiate between the two intrageneric clusters²². For instance, species assigned to the *P. fluorescens* cluster are saprophytic, plant pathogens, plant associated or associated with mushrooms, and found in soil and water. In contrast, those belonging to the *P. aeruginosa* cluster grow well at higher temperatures and can be opportunistic human pathogens, are generally not plant-pathogens and non-plant -associated²².

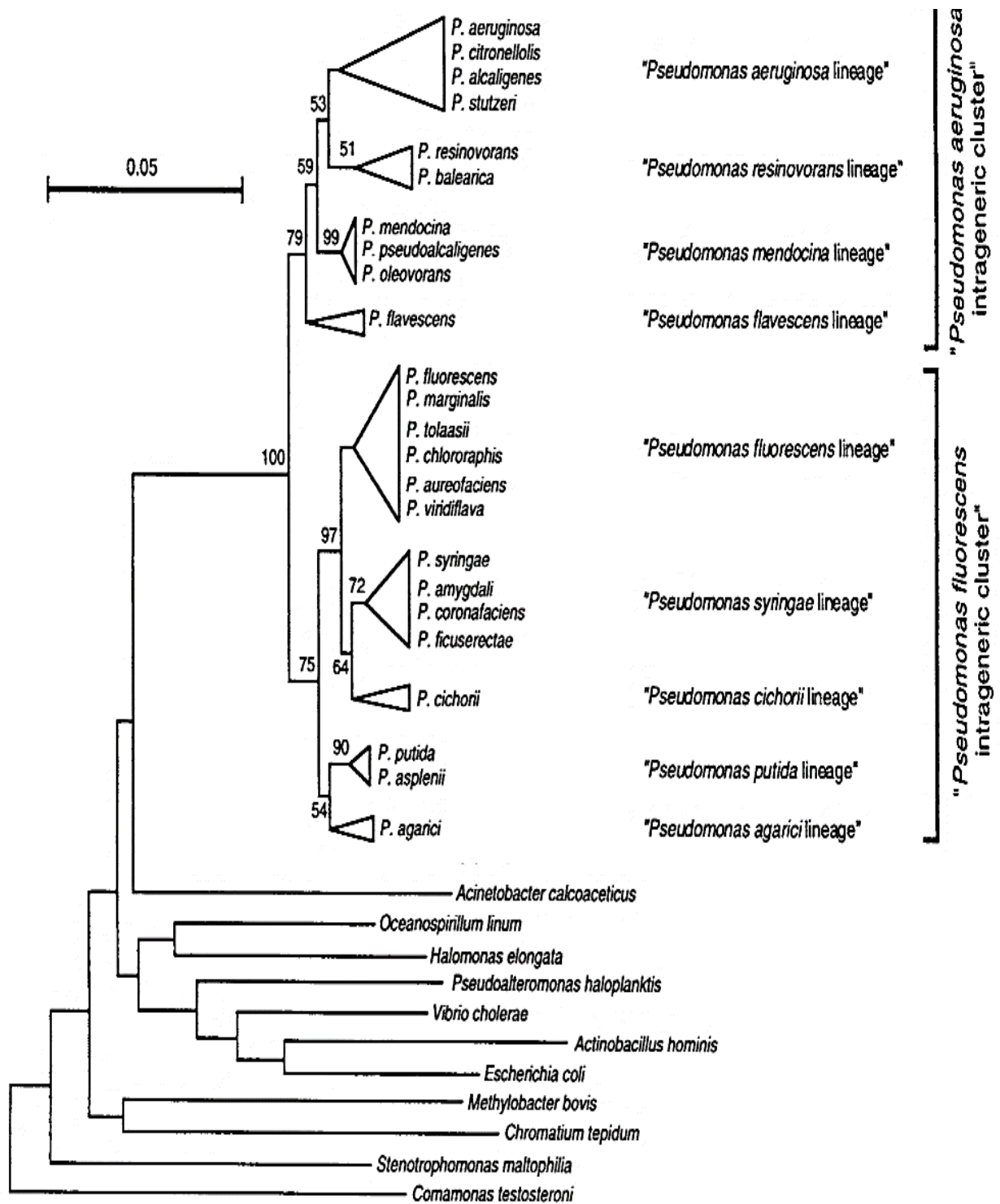


Figure 1-2 Phylogenetic relationships within the *Pseudomonas strictu sensu* group as well as other *Gammaproteobacteria* based on 16S rRNA hypervariable regions

Two major *Pseudomonas* clusters are identified based on 16S rRNA analysis: *P. aeruginosa* and *P. fluorescens*. This method distinguishes groups of species, defined as lineage but does not distinguish species within each lineage. The neighbour-joining clustering method was used to generate the dendrogram. The clade's accuracy was assessed using the bootstrap technique with (confidence levels in brackets). Only branches with bootstrap proportions of confidence higher than 50 % are displayed. (Source: 22, p.481).

These phylogenetic relationships do not allow high resolution determination of these intragenic relationships due to the slow rate of evolution of 16S rRNA genes. DNA gyrase B subunit (*gyrB*) and σ^{70} factor (*rpoD*) are ubiquitous and exhibit a higher evolutionary rate³⁴. Application of these genes to determine phylogenetic relationships shows that the *Pseudomonas* genus is monophyletic and corresponds to Palleroni's subgroup RNA I³⁴. They also cluster into two intragenic clusters named *P. aeruginosa* Cluster I and *P. fluorescens* Cluster II (Figure 1-3). These clusters match the clusters initially established using 16S rRNA gene similarities³⁴ (Table 1-1), but the complexes identified within these clusters are slightly different to the lineages as determined using 16S rRNA sequences (Figure 1-2). *P. fluorescens* Cluster II is more diverse than *P. aeruginosa* Cluster I, and is divided into three monophyletic subclusters: *P. putida* complex, *P. syringae* complex and *P. fluorescens* complex³⁴. The *P. fluorescens* complex (Table 1-2) is divided into two lineages: *P. fluorescens* and *P. chlororaphis*³⁴, although there are common cluster characteristics.

Table 1-1 Cluster characteristics based on phylogenetic relationships for *gyrB* and *rpoD* (Yamamoto et al.³⁴)

Intragenic Complex	Characteristics
Cluster I or <i>Pseudomonas aeruginosa</i>	Single polar flagellum
	High G+C contents (60.6 - 66.3 mol %)
	Growth at 41 °C. Exception <i>P. straminea</i>
	No fluorescent pigment. Exception: <i>P. aeruginosa</i> and <i>P. straminea</i>
Cluster II or <i>Pseudomonas fluorescens</i>	More than one polar flagellum
	Lower G+C contents (59.0 - 63.6 mol %)
	No growth at 41 °C. Some strains can grow at 4 °C
	Most of the strains produce fluorescent pigments

Table 1-2 Characteristics of *P. fluorescens* complex

<i>P. fluorescens</i> complex	Strain SBW25	Reference
Gram negative, rod-shaped bacilli		36
Motile via polar flagella		36
Non-spore forming		36
Secrete exopolysaccharides and form biofilms		36
Generally fluorescent except for <i>P. corrugate</i>	Fluorescent	34
Many are saprophytic	Saprophytic	34
Some are pathogens of plants and fungi	Non pathogenic; PGPB	34
Generally associated with food spoilage between 1 °C to 10 °C		34
Obligate aerobes		36
They can use nitrate in lieu of oxygen as terminal electron acceptor.		36
Optimal temperature growth in environmental isolates is 25 °C - 30 °C. Optimal temperature growth for mammalian isolates is 34 °C – 37 °C	Growth range of 4 °C to 28 °C. Impossible to grow at 37 °C	36
Many are psychrophilic (growth at 4 °C)		34
Oxidase positive		36
Catalase positive		36
	Arginine dihydrolase positive; gelatinase positive	39
Grow on trypticase soy agar (TSA) and Luria-Bertani (LB)	LB, King's medium B (KB), TSA	36
No haemolytic activity in environmental isolates. Haemolytic activity only for some mammalian isolates, e.g. MFN1032	Haemolytic activity ³⁷	36
	Secretes a hemophore protein to chelate heme	37
Small white convex colonies	Round smooth colonies in KB medium ²¹¹ ; round smooth yellow colonies in LA medium	36
	Produce furanomycin	46
They can carry genetic mobile elements.	No mobile genetic elements	9

genus *Pseudomonas*

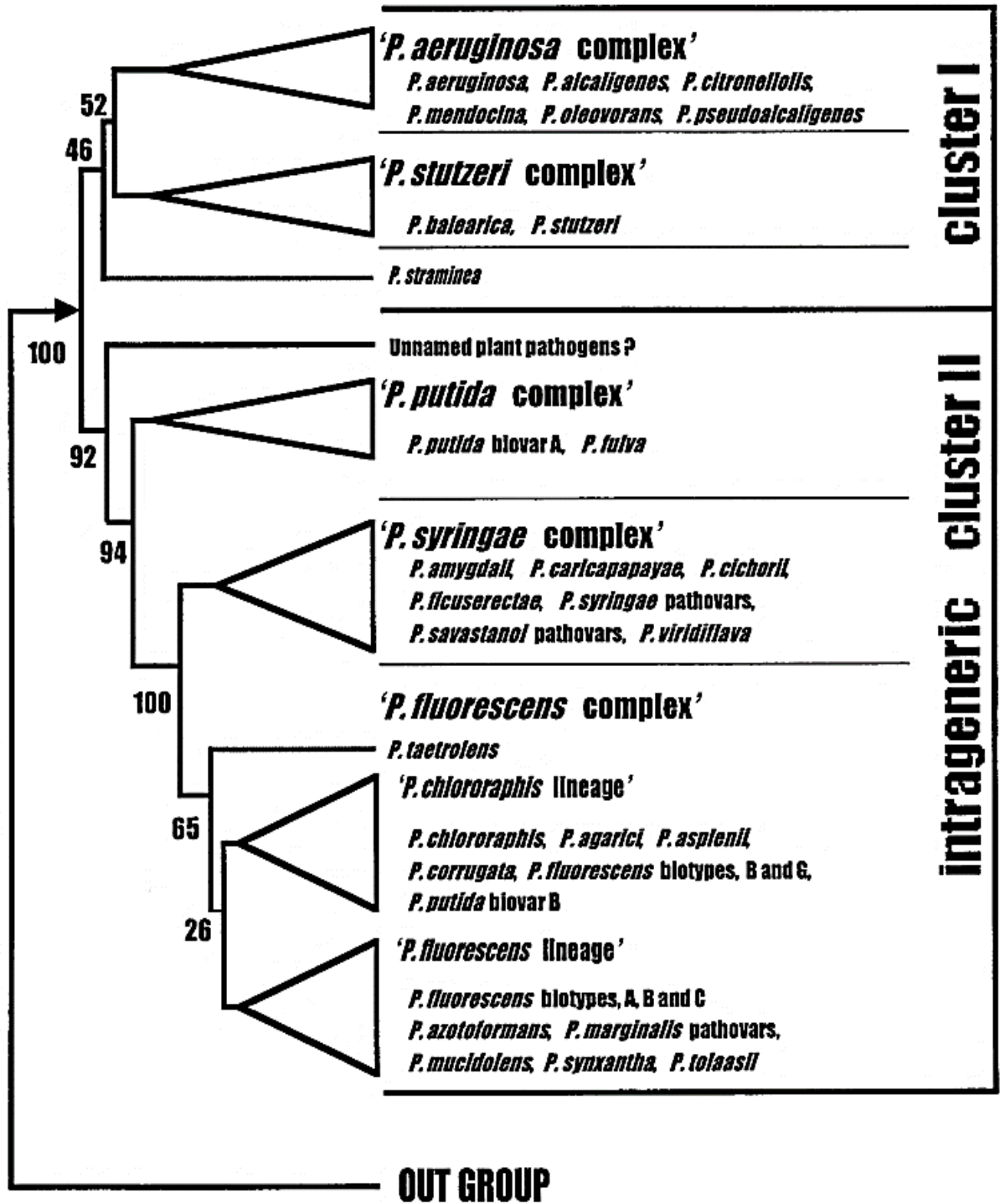


Figure 1-3 Phylogenetic intrageneric relationships of species from the *Pseudomonas* genus based on *gyrB* and *rpoD* gene

On the basis of 125 strains and 31 *Pseudomonas* species, the phylogenetic tree displays a couple of clusters: *P. aeruginosa* Cluster I and *P. fluorescens* Cluster II. The latter is more diverse and hence, split into three complexes: *P. syringae*, *P. putida* and *P. fluorescens*. (Source: 34, p.2391).

From recent estimates, the genus *Pseudomonas* is still comprised of 144 recognised species and 10 subspecies, making it the largest group of Gram-negative bacteria³³. This current number of accepted species was determined after the implementation of a polyphasic taxonomy^{22,34}, which uses chemosystematics, physiological, nutritional, metabolic and morphologic characteristics, ecological characteristics, antigenic structure, DNA:DNA homologies, rRNA-DNA and 16S rRNA similarities, and multi-locus sequence analysis (MLSA), to identify a genus and distinguish between species belonging to the same genus^{22,31,34}. There is a high variability at the species level in *Pseudomonas* as there are many subspecies and strains that differ considerably and require assignment to the category of genomovars³¹.

Throughout these phylogenetic studies the extensive genomic variability of the *Pseudomonas* genus had been demonstrated²⁵. Genomic comparisons conducted among strains representing four *Pseudomonas* species showed that only 2468 genes were conserved (core genome or orthologous coding sequences)²⁵ (Figure 1-4). On the other hand, the percentage of shared conserved genes in those species assigned to the *Pseudomonas fluorescens* group is about 54 %. These core genes include house-keeping genes essential for indispensable cellular functions. The remaining genes, between 45 % to 52 %³⁷, are specific to species and strains and encode unique traits, hence facilitating adaptation to different environments^{17,25}. Most of the species-specific genes are believed to have been acquired via horizontal gene transfer²⁵.

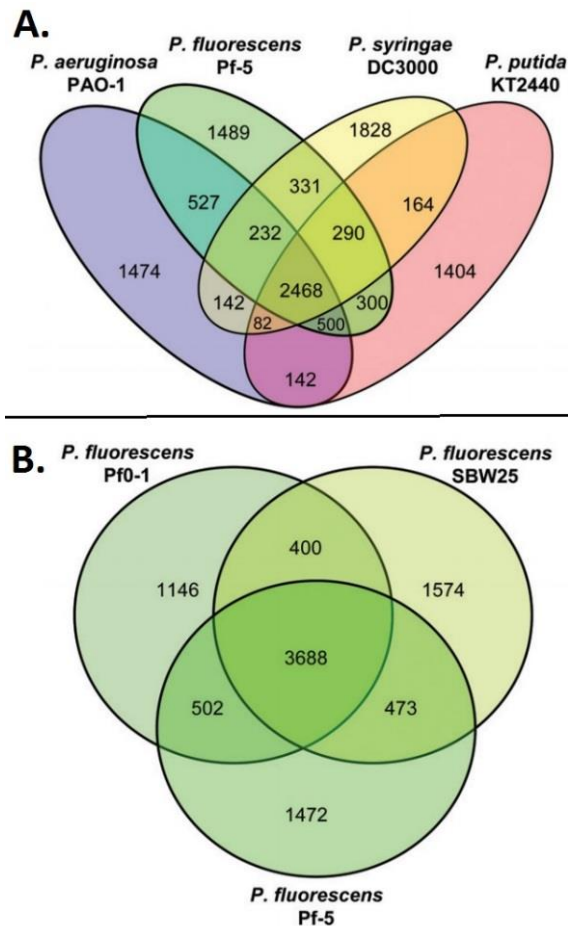


Figure 1-4 Number of shared conserved protein-coding genes within different *Pseudomonas* species and with different *P. fluorescens* strains

(A) Four *Pseudomonas* species. (B) Three strains of plant associated *P. fluorescens* only shared 3688 genes (61 %) of their genome: Pf-5 isolated from cotton, SBW25 isolated from sugar beet phyllosphere, and Pf0-1 isolated from soil. (Source: 25, p.1410).

P. fluorescens is broadly distributed on plant surfaces and in their tissues, and is also found in different habitats, such as soil, organic matter, water²⁵, and the surface of animals³⁸ and humans^{36,38}. *P. fluorescens* is a genetically diverse species³⁹, as demonstrated when comparing the three *P. fluorescens* strains: Pf0-1, SBW25 and Pf5²⁵. These strains share only 3688 protein-coding genes and possess strain specific genes resulting from their different lifestyles²⁵.

P. fluorescens SBW25, which belongs to rRNA group I, is an aerobic and motile saprophytic bacterium with polar flagellum³⁹. This strain was isolated from a sugar beet phyllosphere⁹. It has a genome of 6.7 Mb consisting of 6009 genes with a GC content of 60.5 %²⁵ (Table 1-3). The original strain was plasmid free; however, after being released in field experiments SBW25 acquired the plasmid pQBR^{9,103}.

Table 1-3 Architecture of the *P. fluorescens* SBW25 genome

	Feature	Reference
Number of bases	6,722,539	9
Number of CDSs	6,009	9
Average CDS length (nt)	999	37
Pseudogenes	88	9
Coding percentage	88.3 %	9
% GC	60.5	9
tRNAs	66	9
rRNA (clusters)	16	9
Intergenic repeat families^a	6	9
Predicted genes unique	1195	17
Flagellar synthesis gene clusters	PFLU_4437- PFLU_4456 PFLU_4728- PFLU_4731	42

^aIntergenic repeat families are short sequences approximately 21 bp – 65 bp¹⁷. This repetitive extragenic palindromic elements (also known as REP) are binding sites for DNA polymerase I and DNA gyrase¹⁷. In addition, REP are targets for transposases, recombinases and integration host factors¹⁷.

P. fluorescens SBW25 is a non-pathogenic⁴⁴ root coloniser and a plant growth promoter¹⁷, which is involved in the turnover of organic matter⁴⁷. It is able to modulate plant host metabolism, promote plant growth, and initiate induced systemic resistance³⁹; Figure 1-5 is from a comparison by Loper et al.³⁷ of genes associated with secreted products from ten different strains of *P. fluorescens*. It highlights the ability of *P. fluorescens* SBW25 to synthesize secondary metabolites, such as the cyclic lipopeptide viscosin³⁷, alginates (negative charged polymer)⁴⁴, partially acetylated cellulose necessary for biofilm formation and fast surface spreading⁴⁵ and a non-proteinogenic amino acid named 4-formylaminoxyvinylglycine (FVG), which has antimicrobial and herbicide activity⁴⁶. However, in contrast to many *P. fluorescens* strains which produce a plethora of antimicrobial compounds, such as 2,4-diacetylphloroglucinol (2,4-DAPG), phenazine-1-carboxylic acid (PCA)^{40,41}, pyrrolonitrin, pyoluteorin⁴², toxins, and products involved in plant–bacteria communication, this study suggested that SBW25 produces none of these products.

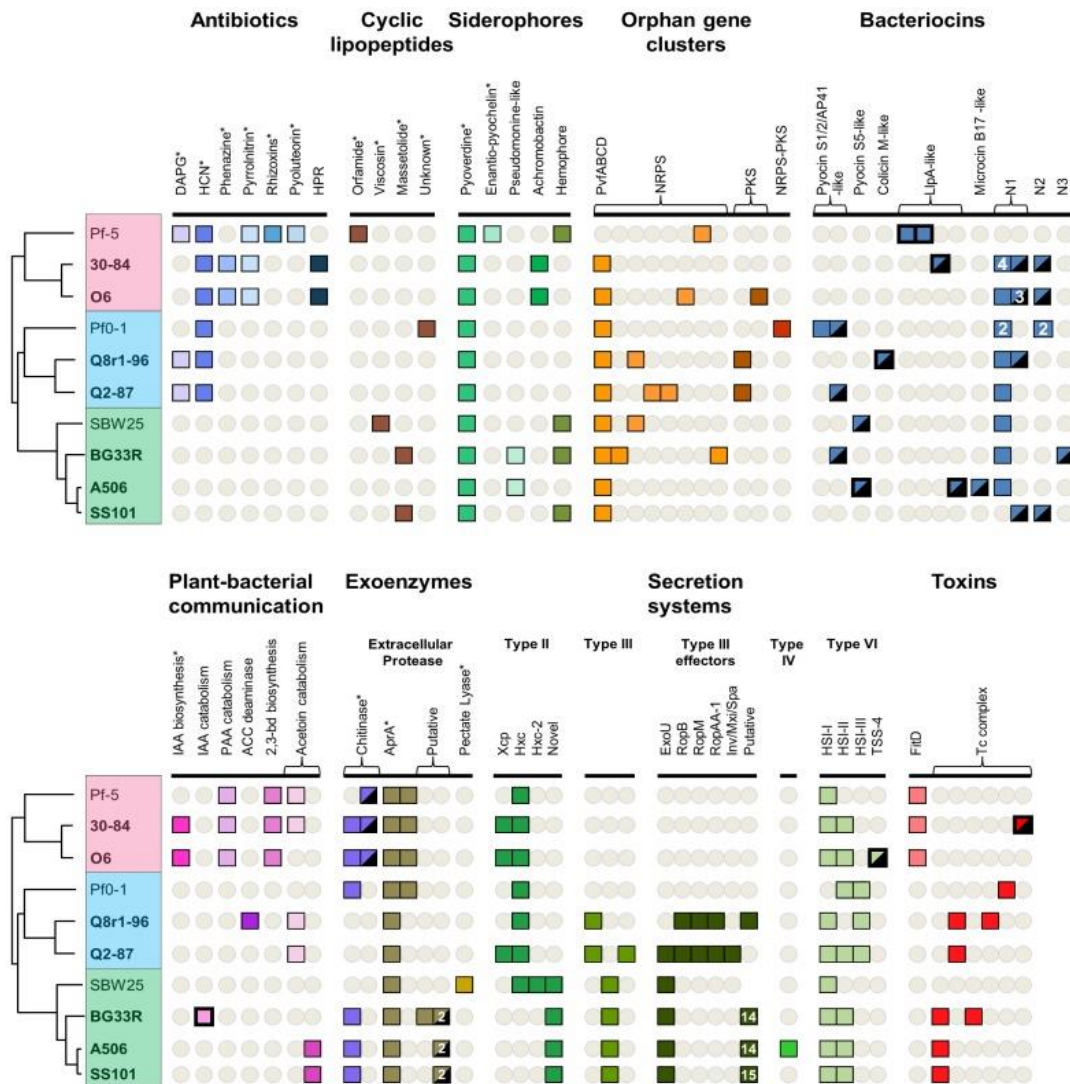


Figure 1-5 Presence of selected biosynthetic/catabolic genes or gene clusters in ten different strains

The coloured boxes denote the presence of a gene or gene cluster; a grey circle represents absence. Numbers within a box denote the number of copies that exist within this genome. Bold box outline indicates genes exist on a mobile genetic; genes that are inside the atypical trinucleotide content's regions have 50 % of the boxes blackened. Meanwhile plant-bacterial communication gene clusters comprise of: *iacR*, an ABC transporter, *iaaMH* (IAA biosynthesis); *iacHABICDEFG* (or IAA catabolism); *acdS* (ACC deaminase); *paaCYBDFGHIJKWLN*. (PAA catabolism); *acoRABC+acoX+bdh* (light pink, acetoin catabolism); *budC/ydJL + ilvBN* (2,3-butanediol biosynthesis); as well as *acoRABC + budC* (acetoin catabolism; dark pink). Their abbreviations are: hydrogen cyanide (HCN); 2,4-diacetylphloroglucinol (DAPG); rhizoxin derivatives (Rhizoxins); nonribosomal peptide synthetase (NRPS); 2-hexyl-5-propyl-alkylresorcinol (HPR); novel groups 1–3 of the pycocin and carocin like bacteriocins (N1, N2, N3); polyketide synthase (PKS); indole-3-acetic acid (IAA); aminocyclopropane-1-carboxylic acid (ACC); phenylacetic acid (PAA); and type VI secretion systems that are found in virulence loci HSI-I, HSI-II, and HSI-III of *P. aeruginosa* (HSI-I, II, II) as well as TSS-4 from *Burkholderia pseudomallei* (TSS-4). The asterisks suggest that this phenotype exists in the strains within this study, and was already known or have been detected in this research, then suggested genes or gene clusters are indicated. (Source: 37, p.11).

The rhizosphere environment has been shown to trigger the expression of 100 genes within *P. fluorescens* SBW25⁴⁸. These rhizosphere induced genes can be divided into six types: nutrient acquisition, stress response, attachment and surface colonisation, antibiotic production, secretion, and unknown⁴⁸. One of the rhizosphere induced genes is *rscC*⁴⁸, which encodes part of a type III protein secretion system (T3SS)⁴⁸. *P. fluorescens* SBW25 harbours other genes and putative effector proteins related to the T3SS⁴⁹.

T3SS is a nanomachine that delivers bacterial protein effectors (toxins or enzymes) into the cytosol of host eukaryotic cells, such as protists, fungi, plants and animals^{50,51}. This nanosyringe-like structure is a highly ordered structure and is genetically related to flagella apparatus⁵⁰. Both organelles are constructed from a series of membrane-spanning rings and are found embedded into the outer and inner membranes of Gram-negative bacteria⁴⁸. These organelles have a similar construction: a cytoplasmic component, basal body and extracellular segments (Figure 1-6). In T3SSs the extracellular needle shaped structure serves as a secretion channel through which to inject effectors into eukaryotic host cells⁵². Five groups of T3SS have been defined; Ysc, Hpr1, Hpr2, Inv/Mxi/Spa, and Esa/Ssa³⁶. Two families have been identified in the *P. fluorescens* complex, Inv/Mxi/Spa (known as SPI-1 in *Salmonella*) and Hpr1³⁶. The most common family of T3SS in *P. fluorescens* strains belong to group Hpr1³⁶. This type of T3SS is involved in plant pathogenicity³⁶ and is found in non-aeruginosa *Pseudomonas* spp and *Erwinia* spp³⁶. The Hpr1 family has a long flexible pilus that transpierces plant cell walls in order to deliver effectors⁵². T3SS is generally associated with virulence, although *P. fluorescens* SBW25 is non-pathogenic. *P. fluorescens* SBW25 encodes a functional Hrp1 T3SS that can secrete effectors and is expressed in the sugar beet rhizosphere³⁶; in tobacco it triggers a hypersensitive response³⁶. *P. fluorescens* SBW25 produces the effector ExoY, which is also expressed in *P. aeruginosa* to target the actin cytoskeleton of eukaryotic cells³⁶. The way in which a T3SS aids survival of *P. fluorescens* SBW25 in the rhizosphere remains to be elucidated.

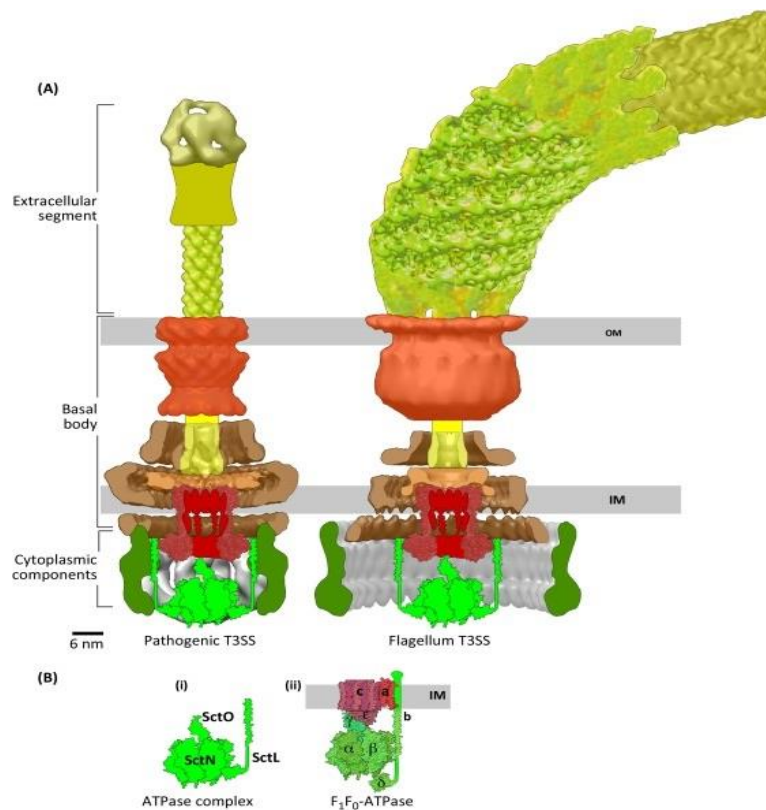


Figure 1-6 Structural comparison of the flagella and injectisome

(A) The pathogenic injectisome includes the following: a basal body, cytoplasmic component as well as a needle (extracellular segment); meanwhile the flagellum features a basal body, a cytoplasmic component (cytoplasmic-ring), a filament and a hook. Homologous components are depicted within the same colour. (B) The schematic shows a comparison between (i) the ATPase complex of T3SS as well as (ii) F₁F₀ ATPase synthase. In both systems the extracellular components are secreted via their own secretion system; the injectisome is believed to be the flagella's exaptation. (Source: 50, p.178).

1.4 Viscosin Is a Biosurfactant Involved in Swarming Motility

The antimicrobial viscosin is a surface-active agent, which improves swimming motility in *Pseudomonas* as the viscosity of the medium alters^{230,231}. In addition, viscosin aids in bacterial dispersion on hydrophobic surfaces (e.g. cuticle of leaves) due to its high wettability, and also this wetting capacity facilitates diffusion and solubilisation of nutrients present in the phytosphere (spermosphere, rhizosphere and phyllosphere)²³⁰. Viscosin is also involved in swarming, swimming and twitching motility²³¹. The mutant strains impaired for biosynthesis of viscosin only diminish motility but do not become non-motile²³¹. In *P. fluorescens*, viscosin production takes place at late exponential or stationary growth phase, and is regulated by the two-component system GacS/GacA and cell density²³⁰.

1.4.1 Classes of cyclic lipopeptides produced by *Pseudomonas*

Pseudomonas produces six different classes of cyclic lipopeptides: viscosin, syringomycin, amphisin, putisolvin, syringopeptin, and tolaasin⁴³. The viscosin-group includes the cyclic lipopeptides: viscosin, viscosinamide, massetolide A, pseudophomin A, and pseudodesmin A⁴³ (Table 1-4).

Table 1-4 Structure of viscosin-group of cyclic lipopeptides

Cyclic lipopeptide	Structure
Viscosin	FA-β-OH-L-Leu-D-Glu-D-aThr-D-Val-L-Leu-D-Ser-L-Leu-D-Ser-L-Ile
Viscosinamide	FA-β-OH-L-Leu-D-Gln-D-aThr-D-Val-L-Leu-D-Ser-L-Leu-D-Ser-L-Ile
Massetolide A	FA-β-OH-L-Leu-D-Glu-D-aThr-D-alle-L-Leu-D-Ser-L-Leu-D-Ser-L-Ile
Pseudophomin A	FA-β-OH-L-Leu-D-Glu-D-aThr-D-Ile-D-Leu-D-Ser-L-Leu-D-Ser-L-Ile
Pseudodesmin A	FA-β-OH-L-Leu-D-Gln-D-aThr-D-Val-D-Leu-D-Ser-L-Leu-D-Ser-L-Ile

Note: The cyclic peptide is closed as the hydroxyl group of aThr (allothreonine) or Thr forms an ester bond with the carboxyl group of the C-terminal amino acid. (Source: 43, p.145).

1.4.2 Viscosin: properties and ecological importance

Viscosin is a cyclic lipopeptide comprised of 3-hydroxydecanoic acid modified with two amino acids and connected to a nine amino acid cyclic peptide^{53,54}. Viscosin is amphiphilic due to the presence of the hydrophobic lipid moiety and hydrophilic as a result of the lactone ring⁵³. This lipopeptide is described as a surface active agent or biosurfactant because it diminishes the surface tension of water⁵⁶. This physical property has many biological implications because it helps the bacteria to overcome the interfacial surface tension of hydrophobic waxes present on plant surfaces and also to disrupt plant cell membranes releasing their nutrients⁵⁶. The strong surface activity and low density of viscosin changes the local soil-water distribution which has ecological implications because water is involved in nutrient diffusion, oxygen availability, microbial communication and bacterial motility⁵⁷. Viscosin has zoosporocidal activity against plant-pathogen oomycetes like *Phytophthora infestans* and *Pythium ultimum*⁵⁷, and serves as a defence to evade protozoan predation⁵⁸. In addition, it is necessary for biofilm formation and also facilitates swarming motility, and spidery-spreading⁵⁹.

1.4.3 Viscosin biosynthesis in *P. fluorescens* SBW25

Viscosin biosynthesis is governed by a multifunctional non-ribosomal peptide synthetase (NRPS)⁴³. This NRPS multienzymatic complex consists of a series of

repeat modules encoded by the genes *viscA*, *viscB* and *viscC* (Figure 1-7). Each module incorporates a specific amino acid in a stepwise fashion into the peptide chain and possesses three catalytic activities: condensation domain (C), adenylation domain (A), and peptidyl carrier domain (PCP or thiolation domain T). *ViscA* modifies the lipid moiety with Leu and Glu, *ViscB* synthesis the tetrapeptide sequence Thr, Val, Leu, Ser and *ViscC* completes the cyclic peptide with addition of Leu, Ser and Ile. This multienzymatic complex demonstrates collinearity because the number of modules is the same as the number of amino acids incorporated into the peptide moiety of viscosin⁴³ and their order in the chromosome parallels the peptide sequence⁶⁰. The gene *viscA* is located approximately 1.5 Mb upstream of *viscB* and *viscC*^{43,60} with a separate putative promoter. Assembly of the NRPS is due to specific domain-domain interactions and does not require physical linkage of the viscosin operon⁶⁰. GacS (the sensor kinase of the two-component Gac system) regulates the expression of viscosin⁶⁰. Viscosin is necessary for swarming and biofilm formation, which has been shown in experiments using site-directed mutagenesis of the *viscABC* operon, where mutants unable to synthesise biosurfactant were found to be sessile and did not form biofilms⁶⁰ (Figure 1-8).

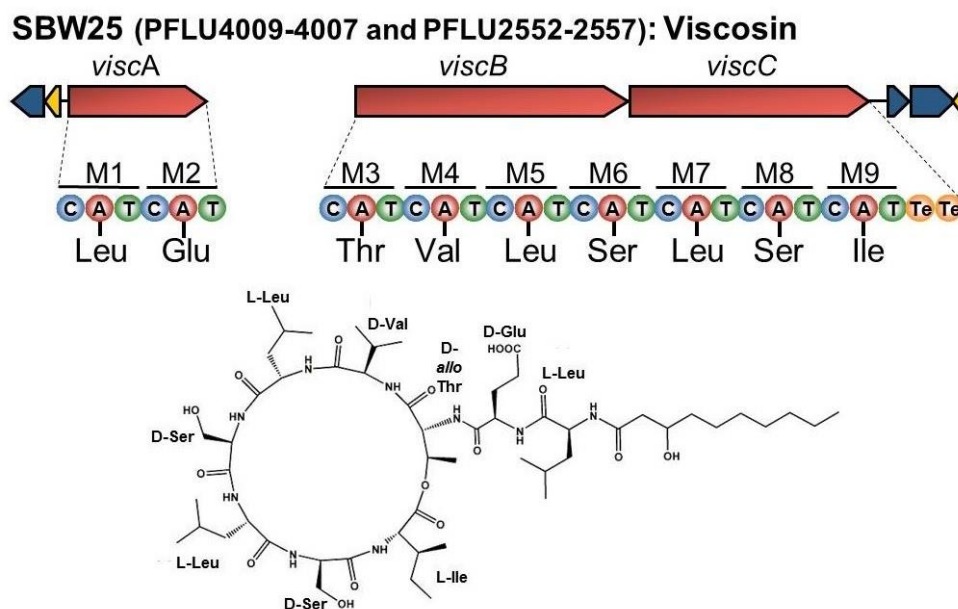


Figure 1-7 Viscosin operon and structure

Viscosin biosurfactant is a lipopeptide with a fatty acid chain connected to a cyclic peptide of nine amino acids. Viscosin is synthesised by a non-ribosomal peptide synthetase complex of gene products of the three unlinked genes *viscA*, *viscB*, and *viscC*. Peptides are synthesised in a stepwise fashion by modules M1-M9, each of which has three catalytic domains: adenylation (A), condensation (C), and thiolate or peptidyl carrier (T). Each module adds the specific amino acid shown. (Source: 37, p.13).

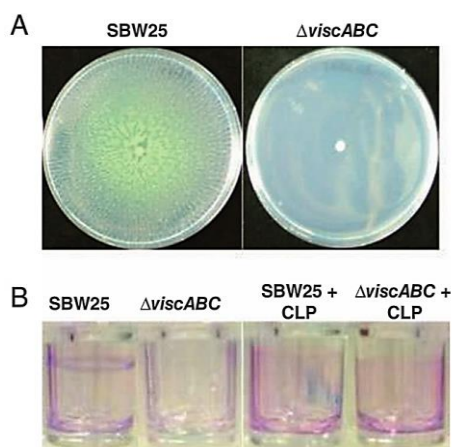


Figure 1-8 Viscosin is important for swarming and biofilm formation

(A) Swarming motility of SBW25 and impaired motility of SBW25 *viscABC* (viscosin minus) on 0.6 % agar w/v standard succinate medium (SSM). (B) Biofilm formation of SBW25 in microtitre wells; absence of biofilm with SBW25 *viscABC* and complementation by addition of CLP: cyclic lipopeptide viscosin. Biofilms were stained with crystal violet. (Source: 60, p.424).

1.4.4 Quorum sensing

Quorum sensing is a bacterial social behaviour that is dependent on the accumulation of a specific product of low molecular weight (e.g. N-acylhomoserine lactones – AHL) that, after reaching the threshold level (quorum)²³⁴, induces the expression of certain operons such as viscosin²³⁸. AHL is produced by some *P. fluorescens* strains like NCIMB 10586²³⁵, F113²³⁷, 5064²³⁸ and 2–79²³⁶; however is not produced by *P. fluorescens* SBW25²²⁹. Thus, its quorum sensing is not regulated by AHL.

Quorum sensing was initially elucidated in the *Vibrio fischeri*, and hence, any mechanism of the bacterial communication that is similar to the *V. fischeri* is known as the LuxI/LuxR type. LuxI is the enzyme that synthesizes an autoinducer, a small signalling molecule that belongs to the class of the N-acylated homoserine lactone (AHL), which is used to monitor the cell population. This autoinducer diffuses freely to-and-fro the cell, and upon reaching a certain intracellular concentration level (quorum), circa 10 nM, binds itself to the transcription factor LuxR. This complex LuxI-LuxR attaches and activates the luciferase operon (*luxICDABE*) expression. The *P. aeruginosa* has the quorum sensing type LuxI/LuxR, and their respective homologous proteins are LasI/LasR and RhII/RhIR; both of the quorum sensing systems belong to a hierarchy of the quorum sensing expression. Initially, the system LasI encodes the autoinducer [N-(3-oxododecanoyl)-HSL], which upon achieving the quorum binds itself to the transcription factor LasR that triggers the expression of *rhIR* (the second quorum

sensing system receptor) and the virulence factors such as elastase (*lasB*), protease (*lasA*), exotoxin A (*toxA*), alkaline phosphatase (*aprA*), and LasI (*lasI*), thus raising the autoinducer concentration. The RhIR attaches itself to the autoinducer N-butyryl-HSL produced by the RhII to target the operon *lasB*, rhamnosyltransferase (*rhlAB*), stationary phase sigma factor σ^S (*rpoS*), genes for pyocyanin antibiotic synthesis, cytotoxic lectin (*lecA*), and RhII (*rhlI*).

1.5 The Importance of Flagella in Bacterial Ecology

Flagella are important organelles involved in motility⁶³, and are required for many tactic responses, such as chemotactic (towards root exudates)^{64,65}, aerotactic (towards optimal oxygen levels) and magnetotactic responses^{66,67}. In addition, flagella driven motility has been shown to improve root colonisation, as flagellated bacteria find suitable binding sites more quickly compared to flagellaless mutants, which must rely on chance⁶⁸. Turnbull et al.⁶⁸ conducted experiments to determine the probability of survival between flagellated and aflagellate strains of *P. fluorescens* SBW25 upon inoculation of equal proportions of both strains in seeds. The motile bacteria moved towards the root system and colonised rhizosphere soil in a higher proportion compared to the non-flagellated strain, proving that flagella improves survival probability⁶⁸. Transposon mutagenesis experiments conducted by De Weger et al.⁶⁹ produced aflagellate *P. fluorescens* strains unable to colonise potato plant roots and studies with tomato root exudate have shown that malic acid and citric acid are the principal chemoattractants for *P. fluorescens* strain WCS365⁷⁰ and flagella-driven motility towards tomato root exudate. However, the non-motile flagellaless *P. fluorescens* strains R1a-4m, R4a-33m and R1a-1m are able to colonise wheat roots and suppress the pathogen *Gaeumannomyces graminis* var. *tritici*⁷¹. Therefore, while for many *P. fluorescens* strains flagella are an important organelle involved in root colonisation, and can contribute to improving crop yield by protection of crops from pathogens⁷², this flagellar driven motility is apparently not necessary for symbiotic association of all strains.

Furthermore, flagella are involved in biofilm formation, adhesion to substrates, virulence processes⁷⁵, and survival from bacterivores, which are bacteria predators such as protozoa or nematodes⁶⁷. This organelle facilitates relocation within microenvironments like soil pores or the root surface⁶⁸, and competition with other microorganisms present⁷⁵. Root colonisation can be achieved through passive or

active bacterial movement; passive movement is via soil water fluxes, whereas active translation is due to chemotaxis driven by flagella. Flagella-motility is an active mechanism of bacterial translocation in the direction towards their host, nutrients or root exudates. The composition of root exudates differs in different plant species and consists of amino acids, organic acids, sugars, vitamins, purines/nucleosides, enzymes, inorganic ions and gaseous molecules⁶⁸. This chemotaxis is driven by flagella and is coupled with a chemosensory system⁷⁶. Chemotaxis confers an evolutionary advantage because bacteria move directionally⁶⁸ and do not waste energy through random movements⁷⁷. There are two types of mediated chemotaxis in *Pseudomonas* that via the flagella-pathway or the pili mediated system⁷⁶.

1.6 Overview of Bacterial Motility and Chemotaxis

Chemotaxis is bacterial movement in response to alterations in low chemical gradients present in the environment, and this behaviour obeys the Weber-Fechner Law¹. The bacterial cell does not directly measure levels of chemoeffector (chemicals responsible for driving a chemotaxis response), rather it relies on an adaptation process by the receptors to these gradients, which means that if a cell is present in an area with a certain attractant concentration, then after a few seconds/minutes the receptors will become desensitised to the chemoeffector concentration, and thus a cell predominantly moves by tumbling and remains in that location. However, dramatic changes in the level of a chemoeffector will trigger bacteria to initiate swimming movement via short tumbling and long runs to move out from that area (Figure 1-9). Chemoeffector can be attractants or repellents, and based on this the bacterial response of chemotaxis is positive if there is a move towards high levels of a chemical (attractant) or negative if the cells translocate towards a lower concentration of a chemoeffector (repellent). Therefore, bacteria move in response to chemical gradients in order to reach a suitable environment for survival, and this trait is important in order to locate surfaces on which to adhere (e.g. algae, crustaceans), hosts to colonise, or for moving towards sources of nutrients available within a niche. Furthermore, plant-microbe interactions are directly related to the presence of certain compounds, such as amino acids which are strong chemoeffector for pseudomonads, and are abundant

¹ The Weber-Fechner law states that an organism will respond to a stimulus if it is above a certain threshold which distinguishes it from the environment.

in seeds and the rhizosphere. In addition, chemotaxis is necessary for plant-microbe interactions, the pathogenesis of infection, biodegradation, symbiosis and biofertilisation.

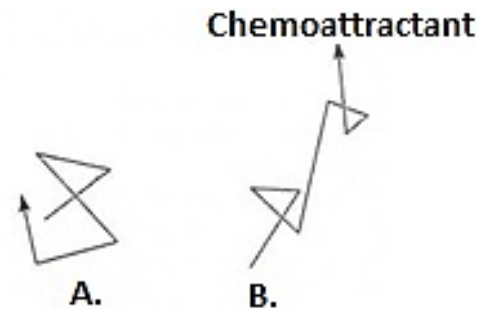


Figure 1-9 Bacterial motility in response to chemical gradients: chemotaxis

(A) In the absence of chemoeffectors the cells perform short runs and are constantly turning, leading to continuous changes in cell direction, and thus the cell remains almost in the same area. (B) Tumbling movement dramatically diminishes and long runs are observed as the result of the presence of a chemoattractant within the medium; when a cell moves towards the attractant then this response is called positive chemotaxis. Bacteria do not swim in a straight line as depicted due to Brownian motion. (Source: 115, p.535).

The chemotaxis system of *Pseudomonas* spp is homologous to that of *E. coli*, and consists of transmembrane methyl-accepting chemotaxis proteins (MCP), and six cytoplasmic Che proteins (CheA, CheB, CheZ, CheW, and CheY) that are localised to the pole of the cell, where their presence was determined by immunofluorescent microscopy. Chemotaxis is related to flagella driven motility because the phosphorylated form of the RR CheY protein (CheY-P) from the chemotaxis signalling cascade interacts with the flagella switch proteins FliM and FliN (Figure 1-10), which causes a change in flagella rotation from the normal counter-clockwise (CCW) direction observed at room temperature, to the clockwise (CW) direction that requires the input of free energy (Figure 1-11). There are more genes encoding MCPs within the *Pseudomonas* genome than *E. coli*; for example *P. aeruginosa* PAO1 has 26 MCPs, *P. putida* KT2440 possesses 26 MCPs, *P. fluorescens* Pf-5 encodes 42 MCPs, and *P. syringae* pv. *syringae* B728a contains 49 MCPs, whereas *E. coli* has only five MCPs¹⁸⁶. There is little research characterising the MCPs encoded by *Pseudomonas*; however, studies in *P. aeruginosa* have shown the presence of three MCPs for amino acid detection: PctA detects 18 amino acids, while PctB detects seven amino acids, and PctC detects two amino acids. The periplasmic domains of these MCPs for the

detection of amino acids are highly similar, and many *Pseudomonas* spp carry homologues to PctA.

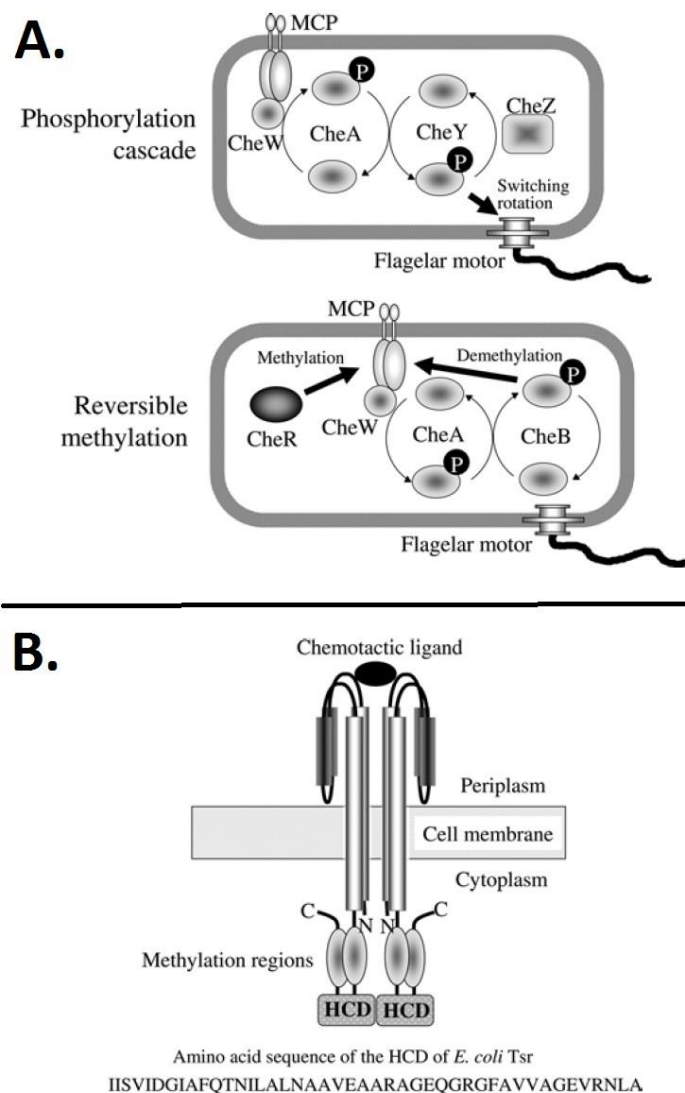


Figure 1-10 Model of chemotaxis signalling and structure of MCP

The chemotactic apparatus in *Pseudomonas* is genetically homologous to *E. coli* and functions similarly^{76,186}. (A) MCP binds to a chemoeffector which triggers a signalling cascade. CheA (histidine kinase) phosphorylation (CheA-P) requires CheW. The phosphate group from CheA-P is transferred to the response regulator CheY, which upon being phosphorylated (CheY-P) binds to the flagellar switch and changes the rotation direction from counter-clockwise to clockwise, causing the cell to tumble. Levels of CheY-P are regulated by CheZ, and this MCP is reversibly methylated at six Glu residues located within the cytoplasmic region, with the amount of methylation regulated by CheB (removes methyl groups) and CheR (adds methyl groups). In the presence of a repellent, methylation decreases, leading to an increase in CheA-P levels due to CheB activity. CheB is a response regulator that passes its phosphoryl group to CheA, thereby increasing levels of CheA-P. In contrast, in the presence of an attractant the methylation level increases and levels of CheY-P drop. (B) MCPs are transmembrane homodimers that interact with a chemoeffector via the periplasmic domain. The highly conserved domain (HCD) is important for the interaction with CheW and CheA. (Source: 186, pp.115-116).

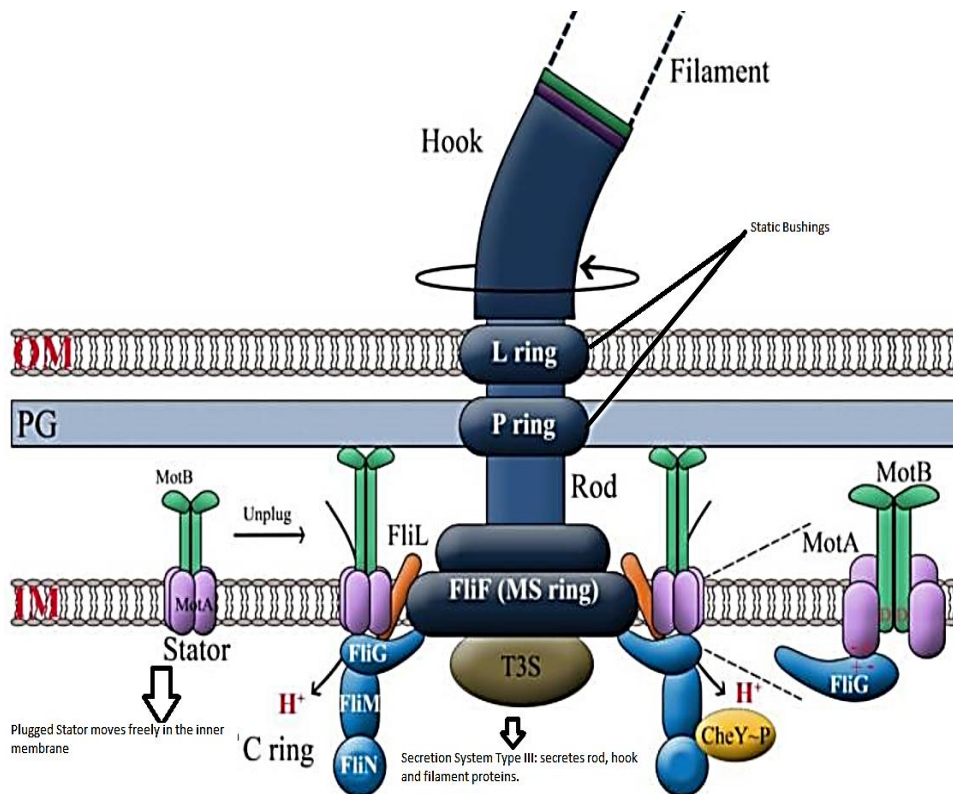


Figure 1-11 Structure of the flagella motor - rotor and stator

The motor consists of two parts: the rotor and stator. The rotor is a mobile structure (C ring, MS ring and rod), whereas the stator is static (MotAB ion channel complex). The P and L rings are bushings, and the flagellar switch (C ring) is comprised of three proteins: FliG, FliN and FliM. FliM and FliN interact with the response regulator CheY-P to change the direction of flagella rotation from counter-clockwise to clockwise by interacting with FliG. MotAB is a proton channel that harnesses energy from PMF in the periplasmic space and transforms it to mechanical energy. This is achieved upon binding of H⁺ to the cytoplasmic region of MotA, which induces conformational changes and triggers charge-charge interactions with FliG, thereby generating a rotational force (torque). This torque is transmitted to the hook via the MS ring and the rod. FliL is like a clutch which interacts with the stator and the rotor, regulating the speed and controlling the rotational direction. OM: outer membrane; PG peptidoglycan wall; IM inner membrane. The direction of rotation is shown with a circle arrow. The direction of flux of a proton is indicated with an arrow. T3S is a type III secretion system through which the hook, rod and filament proteins are secreted. (Source: 187, p.17).

1.6.1 Flagella movement: swimming and tumbling

After the invention of the dark field microscope and a higher numerical aperture enabling better resolution, it was possible to elucidate patterns of bacterial flagellation and motility. MacNab¹⁸⁹ used this technique to determine the average velocity of *Pseudomonas stutzeri* ($48.5 \pm 1.5 \mu\text{m/s}$; mean \pm SD) and *Salmonella typhimurium* ($25.4 \pm 1.5 \mu\text{m/s}$; mean \pm SD), and concluded that slow swimmers have peritrichous flagella and fast swimmers are polar flagellated. In addition, Macnab¹⁸⁹ observed that

tumbling *Pseudomonas* performs a double-reverse movement before reinitiating short or long runs depending on the stimulus present, whereas *Salmonella* after tumbling restart short or long runs depending on the chemoeffector present in the environment.

The bacterial flagellum is a helical rigid filament that moves similarly to an Archimedes' screw, with this movement generated by a proton motive force (PMF) across the inner membrane. In peritrichous flagellated bacteria (e.g. *E. coli*), their flagella form a polar bundle that demonstrates synchronised rotation in a CCW direction and pushes the cell forward when swimming. When the direction of the rotation changes to CW, then the flagella are pushed apart, and this results in a loss of coordination of the flagella movement, and thus the cell changes direction before recommencing short or long runs (flagella again move in a co-ordinated fashion CCW) according to compound responsible for triggering the CW movement (Figure 1-12).

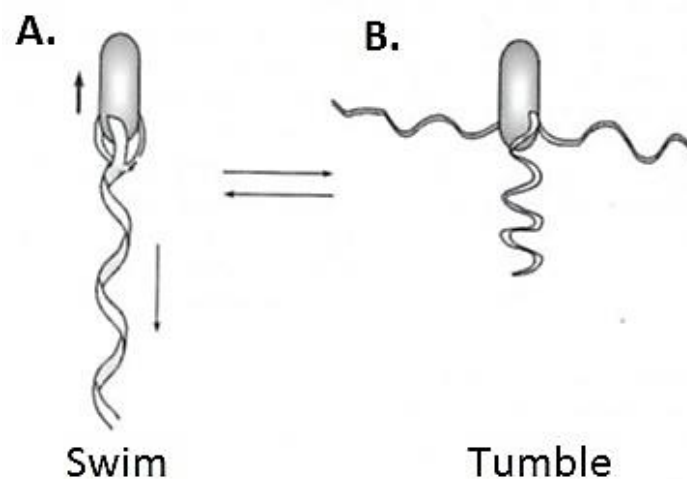


Figure 1-12 Swimming and tumbling in peritrichous *E. coli*

(A) The flagellar motor moves the flagella bundle in a counter-clockwise direction, and hence generates a helical movement that pushes the cell forward, with the physics of this movement being similar to an Archimedes' screw. (B) Whenever the flagella movement changes to the clockwise direction, then this pushes the flagella apart and results in tumbling in a random direction, before a cell then resumes short runs or long runs depending on the chemoeffector. (Source: 115, p.536).

1.6.2 Classic experiments in bacterial chemotaxis

Bacterial movement was first observed under the microscope by Antonie Van Leeuwenhoek, who in 1676 reported swimming organisms (bacteria) to be present in pepper-water. Alterations in bacterial motility due to fluctuations in concentrations of oxygen and carbon dioxide, together with changes in the intensity of illumination, were

observed by Engelmann in 1883. Engelmann called this type of movement *Schreckbewegung*, which in English means gulping or swallowing, because the cells seemed to be frightened when suddenly encountering changes in carbon dioxide and oxygen levels, and also when experiencing any alteration in the light intensity in the medium¹⁸⁵. For example, *Bacterium phatometricum* (purple sulphur bacteria) only swims in the light and is stationary in the dark, and if carbon dioxide is present then this also arrests cell movement, while *Bacterium termo* swims towards high oxygen levels generated by plants, whereas *Spirillum tenue* prefers lower levels of oxygen¹⁸⁵. In addition, Engelman also discovered that *B. phatometricum* only responds to certain light wavelengths after observing their movement behaviour when different wavelengths were used to illuminate the cultures¹⁸⁵.

The German botanist Wilhelm Pfeffer discovered chemotaxis in the 1880s when observing bacterial translocation under the microscope towards a liquid which was diffusing from a 1 μ L glass capillary submerged into a bacterial culture and filled with a solution which was not present in the culture medium. Pfeffer noted that *Spirillum undula* was attracted towards a solution of 1 % asparagine or 1 % meat broth, while the attractive effect of the meat extract or asparagine was overridden by the presence of a repellent such as 4 % potassium nitrate¹⁸⁵. However, when decreasing the amount of this repellent to 0.5 % while maintaining the attractant (meat extract or asparagine) concentration, then *S. undula* again showed chemotaxis towards the capillary; however, fewer bacteria accumulated inside the capillary compared to the initial experiment when the repellent was not present¹⁸⁵. In contrast, *B. termo* demonstrated chemotaxis to 1 % meat extract regardless of the concentration of potassium nitrate¹⁸⁵, and *S. undula* was repelled when the concentration of the meat extract or asparagine was increased to 4 %¹⁸⁵. In conclusion, these experiments show that certain chemicals are repellent to some bacteria, while even attractants can become repellents upon reaching a specific concentration¹⁸⁵. In 1969 Pfeffer' method was modified by Adler¹⁹⁰ in order to quantify the number of bacteria present inside the capillary filled with a chemoeffector, compared to the number of bacteria present in a capillary not containing the chemoeffector. To accomplish this he used a 1 μ L capillary (sealed at one end) filled with a chemical, which was then submerged into a drop of bacterial culture placed onto a microscope slide. The contents of the capillary tubes were then plated out and the number of colonies observed growing on the agar used to determine

the number of bacteria from inside the capillary. However, this method is time consuming and has low precision.

The development of microfluidic technology has allowed the study of bacterial motility within fluids and movement in groups, known as swarming¹⁹². Swarming bacteria move in 'packs' and are elongated (*Clostridium* does not differentiate into larger cells when swarming)¹⁹¹, hyperflagellated, and swim faster than single swimming cells because the cells move in swirling groups joined by their tangled flagella, although the cells are not tightly bound together¹⁹¹. Swarming has ecological implications because it facilitates population dispersion, thus allowing bacteria to reach other regions within their environment in order to acquire nutrients and escape from a harsh environment, as swarming bacteria can barrel through repellents and overcome obstacles (e.g. trapped air in soil). This swarming movement is independent of chemotaxis, whereas swimming is reliant on chemotaxis¹⁸⁷. Swarming bacterial populations tumble less and swim in longer paths¹⁸⁷. Swarming motility can be observed on surfaces and soft-agar² as an extension of a colony (swarming zone), where it has the appearance of a large raft, but this movement is not always conspicuous, and the micro-morphological pattern consists of bands and whirls constructed from bundles of heavily flagellated cells¹⁹¹. Swarming cells do not necessarily express more flagella for swarming, rather they produce alternative motors to propel the cells through viscous fluids and across surfaces. *P. aeruginosa* synthesises an alternative motor for swarming motility, and can also express an additional flagella from the same flagella operon¹⁹³. Therefore, swarming requires a rich environment in order to provide support for flagella synthesis, bacterial growth and surfactant production, which is regulated by quorum sensing¹⁹³. This type of bacterial motility was first observed in *Proteus* grown on nutrient soft-agar, and this technique has been used by Alder to study chemotaxis in *E. coli*, based on the fact that a colony utilises the chemoattractant, and hence creates a gradient so that cells swim towards higher attractant concentrations, and as the swimming movement is outwards then this leads to the appearance of a circular swimming colony¹⁹¹. Bacteria swim through the agar pores within semi-solid media (0.25 % agar) enriched with a chemoeffector, although the agar concentration must not be higher than 0.3 % otherwise the only movement observed will be swarming¹⁹¹.

² Soft-agar implies an agar concentration of 0.25 % within the medium.

The soft-agar plate method to study chemotaxis permits the isolation of chemotactic mutants that have enabled the elucidation of the chemotaxis signalling pathway. Masduki et al.¹⁹⁴ obtained chemotaxis mutants of *P. aeruginosa* following exposure to the mutagenic compound N-methyl-N9- nitro-N-nitrosoguanidine. The isolated mutant strains PC1 (*cheY*⁻) and PC2 (*cheY*⁻ and *cheZ*⁻) expressed flagella and grew like their parent strain PAO1, thus did not possess any metabolic impairment¹⁹⁴. Despite being flagellated the mutant strains did not move and instead formed dense small colonies when grown on semi-solid medium, and it was this phenotype that was used for identification and isolation. These mutants did not tumble as frequently as the parent strain when swimming in chemotaxis buffer (10 mM HEPES), as shown by the low frequency in direction change/sec (< 0.1 change direction/sec) compared to the parent strain PAO1 (0.9 ± 0.4 change direction/sec; mean ± SD). These mutants were not attracted by peptone in a computer assisted capillary assay, which is a technique based on digital image processing that counts the number of cells present in each frame taken at specific time intervals at the mouth of a 1 µL glass capillary filled with a chemoattractant (Figure 1-13).

Hong et al.¹⁹⁵ identified the MCPs Aer and Aer-2 for aerotaxis (movement towards oxygen) in *P. aeruginosa* PAO1, an obligate aerobic bacterium. The well chamber method was employed, and strains harbouring the green fluorescent protein (GFP) carried on a vector (pMRP9-1) were utilised to study the aerotactic behaviour of mutant strains. This technique consists of two wells, whereby the base of the upper well (1 mL) is consists of a polycarbonate filter (pore size 8 µm), which is placed inside the lower well. A GFP expressing bacterial suspension was placed into the lower well and the number of bacteria that migrated towards the upper well was quantified by detecting changes in fluorescence intensity using a fluorescence spectrophotometer (Figure 1-13).

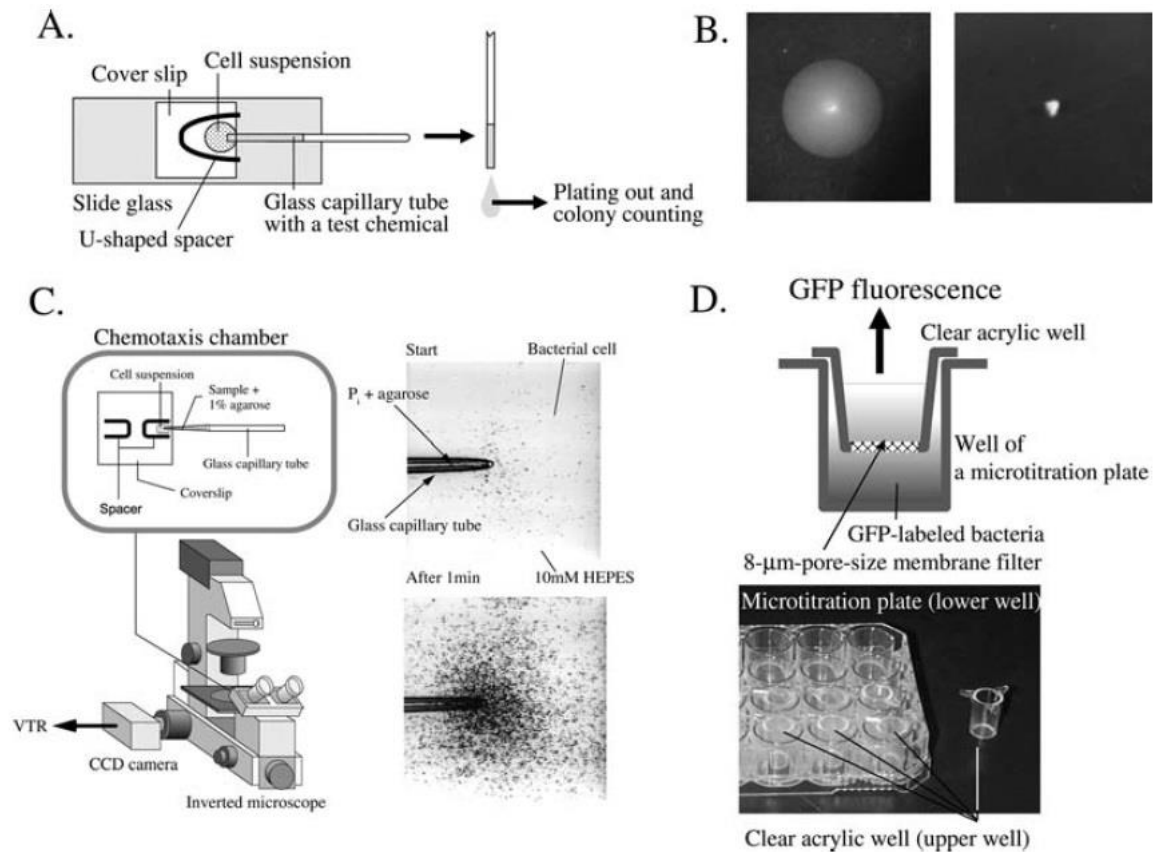


Figure 1-13 Chemotaxis assay methods

(A) The capillary assay. The glass capillary which contains a chemoeffector is inserted into a cell suspension. Following a suitable interval, the total number of bacterial cells in the capillary is gauged by plating out and colony counting. The robustness of the chemotactic response is assessed by the ascertaining the number of bacterial cells within the capillary. (B) The semisolid agar plate assay. Bacterial cells are inoculated onto the semi-solid medium. Following incubation chemotactic cells collectively form swarm rings (left), whereas non-chemotactic or non-motile cells create dense, small colonies (right). (C) The computer-assisted capillary assay. The microscopic images of chemotactic responses are videotaped using an inverted phase contrast microscope that is equipped with a CCD camera. The strength of the chemotactic response is determined by calculating the number of bacteria per videotape frame. (D) The microtitre plate assay. The upper well is an acrylic well that has an 8 μm pore membrane filter as the base, whereas the lower well is that of a 24 well microtitre plate. GFP-labelled bacteria move to the upper well in response to the oxygen gradient, where GFP fluorescence intensity is tracked to measure cell concentrations. (Source: 186, p.110).

1.7 *Pseudomonas fluorescens* SBW25 Movement Is Versatile

Bacterial motility is versatile and uses sensory mechanisms to sense environmental clues and respond to them; thus they can move towards more suitable environments⁷⁷. There are many types of bacterial motility, including swimming, swarming, twitching, and sliding⁷⁸ and this can be achieved using surface appendages, such as flagella or pili. While flagella-driven swimming is the primary mode of motility of *P. fluorescens*,

these bacteria can also move along surfaces by Type IV pili driven twitching and use viscosin to facilitate swimming or promote colony spreading in the absence of flagella.

1.7.1 Flagella driven swimming motility and chemotaxis

Flagella driven motility, the most common organelle involved in bacterial movement, is controlled by a signal transduction cascade that regulates the flagella rotation pattern accordingly to environmental cues⁸⁷. Over 80 % of known bacterial species rely on flagella for translocation and survival⁷⁵. Flagella are coupled to a chemosensory system (Figure 1-14 and Appendix Q: Table Q-1) so that bacterial movement respond to gradients of amino acids, aromatic compounds, organic acids, phosphate, chlorinated compounds, and sugars, among others compounds⁷⁶.

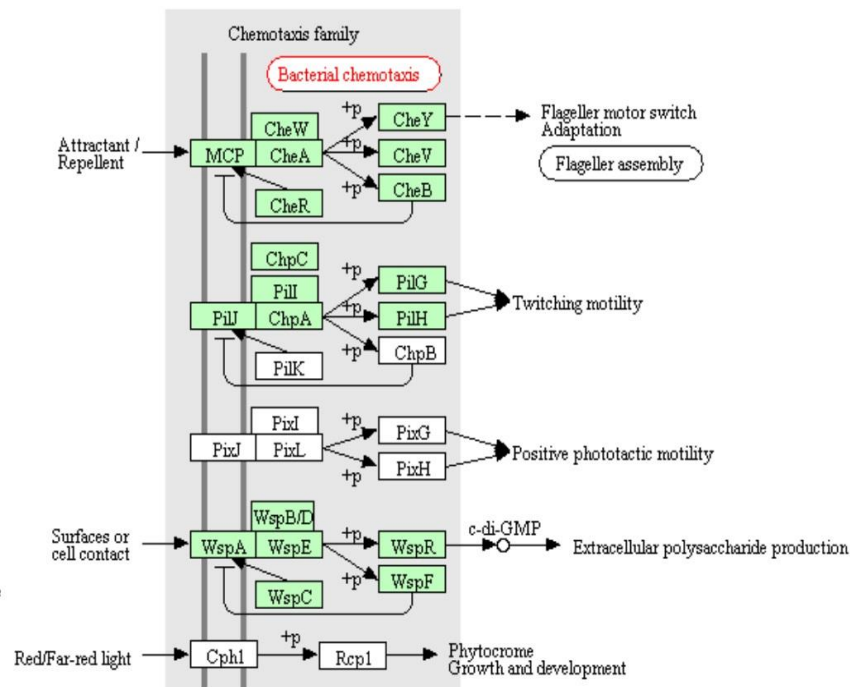


Figure 1-14 Chemotaxis pathway in *P. fluorescens* SBW25

The chemotaxis proteins present in *P. fluorescens* SBW25 are shown in green, whereas those that are absent in this strain are in white.

[Source: KEGG Pathways Database; Retrieved from https://www.genome.jp/kegg-bin/show_pathway?scale=1.0&query=che&map=pfs02020&scale=1.0&auto_image=&show_description=hide&multi_query=].

Comparative phylogenetic studies that were conducted on the genome of 50 strains from the *P. fluorescens* complex revealed that most of them possessed five chemotaxis systems: Wsp, Chp, Che1, Che2 and Che3²¹². *P. fluorescens* SBW25 has only four of these chemotaxis clusters: Wsp, Chp, Che1, Che2²¹². While the chemotaxis system Wsp regulates motility and biofilm production, the Chp cluster is

involved in twitching motility and is in close proximity to the *pil* operon, which is involved in pili biosynthesis regulation²¹². On the other hand, the system Che1 is involved in chemotactic motility; this cluster does not encode any MCP, whereas systems Che2 and Che3 are shown to contain MCPs genes²¹². Systems Che2 and Che3 are not always found to be present within the studied strains from *P. fluorescens* complex and are related to specific functions²¹². As shown in Figure 1-15, *P. fluorescens* F113 has three types of Che clusters. Meanwhile the Che1 cluster is organized into two groups in strain F113.

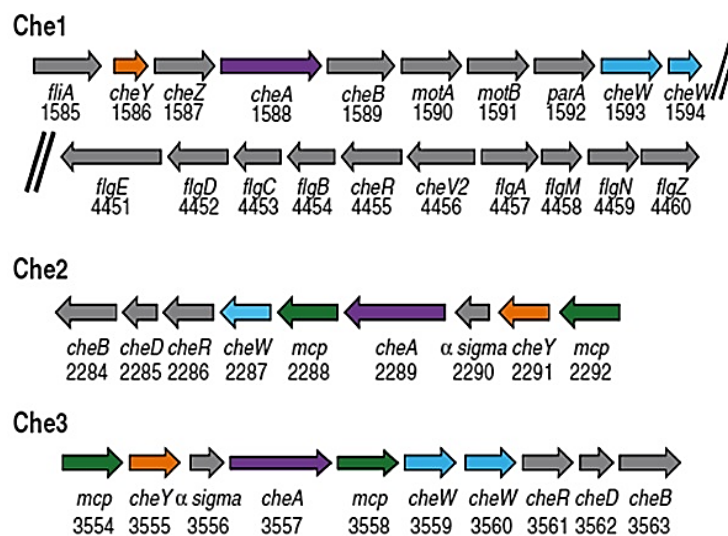


Figure 1-15 Che cluster genes present in the genome of *P. fluorescens* F113

Three Che systems can be seen in strain F113: Che1, Che2 and Che3. Notably, the cluster system Che1 is organized into two groups. Genes denoting the same color are paralogous. The locus tags are indicated below their gene names (PSF113_XXXX). It may be remembered that chemotaxis proteins, CheZ, CheY, and CheB are not indispensable for flagella biosynthesis. (Source: 212, p.8).

1.7.2 Flagella and swimming pattern of *P. fluorescens* SBW25

P. fluorescens SBW25 possesses a polar right-handed flagellum with 2.5 turns per filament, contour length of $8.4 \pm 1.3 \mu\text{m}$ (mean \pm SD), pitch $1.76 \mu\text{m}$ and diameter $0.79 \mu\text{m}$ ²⁴. SBW25 is not strictly monotrichous²⁴ and its average number of flagella per cell is 1.5 ± 1.1 ²⁴, which is lower when compared to other *Pseudomonas* species²⁴. The flagellum is a complex organelle, whose function and synthesis are encoded by at least 40 genes⁹¹ (Appendix P: Table P-1). Some of these are rhizosphere induced, such as *fliF*⁴⁷ which is part of the T3SS, and this suggests that a close interaction exists between SBW25 and plants⁴⁷. The swimming pattern in SBW25 is more complex than in *Escherichia coli* and similar to that of *Caulobacter*²⁴. SBW25 is able

to swim forward (run) and backward (backup), flip the cell body continuously, hover without translocation, and swiftly reorient run or backup movements²⁴ (Figure 1-16). *P. fluorescens* SBW25 is the fastest swimmer in the genera, with an average run rate of colony expansion of 77.6 $\mu\text{m/s}$, and an average backup rate of colony expansion of 18.0 $\mu\text{m/s}$ ²⁴. Jams are prevented by backup movements and collisions are avoided by turning, flipping and hovering²⁴.

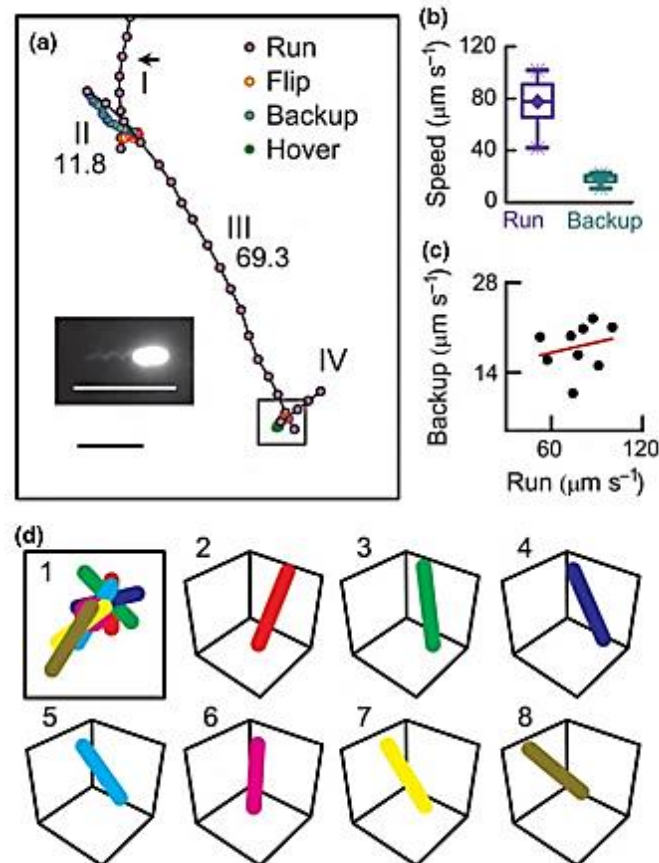


Figure 1-16 The free-swimming behaviour of *P. fluorescens* SBW25

(A) Visual trajectory of a swimming bacterium chemotaxis medium (10^{-2} M potassium phosphate [pH 7], 10^{-4} M potassium EDTA, and 10^{-4} M L-methionine). Scale bar, 10 μm . The inset exhibits a bacterium stained by fluorescence. Trajectory segments are labelled using roman numerals. The run rate and backup of motility ($\mu\text{m s}^{-1}$) is depicted beside segment II and III. Within segment I, the bacterium initially performed a run inside the focal plane before swimming towards the bottom following a turn (arrow). Meanwhile segment II is seen to be corresponding to a backup. A second run ensued (or segment III) which ended in a flip that was followed by a hover. This cell ultimately moved away from the focal plane (or segment IV). (B) Motility average rate of runs ($n = 27$) and backups ($n = 9$). (C) Motility run rates were plotted against backup rate of the same bacterium using a linear fit. (D) Cell orientations. Flip events and seven cell positions captured every 55 ms are superimposed in 1; 2–9 display the cell's three dimensional reconstructions within each frame, the upper ends correspond to the flagellated poles. (Source: 24, p.38).

1.7.3 Regulation of flagella biosynthesis in *Pseudomonas*

Flagellar assembly involves many gene products (Figure 1-17; Appendix P: Table P-1) and requires a large amount of energy. Consequently, expression of flagellar biosynthesis genes are tightly regulated to ensure that each component is produced only when required and in the correct order⁷⁵. A flagellum consists of four main structures: the filament, hook, hook-filament junction, and basal body (Figure 1-18). The filament is a tail-like structure, constructed of the protein flagellin, which is assembled into a helix with a hollow core, while the filament is connected to a hook and anchored to the basal body. The basal body consists of a rod, rotary motor, the flagellar protein export apparatus, and three rings⁶³.

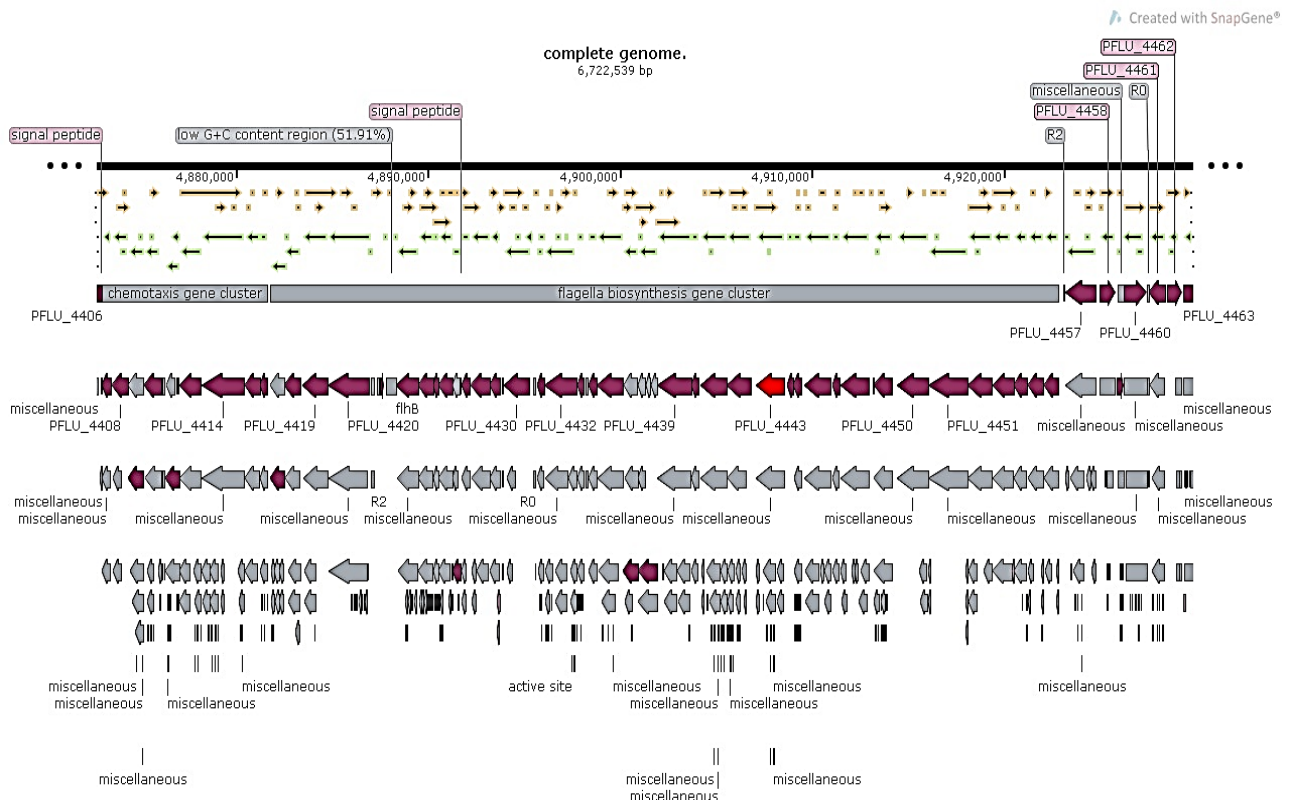


Figure 1-17 Flagella biosynthesis gene clusters in *P. fluorescens* SBW25

The mini-map depicts a zoom of the flagella gene cluster, which demonstrates the involvement of more than 40 genes in flagella synthesis. The flagella gene cluster's localisation within the chromosome is at the position 4,881,793...4,922,870 bp. Importantly, the chemotaxis gene cluster flanks this biosynthetic flagellum cluster. The total size of the flagella cluster is 4078 bp, whereas that of chromosome is 6722539 bp. The FleQ (PFLU_4443; *adnA/fleQ*) coding sequence is shown in red. The *fleQ* gene is located between 4,907,079... 4,908,554 within the complete genome of *P. fluorescens* SBW25, and is 1476 bp with a GC content of 61%; the protein product code is CAY51119.1. FleQ is a protein consisting of 491 aa and has a MW of 55.5 kDa. [Source: SnapGene software (from GSL Biotech; available at snapgene.com)].

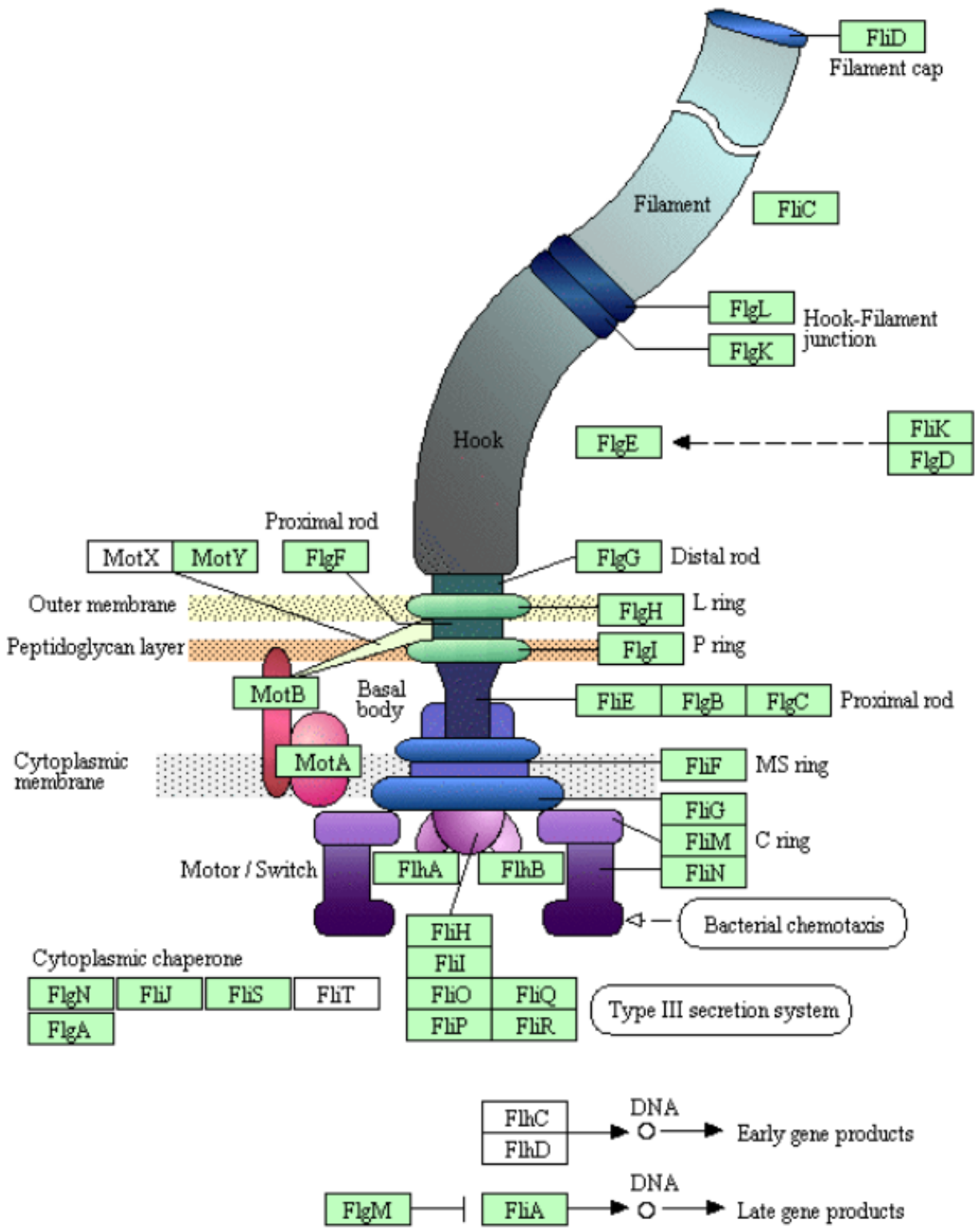


Figure 1-18 Flagella assembly in *P. fluorescens* SBW25

The KEGG map for flagella assembly is indicative of the gene products present in *P. fluorescens* SBW25 - shown in green - whereas those that are absent are in blank. [Source: KEGG Pathways Database; Retrieved from https://www.genome.jp/kegg-bin/show_pathway?pfs02040].

The master regulator FleQ controls expression of flagellar biosynthesis in a four-tiered cascade that includes multiple targets for regulation⁹². This requires hierarchical expression of approximately 40 genes involved in flagella synthesis, which constitute the flagella regulon⁶³ (Appendix P: Table P-1). In *P. aeruginosa* the flagella genes are grouped into four classes according to their transcription order during flagella and chemosensory apparatus assembly: class I, master regulator *fleQ*; class II, hook-basal body genes; and class III, flagellin and chemotaxis genes⁶³ (Figure 1-19; Appendix Q: Table Q-1).

In *P. fluorescens* SBW25, FleQ (also known as *adhA*) is the only class I protein that initiates the expression of class II early structural genes⁶³. The expression of the *fleQ* operon is regulated by environmental factors⁷⁵ and its expression requires σ^{70} . Notably, FleQ dependent activation of Class II genes requires σ^{54} (alternative name NtrA: RNA polymerase sigma factor 54), in contrast to the *Enterobacteriaceae* which use σ^{70} . Class II (or middle) genes encode components of the flagellar export apparatus, basal body and RpoF (σ^{28} ; specific for flagella genes)^{63,75}, with the latter positively regulating the expression of class III or late genes⁷⁵. The regulatory protein FlgM (anti-sigma factor) binds to RpoF to prevent expression of late genes until the basal body-hook structure is formed⁷⁵. Late genes encode regulators like σ^{28} (*fliA*), components of the flagella filament, hook-associated, motor, and chemotaxis proteins⁷⁵. The expression of class IV genes requires σ^{28} ⁷⁵ and these encode flagellin (*fliC*), chemotaxis proteins, and FlgM⁶³ (Figure 1-19).

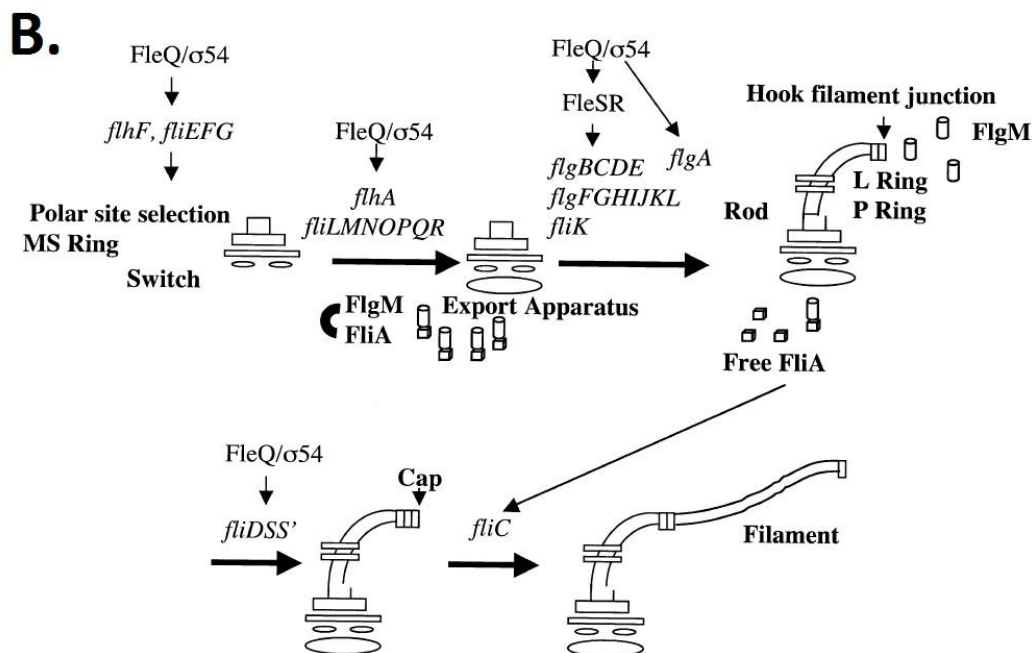
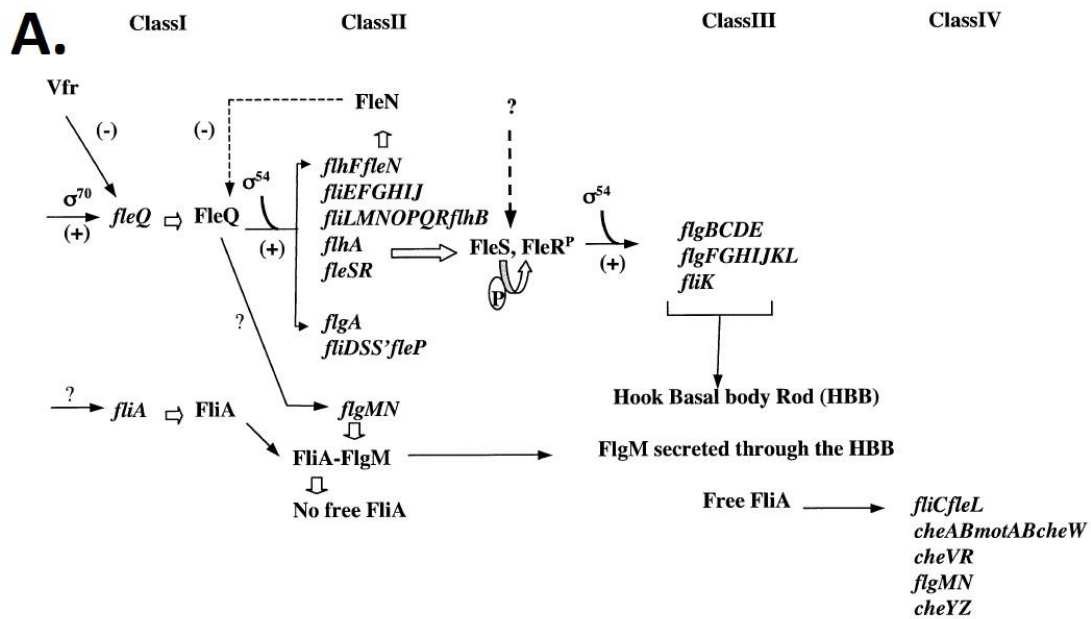


Figure 1-19 Flagella synthesis cascade for polar flagella in *P. aeruginosa*

(A) Flagella operons are expressed hierarchically and are controlled by different regulators such as transcription factor FleQ (Class I gene) that triggers the expression of Class II genes. On the other hand, Class III genes are regulated by TCS FleSR. RNA polymerase sigma factor FliA (PFLU_4417) induces the expression of Class IV genes, and its expression is FleQ independent (Source: 210, p.818). (B) The construction of flagella is initiated with the synthesis of structures embedded into the cytoplasmic membrane (CM) like MS ring and then an export apparatus anchored to the cytoplasmic side of the MS ring. Subsequently, the motor switch is formed and thereafter, a rod that transverses both the periplasmic space and peptidoglycan (P) layer and outer membrane (OM) is formed. It is then added in timely manner across different parts of the flagella. (Source: 210, p.820).

1.8 FleQ Is the Master Regulator of Flagella Expression

AdnA (PFLU_4443; *adnA/fleQ*) is an enhancer binding protein, positioned on the top of the flagella regulon expression hierarchy in *P. fluorescens* SBW25, and also is highly homologous (83 %) to transcriptional regulator FleQ. The FleQ is responsible for initiating the flagella gene expression cascade in *P. aeruginosa*²¹⁵; FleQ's promoter is repressed by the ribbon-helix-helix transcription factor AmrZ (alginate and motility regulator Z; PFLU_4744)⁹³. AdnA in *P. fluorescens* is implicated not only in flagellum biosynthesis but also in biofilm formation, motility, and sand adhesion²¹⁵. FleQ is not phosphorylated and hence does not have any known cognate sensor kinase²¹⁶. It is regulated by the antiactivator FleN (low ATPase activity) and the second messenger c-di-GMP²¹⁷. The Walker A motif of the AAA+/ATPase domain in the FleQ is the binding site for the c-di-GMP, and hence, this molecule competes with the ATP for this site²¹⁷; however, the c-di-GMP did not actually bind itself to the same ATP binding site, but to the one near it due to the larger sized blocks at the ATP entrance²²⁰. Therefore, it strongly dampens FleQ's ATPase activity as compared to when FleN is attached to FleQ. Consequently, both act in concert to arrest the flagella's expression because the FleN enhances the ATPase inhibition in FleQ caused by the c-di-GMP attachment²¹⁷. C-di-GMP levels control the planktonic and biofilm lifestyles of *P. fluorescens*²¹⁸, it was also observed that higher concentrations of c-di-GMP downregulate flagella regulon in *P. aeruginosa*²¹⁷. On the other hand, the expression of enzymes involved in its synthesis (diguanylate cyclase or DGCs) and degradation (phosphodiesterase or PDE) are regulated by AmrZ, a transcription regulator in *P. fluorescens* F113²¹⁹. AmrZ is highly conserved among *Pseudomonas* spp and is also called AlgZ in *P. aeruginosa* because of its involvement in alginate production regulation²¹⁹. Generally, bEBPs enhancement sites are positioned in regions (~100 bp) upstream of promoters¹⁰¹, but FleQ binding site is located in downstream regions of *flhA*, *fliE*, and *fliL* promoters²¹⁸. However, the only operon to which FleQ binds upstream (at 67 bp position) is the *fleSR*²¹⁸ (Figure 1-20).

A

flhA promoter sequence

5' -GAAAAGTTGGAACGGTTCCCTGCAATGACCCGCCCGACGCGCATTCCGGCGTCAAAGTTGTTCGGCGCCACCCACGGGCGCCATACGCAGGGCAGGGG
AGTCGAGAGGTGGATCGCACGCAACTGATC-3'

fliE promoter sequence

5' -CCGACTTGGCACCCCTTGTGCTAACTCCTCTGCAAAAGTGCCGGGCGGCGTCAAAAAAGCCGGCTGTTGGAGGAAGAGTCATGAGTCAGGGTGTTCGAGTC-3'

fliL promoter sequence

5' -CAGAAATTGGCACACCCTTGCTCTGCCCTGTGAAACCCTTCATTGACGCTATAGCGACGGATTTTGGCATGGCTAAGAAAGAGGGCGAC-3'

B

Flagellar promoters

fleSR

FleQ binding sites (3' → 5')

ACAGCCTACTAACTGTC

Figure 1-20 FleQ binding sites in promoters of flagella regulon in *P. aeruginosa*

The complete promoter sequences for the flagella genes are shown where (A) is the downstream region where the FleQ attaches, the sequences are underlined for each flagella promoter and (B) is where only the binding site sequences for *fleSR* promoter are indicated. (Source: 218, p.5256).

1.8.1 Structure and function of FleQ

FleQ (PFLU_4443; *adnA/fleQ*) is a transcription factor (AAA+/ATPase), which belongs to the NtrC subfamily. This transcription factor has a receiver domain (FleQ^R) at its N-terminus, a conserved central AAA+/ATPase domain, and a helix-turn-helix domain (HTH) that binds to DNA (Figure 1-21). FleQ is active when in its dimerised form and generally, does not demonstrate a high degree of polymerisation because the dimer is more stable in comparison to tetramers and hexamers when in solution¹⁷⁹. The AAA+/ATPase activity of FleQ dimers is modulated by c-di-GMP binding¹⁷⁹.

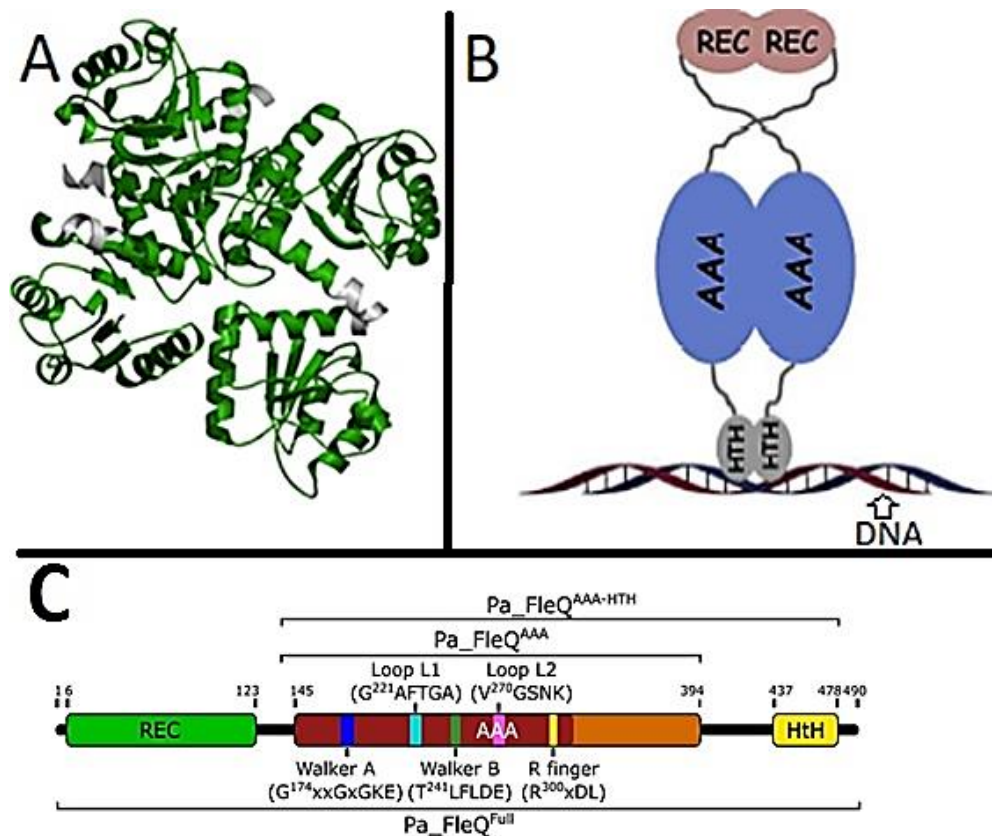


Figure 1-21 FleQ from *P. aeruginosa* PAO1

(A) Ribbon diagram of the FleQ domain from *P. aeruginosa* PAO1. This is a cartoon representation of the amino terminal receiver domain, REC (FleQ^R or FleQ domain). The receiver domain of a response regulator of a two component system is generally conserved, but in FleQ it is different because FleQ^R lacks the conserved Asp54 residue for phosphorylation, and instead has a Ser residue. The FleQ domain (FleQ^R) is not phosphorylated and instead requires binding of c-di-GMP to modulate the ATPase activity of the AAA+/ATPase domain (not shown). FleQ lacks a conserved binding site for c-di-GMP attachment. (Source: EMBL-EBI). (B) This scheme of a FleQ dimer from *P. aeruginosa* PAO1 shows its N-terminal FleQ^R domain, the central AAA+/ATPase domain, and the DNA binding domain containing a helix-turn-helix (HTH) motif. This diagram shows a FleQ dimer attached to a region of DNA (Source: 179, p.12). (C) Domain organization of FleQ: N-terminal receiver domain (REC; Pa_FleQ^{REC}), central AAA+/ATPase domain (Pa_FleQ^{AAA}) and C-terminal HTH DNA binding motif. AAA+/ATPase domain interacts with σ^{54} -RNAP-promoter complex; REC domain is regulated by antagonist ATPase FleN and the second messenger c-di-GMP. (Source: 220, p.E210).

FleQ is a positive regulator at the highest-level of the flagellation cascade (Table 1-5). In addition, it is homologous to NtrC⁹⁷, and is translated by σ^{70} ⁹⁷. FleQ has a DNA binding consensus sequence which is conserved among *Pseudomonas* spp⁹⁸. This DNA motif is 14 bp in size (GTCAATaaATTGAC) and allows this transcription factor to interact with different promoters (e.g. *cdrAB*, *siaABCD*)⁹⁸. FleQ regulates the expression of the *pel* genes (involved in exopolysaccharide synthesis), two-

component *fleSR* genes, flagellar export apparatus assembly, flagellar basal body assembly⁹⁸, and FleN⁹⁹, which controls flagella number. FleQ does not possess a cognate sensor kinase similar to a classic two-component system, such as NtrBC⁹⁷. In addition, FleQ has a Ser residue instead of Asp54 within the conserved receiver FleQ domain (FleQ^R or REC, Figure 1-21) and consequently FleQ activity is not regulated by the characteristic phosphorelay of the NtrC subfamily. FleQ is a bacterial enhancer-binding protein (bEBP) which is necessary for the dissociation of a promoter bound to σ^{54} -RNA polymerase in order to form an open complex¹⁰¹ and allow the hierarchical expression of the flagellar genes¹⁰⁰.

FleQ, the master regulator of flagellar biosynthesis in *P. fluorescens*, can be inhibited in two distinct manners: 1) binding to cyclic diguanosine monophosphate (c-di-GMP)¹⁰³; and 2) sequestration by FleN (P loop ATPase)¹⁰⁴, which in addition to sequestering FleQ, serves to maintain flagellar number⁹⁷. FleN (also termed FlhG and YlxH) dimerises upon binding to ATP and maintains FleQ inactivation (Figure 1-22)⁹¹. The ATPase activity of FleQ is modulated by c-di-GMP⁹⁸, such that under high levels of c-di-GMP the flagellar regulon is down-regulated⁹⁸. This effect is enhanced by the interaction of FleN with FleQ⁹⁹, because FleN dampens ATPase activity in FleQ⁹⁹. It is important to note that FleQ and FleN do not require c-di-GMP or ATP in order to interact⁹⁹.

Table 1-5 Flagellar genes regulated by FleQ in *P. aeruginosa*

Gene	Product Function	Reference
<i>flhA</i>	Flagellar export	181
<i>fliLMNOPQ</i>	Flagellar export	181
<i>flhF</i>	Localisation of flagella apparatus	181
<i>fleSR</i>	TCS for flagellin synthesis. Mucin adhesion and motility	181; 182; 215;216
<i>fliEFG</i>	Basal body, MS ring and motor switch complex	181
<i>fliDS</i>	Flagellar cap and export proteins	181
<i>flgA</i>	P-ring and basal body	181

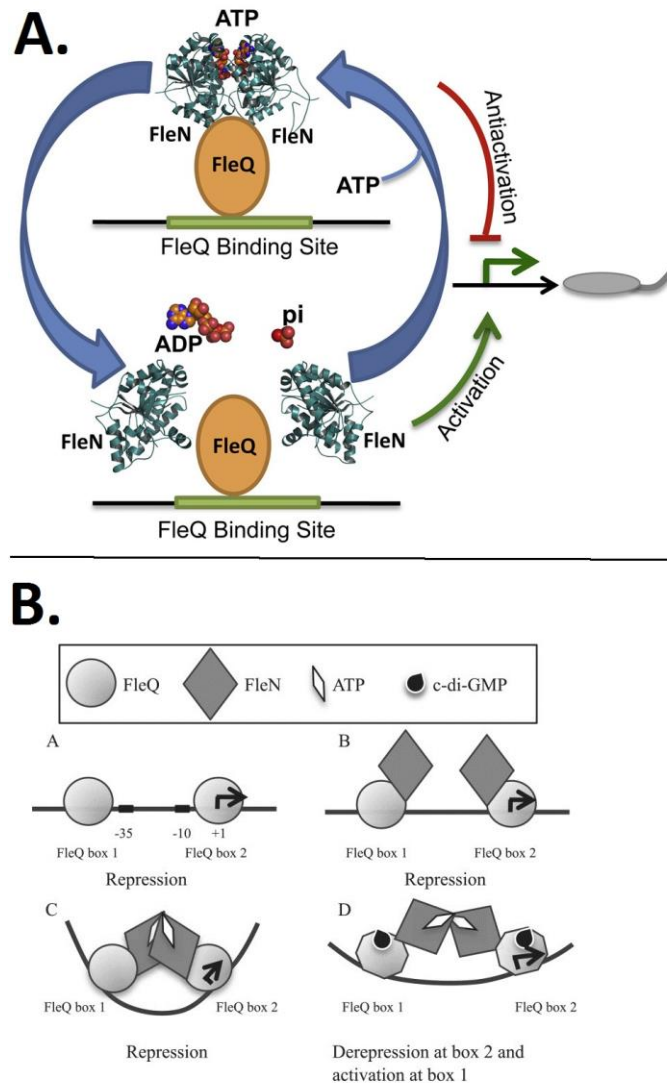


Figure 1-22 Inhibition of FleQ activity via the sequestration by FleN

(A) FleN dimerises on binding ATP and then sequesters FleQ. FleN and c-di-GMP modulates the ATPase activity of FleQ, which is activated upon disassociation from FleN following hydrolysis of ATP (Source: 91, p.243). (B) Regulation of *pel* operon: a) FleQ binds to both FleQ binding boxes located upstream of *pel* operon; b) The subsequent attachment of FleN to FleQ leads to their c) dimerization upon binding ATP to form a kink in DNA to repress the operon; d) FleQ is activated after c-di-GMP binds to FleN-FleQ complex because this molecule induces changes in the tertiary and quaternary conformations of FleQ that trigger *pel* operon expression. (Source: 214, p.7215).

Studies conducted in *P. aeruginosa* have shown that dimerised FleQ requires c-di-GMP binding to regulate its ATPase activity¹⁷⁹. FleQ differs from other bEBPs in that its dimeric form is active, whereas other bEBPs only become active upon polymerisation of phosphorylated forms, as for example NtrC-P polymerises into hexamers which then bind to enhancers in order to isomerise a close promoter complex by interacting with the bound σ^{54} RNA polymerase complex¹⁷⁹. FleQ

regulation is independent of phosphorylation, and this uncommon regulatory mechanism has also been observed in other orthologues, including FlbD, which is a bEBP from *Caulobacter crescentus* and necessary for the expression of σ^{54} dependent flagella promoters. However, FlbD is regulated via physical contact of the trans-acting factor FliX, which lacks histidine kinase activity. A similar regulation mechanism was observed in another FleQ homologue, FlrA, which is involved in flagella regulation in *Vibrio cholerae*.

It is important to note that the REC domain is necessary for activity of FleQ, as observed in experiments using *P. aeruginosa* mutant strain $\Delta fleQ^{179}$. This mutant strain is sessile, and when complemented with the full-length gene *fleQ* via a plasmid, flagella motility was restored; whereas when complemented with a truncated *fleQ* gene (no REC domain) the mutant strain remained sessile¹⁷⁹. Expression of the flagella genes *fleN*, *fleR*, *flhA*, and *fliE* in the mutant strain $\Delta fleQ$ were found to be undetectable; whereas, expression levels were similar to that in the wild type strain *P. aeruginosa* PAO1 when the full length *fleQ* gene was introduced, on a plasmid, into the non-flagellated mutant strain. This was not observed when the mutant strain was complemented with the truncated $\Delta fleQ$ gene containing no REC domain¹⁷⁹.

1.8.2 The second messenger c-di-GMP binds and regulates FleQ

The second messenger cyclic-di-GMP (c-di-GMP) is involved in the regulation of virulence, exopolysaccharide production, biofilm formation and motility in *Pseudomonas*²¹⁹⁻²²⁴. Binding of c-di-GMP occurs at a non-conserved region near the ATP binding site in the AAA+/ATPase domain (Figure 1-23), and so this cyclic dinucleotide does compete with ATP for binding, but does not dramatically affect ATPase activity.

The levels of synthesis and degradation of c-di-GMP are regulated according to environmental cues and the effector proteins to which they bind. C-di-GMP is a second messenger involved in the regulation of biological process, including biofilm formation and motility. It is also known that c-di-GMP is involved in the regulation of cAMP-responsive regulators (Crp families) and ATPases, such as FleQ. The model of FleQ regulation is based on the binding of c-di-GMP to a non-conserved motif nearby the Walker A motif of the AAA+/ATPase domain of FleQ. The attachment of c-di-GMP to FleQ dimers changes the conformation which affects ATPase activity²²⁰. Hence, FleQ

ATPase activity is inhibited upon binding of c-di-GMP and its ability to open the closed promoter complex is impeded¹⁷⁹.

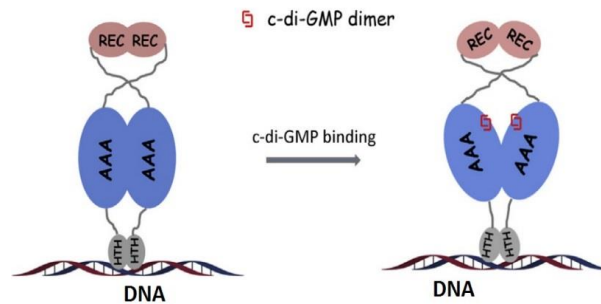


Figure 1-23 C-di-GMP model for FleQ regulation in *P. aeruginosa*

Dimerised FleQ is bEBP active and necessary for isomerisation of the closed promoter complex of the flagella genes operon. FleQ is a transcription factor containing a REC domain, an AAA+/ATPase (shown as AAA) domain, and a HTH (helix-turn-helix) DNA binding domain. The second messenger c-di-GMP upon binding to a non-conserved site near the Walker A motif in the AAA+/ATPase domain causes remodelling of the quaternary structure of the FleQ dimer, thereby inhibiting ATPase activity. (Source: 179, p.12).

1.8.2.1 Diguanilate cyclases and phosphodiesterases regulate the intracellular c-di-GMP levels in *P. fluorescens*

In *P. fluorescens*, switching behavior from free swimming cells to sessile multicellular communities (biofilm) is modulated by intracellular concentration of c-di-GMP in response to changes²²¹⁻²²³ in nutrient levels inside the cells such as phosphate²²³. Also, low concentrations of c-di-GMP (30 pmol/mg of cell extract in *P. aeruginosa*) are present in planktonic bacteria, whereas cells in biofilms have a higher content of c-di-GMP (75–110 pmol/mg of cell extract in *P. aeruginosa*)²²¹. The levels of this second messenger in *P. fluorescens* F113 are mainly controlled by transcriptional regulator AmrZ because it regulates the expression of the enzymes responsible for c-di-GMP production (diguanilate cyclases, DGCs) and degradation (phosphodiesterases, PDEs)²¹⁹. DGCs demonstrate the conserved domain GGDEF, whilst PDEs carry any of the following conserved domains: HD-GYP and EAL. Two molecules of GMP are produced by PDEs as c-di-GMP degradation products, which carry the signature motif HD-GYP, whereas those enzymes with EAL domain release pGpG. Also, *P. fluorescens* encodes 43 different PDEs and DGCs²²². Effectors are proteins or riboswitches to which c-di-GMP attaches, thereby triggering conformational changes necessary to start operon expression or regulate enzyme activity. For example, FleQ

(transcriptional activator) and LapD (transmembrane receptor), both are involved in motility and biofilm formation and regulated by c-di-GMP.

- FleQ: FleQ binds with *pel* operon (exopolysaccharide production), and represses, and the subsequent attachment of FleN to FleQ induces a kink in the DNA, thereby, repressing the operon as well. When c-di-GMP attaches to this FleQ-FleN complex, it triggers tertiary and quaternary changes in FleQ for its activation to start *pel* operon expression.
- LapD: In *P. fluorescens* Pf0-1, the intracellular levels of c-di-GMP are sensed by the transmembrane receptor LapD. When c-di-GMP binds with the cytoplasmic degenerate domain EAL (enzymatic inactive) of LapD, it induces conformational changes in the periplasmic domain HAMP of this receptor²²⁴. Following which, this activated HAMP domain sequesters the enzyme LapG protease in order to prevent degradation of adhesin A, which is necessary to keep the biofilm stuck to the surface and their cells cohesively inside the polysaccharide matrix of this sessile community²²⁴. Phosphate levels inside the cell regulate the c-di-GMP concentration because phosphate starvation triggers expression of RapA (PDE), which in turn, offsets the dispersion of the cells in the biofilm²²⁴.

1.8.3 Enhancers and regulation of the σ^{54} promoters of flagella genes in *Pseudomonas*

Enhancers are regions of DNA which are localised upstream or downstream of a promoter, and are necessary for the attachment of positive activators which in turn promote transcription. It is important to note that σ factors are necessary to confer RNA polymerase complex specificity for certain operons. σ^{54} , as required by FleQ, directs RNA polymerases to conserved sequences located at -24 bp and -12 bp upstream of the +1 transcription start position. This nucleoprotein complex does not spontaneously melt to initiate transcription, as there are thermodynamic and kinetic constraints that require mechanical energy derived from ATP hydrolysis in order to remodel the quaternary structure of the σ^{54} RNA polymerase complex and open the closed operon complex. The ATP-dependent activator protein FleQ gets bound to enhancers and induces DNA kinks or loops in this intervening DNA region upon FleN attaches to FleQ⁹². As a consequence of this DNA bending, FleQ comes in close contact with the stable closed σ^{54} -RNA polymerase promoter complex⁹². Notably, the

promoter isomerisation process necessitates energy that is provided from ATP hydrolysis occurring at the AAA+/ATPase domain of the enhancer binding protein FleQ. Importantly, DNA bending does not always occur if the enhancer is positioned downstream and in close proximity to a promoter's σ^{54} binding site (e.g. 12 bp downstream for gene *fliE*).¹⁸¹ On the other hand, if it is situated upstream, DNA bending becomes necessary for to the commencement of transcription. Jyot et al.¹⁰⁰ observed that in *P. aeruginosa* FleQ binds to the leader sequence of the promoter of the flagellar genes *flhA*, *fliE* and *fliL*, without bending the DNA to trigger expression. However, DNA looping is necessary for the expression of the promoter *fleSR* after attaching of the transcription factor FleQ at two binding sites positioned at -67 bp to -83 bp upstream of the +1 site¹⁸¹ (Figure 1-24).

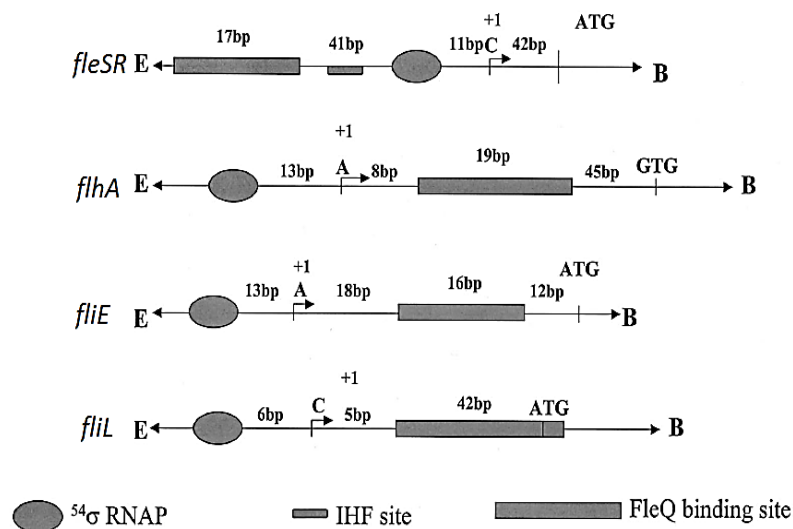


Figure 1-24 Regulation of the σ^{54} promoters of flagella genes in *P. aeruginosa*

The flagellar genes *fleSR* possess a FleQ binding site positioned upstream of the +1 site, whereas the genes *flhA*, *fliE* and *fliL* have enhancers positioned close to the σ^{54} binding site and downstream of the +1 site. Integration host factor (IHF) proteins are necessary for DNA looping to facilitate contact between FleQ and the closed operon complex σ^{54} -RNA polymerase. FleQ binding sites (enhancers) are shown as wide boxes, while ovals represent the holoenzyme RNA polymerase, and the IHF site is represented as a narrow rectangle. (Source: 100, p.5257).

1.8.4 Cryptic flagella operons are absent in *P. fluorescens* SBW25

Cryptic genes or phenotypically silent DNA sequences may be expressed in a small number of cells in a large bacterial population due to activation of pseudogenes or appearance of a functional promoter^{225,226}. Expression of such cryptic genes may occur as a consequence of mutational mechanisms such as deletions, insertions or

chromosomal rearrangements.²²⁵⁻²²⁷ In such cases, maintenance of these cryptic genes is a useful source of variability for the evolution of bacterial populations²²⁷. Generally, the cryptic genes, when active, express a useful phenotype for survival under certain environmental stresses or selective conditions. Hence, they are naturally selected; however, they may eventually become silent if maintaining them active implies a useless energetic cost for the population²²⁶. In such cases, novel expression of certain phenotypic characteristics in a bacterial population is attributed to activation of silent operons and not from the acquisition new gene clusters²²⁶. However, in other cases assignment of loci as 'a cryptic operon' is an artefact, for example when a phenotype is only expressed within a natural habitat and not under laboratory conditions²²⁶.

P. fluorescens SBW25 the flagella locus is controlled by FleQ as its master flagella regulator. Barahona et al.¹⁸¹ reported that a few *Pseudomonas* strains, nearly all from the *P. fluorescens* cluster, have a 'cryptic' flagella operon (45 genes) in addition to the main flagellar operon. Cryptic flagella operons are not expressed under normal laboratory conditions. These cryptic flagellar genes of *Pseudomonas* were shown to be highly homologous to the flagellar genes of *Azotobacter vinelandii* and Enterobacteria. Their expression was controlled by the *flhDC* operon, which is itself controlled by a c-AMP-dependent system and the Vfr protein¹⁸¹. Thus, expression of these cryptic flagellar loci is independent of FleQ. The strains from the *P. fluorescens* cluster that carry this second flagellar apparatus are: *P. fluorescens* F113, *P. extremaustralis* 14-3b, *Pseudomonas veronii* R4, *P. brassicacearum* LBUM300, *P. kilonensis* 1855-344, *P. fluorescens* et76. *P. fluorescens* SBW25 was reported not to carry this cryptic flagella locus¹⁸¹ and re-analysis of the genome confirmed this. The only strain outside the *P. fluorescens* cluster possessing these genes was *P. putida* ATH-43. In the strains that possess this second flagella operon, expression of the 'cryptic' flagella was responsible for a hypermotile and polar hyperflagellated phenotype. This hypermotility has been found to be favourable for root colonisation, and while these strains generally present a single polar flagellum under laboratory conditions, a tuft of flagella are observed when isolated from the rhizosphere¹⁸¹.

1.9 Bacterial Evolution and Adaptation to an Ever Changing Environment

According to Mayr¹⁵², evolution is any hereditary modification to the properties of a population of organisms. Mutations are inherited genetic changes that increase

variability within a population, and are necessary for the evolutionary process because they provide genetic diversity. Existing variants within a population in a specific environment are selected as being the most fit, and this natural selection process leads to the selection of certain advantageous mutations. It is important to highlight that mutations are random and can be advantageous, deleterious or neutral for the organism that carries them. Positive selection occurs whenever a mutation is fixed within a population as a result of the advantage that it confers to those organisms that possess it, whereas negative selection happens whenever the frequency of a mutation drops dramatically, and eventually it will vanish from a population due to its negative impact on the fitness of an organism that carries it. A mutation is neutral if it does not modify the phenotype, and consequently does not impact on the fitness of an organism.

Mutations permanently alter the DNA sequence (Figure 1-25), and there are different types of mutations: point mutations (change in a single base pair), insertions of a single base pair or more base pairs, deletions, duplications of an entire gene or a short sequence, and inversions (alteration in the gene order within the chromosome). These mutational events can be caused by both endogenous and exogenous agents.

- Endogenous factors are those derived from the replication machinery, normal cell metabolism, and spontaneous chemical reactions. For example, spontaneous DNA damage (e.g. DNA base loss and deamination of DNA bases), recombination events, abnormal chromosome separation and partitioning, the movement of genetic elements, DNA damage due to reactive compounds derived from normal cell metabolism (e.g. hydrogen peroxide and S-adenosylmethionine), genome replication inaccuracy and failure to restore the original sequence.
- Exogenous factors are those derived from the environment, such as alterations in pH, changes in temperature, radiation, and chemicals not generated intracellularly. For example, mutagenic compounds that act as DNA base analogues, such as 5-bromouracil, which is an analogue of thymine and when incorporated into DNA mispairs with guanine. DNA can be disrupted due to ionising radiation (e.g. X-rays) or by clastogenic compounds (e.g. bleomycin). For instance, UV radiation is able to form thymine dimers, which if not corrected hinder the activity of DNA polymerase and prevent replication.

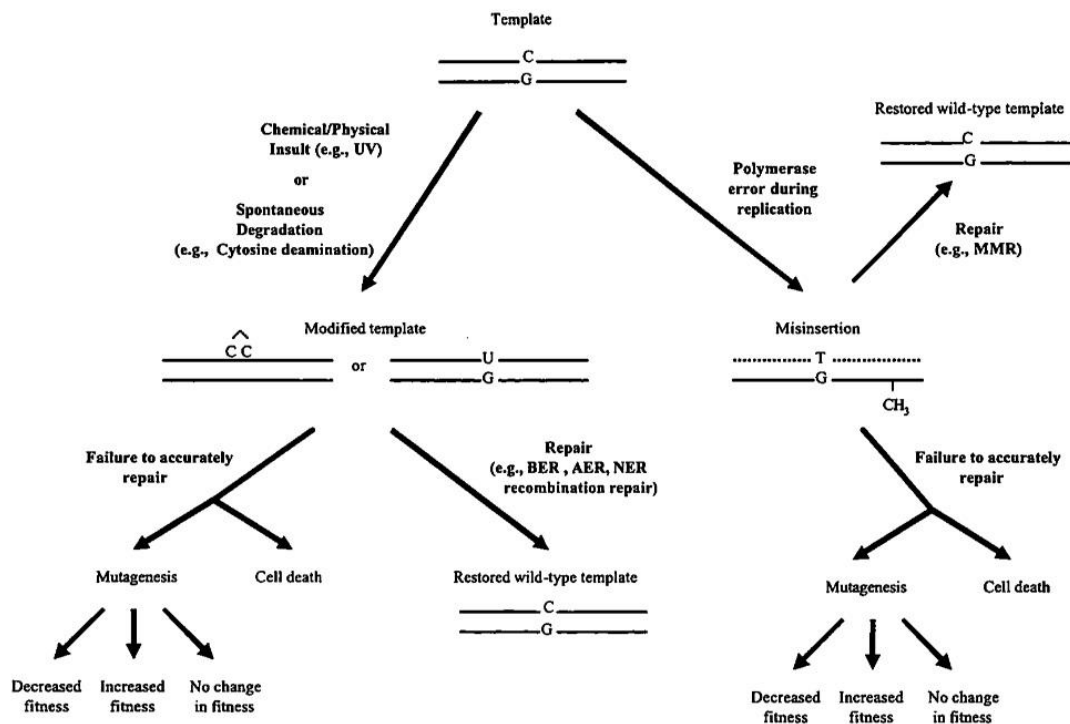


Figure 1-25 Mutagenesis is the source of variability for natural selection

Mutations arise due to endogenous or exogenous factors; endogenous causes include errors during genome replication, whereas exogenous agents refer to any environmental factor that damages DNA and hence alters its sequence. There are mechanisms to reduce the rate of mutation and conserve the DNA sequence, such as the different repair pathways (e.g. BER, AER and NER), which are activated according to nature of a mutational event. (Source: 153, p.4).

The cell has evolved mechanisms to detect mutations and correct them in order to maintain genomic stability; however, mutations are not always detected and repaired. Therefore, this error repair machinery is not fool-proof and does not interfere with the production of genetic variability necessary to drive the process of evolution because a balance exists between genetic repairs and mutations. Consequently, a cell maintains a low spontaneous mutation rate with a mean value of 0.003 mutations per genome per DNA replication, as a result of endogenous agents. This mutation rate has been found to be similar among DNA based microbes¹⁵⁴; therefore the frequency of the appearance of a beneficial adaptive mutation in a population is expected to be 10^{-7} ¹⁵³. However, this spontaneous mutation rate is subject to change as a result of stressful environmental factors that trigger an increase in genetic diversity. Consequently, the evolutionary rhythm of a population increases, which facilitates rapid adaption to a

hostile environment and survival. According to Radman¹⁵⁵ there are two main mechanisms which induce a high mutation rate within a bacterial population:

- Fortuitous inactivation of the fidelity of the genome replication machinery
- Production of low fidelity DNA polymerases

There are small subpopulations of mutants within a population that are outcompeted by the main population that arise as result of random spontaneous mutagenesis (mutation theory). This is a source of genetic diversity upon which selective pressure acts, thus and this favours those mutant phenotypes which are more fit to survive under a particular environmental stress compared to the main population. Mutation theory states that mutations are hereditary and randomly appear within a population. These heritable mutations occur in the absence of any selective agent and the mutant population increases over time within a growing population due to cell division of a previously mutated cell and the appearance of new mutants¹⁵⁶. Generally speaking, mutational events are lethal, neutral or slightly detrimental to population fitness and survival, hence they are considered to be a slow evolutionary parameter¹⁵⁷.

Mutation theory states that mutations arise as result of random spontaneous mutagenesis, are hereditary and randomly appear within a population. These heritable mutations occur in the absence of any selective agent and the mutant population may increase over time within a growing population due to cell division of a previously mutated cell¹⁵⁶. Generally, mutational events are lethal, neutral or slightly detrimental to population fitness and survival, hence they are considered to be a slow evolutionary parameter¹⁵⁷ and are frequently not seen as they are outcompeted by the main population. However, spontaneous mutation is a source of genetic diversity upon which selective pressure acts to favour those mutant phenotypes which are more fit to survive under a particular environmental stress compared to the main population. Bacteria carrying favoured mutations then dominate the population.

1.9.1 Mutational models

According to Poole et al.¹⁶¹, the evolution of organisms follows two different types of selection strategies: r-type and K-type. The r-type occurs in small organisms (e.g. microorganisms), where higher growth rates mean population size can change over a short time, enabling them to thrive in fluctuating environments with variable nutrient

availability. The adaptations that arise in these population are generally modifications to biochemical pathways rather than morphological in nature. K-type selection is observed in large organisms (e.g. vertebrates), where there is slower growth rate, a tendency towards maintaining a stable population size, and a more stable environment that provides a constant nutrient supply. Generally, these adaptations tend to affect the morphology of an organism and to a lesser extent their metabolism, making the modified phenotypes easier to be identified through observations. As bacteria follow the r-type strategy, the term 'adaptation' is used to refer to the appearance of spontaneous mutations after 3 to 7 days or more, under non-lethal conditions within a selective medium where cell division is slow or arrested¹⁵⁸. Adaptability refers to the generation of phenotypic diversity, which is beginning of the evolution process¹⁶¹.

It is widely accepted that mutations are continuous events that occur randomly and without purpose and through natural selection can improve an organism's fitness in response to the environment in which a population is residing. This is known as the classic Darwinian model of mutation^{158,159}. Fluctuation test confirms the classical mutational model: random mutation followed by selection

The classic fluctuation test conducted by Luria-Delbrück¹⁵⁶ showed that mutations are hereditary, random, and appear before exposure to any specific stress. This experiment was based on the fact that *Escherichia coli* strain B divides by binary fission. A broth culture was inoculated with a single colony of this phage sensitive strain in order to study the evolution of resistance to phage T1. The experiment consisted of taking a sample from this broth culture and then many sub-samples for plating out onto solid medium to test for the presence of phage resistant colonies. In a second part to the experiment, multiple sub-broth cultures were made from the initial culture and then plated out to test for the evolution of resistance against phage infection.

The average number of resistant colonies in all the sub-samples was the same and their respective variances were equal to their means. Therefore, the mutants followed a Poisson distribution regarding their random appearance in the population in the absence of a selective agent (phage). However, the outcome of the second part of the experiment did not follow a Poisson distribution as non-resistant cells were present in some sub-cultures and resistant cell in others, so proving the clonal inheritance of mutations. In addition, the average number of resistant bacteria observed in each sub-

culture was different; hence the evolution of resistance had occurred at different growth stages. These results confirmed the randomness of the mutations, their inheritance, and their evolution in the absence of any environmental challenge. This represents the classical mutational model, which states that natural selection acts upon the available diversity but does not trigger the appearance of specific mutations necessary to improve a population's fitness and survival for a specific stress.

1.9.1.1 Cairnsian mutational model: stress induced mutations

There are adaptations that exhibit Cairnsian behaviour, which means that these mutations occur at an apparently higher frequency under certain stress (non-lethal) conditions because they are suitable and favourable for that specific environment. However, these mutations do not show an increase in their frequency in another environment because they are ineffective and do not enhance fitness¹⁵⁹. Cairnsian mutations refer to apparent changes in specific regions in the genome in order to improve fitness under specific stress, hence their name adaptive mutations. Adaptive mutations have been observed in starving populations, and it is interesting to highlight that there is no hypermutation in any of the loci involved¹⁶⁰. This model is based on observations that in *E. coli* strain FC40, which is unable to metabolise lactose, when this sugar is present in the medium then the frequency of Lac⁺ revertants increases¹⁵⁹. In this strain the chromosomal *lac* operon is deleted but it carries the episome F'_{lac}, which contains the fusion allele *lacI-Z33*, which consists of the repressor *lacI* fused to β -galactosidase *lacZ*, but is out of frame with respect to *lacZ*. This frameshift mutation impedes β -galactosidase expression^{159,162}; however, only at very low levels unless there is a mutation, this strain becomes competent to metabolise this sugar when it is present in the medium. Consequently, the mutational revertant frequency (Lac⁺) rises due to an increase in frameshift mutational events when under selective conditions. Experiments conducted by Radicella et al.¹⁶³ showed that this frameshift mutation is dependent upon conjugation, as the proportion of Lac⁺ revertants decreases to 25-50 times the frequency if the fusion mutation is inserted into the chromosome instead of the episome. In addition, it was found that the proportion of Lac⁺ revertants dramatically decreased to less than 25 times its frequency if a detergent was present to impede mating.

Another example of direct mutation is in the studies conducted on strains which carry mutations in the dextrin transportation genes. Dextrin utilisation requires the porin

LamB for the transportation of this type of sugars (e.g. maltose and maltodextrin) into the cell in order to be metabolised. If the gene *lamB* is deleted in *E. coli* strain K12, then this strain becomes unable to metabolise dextrans (phenotype Dex⁻). Benson¹⁶⁴ highlighted that strain K12 ($\Delta lamB$) is unable to take up these large sugars through the pores of the functional porin OmpF. However, mutations in the *ompF* gene led to alterations in its pore size, allowing the diffusion of these large sugars. These mutations were observed to appear at a higher frequency whenever the mutant strain was grown in medium containing dextrans. It is interesting to note that in the double mutant strain $\Delta lamB \Delta ompF$, the diameter of the porin OmpC was mutated to allow dextrin diffusion into the cell. However, this mutant was never observed if the gene *ompF* was not deleted, so it was initially considered to be direct mutation, via a point mutation in the gene *ompF*¹⁶⁵. Further studies on this system showed that OmpF⁻ mutants outgrew the strain Dex⁻, and OmpC⁻ mutants grew slower than OmpF⁻ mutants. Therefore, this system is not providing supporting evidence of direct mutation as initially believed.

The Cairnsian model states that cells 'know' by an unknown mechanism which mutations are favourable, and hence increase their chance of survival. However, most experiments that appear to provide evidence of direct mutation fail due to errors in the experimental design or lack a clear understanding of the genetics behind the processes¹⁶⁵.

1.9.1.2 Adaptive mutations

Adaptive mutation implies that the bacterial populations under stress alter their transcriptome⁶¹. Antibiotic resistance signifies an example of adaptive mutation, which can occur due to epigenetic inheritance (DNA methylation) on drug efflux pump genes as well as in modifications in levels of transcription factors necessitated for these drug efflux pump genes' expressions⁶¹. Hence, the antibiotic resistant phenotype is transient and is lost upon the drug's removal; this is explained in light of the fact that overexpressing these efflux pumps entails a detrimental energetic cost that dampens growth; for this reason, a sensitive phenotype is more appropriate⁶¹. These adaptive mutations are not triggered by any mutational event at the DNA level (e.g. duplications, insertions, deletions), which can then be transmitted vertically to the next bacterial generation but are caused in the wake of stochastic changes in genome expression in response to environmental insults⁶¹. For instance, *E. coli* develops antibiotic

resistance after being exposed to gradual increments in antibiotic⁶¹; in addition, the frequency of sensitive revertants is much higher than expected (> 50 %) ¹⁰². Upon the removal of the antibiotic, it is compared with the expected rate as though the resistance were caused by a heritable mutation^{61,102}. Adam et al.¹⁰² found that upon exposing *E. coli* to increasing concentrations of ampicillin, the resistant population increased as a result of the expression of cryptic β -lactamase gene *ampC*, overexpression of glutamate decarboxylase and DAM methylase. DAM methylase is responsible for regulating expression of drug efflux pumps as well as the aforementioned gene encoding enzymes via DNA methylation (epigenetic inheritance)¹⁰². For this reason, an adaptive mutation cannot be deemed as a Cairnsian mutation or direct mutation.

1.9.1.3 Amplification mutagenesis: stress does not alter mutation rate

Gene duplication is a frequent event with a small number of cells in a population carrying any duplication^{166,167}. As with other mutations, this requires some form of selective pressure to amplify and maintain mutated cells in the population⁵⁵. In the absence of a positive impact on fitness, duplications are likely to be lost^{55,232}.

However, gene duplication and amplification some genes are duplicated and selected, however, the mutational process that produces them is not induced because they are favourable. These duplication events can lead to the selection of point mutations in any of the duplicated genes or in any other mutational event that occurs nearby these tandem duplication events and improves fitness in a bacterial population. The mutated gene (source of a new gene) or any mutational event nearby previously duplicated genes, are only maintained if they have a positive impact on fitness (Figure 1-26).

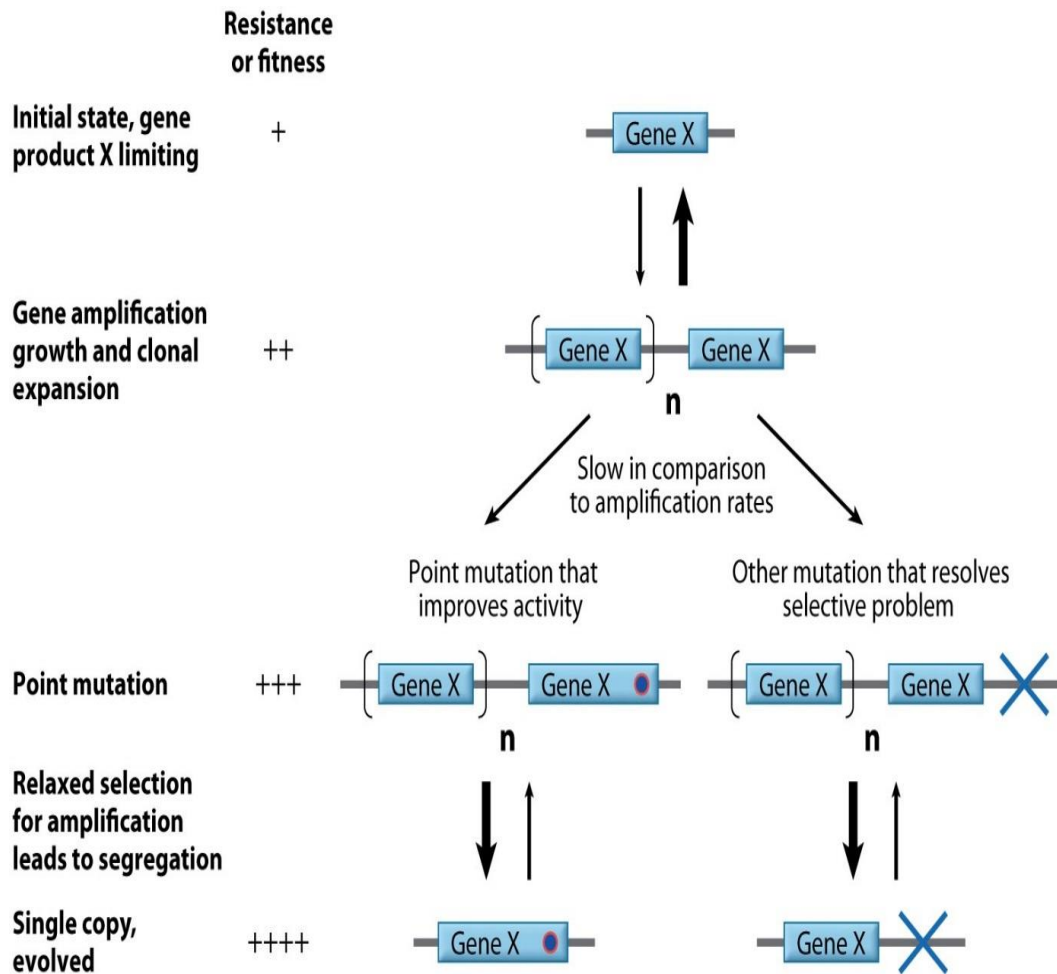


Figure 1-26 Amplification mutagenesis is temporal

Certain genes are subject to tandem duplication. Eventually, copy will undergo a point mutation, while another mutational event nearby a tandem repeat will improve the phenotype. After the selective pressure is relieved tandem repeats are lost, and the population only retains the mutated copy and the point mutation in the nearby gene is maintained. (Source: 166, p.189).

Some cells of the *E. coli* strain FC40 studied by Cairnsian are able to express low levels of β -galactosidase, despite a frameshift mutation within the *lacI* promoter. These are leaky mutants that survive the selective agent, but due to gene duplication of *lacZ*, the amount of this enzyme is increased and the population is able to increase its growth. However after the selective pressure is removed then these tandem duplications are lost, and the cells return to their initial phenotype (Figure 1-27).

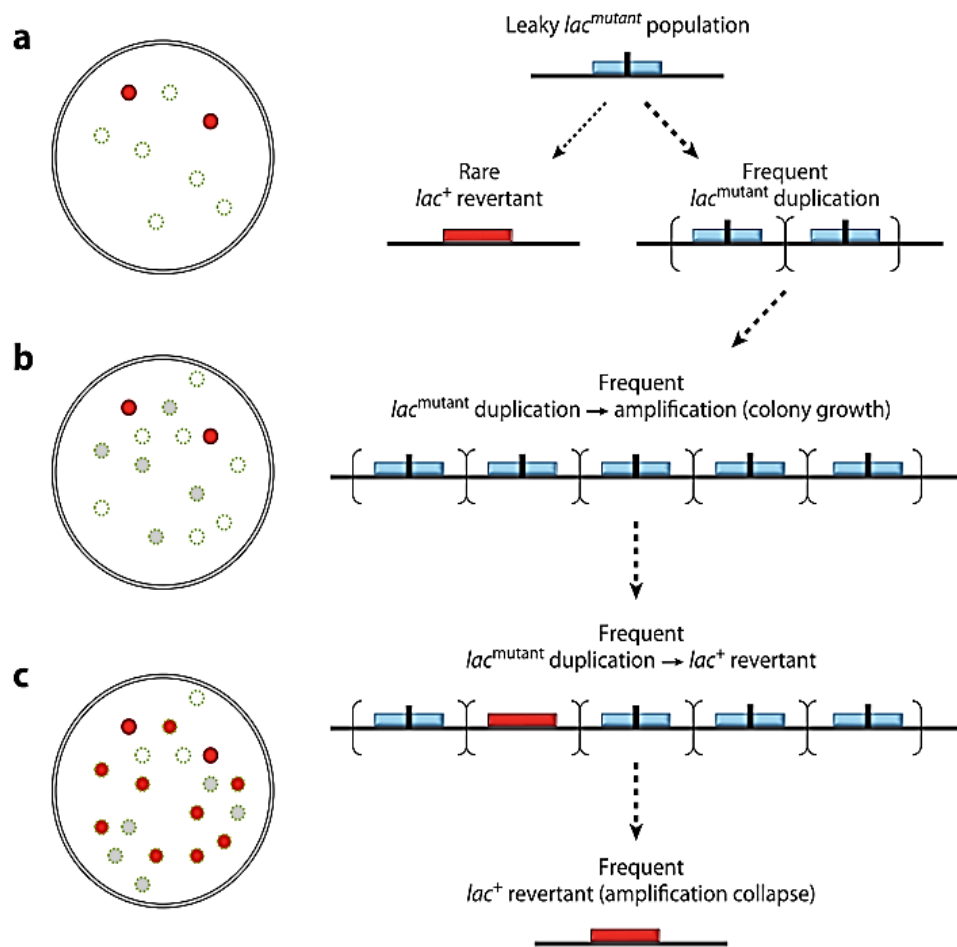


Figure 1-27 Amplification mutagenesis and evolution of leaky *lac* mutant

The *lacZ* was deleted from the chromosome of *E. coli* strain FC40. This strain carries a conjugative plasmid carried the chimeric gene *lacI-lacZ33* which carries a frame mutation in *lacI* that blocks *lacZ* expression. However, there are leaky mutants that are able to express low levels of β -galactosidase despite the frameshift mutation. The levels of required enzyme for optimal growth are achieved by gene amplification, and eventually one of these copies will mutate. After the selective pressure disappears the tandem repeated genes are eventually lost, and only the mutant chimeric gene (with the frameshift mutation) is retained. (Source: 166, p.187).

1.9.2 Rewiring of the nitrogen pathway to restore flagella in sessile mutants

Alsohim et al.¹⁰⁷ isolated non-motile IS- Ω -Km/hah transposon mutants (AR2 and AR1) from the sliding strain SBW25 Δ *fleQ*. In SBW25 Δ *fleQ* the flagella transcription regulator *fleQ* had been knocked out, so that flagella are not expressed and the strain is unable to swim. The non-ribosomal peptide synthase mutants AR2 and AR1 are sessile as a result of both the deletion of *fleQ* and the insertion of the transposon into the viscosin operon causing a loss of viscosin production¹⁰⁷.

It was observed that mutants of these non-motile strains, AR2 and AR1, began to swim in swarming medium after four days, and these mutants were named AR2S (slow motility) and AR2F (fast motility, a mutant derived from a bleb of AR2S)¹⁰⁸ (Figure 1-28). These isolates that had evolved from an aflagellate, non-motile parent expressed flagella but did not produce viscosin¹⁰⁹. Genome sequencing of both evolved mutants identified an *ntrB* mutation in AR2S and the same *ntrB* mutation plus a mutation in *ntrC* in AR2F. Thus, mutation of the regulators of nitrogen metabolism had mutated in a two-step manner to restore flagella driven motility¹⁰⁸. This is an example of the rich physiological and behavioural sophistication of microbial populations, which are able to adapt in order to survive in any environment¹¹⁰.

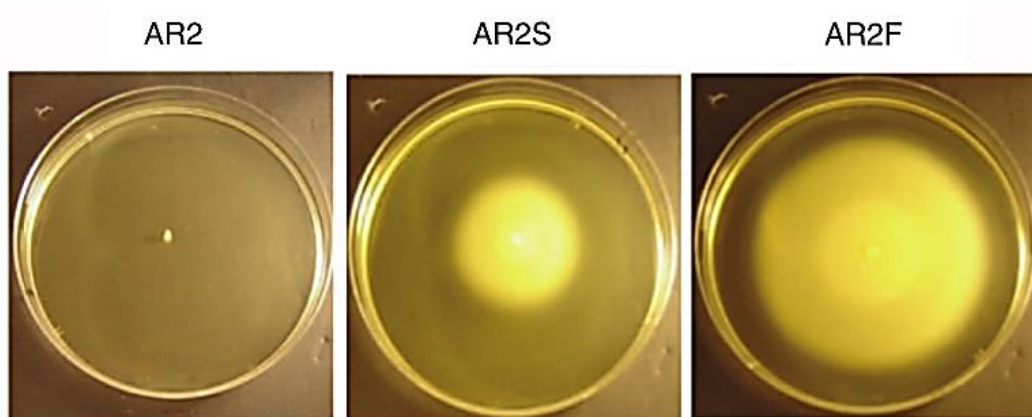


Figure 1-28 Motility phenotype of sessile parent and evolved strains in swarming medium

Evolved mutants AR2S (slow swimmer) and AR2F (fast swimmer) recovered from the non-motile parent *P. fluorescens* SBW25 Δ *fleQ* *viscC*:: IS- Ω -Km following 4 days on swarming medium. Image shows motility of each following central inoculation of motility plates. (Source: 108, p.1015).

Paralogous genes may act as substitutes for defective genes, enabling them to take over their function, thus permitting the survival of a mutant organism¹¹¹. FleQ belongs to the NifA/NtrC family of σ^{54} (RpoN)-dependent transcription activators¹⁰⁰ (Figure 1-29). It not only positively controls the flagella regulon^{92,112} but also the *pel* operon, which is responsible for biofilm development in *P. aeruginosa*⁹². FleQ and NtrC function in a similar way. Both of these bEBPs are required for the isomerisation of the closed promoter in the RNAP- σ^{54} complex to an open, transcriptionally active form in order to initiate the expression of their respective regulons¹⁰¹. Consequently, it was proposed that NtrC acquired a new role as a bEBP to restore flagella biosynthesis¹⁰⁸

As stated previously, flagella-motility is important for survival as it helps bacteria to move towards a more suitable environment⁷⁵. Hence, a detrimental environment will exert a selective pressure on non-motile sessile transposon mutants to favour any mutation able to restore motility, as this would confer a substantial advantage permitting cells to switch niche and avoid metabolic stresses such as starvation¹⁰⁸. Thus mutations in the Ntr system confer a substantial selective advantage allowing former sessile bacteria to move from a harsh starving environment to fulfil their nutritional requirements¹¹³.

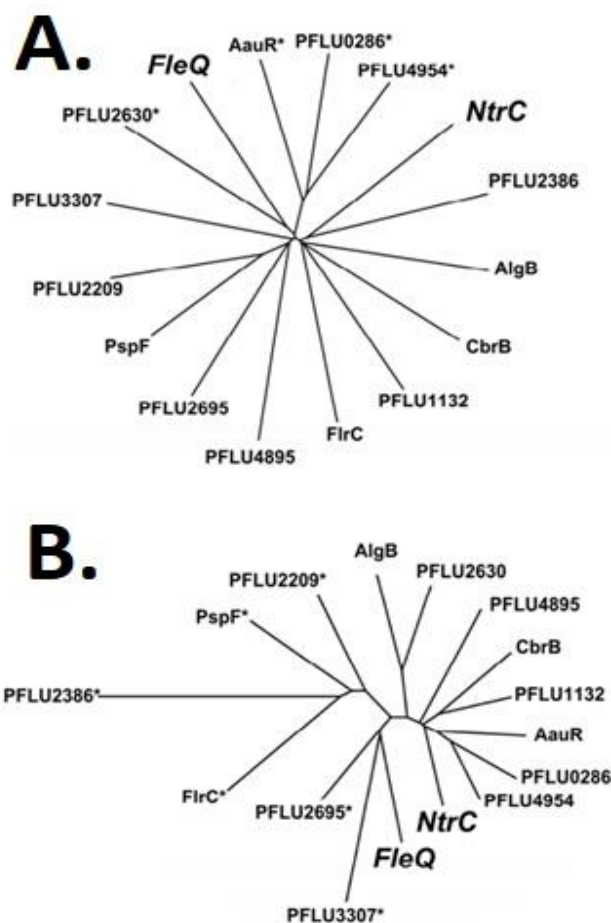


Figure 1-29 Star phylogenies showing a comparison of the full length protein sequences that are homologous to FleQ

(A) Protein sequences (Clustal Omega) and (B) Predicted 3D structure (Neighbor joining) of bEBPs that are RpoN-dependent in *P. fluorescens* SBW25. Proteins positioned at the shortest distances along the branches from the same node are the most similar. However, other proteins are more similar in terms of both structure and sequence to FleQ, with the most similar denoted by an asterisk, but in non-flagellated and non-viscosin strains these did not assume the role of FleQ in its absence under starvation conditions. (Source: 197, p.257).

1.10 Bacterial Regulators and Signalling

Bacterial signalling is necessary to sense the environmental cues to regulate metabolism, cell morphology, gene transcription, flagella expression, cell behaviour¹¹⁵, and other key stages of the cell cycle (e.g. sporulation, biofilm formation)¹¹⁶ in response to a changing environment^{115,116}. An everchanging environment presents fluctuations in carbon, phosphate and nitrogen levels, the availability of respiratory electron acceptors, shifts in osmolarity, variations in temperature, and different types of growth medium (e.g. liquid or solid)¹¹⁵. Therefore, signalling is important for survival and adaption to any stress or habitat alteration^{115,116} because it enables optimisation of the amount and repertoire of proteins and enzyme activity appropriate to the perceived stimuli to complete a cell cycle¹¹⁶. Signalling pathways transmit external stimuli (e.g. metabolites, toxins, cell density, changes in pH, light, gases) to specific downstream cellular targets¹¹⁵ and are involved in a plethora of developmental pathways, for example sporulation, swarming, cell differentiation, and virulence¹¹⁶. This is accomplished by interactions of the stimuli with specific receptors, which cause temporary conformational changes and covalent modifications, such as autophosphorylation. A phosphorylated sensor relays its phosphate group to a cognate response regulator in order to become active. An activated response regulator is active if the stimuli is present and able to trigger an adequate response for survival and homeostasis. Examples of response regulators include transcription factors or a motor protein in flagella¹¹⁵. There are three types of signalling systems used in prokaryotes: single-component, two-component (also known as HAP: histidyl-aspartyl phosphorelay)¹¹⁷ and three-component¹¹⁶ (Figure 1-30).

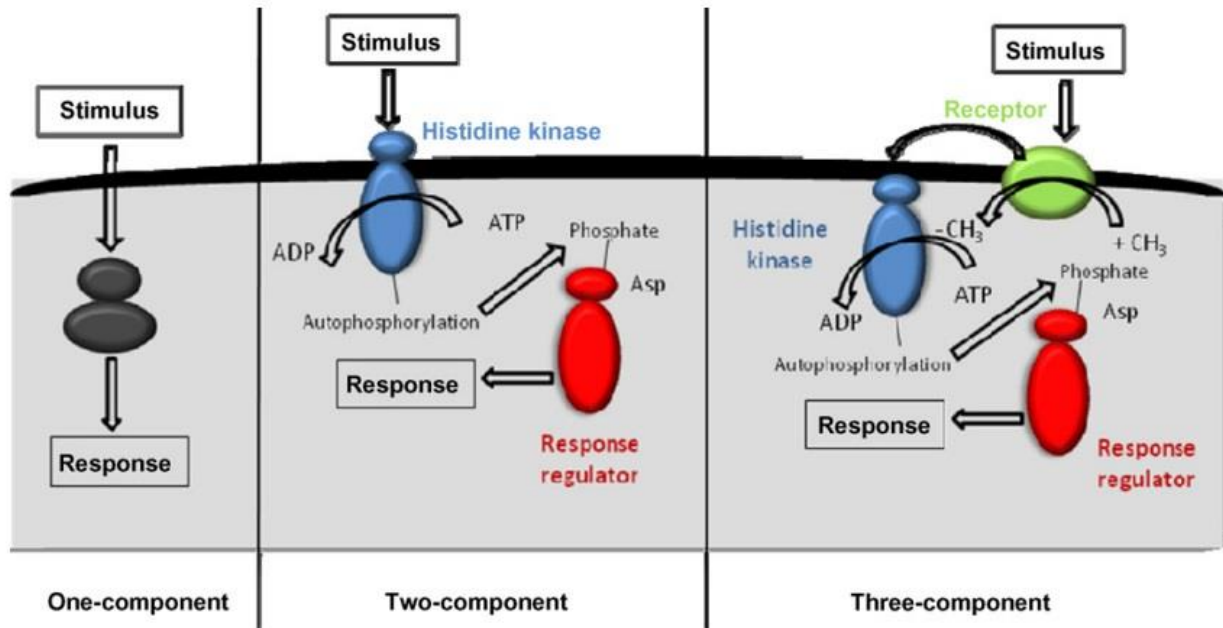


Figure 1-30 The different types of signalling transduction systems in prokaryotes

One-component systems entail a single protein with fusion of the input and output domain; they are essentially cytosolic proteins. On the other hand, two-component systems consist of a histidine kinase (or HK) receptor (cytosolic protein or membrane bound) that is autophosphorylated after receiving a stimulus before relaying the phosphoryl group into a cognate response regulator (RR). Meanwhile an activated RR gains control over the populations of enzymatic activity and engages with other cellular targets in order to regulate their activity. Finally, three-component systems are premised upon a two-component system; however, they need a transmembrane receptor that is de-methylated after receiving the stimulus and triggers HK's kinase activity, before it phosphorelays into a RR which controls the expression or activity of downstream cellular targets. (Source:116, p.96).

Single-component: a single protein with two domains, one for the input signal and the other for the output response. This signalling system is localised in the cytosol, and here must sense all stimuli (e.g. light, amino acids)¹¹⁶. The main output response consists of the binding of its output domain to an upstream region of an operon to initiate transcription¹¹⁶. RocR is a transcriptional activator (Figure 1-31) that regulates the expression of enzymes pertaining to the arginine degradation pathway (operon *rocABC*)¹¹⁸, and ornithine catabolism (operon *rocDEF*) in response to the presence of arginine, citrulline, ornithine or proline¹¹⁹. This regulatory protein in *Bacillus subtilis* belongs to the NtrC/NifA family of transcription factors and is dependent on a σ^{54} -dependent promoter¹¹⁸. Its binding sequence is highly similar to those for NtrC in *E. coli*¹¹⁸.

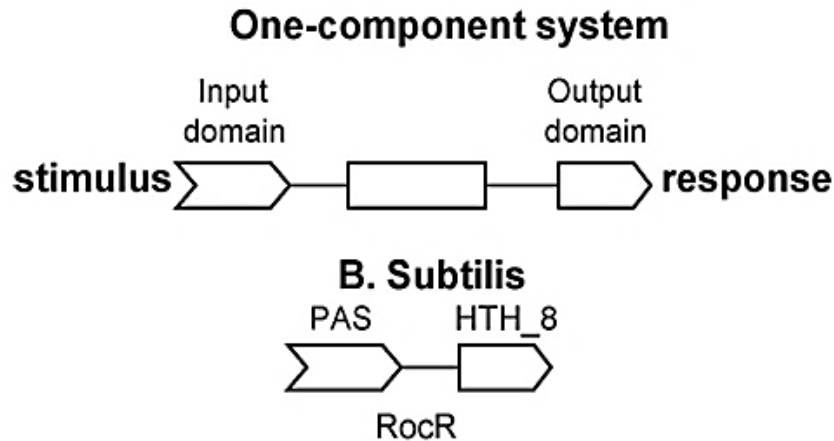


Figure 1-31 A one component system (OCS)

A single component system comprises of one protein that is built input and output, the two fused domains. After the interaction of a stimulus with the input domain, a conformational, transient change is effected on the output domain, which makes it active as a prominent transcription factor in order to the trigger the expression of specific operons that are paramount to produce enzymes for the pathway which are indicated by the metabolite bound into the input domain. RocR refers to a transcriptional activator for citrulline catabolism and the arginase pathway. After the amino terminal domain (PAS) interacts with citrulline metabolites arginine, or proline, it induces the transcriptional activation of DNA binding domain HTH_8¹¹⁹. This OCS is capable of interacting with σ^{54} -RNA polymerase holoenzyme in order to express the operons *rocDEF* and *rocABC*. (Source: 116, p.97).

Two-component or HAP: consists of a modular sensor histidine kinase (HK), with a conserved kinase core, and a cognate response regulator (RR)¹¹⁷. A stimulus triggers a conformational change in HK to undergo ATP-dependent autophosphorylation on a specific histidine residue. This phosphoryl group is then relayed to an aspartate residue in the RR producing changes in its biochemical, genetics or mechano physical properties¹¹⁷. HKs have multiple localisations within the cell and generally are membrane associated (e.g. EnvZ), but can also exist as soluble cytoplasmic proteins, for example CheA and NtrB¹¹⁷. This is the most common signal transduction system used in prokaryotes¹¹⁷. One example is the NtrBC system, which is used under limiting nitrogen conditions when ammonium ions are not available and amino acids are the sole nitrogen source¹²⁰. NtrC, a bEBP, is phosphorylated at Asp54¹²¹ by the sensor NtrB (HK) under nitrogen limited conditions. This activated state (NtrC-P) forms oligomers that bind *glnA* enhancers (Upstream Activator Sequence, UAS), and contact σ^{54} -RNA polymerase holoenzyme bound to this promoter through DNA-looping¹²¹. This bending is assisted by other proteins, such as integration host factors (IHF)¹⁰¹.

The initial formed closed complex isomerises into an open polymerase-promoter via energy derived from the hydrolysis of ATP or GTP^{101,121} (Figure 1-32).

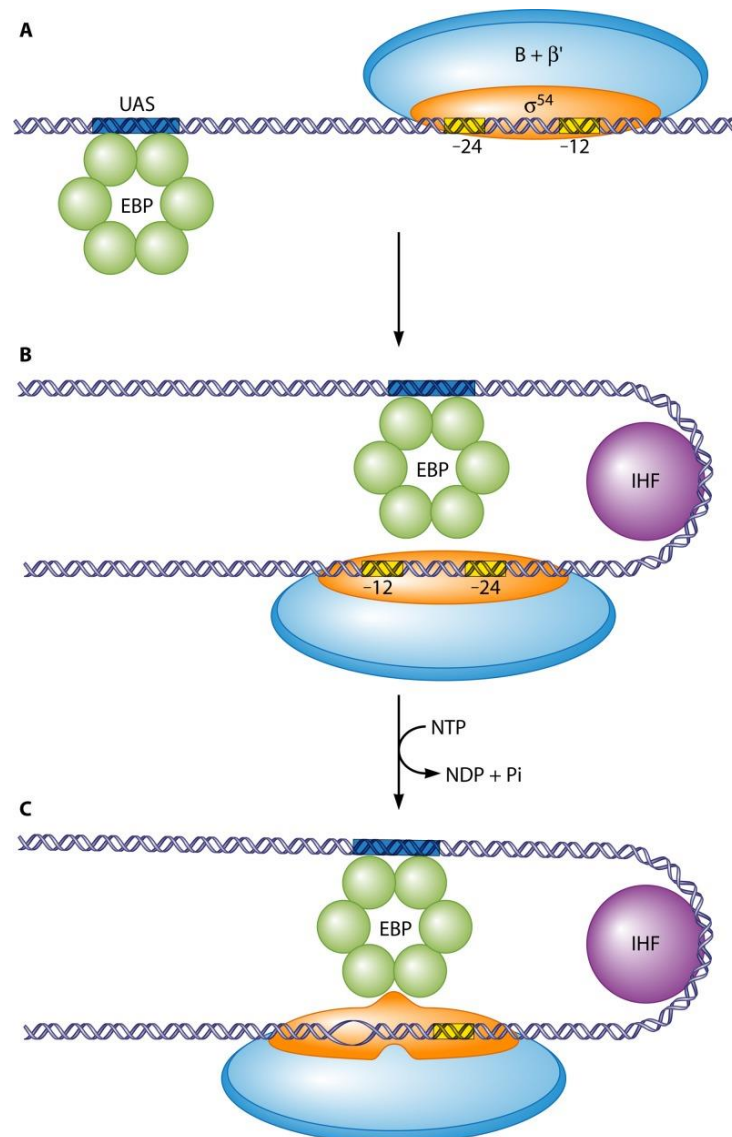


Figure 1-32 Isomerisation of transcription bubble:RNAP-σ⁵⁴ holoenzymes

(A) A bacterial enhancer binding protein (or bEBP) establishes contact with the σ⁵⁴-RNAP holoenzyme that is bound at -12 as well as -24 promoter elements. Initially, it interacts with the upstream activator sequences (UAS) and creates dimers or hexamers. (B) DNA bending takes place and triggered by proteins like integration host factors. (or IHFs). (C) Nucleotide hydrolyses meanwhile is facilitated by the bEBP and following the release of energy, it allows the creation of an open complex so as to initiate transcription. (Source: 101, p.499).

Three-component: this is a two-component system that incorporates a non-kinase receptor. This receptor upon sensing an environmental cue triggers the autophosphorylation of a cytoplasmic HK. Upon activation, the phosphate is phosphorelayed to a RR¹¹⁶. An example of this system are the proteins involved in chemotaxis¹¹⁶ (Figure 1-33) that control movement¹²² according to chemical

gradients⁷⁶. This type of controlled movement acts via flagella or pili⁷⁶, so that motile bacteria are able to respond accordingly to their changing environment¹²³.

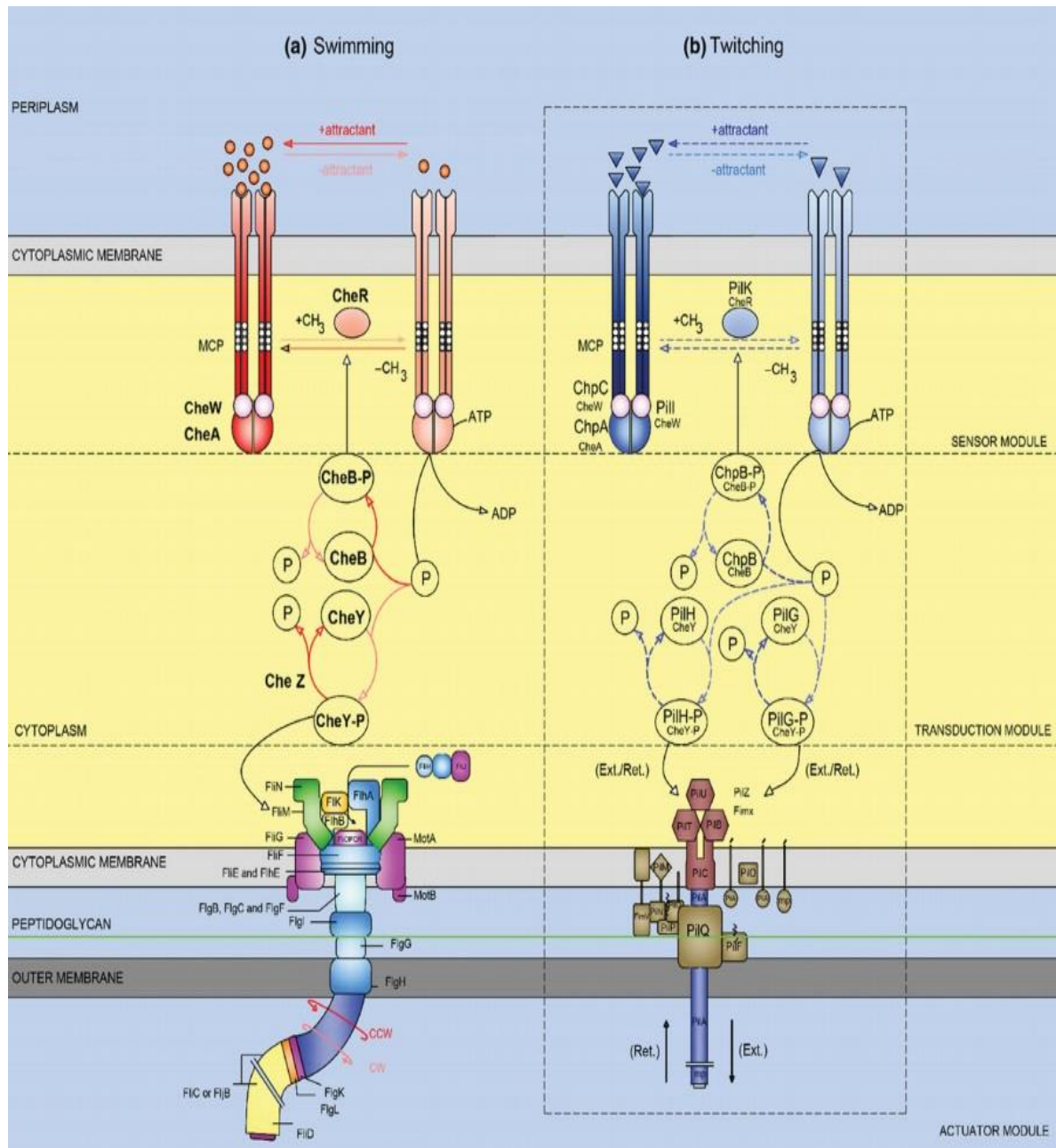


Figure 1-33 Chemotaxis alters the direction of flagella rotation and changes the swimming direction

After a chemoattractant is bound into a dimerised chemotaxis receptor (Methyl-accepting chemotaxis proteins or MCP) that is localised within the cell membrane; this triggers the activation of a CheA (cytoplasmic histidine kinase) in order to undergo autophosphorylation. After CheA-P relays its phosphoryl group to CheY, the activated CheY-P establishes contact with the motor protein FliM within the flagella apparatus so as to change the direction of flagella rotation. CheB removes the CheY's phosphoryl group and is also responsible for undertaking the regulation of the methylation level of MCPs as a response to the level of chemoattractant. (Source: 76, p.20).

1.11 Nitrogen metabolism, regulation and types of nitrogen sources

Nitrogen (N) is an essential element for microorganisms because it is part of important compounds, such as amino acids and nucleotides³⁰⁶. This nutrient is not abundantly available within rocks and soils, whereas in the Earth's surface atmosphere it is present as dinitrogen ($N_{2(g)}$) at a concentration of 78 %²⁹¹. The stable nature of the triple bond of $N_{2(g)}$ renders this gas unreactive,³ and consequently it is unavailable for living organisms²⁹¹. However, there are microorganisms which are able to break this triple bond at room temperature and lower pressure in order to reduce it to the ammonium ion (NH_4^+) and ammonia (NH_3).

In general, microbes live in fluctuating oligotrophic environments, and consequently their metabolism needs to be appropriately regulated in response to starvation. This is accomplished by certain metabolic pathways being 'turned on/off' in response to the available nitrogen source, the concentration of carbon/nitrogen, and the energy status (reflected by the ATP/ADP). Such metabolic regulation is accomplished by controlling the enzymes within these metabolic routes at two different levels:

- Enzyme synthesis: enzyme concentration affects the reaction rate, and mechanisms used to control enzyme production are at the transcriptional and translational levels.
- Enzyme activity: enzymes are active only when needed, and only after being correctly localised within a cell. This mechanism of regulation depends on signal molecules that reversibly bind to an enzyme at specific regulatory sites leading to a range of activities, and are also able to cause inhibition or activation in response to the energetic status of a cell and concentration of specific metabolites.

1.11.1 Transport of ammonia/ammonium (NH_3/NH_4^+) and amino acids glutamate and glutamine

Ammonium, glutamate and glutamine are the key substrates in nitrogen assimilation in the many bacteria, with ammonia/ammonium identified as the preferred source (see sections 1.12 and 1.12.2). Ammonium (NH_4^+) is a 'rich-nitrogen' source and supports

³ N_2 (dinitrogen) is apolar and isoelectronic with CO. Hence, dinitrogen is able to form compounds with transition metals (e.g. ruthenium), which are similar to compounds formed between CO and these metals²⁹¹. Dinitrogen is not very water-soluble, and tends to be unreactive towards most elements and compounds²⁹¹.

a high growth rate of *Enterobacteriaceae* under aerobic conditions³⁰⁶ in comparison to 'poorer-nitrogen' sources such as glutamine or glutamate^{306,134}. At high concentrations $\text{NH}_3/\text{NH}_4^+$ readily diffuses into the cell and at very low concentrations an ammonium channel (AmtB) is required for passive or active diffusion¹³⁴.

AmtB of *E. coli* belongs to the Amt/MEP/Rh superfamily of ammonium channels. Figure 1-34 summarises models for the uptake of ammonium by *E. coli* via diffusion through the bilayer (the primary mode at high ammonium concentration) or binding and uptake through the AmtB channel. The consensus opinion is that diffusion through the membrane or hydrophobic channel of AmtB is as the uncharged molecule ammonia (NH_3)¹³⁴, not requiring metabolic energy. At very low concentrations of ammonium (NH_4^+), there is a marked increase in expression of the ammonia channel encoded by *amtB*¹³⁴. Transport at low concentrations implies a high affinity binding of AmtB for ammonia or the ammonium ion ($K_m \sim 10 \mu\text{M}$)³¹⁵. Only at these low concentrations might metabolic energy be used for ammonium uptake. Whether uptake via AmtB is purely via facilitated passive transport or active transport requiring energy remains a matter of debate (Figure 1-34). Models of transport include electroneutral transfer of NH_3 or electrogenic transfers eg uniport of NH_4^+ or symport of NH_3/H^+ ^{134,261,262}. Disruption of the proton motive force would occur if there was an excess of the charged molecule NH_4^+ in the cytosol owing to the diffusion of uncharged compound NH_3 outside the cell²⁶². Notably, this undesirable disequilibrium in $\text{NH}_3/\text{NH}_4^+$ is prevented by the incorporation of the ammonium ion into glutamate by glutamine synthetase (GS) to form glutamine²⁶².

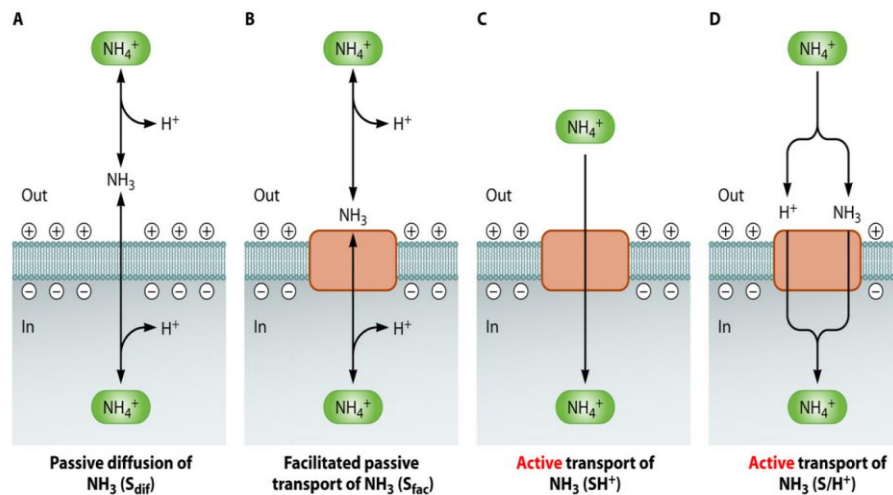


Figure 1-34 Mechanisms of transport for ammonia/ammonium (NH₃/NH₄⁺) in *E. coli*

The rectangle (beige rounded) denotes the transporter AmtB. Meanwhile the four mechanisms of transport include: (A) Mode S_{dif}: transportation of NH₃ through passive diffusion. (B) Mode S_{fac}: transportation of NH₃ after deprotonation of NH₄⁺ by phosphates or carbonates located in the periplasm; this transport use an ammonia-conducting channel and the transportation is electroneutral. (C) Mode S^{H+} or uniporter: active transportation of NH₄⁺ through the AmtB carrier, as there is charged molecule transversing the channel this transport is electrogenic. (D) Mode S/H⁺ or NH₃/H⁺ co-transporters: active transportation of NH₃ whereby NH₃ as well as the symported H⁺ follow distinct routes and the carried H⁺ rejoins NH₃ at the pore exit releasing NH₄⁺. This transport is electrogenic as a net charge is transporter through the channel. In panels A as well as B, H⁺ illustrated at the vertical arrows represents the consumption or production of chemical or scalar protons (protons released as result of chemical reactions). (Source: 134, p.643).

Channel activity of AmtB is blocked by the trimeric GlnK regulator (PII) via the insertion of a loop into each pore of the trimer, thereby exposing a conserved Arg47 residue that impedes the passage of ammonia¹⁴¹ (Figure 1-35). The stability of the GlnK-AmtB complex is affected by the levels of Mg²⁺, 2-oxoglutarate (2-OG), ATP and ADP¹³⁴. A reduction in the amount of 2-OG and changes in ATP/ADP ratio initiates dissociation, thereby allowing ammonia to flow into the cytosol¹³⁴. GlnK is transiently uridylylated by the bifunctional uridylyltransferase/uridylyl-removing enzyme (UTase/UR), which, in turn, is regulated by the glutamine concentration in the cell. Low glutamine concentrations stimulates UTase activity, while high concentrations stimulate UR activity and UMP removal. Since uridylylated-GlnK is unable to interact with AmtB, transport of ammonium in addition to GS activity and gene expression (Figure 1-35) is a point of control of nitrogen assimilation.

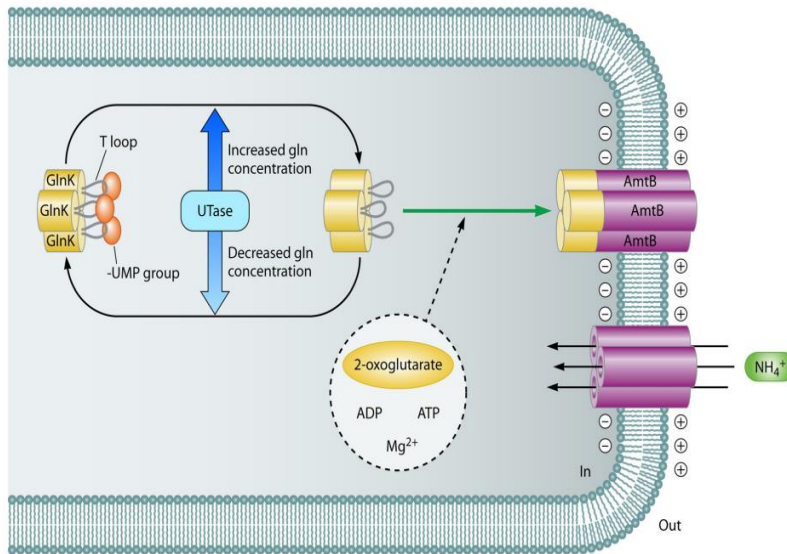


Figure 1-35 Ammonium channel (AmtB) is regulated by sensor protein GlnK

The trimeric regulator protein GlnK (PII) T loop is modified at a Tyr residue by addition of a UMP group (uridine 5'-monophosphate) which can be covalently added or removed by uridylyltransferase/uridylyl-removing enzyme (UTase/UR). This enzyme responds to an upshift (dark blue) or downshift (light blue) in the amount of glutamine by removing or adding the UMP group, respectively. The intracellular glutamine pool reflects the nitrogen status, while the level of 2-oxoglutarate (2-OG) indicates the carbon status in the cell. At higher nitrogen concentrations (high glutamine amounts), the non-uridylyated GlnK is able to interact with AmtB carrier and block the channel in order to stop ammonia influx. An increase in 2-OG (implying low N:C ratio) and change in both ATP/ADP ratio and ion Mg^{2+} destabilises the complex GlnK-Amt and GlnK is released. GlnK-UMP is unable to interact with AmtB. (Source: 34, p.649).

In contrast to ammonium uptake, amino acids like glutamine (Gln) and glutamate (Glu) are unable to diffuse through the cytoplasmic membrane and require active transport via dedicated transporters for assimilation. These show specific and often high affinity for the substrate, permitting scavenging during amino acid shortage^{264,265}. *P. fluorescens* is known to actively transport the neutral amino acids proline, β -alanine as well as L-alanine through permeases²⁶⁶. In the *P. fluorescens* SBW25 genome, a putative glutamine high affinity ATP-binding cassette (ABC) transporter has been annotated (locus tags: PFLU_RS12785, PFLU_RS12790, PFLU_RS12795, PFLU_RS12800), a second putative glutamine ABC transporter is encoded by the loci PFLU_RS17465, PFLU_RS17470, PFLU_RS17475 and two putative transporters for glutamate have been identified (Table 2-7). A putative glutamate/aspartate ABC transporter is encoded by genes *gltJKL* (*gltJ* locus tag: PFLU_RS05640; *gltK* locus tag: PFLU_RS05635; *gltL* locus tag: PFLU_RS05630) and a putative glutamate ABC

transport system is encoded by PFLU_RS01120, PFLU_RS01125, PFLU_RS01130, and PFLU_RS01135 (Appendix O: Figure O-8 and Figure O-9). In addition, *P. fluorescens* SBW25 uses a periplasmic glutaminase (gene *glsA*, locus tag: PFLU_RS17490; Appendix O: Figure O-10) to catalyse the hydrolytic deamination of glutamine releasing ammonium and glutamate¹³³ which can then be taken up by a glutamate transport system. A *P. putida* strain with a disrupted PGA (periplasmic glutaminase/asparaginase) gene was unable to grow on glutamine but could still grow well on glutamate¹³³. This suggests that this strain was not able to transport glutamine.

1.11.2 Overview of nitrogen assimilation

In bacteria, ammonium (NH₄⁺) is generally the preferred nitrogen source. The nitrogen regulator (Ntr) system is induced by nitrogen sources other than ammonium (NH₄⁺)^{133,175,285,293-295}. This is defined as nitrogen limitation leading to induction of the Ntr system for expression of enzymes and transporters involved in nitrogen assimilation^{285,306}. As their mechanisms of regulation are similar in *Pseudomonas*²⁸⁵⁻²⁸⁸, the protein nomenclature can be used interchangeably²⁸⁵. In *P. fluorescens* SBW25, the gene loci PFLU_RS01690 and PFLU_RS01685 share a high percentage of homology to genes *ntrB* (nitrogen regulator NRII) and *ntrC* (nitrogen regulator NRI), respectively, from *E. coli* K12¹⁷⁵. The gene locus PFLU_RS01690 has a 45 % similarity with gene *ntrB*, while gene locus PFLU_RS01685 has a 69 % homology to *ntrC*¹⁷⁵. Therefore, these *P. fluorescens* SBW25 gene loci were named after the *E. coli* K12 genes as *ntrB* and *ntrC*, respectively¹⁷⁵. NtrB (also known as GlnL or NRII) is an HK receptor that phosphorylates the transcription factor NtrC, which is necessary to initiate the transcription of the nitrogen genes¹³⁷ (Appendix O: Figure O-5). Thus in addition to regulating adenylation of GS, glutamine:2-OG levels also regulate the phosphorylation state of NtrC¹³⁸. Glutamine (Gln or Q) concentrations of 0.2 mM to 4 mM diminish the NtrC-P concentration and increase GS-AMP levels¹³⁸. NtrC (also known as NRI or GlnG) is the response regulator for the two-component system NtrB/NtrC¹³⁵ (Figure 1-37 and Appendix O: Figure O-5). This system senses the signals for the carbon and nitrogen status within a cell, via interaction with PII, and regulates the transcription of genes involved in the metabolism of nitrogen¹³⁵⁻¹³⁷ (Appendix O: Figure O-1). Glutamine and 2-OG are the key nitrogen and carbon signals, detected by GlnD (UTase/UR or uridylyltransferase/uridylyl-removing enzyme) and PII, respectively¹³⁷. PII requires the glutamine sensor UTase/UR¹⁴¹, in

order to regulate modification or demodification of the enzyme glutamine synthetase (GS) and the transcription of the *ntr* genes^{120,141}, which are expressed under nitrogen limiting conditions¹²⁰. Glutamate (Glu or E) and 2-oxoglutarate (2-OG) are used as channels for the assimilation of inorganic nitrogen (NH₄⁺/NH₃) via two metabolic pathways: glutamate dehydrogenase (GDH) and GS/GOGAT [glutamine synthetase (GS)/glutamate synthase (GOGAT)] (Figure 1-36 and Figure 1-37). The major carbon skeleton donor for nitrogen assimilation is 2-OG, a key intermediate of the Krebs cycle (Figure 1-38). Therefore, 2-OG is the signal for carbon status inside a cell, and is responsible for linking carbon and nitrogen metabolism. Levels of 2-OG can fluctuate rapidly, approximately 1 min after a change in the nitrogen status, between 1.5 mM (low nitrogen) to 0.1 mM (high nitrogen)¹⁴¹. 2-OG signals the carbon status by interacting with the signal transduction protein PII (encoded by gene *glnK*; Appendix O: Figure O-2) and altering its conformation (Figure 1-39). PII conformation is important for the interaction of PII with adenylyltransferase (ATase) and the nitrogen regulator NtrB (NRII). The different conformations of PII depend on the number of 2-OG and bound uridine 5'-monophosphate (UMP).

A. GDH pathway



B. GS/GOGAT pathway

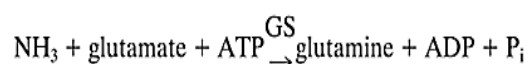


Figure 1-36 Ammonia assimilation pathways

(A) The GDH pathway occurs under high nitrogen levels (high intracellular glutamine pool and high ammonium levels in the milieu) as the enzyme glutamate dehydrogenase (GDH) has low affinity for ammonium ($K_m \approx 1$ mM). This route is not used under conditions of nitrogen limitation, which means a low glutamine/2-OG ratio that triggers overexpression of *glnAntrBC* operon. This nitrogen limitation is caused by low amounts of ammonium in the media or amino acids used as nitrogen sources e.g. glutamine (nitrogen signal) or glutamate (forms 2-OG and uses up glutamine pool). (B) The glutamine synthetase (GS)/glutamate synthase (GOGAT) pathway is regulated by the Ntr system and is used under low levels of ammonium due to the high affinity of the enzyme glutamine synthetase (GS), which has a $K_m \approx 0.1$ mM. This metabolic route is used under conditions of nitrogen limitation and as it uses ATP requires a high energy. 2-oxoglutarate (2-OG) has alternative names, including 2-ketoglutarate, α -ketoglutarate, 2-ketoglutaric acid and oxoglutaric acid. (Source: 169, pp.605-606).

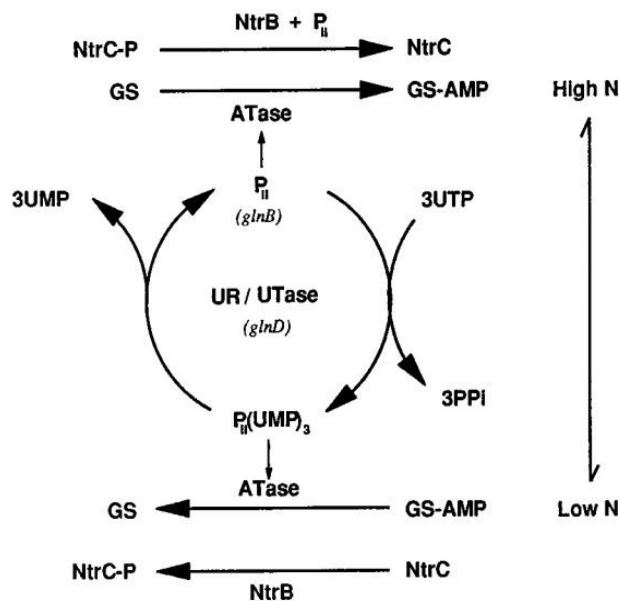


Figure 1-37 Nitrogen regulation of the glutamine synthetase (GS) pathway

At high levels of nitrogen the assimilation of ammonia through the GS pathway is arrested as GS becomes adenylated (GS-AMP) by the bifunctional enzyme adenylyltransferase (ATase; encoded by *glnE*). GS-AMP is inactive. PII (encoded by *glnK* in *Pseudomonas*, and both *glnK* and *glnB* in Enterobacteria) is a sensor of the nitrogen and carbon status within a cell. PII is uridylylated or deuridylylated by the bifunctional uridylyltransferase/uridylyl-removing enzyme (UTase/UR) in response to the nitrogen/carbon ratio. Non-uridylylated PII interacts with ATase to induce its adenylation activity; PII(UMP)₃ induces removal of the AMP groups from GS activating it in preparation for nitrogen assimilation. PII also interacts with NtrB, and leads to an increase in dephosphorylation of the active transcription factor NtrC-P, and an arrest in the expression of *glnA* which encodes GS. AMP: adenosine 5'-monophosphate. UMP: uridine 5'-monophosphate. (Source: 169, p.607).

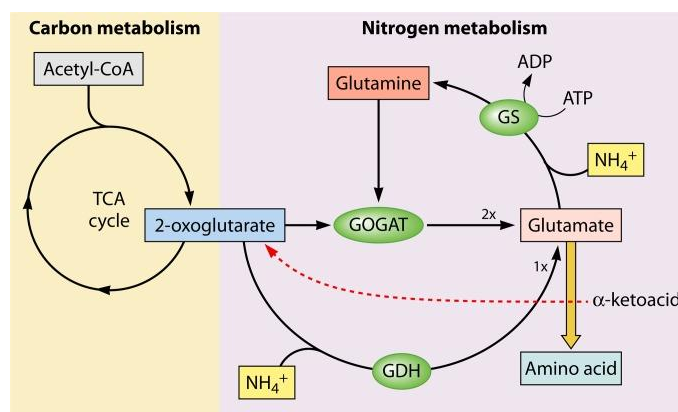


Figure 1-38 Carbon and nitrogen metabolism are interconnected by 2-OG

Ammonium (NH₄⁺) is incorporated into 2-oxoglutarate (2-OG) by glutamate dehydrogenase (GDH) and produces one molecule of glutamate, but when it is assimilated into glutamate by the enzyme glutamine synthetase (GS), it forms glutamine. The enzyme glutamate synthase (GOGAT) synthesises two molecules of glutamate via a transamination reaction between glutamine and 2-oxoglutarate. Anaplerotic reactions provides α-ketoacid to replenish the pool of 2-OG diverted towards nitrogen metabolism. Therefore glutamate can be synthesised by GOGAT or GDH. TCA: Krebs cycle. (Source: 170, p.420).

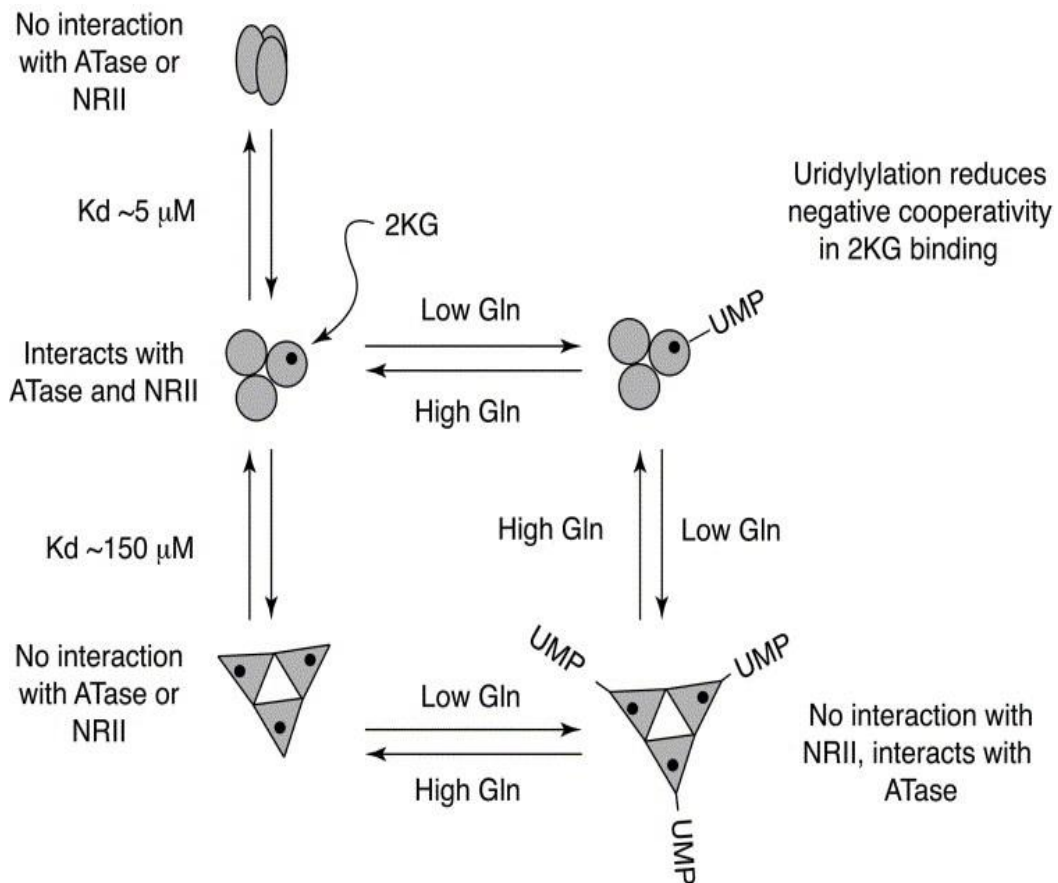


Figure 1-39 Conformational state of PII regulates nitrogen metabolism

PII is a trimeric sensor protein that binds 2-OG (2KG), UMP and ATP (not shown). These signalling molecules alter PII conformation upon binding, thus changing the capacity of PII to interact with NtrB (NRII) and adenylyltransferase (ATase) in response to the carbon and nitrogen status of a cell. If all the regulatory sites for 2-OG are occupied, then PII is unable to interact with NtrB (NRII) and ATase. At low nitrogen (low glutamine) and high carbon levels (abundant 2-OG), the bifunctional uridylyltransferase/uridylyl-removing enzyme (UTase/UR) adds UMP groups to PII to form PII-(UMP)₃, which interacts with ATase to induce the removal of AMP from inactive GS-AMP. The K_d (dissociation constant) increases dramatically ($\approx 150 \mu\text{M}$) upon binding of 2-OG, which reflects the anti-cooperative binding of 2-OG, which is reduced following the removal of UMP. The small black dots in the figure represent 2-OG, while the different conformational states of PII are shown as ovals, triangles and circles. UMP: uridine 5'-monophosphate. AMP: adenosine 5'-monophosphate. (Source: 135, p.174).

PII regulates the enzymatic activity of GS and its biosynthesis indirectly by interacting with adenylyltransferase (ATase) and NtrB, respectively. NtrB is a histidine kinase (HK) that regulates the phosphorylation state of the transcription factor NtrC (nitrogen regulator I or NRI). When NtrB is bound to PII, phosphorylation is prevented. When free, NtrC-P is phosphorylated. Upon phosphorylation, the gene expression of *glnA*, which encodes GS, is triggered (Appendix O: Figure O-5); this, in turn, increases the amount of this enzyme.

NtrC (bEBP) is the master regulator of nitrogen metabolism¹⁷¹. It is interesting to highlight that NtrC of *P. putida* is functionally equivalent to NtrC from *E. coli*, as shown in complementation experiments. On introducing the wild type *P. putida ntrC* gene into *E. coli ΔntrC*, it was observed that expression of the *E. coli* Ntr system was upregulated under conditions of nitrogen limitation¹⁷¹. Mutations in NtrC (D55E, S161F) from *P. putida* confer the same phenotype as similar mutations in NtrC (D54E, S160F) from *Salmonella enterica*¹⁷¹. This mutant phenotype leads to NtrC activation independent of phosphorylation by NtrB and thus to overexpression of the Ntr system independently of the nitrogen source or nitrogen status within the cell¹⁷¹.

The multimeric enzyme GS is sequentially adenylylated by ATase under levels of high nitrogen, thus progressively inactivating the enzyme. The activity of the bifunctional enzyme ATase is controlled by PII in response to the nitrogen/carbon status of a cell (Figure 1-37). ATP or ADP binds to PII in addition to 2-OG, thereby making this protein a sensor of the energy status of the cell. Binding of ATP is in cooperation with binding to 2-OG, whereas ADP binding prevents 2-OG binding¹⁴¹. PII assumes alternative conformations in response to 2-OG and ATP/ADP availability¹⁴¹. Studies conducted in *E. coli* have shown that other effector molecules, such as pyruvate and oxaloacetate, can bind to PII although in a more labile fashion compared to 2-OG¹⁴¹.

1.11.3 Function of regulatory protein PII (GlnK)

The regulation of nitrogen assimilation is through sensing of the ratio of nitrogen/carbon (glutamine/2-oxoglutarate) by the trimeric protein PII (GlnK: sensor of 2-OG)²⁹⁶. If this ratio is high then it implies there is a sufficient nitrogen supply and low carbon, whereas a low ratio indicates the opposite. PII (GlnK) regulates activity of its target proteins, NtrB (His kinase sensor)^{138,139}, GlnE (ATase/AR) and AmtB (ammonium channel; Appendix O: Figure O-1 and O-2) by direct interaction via the flexible T-loop. This loop was named after identifying Tyr-51¹⁴¹ as the site of uridylylation (UMP binding). Modification of PII at this site prevents interaction with these target proteins (Figure 1-35). The level of reversible uridylylation (UMP binding) in PII is regulated by UTase/UR (GlnD). Glutamine is an allosteric effector of UTase/UR, and activates UR activity and UMP removal, while at low glutamine levels UTase activity predominates¹⁴¹. The structure of the homotrimeric allosteric effector PII from *E. coli* is shown in (Figure 1-40).

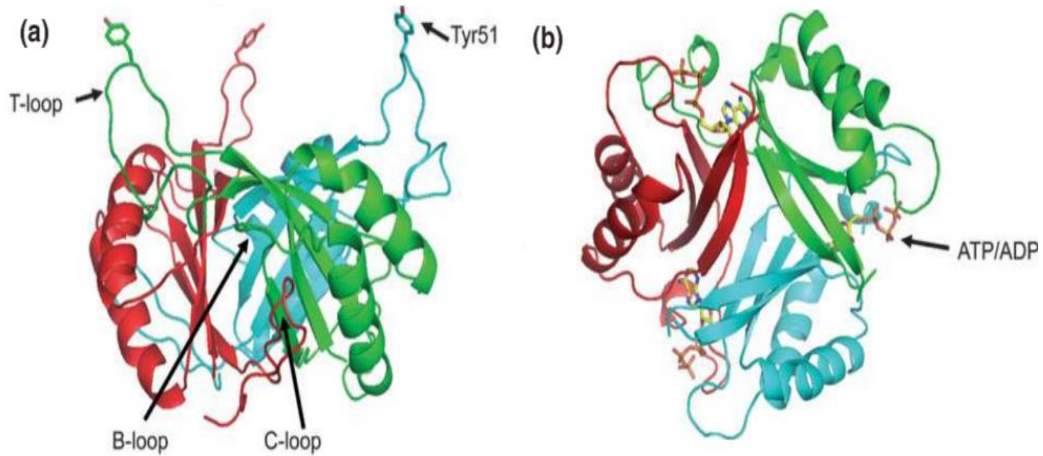


Figure 1-40 Ribbon diagram illustrating the structure of PII in *E. coli*

(A) Side view of the homotrimeric protein PII, arrows indicate the T-loop, B-loop and C-loop. The flexible T-loop has a residue at position Tyr51 to which reversible uridylation occurs. The B-loop is a Walker A motif, and is where ATP/ADP binding takes place. The C-loop is the carboxy terminal region of PII. (B) This is a top view of PII, showing the T-loop at the top. There is an arrow indicating the binding site for ATP/ADP within the cleft formed between the two subunits. (Source: 141, p.256).

1.11.4 Nitrogen regulation: sensor histidine kinase (GlnL or NtrB)

NtrB is the signal transduction protein responsible for phosphorylating the response regulator NtrC under nitrogen limitation conditions. This in turn activates expression of the *ntr* regulon. NtrB functions as a dimer. It has autokinase activity and phosphatase activity that is involved in dephosphorylating NtrC-P. Nonuridylylated PII locks NtrB in a conformation that activates the phosphatase activity³¹⁸. NtrB has three specific domains: Per-ARNT-Sim (PAS), HisKA and HATPase_c (Figure 1-41, Figure 1-42).

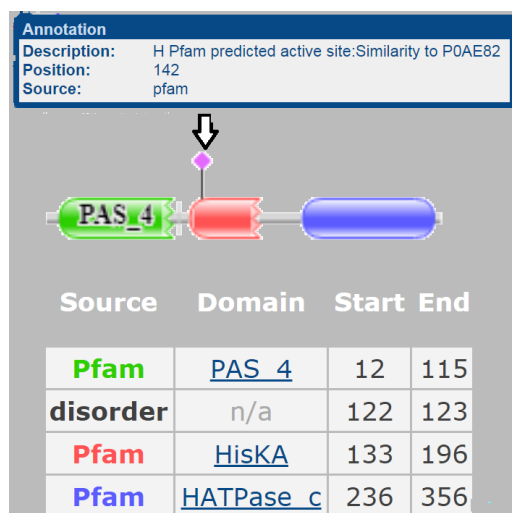


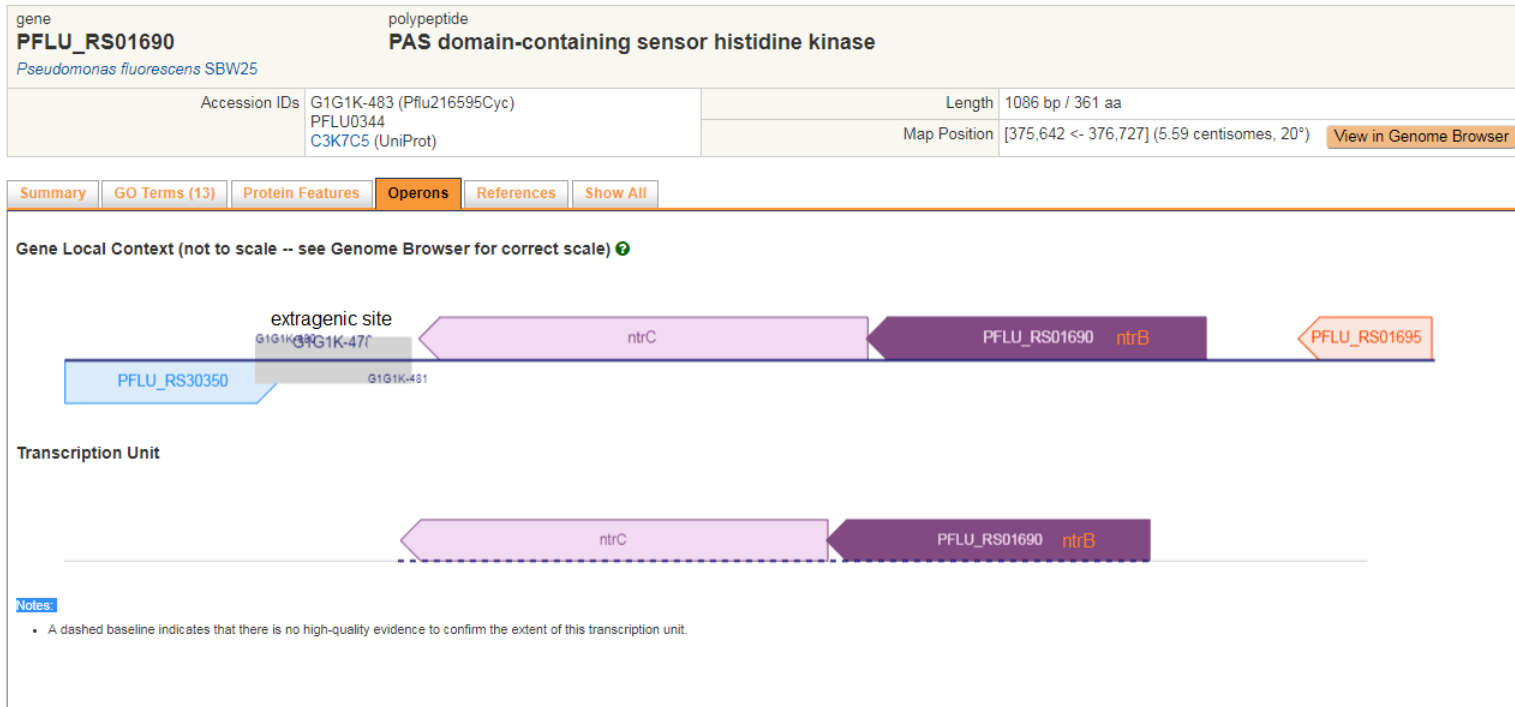
Figure 1-41 Structure of NtrB of *P. fluorescens* SBW25

[Source: <http://pfam.xfam.org/protein/C3K7C5>]

a) PAS domain: this is located in the N-terminal region of the protein and is known as the sensor. While in many sensor:regulator pairs, the PAS domain of the sensor binds a small molecule, no binding partner for the PAS domain of NtrB has been recognized¹³⁷. A T97P mutation towards the end of this domain was shown to overactivate the Ntr response in the evolved swimming mutant *P. fluorescens* Δ *fleQ* AR2S¹⁰⁸.

b) HisKA domain: this is the histidine kinase domain and the phosphorylated histidine is located at position 142. This domain is responsible for interacting with the receiver domain of NtrC to promote phosphorelay at the conserved aspartate residue in NtrC. The phosphotransfer domain is dimeric. A point mutation at position A129T of *Klebsiella pneumoniae* NtrB was shown to diminish its phosphatase activity and removal of the bound phosphate group from NtrC-P³⁰⁹. However, this point mutation did not alter the nature of NtrB interaction with PII³⁰⁹. Mutations in this domain have also been identified in evolved swimmers in a *P. fluorescens* (*Fla*⁻, *Visc*⁻) strain (Table 1-6).

c) HATPase_c: ATPase domain is responsible for ATP binding and hydrolysis. The γ -phosphate of ATP, the substrate for phosphorylation, is subject to nucleophilic attack by the histidine-142 of the HisKA domain. Consequently, NtrB becomes autophosphorylated. There is evidence that this domain is involved in PII interaction to stimulate phosphatase activity^{136,137} and that mutations in this region lead to decreased phosphatase activity and overstimulation of Ntr regulon (Figure 1-43 and Table 1-6).



Sequence Features

```

1  MTISDALHRL  LDNLTTATI  LLNDDLRLEY  MNPAAEMLLA  ISGQRSHGQF  ISELFTESAE  ALSSLRQAVE  QAHFPFKREA  MLTALTGQTL  TVDYAVTPIL  100
101 SNGATLLLLLE  VHPRDRLLRI  TKEEAQLSKQ  ETSKMLVRGL  AHEIKNPLGG  IRGAAQLLAR  ELPEEHLKDY  TNVIEEADR  LRNLVDRMLG  SNKLPSLAMT  200
201 NVHEVLERVC  HLVEAESQGC  ITLVRDYDPS  IPDVLIDREQ  MIQAVLNIVR  NAMQAISSQN  ELRLGRISLR  TRALRQFTIG  HVRHRLVTKV  EIIDNGPGIP  300
301 VELQETIFFP  MVSGRPDGTG  LGLAITQNI  SQHQGLIECE  SHPGHTTFSI  FLPLEQGAPS  T

```

Feature Class	Location	Citations	Comment
Pfam-PF08448	12->107	[Finn16]	PAS_4 : The PAS fold corresponds to the structural domain [More...]
Pfam-PF00512	136->189	[Finn16]	HisKA : Dimerisation and phospho-acceptor domain of histid [More...]
Pfam-PF02518	237->355	[Finn16]	HATPase_c : This family represents the structurally related AT [More...]

Figure 1-42 NtrB sequence features and transcript unit in *P. fluorescens* SBW25

[Source: <https://biocyc.org/gene?orgid=PFLU216595&id=G1G1K-483#tab=TU>]

The point mutations in NtrB and their respective effects are shown Figure 1-43 and Table 1-6.

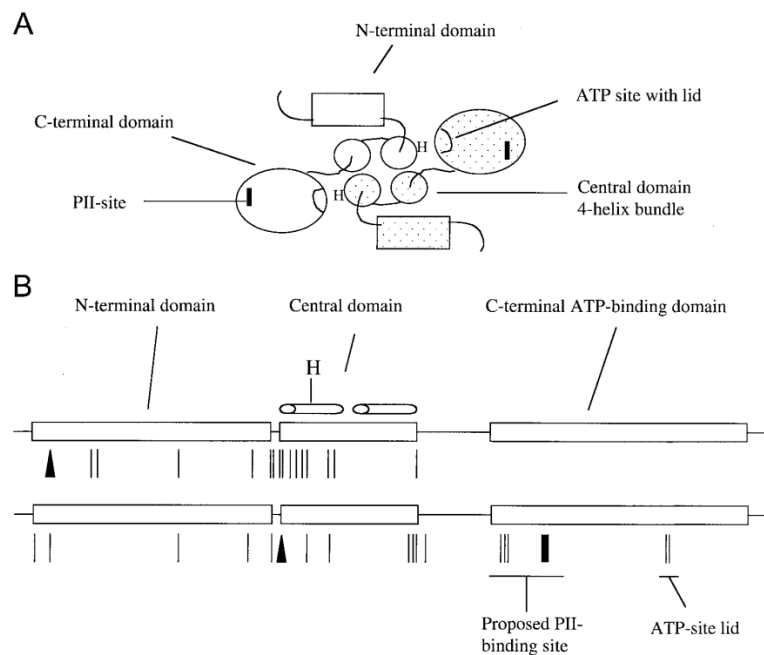


Figure 1-43 Diagram of NtrB dimers, PII binding site and localisation of mutations that dampen phosphatase activity in *E. coli*

A) The nonmodified form of PII is proposed to interact close to the beginning of the C-terminal ATP binding domain. Binding of PII triggers phosphatase activity of NtrB resulting in removal of phosphate groups bound to NtrC-P. In the presence of PII-UMP (flags poor nitrogen levels), the autokinase activity of NtrB is enhanced to raise the NtrC-P levels. B). Linear map of the NtrB domains indicating localisation of mutations that alter its phosphatase activity. Lines signify amino acid substitutions, bars deletions, and triangles insertions. (Source: 316, p.1300).

Table 1-6 NtrB point mutations and their effects

Mutation Position	Effect	Bacterium	Reference
A129T	Phosphatase activity in the absence of PII	<i>E. coli</i>	312
G313A	Slow dephosphorylation of NtrC-P even in absence of PII. Phosphatase activity stimulated by ATP. Does not bind ATP. Lower rate of autophosphorylation		312
H139N	Increased phosphatase activity even in absence of PII. Phosphatase activity is stimulated by ATP. Phosphatase activity is dramatically higher in the presence of PII.		312
D287N	Does not phosphorylate NtrC		312
G289A	Dampens phosphorylation activity but is still able to phosphorylate NtrC.		312

Mutation Position	Effect	Bacterium	Reference	
G291A	Dampens phosphorylation activity but is still able to phosphorylate NtrC		312	
Y302N	Alters the lid that covers the ATP binding site. Lower phosphatase activity. It does bind to PII, but its phosphatase activity is not induced.		316	
S227R	Lower phosphatase activity. Does not bind to PII.		316	
L16R	Lower phosphatase activity. Binds to PII, but phosphatase activity is not induced.		316	
L126W	Reduced phosphatase activity. The NtrB system remains constitutively active, and growth in glucose/TCA intermediates in the presence of ammonium as sole nitrogen source decreases.	<i>P. aeruginosa</i>	174	
D227A				
P228L				
S229I				
A129T	Dampens phosphatase activity	<i>Klebsiella pneumoniae</i>	309, 318	
Mutation Position	Domain	Documented Effect	<i>P. fluorescens</i> Δ <i>fleQ</i> strain	Reference
T97P	N-terminal PAS	Slow swimming, upshift in Ntr regulon	AR2S	108
D228A	Beginning of ATPase domain	Slow swimming	Pf0-2xS	108
V185K	HisKA	Slow swimming	AR2S	108
D179N	HisKA	Slow swimming	AR2S	108
L184Q/V185I	HisKA	Slow swimming	AR2S	108

1.11.5 Nitrogen metabolism: NtrC and regulation at the genetic level

NtrC is the DNA binding regulator of the Ntr regulon. Nitrogen regulation in *Pseudomonas* is very similar to that in Enterobacteria¹⁶⁸. GDH (encoded by *gdhA*) is the enzyme responsible for assimilating ammonia at high levels due to its low affinity (high $K_m \approx 1$ mM). The reaction catalysed by GDH aminates 2-OG using the cofactor NADPH to produce glutamate. Under nitrogen starvation, a reverse reaction by *gdhB* produces ammonia and 2-OG¹⁶⁸. NtrC negatively regulates the expression of GDH through an interaction with four boxes surrounding the *gdhA* promoter in a cooperative manner. NtrC dimers bound to downstream boxes interact with those attached to

upstream boxes in order to form a repressor loop and prevent an open complex, thus hindering transcription¹⁶⁸ (Figure 1-44). The regulatory nature of this repression is dependent upon an abundance of the repressor NtrC. Expression of *ntrBC* increases under nitrogen limitation conditions. Repression of *gdh* transcription is also independent of the phosphorylation status of NtrC, as shown in a study conducted with *P. putida*¹⁶⁸. The high levels of NtrC achieved under nitrogen limitation conditions decreases after cells are exposed to a medium containing a high level of ammonium because of turnover of NtrC and dilution due to growth¹⁶⁸. In addition, it is interesting that in *Pseudomonas* PII (*glnK*) expression is also regulated by NtrC¹⁶⁸.

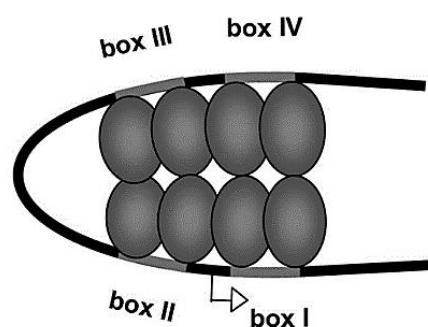


Figure 1-44 DNA looping due to NtrC dimers binding to boxes around the *gdhA* promoter

DNA looping due to interactions between NtrC dimers bound to different boxes (upstream and downstream of promoter) inhibits transcription and impedes isomerisation of closed complexes. The arrow indicates the site of transcription initiation within the *gdhA* promoter. (Source: 168, p.314).

The expression of the bifunctional enzyme ATase (GlnE) is constitutive in *E. coli*¹⁴¹. Adenylyltransferase (ATase) has two homologous nucleotidyltransferase domains connected by a linker region; the domain responsible for adenylylation (AT domain) is at the C-terminal, and the domain responsible for deadenylylation (AR domain) is located at the N-terminal. At high levels of glutamine, non-modified PII interacts with the AT domain triggering adenylylation of GS in order to accumulate GS-AMP. A stable complex formed of GlnB-GlnE is formed upon glutamine binding.

The *glnK* gene (PII) is genetically linked to the *amtB* gene to form an operon (*glnKamtB*) which is expressed under low nitrogen levels¹⁴¹. The product of the *amtB* gene is an ammonia channel¹⁴¹, which is also regulated by PII see above (Figure 1-45). In a rich nitrogen environment such as minimal medium M9 with ammonium/glucose, the sensor PII interacts with ammonium channel (AmtB) impairing ammonium transportation³⁰⁶. With a transition to nitrogen limitation conditions (e.g. glutamine as

nitrogen source), the PII-UUMP level increases and PII-UUMP no longer interacts with AmtB or with NtrB. Consequently, NtrB phosphorylates NtrC and the levels of NtrC-P increase resulting in upregulation of *glnKamtB* locus as well as the *glnAntrBC* locus³⁰⁶. Additionally, acetyl phosphate is able to transfer its phosphate group to NtrC³⁰⁶.

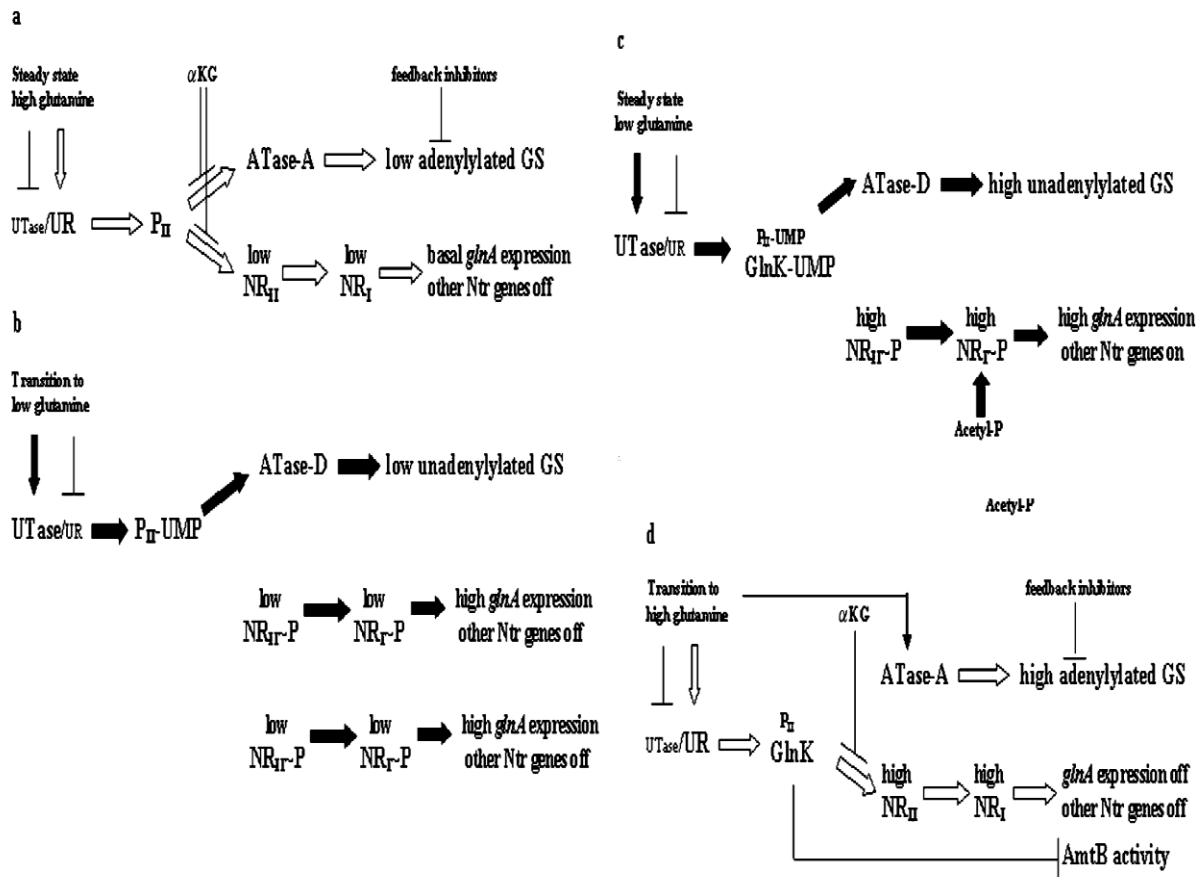


Figure 1-45 Nitrogen regulation in *E. coli* under nitrogen limitation conditions

Glutamine controls the activities of individual regulators of nitrogen regulator (Ntr) cascade. These regulators are PII and NtrB. Glutamine also controls the activities of the bifunctional enzymes UTase/UR and ATase. The NtrC-P upshifts *glnAntrBC* operon expression. NRI: NtrC or GlnG. NRII: NtrB or GlnL. GS: glutamine synthetase or GlnA. ATase: adenylyltransferase. ATase A: adds AMP groups. ATase D: removes AMP groups. PII: GlnK. AmtB: ammonium channel. UTase/UR: uridylyltransferase/uridylyl-removing enzyme or GlnD. α KG: 2-OG or 2-oxoglutarate. AMP: adenosine 5'-monophosphate. UMP: uridine 5'-monophosphate. (Source: 306, p. 163).

In *E. coli*, *glnL* and *glnG* encoding NtrB and NtrC are constitutively expressed at basal levels when expressed from the σ^{70} dependent promoter *glnLp*¹⁶⁹. This promoter is located between *glnA* (encoding GS) and *glnL*¹⁶⁹ (Figure 1-46). In addition, there are two promoters for *glnA*: *glnAp1* and *glnAp2*¹⁶⁹. The promoter *glnAp1* requires σ^{70} and is functional at high nitrogen concentrations, but only *glnA* is transcribed and only low levels of GS (GlnA) are produced compared to when the cell is under nitrogen

starvation conditions¹⁶⁹. In contrast, promoter *glnAp2* is dependent upon factor σ^{54} (alternative name NtrA: RNA polymerase sigma factor 54) and drives expression under nitrogen limiting conditions. In this case, *glnAp1* is blocked due to binding of NtrC-P and the entire locus is transcribed at higher levels from *glnAp2*. Hence, expression of NtrBC is increased together with production of GS¹⁶⁹. NtrC-P also activates other operons involved in nitrogen assimilation such as *glnHPQ* operon (high affinity glutamine ABC transporter) and GOGAT encoding genes (*gltB* and *gltD*)¹³⁴.

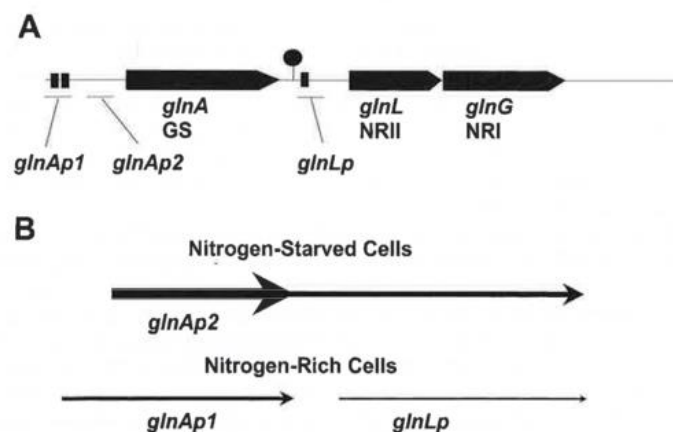


Figure 1-46 Promoters of *glnALG* operon are regulated by the nitrogen status

(A) In *E. coli* There are two promoters (*glnAp1* and *glnAp2*) which function in response to the nitrogen status in a cell. NtrC (NRI) in its phosphorylated form binds (shown as two bars) to *glnAp1* under poor nitrogen levels, and σ^{54} dependent transcription starts at *glnAp2* allowing read through of *glnA* (GS), *glnL* (NtrB or NRII) and *glnG* (NtrC or NRI). Under high nitrogen concentrations, the operon is transcribed from *glnAp1* but stops after *glnA* (circle indicates terminator). The expression of *glnL* is constitutive but lower, via the promoter *glnLp* (*pntrBC*). (B) The amount of GS, NRII and NRI is higher when expressed from *glnAp2* (nitrogen starved). Low levels of GS and a basal level of NRII and NRI are produced under nitrogen rich conditions. (Source: 172, p.33).

NtrC (NRI) (Figure 1-47, Figure 1-48) interacts with the RNA polymerase holoenzyme containing factor σ^{54} upon phosphorylation by NtrB. NtrC-P is then able to form dimers and tetramers that bind to an enhancer positioned upstream of the Ntr system (Figure 1-49). NtrC-P tetramers interact with σ^{54} RNA holoenzyme via a DNA loop causing isomerisation of the closed complex (Figure 1-50). The nucleoid-associated protein integration host factor (IHF) is necessary for DNA bending which brings together NtrC-P tetramers attached to a distant enhancer with the σ^{54} RNA polymerase holoenzyme positioned at the closed promoter¹⁷¹. Studies in *Pseudomonas* have demonstrated that NtrC regulates the expression of other operons, including those involved in nitrite and trinitrotoluene utilisation by *P. putida* JLR11, nitrogen fixation by *P. stutzeri*, and the

atzDEF operon for utilisation of cyanuric acid as a nitrogen source¹⁷¹. In addition, the NtrBC system regulates the two component system CbrA/CbrB, which belongs to the NtrBC family¹⁷⁴ and controls amino acids utilisation¹⁷¹. CbrB is a bEBP and is necessary for the isomerisation of σ^{54} promoters¹⁷⁴. The binding site for CbrB is also recognised by NtrC, which has a dyad symmetry consensus sequence (5' TGCACC TGGTGCA 3') for the binding site of Enterobacteria¹⁷⁶.

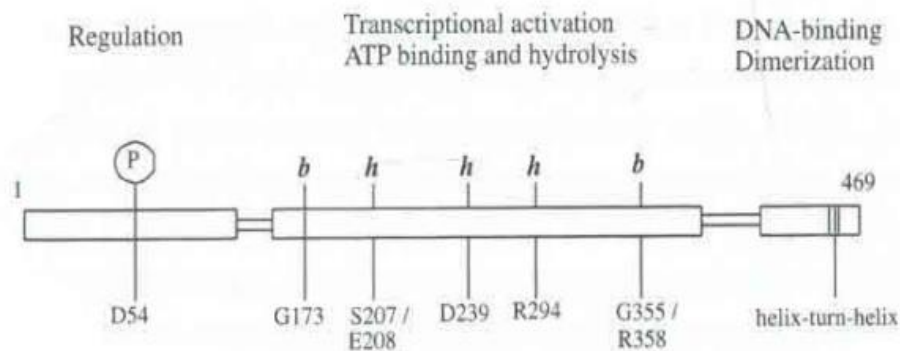


Figure 1-47 NtrC domain structure in *E. coli*

The domain structure of the NtrC protein is composed of three functional domains: An amino-terminal regulatory domain is phosphorylated at aspartate 54 (D54), a central catalytic domain binds and hydrolyses ATP in order to trigger open complex formation, and finally a carboxy-terminal (helix-turn-helix) DNA binding domain. Residues within the central catalytic domain are necessary for magnesium ATP (MgATP) binding and are indicated by b. While residues (indicated by h) are non-binding, but are still required for ATP hydrolysis. Highly conserved residues G173, S207/E208, D239, R294, and G355/R358 interact with σ^{54} -holoenzyme. (Source:173, p.163).

gene	polypeptide		
ntrC	nitrogen regulation protein NR(I)		
<i>Pseudomonas fluorescens</i> SBW25			
Accession IDs	G1G1K-482 (PflU216595Cyc) PFLU_RS01685 PFLU0343	Length	1437 bp / 478 aa
		Map Position	[374,209 <- 375,645] (5.57 centisomes, 20°) View in Genome Browser

Summary | [Protein Features](#) | [Operons](#) | [References](#) | [Show All](#)

Summary

Derived by automated computational analysis using gene prediction method: Protein Homology.

Molecular Weight of Polypeptide: 53.17 kD (from nucleotide sequence)

Unification Links

NCBI-Protein: [WP_03218003.1](#)
UniProt-via-RefSeq: [WP_03218003.1](#)

Relationship Links

Pfam in-Family: [PF00072](#), [PF00158](#), [PF02954](#)

Sequence Features

```

1  MRSSETVWIV  DDDRSIRMWL  EKALQEGMT  TQSFDSADGV  MSRLARQOPD  VIISDIRMPG  ASGLDLLARI  REQHPRLPVI  IMTAHSDLDS  AVASYQGGAE  100
101 EYLPKPFDDVD  EAVLVKRRAN  QHAQEQNQE  APPALTRTPE  IGEAPAMQE  VFRAIGRLSH  SNITVLINGE  SGTGKELVAH  ALHRHSPRAA  SFFIALNMAA  200
201 IPKDLMESEL  FGHEKGAFTG  AANLRRGRFE  QADGGTLFLD  EIGDMPADTQ  TRLLRVLADG  EFYRVGGHTP  VKVDVRIIAA  THQNLLETLVH  AGKFREDLFH  300
301 RLNVIRIHIP  RMSDRREDIP  TLARHFLSRA  AQELAVEPKL  LKSETEEYLK  NLPWPGNVRQ  LENTCRWITV  MASGREVHIS  DLPPELLSLP  QDSAPVTNWE  400
401 QALRQWADQA  LARGQSNLLD  SAVPAFERIM  IETALKHTAG  RRRDAAVLLG  WGRNTLTRKI  KELGMKVDGG  DDDEGDEG

```

Feature Class | **Location** | **Citations** | **Comment**

[Pfam-PF00072](#) | 7->116 | [\[Finn16\]](#) | [Response_reg](#): This domain receives the signal from the sensor pa [More...]

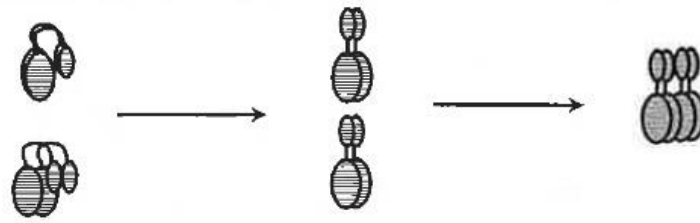
[Pfam-PF00158](#) | 141->308 | [\[Finn16\]](#) | [Sigma54_activat](#): Sigma-54 interaction domain [More...]

[Pfam-PF02954](#) | 423->463 | [\[Finn16\]](#) | [HTH_8](#): Bacterial regulatory protein, Fis family [More...]

Figure 1-48 NtrC sequence features in *P. fluorescens* SBW25

[Source: <https://biocyc.org/>]

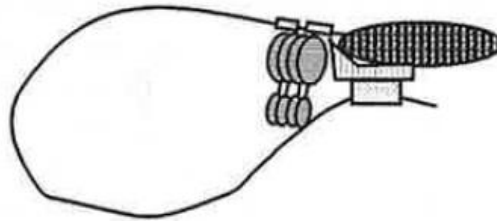
Mechanism of Regulation of Ntr Gene Transcription



Unphosphorylated NRI dimers become phosphorylated, resulting in tetramerization.



NRI~P binds to the upstream enhancer. RNA polymerase containing sigma 54 forms a stable closed complex at the promoter



A DNA loop permits the interaction of NRI~P and the polymerase. This interaction causes RNA polymerase to melt the DNA strands and begin transcription.

Symbols:



unphosphorylated NRI dimer



phosphorylated NRI dimer



sigma 54



enhancer sequences



promoter sequences



core RNA polymerase

Figure 1-49 Molecular regulation: *glnALG* operon transcription by NtrC in *E. coli*

Upon phosphorylation, NtrC (NRI) dimers polymerize to form tetramers which bind to upstream enhancers. These NtrC-P tetramers interact with the holoenzyme RNA complex located at the promoter *glnAp2* of the operon *glnALG*. This interaction occurs via a DNA loop, and the bEBP NtrC-P interaction with the closed complex, causes melting and enables transcription to commence. bEBP: Bacterial Enhancer-Binding Protein. *glnA*: glutamine synthetase (GS). *glnL*: NtrB or nitrogen regulator II (NRII). *glnG*: NtrC or nitrogen regulator I (NRI). Ntr: nitrogen regulation. (Source: 172, p.33).

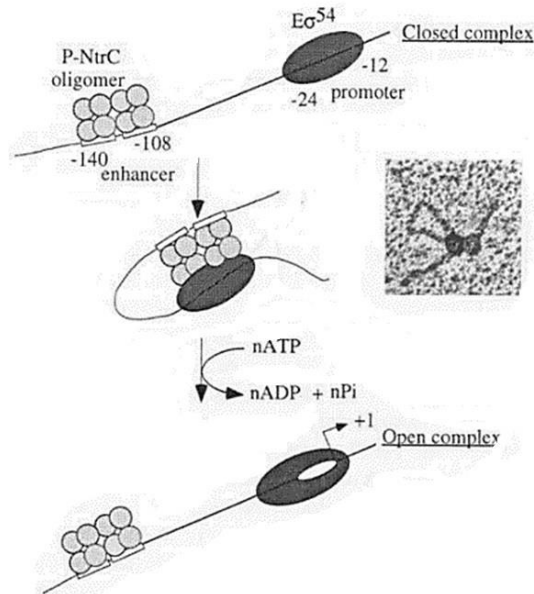


Figure 1-50 Closed complex isomerisation of the promoter for *glnALG* operon expression

Polymerised NtrC-P binds to an enhancer positioned at -140 and -108 upstream of the promoter for the *glnALG* operon, while holoenzyme RNA binds to positions -24 and -12 of the promoter. Factor σ^{54} ($E \sigma^{54}$) is unable to open the promoter. Binding of bEBP NtrC-P and energy (ATP) are required to melt the promoter and initiate translation. bEBP: Bacterial Enhancer-Binding Protein. *glnALG* operon: genes *glnA*, *glnL* and *glnG*. *glnA*: glutamine synthetase (GS). *glnL*: NtrB or nitrogen regulator II (NRII). *glnG*: NtrC or nitrogen regulator I (NRI). Ntr: nitrogen regulation. (Source: 173, p.157).

1.11.6 Nitrogen regulation at the enzymatic level

The main role of the NtrBC system is for nitrogen utilisation, while the principal role of the CbrAB system is carbon utilisation, as shown in studies conducted with knock-out mutants for these two-component systems in *P. aeruginosa*¹⁷⁴. Mutant strains of *P. aeruginosa* $\Delta ntrBC$ cannot metabolise compounds that only contain nitrogen, such as nitrite, nitrate, and urea, together with certain organic compounds with unique nitrogen/carbon sources, such as uridine and cytidine¹⁷⁴. Whereas *P. aeruginosa* strain PAO5100 ($\Delta cbrAB$) is unable to metabolise compounds such as sugars and acetate as a source of carbon. This mutant strain PAO5100 also shows impaired utilisation of compounds such as arginine, histidine, and proline as nitrogen/carbon sources¹⁷⁴. Taken together, these results support the proposed roles for these systems in the regulation of carbon and nitrogen assimilation in *Pseudomonas*.

Although the GDH, GS, GOGAT pathways are the primary route of ammonium assimilation, several other enzymes in *P. fluorescens* SBW25 are able to assimilate

ammonium (NH_4^+) into organic biomolecules. These enzymes include NAD synthetase (encoded by *nadE*), carbamoyl phosphate synthetase (encoded by *carAB*) along with two asparagine synthases¹³⁴. According to Wei et al.¹⁷⁴, certain intermediates of the Krebs cycle and other metabolites that are not more than two steps away from this cycle, are not under CbrAB regulation but instead are controlled by the NtrBC system. These metabolites are succinate, L-aspartate, glycerol, L-glutamate, L-asparagine, fumarate, 2-OG, and L-glutamine¹⁷⁴.

It is important to mention that glutamate (Glu) and glutamine (Gln) are key donors of amino groups in transamination and transamidation biosynthesis reactions, and also that these amino acids can be entirely (or part of their carbon skeletons) incorporated into metabolites. Important metabolites that require Glu or Gln for their production include: coenzyme NAD^+ , nucleotides, aspartate, serine, histidine, tryptophan, asparagine, and alanine. Cells must activate the appropriate metabolic route to ensure that nitrogen assimilation does not deplete 2-OG levels and thereby halt growth.

There are two forms of glutamine synthetases: GS1 and GS2²⁸⁴. Type I class or GS1 is only present in prokaryotes, whereas type II or GS2 is found in both eukaryotes and prokaryotes²⁸⁴. The enzyme GS in *P. fluorescens* and *E. coli* belongs to the type I class, as it is a dodecamer consisting of two superimposed hexamers held together by non-covalent interactions. GS has a pivotal role in nitrogen assimilation under low levels of nitrogen availability. Its regulatory mechanism is based on feedback inhibition and a cyclic cascade of adenylation and deadenylation catalysed by the enzyme adenylyltransferase (ATase or GlnE) in response to the ratio of glutamine/2-OG sensed by the signal transduction protein PII (GlnK). The mechanisms of regulation of GS (GlnA) in *Pseudomonas* are similar to those in *E. coli*. For example, GS extracted from *P. fluorescens* grown in ammonia rich (10 mM) medium is adenylylated as it can be precipitated using anti-AMP antibodies, whereas if the extracted enzyme is treated with phosphodiesterase to remove all AMP groups bound then this capacity is lost¹⁷⁷. Therefore, GS from *P. fluorescens* is subject to covalent modification (attachment of AMP), while the adenylation state (number of bound AMP groups: 0, 6 or 12) affects the activity of the enzyme¹⁷⁷. Fully adenylylated GS extracted from *P. fluorescens* is essentially inactive in comparison to non-adenylylated GS. The only difference between GS from *P. fluorescens* and *E. coli* is different K_m values for ADP observed

for the GS-AMP state; GS-AMP from *P. fluorescens* at pH 8.45 has a K_m of 4 μM for ADP, whereas for *E. coli* GS-AMP at pH 7.57 the K_m is 30 μM ¹⁷⁷.

Each subunit of GS is catalytically active and subject to regulation through reversible covalent modification of a Tyr residue by adenylation via ATase, and by cumulative feedback inhibition of products derived from glutamine metabolism. GS activity decreases upon interaction with the products of glutamine metabolism, such as cytidine triphosphate (CTP), histidine, glucosamine-6-phosphate, adenosine 5'-monophosphate (AMP), carbamoyl phosphate, and tryptophan (Figure 1-51). The amino acids glycine and alanine also inhibit GS activity despite not being metabolites derived from glutamine metabolism, but they are indicators of the amino acid pool. The inhibitory effect of these metabolites on the activity of GS is increased upon adenylation of the enzyme. At high nitrogen levels the PII-ATase complex produces high levels of inactive GS-AMP; whereas, with limited nitrogen, the PII(UMP)₃-ATase complex is formed and is stable. It stimulates activity of the ATase AR domain to remove AMP groups from GS, resulting in high levels of GS activity.

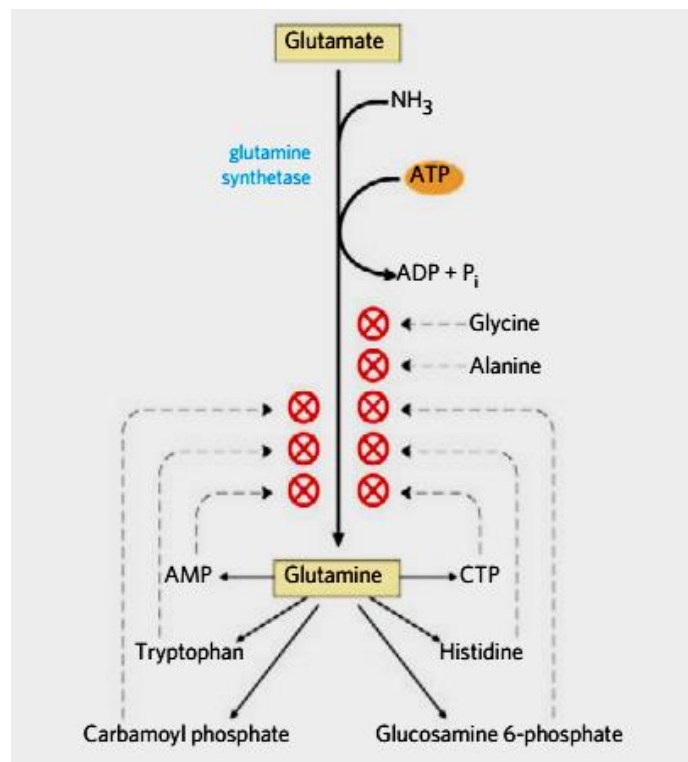


Figure 1-51 Cumulative feedback inhibition of GS

Metabolites derived from glutamine metabolism interact with GS to inhibit its activity (indicated by a red cross). The amino acids glycine and alanine also inhibit GS activity, and are indicators of the amino acid pool within a cell. CTP: cytidine triphosphate. GS: glutamine synthetase. AMP: adenosine 5'-monophosphate. (Source: 178, p.889).

1.12 Carbon and Nitrogen Metabolism in *Pseudomonas*

Catabolic operons are regulated and often expressed only in the presence of a selective substrate so that energy can be harnessed efficiently and not wasted transcribing unnecessary enzymes¹²⁴. Bacteria often show a preference for certain substrates as carbon source and repress expression of enzymes involved in uptake and metabolism of less preferred substrates by catabolite repression. Catabolite repression in *Pseudomonas* results in preferred utilisation of certain amino acids over glucose by preventing the expression of genes for glucose metabolism²³. This strategy known as carbon catabolite repression (CCR), optimises metabolism, energy utilisation and improves the growth rate^{26,27}. In addition, CCR leads to the hierarchical utilisation of amino acids, as observed in *P. putida* in complete medium, where the preference is: catabolism of Pro, Ala, Glu, Gln, His, Arg, Lys, Asp and Asn over Val, Ile, Leu, Thr, Phe, Tyr, Gly and Ser¹²⁵.

The CCR system in *Pseudomonas* is comprised of the following factors: Crc protein, CbrA, CbrB and CrcZ (small RNA)¹²⁵. The global regulator of CCR is Crc protein¹²⁶, which represses the expression of the transporters and enzymes required for the utilisation of the non-preferred carbon sources and redirects metabolism to the metabolise and transport of available preferred carbon sources¹²⁵. Crc protein inhibits gene expression at the post-transcriptionally level by binding to the 5' end of mRNA¹²⁵. The function of Crc is controlled by non-coding CrcZ sRNA which forms complexes when grown in conditions that do not trigger CCR¹²⁵. The expression of the gene *crcZ* which encodes CrcZ, is controlled by the two-component system CbrA/CbrB¹²⁵ (Figure 1-52).

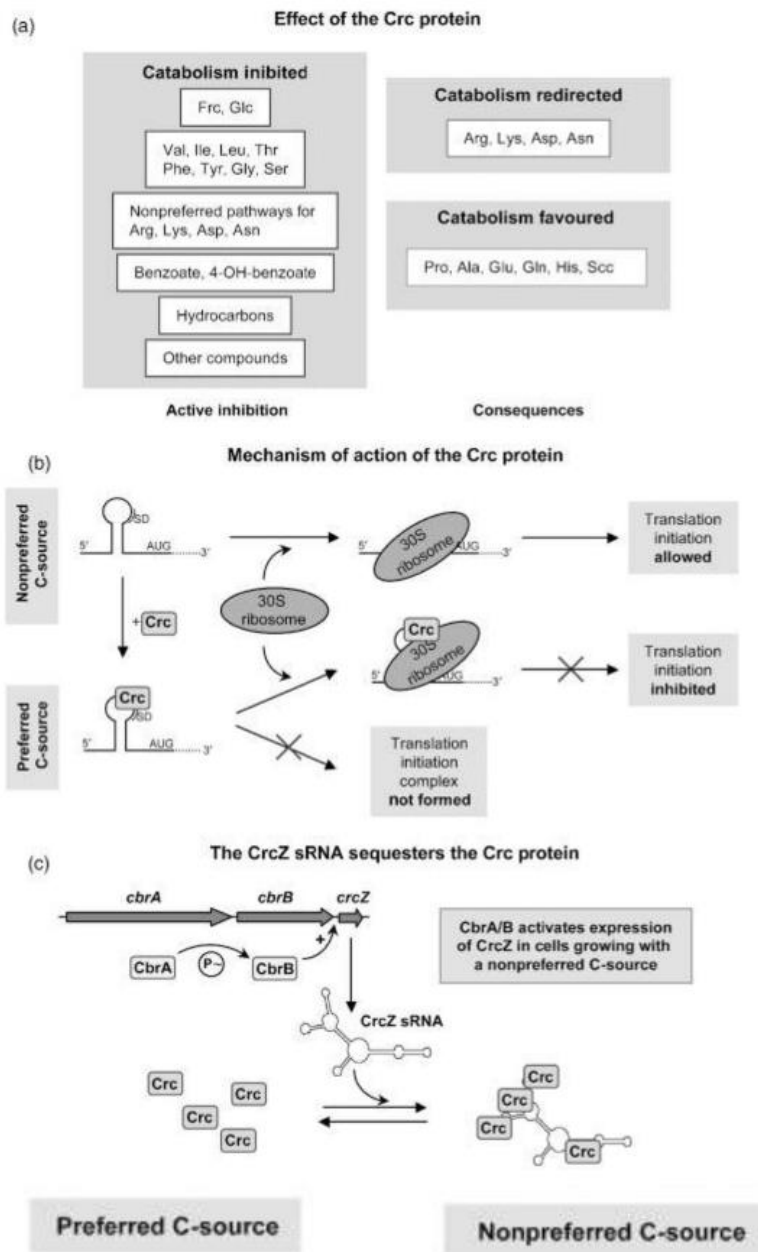


Figure 1-52 The repression of carbon catabolite in *Pseudomonas*

(A) The impact of Crc protein in complete medium containing all 20 amino acids; the metabolism is redirected by the Crc for transporting and catabolising the favoured carbon sources within the medium. (B) The underlying mechanism of the Crc protein’s action which binds, but does not degrade the mRNA that is necessary to utilise non-preferred carbon sources.(C) CrcZ sRNA facilitates the modulation of Crc protein availability.(Source:125, p.666).

The CbrA/CbrB system consists of a sensor kinase (CbrA) and a response regulator (CbrB)¹²⁷. CbrB is an enhancer binding protein for operons that require σ^{54} factor for expression¹²⁷. CbrA/CbrB is involved in biofilm development, chemotaxis, motility, resistance to metals and as well as the regulation of carbon/nitrogen metabolism, such

as amino acids and polyamines¹²⁷. Experiments conducted in *P. putida* mutants demonstrated that CbrA/CbrB regulates carbon/nitrogen metabolism because utilisation of many amino acids (e.g. His, Orn, and Tyr) was impaired in *cbrB* mutants¹²⁷. Amador et al.¹²⁷ showed that an interaction exists between the NtrBC system and the CbrA/CbrB system, as *P. putida* double mutants in genes *ntrC* and *cbrB* were unable to use proline, whereas single mutants in either gene could¹²⁷. The CbrA/CbrB system is important for the regulation of levels of CrcZ sRNA in response to available carbon sources; CrcZ sRNA levels decrease when favourable carbon sources are available (e.g. succinate, citrate) and this triggers CCR for encoding aliphatic amidase (*amiE*) which prevents catabolism of other carbon sources¹²⁸. The CCR response is blocked when grown in poor carbon sources (e.g. mannitol), and this leads to an increase in CrcZ sRNA levels, which is necessary to de-repress expression of genes such as *amiE*¹²⁸. The expression of *amiE* and CrcZ sRNA are intermediate when glucose is present in the medium because this is a secondary carbon source¹²⁸. Krebs cycle intermediates induce CCR to block degradative pathways for sugars, amino acids and other carbon sources (e.g. alkane)¹²⁸.

Acetate or succinate is involved in the repression of the expression of genes necessary for the metabolism of gluconate, glycerol, fructose and mannitol²⁶. Succinate is the preferred carbon source for *Pseudomonas* and represses the expression of genes necessary for the degradation and transport of histidine, glucose and mannitol²⁶. Glucose is not the preferred carbon source and in the presence of succinate the key metabolism enzymes are repressed, including glucose-6-phosphate dehydrogenase and 2-keto-3-deoxy-6-phosphogluconate²⁶. *Pseudomonas* glucose metabolism inhibits the regulons for other carbon sources, such as mannitol, histidine, toluene, methylphenol, phenylacetic acid and styrene. In addition, glucose inhibits the expression of enzymes such as amidase²⁶.

P. fluorescens lacks 6-phosphofructokinase and so is unable to metabolise glucose to triose phosphate via the Embden-Meyerhof pathway^{9,129,240}; however it carries the genes necessary to use glucose via the phosphorylative Entner-Doudoroff pathway⁹, which converts glyceraldehyde-3-phosphate to pyruvate through the intermediate production of 6-phosphogluconate (Figure 1-53).

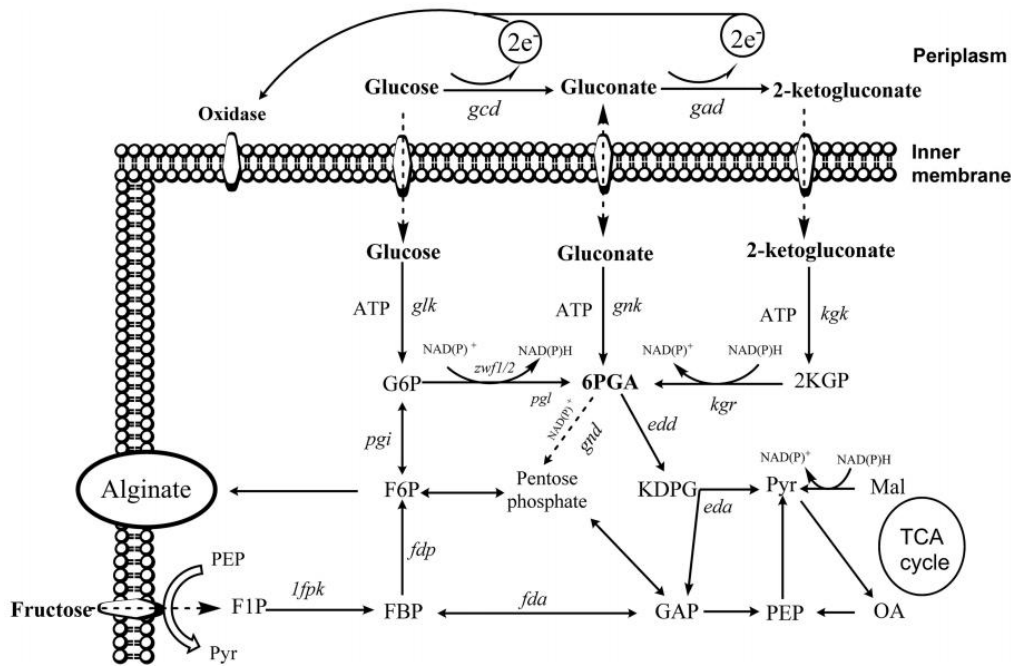


Figure 1-53 Enzymes pertaining to glucose and fructose utilisation in *Pseudomonas fluorescens*

Pseudomonads lack the gene to encode the enzyme 6-phosphofructokinase of the Embden-Meyerhof-Parnas pathway. As a result, glucose is metabolized via Entner-Doudoroff (ED) pathway to form the glyceraldehyde-3-phosphate (GAP) and pyruvate (Pyr) through intermediate production of 6-phosphogluconate (6PGA). Glucose is transported by active transport, whereas fructose makes use of phosphoenolpyruvate (PEP) dependent phosphotransferase system for the transportation. Glucose-6-phosphate dehydrogenase (G6PD) is encoded by genes *zwf-1* and *zwf-2*. Alginate is a polysaccharide produced from fructose-6-phosphate (F6P). This polysaccharide is secreted into the outer membrane through porin AlgE. Abbreviations: G6P, glucose-6-phosphate; 6PGA, 6-phosphogluconate; 2KGP, 2-keto-6-phosphogluconate; KDPG, 2-keto-3-deoxy-6-phosphogluconate; F6P, fructose-6-phosphate; FBP, fructose-1,6-bisphosphate; F1P, fructose-1-phosphate; GAP, glyceraldehyde-3-phosphate; Pyr, pyruvate; DPGA, 1,3-diphosphoglycerate; 3PGA, 3-phosphoglycerate; 2PGA, 2-phosphoglycerate; PEP, phosphoenolpyruvate; OA, oxaloacetate; Mal, malate; Gad, gluconate dehydrogenase; Gcd, glucose dehydrogenase; Kgk, 2-ketogluconate kinase; Gnk, gluconokinase; Glk, glucokinase; Kgr, 2-KGP reductase; Gnd, 6PGA dehydrogenase; Zwf1-2, G6P dehydrogenases; Pgi, phosphoglucose isomerase; Pgl, 6-phosphogluconolactonase; Edd, 6PGA dehydratase; Eda, KDPG aldolase; 1Fpk, 1-phosphofructokinase; Fdp, fructose-1,6-bisphosphatase; Fda, fructose-1,6-bisphosphate aldolase. (Source: 240, p.2).

Pseudomonas does not use the PTS-sugar transport system to import carbohydrates from the medium into the cell as in Enterobacteria and Firmicutes¹²⁵, except for fructose, which is the only sugar transported by PTS. That is not subject to CCR¹²⁵. The diffusion of glucose across the outer membrane into the periplasmic space is facilitated by the OprB-1 porin^{125,292}. Glucose can then be transported directly into the

cell or converted into gluconate or 2-ketogluconate, which in turn are internalised into the cell by specific transporters¹²⁵.

Sucrose is not a good carbon source for *P. fluorescens* as a transporter to internalise this sugar is not expressed¹³⁰, although the cytoplasmic enzyme levansucrase (locus tag PFLU_RS11270; old locus tag PFLU_2294), which is necessary for sucrose degradation, is expressed¹³¹. *P. fluorescens* is only able to catabolise this sugar when the cell membrane becomes leaky, allowing the release of levansucrase into the surrounding medium¹³⁰.

Amino acids are sources of carbon and nitrogen, and are also key intermediates in nitrogen and carbon metabolism¹³². In *P. fluorescens*, the acidic amino acids (Asp and Glu) and their respective amides (Asn, and Gln) support fast growth when used as the sole carbon and nitrogen sources, and also when used as the nitrogen source when glucose is the carbon source¹³³. Other amino acids used as unique carbon-nitrogen sources that support rapid growth are Ala, Ser, Arg, and Pro (Table 1-7). Periplasmic glutaminase/asparaginase (PGA) is strongly upregulated by their substrates Gln and Asn, and their respective reaction products Asp and Glu¹³³. PGA is also subject to CCR by glucose and Krebs cycle intermediates (e.g. pyruvate, succinate and 2-OG), and expression of the gene *ansB*, depends on the transcription factor σ^{54} ¹³³. Glutamine and glutamate are intermediate products of ammonium assimilation, and both these amino acids are nitrogen donors for other metabolites¹²⁰ (Figure 1-54). Glutamate is the nitrogen donor for ~72 % of all nitrogen containing metabolites in the cell¹²⁰. In addition, this amino acid contributes to controlling pH as glutamate decarboxylation consumes a proton and forms γ -aminobutyrate, which is pumped out of the cell in exchange for uptake of a glutamate molecule¹²⁰. Glutamine is the nitrogen donor for ~28 % of metabolites, including histidine, tryptophan, asparagine, purines, pyrimidines, amino sugars, and p-aminobenzoate¹²⁰.

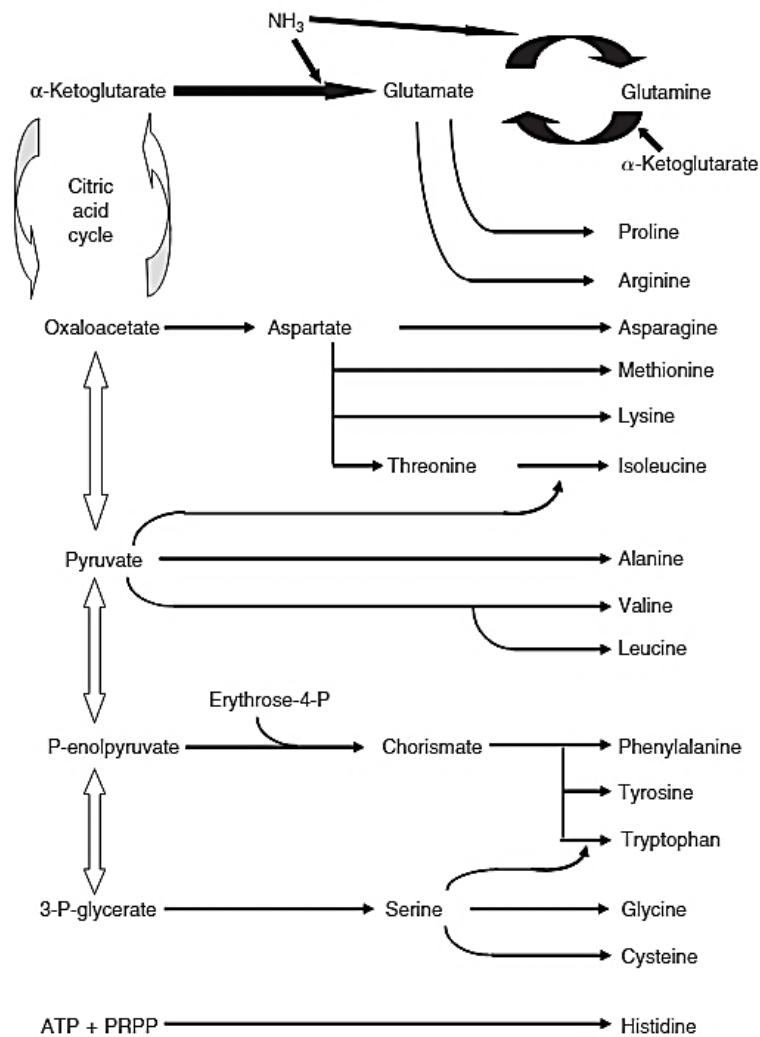


Figure 1-54 Assimilation of ammonium and the synthesis of other metabolites

The thick black arrows illustrate the assimilation of ammonium during nitrogen starvation, albeit with plenty of carbon since this pathway requires ATP input; as a result, the milieu needs to be rich in energy. The metabolite α -ketoglutarate signifies an intermediate of the Krebs cycle and incorporates ammonium. Glutamate's carbon skeleton is used for synthesizing the amino acids: proline and arginine. The other amino acids shown are derived from metabolites from Entner–Doudoroff pathway: P-enolpyruvate, pyruvate, and 3-P-glycerate. Oxalacetate, which is a Krebs cycle metabolite, is a carbon skeleton for aspartate, and is capable of being transformed to pyruvate and vice-versa. Oxalacetate synthesis is catalysed by two different enzymes: biotin-dependent pyruvate carboxylase (EC. 6.4.1.1) as well as biotin-independent phosphoenolpyruvate carboxylase (EC. 4.1.1.31)¹⁹⁶. Concomitantly, both enzymes are present in *P. fluorescens*, and their activity gets regulated by the available carbon source¹⁹⁶. Pyruvate carboxylase presents heightened activity whenever these cells are grown in pyruvate or glucose, while phosphoenolpyruvate carboxylase is highly active in acetate. Under such conditions, the glyoxylate cycle gets turned on, with the enzyme malate (from Krebs cycle) being repressed by acetate. PRPP is the precursor for biosynthesis of histidine and nucleotides. The enzyme PRPP synthetase regulates the production of PRPP and is prone to the regulation of feedback inhibition by their products. PRPP: phosphoribosyl pyrophosphate. (Source: 120, p.3).

Table 1-7 Growth of *Pseudomonas* strains on amino acids

AA	<i>P. fluorescens</i> ATCC 13525		<i>P. fluorescens</i> Pf-5		<i>P. putida</i> ATCC 12633		<i>P. putida</i> KT2440
	N	C and N	N	C and N	N	C and N	C+N
Asp	++	++	++	++	+++	++	++
Asn	+++	+++	+++	+++	+++	++	+++
Glu	++	+	++	+	+	+	++
Gln	+++	+	+++	++	+++	+	++
Ala	++	++	+++	++	++	++	++
Ser	++	++	++	+	+++	++	+
Pro	+	(+)	++	+	-	+	++
His	-	-	-	-	-	-	-
Lys	-	-	-	-	-	-	<i>n.d.</i>
Arg	++	+	++	++	++	++	<i>n.d.</i>
Val	(+)	+	+	+	(+)	+	<i>n.d.</i>
Leu	(+)	(+)	+	+	-	(+)	-
Ile	(+)	(+)	+	+	(+)	(+)	<i>n.d.</i>
Trp	-	-	+	(+)	-	-	-
Cys	-	+	-	+	-	-	-

Note: These cells were pre-grown on M9-NH₄⁺ /glucose medium overnight before being transferred into M9 minimal medium and were supplemented with 10 mM amino acid or 22 mM glucose + 10 mM amino acid as the only source of the combination of carbon and nitrogen (C+N). The estimation of relative growth rates was done from the rise in absorption at 595 nm between 3 h and 5 h after being transferred into fresh medium; (+) < 0.05, + 0.05–0.1, ++ 0.1–0.2 and +++ >0.2. *n.d.* (not determined). (Source: 133, p.153).

Glutamine is synthesised by different enzymes: glutamine synthetase (GS), glutamate dehydrogenase (GDH) and glutamate synthase (GOGAT). Assimilation of ammonium using the GDH pathway does not require energy, whereas the GS pathway is energy consuming. Their respective K_m values are remarkably different, for GS it is 0.1 mmol/L ammonium and for GDH it is 2 mmol/L ammonium; hence, the GS pathway is used under low concentration levels of ammonium and high energy, whereas the GDH pathway is turned on under high levels of ammonium (> 1 mM NH₄⁺)³⁰⁷ in a poor energy environment¹³³ (Figure 1-55). The activity of GDH was not affected by the nitrogen source utilised when cells were grown in minimal medium using glucose as the carbon source and ammonium or amino acids (Glu or Gln, or Asp or Asn) as the nitrogen source. In contrast, GS activity under the same nutritional conditions is notably increased when amino acids were present in the medium, but not with ammonium. In contrast GOGAT was enhanced only when ammonium was the nitrogen source (Figure 1-56 and Figure 1-57).

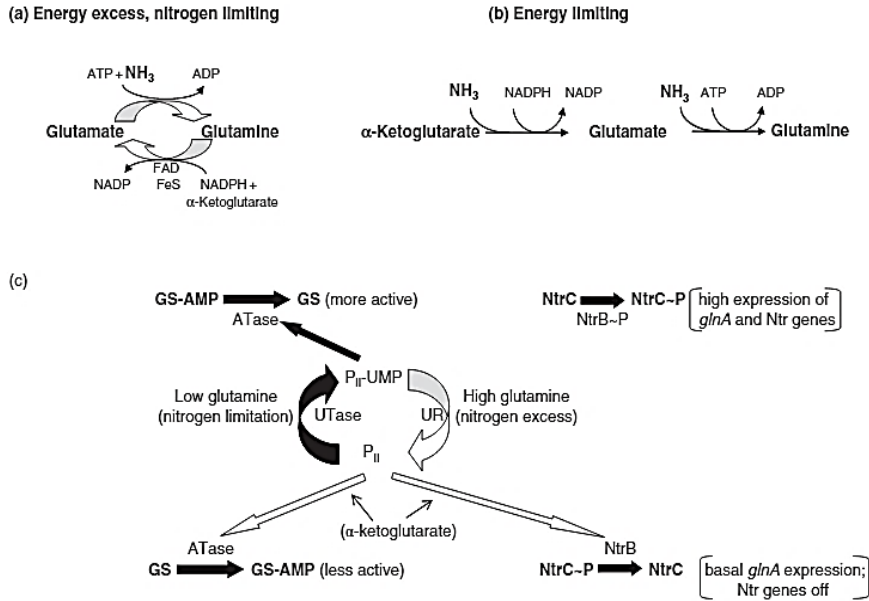


Figure 1-55 Ammonium assimilation, synthesis of glutamine and glutamate, and their control

(A) Shows the reactions in the face of excessive energy whereas (B) depicts the reactions manifesting during energy-constrained growth. (C) The regulatory proteins controlling GS adenylation, GS synthesis, as well as the Ntr system response. Solid symbols show nitrogen limitation, while open symbols exhibits nitrogen excess. - The actions of PII are antagonized by ketoglutarate under nitrogen excess conditions. α -ketoglutarate: 2-oxoglutarate. *glnA*: encodes glutamine synthetase. AMP: adenosine 5'-monophosphate. UMP: uridine 5'-monophosphate. NtrC: nitrogen regulator I or NRI. NtrB: nitrogen regulator II or NR II. ATase: adenylyltransferase. GS: glutamine synthetase (Source: 120, p.5).

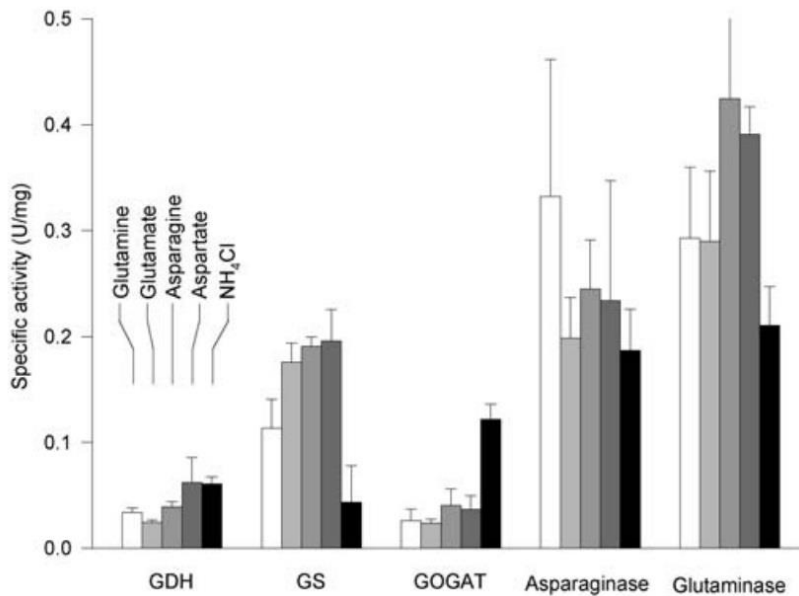


Figure 1-56 Specific activities of important enzymes of nitrogen metabolism within *P. fluorescens* ATCC 13525

Cells were grown in medium M9 during the late exponential phase and were supplemented with 20 mM glucose and nitrogen source as indicated (10 mM each). The extracts of crude cells procured through sonication were then assayed for activities of glutamine synthetase (GS), glutamate dehydrogenase (GDH), glutamate synthase (GOGAT), asparaginase as well as glutaminase. (Source: 133, p.154).

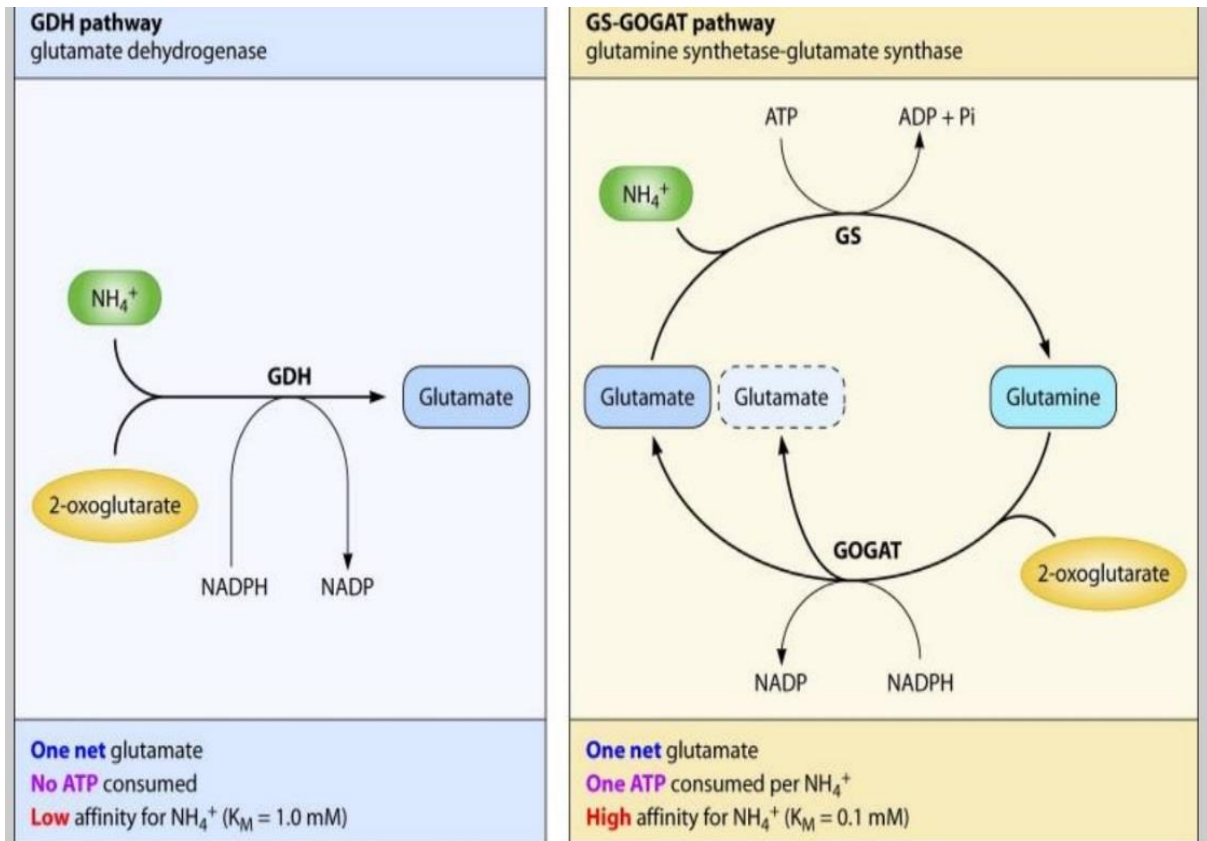


Figure 1-57 Glutamine and glutamate synthesis pathways: GS-GOGAT and GDH

The traits for each pathway are depicted within the box that lies below the scheme. The GDH pathway, used with high levels of ammonium, consists of just one enzyme GDH; the GS/GOGAT pathway, used with low levels of ammonium, comprises of two enzymes - glutamate synthase (GOGAT) and glutamine synthetase (GS) and consumes energy. (Source: 134, p.631).

1.12.1 Roles of glutamine and glutamate in bacterial metabolism

The roles of glutamine and glutamate in bacterial metabolism are the following: primary products of ammonia assimilation, building blocks of a plethora of nitrogen containing compounds and in addition glutamine is a signalling molecule for the regulation of nitrogen metabolism²⁷⁰. An indication of the significance of glutamine is the fact that during protein synthesis, glutamine is not depleted from the cytosolic pool since the enzyme glutamyl-tRNA synthetase uses glutamate to aminoacylate its correspondent glutamine t-RNA^{Gln} 270. Glutamine is a signal molecule that regulates the post-translational modifications of glutamine synthetase (GS) by binding to the single glutamine binding site on uridylyltransferase/uridylyl-removing enzyme (UTase/UR)²⁷⁰. The UR activity adds UMP to the signal integrator molecule PII when

levels of glutamine are low. High glutamine concentrations trigger the reverse activity of this bifunctional enzyme removing the UMP groups of PII²⁷⁰. Notably, the complex PII-UMP interacts poorly with NtrB (histidine kinase). Hence, with low glutamine (N limitation) NtrB is free to phosphorylate its response regulator NtrC leading to activation of the Ntr regulon; whereas, in the presence of high glutamine, the free PII attaches to NtrB, thereby inhibiting its kinase activity and activating dephosphorylation of NtrC-P²⁷⁰. Additionally, PII interacts with bifunctional adenylyltransferase enzyme (ATase) to adenylylate GS in order to inhibit its activity. Adenylylated GS (GS-AMP) is inactive and needs the interaction of PII-UMP along with ATase to remove the AMP groups in order for the enzyme to become active²⁷⁰. NtrC-P is able to initiate the expression of operons involved in nitrogen metabolism such as *glnKnrBC* which is a high affinity operon, responding to low amounts of NtrC-P for expression, whereas the low affinity operon *glnKamtB* needs a much higher concentration of NtrC-P for expression²⁷⁰. Once expressed, the high affinity ammonia channel (AmtB) facilitates scavenging of the small amounts of ammonium present in the milieu²⁷⁰. This is the way in which the NtrBC system is turned on/off (primed) according to glutamine levels²⁷⁰. Studies in *E. coli* growing in minimal media M9 with glucose as a carbon source and glutamine as a nitrogen source concluded that bacteria senses nitrogen limitation because glutamine is imported at a lower rate; thus, the drop in cytosolic levels stimulates the NtrBC system²⁷⁰ (priming). Tian et al.²⁷¹ when conducting experiments with *E. coli* growing in minimal media M9 with glutamine and glucose observed an NtrC dependent increase in the expression levels of *glnA*. This upshift did not occur if the carbon source was poor e.g. fructose or glycerol. Thus, highlighting the link between carbon and nitrogen metabolism through 2-oxoglutarate (2-OG), a metabolite of Krebs cycle and substrate for glutamate synthesis. The enzyme glutamate dehydrogenase (GDH) activity is down regulated by glucose^{272,273}.

Glutamate serves as the counter ion for intracellular potassium (K⁺); thus, it is important for osmoregulation²⁷⁹, and also attaches to glutamate dehydrogenase (GDH), inhibiting its activity²⁷⁴. Glutamate undergoes reductive amination by the enzyme glutamine synthetase (GS) in order to synthesize glutamine. Glutamate is also the main intracellular donor of nitrogen groups²⁷⁵ for all amino acids. Under C-limited conditions glutamate can also be used for production of 2-OG and feeding the Krebs cycle²⁶⁰.

1.12.2 Nitrogen Limitation in *Pseudomonas*

The terms poor and rich nitrogen sources were initially coined in *Enterobacteriaceae* because ammonium (NH_4^+), a rich or preferred N-source, supports a higher growth rate under aerobic conditions³⁰⁶ as compared to poor-nitrogen sources such as glutamine or glutamate^{134,306}. In addition to this, physicochemical constraints mean that while ammonium/ammonia can diffuse across the membrane without the use of energy, amino acids require an energetically expensive transport system (section 1.11.1). Ammonium is assimilated using GDH and NADPH, while glutamate and glutamine use only the GS/GOGAT pathway that requires one ATP per NH_4 assimilated (Figure 1-37). Thus, lower energy requirements and rapid uptake during growth on ammonium would contribute to faster growth. Of central importance for maximum growth, however, is maintenance of an optimum carbon: nitrogen status within the cell. As detailed in sections 1.11.2 and 1.11.3. The status of nitrogen inside the cell is determined by the intracellular concentration of glutamine via UTase/UR, which acts as a signal of excess nitrogen^{270,279} and this is tightly linked via the PII sensor to the carbon and energy status of the cell via 2-OG concentrations (see section 1.11.2 for details). Hence, with growth in nitrogen 'rich' (also termed nitrogen replete) conditions ie with ammonium as primary N source, the 2-OG:Gln ratio is low, PII is de-uridylylated and the Ntr regulon is downregulated. In contrast, growth with glutamine or glutamate as N source correlates with low ammonia i.e. poor or nitrogen limited conditions. Nitrogen limitation is reflected in a high 2-OG:Gln ratio, PII uridylylation, and NtrBC induced expression of *glnKamtB*, *glnAntrBC* operons²⁷⁰ and other loci of the Ntr regulon. Along with upregulated gene expression, GS is activated by de-adenylation, under N-limited conditions.

The same basic pathway of N-assimilation and interlinked control of the N and C status of the cell is assumed to occur in many bacteria, including *Pseudomonas*¹⁷⁵. Annotation of the SBW25 genome has identified genes encoding each of the key players in N-assimilation and regulation^{9,38}, as follows: NADP specific GDH (*gdhA* PFLU_RS26175), GS (*glnA*, PFLU_RS01710), GOGAT(*gltBD*, PFLU_RS02045 and PFLU_RS02050), PII (*glnK*, PFLU_RS29305), UTase (*glnD*, PFLU_RS06265), ATase (*glnE*, PFLU_RS02280), NtrB (*glnL*, PFLU_RS01690), NtrC (*glnG*, PFLU_RS01685), AmtB (*amtB*, PFLU_RS29300) as well as transporters for glutamate and glutamine (see 1.11.1 above). Genetic organisation of *glnK-amtB* is conserved. The key genes

glnA and *ntrBC* are also closely linked, but unlike in *E. coli* in *P. fluorescens* *glnA* is separated from *ntrBC* by 3 additional ORFs (Figure 1-58). However, expression of all three genes has been shown to be upregulated in *P. fluorescens* by NtrC-P^{108,172} SBW25, like other *Pseudomonas*, possesses only the one gene (*glnK*) encoding the PII sensor and no *glnB* gene^{136,281}. In *E. coli*, GlnB is produced constitutively while GlnK is produced under N-limiting conditions and the two forms of PII are at least partially redundant¹³⁴. In SBW25, *glnK* is also induced under N-limiting conditions, in an NtrC dependant manner^{108,281}. As with enteric bacteria, GS of *P. fluorescens* is regulated by adenylation and deadenylation¹⁷⁷ and is expressed at a low level when grown with ammonium as sole carbon source and at much higher levels with glutamine and glutamate¹³³ (Figure 1-55). The combined action of the enzymes GS and GOGAT have been shown to represent the main pathway of ammonium assimilation under nitrogen limitation in *P. aeruginosa*²⁷⁴ and *P. fluorescens* ATCC13525, although when grown on Glu or Gln, as sole C- source only GS appeared to be critical to this strain of *P. fluorescens*¹³³ (Figure 1-56).

Nitrogen limitation also downregulates the expression of GDH, the NADP-specific glutamate dehydrogenase, used for ammonium assimilation under nitrogen replete (rich) conditions²⁷⁴. Tokushige et al.²⁷⁸, characterised the *P. fluorescens* NAD-GDH (*gdhB*, EC 1.4.1.2)²⁷⁷ (required for oxidative degradation of glutamate with production of 2-OG and ammonium), as well as the NADP-GDH (*gdhA*, EC 1.4.1.4)²⁷⁷. Arginine is a preferred amino acid nutrient of *P. aeruginosa* and both *gdhA* and *gdhB* were shown to be part of the Arg regulon, with repression and induction, respectively in the presence of arginine^{274,277}. Thus, with growth on arginine as sole carbon source metabolism is directed towards maintenance of 2-OG and energy levels.

As the intracellular pools of glutamine, the nitrogen signal molecule, and glutamate are depleted due to use as a nitrogen donor group or carbon skeleton²⁷⁹, they need to be constantly replenished during growth. Production of glutamine from glutamate requires ammonium, and the enzyme glutamine synthetase (GS), thus as decrease in glutamine signals nitrogen starvation it induces upregulation of the *glnAntrBC* operon to increase levels of GS²⁸⁰. The intracellular glutamate pool is replenished by GDH (nitrogen replete) and GOGAT, (nitrogen limited) activity, whereas it is reduced by GS. Glutamine and glucose when used by *P. fluorescens* as nitrogen and carbon sources, respectively, up-regulate the GS pathway for nitrogen metabolism^{133,148}. However, this is dampened if a poor carbon source, such as mannitol, is present^{133,148}. The presence of poor carbon sources induces the expression of periplasmic glutaminase/asparaginase (PGA)¹³³, and glutamine is then utilized as the carbon source²⁶⁵.

For *E. coli*, growth on minimal medium with glucose and glutamine has been routinely used as nitrogen limited conditions and with glucose and ammonium as nitrogen replete conditions. The anomaly that cells growing in Gln induce a strong nitrogen limited response has been attributed to poor uptake of Gln^{135,137,138,169,170}. However, one study reported high intracellular concentrations of Gln and stressed the greater significance of 2-OG and importance of the relative ratio of 2-OG:Gln^{135,137,138,169,170} in signalling the N status of the cell. Utilisation of Gln as a carbon skeleton involves oxidative degradation of glutamate with production of 2-OG and ammonium, hence increasing the 2-OG:Gln ratio. In *Pseudomonas*, some amino acids, including glutamine and glutamate appear to be metabolised in preference to glucose. Transport and metabolism of Gln is not well understood in *P. fluorescens*, irrespective of this,

growth on minimal medium with glucose and glutamine induces a classic nitrogen limited response with enhanced GS activity¹³³ (Figure 1-57).

1.13 General Aims and Research Hypothesis

Evolution of a population is a consequence of random mutations in the genome. However, under adverse conditions if the benefit of a mutation for survival of bacterial cells is higher than the cost of detrimental effects, the frequency of occurrence of this mutation will increase as the population of bacterial cells grows. As selection of cells carrying this mutation increases, the genotype may become fixed in the population. Multiple evolutionary paths may lead to the same beneficial phenotype. The frequency with which a specific evolutionary pathway occurs is likely to be a consequence of many different factors. As well as the benefit:fitness cost of specific mutation(s), the number of mutational events required to reach the beneficial phenotype and also the physiological status of the cell and level of expression of mutated genes are likely to influence the evolutionary outcome.

In the recent study of Taylor et al.¹⁰⁸ evolved swimming mutants derived from a FleQ deficient *P. fluorescens* strain were shown to carry mutations in the NtrBC sensor:regulator system which responds to nitrogen status of the cell. Evolution was a two step process; initially in the NtrB sensor resulting in high overexpression of the Ntr regulon and slow swimming migration on swarming medium, followed by a second mutation in the DNA binding domain of NtrC with a lowered Ntr regulon response and faster motility on swarming medium (see Figure 1-59, and sections 1.9.2 and 1.11.5/6 for more detailed description). The conclusion was that the NtrB mutation resulted in accumulation of high levels of NtrC-P and that NtrC-P could then bind to the FleQ binding site and activate flagella synthesis¹⁰⁸. One can predict that the frequency of appearance of evolved swimmers from non-motile *P. fluorescens* $\Delta fleQ$ strains would be relatively high as it involves only two mutational steps and that this adaptation is beneficial despite the metabolic cost as it permits an initially aflagellate population to respond to chemotaxis cues and access fresh nutrients^{70,76,193,244-247}.

As these evolved swimming $\Delta fleQ$ strains carried mutations in nitrogen sensing or utilisation genes¹⁰⁸ it was hypothesized that nitrogen limitation represents a key force of evolution and may influence the pathway to suppression of the non-motile phenotype. Under nitrogen limitation conditions (high intracellular OG:glN ratio), the

NtrBC system is primed and *glnA*, *ntrB*, *ntrC*, *glnK* are all expressed at higher levels in *P. fluorescens* SBW25¹⁰⁸. Hence it was predicted that when grown with glutamine or glutamate as the sole nitrogen source (nitrogen limiting conditions) there would be a higher probability of identifying mutants in *glnA*, *ntrB*, *ntrC* or *glnK*. On the other hand, when grown on the 'rich' nitrogen source ammonium (low intracellular OG:gln ratio), expression of these genes should be lower and hence recovery of evolved swimming mutants would also be predicted to be lower.

NtrC and FleQ belong to the same family of bEBPs (Figure 1-29) and this is assumed to be the basis of resurrection of swimming motility in the non-motile *P. fluorescens* SBW25 $\Delta fleQ$ *viscB::IS- Ω -Km/hah* strain, AR2¹⁰⁸. *P. fluorescens* SBW25 genome contains genes for a number of other bEBPs, some more closely related to *fleQ*. The possibility that an alternate evolutionary pathway(s), for example involving a different bEBP, may also lead to resurrection of flagella driven motility under nitrogen replete growth conditions or in the aflagellate but motile strain, SBW25 $\Delta fleQ$, was also considered. This possibility is depicted in Figure 1-59.

To address these aims, the project monitored evolution of swimming motility of the two non-motile strains previously studied¹⁰⁸, AR1 ($\Delta fleQ$ *viscC::IS- Ω -Km/hah*) and AR2 ($\Delta fleQ$ *viscB::IS- Ω -Km/hah*), but using minimal media with replete (ammonium) or limiting (glutamate and glutamine) nitrogen sources. The evolution pathway of the aflagellate, viscosin producer SBW25 $\Delta fleQ$, which could spread but not swim, was also monitored in the same way. The project commenced with confirmation of the phenotype and establishing a time-lapse recording system to quantify the motility of the wild type strain SBW25 and each parent strain to be used in the evolution study. The efficiency of the restoration of motility for the different nitrogen sources was then tested for all three parent strains, and the motility properties of all the mutants successfully isolated were recorded. PCR and sequencing were used to target predicted mutations within *glnK*, *ntrB* and *ntrC*, and finally WGS of selected strains was performed to identify any additional genomic mutations that may have contributed to the restored swimming phenotype.

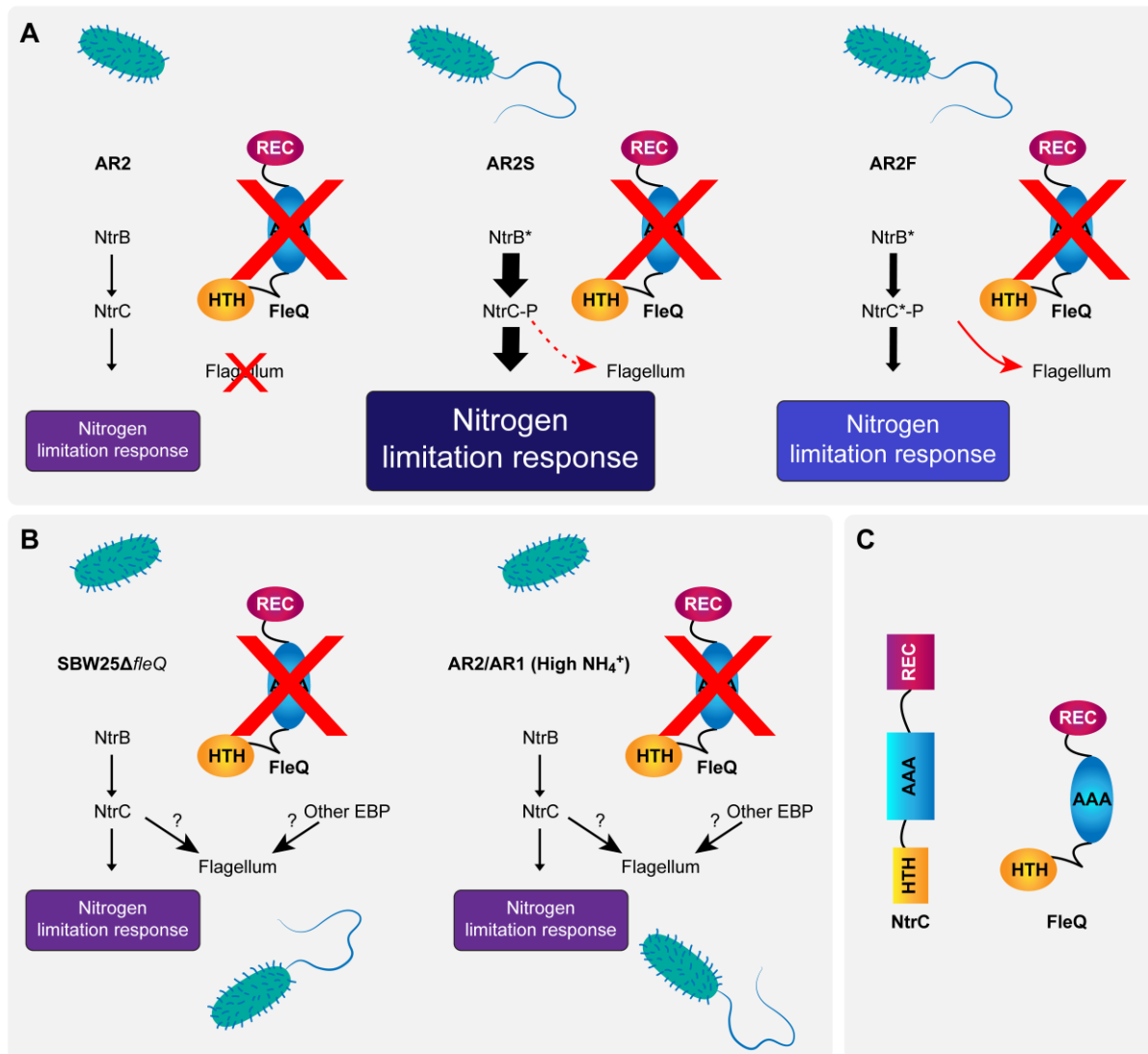


Figure 1-59 Proposed Ntr driven pathways of evolution of swimming motility in $\Delta fleQ$ strains

(A) Previously reported route of evolution of swimming motility in the non-motile parent strain, AR2 $\Delta fleQ$ *viscC::IS- Ω -Km/hah*, on rich medium LA (Taylor et al.¹⁰⁸). Cells (AR2S) with a mutated NtrB* overexpress genes that are upregulated in response to nitrogen limitation (dark navy blue), presumed to be a result of over-accumulation of NtrC-P. NtrC-P replaces the missing flagellar regulator FleQ to also trigger expression of the flagella regulon. The fitness cost of overexpression of Ntr regulated genes in AR2S led to selection of cells (AR2F) carrying a mutated NtrC* which dampens overexpression of the nitrogen limitation regulon (bright blue) to an intermediate level. Nitrogen limitation response (light purple) represents the low Ntr response of the parent strain AR2, under N replete conditions. (B) Hypothesis that other bEBPs might complement loss of FleQ. Under nitrogen replete conditions (high NH₄⁺), *glnAntrBntrC* transcription is low. Can evolution to swimming motility also occur via mutation in the *ntrB/C* pathway when grown in high NH₄⁺? Is there an alternate evolution pathway via mutation of other bEBPs (Bacterial Enhancer Binding Protein)? Does the spidery-spreading but aflagellate strain, SBW25 $\Delta fleQ$, evolve swimming motility and if so is this via the *ntrB/C* or involve an alternate pathway eg via an alternate bEBP? (C) Similarity of NtrC and FleQ domain structure. REC, receiver domain; AAA, ATP binding and hydrolysis domain; HTH, helix-turn-helix, DNA binding domain. Despite domain homology, unlike the NtrB-C sensor regulator pair, FleQ regulator functions independently of a cognate sensor (see section 1.8.1).

2 General Methods

2.1 Strain History

The control strain SBW25 was a wild type *P. fluorescens* isolated from a sugar beet (*Beta vulgaris*) leaf¹⁴³, and this strain is plasmid free⁹, non-pathogenic and motile¹⁴³. The flagella master regulator FleQ had been knocked-out in the isolate *P. fluorescens* SBW25 Δ fleQ¹⁰⁷. This strain was used as parent of evolved strains described in Chapter 4. AR1 and AR2 are IS- Ω -Km/hah transposon mutants derived from *P. fluorescens* SBW25 Δ fleQ, isolates obtained by Alsohim et al.¹⁰⁷ (Appendix X: Figure X-1). AR1 and AR2 were the parent strains of evolution studies described in Chapter 5. The characteristics of parent strains used in this study are shown in Table 2-1 and of evolved strains in Table 2-2.

Table 2-1 Properties of *P. fluorescens* strains

Strain Name	Genotype/Phenotype	Notes	Reference
*AR1	Δ fleQ <i>viscC</i> :: IS- Ω -Km/hah Fla⁻, Visc⁻	Sessile	107,109
*AR2	Δ fleQ <i>viscB</i> :: IS- Ω -Km/hah Fla⁻, Visc⁻	Sessile	107,109
AR9	Δ fleQ <i>PFLU_0129</i> ::IS- Ω -Km/hah Fla⁻, Visc[]	Dendritic (yellow). The colony was not branched as extensively, and entailed wider tendrils. Viscosin overproducer. Spidery-Spreading	107,109
*SBW25	WT	Colony edge erose. Plasmid free, non-pathogenic strain isolated from the phyllosphere of sugar beet. Swims and swarms	9,38,107,143
*SBW25C	<i>viscC</i> ::TnMod-OKm. Fla⁺, Visc⁻	Colony edge entire. Obtained by random transposon mutagenesis using a natural SBW25 rifampicin-resistant isolate. Swims	107

Strain Name	Genotype/Phenotype	Notes	Reference
*SBW25 Δ <i>fleQ</i>	Δ <i>fleQ</i> <i>Fla</i>⁻, <i>Visc</i>⁻	Dendritic (yellow). The colony was branched more extensively, whereas the tendrils were slender. Spidery-Spreading [Also known as SBW25Q or FleQ]	107, 109
*SBW25Q(<i>pfleQ</i>)	Δ <i>fleQ</i> <i>pBBRMCS-5</i> , <i>Gm</i> ^R <i>Fla</i>⁺, <i>Visc</i>⁺	SBW25 Δ <i>fleQ</i> complemented with full length SBW25 <i>fleQ</i> on the 4768 bp plasmid <i>pfleQ</i> , (<i>Gm</i> ^R). Swims	107
SBW25Qp	<i>pBBRMCS-5</i> , <i>Gm</i> ^R <i>Fla</i>⁺, <i>Visc</i>⁺	SBW25 Δ <i>fleQ</i> complemented with the vector <i>pBBRMCS-5</i> , <i>Gm</i> ^R . Spidery-Spreading	This study
SBW25p	<i>pBBRMCS-5</i> , <i>Gm</i> ^R <i>Fla</i>⁺, <i>Visc</i>⁺	SBW25 strain complemented with the vector <i>pBBRMCS-5</i> , <i>Gm</i> ^R . Swims	This study
*AR2S	Δ <i>fleQ</i> <i>viscB</i> :: <i>IS-Ω-Km/hah ntrB</i> <i>Fla</i>⁺, <i>Visc</i>⁻	Previously evolved mutant from AR2. Mutation in <i>ntrB</i> , T97P in PAS domain. Slower rate of colony expansion compared to AR2F. Swims	108
*AR2F	Δ <i>fleQ</i> <i>viscB</i> :: <i>IS-Ω-Km/hah ntrB ntrC</i> <i>Fla</i>⁺, <i>Visc</i>⁻	Previously evolved mutant from AR2S. <i>NtrB</i> -T97P, plus mutation in <i>ntrC</i> , R442C in HTH domain of <i>NtrC</i> . Faster rate of colony expansion compared to AR2S. Swims	108

Note: *Fla*⁻: no flagella, *Fla*⁺: flagella, *Visc*⁻: no viscosin production, *Visc*⁺: viscosin production, *Visc*^{*}: viscosin overproducer, *WT*: wild type. *Provided by University of Reading (UK).

2.2 Evolved Strains

The evolved strains obtained in this research are presented in Table 2-2, and they were grouped according to the source treatment (carbon/nitrogen) through which they evolved swimming motility.

Table 2-2 Properties of evolved strains

*Group of strains	History of Strains	Reference
FleQS1, FleQS2, FleQS3, FleQS4, FleQS5, FleQS6	Strains evolved from the aflagellate parent strain SBW25 Δ fleQ when treated with <i>ammonium</i> and <i>glucose</i> ; exhibited spidery and/or wild swarming.	This study
FleQS7, FleQS8,	Strains evolved from the aflagellate parent strain SBW25 Δ fleQ when treated with <i>glutamate</i> and <i>glucose</i> ; exhibited spidery swarming	This study
FleQS9	Strain evolved from the aflagellate parent strain SBW25 Δ fleQ when treated with <i>glutamine</i> and <i>glucose</i> ; exhibited spidery swarming	This study
FleQS7D, FleQS7W	Isolated from FleQS7 grown on 0.25 % agar LA; FleQS7D was obtained from the swimming disc and FleQS7W was isolated from the spidery swarming region of the colony.	This study
AR1S1, AR1S2, AR1S3	Stains evolved from the sessile parent strain AR1 when treated with <i>ammonium</i> and <i>sucrose</i> amended with kanamycin; exhibited spur swarming.	This study
AR1S4, AR1S5	Strains evolved from the sessile parent strain AR1 when treated with <i>glutamine</i> , <i>glucose</i> and added kanamycin; exhibited spur swarming.	This study
AR1S6	Strain evolved from the sessile parent strain AR1 when treated with <i>glutamine</i> and <i>sucrose</i> treatment supplemented with kanamycin. Exhibited spur swarming.	This study
AR2S1, AR2S3, AR2S4	Strains evolved from the sessile parent strain AR2 when treated with <i>ammonium</i> and <i>glucose</i> treatment supplemented with kanamycin. Exhibited spur swarming.	This study

*Group of strains	History of Strains	Reference
AR2S10, AR2S11, AR2S12, AR2S13, AR2S14, AR2S15, AR2S16, AR2S17, AR2S18, AR2S19, AR2S20, AR2S22, AR2S23, AR2S24, AR2S25, AR2S26, AR2S27, AR2S28, AR2S29, AR2S30, AR2S31, AR2S32, AR2S33, AR2S34, AR2S35, AR2S8, AR2S9	Strains evolved from the sessile parent strain AR2 when treated with <i>glutamine</i> , <i>glucose</i> treatment reformed with kanamycin; exhibited spur swarming.	This study
AR2S6, AR2S7	Strains evolved from the sessile parent strain AR2 when treated with <i>ammonium</i> and <i>sucrose</i> treatment reformed with kanamycin; exhibited spur swarming.	This study
AR2S20D, AR2S20W	Isolated from the same colony AR2S20 in 0.25 % agar LA. AR2S20D isolated from the swimming colony disc. AR2S20W was obtained from swarm spur region.	This study

*Note: Properties of evolved strains grouped according to treatment from which they evolved.

2.3 Culture of *P. fluorescens* Strains

The culture medium used for the purpose of propagation and isolation experiments was rich medium Luria-Bertani agar (LA) containing 1.5 % w/v agar. Bacteria were stored as frozen stocks in Luria-Bertani broth (LB) containing 20 % w/v glycerol, at -80 °C. For reculture, a sample from stocks was streak plated onto LA medium, and incubated at 26 °C for 24 h. When required, the culture medium was supplemented with kanamycin or gentamycin at a concentration of 50 µg/mL. The colony expansion studies were routinely conducted using swarming medium (LA with 0.25 % w/v agar) to detect swimming and/or swarming motility¹⁰⁷. In some circumstance, where indicated, 0.1 strength LB was used with 0.25 % w/v agar (swimming medium) to monitor swimming¹⁰⁷. Evolution experiments were conducted in minimal medium M9 0.25 % w/v agar using different sources of carbon/nitrogen, refer to Table 2-3.

2.3.1.1 Luria-Bertani Agar (LA)

Reagents: 10 g tryptone; 5 g yeast extract; 5 g NaCl; 15 g Difco agar (1.5 % or 0.25 % w/v agar for motility).

The medium was prepared by adding all the reagents to deionised water and bringing the volume up to 1 L and mixing thoroughly. The pH was adjusted to 7.5.

2.3.1.2 Luria-Bertani Broth (LB)

Reagents: 10 g tryptone; 5 g yeast extract; 5 g NaCl; 1 g glucose

This culture medium was used for propagation or the preparation of strain stocks. The medium was prepared by adding all the reagents to deionised water and bringing the volume up to 1 L and mixing thoroughly. The pH was adjusted to 7.5.

2.3.1.3 Minimal medium M9 based agar 0.25 % w/v (200 mL) for evolution experiment

This medium was prepared by autoclaving 100 mL of 0.5 % w/v water-agar in a 200 mL Duram[®] bottle. Firstly, 20 mL of 10× M9 salts was aseptically added to the sterile 100 mL 0.5 % w/v water-agar, followed by stock solutions as listed in Table 2-3. The final volume was made up to 200 mL with autoclaved deionised water. The medium was thoroughly mixed by swirling before preparing plates as below. The final concentration of the source of nitrogen in the medium was 10 mM; there was only one type of carbon source (glucose or sucrose) and nitrogen source (ammonium, glutamate or glutamine). The treatment of glutamate/sucrose was not performed.

Table 2-3 Stock solutions and preparation of 200 mL semi-solid medium M9

	Stock solutions	Volume		Final Concentration
		µL	mL	mM
	1 M MgSO ₄	400		2.00
	1 M CaCl ₂	20		0.10
Nitrogen Sources	1 M NH ₄ Cl		2	10
	0.25 M glutamine		8	10
	0.25 M glutamate		8	10
Carbon Sources	20 % w/v glucose		2	11.10
	20 % w/v sucrose		2	5.84

Note: Sources of ammonium (NH₄Cl), glutamine (L-glutamine) and glutamate (L-glutamic acid monosodium salt hydrate) were Sigma-Aldrich; NH₄Cl, glutamine and glutamate stock solutions were filter sterilised using a syringe filter with a 0.22 µm pore size. Components were added and mixed thoroughly before making the volume up to 200 mL with autoclaved deionised water.

Summary of media used:

- Minimal media signifies the defined M9 medium with different carbon sources (glucose or sucrose) and nitrogen sources (glutamine, glutamate or ammonium).
- Motility and swarming medium: semi-solid medium LA (0.25 % w/v agar, generally 9 cm diameter Petri dish or 15 cm where indicated).
- Propagation medium: LA in which agar was added to a final concentration of 1.5 % w/v.
- Rich medium signifies a complex medium (LA or LB) with multiple carbon and nitrogen sources.
- Semi-solid medium: any medium in which agar was added to a final concentration of 0.25 % w/v.
- Swimming medium: semi-solid medium of 0.1× LB, 0.25 % w/v agar. This was used only in Chapter 3 for confirmation of absence of swimming and complementation of SBW25Δ*fleQ*.

Petri dish:

The Petri dishes of 9 cm and 15 cm diameter that were used in motility experiments were bought at Thermo Fisher Scientific (catalog number for 9 cm disposable Petri dish: 101VR20) and Sigma-Aldrich (catalog number for 15 cm single use Petri dish: P5981). These plates have ventilation ribs, which permit free air circulation whilst reducing condensation during the incubation process. Technically speaking, this air flow should permit uniform access to oxygen throughout the experiment. This is important because *P. fluorescens* is aerobic and oxygen is required for respiration and hence motility.

Chemicals:

All chemicals were purchased from Sigma-Aldrich (St. Louis, MO).

Agar: Fisher Chemical BP14232 Agar (Granulated/Molecular Genetics).

2.3.2 Growth curves

Growth curves were conducted using the honeycomb 100-well plates and 4-6 biological replicates per treatment and strain. A 5 µL volume from an overnight (ON) culture in the test medium was added to 395 µL of the same test culture medium. The inoculated plates were incubated for 24 h at 26 °C with continuous vigorous shaking

(Shaking mode: strong intensity 80; command length: 80 pulse 0 milliseconds; type built in; pulse override: no) in a Bioscreen C™ growth curve analysis system. Growth was monitored every 20 min by measuring the turbidity (OD₆₀₀) with a wide-band filter (primary filter number 8) and assessed using the Norden Lab Professional software. The zero time absorbances were normalised to 0.008 and the blank values were averaged for each growth medium treatment (at least 10 replicates) before being subtracted from their corresponding growth curve.

2.4 Assessment of Colony Expansion

2.4.1 Preparation of motility plates

Agar plates (0.25 % w/v agar) were prepared using either LA (see section 2.3.1.1) or M9 medium (prepared as described in 2.3.1.3) according to the type of experiment, supplemented with 50 µg/mL kanamycin when required. The medium was aseptically pipetted as 30 mL aliquots of molten agar into 9 cm plates or 70 mL into 15 cm plates. Plates were left uncovered in a Class II laminar-airflow cabinet for 20 min in order to remove any surface condensation before replacing the lids, and allowed to settle for 4 h prior to inoculation of a single bacterial colony. Inoculation was centrally into the agar, with a platinum inoculation straight wire through the agar to the bottom of the Petri dish. Non-inoculated plates were included in all the experiments to confirm the sterility of the medium.

2.4.2 Low strength nutrient plates to confirm swimming motility

For the complementation study to confirm genotype of the SBW25Δ*fleQ* strain culture in plates with 0.1 strength LB and 0.25 % w/v agar (swimming medium), supplemented with 50 µg/mL kanamycin or gentamycin as required, were used (see 2.4.1 for preparation of plates). These were left to dry for 30 min after pouring. Using a pipette tip each plate was inoculated through the agar at the bottom, with 3 µL of an ON LB bacterial culture (OD₆₀₀ = 1) and incubated at 26 °C in a walk-in incubator⁴ in the dark on a bench without stacking. This method of inoculation permits visualisation of swimming motility through the agar without surface sliding-spiderly motility. The area of colony expansion (mm²) was measured as described in sections 2.4.3.1 and

⁴ The walk-incubator despite of being set at 26 °C, demonstrated a temperature fluctuation of around 24 °C - 26 °C on the bench top.

2.4.3.2. To confirm the sterility of the medium, plates were inoculated with sterile LB and treated in the same manner as the bacterially inoculated plates.

2.4.3 Recording colony expansion

The time of initiation of visible swarming or spreading-spiderly phenotype was recorded following visual examination. The area of motility was recorded using two techniques:

- ❖ Hand-Drawn
- ❖ Time-Lapse photography

2.4.3.1 Hand-Drawn method

This involved marking the border of the colony every 2 h using a permanent marker so as to measure the area (mm²). Importantly, the plates were incubated in the dark. All plates were incubated in a walk-in incubator at 26 °C in the dark on a bench and without stacking. Every 2 h for a period of either 22 h or 28 h depending on the strain, the borders of the growth was marked using a Lumocolor permanent superfine 0.4 mm marker. A jeweller's illuminated high-power magnifier (10×) visor was used to observe the colony borders against the light supplied by a table lamp. Each border was marked with a different colour to differentiate it from the previous marked border, as shown in Figure 2-1. The plates were scanned using a colour image scanner (Canon CanoScan 9000F MKII) in order to measure the area of spread of the colony to the expansion border using the software ImageJ 1.48i for Windows 8 (Wayne Rasband, National Institute of Health, USA). The area of each marked region, each time-point, was calculated using the function *Analyse*. Data was used to create colony expansion curves as described below, section 2.5.

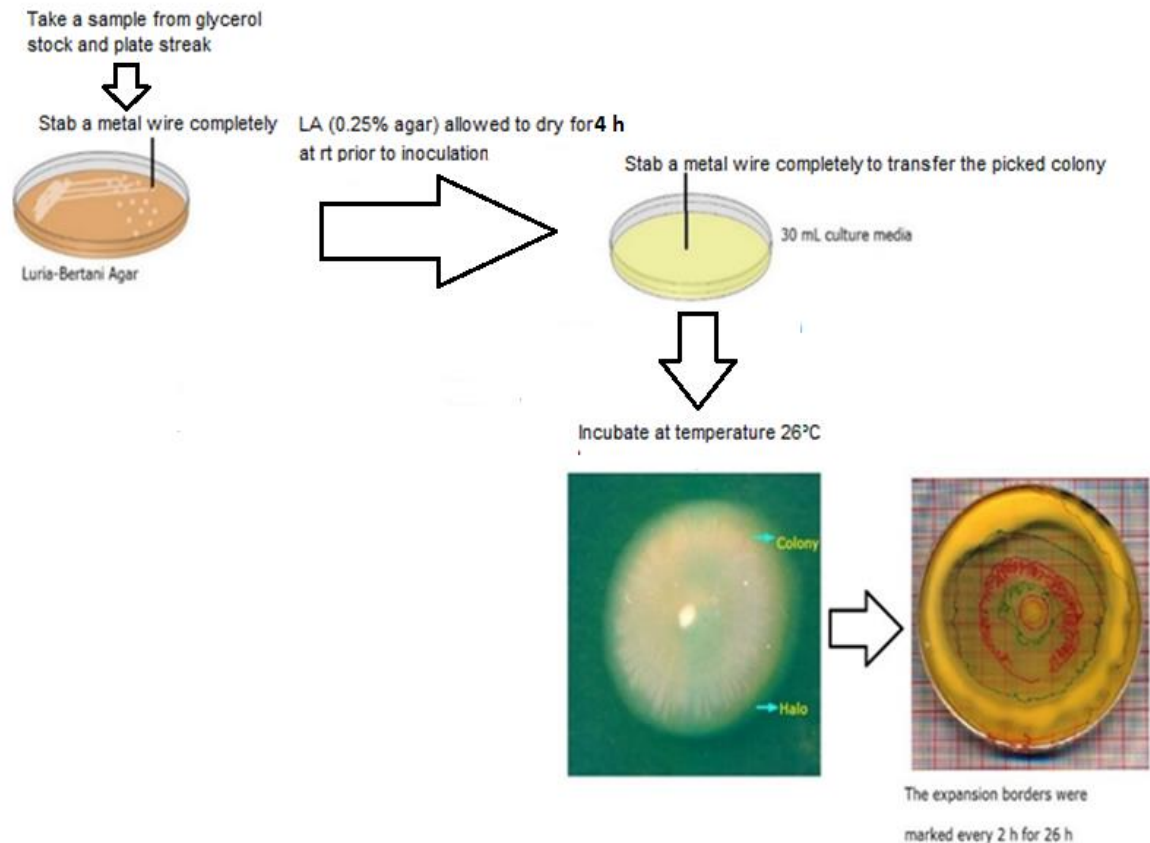


Figure 2-1 Hand-Drawn method to assess colony expansion

A single colony was picked with a metal wire and stab-inoculated into the middle of a 0.25 % w/v agar plate and the colony borders marked every two hours using a permanent marker. After 22 h or 28 h the plates were scanned to measure the indicated areas (mm²) using ImageJ software. Halo indicates viscosin production.

2.4.3.2 Time-Lapse photography

This required taking pictures automatically every 2 h to measure the area (mm²) that was covered by the colony. There was constant illumination to take pictures, and desk lamps were used for illumination using LED bulbs (4 W, ~ 250 lm). This would create heat, loss of moisture that may affect colony expansion. One reason why best to compare always same plates sizes. A Sony SLT-A65V camera was set up on a tripod at distance of 32.8 cm to automatically take a photograph every two hours of either six 9 cm plates or a single 15 cm plate. Plates were placed on a black muslin cloth to prevent reflection and a circular polarizing filter (Hoya) was put on the lens to diminish glare and reflections. The ARW picture files were converted to TIFF (600 dpi) so as to facilitate analysis using the software ImageJ 1.48i for Windows 8 (Wayne Rasband, National Institute of Health, USA). After conversion, the area for each replicate over a period of 24 h-38 h was measured. The scale was set, based on the plate size and

the freehand selection tool was used to outline the colony borders. The area of this marked region of the picture was obtained using the function *Analyse* as above 2.4.3.1.

With the larger Petri dishes (diameter 15 cm), when used for the time-lapse photography, replacement of the lids (aseptically in a cabinet laminar flow) every ~7 h was required as accumulated condensation on the lid impeded clear recording of colony expansion.

2.5 Quantitation and Classification of Colony Expansion Rate

To characterise parent and different evolved mutants, images of either hand-drawn or time-lapse recorded plates were used to measure the total area of motility at a given time-point with data presented as area (mm²) over time, as described 2.4.3.1 or 2.4.3.2. For each strain tested, data from replica plates was plotted and the geometric mean (geomean) of motility was calculated using Excel version 2016 and GraphPad PRISM version 8. Thus, colony expansion curves were created using the average (Gaussian distribution) or geometric mean (Log-Normal distribution) of replicates at each time point, while all replicates were also plotted to show the variability.

Classification of evolved swimming mutants:

Because of variable time of swarming (see Chapter 3 and 4) on replica plates, geomean-based characterisation of evolved swimming mutants were broadly classified according to the rate of colony expansion between 2 h and 8 h. The geomean data was used to calculate the mean rate of colony expansion per hour between 2 h and 8 h growth. The average rate of colony expansion per hour (Equation 2-1)^{183,184} was calculated for each 2 h window (2 h- 4 h, 4 h- 6 h and 6 h- 8 h) and then these 3 values were averaged to give average colony expansion per hour (mm²/h) over the period 2 h -8 h. Within groups of strains evolved from the same parent, the early swimming dependant median colony expansion value was determined. Based on this, strains within each group were classified as fast, medium and slow swimmers. The 2-3 strains closest to the median value were defined as medium motility, strains with colony expansion rates faster than this as fast and those lower than the medium group as slow.

The average rate of the colony expansion (mm²/h) was plotted against average time points^{183,184} (Equation 2-2). Analysis of the geomean data was extended to monitor

acceleration (mm²/h²) changes of colony expansion with time. This was determined by calculating the difference in the averaged rate of colony expansion between two consecutive points (Equation 2-3) which was then divided by the difference between their respective averaged times (Equation 2-4 and Equation 2-5)¹⁸³⁻¹⁸⁴.

$$\text{Averaged Rate of Colony Expansion (for Time A)} = \frac{\text{Area (at Time 2)} - \text{Area (at Time 1)}}{\text{Time 2} - \text{Time 1}} \quad (2-1)$$

$$\text{Averaged Time A} = \frac{\text{Time 2} + \text{Time 1}}{2} \quad (2-2)$$

$$\text{Averaged Acceleration} = \frac{\text{Rate of Motility (at Time B)} - \text{Rate of Motility (at Time A)}}{\text{Time B} - \text{Time A}} \quad (2-3)$$

$$\text{Averaged Time B} = \frac{\text{Time 3} + \text{Time 2}}{2} \quad (2-4)$$

$$\text{Averaged Time C for averaged acceleration} = \frac{\text{Time B} + \text{Time A}}{2} \quad (2-5)$$

2.5.1 Swimming and swarming rates of wild type and parent strains

Wild-type and parent swimming and swarming/ spidery spreading dependent rates of colony expansion were also calculated by averaging data from replica plates (Chapter 3). The colony expansion rates were calculated (Equation 2-1) for each 2 h interval (Equation 2-2) for every replica plate until colonies reached the edge of the plate. The time point of initiation of visible swarming/ spidery spreading was recorded for each plate. The wild-type swimming dependant rate of expansion was calculated by averaging rates/h from 2 h up to visible swarming, for each plate. Swarming dependant expansion rates were calculated from data post visible swarming. Data for each plate was presented as individual box plots. The average swimming and swarming/ spreading rate for each strain was then calculated by averaging mean rates (mm²/h) from each replica plate. These calculations also highlighted three different phases of colony expansion of SBW25 (see Table 3-1 and Figure 3-13).

2.5.2 Sliding and spidery-spreading for individual plates

The colony expansion rates were calculated (Equation 2-1) for every point in time (Equation 2-2) for every plate only during the time when the sliding colony did not develop its spidery phenotype. An average of all sliding (colony without spidery phenotype) rates per plate was calculated and showed as individual box plots. To indicate the sliding rate (before acquiring the spidery-spreading phenotype) for the

strain the average (not geomean) of all rates was calculated per plate. An average of all sliding rates per plate was calculated and shown as individual box plots. To indicate the sliding rates (before the colony acquired spidery shape) for the strain the average (not geomean) of all rates was calculated. However, this data was not used for classification.

The colony expansion rates were calculated (Equation 2-1) for every point in time (Equation 2-2) for every plate only when the sliding colony developed its spidery phenotype. An average of all spidery-spreading rates per plate was calculated and shown as individual box plots. To indicate the spidery-spreading rate for the strain the average (not geomean) of all rates was calculated. However, this data was not used for classification.

2.6 Experimental Evolution Assay

Parent strains SBW25 Δ *fleQ*, AR1 or AR2 (Table 2-1), stored at -80 °C in glycerol were streaked for single colonies on LA (propagation medium) and incubated for 24 h at 26 °C. Kanamycin (50 µg/mL) was included for plates inoculated with AR1 or AR2 to ensure transposon was not lost. For evolution experiments, twelve replica plates of each test medium were inoculated with a single colony (a different colony for each plate), as shown in Figure 2-1, incubated at 26 °C and monitored for evolution of swimming motility up to 26 days. Plates were minimal medium M9 0.25 % w/v agar with 20 % w/v glucose solution as carbon source and either 10 mM ammonium, 10 mM glutamine or 10 mM glutamate as nitrogen source, as described in Table 2-3. Medium with 20 % w/v sucrose solution and either 10 mM ammonium or 10 mM glutamine were also tested. The incubated plates were observed several times a day and photographed using a Sony SLT-A65V camera. For replicates that evolved swimming motility a hand-drawn colony expansion was constructed as described in section 2.4.3.1. To calculate swimming motility on evolution plates, a normalisation method was used as replicates did not all evolve at the same time. Normalisation involved subtracting the first area (bacterial growth) marked from all consecutive observations of the respective replicates. Consequently, it was possible to obtain colony expansion curves for evolved strains and their replicates that did not move (swimming) at the same time. This colony expansion was recorded over a period of 10 h. All inoculated plates were monitored for evolved motility for 1 month.

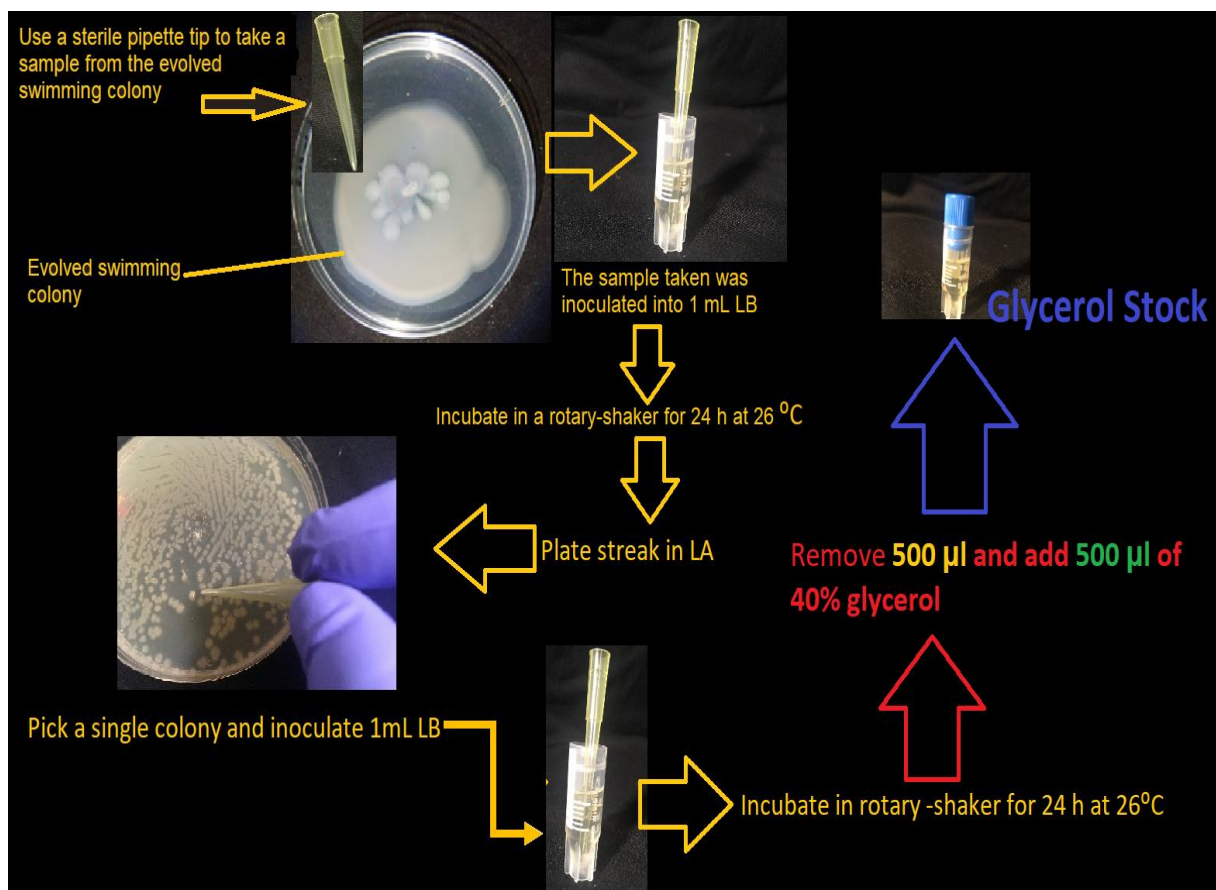


Figure 2-2 Isolation of evolved strain and preparation of glycerol stock

A sterile pipette tip was used to take a sample from the evolved swimming colony. This tip was immersed into 1 mL LB, incubated for 24 h in a rotary shaker at 26 °C and 20 µL then streaked out onto an LA plate (1.5 % w/v agar) for single colonies. An isolated colony was then transferred to 1 mL LB and a glycerol stock prepared after 24 h incubation at 26 °C.

2.6.1 Isolation and testing of evolved mutants

To isolate evolved mutants, a sample of agar plus bacteria was picked from the border of the swimming area (see Figure 2-2) or from blebs (see Figure 5-3) of an evolved swimming colony using a sterile yellow tip. This was inoculated into 1 mL of LB (plus kanamycin for AR1 and AR2 mutants) and incubated at 26 °C for 24 h on an orbital platform shaker at 222 rpm. Approximately 1 – 6 samples were picked from each plate. Each culture was streaked out on LA for single colonies. One colony from each plate was picked and grown for 24 h at 26 °C in LB. Each pure culture was stocked in 20 % v/v glycerol and stored at -80 °C. The -80 °C stock cultures were then tested for swimming motility, using the same medium in which they were isolated, but otherwise as described in Figure 2-1. All strains that swam within 24 h were considered to be evolved swimmer strains and used to conduct further investigations.

2.7 Agarose Gel Electrophoresis

Electrophoresis was performed at constant voltage (80 mV) at rt with 1 % or 0.75 % w/v agarose gels. The molecular ladders 1 Kb HyperLadder™ and 25 bp HyperLadder™ were purchased from Bioline. The running buffer for the gels was 1× TAE, which was prepared from a 50× TAE concentrated stock solution (Table 2-4) stored at rt.

For nucleic acid visualisation, GelRed™ (10,000× stock solution, Biotium) was diluted 1:10000 in molten agar, which was then mixed thoroughly by swirling before pouring gel. Following electrophoresis, the gel was imaged using a transilluminator G:Box Chemi XX6/XX9 (Syngene), where a wavelength of 312 nm was selected and a SYBR® filter applied in order to observe the DNA bands.

Table 2-4 Recipe for 50× TAE buffer

tris(hydroxymethyl)aminomethane	242 g
glacial acetic acid	57.1 mL
Na ₂ EDTA	7.43 g
Dissolved in 1 L deionized H ₂ O	
Final pH adjusted to 8.3	

Taken from Sambrook et al.¹⁸⁸ p.1078.

2.8 Plasmid Isolation from *Escherichia coli* DH5α

Escherichia coli DH5α was used for storage and propagation of the plasmid pBBR1MC-5A¹⁴⁴. A single colony of *E. coli* DH5α was inoculated into 3 mL of LB plus gentamycin, and incubated in a rotary shaker (220 rpm) at 37 °C for 24 h. The plasmid was extracted using a kit GE Healthcare Illustra plasmid Prep Mini Spin kit (GE Healthcare), and the extracted DNA analysed by agarose (0.75 %) gel electrophoresis gel at 80 mV for 1 h.

2.8.1 Plasmid purification

Extracted plasmid DNA (see section 2.8) was purified by ethanol precipitation; 2 volumes of 95 % v/v ethanol was added to the plasmid solution together with 0.1 volume of 3 M sodium acetate (pH 4.8). The solution was mixed by inversion and incubated at -80 °C for 30 min to aid DNA precipitation, before being subjected to centrifugation at 12000 rpm for 20 min at 4 °C. The supernatant was discarded and

the pellet washed with 500 μ L ice cold 70 % ethanol before being subjected to centrifugation at 12000 rpm for 5 min at rt. The supernatant was again discarded and the tube left inverted for 20 min in order to dry the pellet. The DNA was resuspended in 50 μ L of sterile deionised water and assessed via gel electrophoresis. The DNA concentration was determined using a NanoDrop™ 1000 Spectrophotometer (Thermo Scientific).

2.8.2 Electroporation of *Pseudomonas* strains

A single colony was inoculated into 1.5 mL LB and grown ON at 26 °C on a rotary shaker at 220 rpm. The bacterial culture was harvested and the pellet washed three times using 750 μ L of ice cold 0.5 M sucrose, before resuspending in 100 μ L of 0.5 M sucrose. The cells were transferred to a sterile electrophoretic cuvette, 10 μ L of plasmid solution added and the cell mixture incubated on ice for 30 min prior to electroporation. The electroporation conditions were: 200 Ω , 10.0 kV/cm (i.e. 2000 V), 25 μ F and a time constant of approximately 4.4 s. After conducting the electroporation 1 mL of LB was immediately added and the cell mixture transferred to a 15 mL tube and incubated at 26 °C on a rotary shaker at 222 rpm for 3 h. The bacterial culture was subjected to centrifugation at 12000 rpm for 1 min. The cell pellet was resuspended in 100 μ L LB and 20 μ L was plated onto selective medium, LA supplemented with gentamycin. Two electroporation controls were included, cells without the plasmid vector (only with 0.5 M sucrose), and a solution of sucrose and the DNA vector (no cells). After incubation at 26 °C for 24 h glycerol stocks were prepared from the transformant colonies present.

2.9 DNA Amplification and Sequencing of Target Regions of *ntrB*, *ntrC* and *glnK*

DNA amplification was performed using the primers shown in Table 2-5 and Table 2-6. The DNA template consisted of a single colony inoculated into 50 μ L of PCR reaction mix. Alternatively, a colony was resuspended into 9 μ L of sterile deionised water, and 2 μ L of this was added to 48 μ L of PCR reaction mix.

The polymerase chain reaction (PCR) conditions were the same for the genes *ntrB* and *ntrC*: an initial denaturation step of 95 °C for 1 min, followed by 30 cycles of denaturation at 95 °C for 15 s, annealing at 60 °C for 10 s, and extension at 72 °C for

10 s. The PCR conditions for *glnK* consisted of an initial denaturation step of 95 °C for 1 min, followed by 30 cycles of denaturation at 95 °C for 15 s, annealing at 55 °C for 15 s and extension at 72 °C for 10 s. The polymerase MyTaq™ (Bioline) was utilised and the PCR products were assessed via agarose gel electrophoresis (1 % or 0.75 v/v %), using the nucleic acid tracking dye GelRed™ (Biotium). The products were purified using a QIAquick PCR purification kit (Qiagen) according to the manufacturer's instructions before sending the amplicons for sequencing at Eurofins Genomics. DNA Sequencing and Analysis was performed with DNADynamo software (Blue Tractor Software Ltd., North Wales, UK).

Table 2-5 Primer sequences for the nitrogen regulation genes¹⁰⁸

Gene	Forward (5' →3')	Reverse (5' →3')	Expected Size
<i>nrB</i>	CTTGCGCCTTGAGTACATGA	ATGCGGTCTACCAGGTTACG	489 bp
<i>nrC</i>	CTTCATCCCCAACTCCTTGA	AAGCTGCTGAAAAGCGAGAC	384 bp
<i>glnK</i>	GCCGGGCATTACGATAGACA	TGCGCTTAGACTTGAGTCGG	1045 bp

Table 2-6 Region of the genes amplified by PCR

Gene	Alternative names	Locus Tag	Size bp	Protein Size	Location in Genome	Binding site Primers	aa residues
<i>nrB</i>	<i>glnL</i> NRII	PFLU_RS01690	1086	361 aa 40.1 kDa	375642...376727	Forward: 376634...376653 Reverse: 376165...376184	35 -175
<i>nrC</i>	<i>glnG</i> NRI	PFLU_RS01685	1437	478 aa 53.2kDa	374209...375645	Forward: 374248...374267 Reverse: 374612...374631	350 -455
<i>glnK</i>	PII	PFLU_RS29305	339	112 aa 12.3 kDa	6509024...6509362	Whole gene	Whole protein

2.10 Analysis of Single Colony

A single colony was suspended in 9 µL of sterile deionised water and then 2 µL was inoculated onto a 9 cm 0.25 % w/v agar LA plate ($n = 3$) prepared as described previously. Time-Lapse photography was performed as described in section 2.4.3.2 to assess motility (Figure 2-3) and 2 µL of the single colony suspension was used as the DNA template in order to amplify the *nrC* gene.

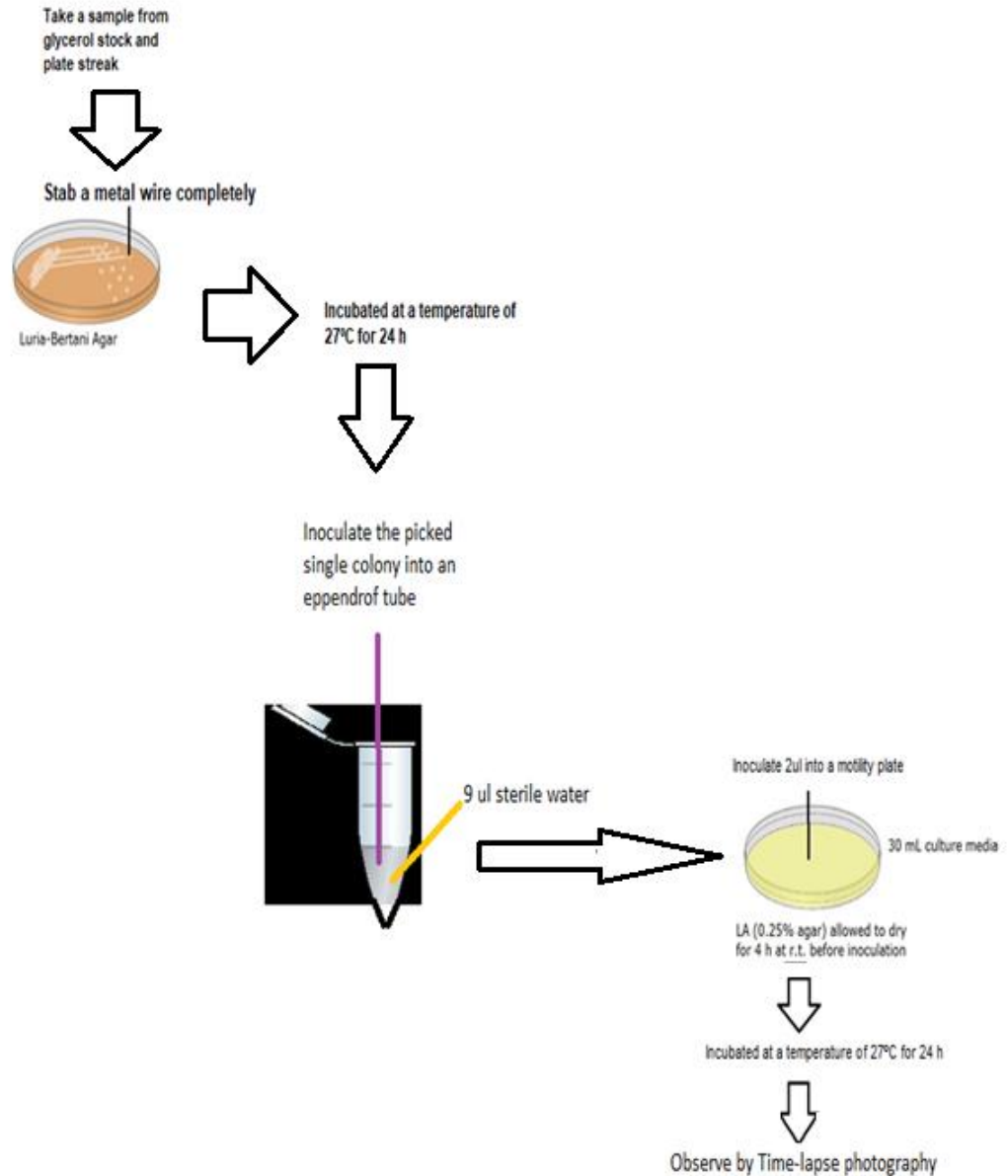


Figure 2-3 Study of single colony of *Pseudomonas* strain

A single colony was resuspended in 9 µL sterile deionised water, and 2 µL was used to inoculate a 0.25 % agar LA plate. Replicates were incubated at 26 °C and observed via time-lapse photography. The *ntrC* gene was amplified using 2 µL of the colony suspension as the template.

2.11 Concurrent Assessment of Colony Expansion of Multiple Colonies on the Same Plate

Separate individual colonies from the same strain were inoculated onto a single 15 cm 0.25 % agar LA plate prepared as described previously and incubated at 26 °C in a walk-in incubator. Colony expansion was observed using time-lapse photography as described in section 2.4.3.2 (Figure 2-4).

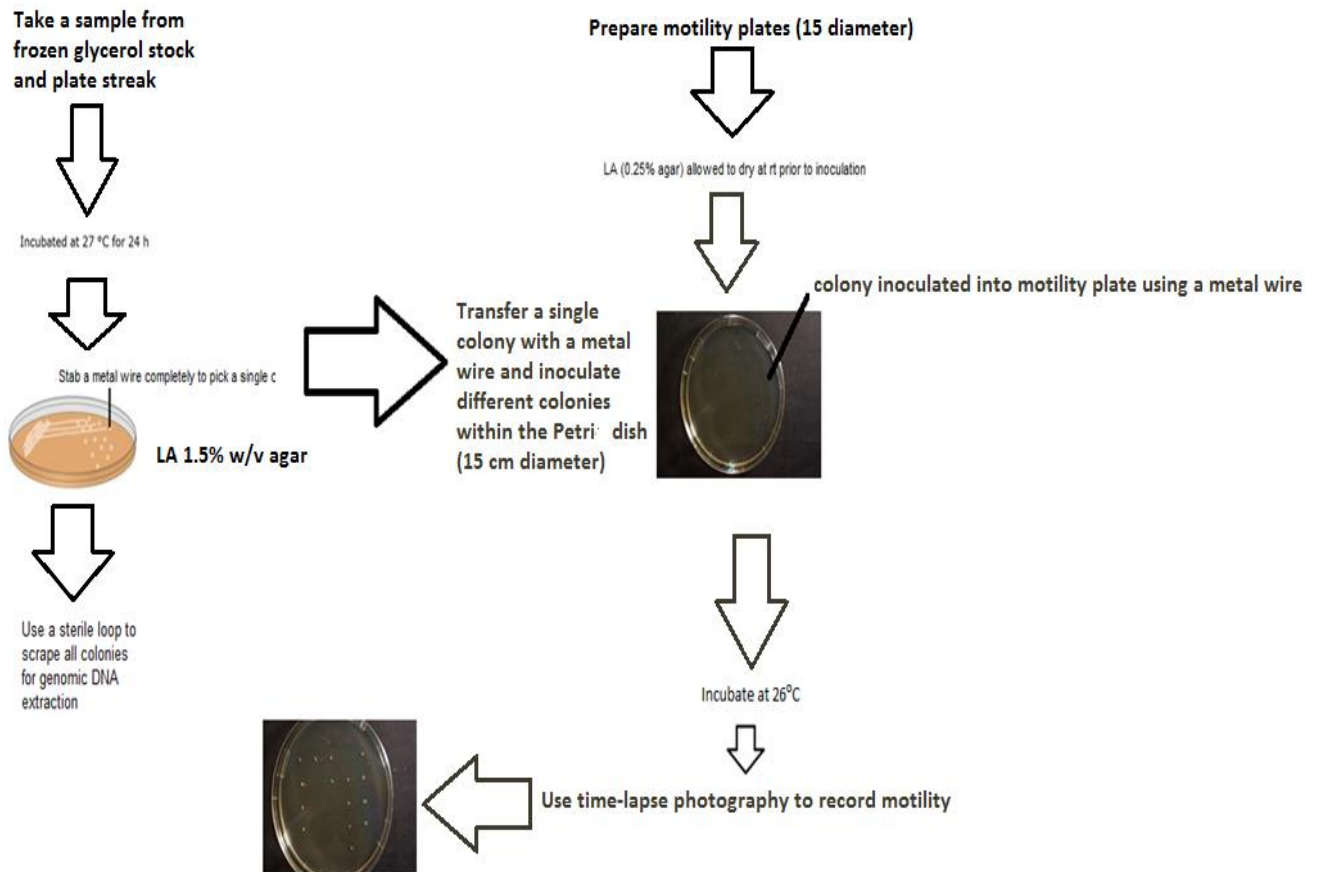


Figure 2-4 Concurrent assessment of colony expansion for multiple colonies on the same plate

2.12 Whole Genomic DNA Extraction, Sequencing and Concurrent Assessment of Colony Expansion of Multiple Colonies on a Single Plate

2.12.1 From an overnight broth culture

A single colony was inoculated into 12 mL LB in a conical flask and incubated at 26 °C on a rotary shaker at 220 rpm for 24 h. Genomic DNA from 11 ml broth culture was isolated using a GenJet genomic kit (Thermo Scientific) and further purified using a Genomic DNA Clean & Concentrator™ kit (Zymo Research). DNA was and eluted in 100 µl of 10 mM Tris-HCl pH 8.5 (Elution Buffer: EB). The ON culture (500 µL) was also used to make a glycerol stock. To monitor motility, 20 µL of the ON culture was also plated onto a 15 cm LA plate which was incubated at 26 °C for 24 h. Individual colonies were picked and used to inoculate a single 15 cm 0.25 % agar LA plate

(Figure 2-5) and colony expansion was observed using time-lapse photography as described in section 2.4.3.2.

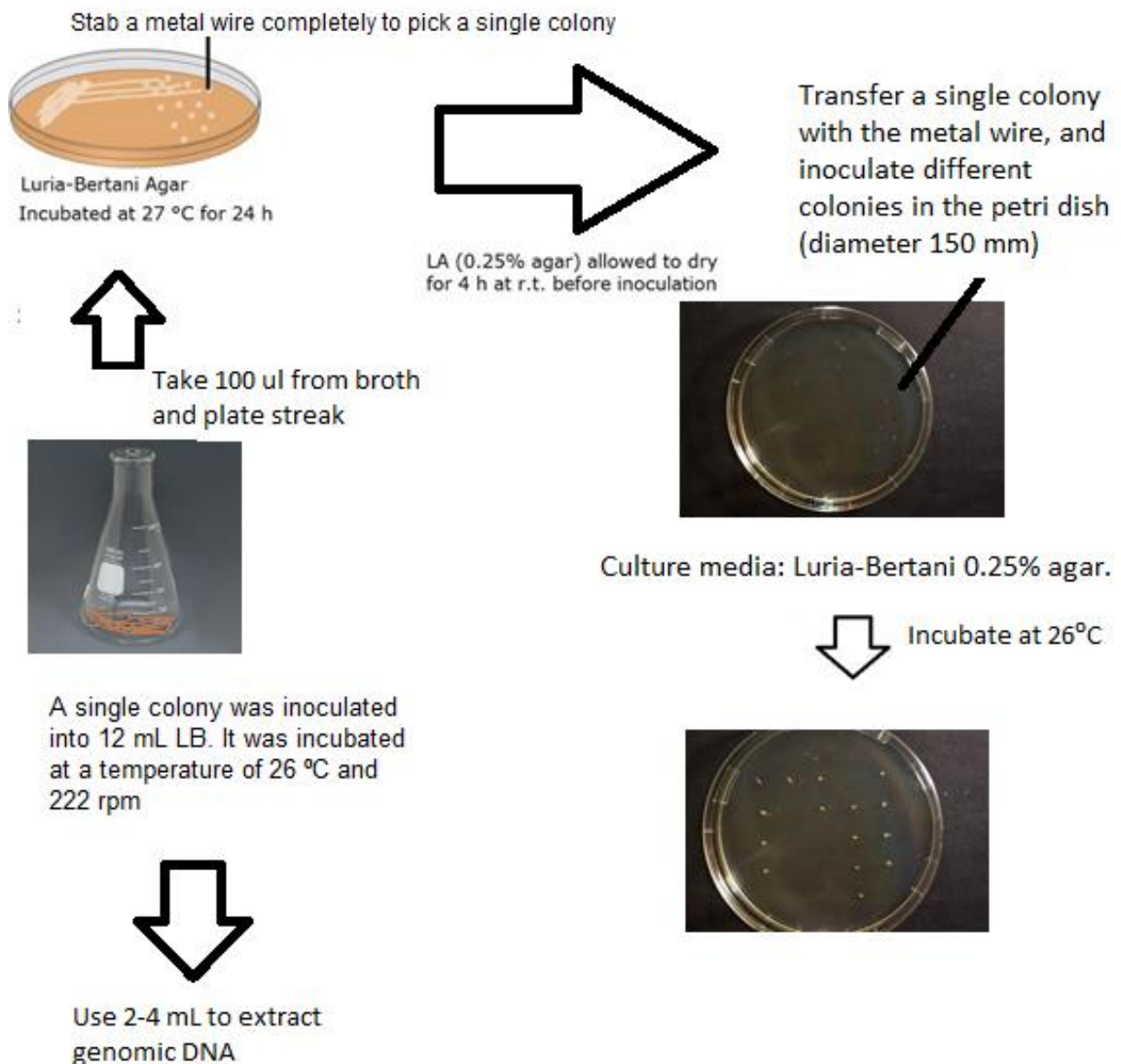


Figure 2-5 Assessment of colony expansion for multiple colonies on the same plate from an overnight broth culture

Genomic DNA extraction and concurrent assessment of colony expansion for multiple colonies on the same plate from an overnight broth culture.

2.12.2 From an overnight agar culture

A sample of frozen glycerol stock was streaked onto LA medium and incubated at 26 °C ON. Individual colonies were picked using a metal wire and used to inoculate one 15 cm 0.25 % agar LA plate as in Figure 2-5. Colony expansion was observed using time-lapse photography as described in section 2.4.3.2. To isolate genomic DNA, a

sterile loop was used to scrape all remaining cells from the agar plate. Cells were resuspended in 2 mL sterile phosphate buffered saline (PBS), recovered by centrifugation and resuspended in mL lysis buffer from a GenJet genomic DNA kit (Thermo Scientific). Genomic DNA was recovered using this kit and further purified using a Genomic DNA Clean & Concentrator™ kit (Zymo Research) and eluted in 10 mM Tris-HCl pH 8.5 (Elution Buffer: EB) in a volume of 100 µL.

2.12.3 Illumina technique for whole genome sequencing

Genomic DNA isolated from broth and plate cultures were sent to MicrobesNG (<http://www.microbesng.uk>), supported by the BBSRC (grant number BB/L024209/1), for Illumina sequencing. Genomic DNA concentration was quantitated by Nanodrop and integrity of the DNA was evaluated by running on a 0.75 % agarose gel. DNA was sent at a concentration of 10 - 100 ng/µL. The procedure used by MicrobesNG was essentially as follows: Genomic DNA was quantified in triplicate using the Quantit dsDNA HS assay in a plate reader (Ependorff AF2200). Genomic DNA libraries were then prepared using a Nextera XT Library Prep Kit (Illumina, San Diego, USA) by complying with the protocol of the manufacturer with these modifications: two nanograms of DNA rather than one were utilised as input, and PCR elongation time was raised to 1 min from 30 s. DNA quantification/library preparation was conducted on a Hamilton Microlab STAR automated liquid handling system. Pooled libraries were quantified with the Kapa Biosystems Library Quantification Kit for Illumina on a Roche light cycler 96 qPCR machine. Finally, libraries were sequenced on the Illumina HiSeq following a 250 bp paired-end protocol, with > 30x sequence coverage. DNA sequence reads were adapter trimmed with Trimmomatic 0.30 using a sliding window quality cutoff of Q15. *P. fluorescens* SBW25 (NC_012660.1/AM181176.4) genome sequence was used as reference sequence during assembly. De novo assembly was conducted on the samples using SPAdes version 3.7. Contigs were annotated by utilising Prokka 1.11.

Buffers:

Phosphate-buffered saline (PBS): dissolved 8 g NaCl, 0.2 g KCl, 1.4 g Na₂HPO₄, and 0.24 g KH₂PO₄ in 800 mL deionized H₂O. Final pH adjusted to 7.4 with HCl prior to adjust the volume to 1 L with deionized H₂O²⁵⁰.

Elution Buffer (EB) 10 mM Tris-HCl: dissolved 1.2114 g tris(hydroxymethyl)aminomethane (Tris base) in 800 mL deionized H₂O. Final pH adjusted to 8.5 with HCl before adjusting the volume to 1 L with deionized H₂O²⁵⁰.

2.13 Observation of Swimming via Light Microscopy

A single colony was inoculated into 3 mL of LB which was incubated at 26 °C on a rotary shaker at 220 rpm ON. This ON broth (100 µL) was added to 200 µL of LB in a well of a 6 well plate and observed at ×40 magnification under an inverted microscope to examine for swimming motility.

2.14 Observation of Flagella via Transmission Electron Microscopy

A single colony was inoculated into 3 mL LB (poured into 50 mL conical centrifuge tube) and incubated ON at 26 °C on a rotary shaker at 95 rpm²⁵². Glow discharged copper grids (carbon films on copper grids, 300 mesh, EM resolution) were placed on sterile Whatman no. 1 filter paper and 15 µL of the bacterial culture was added to each grid, which were left to air dry for 15 min. The samples were stained with 1 % w/v uranyl acetate solution for 1 min and then washed three times in sterile 1 % w/v ammonium acetate solution (pH 7)²⁵². The grids were left to air dry for 4 h before being examined by TEM (JEM 2100 plus TEM; magnification ×2,000).

2.15 Bacterial Staining with Fluorescent NanoOrange Dye

The method of Grossart¹⁴⁵ was used to observe bacterial morphology. A single colony was inoculated into 3 mL LB and incubated ON at 26 °C on a rotary shaker at 220 rpm. A NanoOrange stock solution was prepared using a NanoOrange Protein Quantitation kit (Thermo Fisher Scientific) according to the manufacturer's instructions. Between 0.5 µL and 10 µL of the ON bacterial culture was placed on a microscope slide, which was left in the dark for 30 min at rt before adding either 20 µL of 30 % w/v polyvinylpyrrolidone solution or a loopful of polyvinylpyrrolidone. It was then covered with a cover slip and the edges sealed with clear nail polish. Cells were viewed using a Zeiss AxioImager epifluorescence microscope, with an excitation wavelength of 490 nm and an emission wavelength of 520 nm.

2.16 Multivariate Analysis of the Strains: Discriminant

The growth data (OD₆₀₀) was considered at 10 h from all biological replicates used to obtain growth curves, the used colony expansion information was contained in the area (mm²) that was covered by the colony in swarming medium after different time points. The time points were 2 h, 4 h, 6 h, 24 h. This area data was obtained from each replicate from their respective colony expansion curve. These strains underwent discriminant analysis (discriminant function: linear) via the following factors: growth under different nitrogen treatments (ammonium, glutamine and glutamate) with the usage of glucose as carbon source, growth in rich medium LB, and the colony covered area in swarming medium at varying time points. MiniTab (version 19) was used as the statistical software.

2.17 Databases

The databases used to obtain the sequence, cellular localisation, physicochemical properties, function of proteins were UniProt Knowledgebase (UnitProtKB: <https://www.uniprot.org/help/uniprotkb>), European Bioinformatics Institute (EMBL-EBI: <https://www.ebi.ac.uk/>) and BioCyc Database Collection (<https://biocyc.org/>)³¹⁷. The KEGG Pathways Database was used to find the function of proteins and their localization in the cell as well as to identify which proteins or enzymes are expressed in *P. fluorescens* SBW25. Gene browsing of the whole genome and construction of the mini-maps in order to depict the localization of the genes in relation to the entire genome of *P. fluorescens* SBW25 were undertaken using SnapGene software (from GSL Biotech; available at snappgene.com). In addition, the gene symbols, sequences, products and their respective locus tags were obtained in database NCBI for genes (<https://www.ncbi.nlm.nih.gov/gene>) whereas the database *Pseudomonas* Genome DB (<http://beta.pseudomonas.com>) was used for information of gene products and their localisation in the whole genome of *P. fluorescens* SBW25. The protein sequences for alignments were obtained from database NCBI for proteins (<https://www.ncbi.nlm.nih.gov/protein/>).

The whole genome of *P. fluorescens* SBW25 was downloaded from database NCBI for nucleotides (<https://www.ncbi.nlm.nih.gov/nucleotide>). The GenBank genome accession of *P. fluorescens* SBW25 was AM181176 and version AM181176.4. The proteins and genes sequences were aligned using the Basic Local Alignment Search

Tool (BLAST) from U.S Library of Medicine (NCBI: <https://blast.ncbi.nlm.nih.gov/Blast.cgi>). Meanwhile the modeling of proteins was undertaken using the homology –modelling server provided by ExPasy at <https://swissmodel.expasy.org/>. The locus tags of the genes cited or studied in this research are shown in the Table 2-7 below.

Table 2-7 Gene symbol, description and locus tags

Gene symbol and description	Locus tag	Old locus tag
polar amino acid ABC transporter permease (glutamate ABC transporter)	PFLU_RS01120	PFLU_0227
glutamine ABC transporter permease	PFLU_RS01125	PFLU_0228
glutamine ABC transporter ATP-binding protein	PFLU_RS01130	PFLU_0229
amino acid ABC transporter substrate-binding protein	PFLU_RS01135	PFLU_0230
<i>glnG</i> (<i>ntrC</i>)	PFLU_RS01685	PFLU_0343
<i>glnL</i> (<i>ntrB</i>)	PFLU_RS01690	PFLU_0344
<i>glnA</i> , glutamine synthetase	PFLU_RS01710	PFLU_0348
<i>gltB</i> (glutamate synthase subunit alpha)	PFLU_RS02045	PFLU_0414
<i>gltA</i> (glutamate synthase subunit beta)	PFLU_RS02050	PFLU_0415
<i>glnE</i> , bifunctional glutamine synthetase adenylyltransferase/adenylyl-removing enzyme	PFLU_RS02280	PFLU_0461
<i>gltL</i> , arginine ABC transporter ATP-binding protein	PFLU_RS05630	PFLU_1136
<i>gltK</i> , glutamate/aspartate transporter permease	PFLU_RS05635	PFLU_1137
<i>gltJ</i> , amino acid ABC transporter permease	PFLU_RS05640	PFLU_1138
<i>glnD</i> , bifunctional uridylyltransferase/uridylyl- removing enzyme	PFLU_RS06265	PFLU_1268
ammonium channel	PFLU_RS08590	PFLU_1747
<i>lsc</i> , levansucrase [function: glycosyltransferase]	PFLU_RS11270	PFLU_2294
ABC transporter substrate-binding protein	PFLU_RS12785	PFLU_2617
amino acid ABC transporter permease	PFLU_RS12790	PFLU_2618
ABC transporter permease	PFLU_RS12795	PFLU_2619
arginine ABC transporter ATP-binding protein	PFLU_RS12800	PFLU_2620

Gene symbol and description	Locus tag	Old locus tag
glycosyltransferase [function: mannosyltransferase activity]	PFLU_RS14795	PFLU_3035
short chain dehydrogenase (oxidoreductase)	PFLU_RS16245	PFLU_3332
<i>gdh</i> glutamate dehydrogenase [glutamate dehydrogenase (NAD ⁺) activity]	PFLU_RS17095	PFLU_3504
ABC transporter substrate-binding protein	PFLU_RS17465	PFLU_3582
amino acid ABC transporter permease	PFLU_RS17470	PFLU_3583
<i>glnQ</i> (arginine ABC transporter ATP-binding protein)	PFLU_RS17475	PFLU_3584
<i>glsA</i> (glutaminase)	PFLU_RS17490	PFLU_3587
L-asparaginase II	PFLU_RS20385	PFLU_4161
putative filamentous adhesin	PFLU_RS20605	PFLU_4201
<i>gdhA</i> , glutamate dehydrogenase [NAD or NADP as acceptor]	PFLU_RS26175	PFLU_5326
<i>fusA</i> (elongation factor G)	PFLU_RS27180	PFLU_5530
<i>pill</i> (type IV pili signal transduction protein/twitching mobility protein)	PFLU_RS28305	PFLU_5750
<i>algP1</i> (transcriptional regulatory protein algp; alginate regulatory protein algr3)	PFLU_RS31200	PFLU_5927
<i>amtB</i> (ammonium channel)	PFLU_RS29300	PFLU_5952
<i>glnK</i> (PII)	PFLU_RS29305	PFLU_5953

3 Active and Passive Movements

3.1 Introduction

Bacteria demonstrate passive and active movements^{193,233}. Active movements are reliant on appendages (e.g. flagella, pili) in order to move through fluids, while passive movements are organelle independent and are mainly depend on cell growth (expansion of a colony border due to the force exerted by cell division) and the production of compounds to facilitate colony sliding²³³ (Figure 3-1). Passive movements, which can be observed on semi-solid surfaces (e.g. swarming medium) have been classified into three types based on the chemicals released by cells to accelerate sliding over a surface²³³:

- ❖ **Group I:** Surfactant production. For example, viscosin in the aflagellate strain *P. fluorescens* SBW25 Δ *fleQ* (refer to section 1.4), see Figure 3-2.
- ❖ **Group II:** Exopolysaccharide production. For example, sliding colonies of *Bacillus subtilis* release an exopolysaccharide that functions as a biosurfactant.
- ❖ **Group III:** Other mechanisms that are independent of surfactant production. For example, *Salmonella enterica* serovar Typhimurium slides with the assistance of the protein PagM.

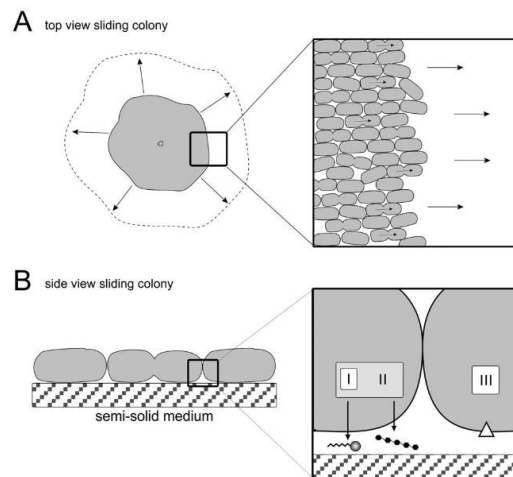


Figure 3-1 Illustration of the mechanism for sliding motility in aflagellate strains

(A) A sliding colony on top of soft-agar being viewed from above. The inset indicates the expansion of its border due to the force exerted by the dividing population. (B) This scheme depicts the side view of the border of the same colony; the inset shows that sliding is promoted by the production of the different chemicals and classed on three groups: I (e.g. viscosin), II (exopolysaccharide) and III (e.g. proteins). (Source 233, p. 2540).

Group	Bacterium	Sliding facilitating component	Sliding morphology
I	<i>Serratia marcescens</i>	lipopeptide surfactant serrawettin	
	<i>Pseudomonas aeruginosa</i>	rhamnolipid biosurfactant	
	<i>Pseudomonas syringae</i> pv. tomato DC3000	lipopeptide surfactant syringafactin	
	<i>Pseudomonas fluorescens</i> SBW25	lipopeptide surfactant viscosin	
	<i>Legionella pneumophila</i>	unidentified surfactant	
II	<i>Bacillus subtilis</i>	surfactin, exopolysaccharides, protein BslA	
	<i>Sinorhizobium meliloti</i>	siderophore rhizobactin, exopolysaccharide EPSII	
III	<i>Salmonella enterica</i> serovar Typhimurium	protein PagM	
	<i>Mycobacterium smegmatis</i>	acetylated glycopeptidolipids	

Figure 3-2 Sliding colony phenotypes classed based on the type of chemical released

Group I: sliding colonies produce surfactant, e.g. viscosin. Group II: exopolysaccharides released promote sliding. Group III: compounds distinct as surfactants such as protein PagM utilized for sliding. The typical viscosin dependent spidery-spreading (sliding) phenotype of *P. fluorescens* is only seen in the absence of flagella, see Figure 3-17 below. (Source 233, p. 2451).

P. fluorescens SBW25 exhibits the following types of active motility: swimming, swarming and twitching^{76,246}. In the absence of flagella, *P. fluorescens* SBW25 Δ *fleQ* exhibits a spidery-spreading (dendritic-like sliding)^{107,233} passive motility.

Swimming:

Swimming is a flagella-dependent movement of free cells in liquid media or through a semi-solid medium with low agar content such as swarming medium (0.25 w/v % agar, LA) or swimming medium (0.1 strength LB 0.25 w/v % agar). When swimming through a semi-solid medium, the bacterial population (colony) has the appearance of a circle²⁴⁶, which expands evenly over time. The circular appearance of this relocating population is caused by nutrient gradients, individual cells move in different directions in response to these gradients (chemotactic response)²⁴⁶, and hence the appearance of the colony remains circular as the total area (mm²) increases over time (see section

1.6.2 for more detailed explanation). The lower nutrient availability in swimming media substantially reduces initiation of swarming.

Swarming:

Swarming, which can be seen just below the surface in the semi-solid swarming medium, refers to swimming in groups^{93,243,244} and at higher speeds (cover more area)²⁴⁴ compared to a swimming colony. Swarming generally initiates at a single point of the swimming colony. The swarming in *P. fluorescens* accelerates biomass production and allows for the colonization of nutrient-rich areas²²⁹. In *P. fluorescens* SBW25 viscosin facilitates this swarming⁵⁴. The antimicrobial, surfactant viscosin is encoded by the operon *viscABC* operon and transcription is upregulated by population cell density (quorum sensing)^{193,238,244}. Viscosin is a wetting agent that is required to trigger the disassemble of the biofilm under carbon starvation conditions. The inability to disperse biofilms has been observed in mutant strains of SBW25, which no longer produce viscosin due to an impaired *viscA* gene⁵⁴.

Spidery-Spreading:

In the absence of flagella, *P. fluorescens* exhibits spidery-spreading (sliding motility), which gives the colonies a dendritic appearance¹⁰⁷. The force of cell division expansion in the presence of viscosin facilitates dispersion of the dividing cells²³³ (Figure 3-2). The aflagellate colony slides on the top of 0.25 % agar in swarming medium to give the colony a spidery shape.

Twitching:

Twitching motility depends on retraction of flexible T4P pili (encoded by the gene *pilI*; locus tag PFLU_RS28305, old locus tag PFLU_5750) and can be observed on moist semi-solid and solid surfaces²²⁸. In *P. fluorescens* SBW25, it is possible to observe twitching motility after inoculating bacteria on the bottom of a soft-medium (e.g. swarming medium) and incubating plates for several hours. Following careful removal of agar twitching motility can be observed as a circle on the bottom of the plate by staining with crystal violet²²⁸.

Movements like swimming and swarming permit a colony to expand rapidly and to respond in an effective manner for population nutritional requirements by translocating to a less harsh and more favourable environment for survival^{70,86,113,239,241,247}. The viscosin dependent passive spidery-spreading movement on the surface of swarming

medium is not a consequence of a chemotactic response as in swimming, but is a result of the physical expansion of the dividing cells on the wet surface²³³. This fundamental difference in the mechanisms of swimming and spidery-spreading motility helps explain the very different appearance of swimming dependant and spidery-spreading dependant colony expansion – an expanding circle with the former and dendritic appearance with the latter.

Viscosin production in planktonic cells:

In *Pseudomonas* spp, quorum sensing plays an important role to regulate the cyclic lipopeptide (e.g. viscosin) production⁸⁹. *P. fluorescens* synthesizes these lipopeptides in the late exponential or stationary growth phase⁸⁹. However, viscosin production in *P. fluorescens* SBW25 is lower in the planktonic cells as compared to that in the biofilms⁵⁴. In addition to this, carbon starvation upregulates *viscA* expression in biofilms, and thus induces the biofilm dispersal process⁵⁴.

Active and passive movements monitored in this project include swimming, swarming and spidery-spreading dependant colony expansion. Before commencing the experimental evolution investigation, a study was conducted to monitor the phenotypic characteristics of wild type strain SBW25 as well as the parent strains AR1 ($\Delta fleQ$ *viscC::IS- Ω -Km/hah*), AR2 ($\Delta fleQ$ *viscB::IS- Ω -Km/hah*) and SBW25 $\Delta fleQ$. The characteristics and differences between flagella-driven colony expansion, viscosin driven sliding (spidery-spreading) motility and cumulative growth in sessile bacteria were established. In addition, the impact of viscosin on bacterial movement was assessed. The objectives of these experiments were as follows:

- To differentiate between flagella-driven swimming and swarming motilities, viscosin dependent sliding and cumulative growth.
- To establish an imaging based colony expansion assay and to quantitate and document the colony expansion phenotype of each strain to be used as parent in the evolution studies.
- To complement the SBW25 $\Delta fleQ$ mutant with plasmid-encoded *fleQ* to confirm that the defined $\Delta fleQ$ mutation was solely responsible for the loss of flagella-driven motility.

- Using the hand-drawn based motility assay, define motility of the previously evolved motile strains AR2S (*Fla*⁺, *Visc*⁻; Δ *fleQ ntrB*) and ARSF (*Fla*⁺, *Visc*⁻; Δ *fleQ ntrB ntrC*)¹⁰⁸ to obtain the colony expansion curves.
- Monitor the impact of viscosin on bacterial movement by comparing the colony expansion curves of wild type SBW25, a viscosin overproducing strain AR9 (*Fla*⁻, *Visc*^{*}), the aflagellate strain SBW25 Δ *fleQ* (*Fla*⁻, *Visc*⁺) and non-viscosin producer strain SBW25C (*Fla*⁺, *Visc*⁻).
- Establish growth properties of wild type and parent strains in rich medium LB and minimal medium M9 plus glucose with different nitrogen sources (glutamine, glutamate, and ammonium) to document any differences in nitrogen metabolism.
- All strains were compared using discriminant analysis of these phenotypic characteristics.

3.2 Complementation of SBW25 Δ *fleQ* with plasmid (*pfleQ*)

Swimming and swarming are both flagella driven motilities^{107,243} present in the wild type strain, SBW25. Swimming medium can be used to clearly differentiate between swimming and swarming¹⁰⁷. When the wild type strain SBW25 was checked for swimming and swarming motility in swimming medium, all plates showed the typical swimming expansion circle (Figure 3-3), but only one out of six replicates was observed to swarm, confirming the low frequency of swarming of wild type in this medium. The maximum area of colony expansion was recorded every two hours, for all 6 replicates, as described in section 2.5, and plotted to produce colony expansion curves (Figure 3-4). With the exception of replica plate 2 which initiated swarming between 14 h and 16 h, there was no swarming in swimming medium. There was slightly more variability (coefficient of variation of colony's area at 24 h = 26.61 %) in colony expansion areas among the replicates (Figure 3-3 and Figure 3-4) compared with the results of the strains SBW25p and SBW25Q(*pfleQ*) discussed below (Appendix ZT: Table ZT-2 and Figure ZT-4). There was an initial low rate of expansion up to about 8 h-10 h, followed by a more rapid expansion of the circumference after 14 h. The geometric mean (geomean) from all 6 replicates was calculated and data from 2 h – 8 h of the geomean (before any visible swarming) used to determine the

average initial swimming dependent expansion rate (mm^2/h) up to 8 h. This was calculated as $27.2 \text{ mm}^2/\text{h}$ (mean).

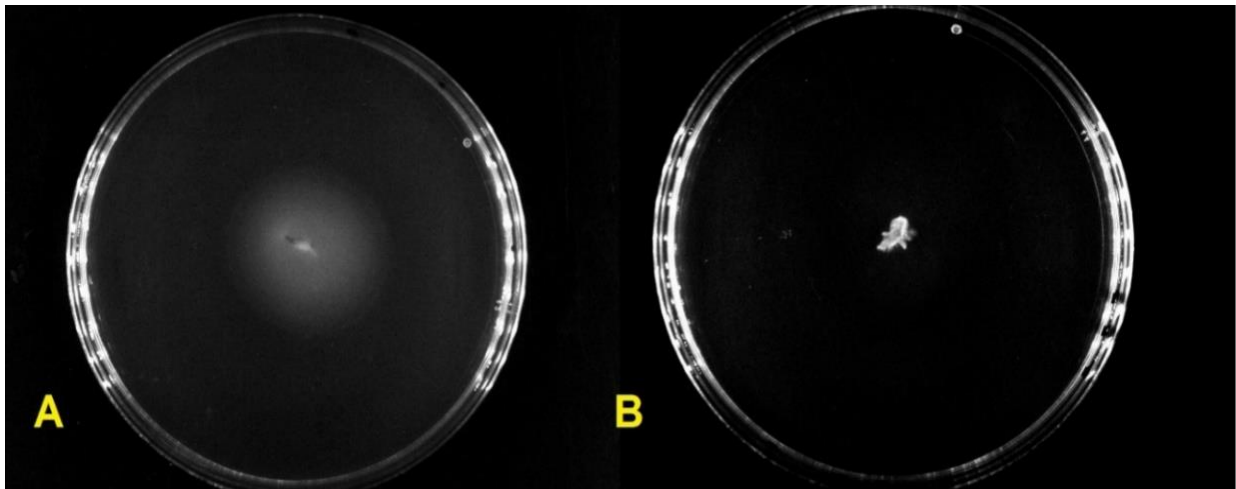


Figure 3-3 Colony phenotype of strains in swimming

Strains in swimming medium grown on 9 cm diameter plates. (A) Wild type strain SBW25: swimming motility. (B) Strain SBW25 Δ *fleQ* (*Fla*⁻, *Visc*⁺): non motile. Picture was taken after 24 h using a gel imaging system (G:BOX Chemi XX6).

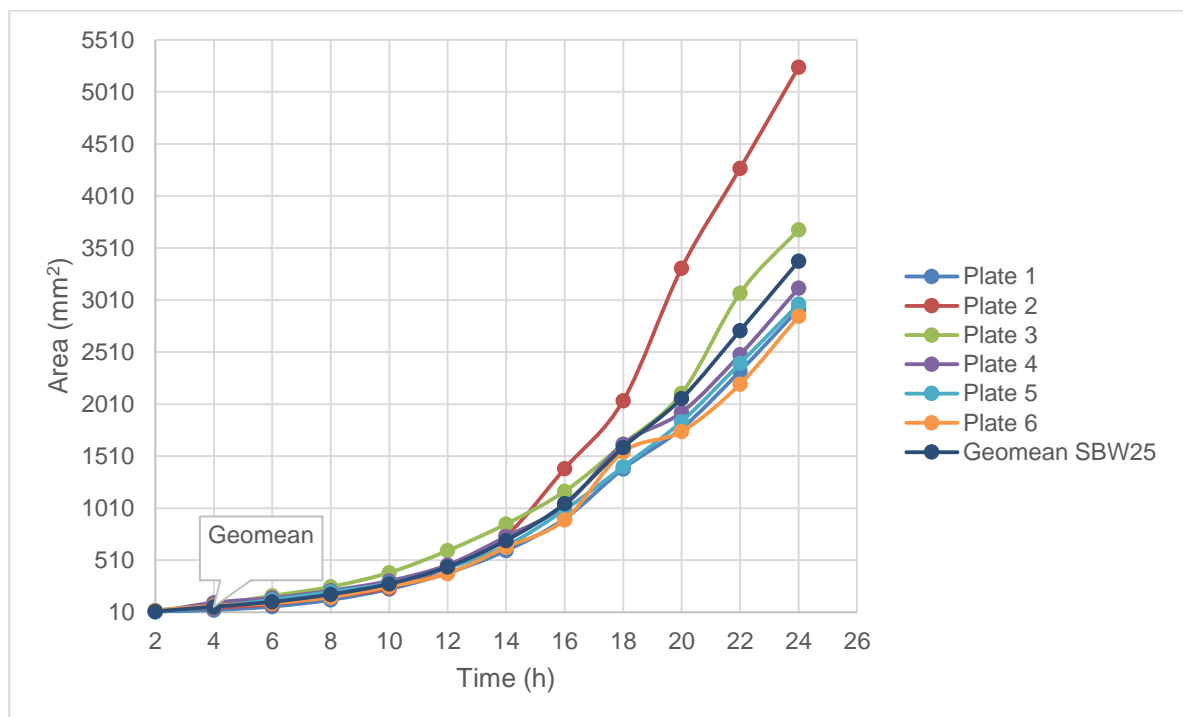


Figure 3-4 Colony expansion curve of wild type strain SBW25

Strain SBW25 in swimming medium on 9 cm diameter plates. Individual colony expansion curves per replicate. The base of the plate was inoculated with $3 \mu\text{L}$ of bacterial culture ($\text{OD}_{600} = 1$) grown in LB before incubating the plates at 27°C in a walk-in incubator in the dark, placed on a bench without stacking. The plates were visually inspected against the light using a jeweller's lighted high-power magnifier ($10\times$) visor and the colony borders marked and measured every 2 h for 16 h as described in section 2.4.3.1. Each replicate was a different colony. The geomean of all replicates was determined and the mean rate of colony expansion over a period of 8 h was calculated as $27.2 \text{ mm}^2/\text{h}$. The area of 9 cm diameter plate diameter is 7226.4 mm^2 .

In comparison to the wild type strain, the aflagellate strain SBW25 Δ *fleQ* did not move in swimming medium for the first 24 h despite producing visible viscosin rings (Figure 3-3). After 24 h SBW25 Δ *fleQ* colonies began to form the typical spidery-spreading phenotype seen in swarming medium (not shown). This may reflect the necessity of some form of motility to access sufficient nutrients for division and growth.

To confirm that the deletion of *fleQ* alone was responsible for the non-swimming phenotype of SBW25 Δ *fleQ*, this strain was complemented with the plasmid *pfleQ* which encodes the full length SBW25 *fleQ* gene cloned into pBBRMCS-5¹⁴⁴. Plasmid encoded *fleQ* efficiently complemented the motility defect in SBW25 Δ *fleQ* (Figure 3-5). SBW25Q (*pfleQ*) was able to swim as efficiently as wild type SBW25p, a control strain carrying the empty plasmid pBBRMCS-5 (Gm^R) (see also Movie 11 and Movie 25 respectively). The swimming colony expansion curve of SBW25Q (*pfleQ*) showed little variability among the replicates (coefficient of variation of colony's area at 24 h = 4.69 %) and did not swarm (Figure 3-6). Similarly, the colony expansion curve for strain SBW25p showed slight variability among the replicates (coefficient of variation of colony's area at 24 h = 13.09 %) and no swarming (Figure 3-6), refer to Appendix ZT: Table ZT-2. The average area covered in 24 h by strain SBW25p was 1341.8 mm² (*SD* = 175.6 mm², *n* = 6; data analysed from Figure 3-6). This was not statistically significantly different (*P-value* 0.052 > 0.050) from the average area that was covered by strain SBW25Q(*pfleQ*), which stood at 1498.1 mm² (*SD* = 70.2 mm², *n* = 7; data analysed from Figure 3-6), please refer to Appendix ZT: Table ZT-1 and Figure ZT-3.

To determine if the plasmid pBBRMCS-5 (Gm^R) was able to restore swimming motility without requiring the full length *fleQ* gene, strain SBW5Qp was used. Strain SBW5Qp is strain SBW25 Δ *fleQ* carrying the vector pBBRMCS-5, Gm^R (refer to section 2.8.2). This strain did not swim (Movie 12) and showed only cumulative growth (Figure 3-3; Figure 3-6). Therefore, the conclusion was made that the loss of gene *fleQ* was the only mutation in SBW25 Δ *fleQ* leading to the non-swimming phenotype. Therefore, this strain was suitable as parent for the experimental evolution studies investigating restoration of expression of flagella and swimming motility.

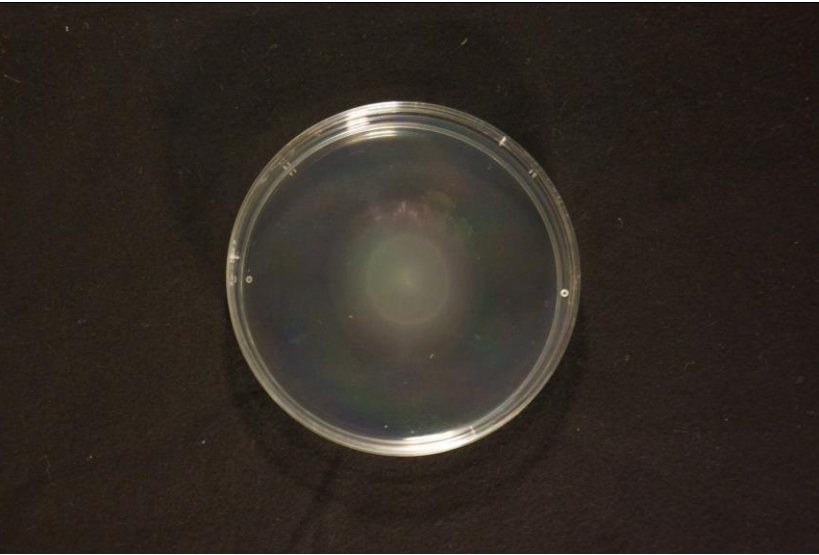
<p>SBW25Q (p<i>fleQ</i>) (<i>Fla</i>⁺, <i>Visc</i>⁺) Δ<i>fleQ</i> <i>fleQ</i> gene cloned into pBBRMCS-5</p>	
<p>SBW25p (<i>Fla</i>⁺, <i>Visc</i>⁺) pBBRMCS-5 (Gm^R)</p>	
<p>SBW5Qp (<i>Fla</i>⁺, <i>Visc</i>⁺) Δ<i>fleQ</i> pBBRMCS-5 (Gm^R)</p>	

Figure 3-5 Phenotype of *P. fluorescens* strains at 22 h
Plates (9 cm diameter) inoculated and incubated as described in Figure 3-6.

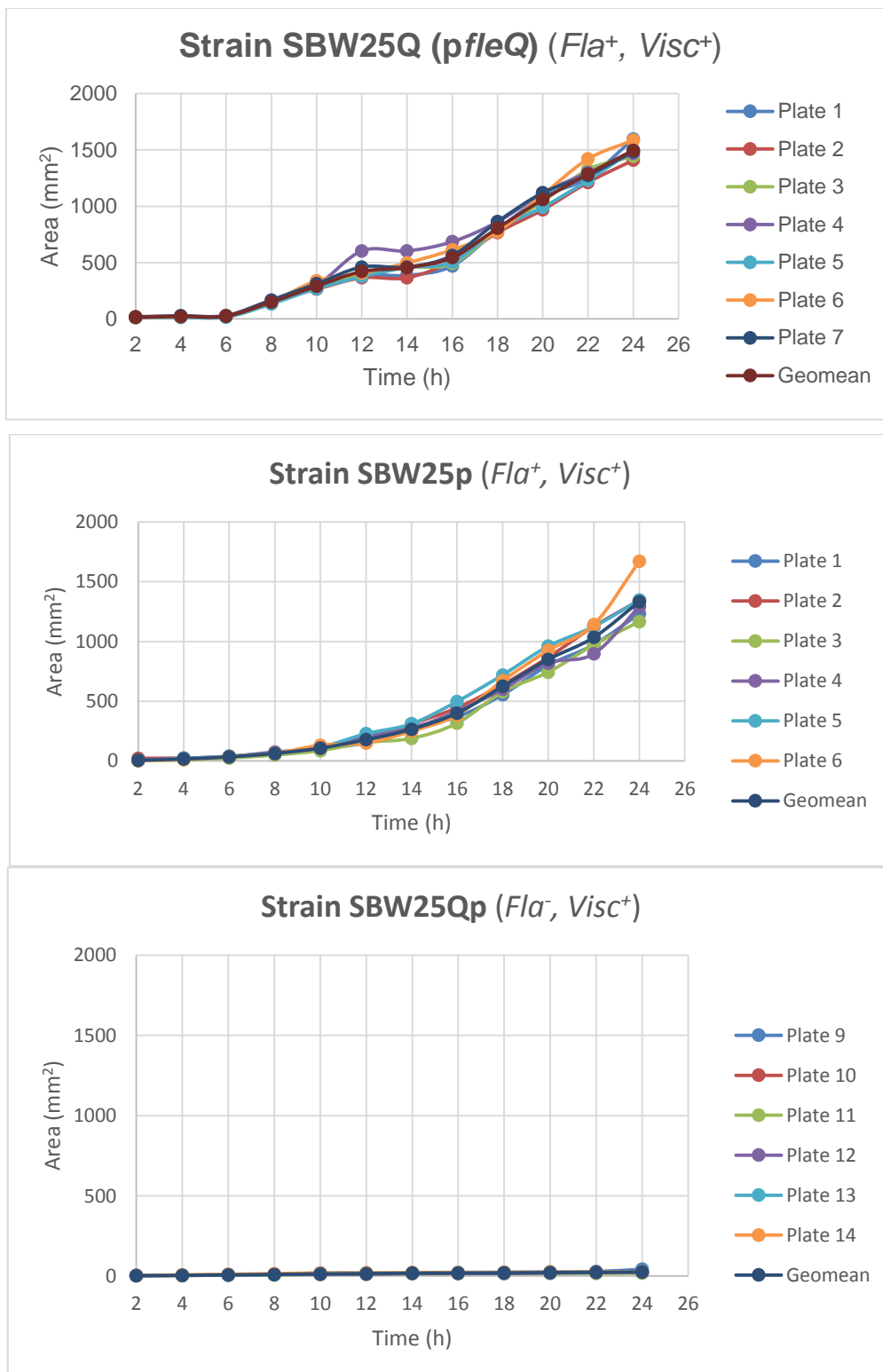


Figure 3-6 Colony expansion of *P. fluorescens* strains

All individual colony expansion curves per replicate. The base of the plate was inoculated with 3 μ L of bacterial culture ($OD_{600} = 1$) grown in LB (supplemented with gentamycin) before incubating the plates at 26 $^{\circ}$ C in a walk-in incubator in the dark, placed on a bench without stacking. The plates used had a 9 cm diameter and an area of 7226.4 mm². All plates run together using the hand-drawn method or time-lapse photography technique. Strains grown on swimming medium with gentamycin.

3.3 Active Movements in the *P. fluorescens* strains

3.3.1 Swimming and swarming motilities of the wild type strain SBW25

TEM visualised the wild type strain SBW25 as a rod-shaped Gram-negative bacillus with 2 or 3 polar flagella (Figure 3-7). This was found to be consistent with reports in the literature of 1-3 polar flagella/cell^{18,23}. Rapid, directional swimming in Luria-Bertani broth was recorded (Movie 24). This strain is also known to exhibit twitching motility at the bottom of microtitre wells because it expresses T4P¹⁰⁹.

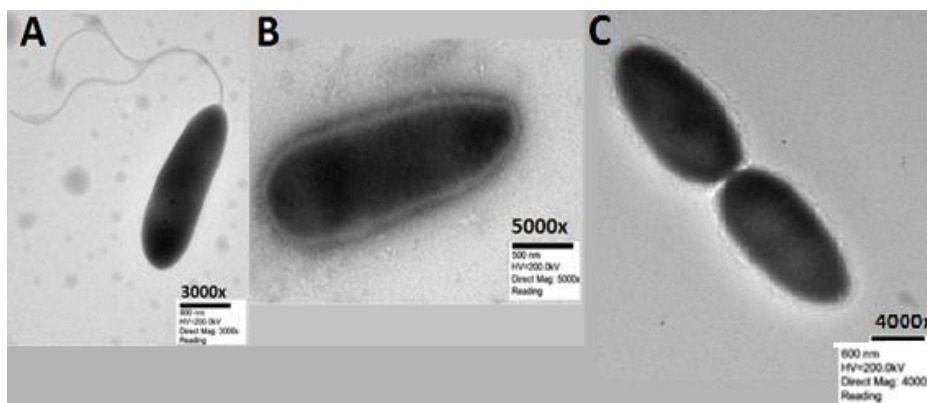


Figure 3-7 TEM image of wild type strain SBW25 and aflagellate strains SBW25 Δ *fleQ* and AR2

(A) The wild type strain SBW25, polar flagella and rod shaped bacillus. (B) SBW25 Δ *fleQ*, aflagellate rod shaped bacillus. (C) AR2, rod shaped non-flagellate bacillus. Cells of all strains were grown overnight in LB at 26 °C with shaking at 95 rpm then stained with 1 % w/v uranyl acetate and imaged by TEM, as elucidated in section 2.14.

3.3.1.1 Swimming and swarming motilities in swarming medium

Swimming and swarming of the SBW25 strain, was recorded in swarming medium (0.25 % agar LA) as described in section 2.4.1. Figure 3-8 illustrates a typical result following 22 h growth at 26 °C. The swimming population can be identified as a round white circle within the agar. Gradually, this acquired a yellow hue at around 8 h. The swarming cells radiated out from one side of the swimming colony (Movies 8-10) and with time expanded, with a doughnut like appearance, to surround the colony and cover the entire plate. In this experiment, colony expansion on nine replica 9 cm plates and 6 replica 15 cm plates was recorded every 2 h over 24 h and 30 h, respectively. In the wake of the extensive swarming of the wild type strain, 15 cm diameter plates, were also tested and recorded using time-lapse photography (Figure 3-9), refer to section 2.4.3.2. The geometric mean (geomean) of all replicates was calculated and

plotted for both the 15 cm replica plates (Figure 3-9) and the 9 cm replica plates (Figure 3-10).

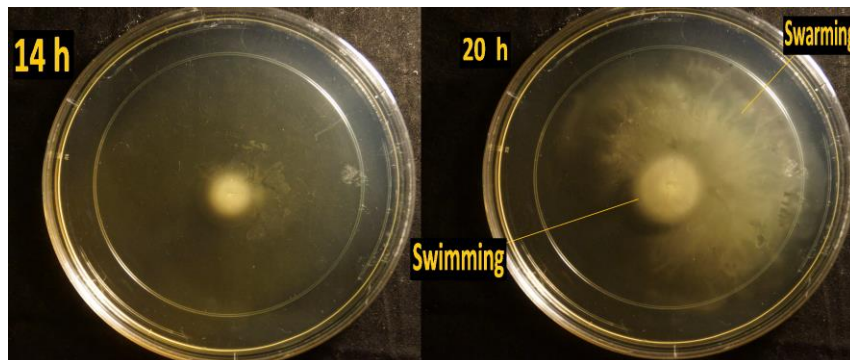


Figure 3-8 Swimming and swarming of the wild type strain SBW25

Strain SBW25 was inoculated from a single colony into swarming medium in a 15 cm diameter plate and grown at 26 °C, as described in section 2.4.1. The white circle showed the swimming bacterial population (colony) as the bacteria swam through the agar. Swarming was fast and began after 14 h from one point of the swimming colony border. The plate shown is replicate plate 12 from the motility assay (below), images at 14 h and 20 h are shown.

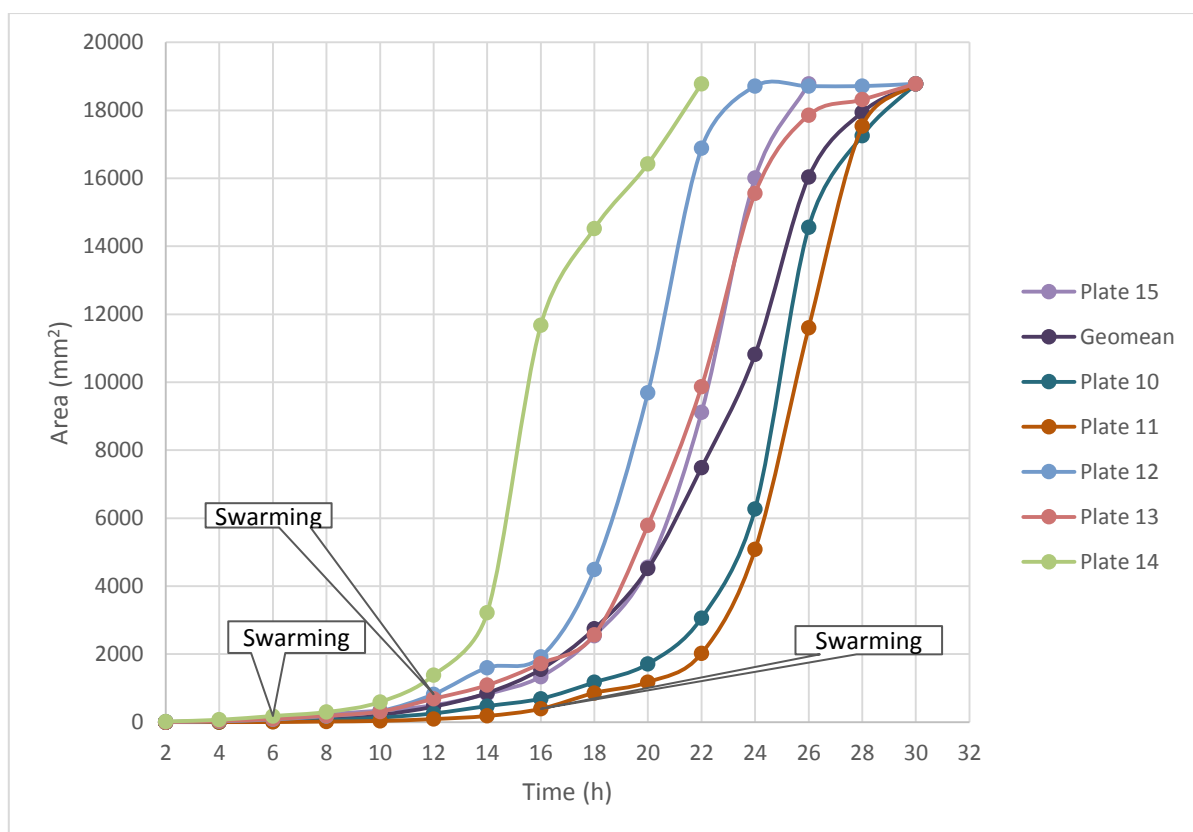


Figure 3-9 Colony expansion curves of strain SBW25 on swarming medium

Replica plates (15 cm) were inoculated with strain SBW25, as described in Figure 2-1, and incubated and imaged separately using the time-lapse photography method. Plate 14 initiated swarming at 6 h, and plate 12 at 12 h, while all other plates were seen to be initiating swarming at 14 h or 16 h. Geomean curve represents the geometric mean of all individual expansion curves. The area of a 15 cm diameter plate is 18783.4 mm².

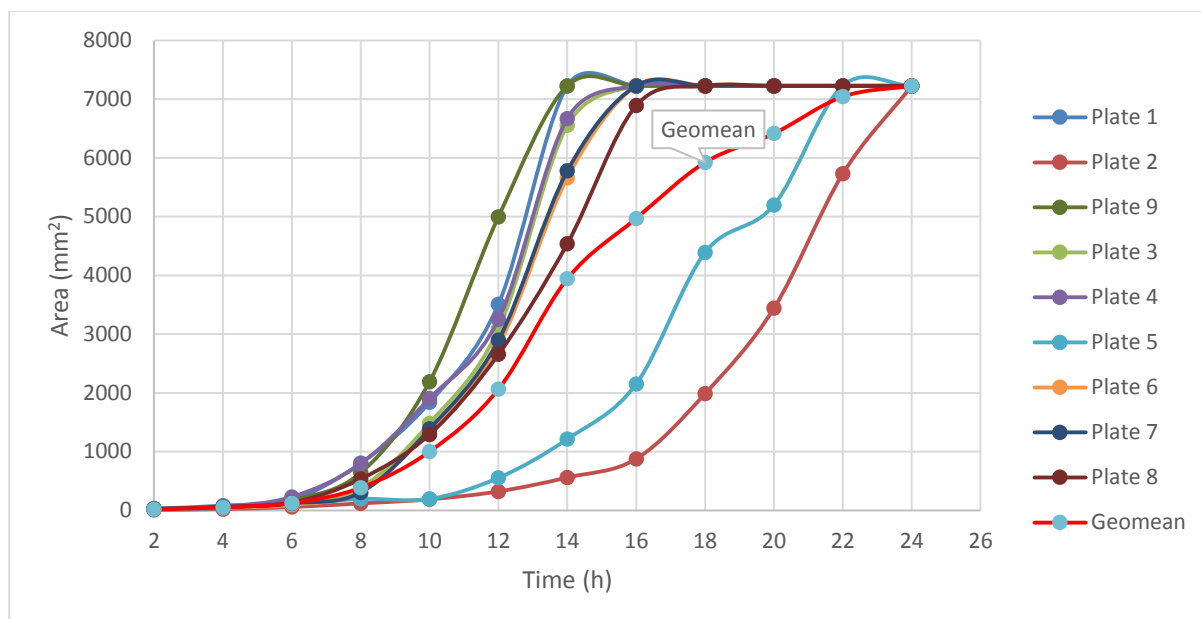


Figure 3-10 Colony expansion curves for strain SBW25 on swarming medium

Replica plates were inoculated and the total area of bacterial spread was imaged, as shown in Figure 2-1. The 9 cm diameter plates were grown concomitantly; bacterial spread was recorded using the hand-drawn method (section 2.4.3.1). Plates 1, 3, 4, 6, 7, 8 and 9 and visibly swarmed at 8 h; whereas plate 5 swarmed at 12 h and plate 2 at 16 h. The geomean of all replicates is shown. The averaged swarming time for these plates was 9.3 h ($SD = 2.8$ h). The area of a 9 cm diameter plate is 7226.4 mm².

Time-Lapse images of the two 15 cm diameter motility plates, as illustrated in Figure 3-11, highlight variation in initiation of swarming. In this project, it was considered as an early swarmer whenever any of the replicates swarmed before 14 h. The swarming was studied and visually determined in Petri dishes 15 cm and the colony movement was as described in section 2.4.3.2. Swarming was observed as a fast and diffuse movement initiated from one point of the swimming colony that took place underneath the surface of the swarming medium (surface motility) because the bacteria moved as group (e.g. flagella entangled or hooking between cells via pili). There was one exception where a replicate swarmed from different points on the swimming colony (plate 14 in Figure 3-11). The wild type strain SBW25 exhibited continued swimming motility for 30 h (total observation time in 15 cm diameter plates) as a yellow swimming disc through the agar and under the swarming population.

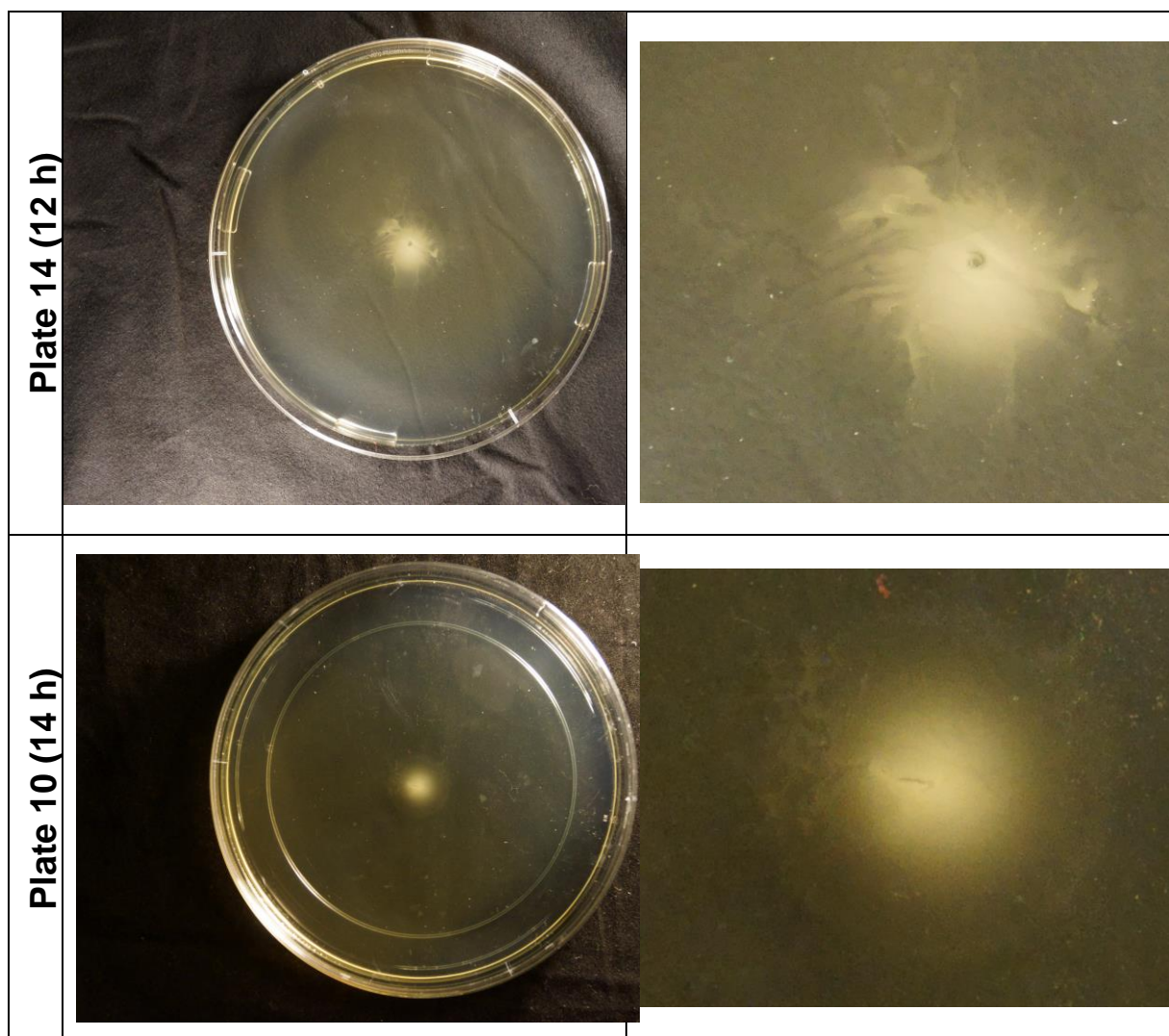
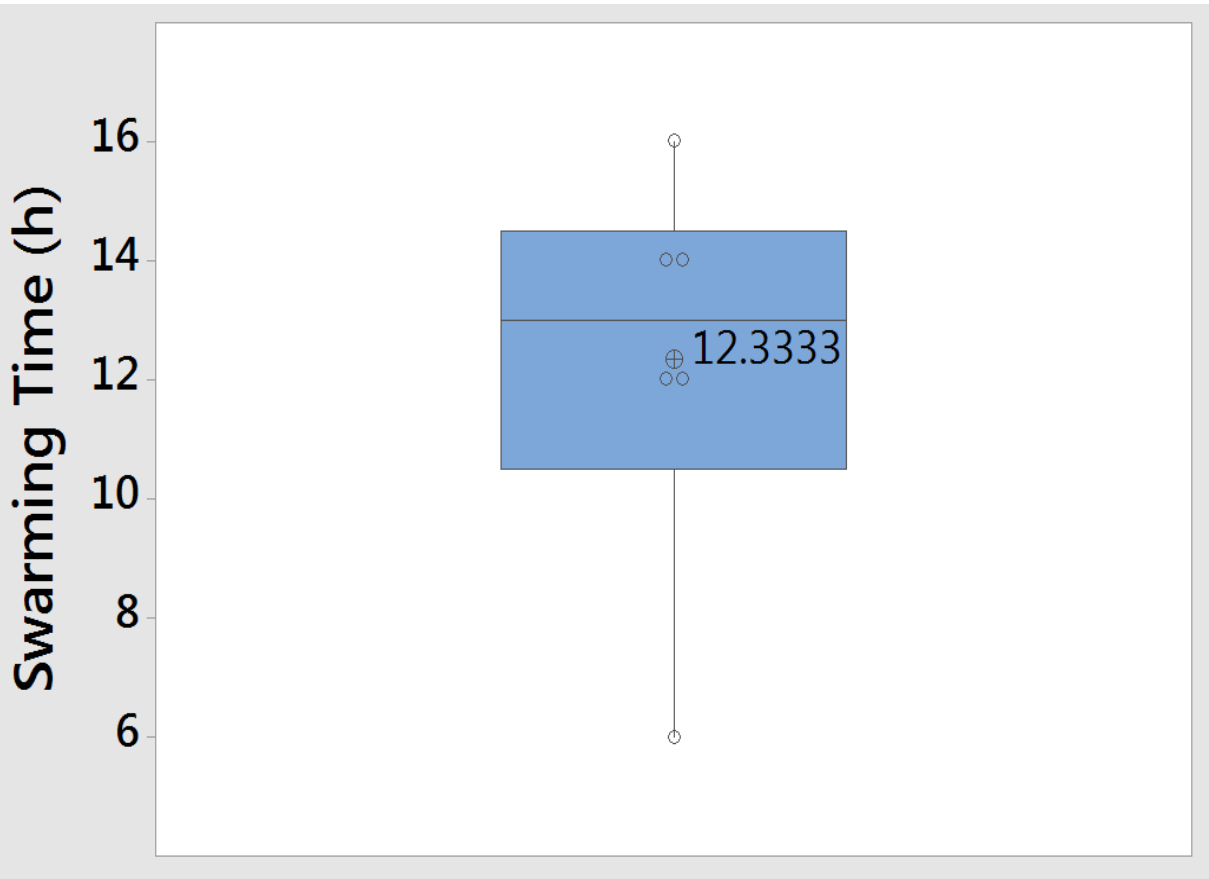


Figure 3-11 Swimming and swarming of the wild type strain SBW25

Swarming medium on 15 cm diameter plates, as shown in Figure 3-9. See Figure 2-1 and section 2.4.3.2 for details of inoculation and recording colony's area. Images were taken at time points shown. Plates 14 and 10 represent respectively early, and intermediate initiation of swarming. The colony grown on the plate is zoomed in the right column.

The 15 cm diameter plates showed great variation at times when swarming motility was initially visible. This varied from very early at 6 h up to 16 h, post-inoculation. Presentation of the data in the box plot (Figure 3-12) shows a mean swarming time for SBW25 as 12.3 h ($SE = 1.4$ h) with two swarming populations - one that initiated visible swarming at 12 h, and other at 14 h and the two outliers swarming at 16 h and 6 h.



Descriptive Statistics: Time Statistics

Variable	Total Count	Mean	SE Mean	StDev	CoefVar	Minimum	Q1	Median	Q3	Maximum
Time	6	12.33	1.41	3.44	27.93	6.00	10.50	13.00	14.50	16.00

Variable	Range	IQR	Mode	N for Mode
Time	10.00	4.00	12, 14	2

Figure 3-12 Box plot: The swarming time of the wild type strain SBW25

The analysed data is from Figure 3-9. Strain SBW25 was inoculated in swarming medium. The time-lapse-photography method was used in order to evaluate the 15 cm diameter plates. Notably, these plates were not observed concomitantly. The average swarming time (12.3 h) is illustrated inside the box plot. CoefVar: coefficient of variation (%).

Data from the 9 cm diameter plates (Figure 3-10) were obtained in accordance with the hand-drawn technique (section 2.4.3.1). The plates did not swarm concomitantly. Plates 1, 3, 4, 6, 7, 8 and 9 swarmed around 8 h; on the other hand, plate 5 swarmed at 12 h and on plate 2 at 16 h. This variation in swarming time meant that the experimental population data for all replicates had a Log-Normal distribution, with a similar profile for 9 cm and 15 cm plates. No significant statistical differences (Appendix ZZ: Table ZZ-1; *P-value* 0.087 > 0.050) were found at the start of swarming

between both plate sizes (9 cm and 15 cm diameter); plates 9 cm diameter swarmed at 9.3 h ($SD = 2.8$ h), whereas those in 15 cm diameter swarmed at 12.3 h ($SD = 3.4$ h). However, there was slightly more variability in the swarming time data from the plates of 9 cm diameter (coefficient of variation = 30.11 %) compared with the 15 cm diameter plates (coefficient of variation = 27.64 %).

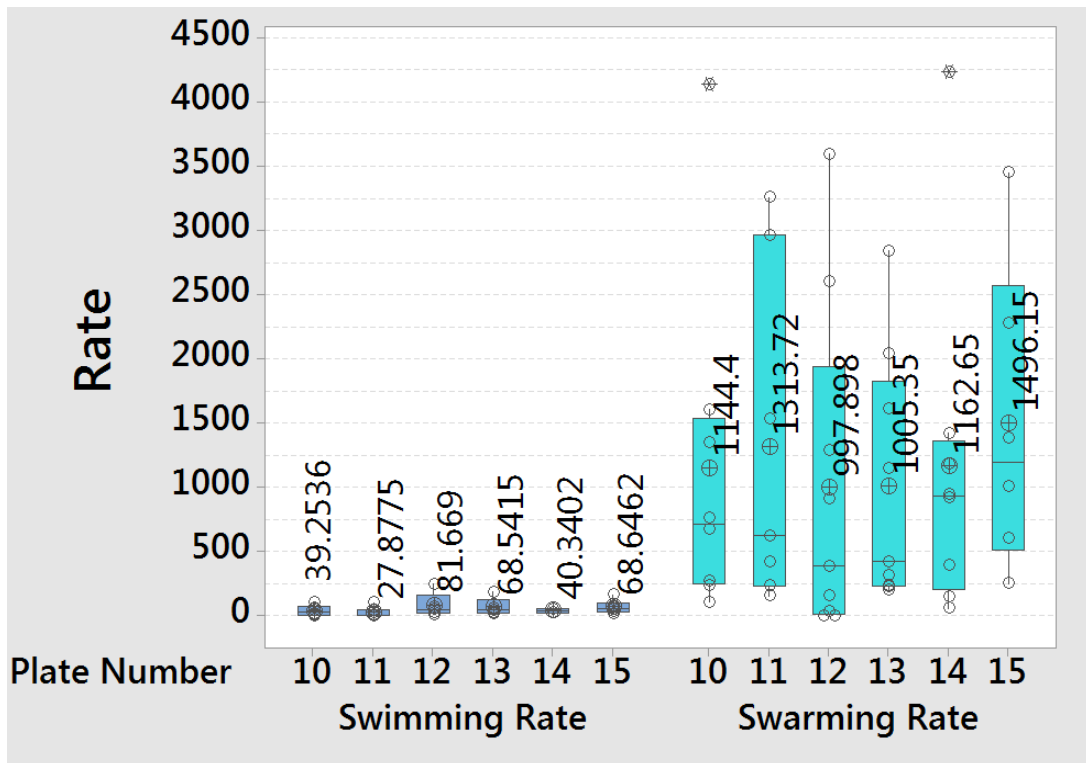
The swimming dependent and swarming dependent colony expansion rates were determined for each 15 cm diameter plates (Table 3-1, Figure 3-13). The increase in area/h is shown for each 2 h monitoring period. Initiation of visible swarming correlated with a distinct lag in increase in colony area. The length of swimming dependent colony expansion varied from the first 6 h growth (plate 14) to the first 16 h growth (plate 11) and the average swimming dependent expansion rate, over these time periods for all plates, was 54.4 mm²/h ($SD = 21.3$ mm²/h, $n = 6$). Following initiation of swarming, colony expansion increased rapidly reaching very high expansion rates, for example 4231 mm²/h as observed in plate 14 at 15 h (Table 3-1). The average rate of swarming dependent colony expansion was 1186.7 mm²/h ($SD = 191.2$ mm²/h, $n = 6$). As published¹⁰⁷, viscosin allows a swimming colony to move farther compared to a colony that can only utilize flagella driven movement, such as strain SBW25C. Viscosin is necessary for swarming of *P. fluorescens*^{83,107}, permitting the bacteria to explore a new environment²⁴⁴. In addition to viscosin it is possible that swarming cells of SBW25 have a transient increase in flagella number, enhancing swarming as *P. fluorescens* strain F113 becomes hypermotile²⁴⁶ and hyperflagellated upon colonizing the plant roots^{181,246}, see section 1.8.4.

Because of the variation in time of initiation of swarming on both 9 cm and 15 cm plates (Figure 3-12), the geomean was unsuitable for calculation of average colony expansion rates after swarming was initiated. Therefore, with strains exhibiting swarming or viscosin dependent spreading, data from the geomean curve from 2 h to 8 h was used for comparison of swimming dependent colony expansion rates (mm²/h). The geomean based swimming rate of SBW25 was calculated as 26.3 mm²/h from 2 h- 8 h, as defined in section 2.5.

Table 3-1 Swimming and swarming dependant rates of colony expansion for individual replicates of SBW25

Plate Number	Time (h)	Swimming Rate (mm ² /h)	Time (h)	Swarming Rate (mm ² /h)
10	3	0.07	15	108.53
	5	8.58	17	240.32
	7	16.58	19	271.93
	9	40.26	21	674.22
	11	62.15	23	1605.00
	13	107.88	25	4141.62
			27	1350.38
			29	763.20
11	3	0.11	17	234.09
	5	0.79	19	157.71
	7	7.25	21	422.90
	9	9.02	23	1530.56
	11	27.62	25	3260.03
	13	45.47	27	2966.48
	15	104.90	29	624.25
	12	3	10.83	13
5		26.82	15	159.47
7		49.33	17	1287.02
9		72.84	19	2599.93
11		248.53	21	3596.20
			23	913.68
			25	
			27	
13	3	16.25	13	200.28
	5	28.96	15	318.62
	7	47.56	17	421.05
	9	62.23	19	1613.81
	11	187.70	21	2038.72
			23	2843.94
			25	1148.51
			27	228.61
14	3	24.57	7	57.93
	5	56.11	9	147.08
			11	394.36
			13	918.83
			15	4231.08
15	3	15.08	15	253.65
	5	33.05	17	603.56
	7	66.28	19	1008.03
	9	51.67	21	2275.66
	11	79.52	23	3451.79
	13	166.28	25	1384.21

Note: Colony expansion rate (mm²/h) is the average hourly expansion rate over each 2 h interval calculated from the data for 15 cm diameter plates (Figure 3-10), calculated as described in section 2.4.3.2 using Equations 2-1 and 2-2. The time (h) shown is the intermediate time between the two recorded time points. 'Swimming rate' is swimming dependent expansion up until visible swarming. 'Swarming rate' is all colony expansion post visible swarming.



Descriptive Statistics: Swimming Rate, Swarming Rate

Statistics

Variable	Plate Number	Total Count	Mean	SE Mean	StDev	CoeffVar	Minimum	Q1	Median	Q3
Swimming Rate	10	8	39.3	16.6	40.6	103.32	0.1	6.5	28.4	73.6
	11	7	27.9	14.2	37.7	135.23	0.1	0.8	9.0	45.5
	12	9	81.7	43.0	96.2	117.75	10.8	18.8	49.3	160.7
	13	9	68.5	30.8	68.9	100.50	16.3	22.6	47.6	125.0
	14	8	40.3	15.8	22.3	55.27	24.6	*	40.3	*
	15	6	68.6	21.7	53.1	77.31	15.1	28.6	59.0	101.2
Swarming Rate	10	8	1144	468	1323	115.62	109	248	719	1541
	11	7	1314	496	1313	99.92	158	234	624	2966
	12	9	998	431	1294	129.69	0	17	390	1943
	13	9	1005	323	968	96.29	200	232	421	1826
	14	8	1163	471	1333	114.61	58	209	934	1362
	15	6	1496	484	1185	79.22	254	516	1196	2570
Variable	Plate Number	Maximum	Range	IQR	Mode	N for Mode				
Swimming Rate	10	107.9	107.8	67.1	*	0				
	11	104.9	104.8	44.7	*	0				
	12	248.5	237.7	141.9	*	0				
	13	187.7	171.4	102.4	*	0				
	14	56.1	31.5	*	*	0				
	15	166.3	151.2	72.7	*	0				
Swarming Rate	10	4142	4033	1293	*	0				
	11	3260	3102	2732	*	0				
	12	3596	3596	1926	0	2				
	13	2844	2644	1595	*	0				
	14	4231	4173	1153	*	0				
	15	3452	3198	2054	*	0				

Figure 3-13 Box plot: Swimming and swarming mean rates for individual plates

Analysis of data presented in Table 3-1 and Figure 3-9. Wild type strain SBW25 on swarming medium from 6 individual replicates (15 cm plates), prepared and analysed consecutively. Mean swimming rate of all swimming rates per replicate: 54.0088 mm²/h (SD = 57.7148 mm²/h, n = 31); mean swarming rate of all swarming rates per plate: 1162.95 mm²/h (SD = 1181.76 mm²/h, n = 47).

3.3.1.2 The flagellated but non-viscosin producing strain, SBW25C swims but does not swarm

Strain SBW25C, which has flagella but does not produce viscosin, was similarly monitored on swarming media to assess the impact of loss of viscosin on colony expansion. The average area covered in 24 h by strain SBW25C was only 766.12 mm² (*SD* = 128.09 mm², coefficient of variation = 16.72 %) (Figure 3-15), which was much less compared to the average area covered by the wild type strain SBW25 [12329 mm² (*SD* = 6204.48 mm²), coefficient of variation = 50.33 %] (Figure 3-10) in the same period. This can be readily explained by the absence of swarming by SBW25C in this assay (Figure 3-14). There was not much variability (coefficient of variation of colony's area at 24 h = 16.72 %) among the twelve replicates studied to construct the colony expansion curve for SBW25C (see also Appendix I: Figure I-1 and Figure I-2) compared with SBW25 (coefficient of variation of colony's area at 24 h = 50.33 %). This can be explained by the fact that SBW25C colonies continued to swim and did not switch to a rapid swarming motility as did SBW25.

The average rate of colony expansion of SBW25C, calculated over a period 2 h - 8 h from the geomean, was 12.1 mm²/h (mean), and was also much less than average rate of colony expansion of SBW25 (mean = 26.3 mm²/h). Therefore, both flagella driven motility and the production of the biosurfactant viscosin were necessary for an effective colony expansion. SBW25C moved slower than SBW25 despite both strains being flagellated. In conclusion, the mutant flagellated strain SBW25C swam but did not swarm because it did not produce the biosurfactant viscosin.

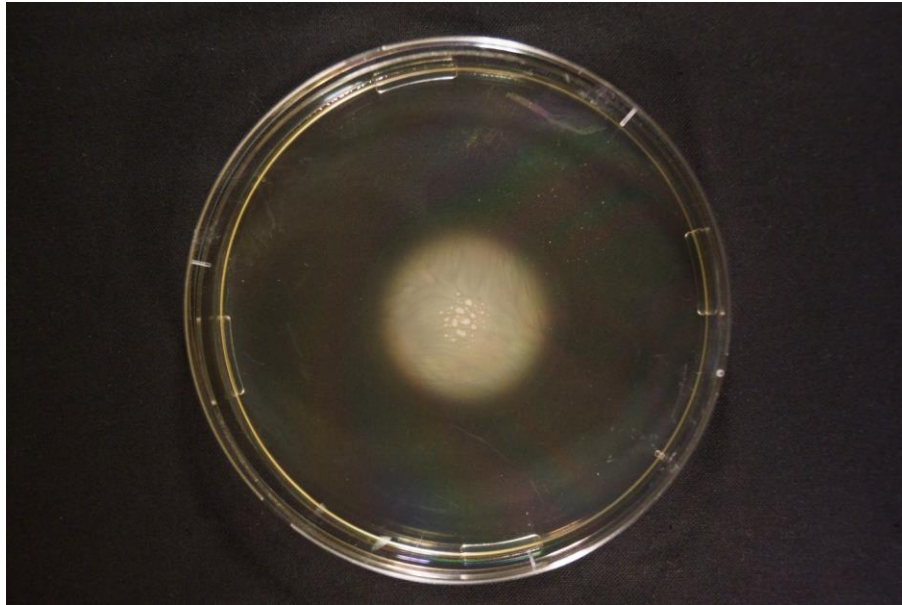


Figure 3-14 Swimming, non-swarming motility of SBW25C

SBW25C (*Fla*⁺, *Visc*⁻) was inoculated from a single colony into swarming medium in a 15 cm diameter plate and grown at 26 °C, as described in section 2.4.1. Swimming motility (white circle) only was observed. This picture was taken after 26 h. No antibiotic added.

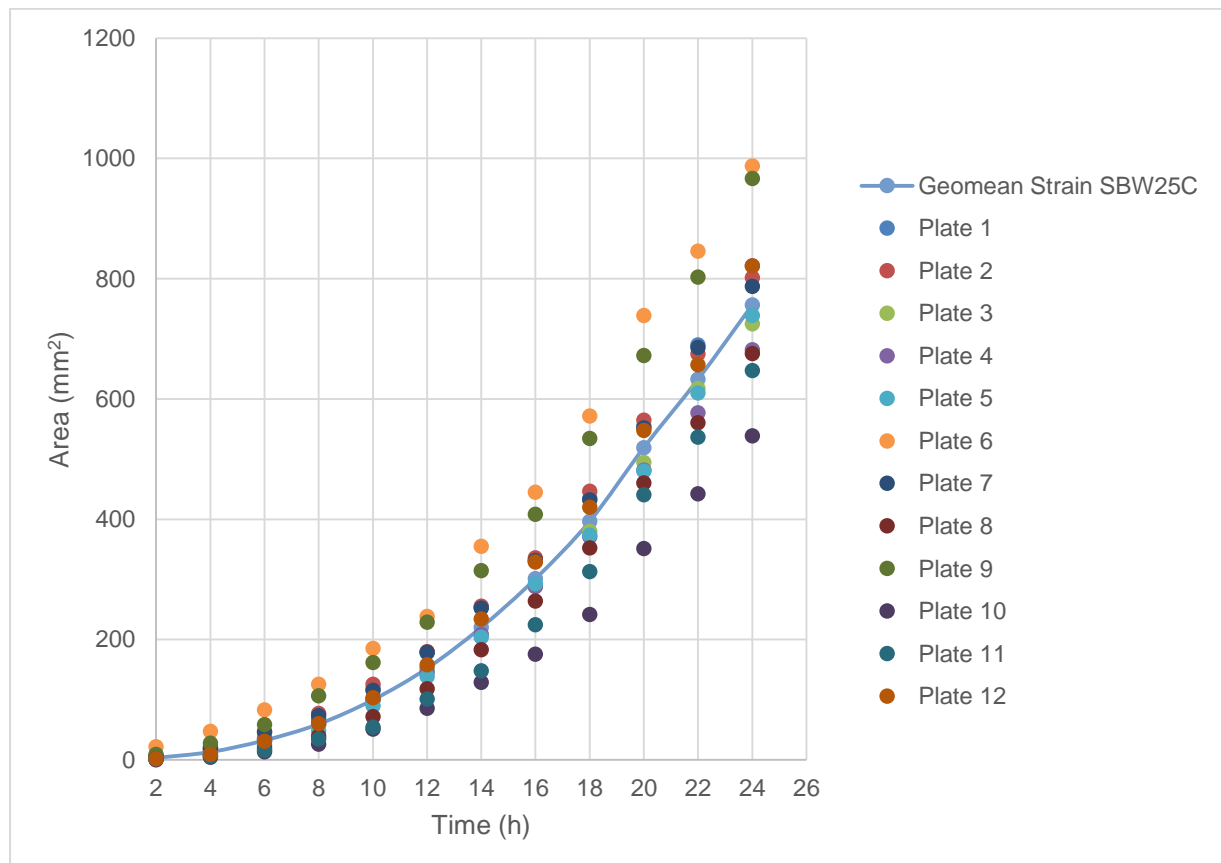


Figure 3-15 Colony expansion curve of strain SBW25C

Strain SBW25C (*Fla*⁺, *Visc*⁻) swam but did not swarm because it did not produce the biosurfactant viscosin. Surface area of a 9 cm diameter plate is 7226.4 mm². Importantly, all replicates were undertaken concomitantly and monitored via the hand-drawn method. Swarming medium without antibiotic.

3.3.1.3 Comparison of the evolved strains AR2S and AR2SF (Taylor et al.¹⁰⁸)

Taylor et al.¹⁰⁸ discovered that the sessile strain AR2 (*Fla*⁻, *Visc*⁻) evolved swimming motility in rich medium (0.25 % agar LA) after 3 days. According to Taylor et al.¹⁰⁸, AR2 re-wired the NtrBC system to express the flagella operon via a two-step process that consisted of an initial single point mutation in the *ntrB* gene, and later a second single point mutation occurred in the *ntrC* gene. Therefore, the initial evolved swimming strain named AR2S¹⁰⁸ was a *ntrB* mutant and was defined as a slow swimmer (mean colony expansion rate from 2 h-8 h: 2.25 mm²/h). The strain AR2SF was isolated from a bleb of an AR2S swimming colony¹⁰⁸. AR2SF swam faster than AR2S because it carried a double mutation in the NtrBC system (Appendix C: Figure C-33; Figure C-34). The evolution of motility in sessile strain AR2 was tested only in rich medium (swarming medium)¹⁰⁸. The evolved strain AR2F was reported to expand much more slowly than other motile strains, such as wild type strain SBW25 or other aflagellate strains, such as SBW25Δ*fleQ*¹⁰⁸. Swimming dependent colony expansion of both evolved AR2 strains was compared to that of SBW25C in swarming media. The very slow swimming motility of AR2S (NtrB T97P) was confirmed (2.25 mm²/h; mean). However, AR2F swam faster (19.1 mm²/h; mean) than SBW25C (12.1 mm²/h; mean), see Figure 3-16 and Figure 3-35.

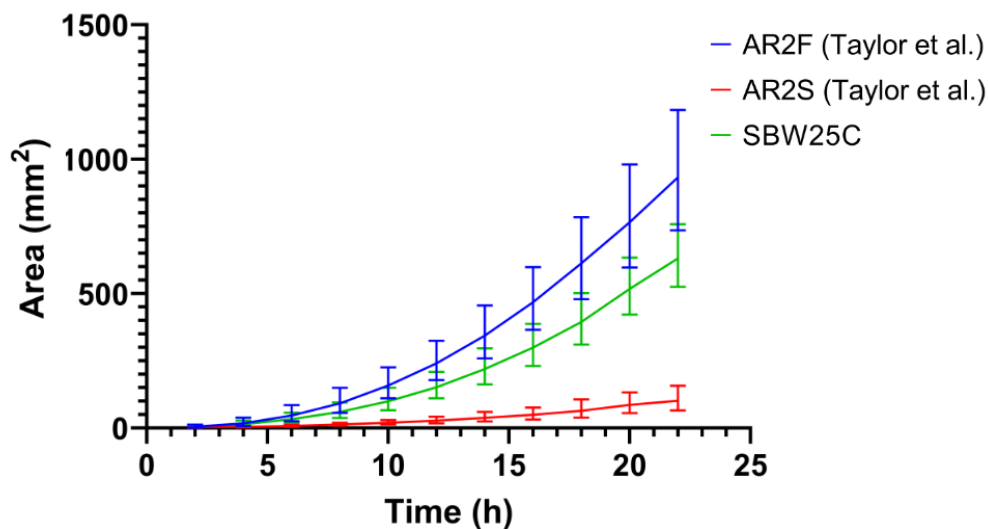


Figure 3-16 Colony expansion of flagellated, non-viscosin producer strains

The evolved strain AR2F was a double mutant (*ntrB ntrC*) while the evolved strain AR2S was a single mutant (*ntrB*). Strain SBW25C (*Fla*⁺, *Visc*⁻) did not produce viscosin and consequently also did not swarm. The graph shows geomean of all replicates ($n = 12$) for each strain and the error bars represent the geometric standard deviation. Method: hand-drawn. Plates: 9 cm diameter on swarming medium without antibiotic.

3.4 Passive Movements in the *P. fluorescens* Strains

3.4.1 Spidery-Spreading movement of strain SBW25 Δ *fleQ* relies on viscosin and cell division to expand the sliding colony

Strain SBW25 Δ *fleQ* was confirmed to be non-flagellate by TEM (Figure 3-7). A large field of bacteria grown and imaged under the same conditions as wild type were viewed. None possessed flagella. Despite the absence of flagella, this strain still spread over the surface of 0.25 % agar LA plates, spreading as a spidery shaped colony (Figure 3-17). Spidery-Spreading movement (Movie 3) has been documented and depends on cell expansion and production of the biosurfactant viscosin to spread a colony over the surface of the agar¹⁰⁷. This biosurfactant facilitated sliding and permitted a colony to rapidly move and cover an extensive area despite a lack of flagella expression¹⁰⁷.

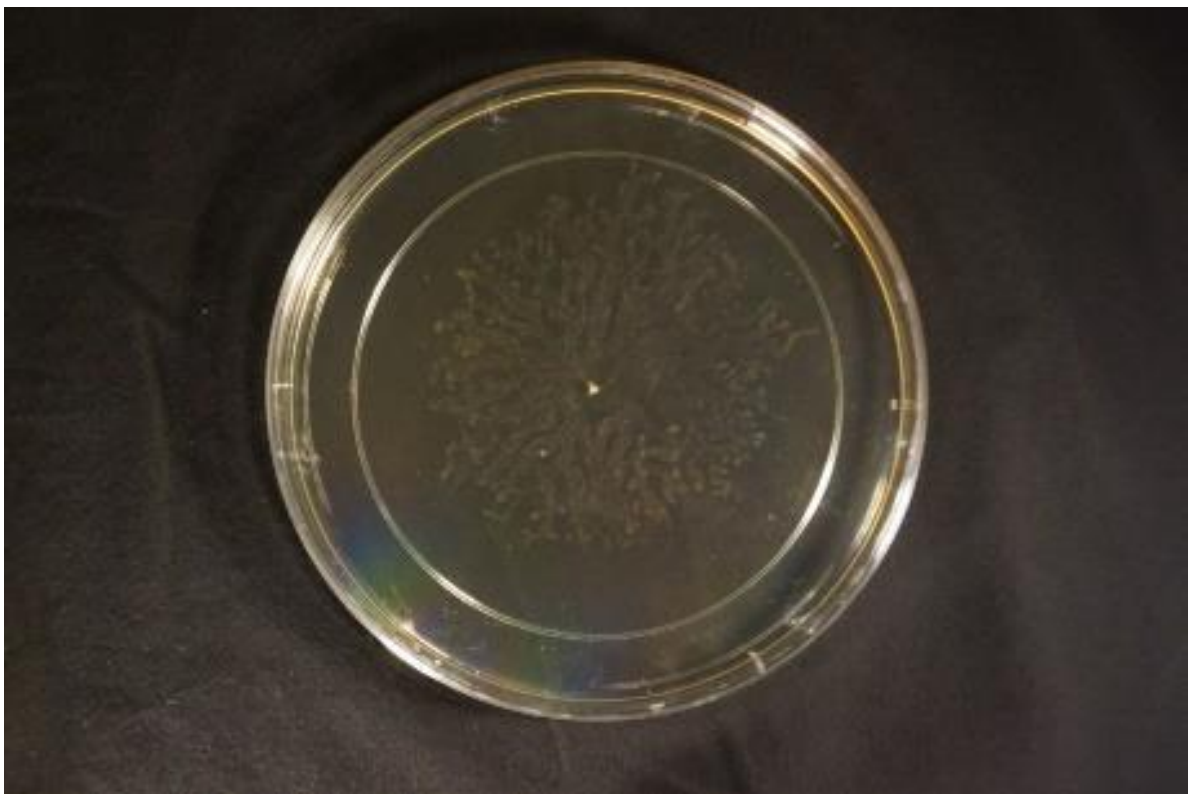


Figure 3-17 Spidery-Spreading growth of strain SBW25 Δ *fleQ*.

SBW25 Δ *fleQ* was inoculated from a single colony into swarming medium in a 15 cm diameter plate and grown at 26 °C, as described in section 2.4.1. Rapid spreading of the colony as spidery-spreading growth over the plate was observed. This picture was taken after 20 h growth.

Hand-Drawn monitoring (section 2.4.3.1) was used for the 9 cm diameter plates and all replicates were done concomitantly (Figure 3-18). With this type of motility, to avoid the boundary effect with 9 cm plates²⁹⁰, as the expanding colony reached the border of the plate the biomass in the tendrils became wider and covered free space still available on the surface of the media²⁹⁰. Hence, with 9 cm plates, space for the front of the sliding colony to spread was limited, therefore studies with SBW25 Δ *fl*eQ used 15 cm diameter plates. The time-lapse photography method was employed for larger plates (15 cm) with plates incubated and imaged consecutively (Figure 3-19). The replicates studied followed a Log-Normal distribution as some replicates developed the spidery phenotype earlier than others. Since this spidery-spreading phenotype did not appear concomitantly in all replicates (Figure 3-20), it was used the geomean instead of the average to construct the colony expansion curve.

The individual colony expansion curves for each replicate (9 cm diameter plates) showed a difference at the commencement of spidery phenotype (Figure 3-18); for example, the colony in plate 2 became spidery shaped at 4 h, whereas the plates 4 and 9 at assumed this shape at 10 h, respectively. The spidery-spreading phenotype enhanced the rate of the aflagellate colony's sliding movement as observed in plate 9 (Figure 3-18) covering a higher area (5653 mm²) after 26 h as compared to the other plates except plate 4, which attained the plate border at 16 h (7226 mm²). No statistical significant differences (*P-value* 0.913 > 0.050; Table 3-2) appeared during the time to appear as spidery-phenotype in the colonies inoculated in 9 cm diameter (mean = 13.40 h, *SE* = 1.79 h) as compared to those inoculated into 15 cm diameter plates (mean = 13.67 h, *SE* = 0.61 h). However, there were more variability in spidery time data among replicates of 9 cm diameter plates (coefficient of variation = 41.40%) compared with replicates of 15 cm diameter plates (coefficient of variation = 11.02 %). This variability might be caused by physicochemical properties of the medium²⁹⁰ or pH changes²⁵⁶. Hence, quantification of the individual rates of expansion for each replica 15 cm diameter plate were useful to identify the time points with less variability to be used to classify the motility phenotype to facilitate comparison with other strains growing in the same swarming medium.

Table 3-2 One-way ANOVA: Initiation of spidery phenotype time (h) versus plate diameter

Null hypothesis	All means are equal						
Alternative hypothesis	Not all means are equal						
Significance level	$\alpha = 0.05$						
<i>Equal variances were assumed for the analysis.</i>							
Factor Information							
Factor	Levels	Values					
Plate diameter	2	9 cm, 15 cm					
Analysis of Variance							
Source	df	Seq SS	Contribution	Adj SS	Adj MS	F-value	P-value
Plate diameter	1	0.267	0.09%	0.267	0.2667	0.01	0.913
Error	14	299.733	99.91%	299.733	21.4095		
Total	15	300.000	100.00%				
Model Summary							
S	R-sq	R-sq(adj)	PRESS	R-sq(pred)			
4.62704	0.09%	0.00%	372.369	0.00%			
Means							
Plate diameter	N	Mean	SD	95% CI			
9 cm	10	13.40	5.66	(10.26, 16.54)			
15 cm	6	13.667	1.506	(9.615, 17.718)			
<i>Pooled SD = 4.62704</i>							

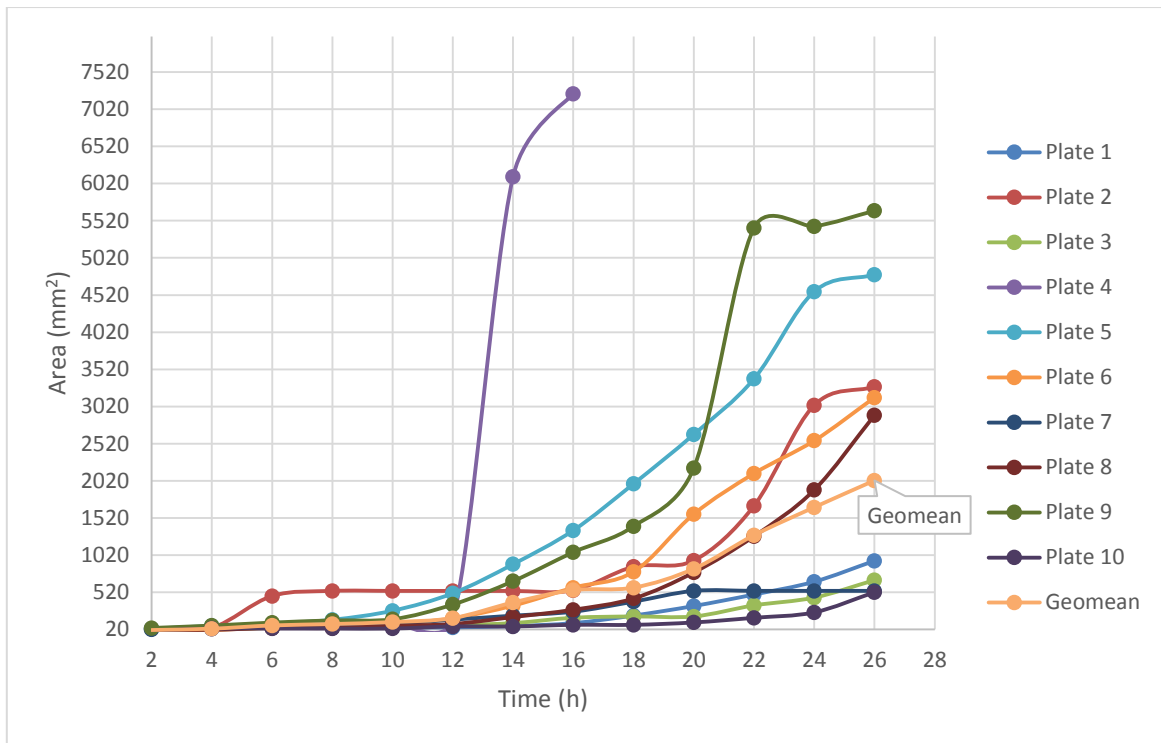


Figure 3-18 Spread of aflagellate strain SBW25ΔfleQ

Strain SBW25ΔfleQ was inoculated in swarming medium on 9 cm diameter plates. Area of a 9 cm plate is 7226.4 mm². Individual colony expansion curves were done for all the replicates, which were done concomitantly via the hand-drawn method. Plate 4 looked like others morphologically. Geomean of all plates is shown.

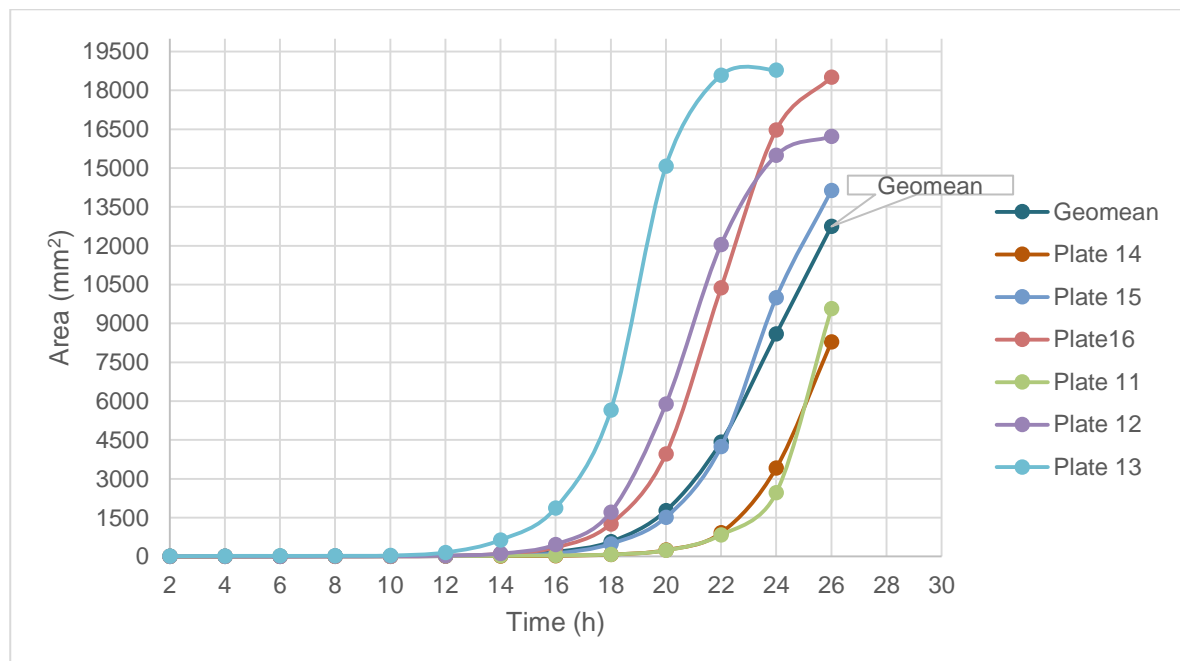


Figure 3-19 Spread of individual replicates of SBW25ΔfleQ

Swarming medium on 15 diameter plate. These colony expansion curves indicated that most of the replicates slid faster on the agar surface about 14 h - 16 h. Plates 13, 16, and 12 spidery-spread faster than other replicates, reaching the plate border at 26 h, whereas other plates not. A 15 cm diameter plate has an area of 18783.4 mm². Method: time-lapse photography. Geomean of all replicates is shown.

Time (h)	Plate 11	Plate 13
16 h		
18 h		
24 h		
28 h		

Figure 3-20 Development of spidery-spreading phenotype of strain SBW25 Δ *fleQ*.

SBW25 Δ *fleQ* was inoculated into swarming medium in a 15 cm diameter plate and grown at 26 °C, as described in section 2.4.1. Time-Lapse images were taken at 2 h intervals from 2 h - 36 h and used for quantitation of colony expansion. Selected images shown here highlight development of spidery-spreading phenotype. These replicates were from the colony expansion curve shown in Figure 3-19.

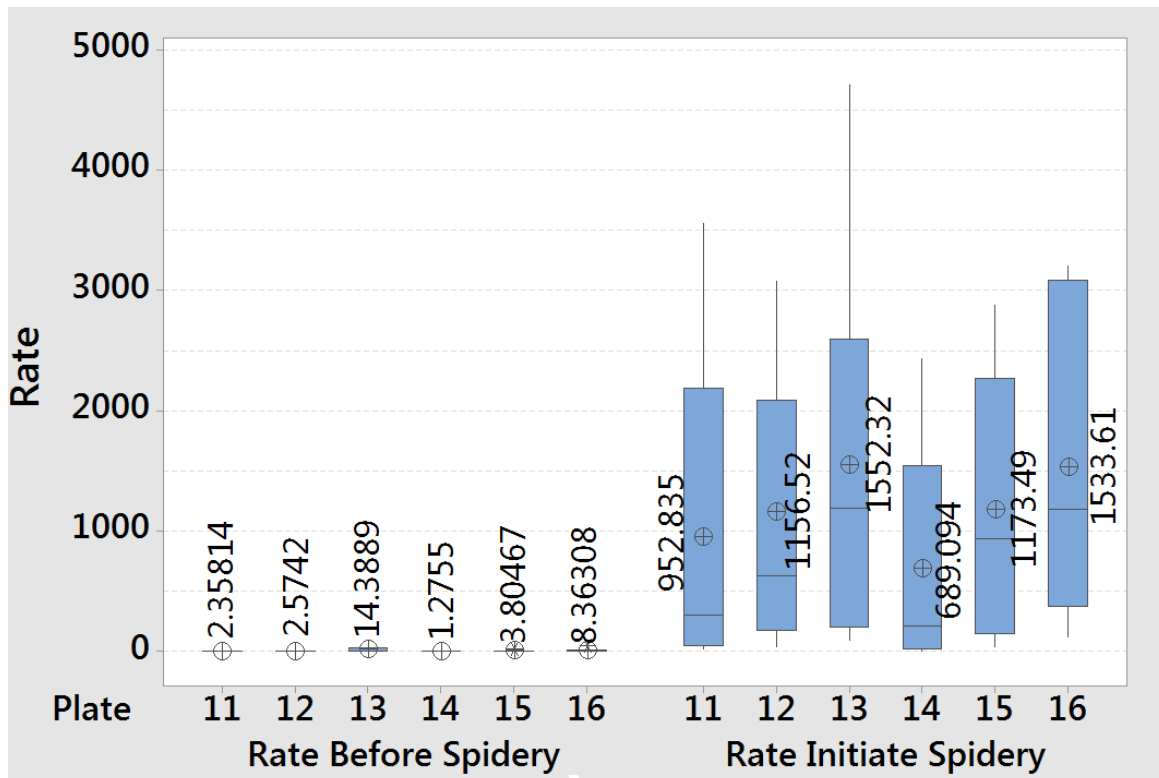
Assessment of rate of colony expansion (section 2.5: Equation 2-1 and Equation 2-2) was performed only on data obtained from replicas 15 cm diameter plates (Figure 3-21; Appendix I: Figure I-3). The averaged rate of all colony expansion rates of all replicates before the spidery phenotype developed was minimal (mean = 5.20 mm²/h) compared with the rate achieved (mean = 1182 mm²/h) after the colony first visibly showed spidery/dendritic phenotype. The spidery phenotype achieved rates as high as 4713 mm²/h as observed in plate 13 at 19 h (Figure 3-19; Table 3-3). The expansion rate immediately before the spidery phenotype was visible was 58.50 mm²/h in the same plate 13 at 11 h (Table 3-3). Notably, there was lesser variability in the spreading rates after the spidery phenotype developed as the coefficient of variation per each plate dropped, as shown in box plot (Figure 3-21). In addition to this, there were no statistical significant differences (Appendix ZZ: Table ZZ-2; *P-value* 0.405 > 0.050) between the time of starting swarming (mean = 13.7 h, *SD* = 1.7 h) and developing the spidery phenotype (mean = 12.3 h, *SD* = 3.4 h), when comparing time data from both strains (SBW25 and SBW25Δ*fleQ*) when grown on swarming medium in 15 cm diameter Petri dishes.

Table 3-3 Colony expansion rates per plate before and after the spidery phenotype developed

Plate	Time Before (h)	Colony Expansion Rate Before Spidery Phenotype (mm ² /h)	Time After Initiation (h)	Colony Expansion Rate After Initiation Spidery Phenotype (mm ² /h)
11	3	0.675	17	19.071
	5	4.538	19	77.950
	7	1.127	21	299.078
	9	1.207	23	814.223
	11	0.614	25	3553.851
	13	1.255		
	15	7.094		
12	3	0.490	13	40.628
	5	0.750	15	175.584
	7	3.004	17	626.114
	9	1.132	19	2088.020
	11	7.495	21	3076.058
			23	1725.832
			25	363.432

Plate	Time Before (h)	Colony Expansion Rate Before Spidery Phenotype (mm ² /h)	Time After Initiation (h)	Colony Expansion Rate After Initiation Spidery Phenotype (mm ² /h)
13	3	5.483	13	241.601
	5	0.290	15	618.452
	7	1.376	17	1887.534
	9	6.292	19	4713.044
	11	58.504	21	1757.150
			23	96.157
14	3	1.170	1	4.592
	5	1.308	17	24.771
	7	0.735	19	85.202
	9	0.625	21	334.231
	11	2.787	23	1251.969
	13	1.028	25	2433.800
15	3	0.416	15	36.485
	5	0.436	17	183.940
	7	0.532	19	512.934
	9	0.948	21	1363.588
	11	3.145	23	2876.160
	13	17.350	25	2067.854
16	3	0.500	15	122.264
	5	0.147	17	453.120
	7	1.704	19	1351.724
	9	0.804	21	3207.676
	11	4.648	23	3050.976
	13	42.376	25	1015.871

Note: The time (h) shown corresponds to the time calculated based on Equation 2-2 and colony expansion rate was done based on the data from colony expansion curve in 15 cm diameter plates in swarming medium and recorded, as explained in section 2.4.3.2. The calculations shown are explained in section 2.5.2.



Descriptive Statistics: Rate Before Spidery, Rate Initiate Spidery

Statistics

Variable	Plate	Total								
		Count	Mean	SE Mean	StDev	CoefVar	Minimum	Q1	Median	
Rate Before_Spidery	11	7	2.358	0.940	2.487	105.45	0.614	0.675	1.207	
	12	7	2.57	1.31	2.92	113.51	0.49	0.62	1.13	
	13	6	14.4	11.1	24.8	172.32	0.3	0.8	5.5	
	14	6	1.276	0.320	0.784	61.47	0.625	0.707	1.099	
	15	6	3.80	2.74	6.72	176.55	0.42	0.43	0.74	
	16	6	8.36	6.83	16.74	200.19	0.15	0.41	1.25	
Rate Initiate_Spidery	11	7	953	665	1487	156.10	19	49	299	
	12	7	1157	436	1154	99.81	41	176	626	
	13	6	1552	704	1724	111.04	96	205	1188	
	14	6	689	398	976	141.61	5	20	210	
	15	6	1173	463	1135	96.74	36	147	938	
	16	6	1534	534	1309	85.34	122	370	1184	

Variable	Plate	N for					
		Q3	Maximum	Range	IQR	Mode	Mode
Rate Before_Spidery	11	4.537	7.094	6.479	3.862	*	0
	12	5.25	7.49	7.01	4.63	*	0
	13	32.4	58.5	58.2	31.6	*	0
	14	1.678	2.787	2.162	0.970	*	0
	15	6.70	17.35	16.93	6.26	*	0
	16	14.08	42.38	42.23	13.67	*	0
Rate Initiate_Spidery	11	2184	3554	3535	2136	*	0
	12	2088	3076	3035	1912	*	0
	13	2594	4713	4617	2389	*	0
	14	1547	2434	2429	1528	*	0
	15	2270	2876	2840	2123	*	0
	16	3090	3208	3085	2720	*	0

Figure 3-21 Box plot: Rates of colony expansion before and after the spidery-phenotype developed in SBW25ΔfleQ

The data shown is from each individual replica 15 cm diameter plate depicted in Figure 3-19 and Table 3-3. The time-lapse-photography method was used in order to evaluate the plates. Notably, these plates were not observed concomitantly. Sliding mean rate of all sliding rates per plate was 5.19949 mm²/h (*SD* = 11.92850 mm²/h, *n* = 35); spidery-spreading mean rate of all spidery-sliding rates per replicate was 1181.97 mm²/h (*SD* = 1250.81 mm²/h, *n* = 36). CoefVar: coefficient of variation (%).

Finally, despite the extremely different initial colony expansion rates of strains SBW25 (swimming dependent) and SBW25 Δ *fleQ* (growth only), it was found that both rapidly covered the entire plate after the swarming of SBW25. SBW25 Δ *fleQ* expanded 7832.7 mm² ($SE = 2884.9$ mm²) when compared to the wild type strain SBW25 (mean = 9956.1 mm, $SE = 2811.6$ mm²) over a 22 h period, when grown on 15 cm diameter plates. Notably, no statistically significant differences (P -value 0.610 > 0.050) were found between the colony's area of both strains at 22 h (data analysed from Figure 3-19 and Figure 3-9; Appendix ZS: Figure ZS-3 and Table ZS-1). However, statistically significant differences were observed in the colony's spreading area at 22 h (P -value 0.015 < 0.050) between both strains SBW25 Δ *fleQ* and wild type strain SBW25 whilst comparing their colonies spreading between the two diameter plates: 9 cm and 15 cm (Appendix ZO: Table ZO-2 and Figure ZO-1). Indeed, strain SBW25 Δ *fleQ* was seen to spread less (mean = 2267 mm², $SD = 2390$ mm²) at 22 h in 9 cm diameter plate as compared to the wild type strain SBW25 (mean = 7060 mm², $SD = 499$ mm²) at 22 h in 9 cm diameter plate (data analysed from Figure 3-18 and Figure 3-10). It is notable that the coefficient of variation of the data set (colony's spreading area at 22 h) for strain SBW25 Δ *fleQ* was higher (105.41 %) in smaller Petri dish plates (9 cm diameter) when compared with larger dishes (15 cm diameter) that had a coefficient of variation of 90.22 % (Appendix ZO: Table ZO-2). Whereas for wild type strain SBW25 more variations were found in the colony's area at 22 h (coefficient of variation = 69.17 %) in larger plates (15 cm diameter) as compared with the smaller ones (9 cm diameter) that had a coefficient of variation of 7.07 %. This difference in the colony's area spreading between the two strains in different Petri dish diameter plates could be attributed to not only the physical chemical properties of the medium (humidity content)^{243,290}, but also due to temperature fluctuations in the walk-in incubator, as temperature affects both swarming and growth. When studied in 9 cm diameter plates, the strains SBW25 Δ *fleQ* and wild type strain SBW25 were studied collectively and all their replicates inoculated at the same time/evaluated using the hand-drawn method. Therefore, during the process of comparing colony spreading (area) between different strains, they should be grown within the same Petri dish diameter and run together.

In contrast, flagella driven motility alone with no viscosin production, as in strain SBW25C, resulted in a much slower overall rate of colony expansion (Appendix I: Figure I-3, Figure I-6) and smaller total area covered even compared to strain

SBW25 Δ *fleQ* in 9 cm diameter plates (*P-value* 0.011 < 0.050; Appendix ZR: Table ZR-1 and Figure ZR-3), which produced viscosin but was aflagellate (Figure 3-35). The strain SBW25C did not swarm and this highlights the important role of viscosin dependent swarming (with flagella) or spidery-spreading (in the absence of flagella) in rapid movement to nutrient rich areas of the plate^{70,76,193, 244-247}.

Strains SBW25, SBW25C (only swims) and SBW25 Δ *fleQ* (spidery-spreads) showed variation as a consequence of different times of initiation of spreading (Appendix I: Figure I-2, Figure I-3). Also, the high variability observed in colony spreading of aflagellate strains was also caused by their dependence on physical properties of the agar and water content on the surface^{243,290} (Table 3-6 and Figure 3-35).

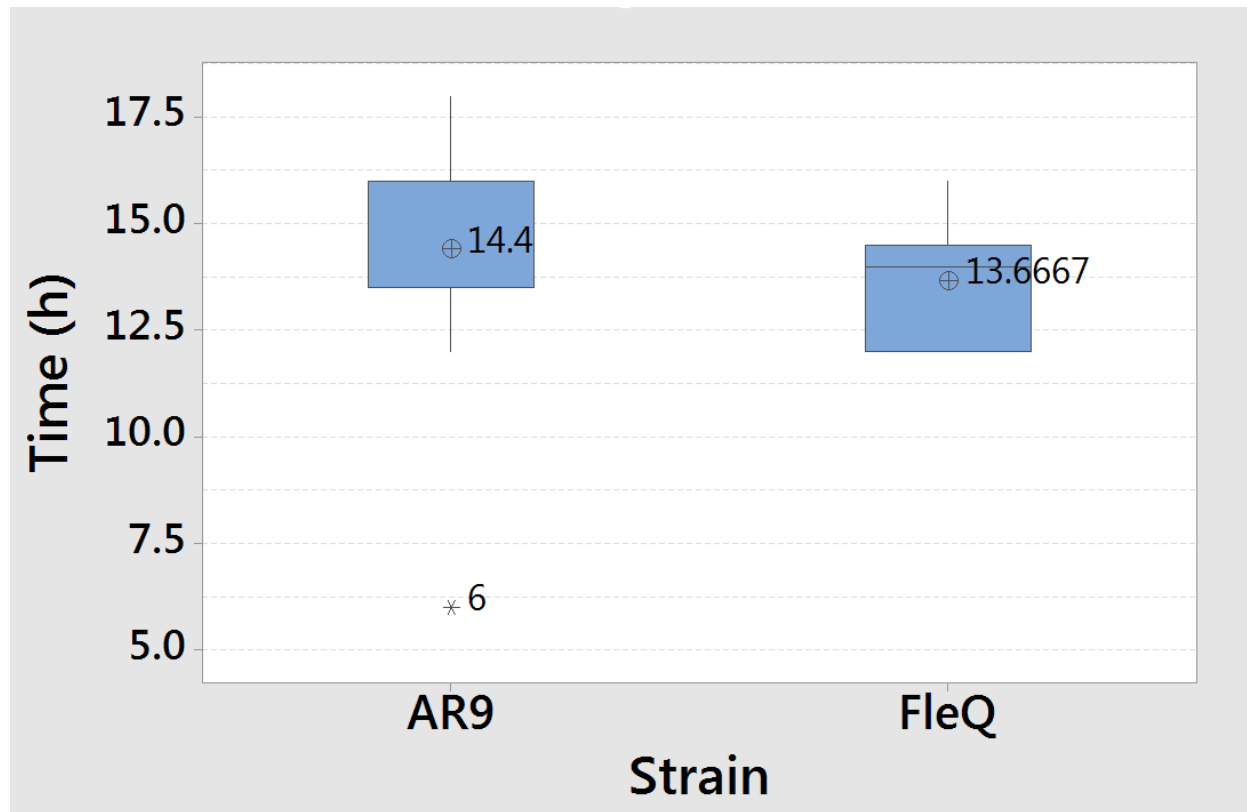
3.4.2 Overproduction of the biosurfactant viscosin hinders spidery-spreading movement in strain AR9

Following transposon mutagenesis of SBW25 Δ *fleQ*, one isolate AR9 (Δ *fleQ* PFLU_0129:: IS- Ω -Km) was shown to overproduce viscosin¹⁰⁷. Colony expansion of this strain on swarming media was also monitored to assess the impact of overproduction of viscosin on spidery spreading motility (Movie 2). The time for development of spidery phenotype was 14.40 h (*SE* = 1.07 h) when grown on swarming medium without kanamycin. This was not statistically different (*P-value* 0.626 > 0.050) from the earlier value obtained for SBW25 Δ *fleQ* (mean = 13.67 h, *SE* = 0.62 h), which produced viscosin at normal levels (Figure 3-22; Table 3-2).

On the other hand, kanamycin appeared to inhibit the motility of AR9. Only one out of ten replicates showed colony spreading, when kanamycin was included in the medium (Figure 3-23B; Appendix I: Figure I-4 and Figure I-5). This might be related to expression and activity of enzyme kanamycin-neomycin phosphotransferase (gene *aphA*) carried in the transposon IS- Ω -Km²⁶⁸. This enzyme deactivates kanamycin to prevent mistranslation or the premature termination of proteins²⁰¹ by catalyzing the transfer of γ -phosphoryl group of ATP to the 3'-hydroxyl of kanamycin²⁶⁹. Therefore kanamycin was omitted from colony spreading experiments for draining metabolic ATP to characterise and compare different strains in swarming medium. Strain AR9 moved slower than SBW25 Δ *fleQ* in the absence of kanamycin, covering less area at 24 h, 916.47 mm² (9 cm diameter plates) when compared to 2156.35 mm² (9 cm diameter plates), respectively (Figure 3-23A; Figure 3-18). Strain AR9 spread slower than

SBW25 Δ *fleQ* in the absence of kanamycin, covering less area at 24 h, 916.47 mm² (9 cm diameter plates: including the outlier replicate 5) as compared to 2156.35 mm² (9 cm diameter plates: replicate 4 covered the plate at 16 h hence, it was not included in the analysis), respectively (Figure 3-23A; Figure 3-18). When comparing the spidery spreading of strains AR9 and SBW25 Δ *fleQ* in motility plates of 9 cm diameter, more variability in the data set of the colony's area was observed at 24 h for strain AR9 (coefficient of variation 137.21 %: including the outlier plate 5) as compared with SBW25 Δ *fleQ* (coefficient of variation 83.08 %: plate 4 was excluded as the colony covered the plate at 16 h), data analysed from Figure 3-18 and Figure 3-23A. Meanwhile, for strain SBW25 Δ *fleQ*, more variability was observed among the different replicates when comparing the colony's area at 24 h in 9 cm diameter (coefficient of variation = 83.08 %) plates with 15 cm diameter plates (coefficient of variation = 62.66 %), see Appendix ZP: Table ZP-1 and Figure ZP-2. This difference in variability in the data (colony's area) from different Petri dish diameters might possibly have arisen not only as variability in the amount of inoculum, but also for temperature fluctuations in the walk-in incubator as well as differences in water content in the plates²⁹⁰ owing to the fact that 15 cm diameter plates were prepared individually and placed in the centre of the laminar flow cabinet during their drying time after pouring the molten swarming medium. On the other hand, the smaller plates (9 cm diameter) were studied together and the plates were put in different positions in the laminar flow cabinet. In order to determine whether there were statistically significant differences in colony's area at 24 h between both strains when both grown in 9 cm diameter plates, the outlier (plate 5: colony's area 4281.704 mm²) was removed from the data set of strain AR9. Statistically significant differences (*P-value* 0.016 < 0.050) were found in the colony spreading between strains AR9 and SBW25 Δ *fleQ* at 24 h - when grown in swarming medium on 9 cm diameter plates (Appendix ZQ: Figure ZQ-4 and Table ZQ-2). If included the outlier plate 5 of strain AR9 (colony's area at 24 h of plate 5 was 4281.704 mm²) and plate 4 of strain SBW25 Δ *fleQ* that covered the 9 cm plate at 16 h (colony's area at 16 h: 7226.4 mm²), it was observed statistically significant differences (*P-value* 0.038 < 0.050) between the colony's spreading areas between both strains at 24 h in swarming medium in 9 cm diameter plates (9 cm diameter plate area: 7226.4 mm²), see Appendix ZQ: Figure ZQ-4 and Table ZQ-2. This might be explained by the overproduction of the biosurfactant impeding cell expansion since the bacteria were looser, and cells must be more compact to slide on the agar surface. It is important to

mention that both strains and their respective replicates were inoculated and studied concomitantly using the hand-drawn method.



Variable	Strain	Total Count	Mean	SE Mean	StDev	CoefVar	Minimum	Q1	Median	Q3
Time (h)	AR9	10	14.40	1.07	3.37	23.42	6.00	13.50	16.00	16.00
	FleQ	6	13.667	0.615	1.506	11.02	12.000	12.000	14.000	14.500

Variable	Strain	Maximum	Range	IQR	Mode	N for Mode
Time (h)	AR9	18.00	12.00	2.50	16	5
	FleQ	16.000	4.000	2.500	14	3

Factor Information

Factor	Levels	Values
Strain	2	AR9, FleQ

Analysis of Variance

Source	DF	Seq SS	Contribution	Adj SS	Adj MS	F-Value	P-Value
Strain	1	2.017	1.74%	2.017	2.017	0.25	0.626
Error	14	113.733	98.26%	113.733	8.124		
Total	15	115.750	100.00%				

Figure 3-22 Box plot: Appearance of the spidery phenotype in aflagellate strains with different levels of viscosin production

Analysed data from Figure 3-18 and Figure 3-23. Both strains were grown on swarming medium (no kanamycin). Plates 15 cm diameter for SBW25Δ*fleQ*; plates 9 cm diameter for AR9. The viscosin overproducer strain AR9 (*Fla*⁻, *Visc*^{*}) formed the spidery phenotype at the same time of SBW25Δ*fleQ* (*Fla*⁻, *Visc*^{*}) which had normal levels of viscosin. The value shown inside each box plots are the mean time to appear the spidery phenotype.

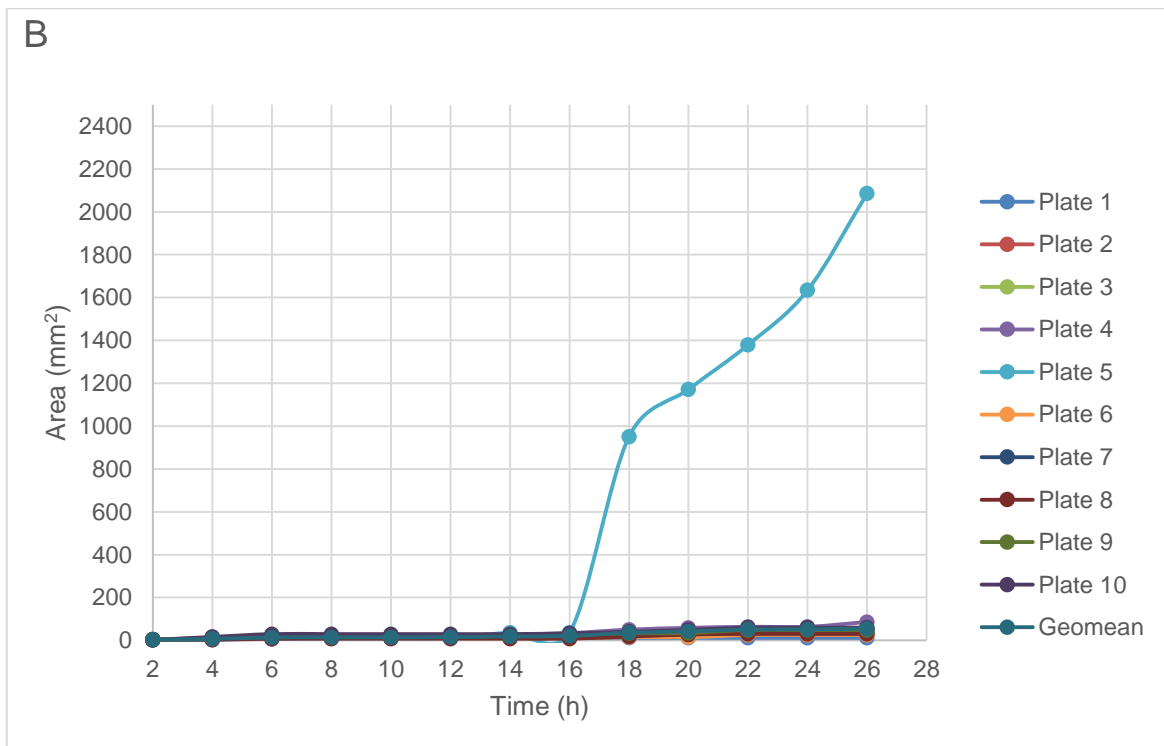
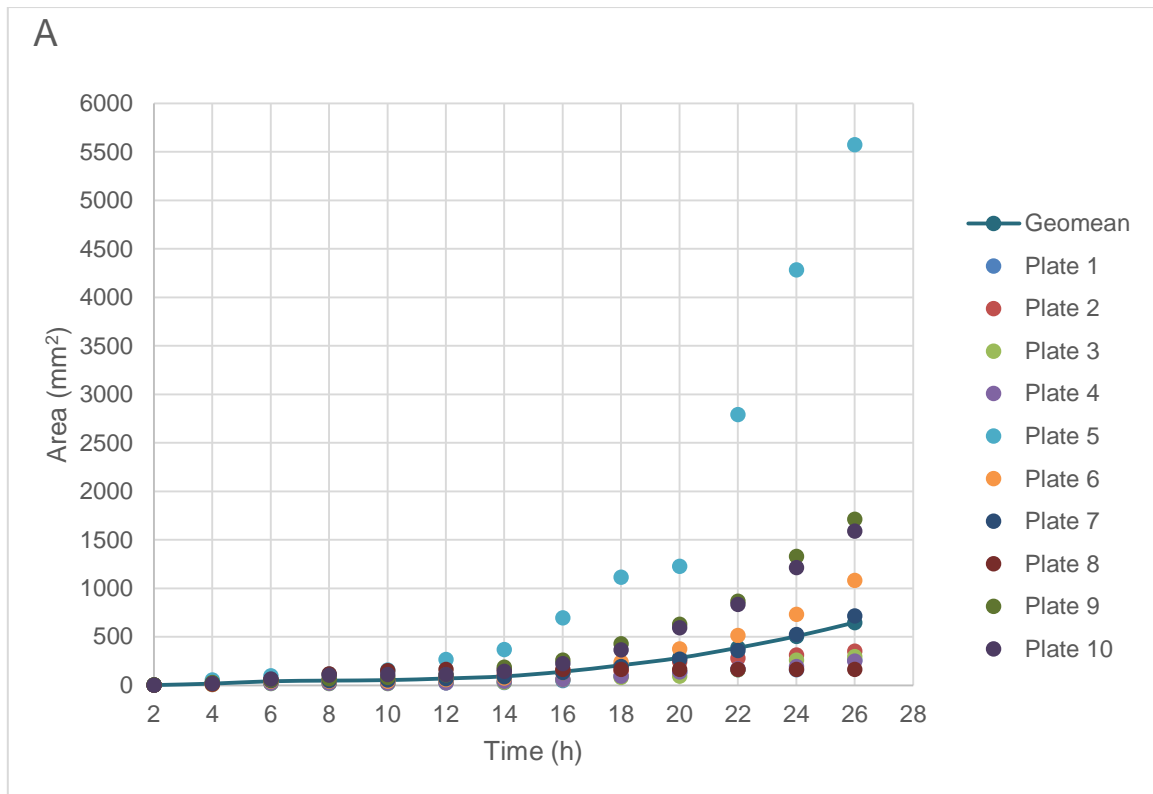


Figure 3-23 Colony expansion curves of strain AR9 in swarming medium with and without kanamycin supplementation

The presence of kanamycin slowed down the spidery-spreading of the colonies. All colony expansion curves were constructed using 9 cm diameter plates (area 7226.4 mm²). (A) No supplementation with kanamycin. (B) Supplementation with kanamycin. Strain AR9 phenotype: *Fla*⁻, *Visc*^{*}.

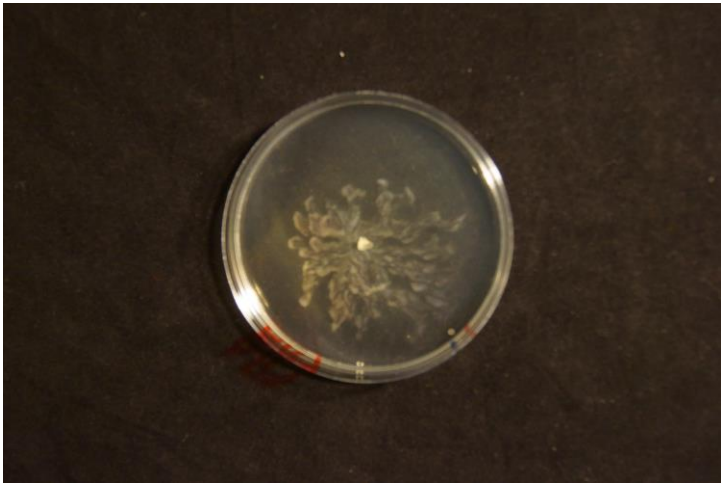
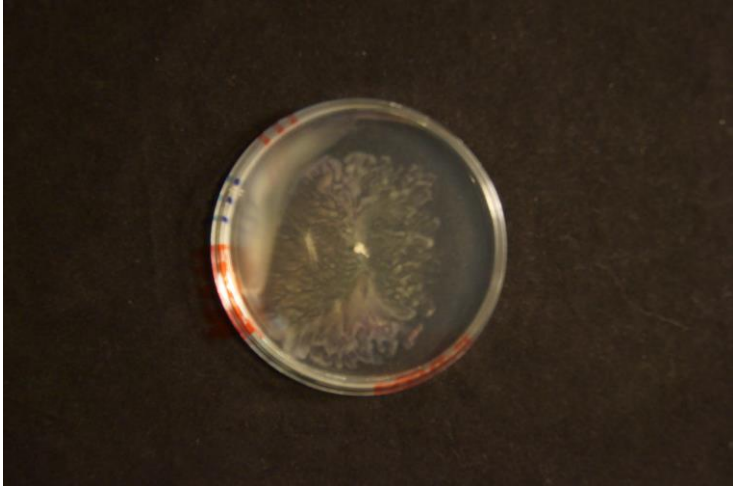
Swarming medium non reformed with kanamycin	
Strain	Time: 24 h
AR9 (<i>Fla⁻</i> , <i>Visc⁺</i>)	
SBW25Δ <i>fleQ</i> (<i>Fla⁻</i> , <i>Visc⁺</i>)	

Figure 3-24 Spidery phenotype of aflagellate strains AR9 and SBW25Δ*fleQ*

Swarming medium (no kanamycin) on 9 cm diameter plates. AR9: a typical dendritic sliding colony is shown. The colony (yellow) was not branched as extensively, and entails wider tendrils, compared to SBW25Δ*fleQ*. AR9 rarely formed these tendrils in medium supplemented with kanamycin. SBW25Δ*fleQ*: sliding colony was dendritic (yellow). The colony was branched more extensively, whereas the tendrils were slender.

3.4.3 Sessile strains AR1 and AR2 exhibit cumulative growth on the surface of agar

The aflagellate strains AR2 (*ΔfleQ viscB*:: IS-Ω-Km/hah) and AR1 (*ΔfleQ viscC*:: IS-Ω-Km/hah) each carry a transposon insertion within a *visc* gene required for viscosin production. Both have been shown not to produce viscosin^{107,109}. When analysed in the swarming medium assay, the colony phenotypes of these strains were identical. Both had a dot shaped appearance due only to cumulative growth (Figure 3-25; Figure 3-26). As they were unable to undergo viscosin dependent spidery-spreading, colonies

these sessile bacteria covered a very small average area (mean = 23.9 mm², SD = 4.5 mm²) compared to the spidery-spreading aflagellate strain SBW25Δ*fleQ* (mean = 11104.5 mm², SD = 6958.5 mm²) following 24 h incubation (Figure 3-35; Table 3-6). Cumulative growth curves, for strains AR1 and AR2 exhibited the same pattern (Figure 3-27 and Figure 3-28) with a slight sigmoidal appearance. These sessile strains also showed a slower initial phase and slightly faster later phase of colony expansion (Figure 3-29 and Figure 3-30). In addition to this, the cumulative growth rates (mm²/h) calculated per replicate and strain showed no differences in rate between both sessile strains (Figure 3-29). Additionally, there were no statistical significant differences (*P*-value 0.103 > 0.050) between colony area covered at 24 h for both sessile strains AR1 and AR2 (Appendix I: Table I-1; Figure 3-25). There were differences in variability in the colony expansion curves of multiple replicates for either of these sessile strains. The coefficient of variation of colony's area at 24 h of strain AR1 was 18.62 %, whereas for strain AR2 was 37.50 %, see Figure 3-27 and Figure 3-28. Therefore, the amount of inoculum, temperature changes in the walk-in incubator, differences in humidity among the motility plates affected the variability of the results and the colony expansion curves for sessile strains (Figure 3-25 and Table 3-6).

It is interesting to note that, despite being sessile, strains AR1 and AR2 (Movie 13) also demonstrated a small change in both their rate of colony expansion (cumulative growth) and acceleration (Appendix I: Figure I-8 and Figure I-9), also at around 10 h. The mean rate of cumulative growth for all the replicates of strain AR1 during the slow phase was 4.55303 mm²/h (SD = 2.09823 mm²/h), whereas the mean rate of cumulative growth for all replicates during the course of the fast phase was 17.7882 mm²/h (SD = 4.29865 mm²/h), see Figure 3-29 and Figure 3-30. For strain AR2, the average rate of cumulative growth for all replicates was 5.63100 mm²/h (SD = 3.46078 mm²/h) during the slow phase and 19.8903 mm²/h (SD = 10.0293 mm²/h) for the fast phase (Figure 3-29 and Figure 3-30). The average cumulative growth rate of all rates calculated per plate for strain AR1 was 11.8531 mm²/h (SD = 7.74820 mm²/h). Meanwhile the mean cumulative growth rate of all rates calculated per replicate for strain AR2 was 16.2265 mm²/h (SD = 10.8013 mm²/h). On the basis of cumulative growth curve (geomean of all replicates), the mean rate of cumulative growth for strain AR1 from 2 h to 8 h was found to be 0.546 mm²/h and 0.707 mm²/h for AR2 (2 h to 8 h). If calculated from 2 h to 24 h, it was 0.968 mm²/h (reported as 1 mm²/h) for strain

AR1 and 1.080 mm²/h (reported as 1.1 mm²/h) for strain AR2. Finally, growth dependent colony expansion of AR1 and AR2 was low, approximately 1 mm²/h based on the data presented in the colony expansion curves (Figure 3-27; Figure 3-28).

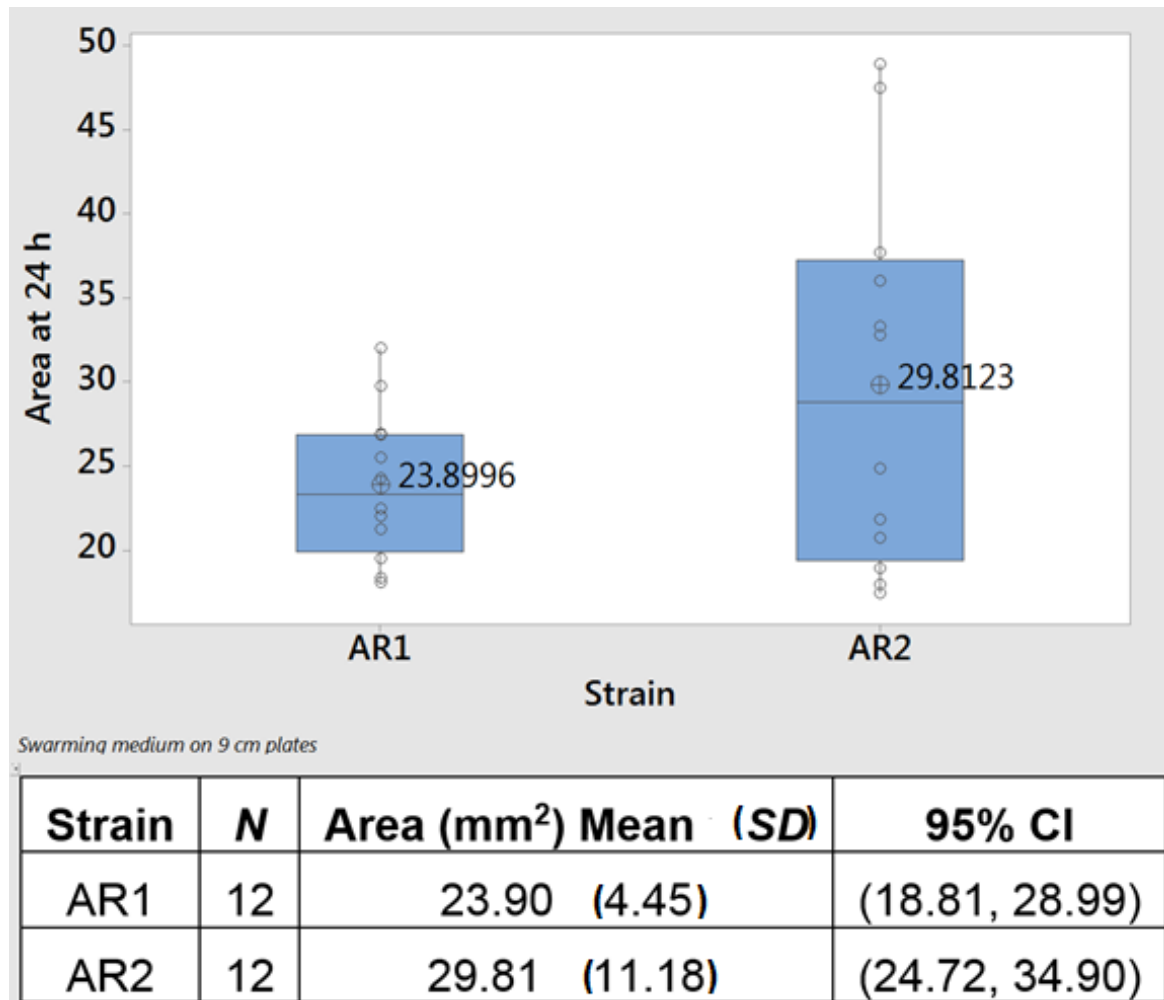


Figure 3-25 Box plot: Comparison of colony's area from both sessile strains AR1/AR2 at 24 h

The data analysed are from the individual cumulative growth curves (Figure 3-27 and Figure 3-28) conducted in swarming medium without kanamycin on plates 9 cm diameter (area: 7226.4 mm²). The value shown inside each box plot is the average colony area (mm²) at 24 h.

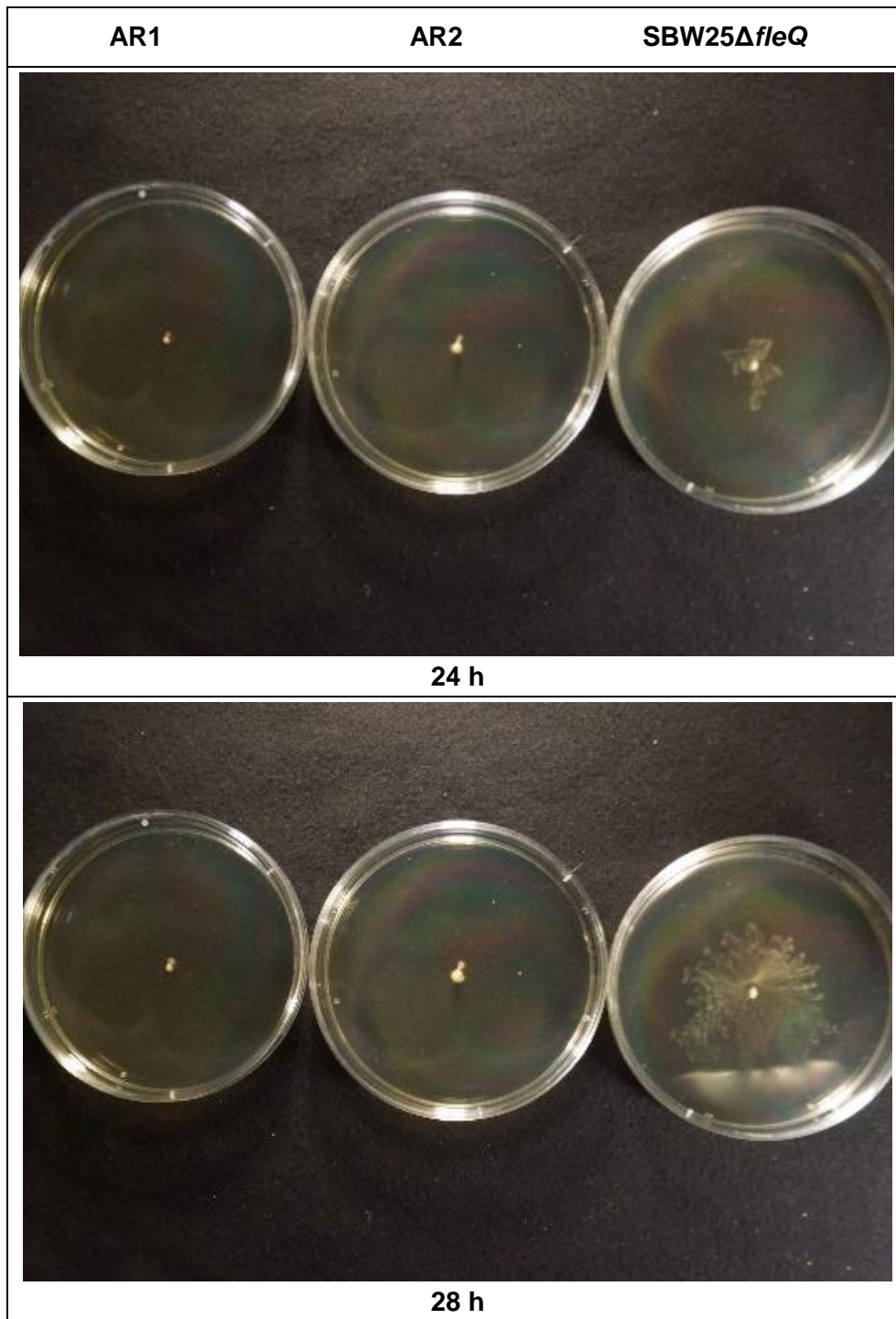


Figure 3-26 Phenotypes of sessile strains AR1, AR2 and the spidery-spreading strain SBW25 Δ *fleQ*

Strains grown on 0.25 % agar LA (no kanamycin) on 9 cm diameter plates. Two example time points are shown.

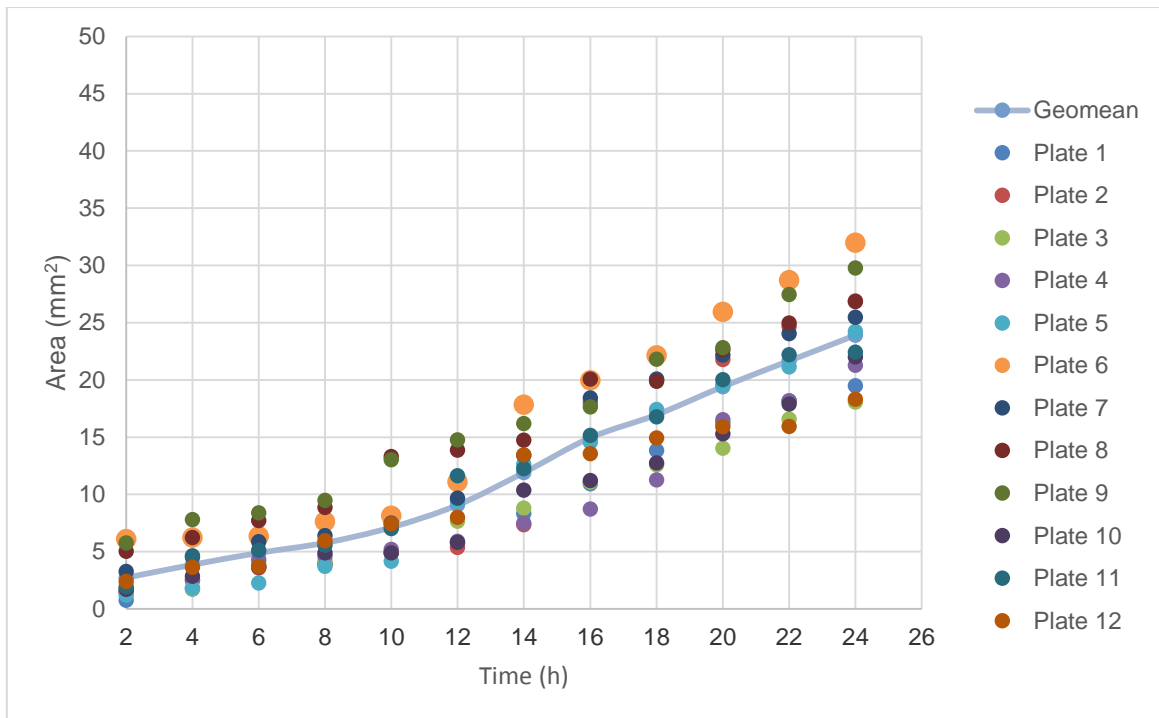


Figure 3-27 Cumulative growth curve of strain AR1

The geomean of all replicates is shown. Methods: hand-drawn (replicates 1 to 6) and time-lapse (replicates 7 to 12). Swarming medium without antibiotic on 9 cm diameter plates.

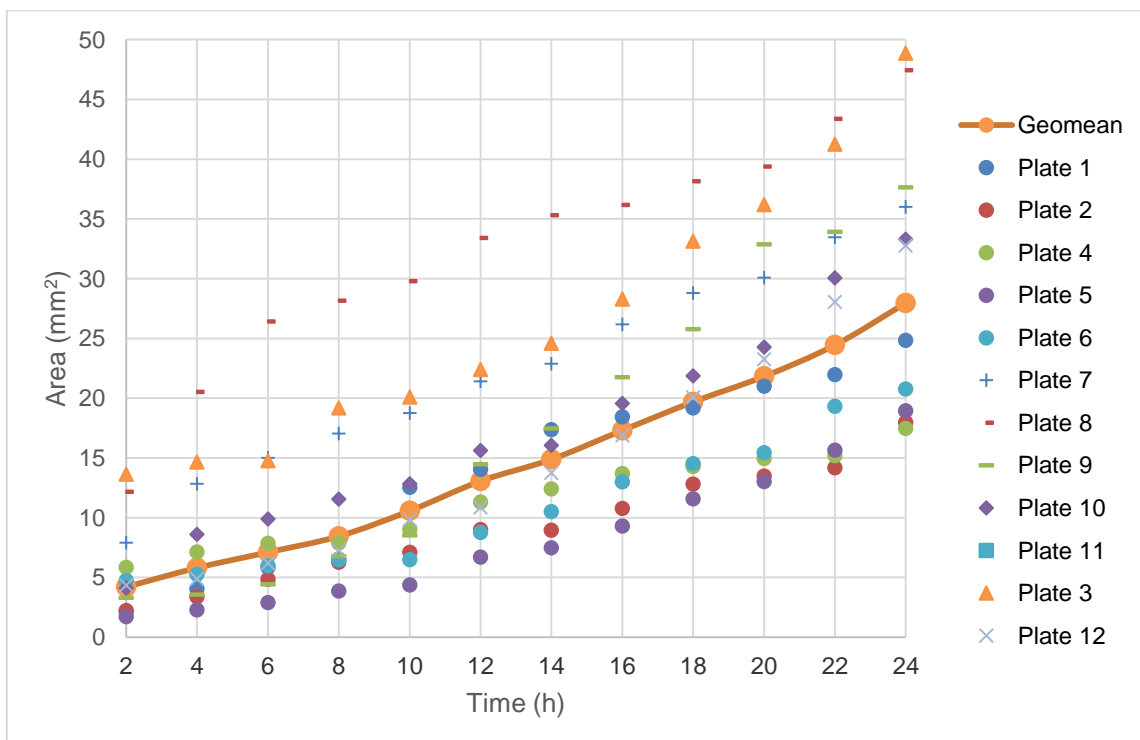


Figure 3-28 Cumulative growth curve of strain AR2

The geomean of all replicates is shown. Methods: hand-drawn (replicates 1 to 6) and time-lapse (replicates 7 to 12). Swarming medium without antibiotic on 9 cm diameter plates.

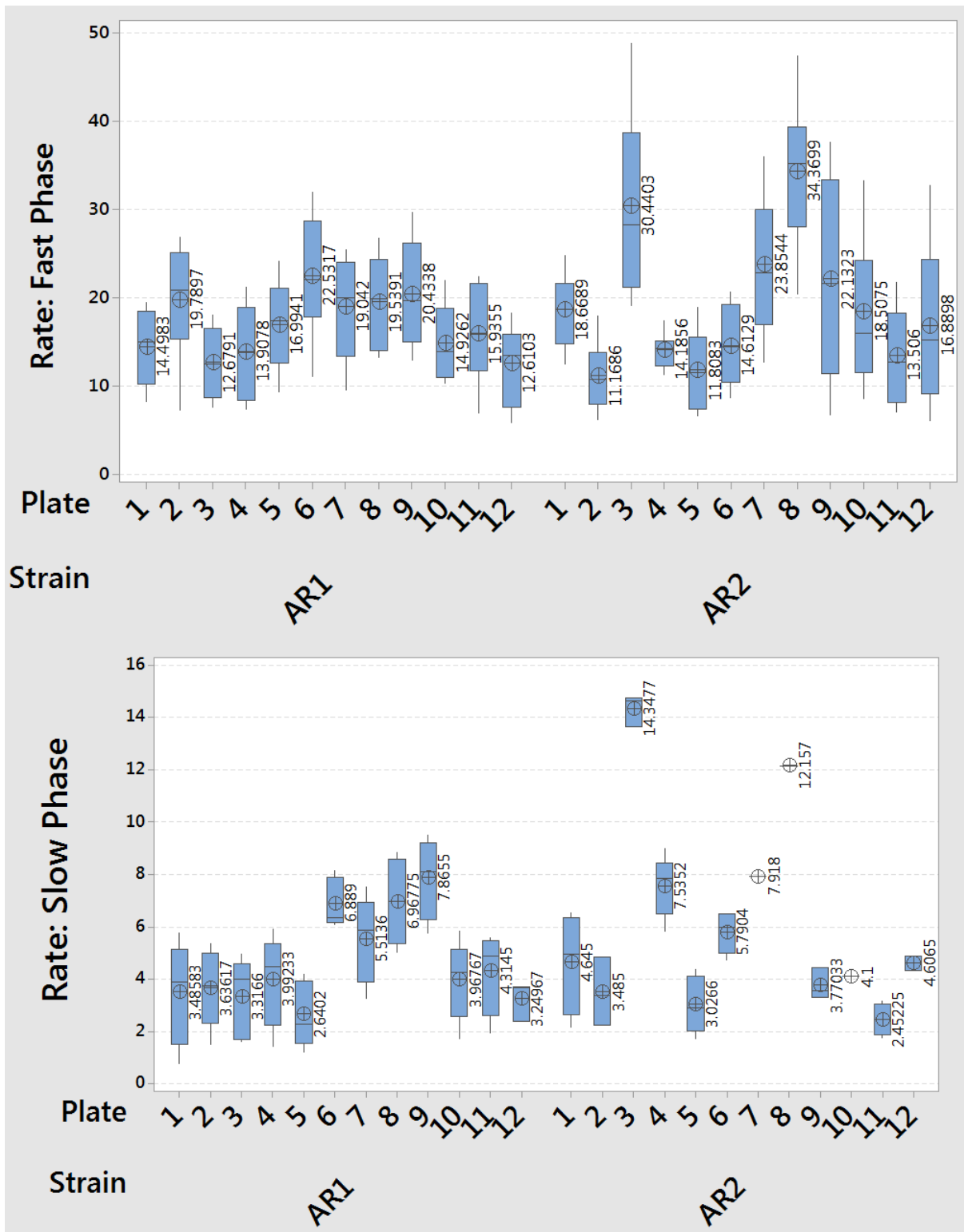
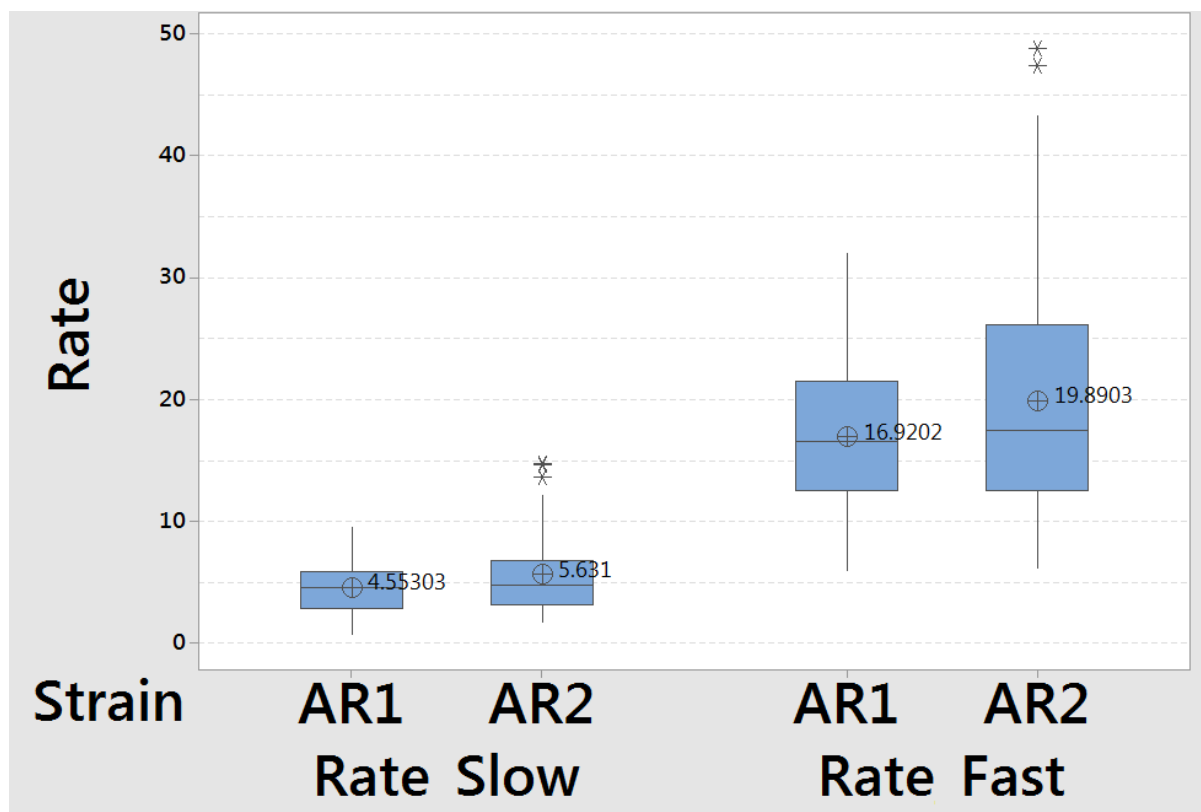


Figure 3-29 Box plot: Cumulative growth rates for sessile strains AR1/AR2

The data analysed correspond to each individual replicate and strain (Figure 3-27; Figure 3-28). The value next to each box plot is the average cumulative growth rate (mm²/h). Swarming medium without antibiotic on 9 cm diameter plates.



Variable	Strain	Mean	SE Mean	StDev	CoefVar	Minimum	Q1	Median	Q3
Rate_Slow	AR1	4.553	0.273	2.098	46.08	0.767	2.845	4.631	5.861
	AR2	5.631	0.569	3.461	61.46	1.720	3.220	4.746	6.828
Rate_Fast	AR1	16.920	0.649	5.979	35.34	5.952	12.601	16.569	21.529
	AR2	19.890	0.970	10.029	50.42	6.205	12.542	17.463	26.162

Variable	Strain	Maximum	Range	IQR	Mode	N for Mode
Rate_Slow	AR1	9.493	8.726	3.016	*	0
	AR2	14.754	13.034	3.608	*	0
Rate_Fast	AR1	31.983	26.031	8.929	20.066	2
	AR2	48.845	42.640	13.620	*	0

Figure 3-30 Box plot: Mean rates of cumulative growth during the slow and fast phases for both sessile strains AR1/AR2

The analysed data were obtained from their respective cumulative growth curves (Figure 3-27; Figure 3-28), obtained in swarming medium without kanamycin on 9 cm diameter plates. The average cumulative growth rate (mm^2/h) of all individual cumulative growth rates per replicate over a period of 24 h, for each phase and strain are presented separately. The value shown inside each box plot is the average colony expansion rate (mm^2/h) for all rates calculated per plate, shown in Figure 3-29; additionally this averaged value is also represented as a cross-circle inside the box plot. The shaded area represents the 25th to 75th percentiles. The median is shown as a line inside the box plot, and the whiskers represent the upper limit ($Q_3 + 1.5 \times \text{IQR}$) and lower limit ($Q_1 - 1.5 \times \text{IQR}$). The stars indicate outliers in the observations that are outside these limits. $Q_1 = 25^{\text{th}}$ percentile, $Q_2 = 75^{\text{th}}$ percentile, $\text{IQR} = \text{Interquartile Range}$.

3.5 Growth Curves and Phenotype

Growth in minimal medium M9 (broth) permits quantitation of efficiency of growth on specific nutrient sources. In this study, the sessile strains AR1 and AR2 (*Fla*⁻, *Visc*⁻) and non-sessile strain SBW25 Δ *fleQ* were to be used as parent strains to assess the influence of different nitrogen sources on evolution swimming mutants via rewiring of the NtrBC system for the expression of the flagella regulon. Hence, it was important to initially establish growth properties of these strains in each of the nitrogen sources to be tested, ammonia, glutamate and glutamine. Each nitrogen source (10 mM) was tested in M9 minimal medium with glucose as a sole (with ammonia) or additional (with glutamate or glutamine) carbon source (see section 2.3.1.3 for recipes). Assays were performed in a microtitre plate assay with strong and continuous shaking to ensure an adequate oxygen supply for these mutant strains because *P. fluorescens* SBW25 is an obligate aerobe gaining energy via aerobic respiration^{18,23,39}.

Growth of the wild type strain SBW25 was initially assessed in each medium (Figure 3-31). SBW25 grew well in the rich medium LB. It rapidly entered exponential phase at around 3 h, reached an OD₆₀₀ of 1.50 (*SD* = 0.12) by 10 h, which represented late-exponential/early stationary phase. In contrast, growth was much lower in M9 medium (broth) with glucose and each of the different nitrogen sources. There was a longer lag phase to around 5 h and a slower exponential increase in density. By around 10 h, as with growth in LB, cultures with glutamine or glutamate as nitrogen source had reached late exponential phase, entering stationary phase between 10 h and 12 h. Growth with ammonium as nitrogen source was slower, although by late stationary phase it did reach the same density as growth on glutamate. As 10 h represented late exponential phase, this was selected as a suitable time point to compare all strains and culture media. With wild-type and glutamine as nitrogen source at 14 h the OD₆₀₀ was 0.8 (*SD* = 0.1), with glutamate it was 0.7 (*SD* = 0.1) and with ammonium as nitrogen source growth at 10 h the OD₆₀₀ was 0.5 (*SD* = 0.0) (Figure 3-31). The same analysis was then repeated for each of the mutant strains (Figure 3-32). Growth of each strain and each medium were then compared using the 10 h value and are shown as box plots (Figure 3-33, for LB; and Figure 3-34, for minimal medium M9 and different nitrogen sources).

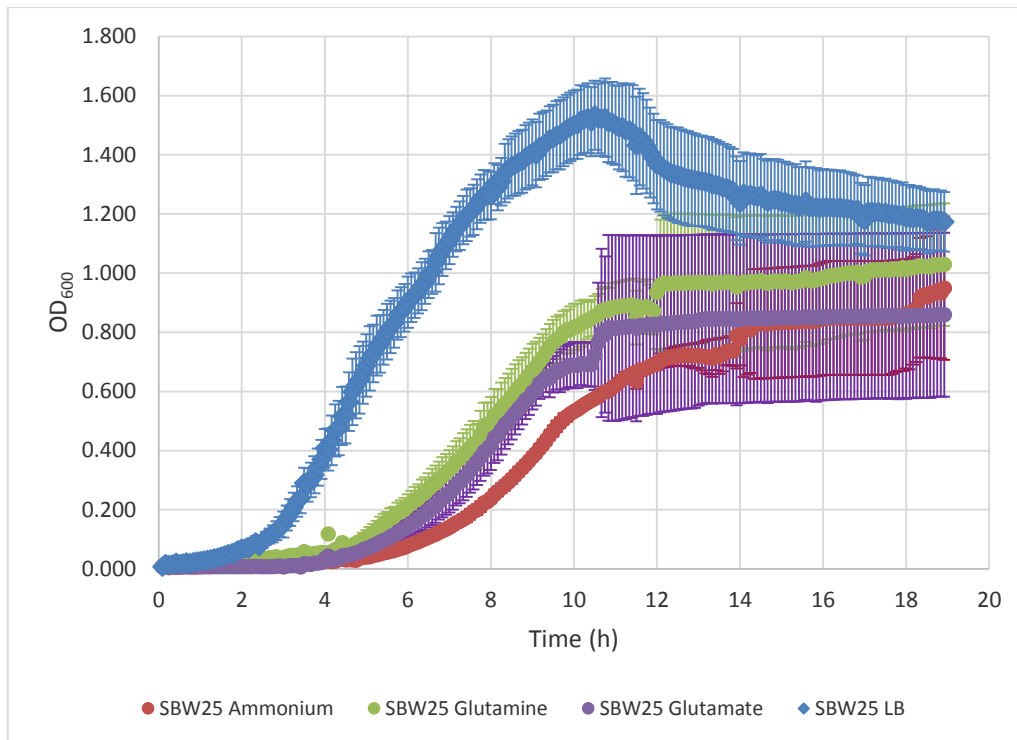


Figure 3-31 Comparison of growth of wild type strain SBW25 in LB or M9 medium (broth) supplemented with different nitrogen sources

Nitrogen sources (10 mM) were as shown and M9 medium also contained glucose (20 % w/v). The data shown is the mean (SD) of $n = 5$ biological replicates. The error bars represent standard deviation. Microtitre plate assay: A 5 μ L volume from an overnight (ON) culture in the test medium was added to 395 μ L of the same test culture medium. The inoculated plates were incubated for 24 h at 26 °C with continuous vigorous shaking in a Bioscreen C™ growth curve analysis system. The zero time absorbances were normalised to 0.008 and the blank values were averaged for each growth medium treatment before being subtracted from their corresponding growth curve.

3.5.1 Rich medium LB

Cultures of the wild type strain SBW25 grew better in LB (Figure 3-31) than all of mutant sessile and non-sessile strains tested (Figure 3-32 and Figure 3-33; Appendix R: Figure R-1, Figure R-2, Figure R-9; Appendix S: Figure S-2). The wild-type strain SBW25 rapidly entered exponential phase at around 3 h, reached an OD₆₀₀ of 1.50 (SD = 0.12) by 10 h, which represented late-exponential early stationary phase. There was no difference in growth of any of the aflagellate strains SBW25 Δ *fleQ*, AR1, AR2, and AR9 (*Fla*⁻, *Visc*^{*}). All reached an OD₆₀₀ of around 1.2 at 10 h. Therefore, despite the fact that flagella expression is energy demanding²⁴², mutants without flagella grew more poorly. This could be a preliminary indication that absence of the master flagella regulator FleQ impairs metabolism. Despite the fact that SBW25 Δ *fleQ* (*Fla*⁻, *Visc*^{*})

produces viscosin at normal levels, AR9 (*Fla*⁻, *Visc*^{*}) is an overviscosin producer strain¹⁰⁹ and the sessile strains (AR1 and AR2) do not produce viscosin¹⁰⁹ there was no difference in growth of these strains in LB.

This was in contrast to growth on swarming medium. In semi-solid media viscosin producer strains without flagella covered a large area comparable to wild type strain SBW25, SBW25 Δ *fleQ* spread over 11104.5 mm² (*SE* = 2.8 mm²) by 24 h in swarming medium (Figure 3-35), reflecting substantial growth; whereas, sessile strains covered a smaller area (~26 mm²) and viscosin overproducer strain, AR9, covered 916 mm² (*SE* = 398 mm²). Overproduction of viscosin impeded the translocation of cells, since bacteria must be more compact in order to slide over the agar surface. An excess of this biosurfactant was responsible for the reduced area of spidery-spreading of AR9 (*Fla*⁻, *Visc*^{*}) compared to the area of spidery-spreading strain SBW25 Δ *fleQ* (*Fla*⁻, *Visc*⁺), whereas AR9 did not grow differently in rich-LB medium to SBW25 Δ *fleQ* (Figure 3-33).

3.5.2 M9 medium containing ammonium and glucose

Wild type strain SBW25, sessile strain AR2 (*Fla*⁻, *Visc*⁻), and non-sessile strains AR9 (*Fla*⁻, *Visc*^{*}) and SBW25 Δ *fleQ* (*Fla*⁻, *Visc*⁺) did not grow differently (Appendix S: Figure S-1, Figure S-2; Appendix R: Figure R-1, Figure R-9); however, these strains grew more than the sessile strain AR1 (*Fla*⁻, *Visc*⁻), see Figure 3-32 and Figure 3-34. In contrast, sessile strain AR1 showed remarkably less growth compared to all the other strains (Figure 3-34). Based on this observation, it can be inferred that the location of the transposon within the genomes of sessile strains AR1 and AR2 affected the assimilation of ammonium differently, due to the fact that the mutant strain AR1 grew much less than all the aflagellate mutant strains and the wild type strain SBW25. The aflagellate strains SBW25 Δ *fleQ*, AR2 and AR9 grew equally to the wild type strain SBW25 despite the expression of flagella being energetically demanding. The wild type strain SBW25 grew remarkably better than the sessile strain AR1 (*Fla*⁻, *Visc*⁻), in spite of producing viscosin and flagella, something that AR1 did not.

3.5.3 Glutamine/Glucose M9 treatment

Strain AR9 grew better than the wild type strain SBW25 and all other mutant strains studied (Figure 3-32; Figure 3-34). While the sessile strain, AR1, exhibited a different metabolic pattern for nitrogen metabolism in rich nitrogen sources (it grew less well in

ammonium when compared to AR2), it grew equally to AR2 when grown in glutamine. The growth of SBW25 Δ *fleQ* and SBW25 was not found to be different in glutamine. Whether the absence of flagella and overviscosin production had any impact on the improved growth of strain AR9 (*Fla*⁻, *Visc*^{*}) in glutamine as nitrogen is unknown. However, the aflagellate strain SBW25 Δ *fleQ* (*Fla*⁻, *Visc*^{*}) grew less than AR9 in spite of producing normal levels of viscosin. AR1 and AR2 grew slightly less than the wild type despite the lack of expression of flagella or viscosin production. In summation, possession of the master flagella regulator FleQ did not appear to affect nitrogen metabolism when grown on minimal media M9 (broth). The better growth in glutamine of the aflagellate strains AR9 (mean = 1.0 OD₆₀₀), when compared to SBW25 Δ *fleQ* (mean = 0.8 OD₆₀₀) and the wild type strain (mean = 0.8 OD₆₀₀), did not imply enhanced motility on swarming medium.

3.5.4 Glutamate/Glucose M9 treatment

No growth differences were found in SBW25 Δ *fleQ* (*Fla*⁻, *Visc*^{*}), sessile strains (AR1, AR2) as compared to the wild type strain SBW25 (Figure 3-32; Figure 3-34). In contrast, strain AR9 (*Fla*⁻, *Visc*^{*}) again grew more than all the strains studied, when supplied with poor nitrogen sources. AR9 was found to grow much more than all other strains. Glutamate did not dampen growth in the wild type strain and other mutant strains SBW25 Δ *fleQ*, AR1, and AR2 as they reached 0.6 OD₆₀₀. Meanwhile growth in glutamine of sessile strains AR2 and AR1 were found to be equal but different to the other strains. In glutamate, both sessile strains (AR1, AR2) were not different to SBW25 and SBW25 Δ *fleQ*.

Strain SBW25 and SBW25 Δ *fleQ*, did not exhibit differences in growth under the different nitrogen treatments studied. They only showed a small difference in growth in the rich medium LB. The colony of overviscosin producer strain AR9 (*Fla*⁻, *Visc*^{*}), in spite of growing more than SBW25 Δ *fleQ* and SBW25 in poor nitrogen sources (glutamine or glutamate), and equally to these strains in rich medium LB, covered less area in swarming medium when compared to SBW25 Δ *fleQ* and wild type strain SBW25 (Figure 3-35; Table 3-7). This is readily explained by its ineffective motility.

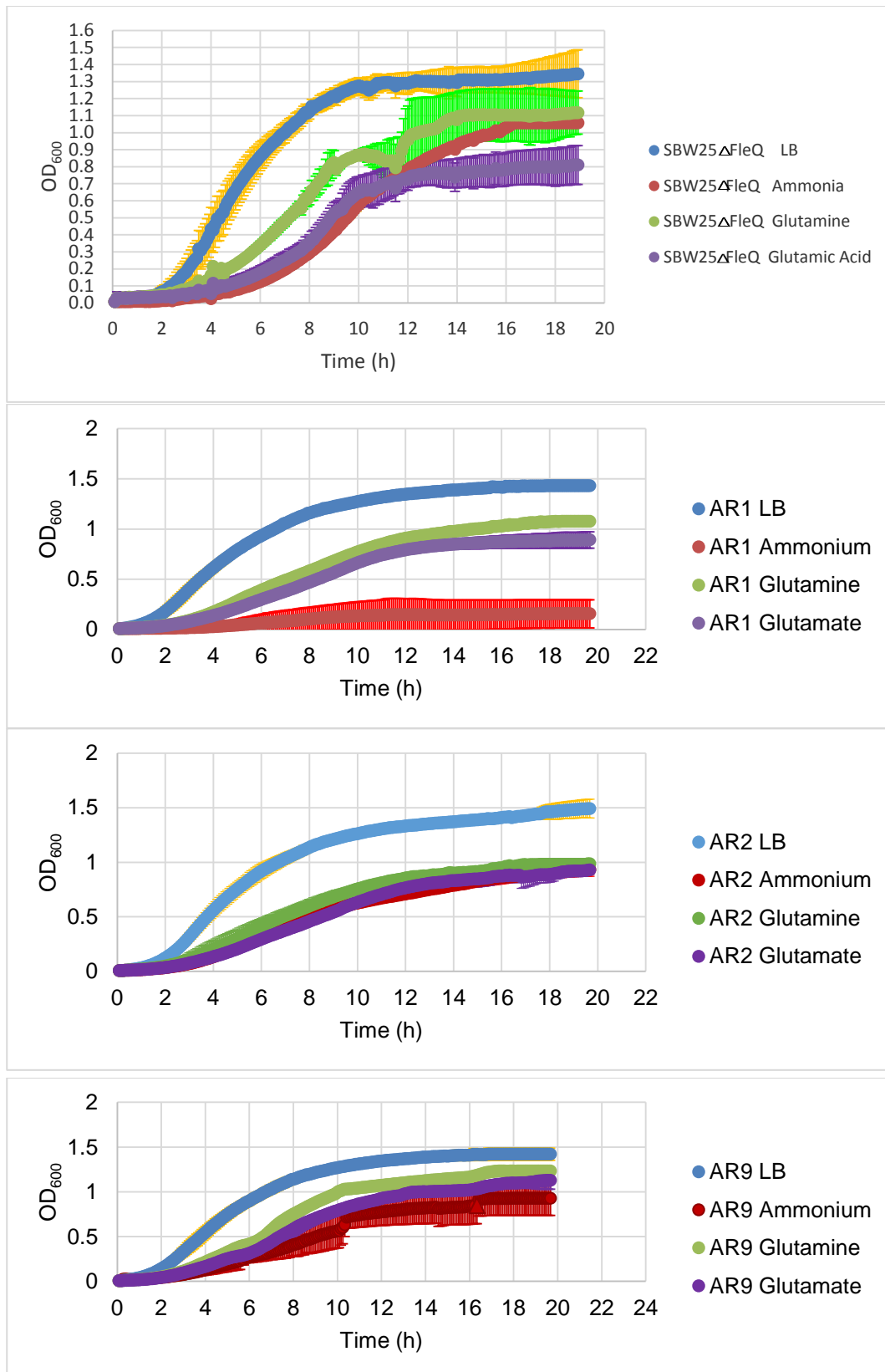
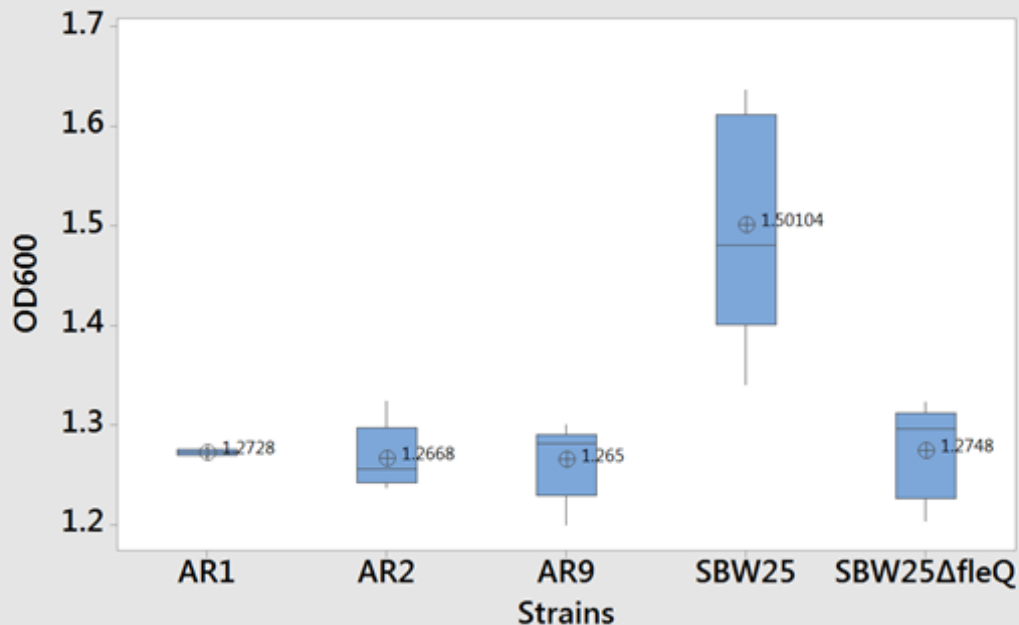


Figure 3-32 Growth curves in rich medium LB and medium M9

The growth curves are the mean of biological replicates ($n=5$), error bars represent standard deviation. See Figure 3-31 for details. Strains are as follows AR1 and AR2 (*Fla*⁻, *Visc*⁻), sessile strains; SBW25Δ*fleQ* (*Fla*⁻, *Visc*⁺) and AR9 (*Fla*⁻, *Visc*⁺). There were different nitrogen/glucose sources. All growth experiments were performed at the same time. AR1 in ammonium was repeated on different occasions. No antibiotic added to any medium.



Luria-Bertani (LB)

Strains	N	OD ₆₀₀ Mean (SD)	95% CI
AR1	5	1.27280 (0.00396)	(1.21748, 1.32812)
AR2	5	1.2668 (0.0342)	(1.2115, 1.3221)
AR9	6	1.2650 (0.0380)	(1.2145, 1.3155)
SBW25	5	1.5010 (0.1154)	(1.4457, 1.5564)
SBW25ΔfleQ	5	1.2748 (0.0477)	(1.2195, 1.3301)

Note: CI: confidence interval.

Figure 3-33 Box plot: Comparison of sessile and non-sessile strains growth in rich medium LB at 10 h

No kanamycin in the medium. Data obtained at 10 h (late exponential / early stationary phase, Figure 3-31 and Figure 3-32) from the growth curves were used for comparison of growth of different strains on LB. AR1 and AR2 (*Fla*⁻, *Visc*^c) denote sessile strains, while SBW25ΔfleQ (*Fla*⁻, *Visc*⁺) and AR9 (*Fla*⁻, *Visc*⁺) represent non-sessile strains. The value shown inside each box plot depicts the average of growth (OD₆₀₀). All growth experiments were performed at the same time.

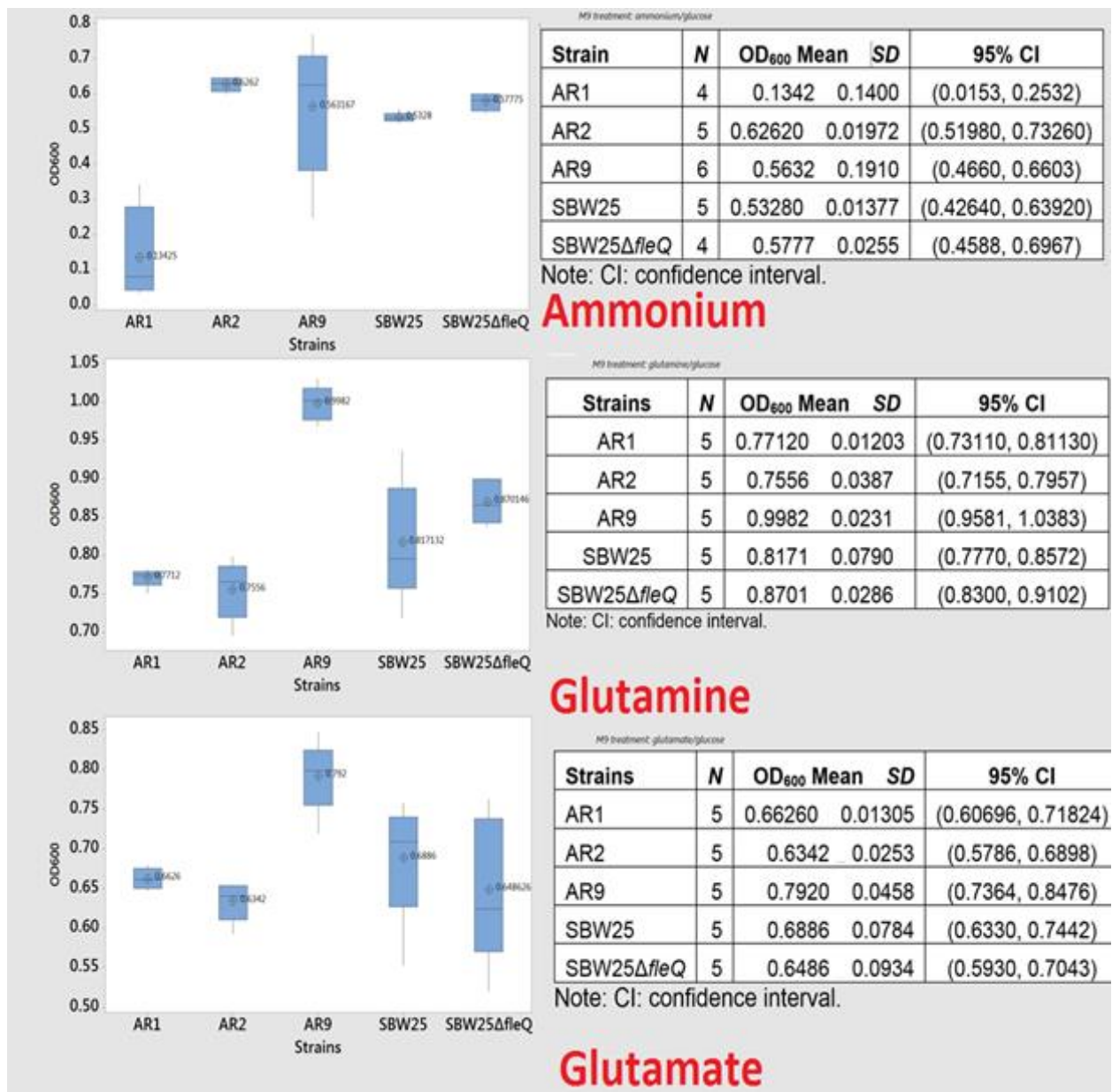


Figure 3-34 Box plot: Comparison of sessile and non-sessile strains growth in nitrogen/glucose M9 medium at 10 h

Data obtained at 10 h from the growth curves (late exponential/ early stationary phase, Figure 3-31 and Figure 3-32) were used for comparison of growth of strains on different nitrogen sources. AR1 and AR2 (*Fla⁻*, *Visc⁻*) denote sessile strains, while SBW25ΔfleQ (*Fla⁻*, *Visc⁺*) and AR9 (*Fla⁻*, *Visc^{*}*) represent non-sessile strains. The value shown inside each box plot denotes the average time of growth (OD₆₀₀). All growth experiments were performed at the same time. No antibiotic added.

3.6 Multivariate analysis: Discriminant

Subsequently, the information obtained from each strain was used in order to conduct a multivariate analysis as described in section 2.16. This statistical analysis identified similar strains and helped in distinguishing from the ones, which are phenotypically different. In accordance with the discriminant analysis, it was deduced that all the analysed strains differed in phenotype (Table 3-4). For example, sessile strains AR1 and AR2 were different despite their passive motility and similar colony phenotype (dot appearance as the cells tended to accumulate in the same place). However, the colony area covered by cumulative growth between both sessile strains at 24 h on swarming medium was not statistically significant different (*P-value* 0.103 > 0.050). Therefore the colony expansion rate was the same for both sessile strains 1 mm²/h (Table 3-7).

The data of the growth (OD₆₀₀) was taken at 10 h of the growth curve of wild type strain SBW25, sessile mutant strains AR1, AR2 (*Fla*⁻, *Visc*⁻) and non-sessile mutant strains AR9 (*Fla*⁻, *Visc*^{*}) along with SBW25Δ*fleQ* (*Fla*⁻, *Visc*⁺). This point of growth curve (10 h) correlates approximately to late exponential phase. At this phase, the population is not influenced by nutrient depletion, or the accumulation of excreted metabolic products in the medium, which triggers changes in their metabolism, phenotype (size and shape), as would occur in the stationary phase. During the stationary phase (starts around 14 h), the rate of cell death is equal to the rate of cell division.

On the contrary, the metabolism of the aflagellate mutant strains (sessile and non-sessile) differed from the wild-type strain SBW25, as they grew less (~1.2 OD₆₀₀ at 10 h) in a rich medium LB than the SBW25 (grew 1.5 OD₆₀₀ at 10 h in a rich medium LB) despite the presence of non-producing flagella, an organelle, which requires a great amount of energy for its production.

Based on the growth observed for different nitrogen sources as well as in rich medium LB, it was possible to infer the existence of metabolic differences between sessile strains (AR1, AR2) and non-sessile strains (SBW25Δ*fleQ*, AR9) as compared to the wild type strain SBW25. In conclusion, all studied strains are phenotypically different as shown in the discriminant analysis (Table 3-4).

Table 3-4 Discriminant analysis**Summary of Classification**

Put into Group	True Group				
	AR1	AR2	AR9	SBW25 Δ <i>fleQ</i>	SBW25
AR1	4	0	0	0	0
AR2	0	5	0	0	0
AR9	0	0	5	0	0
SBW25 Δ <i>fleQ</i>	0	0	0	4	0
SBW25	0	0	0	0	4
Total N	4	5	5	4	4
N correct	4	5	5	4	4
Proportion	1.000	1.000	1.000	1.000	1.000

Correct Classifications

N	Correct	Proportion
22	22	1.000

Note: phenotypes included were growth (OD₆₀₀) under different nitrogen sources with glucose as carbon source, rich medium LB, and colony's spreading area (mm²) in swarming medium at different time points (2 h, 4 h, 6 h, 24 h).

3.7 Summary of the Characteristics of the Strains Studied

The characteristics and phenotype of the studied strains are summarised in Figure 3-35, Table 3-5 and Table 3-7. Colony expansion phenotypes were determined in rich medium 0.25 % agar LA (swarming medium) for all strains, with exception of the initial complementation study of SBW25 Δ *fleQ*, which was studied in swimming medium (0.1 strength LB 0.25 % agar) with the antibiotic gentamycin. *P. fluorescens* SBW25 showed swarming and swimming movement in swarming medium (Movies 8-10), whereas in swimming medium only swimming was observed and very rarely swarming. The swimming medium was used to assess only swimming motility and to corroborate that without flagella a colony is sessile. In contrast, when flagella are expressed swimming results in the formation of circles. Swimming medium helps to determine the difference between swimming and swarming, and the nutritional requirements or percentage of agar to favour any of these different movements¹⁴⁶. Therefore, sliding movement in the aflagellate strain SBW25 Δ *fleQ* occurred independently of the medium used (swarming or swimming medium) because it is completely flagella independent and relies instead on viscosin and cell division and movement over the surface of the medium (Movies 3 and 4).

Both spidery-spreading and flagella-driven movements achieved high rates of colony expansion with maximum rates of expansion at around 25 h (Appendix I). Interestingly,

the colony expansion curves of *P. fluorescens* SBW25 and SBW25 Δ *fleQ* resulting from flagella driven motility and the passive spidery-spreading movement, respectively, exhibited some similarity in phases of colony expansion. The wild-type strain, SBW25, exhibited the following three phases (Figure 3-9, Figure 3-13; Table 3-1):

- An initial or slow phase which lasted for ~10 h, with expansion rate of 26.3 mm²/h up to 8 h. This represented swimming motility and gradually increased, in time. (In the absence, of flagella there was no spread during this period). Swimming dependent spread occurred as a discrete, expanding circle, a consequence of chemotactic response of individual cells.
- A short lag phase where acceleration of expansion decreased or briefly halted. This corresponded with the initial time of visible swarming, average time 12.3 h. A plausible explanation for this might be that many of the cells were undergoing a switch from swimming to the viscosin dependent swarming phenotype and that metabolic changes led to a decrease in motility.
- A final fast phase in which the rate of colony expansion constantly changed and dramatically increased. The duration of this phase was ~15 h or continued till the end of the observation period. This represented the swarming phase. Swarming generally occurred from one side of the swimming circle with rapid initial expansion on one side of the plate, expanding with an average rate of 1162.96 mm²/h. The rapid expansion in area covered is likely to be a consequence of several factors. Bacteria move together as a 'raft' directionally with rapid movement facilitated by viscosin. In addition, diffuse distribution of swarming bacteria would contribute to a rapid increase in area covered, and rapid access to additional nutrients, without necessitating a corresponding increase in bacterial density.

The corresponding three phases with SBW25 Δ *fleQ* (Figure 3-18, Figure 3-21) which exhibited spidery –spreading motility were as follows:

- An initial non-motile growth dependent expansion phase, also generally lasting around 10 h. Expansion in this phase was low ~ 1 mm²/h.
- A short period of visible expansion, corresponding to initial evidence of spidery-spreading phenotype.

➤ A final fast phase of rapid expansion (1182 mm²/h) as cells moved by viscosin dependent sliding as tendrils on the surface of the medium.

In contrast, the sessile aflagellate strains (AR1 and AR2) showed minimal spread (Figure 3-25, Figure 3-29 and Figure 3-30; Table 3-6 and Table 3-7), a consequence of cumulative growth since cells were unable to spread effectively as they produced neither viscosin nor flagella. Unlike motile strains and aflagellate viscosin producer strains, there was no dramatic change in colony expansion rates (highest rate ~50 mm²/h; Figure 3-29, Figure 3-30), although a slow phase (~ 1 mm²/h) comparable to SBW25Δ*fleQ* and later phase with marginally increased rate (~ 2 mm²/h) were recorded.

Both swarming of SBW25 and spidery spreading of SBW25Δ*fleQ* are dependent on viscosin production^{107,233} which in turn has been reported to be controlled by growth phase and quorum sensing^{54,193,238,244}. These factors controlling viscosin production are likely to be a major factor contributing to the similar average time of visible appearance of swarming (12.3 h, SBW25) and spidery spreading phenotype (13. 67 h, SBW25Δ*fleQ*). The reason for the marked variation among replicates in initiation of swarming times in wild-type SBW25 and in spidery spreading of SBW25Δ*fleQ* is less clear. The physicochemical properties of the medium are also likely to have had an impact. In particular, the moisture content of the medium is known to impact swimming and swarming of bacteria through the agar²⁹⁰. For this reason, 0.25 % w/v agar is used. Variation in moisture content could be compounded by the use of lights for photography. For the 15 cm diameter plates which were monitored singly, temperature fluctuations may also have impacted growth density, as growth and imaging was done in a shared walk-in incubator. Oxygen is essential for growth of *P. fluorescens*, each of these factors could impact oxygen availability in individual plates. There was little variation on the swimming dependent colony expansion, therefore it seems less likely that use of a wire stab inoculum had an impact on variation in swarming times.

The growth properties of each parent strain (SBW25Δ*fleQ* and AR2) in minimal media (M9 plus glucose) with the different nitrogen sources (summarised Table 3-7), confirmed the suitability of use of these media as nutrient sources for the evolution study. Growth was best with glutamine, followed by glutamate and then ammonium.

AR2 grew well with both glutamine and glutamate but very poorly when ammonium was the N-source.

Table 3-5 Summary of the characteristics of the studied strains

Strain	Colony Shape	Movement	Phenotype	Mean Rate (mm ² /h) over initial 2 h-8 h	Tranposon	Antibiotic Resistance	Note
SBW25	Circular (yellow)/swarming often from one side	Swimming/Swarming	WT	26.3	None	No	Swarming rate: 1162.95 mm ² /h Swimming rate: 54.01mm ² /h Swarming time: 12.3 h
SBW25C	Circular (yellow)	Swim	<i>Fla</i> ⁺ , <i>Visc</i>	12.1	<i>viscC</i> ::Tn <i>Mod</i> -OKm	^E gentamycin	rate:12.1 mm ² /h
AR1	Dot (yellow)	Sessile	<i>Fla</i> ⁻ , <i>Visc</i>	^A 1.0	<i>viscC</i> ::IS- Ω -Km/hah	^B kanamycin	rate: 1 mm ² /h
AR2	Dot (yellow)	Sessile	<i>Fla</i> ⁻ , <i>Visc</i>	^A 1.1	<i>viscB</i> ::IS- Ω -Km/hah	^B kanamycin	rate: 1.1 mm ² /h
SBW25ΔfleQ	Dendritic (yellow). Extensive branching of colony, with slender tendrils.	Spidery-Spreading	<i>Fla</i> ⁻ , <i>Visc</i> ⁺	1.3	None	No	Sliding-Spidery rate:1182 mm ² /h Spidery phenotype development at 13.67 h
AR9	Dendritic (yellow). Less branching of colony and wider tendrils.	Spidery-Spreading	<i>Fla</i> ⁻ , <i>Visc</i> [*]	6.4	IS- Ω -Km/hah located upstream on PFLU_0129	^B kanamycin	rate: 6.4 mm ² /h
SBW25Q(pfleQ)	Circular	Swimming	<i>Fla</i> ⁺ , <i>Visc</i> ⁺	^c 22.5	None	^D gentamycin	
SBW25Qp	Dot for 24 h, then dendritic	Sessile/Sliding	<i>Fla</i> ⁻ , <i>Visc</i> ⁺	^c 1.2	None	^D gentamycin	
SBW25p	Circular	Swimming	<i>Fla</i> ⁺ , <i>Visc</i> ⁺	^c 9.6	None	No	
AR2S (ΔfleQ ntrB)	Circular	Swimming	<i>Fla</i> ⁺ , <i>Visc</i>	2.2	<i>viscB</i> ::IS- Ω -Km/hah	^B kanamycin	rate:2.25 mm ² /h
AR2F (ΔfleQ ntrB ntrC)	Circular	Swimming	<i>Fla</i> ⁺ , <i>Visc</i>	19.1	<i>viscB</i> ::IS- Ω -Km/hah	^B kanamycin	rate:19.1 mm ² /h

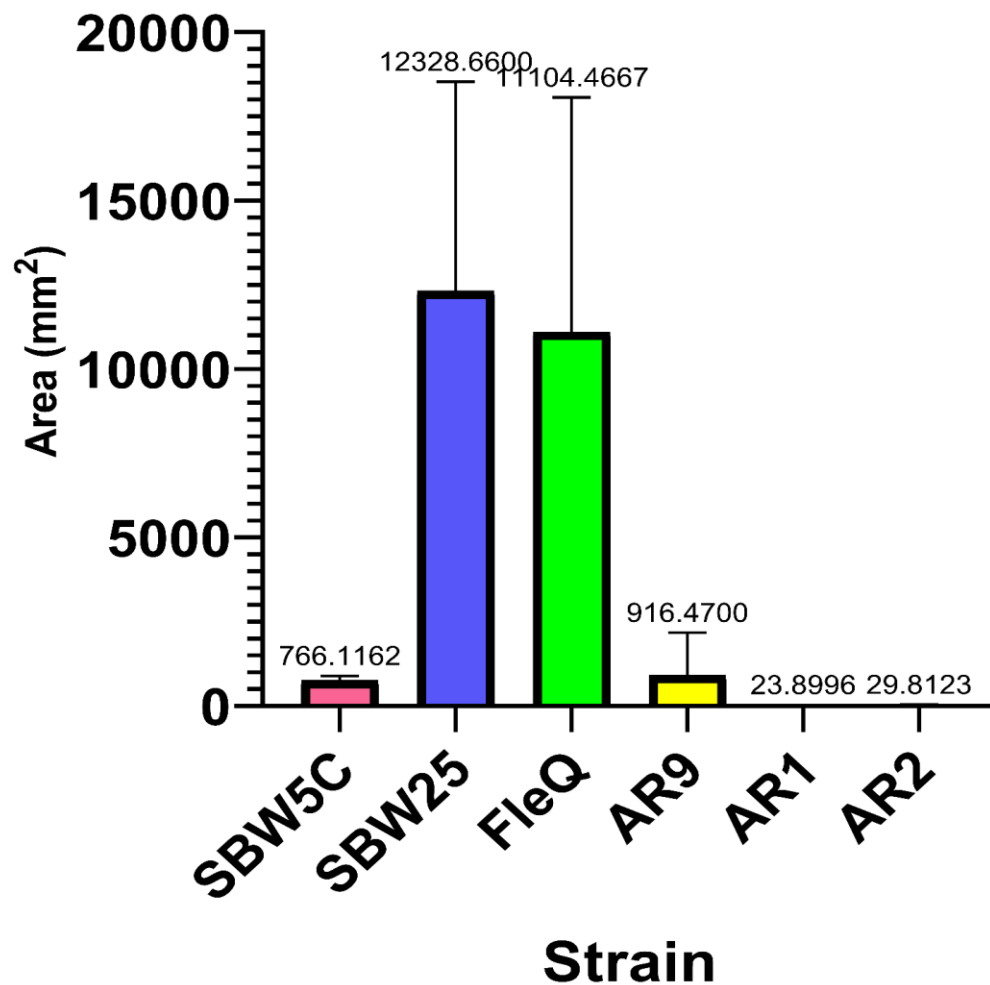
Note: ^AAverage colony expansion rate (mm²/h) over a period of 24 h only for sessile strains AR1/AR2. ^BMechanism of resistance: enzyme aminoglycoside kinase transfers phosphate groups from ATP to kanamycin rendering inactive by diminishing the antibiotic affinity for the bacterial ribosome. This kinase enzyme uses up metabolic ATP. ^CColony expansion rate calculated from data obtained in swimming medium. ^DPlasmid pBBR1MCS-5 carries gentamycin-3-acetyltransferase gene. ^ETn*Mod* plasposon carries gentamycin-3-acetyltransferase gene^{282,283}. *Fla*⁺: flagella, *Fla*⁻: non-flagellated, *Visc*⁺: viscosin, *Visc*⁻: non-viscosin producer, *Visc*^{*}: viscosin overproducer

Table 3-6 Descriptive statistics of colony's area (mm²) at 24 h in swarming medium

Variable	Strain	Total Count	Mean (mm²)	SE Mean	SD	CoefVar (%)	Minimum	Q1	Median	Q3
Area (mm ²)	AR1	12	23.90	1.28	4.45	18.60	18.06	19.93	23.33	26.89
	AR2	12	29.81	3.23	11.18	37.50	17.46	19.40	28.80	37.24
	AR9	10	916	398	1257	137.21	161	185	418	1241
	SBW25Δ <i>fleQ</i>	6	11104	2841	6959	62.66	2460	3179	12745	17052
	SBW25	5	12329	2775	6204	50.33	5082	5677	15560	17364
	SBW5C	12	766.1	37.0	128.1	16.72	538.9	677.2	763.0	821.3

Variable	Strain	Maximum	Range	IQR	Mode	N for Mode
Area (mm ²)	AR1	31.98	13.92	6.96	*	0
	AR2	48.84	31.39	17.83	*	0
	AR9	4282	4120	1056	*	0
	SBW25Δ <i>fleQ</i>	18783	16323	13873	*	0
	SBW25	18713	13632	11687	*	0
	SBW5C	987.2	448.3	144.1	*	0

Note: The data for strains SBW25Δ*fleQ* (*Fla*⁻, *Visc*⁺) and SBW25 were obtained from the colony's expansion curves conducted in 15 diameter plates (Figure 3-9 and Figure 3-19). There were five observations for wild type strain SBW25 because plate 14 swarmed earlier and covered the Petri dish at 22 h. CoefVar: coefficient of variation. SE: standard error. Q₁ = 25th percentile, Q₂ = 75th percentile, IQR = Interquartile Range.



Variable	N	Mean	SE Mean	SD	Coeff'Var	Minimum	Q1	Median	Q3	Maximum	Range
SBW5C	12	796.1	37.0	128.1	16.72	538.9	677.2	763.0	821.3	967.2	448.3
SBW25	5	12328	2775	6204	50.33	5082	5677	15560	17364	18713	13632
FleQ	6	11134	2841	6859	62.65	2480	3179	12745	17052	18763	16323
AR9	10	916	358	1257	137.21	161	185	418	1241	4282	4120
AR1	12	23.90	1.28	4.45	18.63	18.06	19.93	23.33	26.89	31.98	13.92
AR2	12	29.81	3.23	11.16	37.50	17.46	19.40	28.80	37.24	46.84	31.39

Variable	IQR
SBW5C	144.1
SBW25	11687
FleQ	13873
AR9	1056
AR1	6.96
AR2	17.83

Figure 3-35 Average of colony's spreading area in 24 h

Strains SBW25 and SBW25Δ*fleQ* (also known as FleQ) were grown on swarming medium (without antibiotic) on 15 cm diameter plates, while strain SBW25C, AR1, AR2, and AR9 were grown on 9 cm diameter plates. The error bars represent the standard deviation. The value shown above each error bar is the mean.

Table 3-7 Summary of results

Culture Medium								
M9				LB (Mean OD ₆₀₀)	Colony Expansion Rate in 8 h (mm ² /h)	Mean	Area (mm ²) Mean	Observation (swarming medium)
Nitrogen Source								
Strain	NH ₄ ⁺ (Mean OD ₆₀₀)	Glutamine (Mean OD ₆₀₀)	Glutamate (Mean OD ₆₀₀)					
AR1	0.1342	0.7712	0.6626	1.2728	1.0	23.90	Sessile <i>Fla</i> ⁻ , <i>Visc</i> ⁻	
AR2	0.6260	0.7556	0.6342	1.2668	1.1	29.81	Sessile <i>Fla</i> ⁻ , <i>Visc</i> ⁻	
AR9	0.5632	0.9982	0.7920	1.2650	6.4	916.47	Spidery at 14.4 ± 1.1 h (mean ± SE) <i>Fla</i> ⁻ , <i>Visc</i> ⁺	
SBW25Δ <i>fleQ</i>	0.5777	0.8701	0.6486	1.2748	1.3	11104.47	Spidery at 13.7 ± 0.6 h (mean ± SE) <i>Fla</i> ⁻ , <i>Visc</i> ⁺	
SBW25	0.5328	0.8171	0.6886	1.5010	26.3	12328.66	Swarming at 12.3 ± 1.4 h (mean ± SE)	

Note: ^AAverage rate of colony expansion (mm²/h) over a period of 24 h only for sessile strains AR1/AR2. Both sessile strains differ in phenotype. However there were no statistical significant differences between the colony's area covered by both sessile strains in rich medium 0.25 % agar LA (*P*-value 0.103 > 0.050). ^BAverage area (mm²) covered by different strains in 24 h when grown on medium 0.25 % agar LA. ^CGlucose as carbon source. ^DGeomean data used to construct the colony expansion curve was used to calculate the colony expansion rates. The time for development of spidery phenotype for AR9 and SBW25Δ*fleQ* was not statistically different (*P*-value 0.626 > 0.050).

- The strains shaded red grew or the area covered by them was more that the strains shaded yellow.
- The strains shaded blue grew less or the area covered by them was less than the ones shaded yellow.
- The strains shaded green grew less or the area covered by them was less than the strains shaded blue.

4 Evolution of Swimming Motility under Different Nitrogen Sources in the Aflagellate Strain SBW25 Δ *fleQ*

4.1 Introduction

Taylor et al.¹⁰⁸ discovered that the sessile strain AR2 evolved swimming motility upon being starved in a rich medium, 0.25 % agar LA. The evolved strain AR2S¹⁰⁸ eventually formed a bleb, a satellite colony on the border of the main swimming colony, and the strain isolated from this bleb was named AR2F¹⁰⁸. Strain AR2S is a slower swimmer than AR2F, and despite evolving swimming motility¹⁰⁸, these strains swam slower than the wild type strain SBW25. The strains AR2S and AR2F do not produce viscosin due to insertion of a transposon that confers kanamycin resistance. Whole genome sequencing revealed that the mutational event that led to the expression of flagella in the absence of the master flagella regulator FleQ occurred in the NtrBC system in a stepwise manner¹⁰⁸. The slower swimmer, AR2S, possesses a single point mutation in *ntrB*, while the faster swimmer, AR2F has an additional single point mutation *ntrC*; therefore, the faster swimmer AR2F is a double mutant, *ntrB ntrC*¹⁰⁸. The expression profile of nitrogen assimilation genes in AR2S was found to be much higher than the wild type strain SBW25. Thus, it was concluded that nitrogen regulation in this mutant strain is independent of nitrogen levels and over up-regulated¹⁰⁸. In contrast, the expression of the nitrogen assimilation genes in AR2F is more fine-tuned compared to the mutant strain AR2S, and therefore, the second mutational event in *ntrC* has improved the nitrogen regulation in the double mutant strain AR2F¹⁰⁸.

These studies suggest that there has been a re-wiring of the NtrBC system for the nitrogen regulation pathway in order to express the flagella regulon in the absence of the master flagella regulator FleQ. It was hypothesized that the agent of selection was nitrogen limitation; thus triggering the assimilation of nitrogen via the GS/GOGAT [glutamine synthetase (GS)/glutamate synthase (GOGAT)] pathway which is regulated by the NtrBC system. The acidic amino acids aspartic acid (Asp) and glutamate (Glu) and their respective amides asparagine (Asn) and glutamine (Gln) are good substrates to sustain growth in pseudomonads¹⁴⁸. However, only glutamate (Glu) and glutamine (Gln) play a central role¹⁴⁸ for GS/GOGAT pathway, which is the principal route for nitrogen metabolism²⁶⁰. The utilization of glutamine (Gln) and

glutamate (Glu) triggers expression of enzymes e.g. periplasmic glutaminase/asparaginase (PGA)¹⁴⁸ and transporters necessary for their uptake and metabolization, which depend on sigma factor σ^{54} for their expression¹⁴⁸ (refer to section 1.12). Also these amino acids are subject to carbon catabolite repress (CCR) by glucose and Krebs cycle intermediates¹⁴⁸ (refer to section 1.12). As glucose arrests the utilisation of these amino acids as carbon sources, and hence it is necessary to use glucose as the carbon source in order to conduct a study of experimental evolution to determine if the frequency of evolutive rescue depends on the nitrogen source under starvation conditions. Evolutionary rescue is a heritable adaptation selected by natural selection to avoid extinction of a population under deleterious environmental conditions¹⁹⁸.

The first part of this study investigated whether an aflagellate strain SBW25 Δ *fleQ* that could still move by spidery-spreading motility, via viscosin production, also evolved swimming motility and if so if this also involved the same *ntrBC* rewiring mechanism. It also addressed the question of whether the physiological status under different nitrogen sources is the evolutionary force for the re-expression of flagella in non-flagellated strain SBW25 Δ *fleQ* (*Fla*⁻, *Visc*⁺), by testing the strain in minimal medium M9 with rich (ammonium) or poor (glutamate or glutamine) sources of nitrogen, see research hypothesis (Figure 1-59). Switching niches is important for survival as this enables a bacterium to acquire preferred sources of nitrogen and other nutrients²⁴⁹. While a spidery-spreading colony can access nutrients at the surface, swimming motility may facilitate access to more nutrients within the agar.

4.2 Initial Spidery-Spreading Motility of SBW25 Δ *fleQ* with Different Nitrogen and Carbon Sources

To test and isolate evolved swimming mutants from SBW25 Δ *fleQ*, single colonies were inoculated in 0.25 % agar M9 medium with 10 mM glutamine, 10 mM glutamate, or 10 mM ammonium as nitrogen source and 20 % w/v glucose or 20 % w/v sucrose as carbon source and incubated at 26 °C (see sections 2.3.1.3 and 2.6). Twelve replicates were set up for each condition and the plates (see section 2.4) were monitored initially for growth and phenotype of spreading colonies on each medium with different N and C source. They were also monitored for 26 days for evolution of

swimming motility (described in section 2.6). Potential evolved mutants were picked from all plates showing evidence of swimming motility (see sections 2.6.1 and 4.4).

During the first 24 h the SBW25 Δ *fleQ* colonies grew very little and did not spread (cumulative growth or passive movement) despite visible production of viscosin during growth on all nitrogen sources with glucose as the carbon source. Viscosin was visible as a clear ring around colonies. At 24 h colony size on 0.25 % agar medium M9 ammonium was 8.1 mm² ($SD = 4.5$ mm², $n = 12$); average on M9 glutamine 6.5 mm² ($SD = 2.9$ mm², $n = 6$) and on M9 glutamate 5.8 mm² ($SD = 3.6$ mm², $n = 12$ replicates). After 25 h - 30 h for most replicates, colonies began to acquire a butterfly shape, although in a few replicates butterfly shape formation took up to 4 days. Formation of the spidery-spreading phenotype followed butterfly formation but was variable on all media. At 72 h on M9 glucose – glutamine, one of 6 plates (plate 2, 2803 mm²) had spread significantly, while the average spread of the other 5 plates was 681 mm² ($SD = 150$ mm²) (Figure 4-1). On M9 glucose - glutamate 4 plates (7,8,9 and 12) of 12 showed extensive spreading with an average area of 2380 mm² ($SD = 663$ mm²), while the other 9 showed a low level of spreading with an average of 352 mm² ($SD = 131$ mm²), by 72 h (Figure 4-2). Spread on M9 glucose – ammonium was exceedingly low on all 12 replicates, ranging from only 13 mm² to 32 mm² (Figure 4-3), at 72 h. Colony expansion data, as shown in Figure 4-1 to Figure 4-3, was recorded for these sliding colonies from 74 h - 84 h and normalised by subtracting the colony growth area at 72 h from each measurement (see section 2.6). The marked minimal spread on M9 glucose – ammonium medium remained evident at 84 h. There were statistically significant differences between the spreading of the spidery-colony (area) and type of nitrogen source (P -value 0.000 < 0.050; Appendix ZY: Table ZY-2). Colony spreading was not significantly different (P -value 0.148 > 0.050) between M9 glucose-glutamine (at 82 h average colony area was 1817 mm²; Figure 4-1) and M9 glucose-glutamate (at 82 h average colony area was 1177 mm²; Figure 4-2). There were statistically significant differences in colony's area between glutamate and ammonium (P -value 0.001 < 0.050; Appendix ZY: Table ZY-2). The area of spread was dramatically lower when ammonium was compared to glutamate as nitrogen source (at 82 h the average colony area was 40.2 mm²; Figure 4-3 and Figure 4-4).

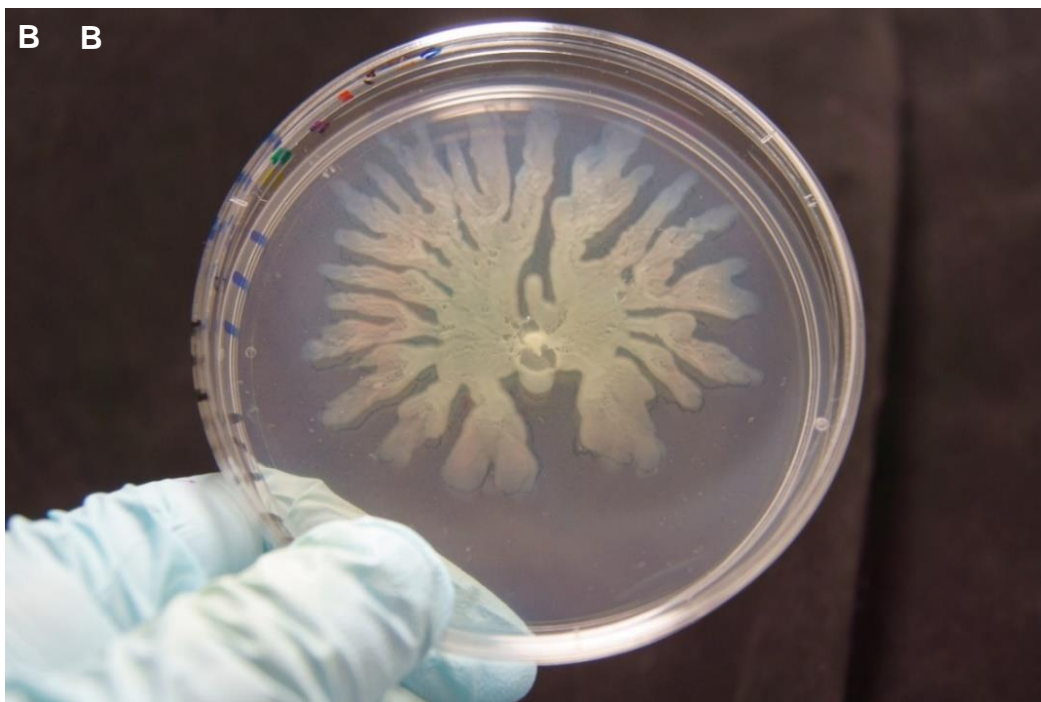
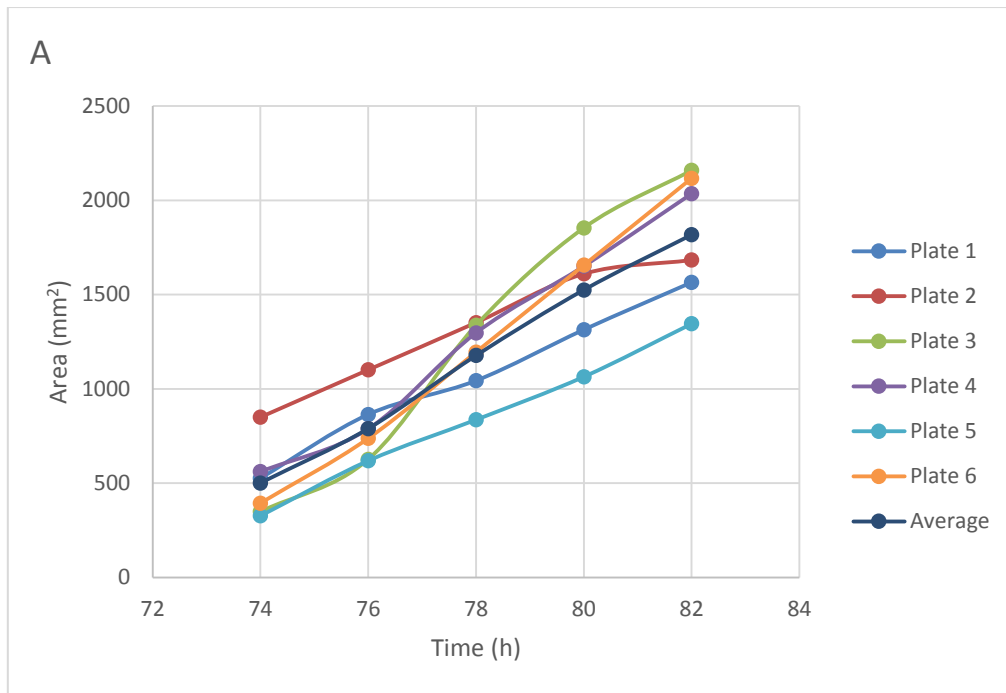


Figure 4-1 Colony expansion of *P. fluorescens* SBW25 Δ *fleQ* on M9 glucose plus glutamine

Colonies grown on minimal medium M9 with glutamine and glucose, as nitrogen and carbon sources respectively. (A) Colony expansion curves were constructed from 74 h - 82 h after inoculation using the hand-drawn method and normalised (see section 2.6), by subtracting the area covered at 72 h (start of measurement) from all consecutive measurements. The area spread for each plate at 72 h used for normalisation is shown in Appendix ZV: Table ZV-1. The average curve shown is averaged of 6 replicates. (B) A sliding spidery-butterfly colony on 0.25 % agar medium M9 at 4 days after inoculation (plate 4). Plate diameter: 9 cm.

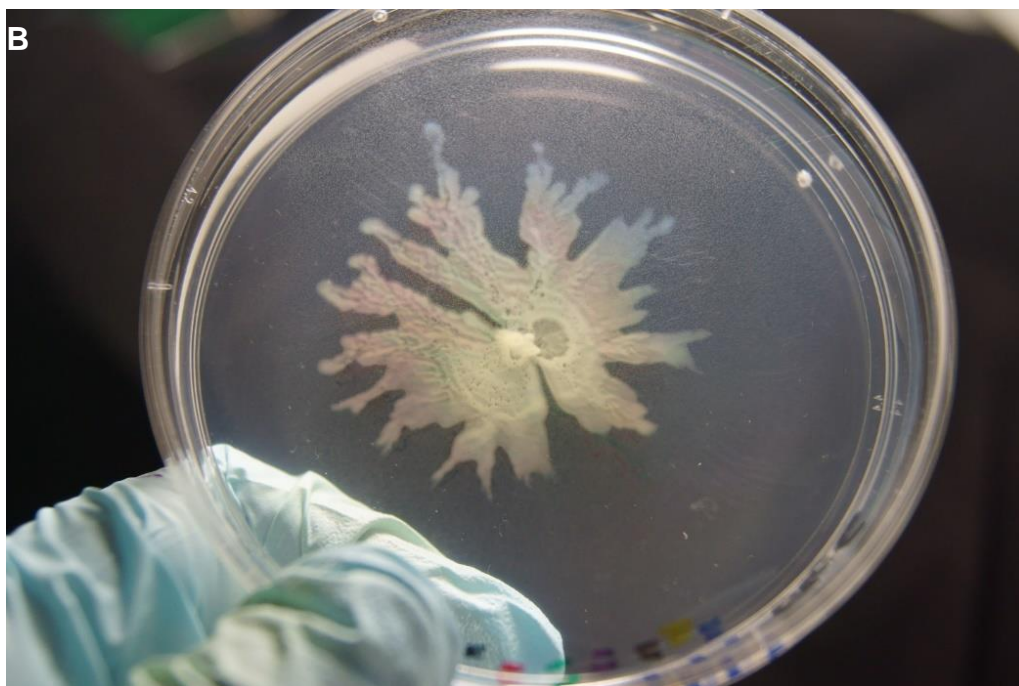
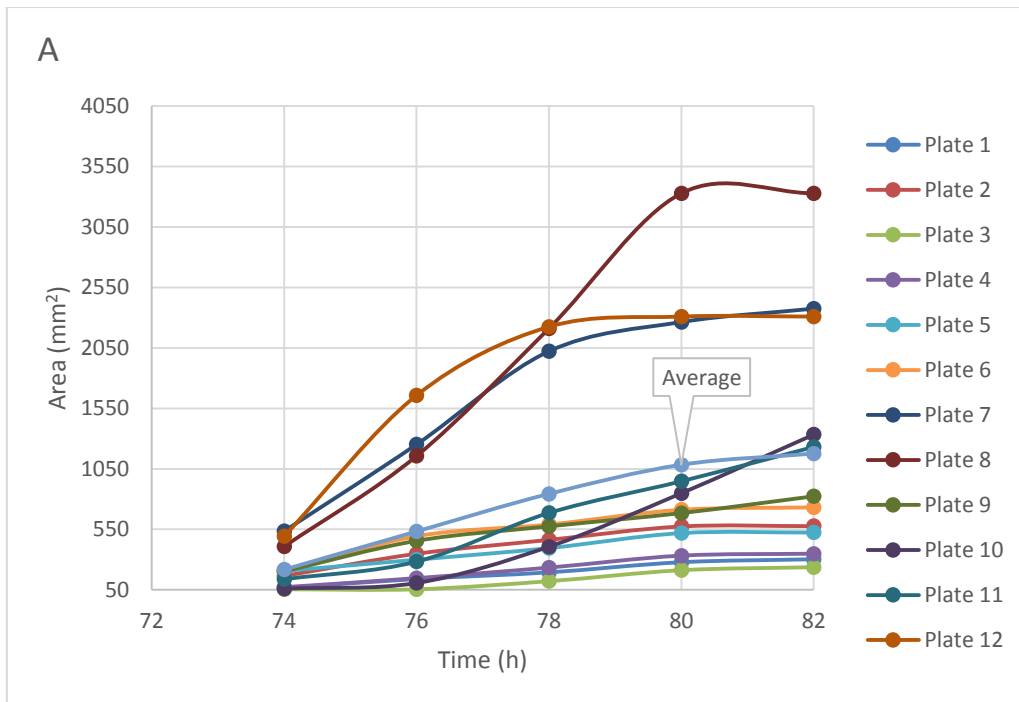


Figure 4-2 Colony expansion of *P. fluorescens* SBW25Δ*fleQ* on M9 glucose plus glutamate

Colonies grown on minimal medium M9 with glutamate and glucose, as nitrogen and carbon sources respectively. (A) Colony expansion curves, constructed from 74 h - 82 h after normalisation for growth at 72 h, see Figure 4-2 and section 2.6 for method and Appendix ZV: Table ZV-1 for details of area spread per plate at 72 h. The average curve shown is from all 12 plates. (B) A sliding spidery-butterfly colony on 0.25 % agar medium M9 at 4 days after inoculation (plate 6). Plate diameter: 9 cm.

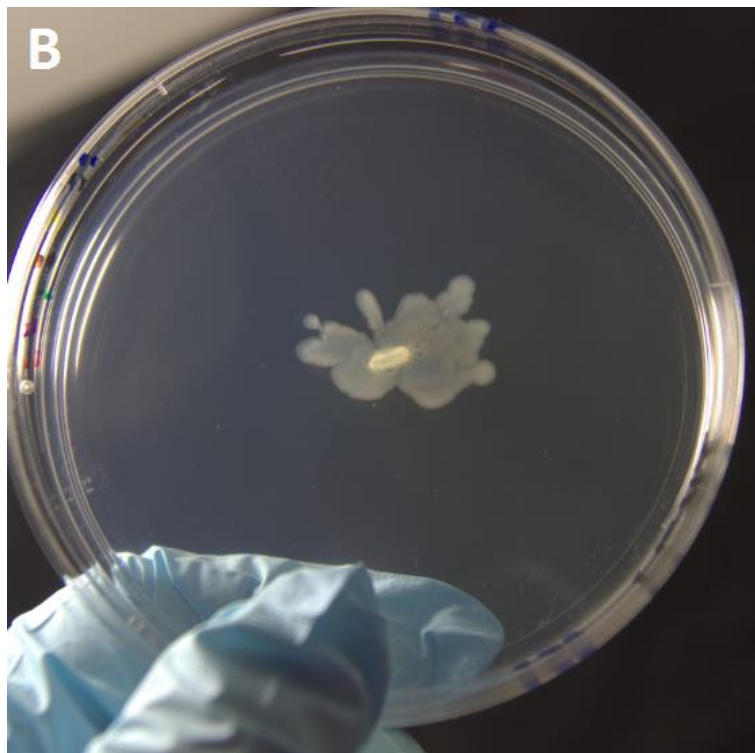
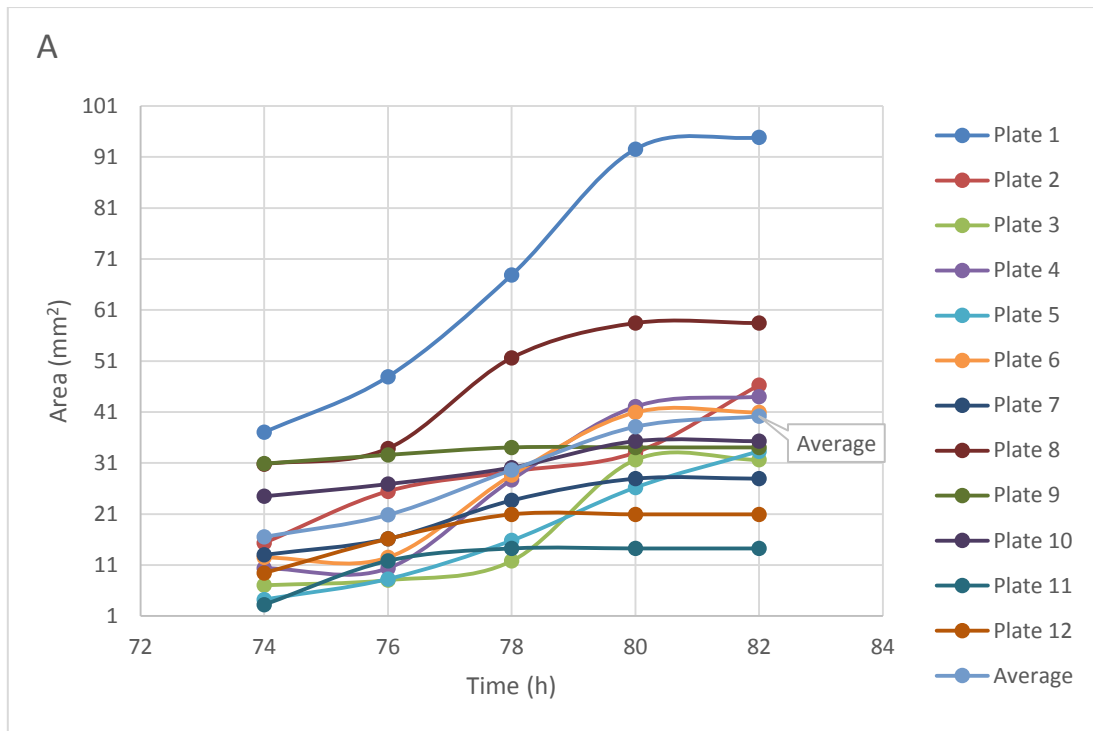


Figure 4-3 Colony expansion of *P. fluorescens* SBW25 Δ *fleQ* on M9 glucose plus ammonium

Colonies grown on minimal medium M9 with ammonium and glucose, as nitrogen and carbon sources respectively. (A) Colony expansion curves, constructed from 74 h - 82 h after normalisation for growth at 72 h, see Figure 4-2 and section 2.6 for method and Appendix ZV: Table ZV-1 for details of area spread per plate at 72 h. The average curve shown is from all 12 plates. (B) A sliding spiderly-butterfly colony on 0.25 % agar medium M9 at 4 days after inoculation (plate 2). Plate diameter: 9 cm.

4.2.1 Comparison of colony expansion between SBW25 Δ fleQ and SBW25:

In contrast to the long delayed initiation of motility of SBW25 Δ fleQ (*Fla*⁻, *Visc*⁺), the wild-type strain SBW25 (*Fla*⁺, *Visc*⁺), exhibited swimming dependent colony expansion shortly after inoculation of M9 medium with glucose and each of the nitrogen sources tested. The impact of each nitrogen source on colony expansion of SBW25 was monitored for the 10 h post inoculation (Figure 4-5). As with strain SBW25 Δ fleQ which demonstrated efficient sliding dependent colony expansion with glutamine as the nitrogen source (1817 mm², 82 h growth), swimming dependent colony expansion of SBW25 was greatest with glutamine as nitrogen source (1514 mm² at 10 h), see Figure 4-5. However, while there was no difference in the area covered by SBW25 with ammonium or glutamate as N source, there was a dramatic difference with sliding dependent expansion of SBW25 Δ fleQ (Figure 4-3). The aflagellate strain SBW25 Δ fleQ showed a statistically significant difference (*P*-value 0.001 < 0.050; Appendix ZY: Table ZY-2) in colony expansion (sliding) between growth on M9/ glucose with glutamate (82 h, colony area 1177 mm²) and M9/ glucose with ammonium (82 h, colony area 40.16 mm²; Figure 4-5; Figure 4-4). On the other hand, there was no statistically significant difference (*P*-value 0.666 > 0.050; Appendix ZY: Table ZY-3) in colony expansion (swimming) between ammonium (10 h, colony area 1125.3 mm²) and glutamate (10 h, colony area 1097.8 mm²) as nitrogen source with the wild type strain SBW25 (Figure 4-4; Figure 4-5). This difference could not be attributed solely to poor growth on M9 glucose with ammonium, as SBW25 Δ fleQ grew equally well in liquid M9 glucose medium whether glutamate or ammonium was provided as the N source (see Chapter 3, Figure 3-32).

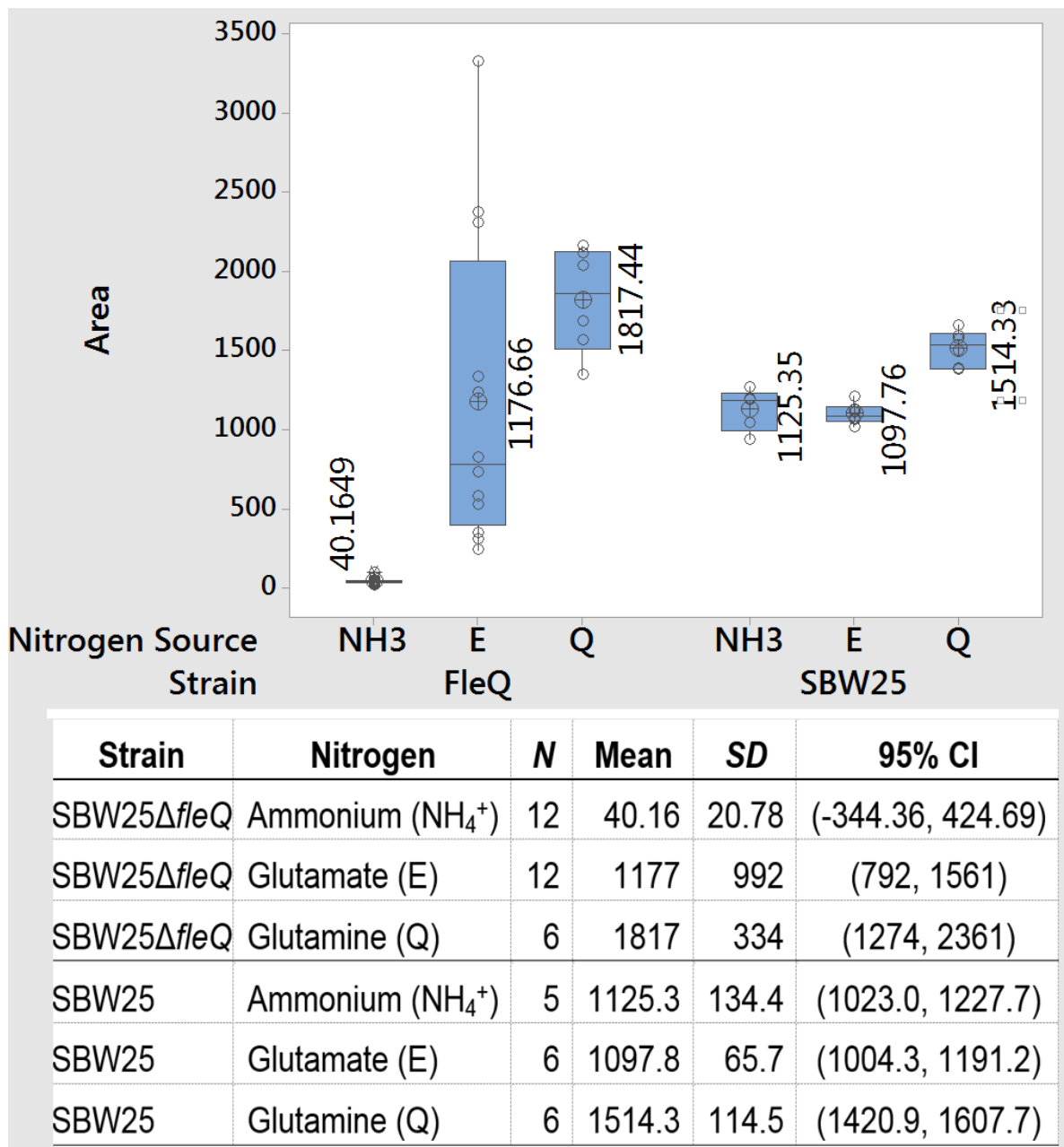


Figure 4-4 Box plots: Comparison of colony expansion area (mm²) between SBW25 and SBW25ΔfleQ under different nitrogen treatments

The analysed data is from colony expansion curves with different nitrogen sources and glucose as carbon source, see Figure 4-5. The aflagellate strain SBW25ΔfleQ (*Fla*⁻, *Visc*⁺) remained sessile during the first 24 h and produced viscosin, whereas the wild type strain SBW25 swam. Also, swarming in strain SBW25 occurred after 2 days – 3 days depending on the nitrogen source (earlier in glutamine). The area shown for SBW25ΔfleQ was obtained from its colony-expansion curve at 82 h and for SBW25 it was obtained at 10 h. The individual values are represented by open circles.

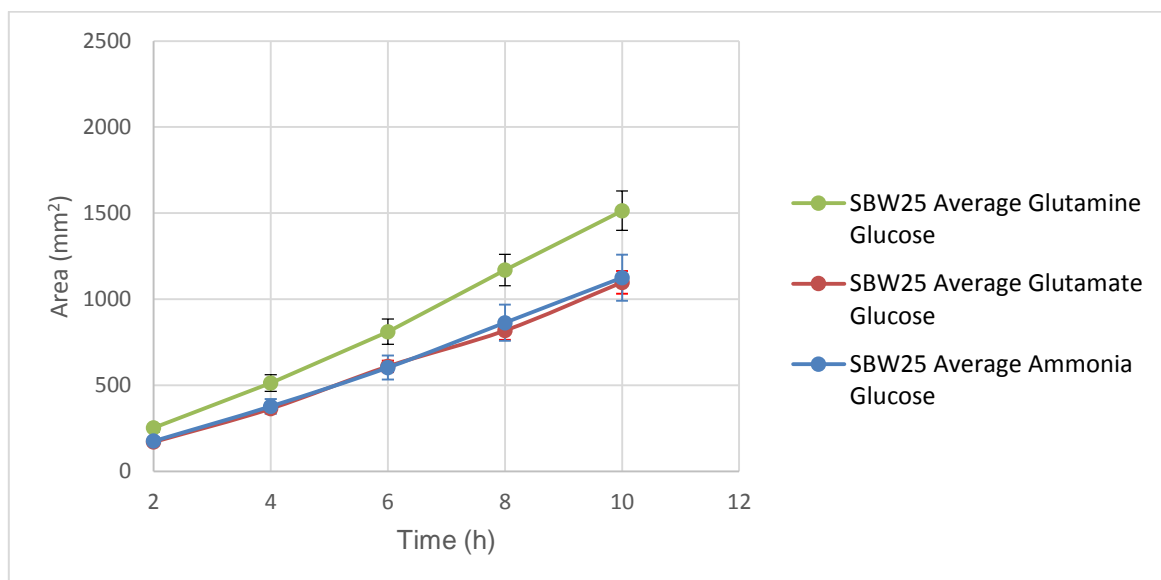
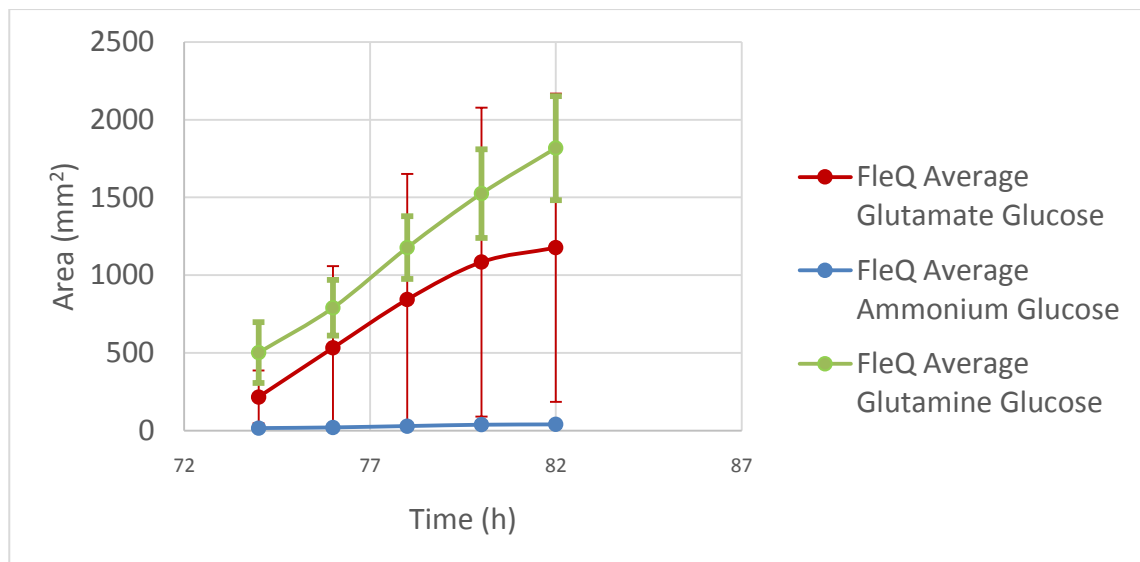


Figure 4-5 Comparison of colony expansion between SBW25 and SBW25ΔfleQ for different nitrogen sources with glucose as the carbon source

A. Area covered by sliding colony of SBW25ΔfleQ on M9 plus glucose with glutamine, glutamate or ammonium as N source. Data from Figures 4-1, 4-2 and 4-3. B. Area covered by swimming colony of SBW25 on M9 plus glucose with glutamine, glutamate or ammonium as N source, monitored over first 10 h. The colony expansion curves are average of all replicates ($n = 6$ or 12 for SBW25ΔfleQ; $n = 6$ for SBW25) and error bars represent standard deviation.

4.2.2 Glutamine as the Sole Carbon and Nitrogen Source for *P. fluorescens*

The strain SBW25ΔfleQ when grown on medium containing sucrose and glutamine initially showed a spidery-butterfly sliding colony phenotype, which gradually changed to a spidery appearance. However, only two plates showed any growth when ammonium and sucrose were used as the nitrogen and carbon sources for strain

SBW25 Δ *fleQ*. This was not surprising as *P. fluorescens* SBW25 is unable to transport this sugar and depends on cell membrane leakage to release the enzyme levansucrase in order to degrade sucrose¹³¹. A similar growth tendency was observed for strain SBW25 when grown on the same nitrogen and carbon sources. When inoculated on M9 ammonium and sucrose agar colonies of SBW25 Δ *fleQ* only became visible after 22 days as small dot and then a few hours later evolved swimming motility became visible. In contrast, *P. fluorescens* can use glutamine as both C and N source²⁶⁵. When grown on sucrose and glutamine colonies were visible 2 h after inoculation but did not move (slide) during the first 24 h although there did appear to be evidence of viscosin rings. Later, these colonies slowly acquired the spidery phenotype and sliding colony expansion curves were constructed after 3 days (Figure 4-6). Colony expansion of SBW25 Δ *fleQ* on M9/ sucrose plus glutamine was similar to expansion on M9/glucose plus glutamine, reaching the same area (Figure 4-1).

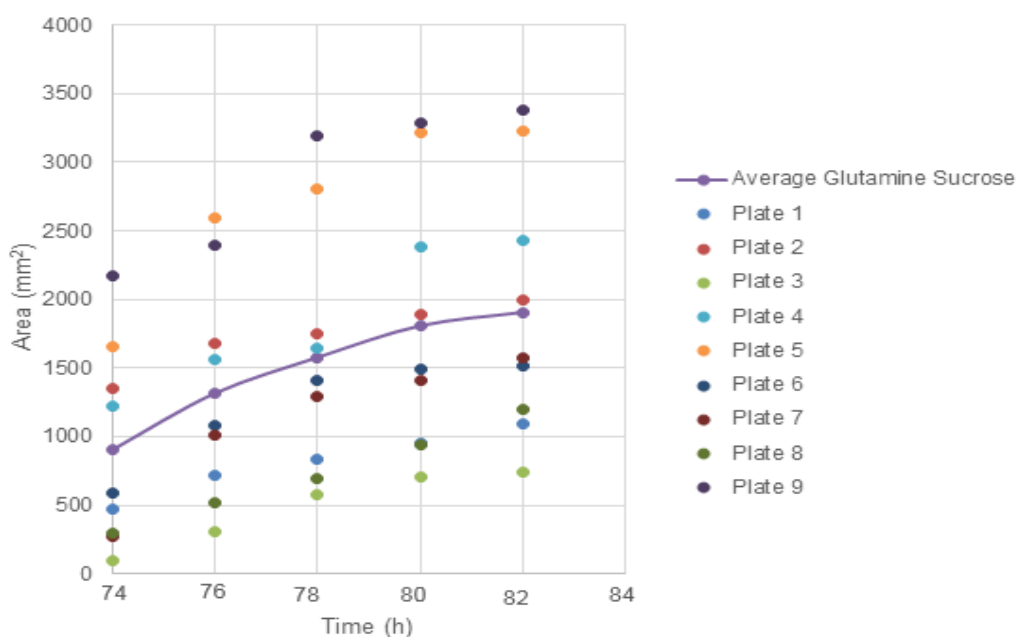


Figure 4-6 Colony expansion of a sliding spidery colony of SBW25 Δ *fleQ* grown on glutamine and sucrose

The colony expansion curve was constructed 3 days after inoculation. The colony expansion curve is the average of 9 replicates.

4.3 Nitrogen Limitation and Evolution of Swimming Motility

As described in section 4.1, replica plates set up for evolution studies, on M9 agar with different N and C sources, did not spread for the first 24 h - 30 h, but then acquired a butterfly appearance that gradually developed a spidery spreading phenotype. Plates

were monitored at 2 days intervals up to 26 days for evolution of swimming. Characteristic swimming dependent expansion, emanating as a circle appeared on most plates (Figure 4-7). This was designated as an evolved swimming phenotype. Evolution of swimming occurred on each different medium with high frequency in this non-sessile aflagellate strain, SBW25 Δ *fleQ* (Figure 4-7; Figure 4-8). This was despite the ability of SBW25 Δ *fleQ* to rapidly slide over the surface with the spidery movement that is reliant on cell division and viscosin production. The centre of the SBW25 Δ *fleQ* colony would be under nitrogen starvation pressure as cells in the centre would be trapped in an area of nutrient depletion. Therefore, it is assumed that the bacteria localised in this region of the colony may have a higher probability of evolving swimming motility to allow them to switch niche and survive.

All replica plates of M9-glucose with either ammonium or glutamate as N source evolved swimming motility, within an average of 4 days or 3 days, respectively. Twelve of 14 replica plates with glutamine as N source evolved swimming within an average of 2.5 days (Table 4-1). There were significant statistical differences (P -value $0.047 < 0.050$; Appendix J: Table J-1) between the different nitrogen sources and the time to evolve swimming motility in this rich energy environment where glucose was the carbon source (Appendix J: Figure J-1, Figure J-2). The evolved swimming phenotype of SBW25 Δ *fleQ* was observed earlier in glutamine and glutamate compared to ammonium (Table 4-1). There was no statistically significant difference (P -value $0.223 > 0.050$; Appendix J: Table J-2) between the times to evolve swimming motility with glutamate or glutamine as N source (Appendix J: Figure J-3). Almost all plates evolved swimming motility as shown in Table 4-1. However, the number of replicates was not enough (at least $n = 17$ replicates per treatment) to conduct a chi-square test for association (Pearson chi-square) to identify if there existed a statistically significant association between the different nitrogen sources and the number of non-evolved replicates.



Figure 4-7 Evolution of swimming motility of the aflagellate strain SBW25 Δ *fleQ* with ammonium as the nitrogen source and glucose as the carbon source

(A) Colony grown on the 0.25 % agar surface. (B) Colony slid over the surface and initially had a butterfly shape, 4 days (plate 5). (C) After six days swimming motility evolved from the centre of the colony and moved much faster through the agar, than the surface sliding colony (picture taken after 11 days; plate 5).

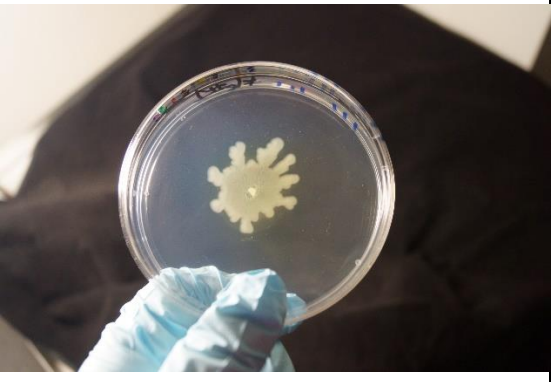
		Nitrogen Source/Glucose		
		Ammonium	Glutamine	Glutamate
		Plate 1	Plate 5	Plate 1
4 days (sliding)				
				
11 days (swimming)				

Figure 4-8 Evolution of swimming motility of spidery-spreading strain SBW25 Δ *fleQ*

Colony slid on 0.25 % agar medium M9 with different nitrogen treatments and glucose as carbon source. The sliding colony initially had a butterfly shape, and gradually acquired a spidery appearance. The plates shown evolved swimming motility under different nitrogen treatments. Pictures were taken after 4 days and 11 days of inoculation. The plates shown correspond to replicates used to obtain the colony expansion curves using hand-drawn method. Plates: 9 cm diameter.

Table 4-1 Evolution of swimming motility under different nitrogen/glucose treatments

Days to evolve swimming motility on different nitrogen sources and glucose as the carbon source						
Nitrogen source		N	Mean (days)	SD (days)	95 % CI	
Glutamate		12	3.000	1.044	(2.415, 3.585)	
NH ₄ ⁺		12	4.000	2.089	(3.151, 4.849)	
*Glutamine		12	2.500	0.905	(1.915, 3.085)	

Note: CI = confidence interval.*Data was averaged only from evolved replicates. There were 14 replicates for glutamine treatment and two plates did not evolve swimming motility.

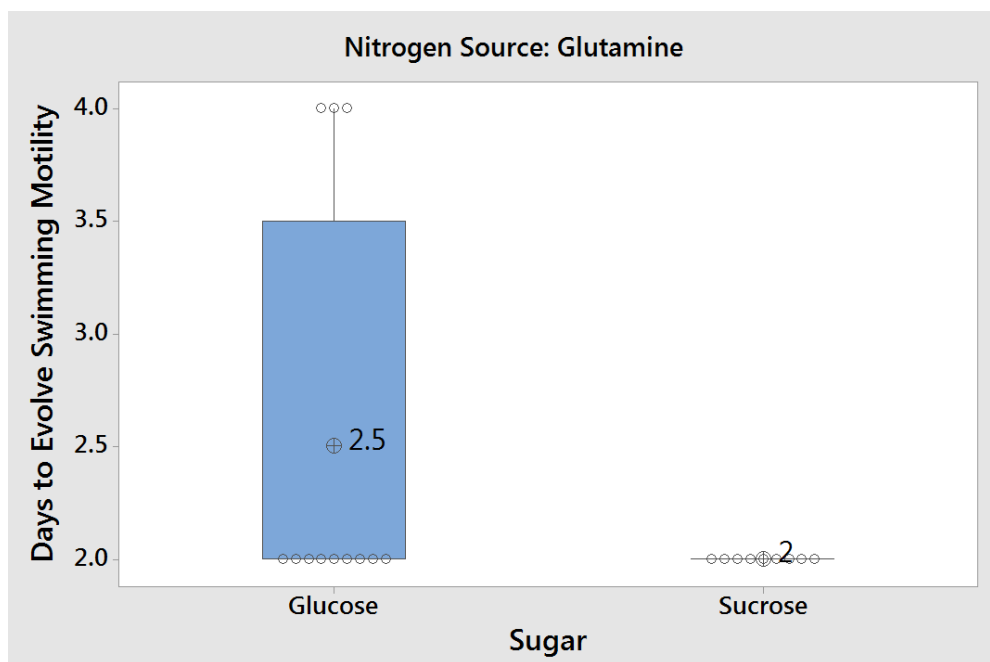
Number of evolved and non-evolved replicates						
Treatment		Days to Evolve Swimming Motility			Non Evolved	Total Replicates per Treatment
Carbon Source	Nitrogen Source	2 Days	4 Days	6 Days		
Glucose	Glutamate	6 plates	6 plates	0 plates	0 plates	12 plates
	Ammonium	6 plates	0 plates	6 plates	0 plates	12 plates
	Glutamine	9 plates	3 plates	0 plates	2 plates	14 plates

4.3.1 Evolution of swimming motility in aflagellate SBW25Δ*fleQ* on a poor carbon source

Much higher growth and increased sliding movement were observed for glutamine and sucrose as compared to ammonium and sucrose. Since a SBW25Δ*fleQ* colony depended on cell division and surfactant to translocate via sliding movement, there would be rapidly depleted glutamine levels, particularly in the centre of spidery-colony, where space was not available in order to reach more glutamine as nitrogen and carbon source because *P. fluorescens* does not release levansucrase for the utilisation of sucrose as carbon source¹³³. Meanwhile in ammonium/sucrose treatment, cells started to starve and die. Consequently levansucrase would be released to provide the growth potential on sucrose by surrounding bacteria. After the

sucrose, degradation was initiated and energy levels increased. The higher levels of ammonium present in the medium signalled sufficiency of N and consequently blocked the up-regulation of the *glnAntrBC* operon¹⁷⁵, which is controlled by NtrC-P^{175,307}. It may be noted that nitrogen limitation was a selective pressure for evolving swimming motility to move towards a more favourable niche (chemotaxis). For this reason, there was a higher probability of selecting earlier a population that had evolved flagella-driven motility when grown on glutamine as compared to ammonium as the nitrogen source. The aflagellate strain evolved swimming motility after 2.0 days ($SD = 0.0$ days) when grown on M9/sucrose plus glutamine. Under these conditions, the bacteria are essentially growing on glutamine as the carbon and nitrogen source because sucrose cannot be transported into the cell and used in spite of the production of the enzyme levansucrase¹³³. Only when cells become leaky is this enzyme released into the milieu permitting metabolism of sucrose by surrounding bacterial cells. Despite sole use of glutamine as carbon and nitrogen source, this evolutive event did not have a statistically significant difference (P -value $0.116 > 0.050$; Figure 4-9) compared to that of growth on glutamine and glucose (mean = 2.5 days, $SD = 0.9$ days) (Appendix J: Figure J-4).

Perhaps not surprisingly, there was a marked difference in the number of plates and time to evolved swimming when bacteria were grown on M9 with either ammonium and glucose or ammonium and sucrose. The latter would have no readily available source of carbon. The absence of growth on ammonium and sucrose would maintain high ammonium levels and ensure repression of the Ntr system. In addition, very poor growth would decrease the probability of mutations occurring and being naturally selected (Table 4-2). The colony expansion curves of the plates showing evolved swimming on M9/ sucrose with ammonium show a similar very low expansion rate for evolved SBW25 Δ *fleQ* (Figure 4-10) and the wild type strain SBW25 (Figure 4-11).



Sugar	N	Mean	SD	95% CI
Glucose	12	2.500	0.905	(2.084, 2.916)
Sucrose	9	2.000	0.000	(1.520, 2.480)

Pooled SD = 0.688247

Factor Information

Factor	Levels	Values
Sugar	2	Glucose, Sucrose

Analysis of Variance

Source	DF	Adj SS	Adj MS	F-value	P-value
Sugar	1	1.286	1.2857	2.71	0.116
Error	19	9.000	0.4737		
Total	20	10.286			

Figure 4-9 Box plot: Comparison of days to evolve swimming motility between different sugars and glutamine

The days to observe evolution of swimming motility of strain SBW25 Δ *flaQ* (*Fla*⁻, *Visc*⁺) grown on M9 with either glucose or sucrose as carbon source and glutamine as nitrogen source.

Table 4-2 Number of evolved and non-evolved replicates

Treatment		Days to Evolve Swimming Motility			Total Replicates per Treatment
Carbon Source	Nitrogen Source	2 Days	28 Days	Non Evolved	
Sucrose	Ammonium		2 plates	4 plates	6 plates
	Glutamine	9 plates		3 plates	12 plates

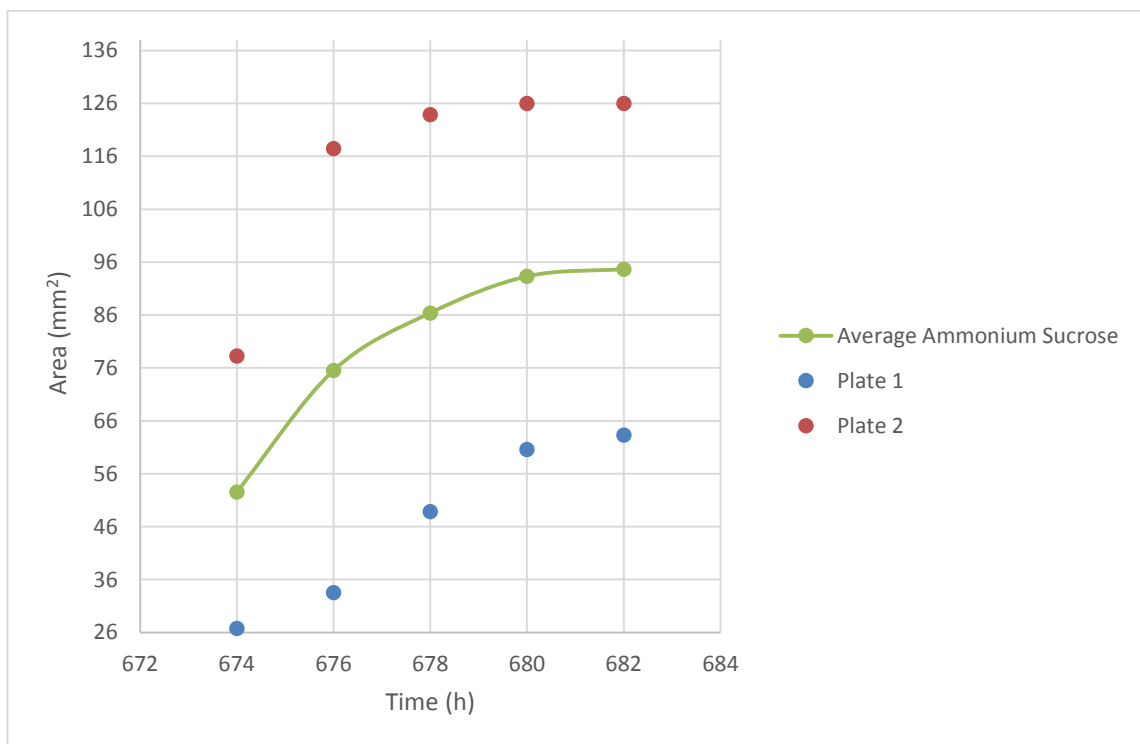


Figure 4-10 Colony expansion of evolved SBW25Δf/eQ swimming colonies grown on ammonium and sucrose

Both replicates evolved the swimming phenotype after 22 days and the colony expansion curve was constructed 28.08 days (674 h) after swimming motility had evolved. The previous area marked was subtracted from all consecutive observations of the respective replicate. The colony expansion curve is the average of 2 replicates.

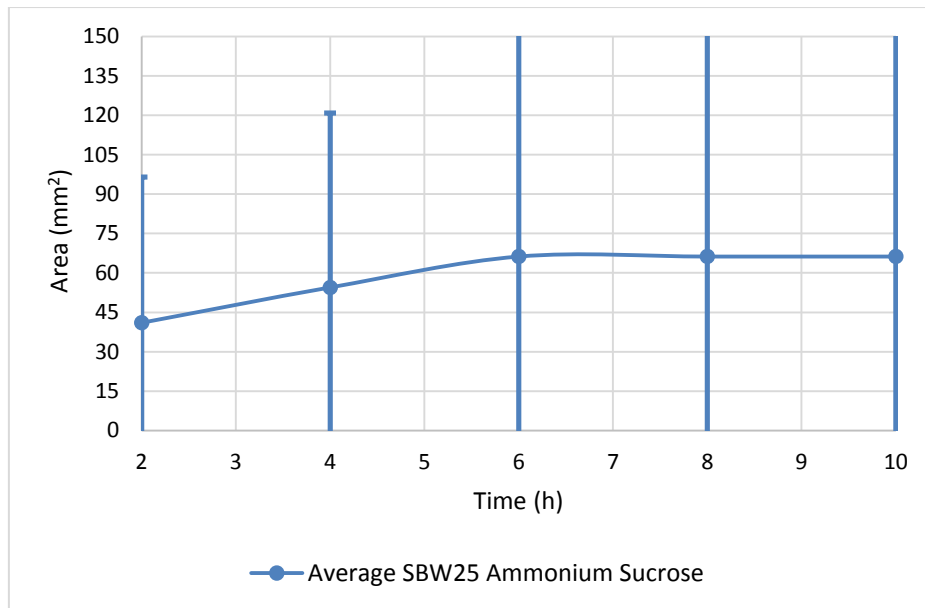


Figure 4-11 Swimming motility of wild type strain SBW25 colonies grown on ammonium and sucrose

The colony expansion curves is the average of all replicates ($n = 3$). The error bars represent standard deviation.

4.4 Purification of Individual Evolved Mutants of SBW25 Δ fleQ

To characterise both phenotype and genotype of evolved mutants, plugs of agar from the colony border (1 plugs per plate) were taken as described in section 2.6.1. Individual colonies were isolated from each plug and a single colony from each plug stocked to confirm the swimming phenotype. The isolated strains predicted to be motility mutants, were tested for swimming motility in the same culture medium in which they had evolved. Only 9 out of 19 tested isolates maintained their swimming phenotype (Table 4-3). The majority of non-evolved isolates were from growth on glutamine or glutamate where spreading growth of the parent SBW25 Δ fleQ may have been present within areas of evolved swimming. This would also explain the 100 % success in purification of only evolved mutants from ammonium/ glucose plates where growth and spreading was much slower. It is important to mention that many isolates (particularly from sucrose plates) were lost due to technical problems. In total, only 9 evolved FleQS strains were recovered from all nitrogen sources examined (Table 4-4). Of these 6 were from ammonium/glucose plates, 2 from glutamate/glucose and only one from glutamine/glucose. None were obtained from blebs.

Table 4-3 Frequency of recovery of motility mutants

	Nitrogen Source						Total Isolates
	Ammonium		Glutamate		Glutamine		
	Carbon Source		Carbon Source		Carbon Source		
	Glucose	Sucrose	Glucose	Sucrose	Glucose	Sucrose	
Non Evolved	0	0	4	0	1	5	10
Evolved Swimming Motility	6	0	2	0	1	0	9
Total Isolates	6	0	6	0	2	5	19

Table 4-4 Swimming phenotype of FleQS strains

Strain Name	*Mean Rate of Colony Expansion (mm ² /h)	Motility Phenotype	Treatment Nitrogen/Glucose	Replicate	Days Isolated
FleQS1	7.2	Fast	ammonium	1	9
FleQS2	8.9	Fast	ammonium	2	9
FleQS3	6.5	Fast	ammonium	3	9
FleQS4	4.1	Slow	ammonium	4	9
FleQS5	5.1	Medium	ammonium	5	9
FleQS6	3.7	Slow	ammonium	6	9
FleQS7	4.4	Slow	glutamate	3	4
FleQS8	5.6	Medium	glutamate	4	4
FleQS9	6.2	Fast	glutamine	5	4

Note: All evolved swimmers were earlier swarmer because some of their replicates swarmed at 18 h or earlier. The replicate number corresponds to the plate number from which they were picked. The isolation was not conducted as soon as evolution of swimming motility occurred, so the number of days means time after inoculation in the plate. Isolation of bacteria was not performed immediately after swimming evolution had occurred in the aflagellate parent strain SBW25Δ*fleQ*. All isolates were obtained from main swimming disc and not blebs. The motility phenotype classified as medium has an expansion rate of ~5 mm²/h. The values below it (from ~4 mm²/h and below) are classified as slow expansion rate, whereas those that above it (from ~6 mm²/h and above) are categorised as fast expansion rate. *The average rate of colony expansion (mm²/h) is based on geomean data from 2 h to 8 h.

4.5 Swimming and Swarming Phenotypes of Evolved FleQS

Strains

The FleQS swimming phenotype was tested in swarming agar and LB broth (Table 4-4 and Table 4-5; Appendix M: Figure M-1, Figure M-2, Figure M-3, and Figure M-4). From broth cultures, it was possible to see swimming by light microscopy for all isolates. Therefore, it was concluded that all evolved FleQS strains express flagella. This was confirmed by electron microscopy for FleQS5 and FleQS7 (see section 4.8). It is interesting to note that two types of swarming on rich medium (0.25 % agar LA) were observed: spidery and wild type (Movies 5-7). The spidery-swarming consisted

of several dendritic extensions that appeared at different places of the swimming colony border, which gave the appearance of a spider to the swimming colony (Figure 4-12), and then gradually moved in multiple directions. This spidery-swarming was very fast and a colony was able to completely cover a plate within a few hours. This was seen with most mutants (FleQS2, FleQS3, FleQS5, FleQS7, FleQS8 and FleQS9) and was shown for FleQS3 in Figure 4-12. The other class of swarming behaviour observed was named as wild as it displayed the same pattern of swarming as SBW25 (Figure 3-8), appearing on one side of a colony (Figure 4-13). Again there was fast and diffuse movement (different directions), and a swarming colony was able to completely cover a plate in a few hours. The strain FleQS3 (Movie 20) and strain FleQS4 (Movie 6 and Movie 7) showed both types of swarming, but this did not occur within the same colony.

Table 4-5 Swarming phenotype of FleQS strains

Strain Name	Swarm Type	Observation
FleQS1	Wild	Only 1 out of 12 replicates swarmed at 18 h. The other plates swarmed at 28 h
FleQS2	Spidery	Swarmed at 12 h, but most plates swarmed at 28 h
FleQS3	Spidery/Wild ^a	Swarmed at 14 h, but most plates swarmed at 28 h
FleQS4	Spidery/Wild ^a	Swarmed at 16 h, but most plates swarmed at 28 h
FleQS5	Spidery	Swarmed at 12 h, but most plates swarmed at 28 h
FleQS6	Wild	Swarmed at 18, but most plates swarmed at 22 h
FleQS7	Spidery	Swarmed at 16 h, but most plates swarmed at 28 h
FleQS8	Spidery	Swarmed at 10 h, but most plates swarmed at 28 h
FleQS9	Spidery	Swarmed at 12 h, but most plates swarmed at 28 h

Note: Swimming was observed on agar and in broth.^aFleQS4 and FleQS3 depicted both types of swarming, although this was absent in the same colony.

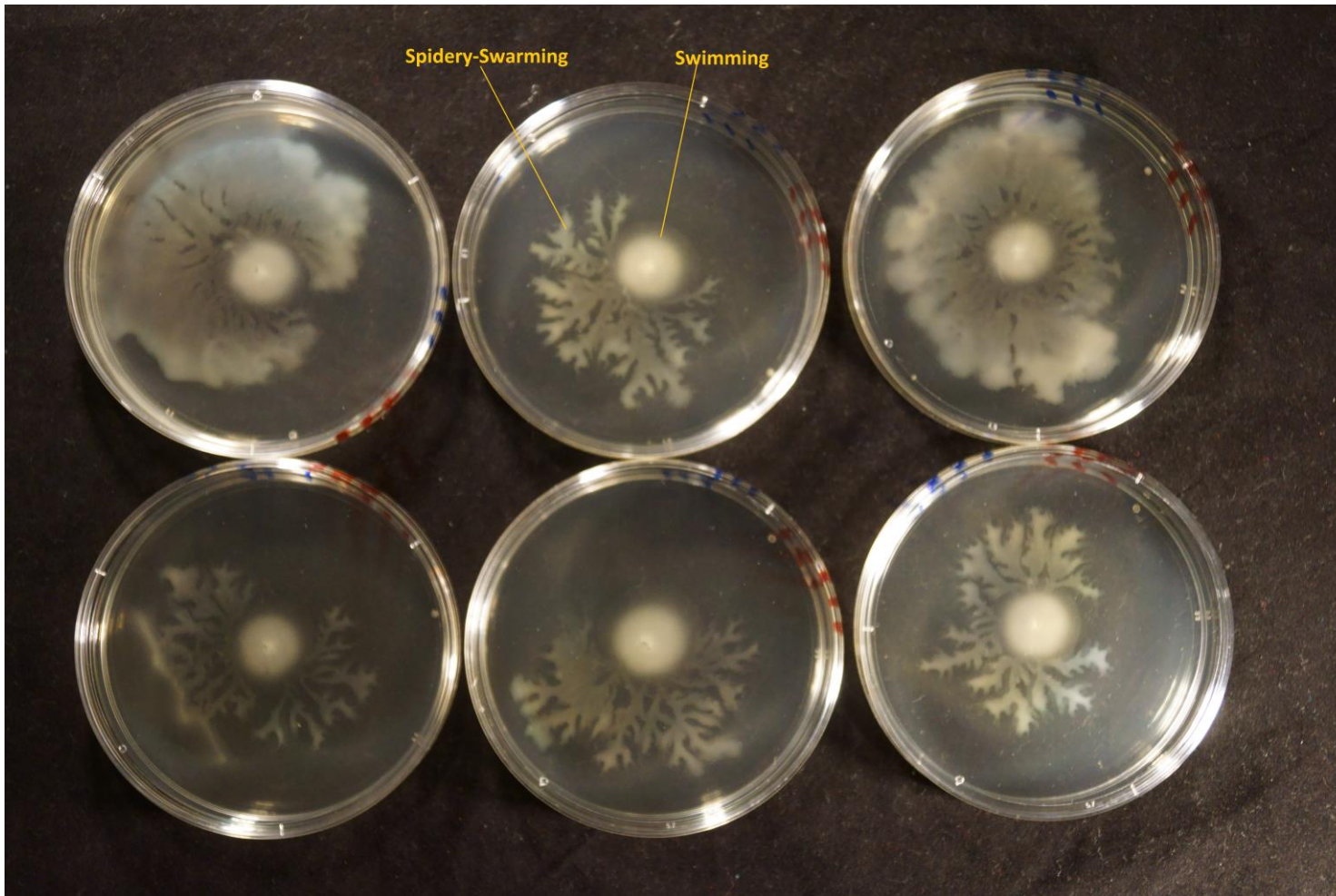


Figure 4-12 Spidery-Swarming of evolved strain FleQS3

A single colony was picked using a metal wire and transferred into a 9 cm diameter motility plate (0.25 % agar LA). Generally, this strain swam for 28 h, except for one plate that swarmed at 14 h. The spidery-swarming was a fast movement compared to the swimming colony and covered the plate within a few hours. This strain was classed among its group as a fast swimmer and showed an averaged colony expansion rate of 6.5 mm²/h for a period of 8 h.

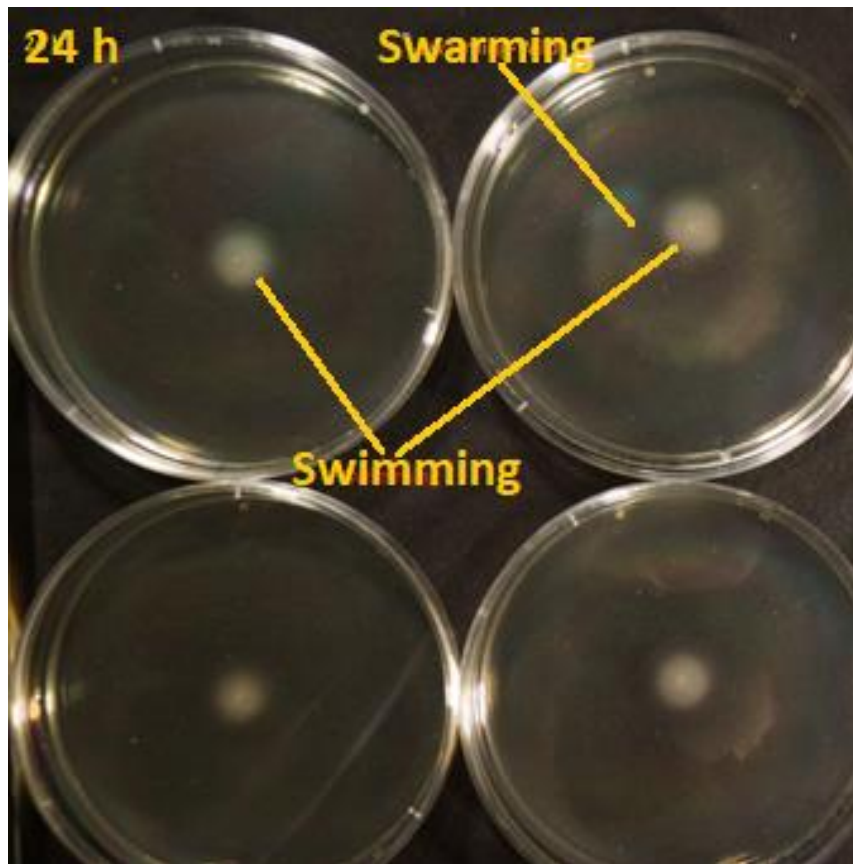


Figure 4-13 Swimming and wild-swarming of strain FleQS6

All motility plates were inoculated concomitantly; however, they did not swarm at the same time. Wild-Swarming was a diffuse movement that always appeared on one side of the swimming colony and resembled the swarming observed in wild type strain SBW25. FleQS6 was classed as a slow swimming type in its group. Its averaged colony expansion rate stood at 3.7 mm²/h over period of 8 h. Motility plate: 0.25 % agar LA. Plates: 9 cm diameter.

Swarming did not occur concomitantly in all the replicates of all the FleQS strains (Figure 4-13), and the replicates in the colony expansion curves reflected this variability as shown for FleQS5 in Figure 4-14. Some replica plates of FleQS5 showed swarming at 12 h, but many exhibited later swarming and all exhibited rapid spidery swarming by 28 h. Colony expansion curves for all FleQS mutants are shown in Appendix A. Most FleQS strains showed a swarming time pattern; for each strain all replicates had always initiated swarming movement by 28 h and were able to cover the surface of a 9 cm plate (area of the plate: 7226.4 mm²) by 40 h - 42 h. Therefore, FleQS strains showed timely swarming. FleQS9 was one exception. It was observed that some replicate colonies of FleQS9 (Movie 23) initiated swimming and then switched to spidery-spreading (sliding) (Figure 4-15, centre lower row), whereas other replicates only exhibited spidery-spreading (Figure 4-15; Appendix A: Figure A-9).

Only the swimming plates of this strain were used obtain the swimming colony expansion curves for FleQS9 (Figure 4-16).

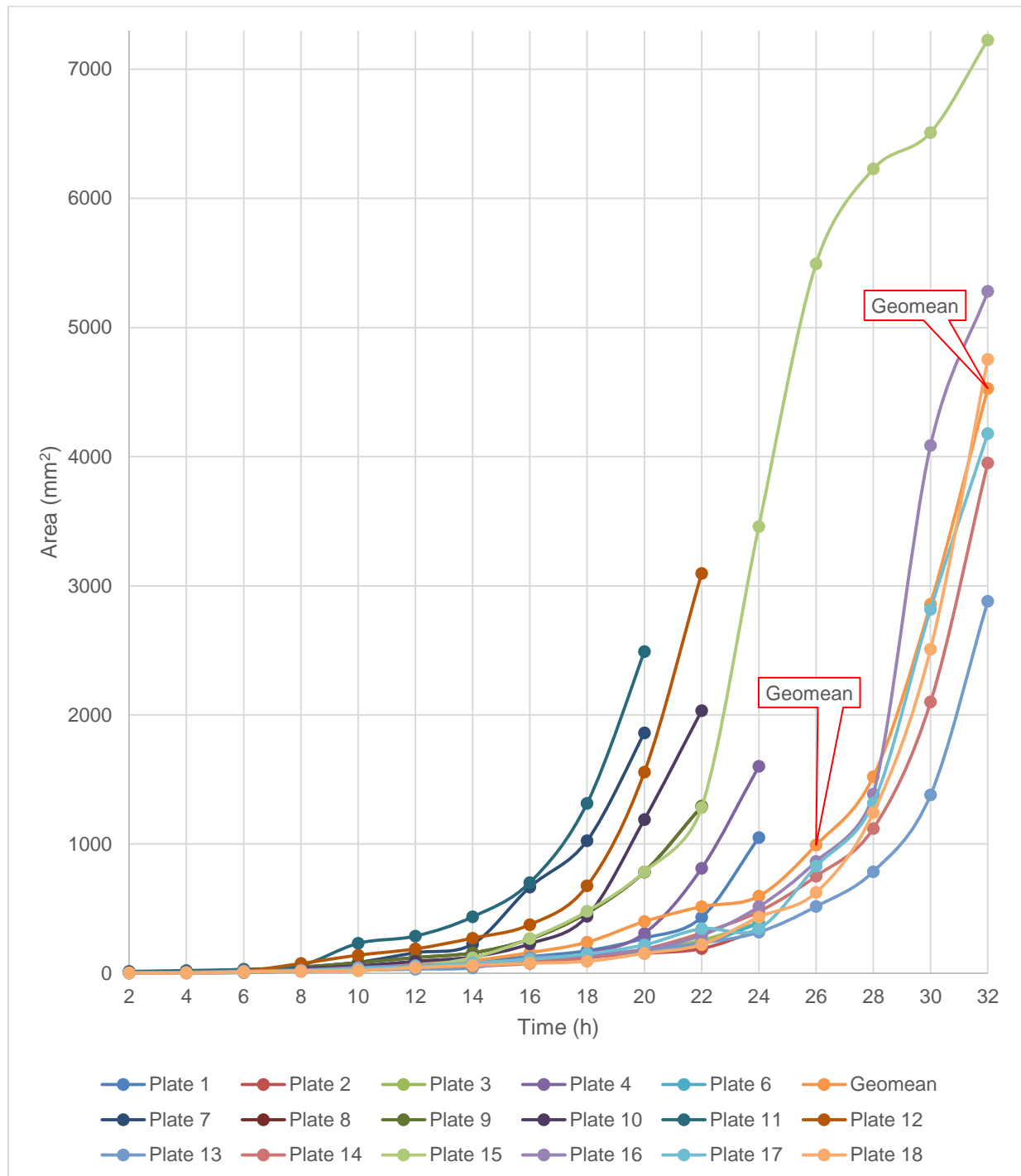


Figure 4-14 Colony expansion of the evolved strain FleQS5

Colony expansion curves were constructed using the hand-drawn method (plates 1 to 12) and time-lapse photography (plates 13 to 18). Replicates were performed in batches of 3 and 6, and the culture medium was 0.25 % agar LA on 9 cm plates (area of the 9 cm plate: 7226.4 mm²). Curves done by hand-drawn method were observed for 20 h -24 h. Whereas the time-lapse photography technique allowed to study the plates for more time (32 h).

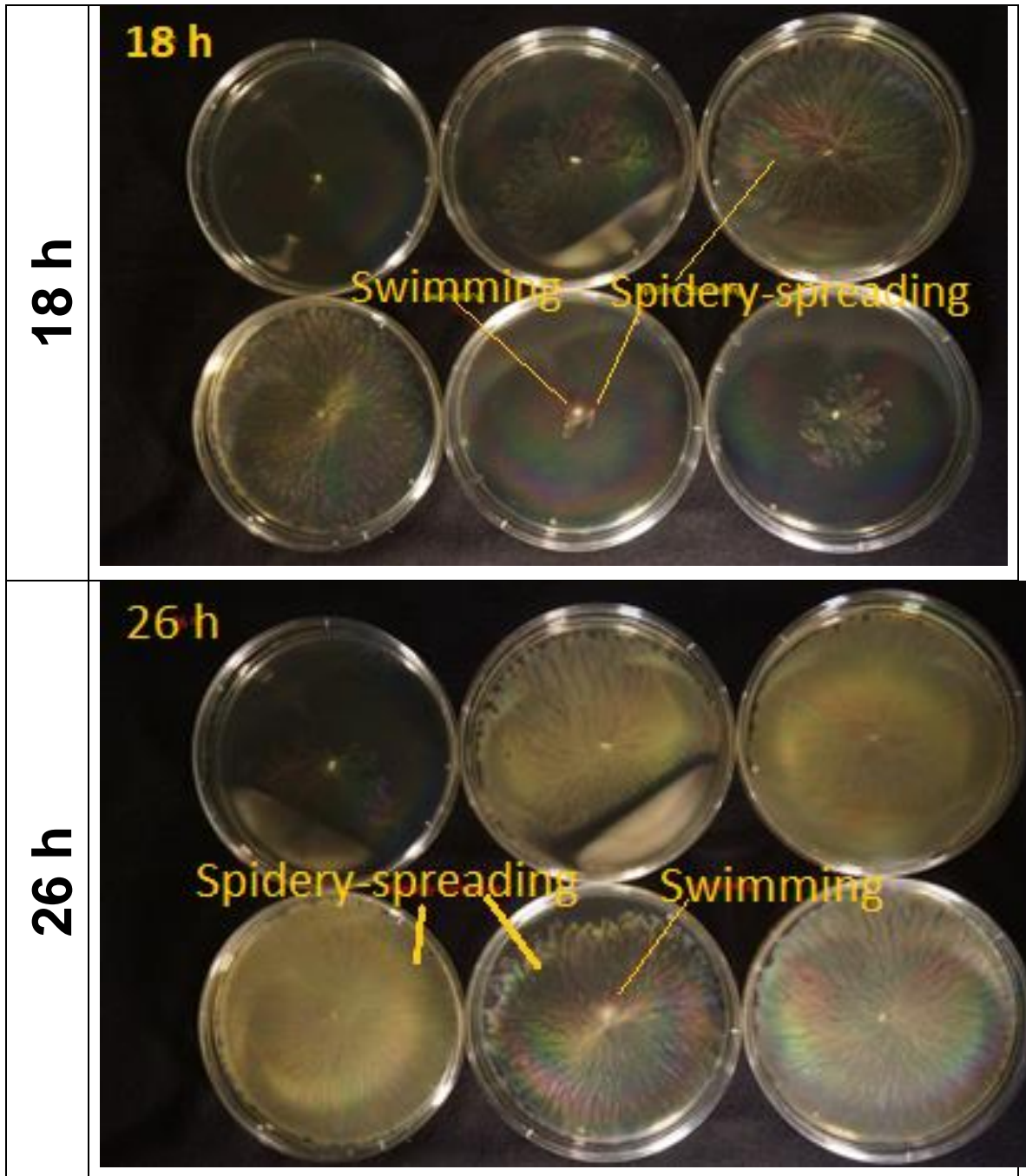


Figure 4-15 Colony phenotype of strain FleQS9

All replicates were inoculated concomitantly and most showed spidery-spreading, with just one swimming. The replicate that showed swimming was beginning to switch to spidery-spreading movement (photo after 18 h). The one replicate that swam (center plate, lower the row) showed both types of movement: spidery-spreading and swimming (photo after 26 h). Plates: 9 cm diameter. Swarming medium: 0.25 % agar LA.

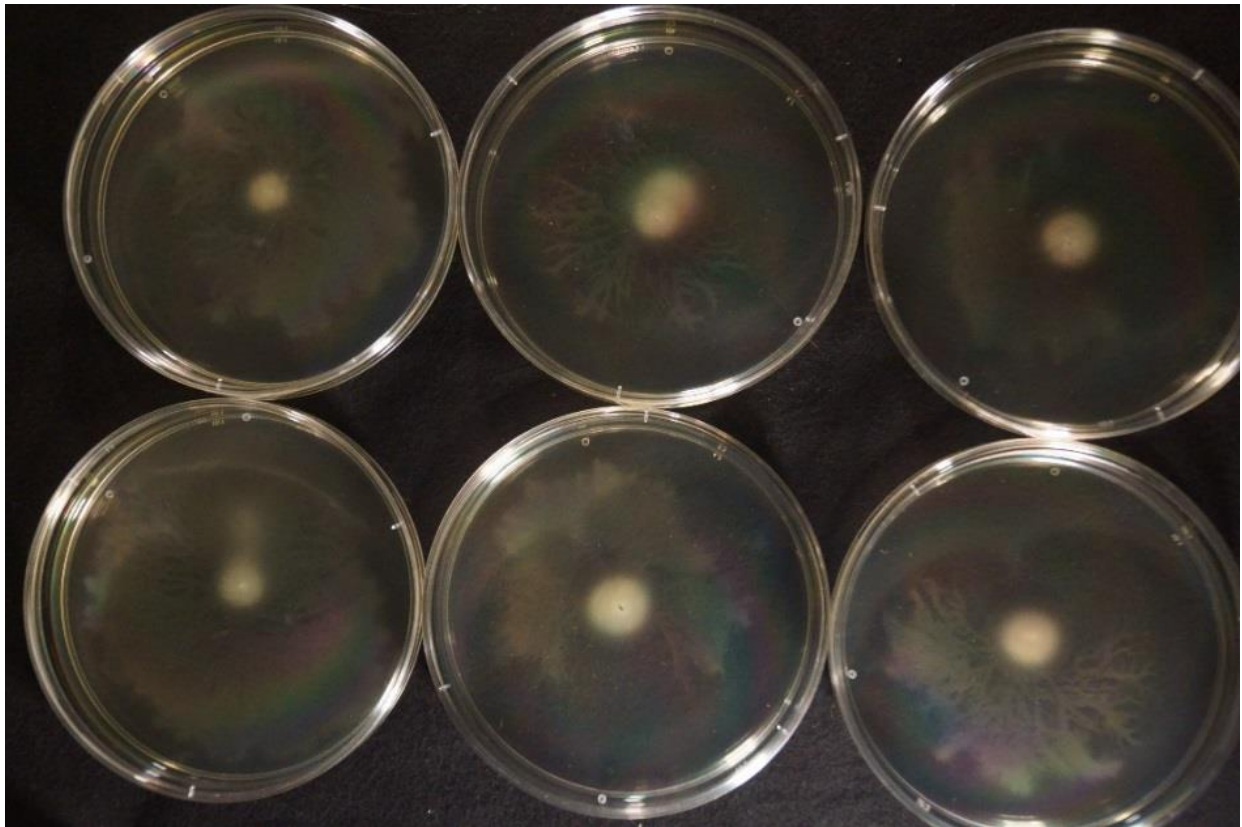


Figure 4-16 Colony phenotype of evolved strain FleQS9

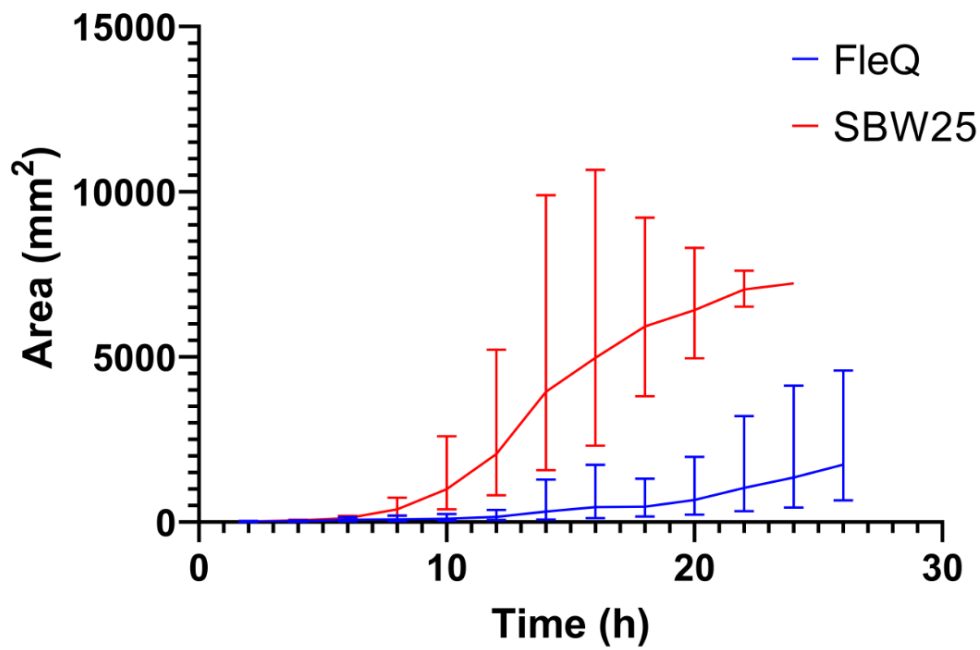
All colonies exhibited swimming motility as well as spidery-swarming. This picture was taken after 28 h and was used to construct the colony expansion curves. It was classified as a fast type in its group. The averaged colony expansion rate over a period of 8 h was 6.2 mm²/h (mean). Method: time-lapse photography. Plates: 9 cm diameter. Swarming medium (0.25 % agar LA medium).

4.5.1 Classification of evolved FleQS strains based on rate of colony expansion

In spite of the ability to swim and spidery-swarm, all evolved strains spread much slower than wild type strain SBW25 on swarming media. By 25 h, while SBW25 had covered the entire 9 cm plate (7226.4 mm²), the maximum area covered by any mutant was just over 1000 mm². The area covered by the FleQS mutants, by 25 h, was less compared to that covered by the aflagellate parent strain SBW25Δ*fleQ*, but much higher than spread of the parent strain in the total period of time observed (40 h) (Figure 3-9; Figure 3-19; Figure 4-17). Thus, the mutation did not fully compensate for loss of the *fleQ* regulator and appeared to reduce total spread area during the initial ~16 h. Movement of mutants was reliant on swimming motility and not on cell division as in the parent aflagellate strain SBW25Δ*fleQ*. Based on the geomean of colony expansion curves the average rate of colony expansion of the strains was calculated

(Equation 2-1). The rate of colony expansion and acceleration of the colonies changed constantly over the time period studied (32 h), and variation was most pronounced when some replicates initiated earlier swarming (Appendix K). Swarming was very fast and dramatically affected the rate of colony expansion curve where plates did not swarm concomitantly. As observed by Tremblay and Déziel²⁹⁰ when studying the effect of water content in the medium on swarming initiation of *P. aeruginosa*, physicochemical properties of the swarming medium are likely to contribute to variation in initiation of swarming. Only mutant FleQS6 exhibited more variability in the motility of replicates (Figure 4-18; Appendix A: Figure A-15) compared with the other FleQS strains (Appendix A: Figure A-19). Hence, it was considered valid to use the geomean data to compare swarming-spreading as well as swimming dependent expansion rates of colony spread.

Based on the swimming dependent initial rate of colony expansion (2 h- 8 h), the evolved FleQS strains were classified as fast, medium and slow swimmers. The fastest strain, FleQS2 (mean = 8.9 mm²/h), exhibited 8 times the rate of colony expansion of the aflagellate parent strain SBW25 Δ *flaQ* (mean = 1.3 mm²/h) over the initial period of 8 h (Appendices A and K), but was 3 times slower than the wild-type SBW25 (mean = 26.3 mm²/h). The swimming colonies of all FleQS strains were rounded and yellow in appearance (Appendix M). Strains that had some replicates that swarmed at 18 h or less were considered to be earlier swarmers. Also, it is important to notice that all strains began to differentiate dramatically from the swimming rate of colony expansion at around 16 h. All FleQS strains tended to decrease their rate of colony expansion at around 17 h and to increase the rate of expansion again between 20 h and 24 h (Appendix K). As with SBW25 this would correlate to a switch from swimming dependent expansion to viscosin dependent swarming (Chapter 3). A second decrease in the rate of expansion between 28 h and 29 h likely correlates with spread approaching the plate border.



FleQS

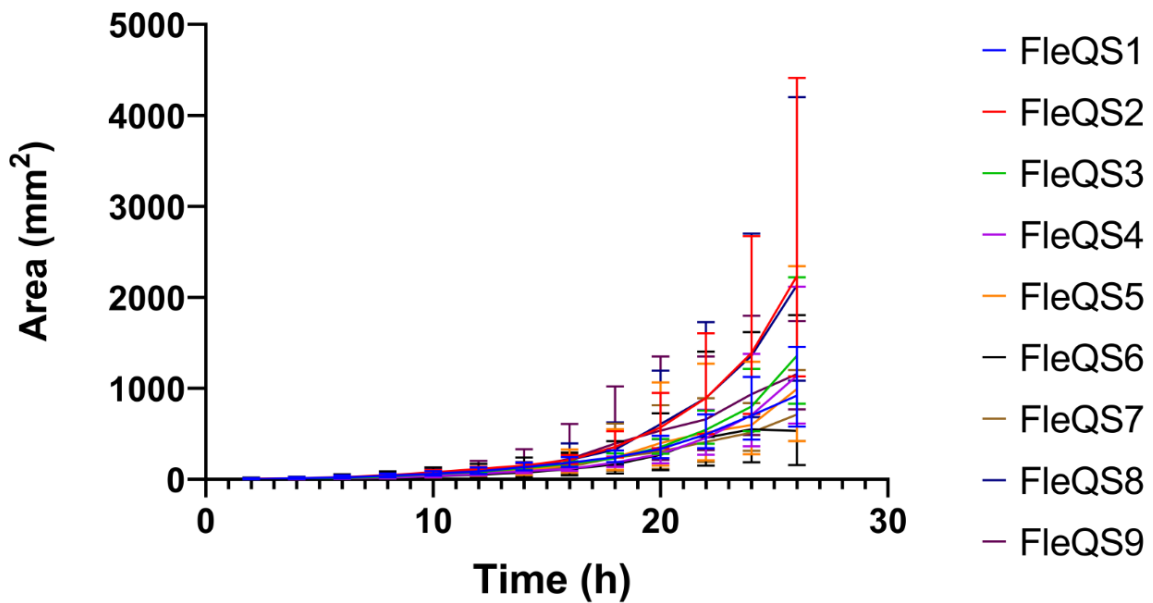


Figure 4-17 Colony expansion curves of the evolved FleQS strains compared to SBW25 and SBW25ΔfleQ

Colony expansion curves were constructed from motility plates (swarming medium) using the hand-drawn method (only for strains SBW25 and SBW25ΔfleQ) and time-lapse photography (only for FleQS strains). All plates shown were 9 cm in diameter (area of the 9 cm plate: 7226.4 mm²). The graph shows geommean of all replicates. The error bars represent the geometric standard deviation. The data shown for SBW25 and SBW25ΔfleQ are from Chapter 3.

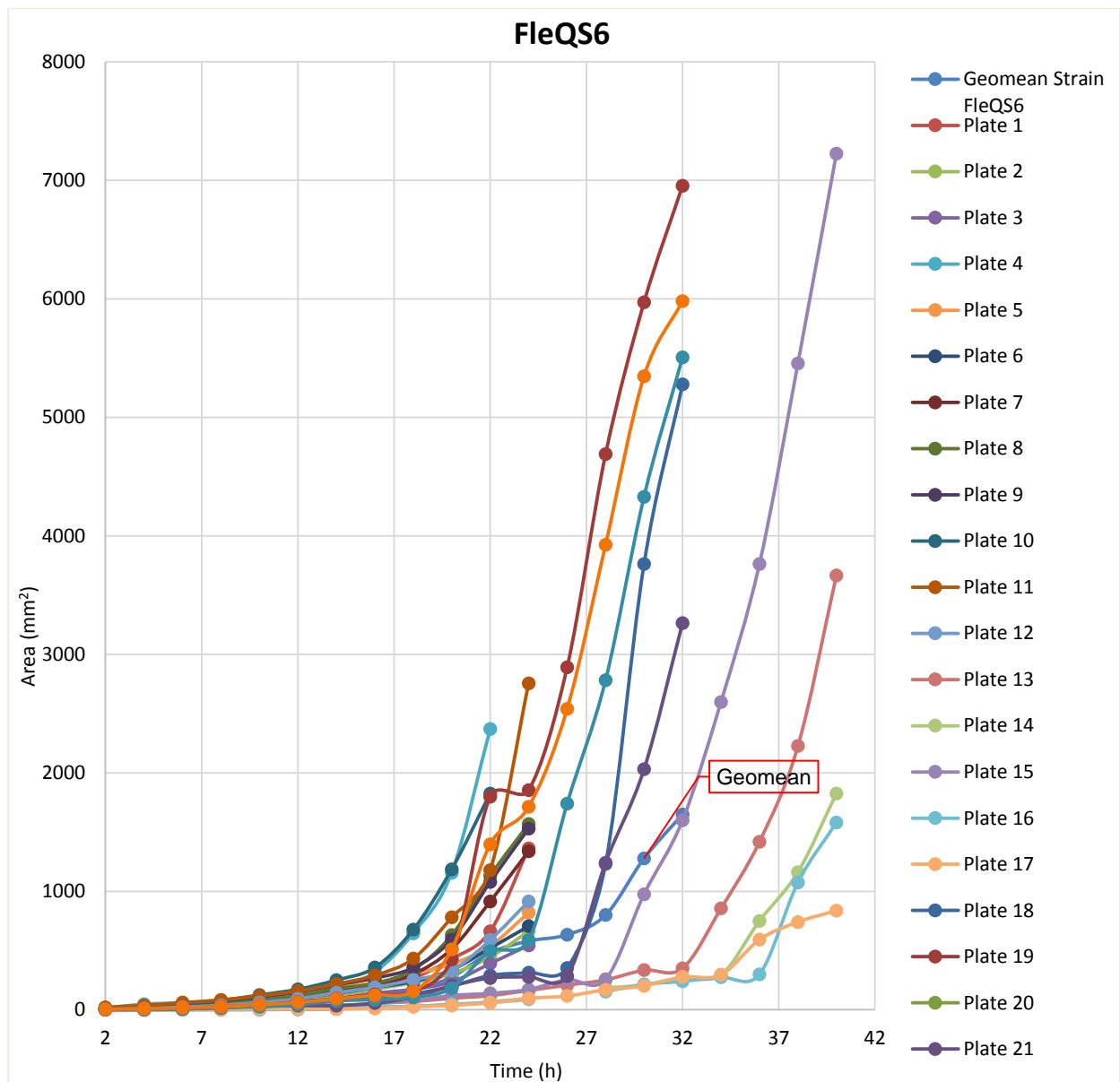


Figure 4-18 Colony expansion curves of evolved strain FleQS6

The colony expansion curves that only were obtained for a period of 24 h were done using the hand written method, and where done concomitantly. The other replicates were studied using time-lapse photography in groups of 6 replicates, and observed for 40 h. The area of the 9 cm plate: 7226.4 mm². Plates: 9 cm diameter. Swarming medium (0.25 % agar LA medium).

4.6 Mutational Changes in the Nitrogen Regulation Pathway (NtrBC) and Evolution of Swimming Motility

Mutations in 3 different genes of the Ntr system, *ntrB*, *ntrC* and *glnK*, were considered to be the most likely suppressors of the non-motile phenotype of SBW25Δ*fleQ*. Suppressor mutations in each of these genes had previously been reported¹⁰⁸. PCR was used to amplify the corresponding segment of each of these putative suppressor

genes (see section 1.9.2 for details). None of the evolved FleQS strains contained mutations within the amplified segment of the *ntrC* and *glnK* genes (refer to Alignments in Supplementary Information). With the exception of FleQS5 and FleQS7, each evolved mutant possessed a point mutation in *ntrB*, A289C. It is interesting to note that each of these evolved strains showed the same single point mutation, encoding a T97P substitution within the PAS domain of NtrB (Table 4-6), previously identified in AR2S, a slow swimming evolved mutant¹⁰⁸. The absence of any identified mutation in FleQS5 and FleQS7 is further investigated in Chapter 6.

Table 4-6 Mutations in *ntrB* and the associated amino acid position changes

Strain	Isolated from treatment	Rate of colony expansion in 8 h (mm ² /h)	Motility Phenotype	Nucleotide Change	Amino Acid Change
	Nitrogen/Glucose	Mean		<i>ntrB</i>	NtrB
FleQS1	ammonium	7.2	Fast	A289C	T97P
FleQS2	ammonium	8.9	Fast	A289C	T97P
FleQS3	ammonium	6.5	Fast	A289C	T97P
FleQS4	ammonium	4.1	Slow	A289C	T97P
FleQS5	ammonium	5.1	Medium	Wild type	Wild type
FleQS6	ammonium	3.7	Slow	A289C	T97P
FleQS7	glutamate	4.4	Slow	Wild type	Wild type
FleQS8	glutamate	5.6	Medium	A289C	T97P
FleQS9	glutamine	6.2	Fast	A289C	T97P

Note: All evolved strains did not show any mutation in the target sequence for *ntrC*, and none of them mutated in *glnK*.

4.7 Growth Comparison of Evolved FleQS Mutants in M9 Liquid Medium for Different Nitrogen Sources and Rich LB Medium

To monitor any impact that mutation(s) in the evolved strains had on growth, all mutants were tested in a microtitre plate assay for growth in rich medium (LB) and in M9-glucose with each of the nitrogen sources used for isolation, as described in section 2.3.2. Bacterial growth refers to the incremental proliferation of bacterial cells through division and growth. During the exponential phase when cells are not starving and should not be under stress from metabolic end products, cell numbers double exponentially at constant rate. In contrast, during stationary phase, the cell death rate is equal to the cell division rate, and cells undergo substantial physiological adaptations. Cells respond to environmental stress caused by the accumulation of waste products, which leads to a modification in the osmolality and pH in the

environment. As a result of these environmental cues, the genetic expression profile changes, with the expression of the alternative sigma factor RpoS, and small non-coding RNAs (sRNAs), and cell metabolism is consequently modified. Hence, bacterial growth properties are generally defined by the growth rate in exponential phase and maximum growth achieved in the stationary phase. Growth curves for all strains and each medium are available in Appendices D (FleQS mutants) and S (SBW25 and SBW25 $\Delta fleQ$ parent), see Figure 4-19. The OD₆₀₀ at 10 h was selected as a time-point for comparison of evolved mutants. The 10 h time point was within the exponential phase, either late or early-to mid exponential phase, on LB and each M9 broth tested. Entry into the stationary phase varied and reflected differences in exponential growth rates in each different medium. This was at around 11 h-12 h for growth on LB or M9-glucose with glutamine, 16 h -18 h for growth on M9- glucose with glutamate and greater than 18 h for growth on M9-glucose with ammonium. A high variability was observed among the biological replicates in any treatment during both the exponential and stationary phases. This observation was noted in all growth curves of the evolved FleQS strains with each different medium (Appendix D: Figure D-1 to D-9), with wild type strain SBW25 (Appendix S: Figure S-1), and the AR1 and AR2 mutant strains (Appendix R: Figure R-1, Figure R-2, Figure R-3) studied. This variability might be explained by diversity in the growth stage of cells in the inoculum from independent overnight cultures and hence variation in the length of the lag phase. If growth curves were constructed using pseudo-replicates i.e. multiple growth curves from a single overnight culture, then this variability was not present. Biological repeats, overnight cultures from individual colonies ($n = 5$ or 6), were used to quantitate growth of each FleQS mutant in LB (rich medium) and M9 – glucose minimal medium with glutamine, glutamate or ammonium as sole nitrogen source.

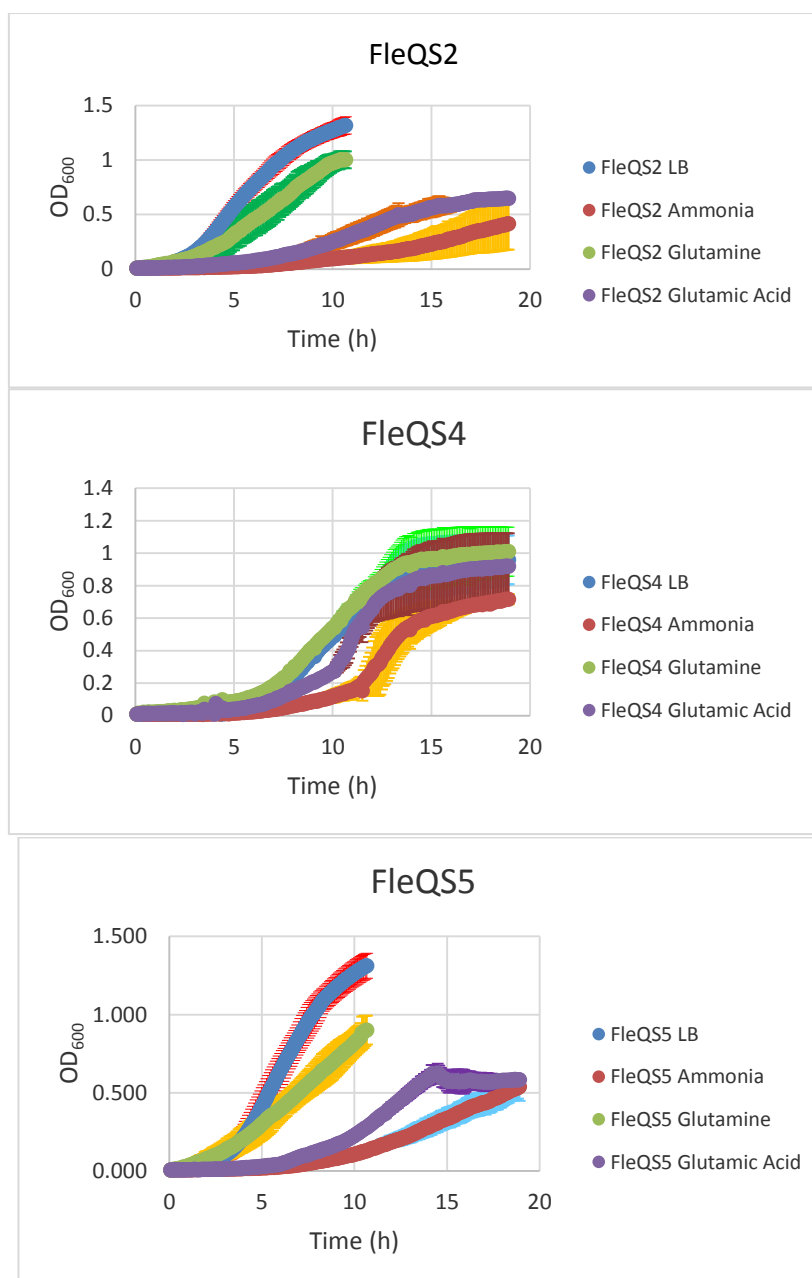


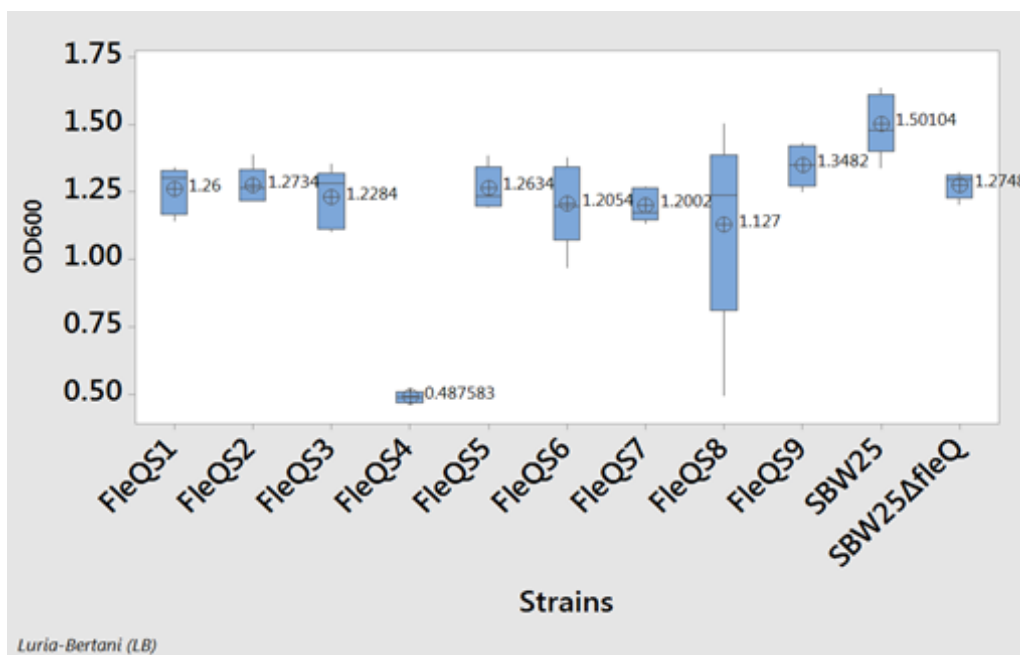
Figure 4-19 Growth curves of FleQS strains in LB and liquid medium M9-glucose

The growth curves shown are the average of all biological replicates and the error bars represent the standard deviation. Nitrogen sources: glutamic acid (glutamate), glutamine and ammonium.

4.7.1 Growth in rich medium LB:

As recorded in Chapter 3, the wild type strain SBW25 grew slightly better than the aflagellate strain SBW25 Δ *fleQ*, with a 10 h optical density of OD₆₀₀ = 1.50 (*SD* = 0.11) and 1.28 OD₆₀₀ (*SD* = 0.05), respectively (Figure 3-31, Figure 3-32, Figure 4-20). Interestingly, evolution to the swimming phenotype via the *ntrB* mutation, had no evident impact on growth of most mutants in rich medium. The parent strain

SBW25 $\Delta fleQ$ and the evolved flagellated strains FleQS1, FleQS2, FleQS3, FleQS5, FleQS6, FleQS7, FleQS8 and FleQS9 showed equivalent growth at 10 h (~1.2 OD₆₀₀), see growth curves in Appendix D: Figure D-19.



Strain	N	OD ₆₀₀ Mean	SD	95% CI
FleQS1	5	1.2600	0.0874	(1.1311, 1.3889)
FleQS2	5	1.2734	0.0696	(1.1445, 1.4023)
FleQS3	5	1.2284	0.1110	(1.0995, 1.3573)
FleQS4	5	0.4876	0.0231	(0.3587, 0.6165)
FleQS5	5	1.2634	0.0799	(1.1345, 1.3923)
FleQS6	5	1.2054	0.1553	(1.0765, 1.3343)
FleQS7	5	1.2002	0.0616	(1.0713, 1.3291)
FleQS8	5	1.127	0.379	(0.998, 1.256)
FleQS9	5	1.3482	0.0772	(1.2193, 1.4771)
SBW25	5	1.5010	0.1154	(1.3722, 1.6299)
SBW25 $\Delta fleQ$	5	1.2748	0.0477	(1.1459, 1.4037)

Note: CI: confidence interval

Figure 4-20 Box plot: Growth comparison between parent strain SBW25 $\Delta fleQ$ and evolved FleQS strains in rich medium LB

Growth data was obtained from the respective growth curves at 10 h in rich medium LB, towards the end of the exponential phase. The value shown inside each box plot is the average growth (OD₆₀₀) at 10 h. The growth data for SBW25 $\Delta fleQ$ and SBW25 are from Chapter 3 (Figure 3-31; Figure 3-32). The growth curves for all evolved FleQS strains are shown in Appendix D.

Only strain FleQS4 exhibited a marked decrease in growth, reaching an OD₆₀₀ of only 0.49 (*SD* = 0.02) by 10 h and a maximum stationary phase optical density of 0.95 (Figure 4-19, Figure 4-20; Appendix D: Figure D-4). This did not correlate with colony expansion data on swarming medium. No impact of poorer growth of FleQS4 was evident on swarming medium. FleQS4 covered a similar area at 18 h (*P-value* 0.092 > 0.050) on swarming medium (mean = 192.1 mm², *SD* = 21.7 mm²) by 18 h; see Appendix ZL: Table ZL-1 and Table ZL-2, as most other evolved FleQS mutants (Figure 4-17, Figure 4-18; Appendix A: Figure A-19). Oxygen depletion would not explain this decrease, as cultures were constantly shaken and the nutrients evenly distributed. FleQS4 possessed the same *ntxB* mutation (A289C) as other evolved FleQS mutants. Thus, the poor growth of FleQS4 in LB was an initial indication that this strain possessed some additional mutation that led to a detrimental impact on metabolism and growth in rich medium.

4.7.2 Growth in ammonium/glucose M9 medium

While the aflagellate parent strain SBW25Δ*flaE*Q grew as well as the wild type strain SBW25 (~0.5 OD₆₀₀ at 10 h) in ammonium/glucose M9 minimal medium (Figure 3-31; Figure 3-32; Figure 4-21), all evolved FleQS strains showed remarkably poor growth with ammonium as sole N source (≤ ~0.1 OD₆₀₀ at 10 h) (Appendix D, Appendix S). In these evolved FleQS strains, ammonium presented a profound negative effect on growth. The pattern of growth curve of FleQS1, FleQS2, FleQS3 and FleQS5 was very similar (shown in Figure 4-19 for FleQS5 and FleQS2). There was an extended lag phase to around 6 h followed by a slow increase in growth to OD₆₀₀ = 0.09 - 0.13 at 10 h, and subsequent steady but slow exponential growth to around OD₆₀₀ = approximately 0.4 at 18 h. Growth of FleQS 6, FleQS7 and FleQS9 was similar but slower, with an extended lag phase to around 8 h, and reaching an OD₆₀₀ of only 0.04 - 0.06 at 10 h and approximately 0.2 at 18 h. As with LB medium, FleQS4 stood out as clearly different (Figure 4-19, Table 4-7). But in contrast to growth in LB, in ammonium/glucose M9 medium FleQS4 grew better than all other FleQS mutants. This mutant exhibited the same slow initial growth reaching only 0.12 OD₆₀₀ at 10 h, but between 11 h and 13.5 h there was rapid exponential growth to an OD₆₀₀ of 0.5 at 13.5 h and continued growth through early stationary phase to OD₆₀₀ of 0.69 at 18 h. This suggested a genotype that was detrimental to growth in LB but permitted better survival and growth in high concentrations of ammonium.

4.7.3 Growth in glutamine/glucose M9 medium

As with the parent strain *SBW25ΔfleQ* and wild type *SBW25* (Table 4-8), all evolved FleQS strains exhibited best growth in M9- glucose medium with glutamine as N source. FleQS1, FleQS2, FleQS3, FleQS5, FleQS6, FleQS7, FleQS8, and FleQS9 grew to ~0.8 OD₆₀₀ by 10 h in glutamine/glucose M9 minimal medium (Figure 4-21). However, as with growth in LB, strain FleQS4 grew less well (0.5 OD₆₀₀ at 10 h). The nitrogen source in which these FleQS strains evolved (Table 4-4) did not correlate with their growth phenotype in glutamine, as FleQS4 was isolated from ammonium/glucose treatment, as were all isolates, FleQS1-6.

4.7.4 Growth in glutamate/glucose M9 medium

In contrast to growth with glutamine but similar to growth with ammonium, all of the evolved FleQS strains grew more poorly than the parent *SBW5ΔfleQ* and wild type *SBW25* strains in glutamate/glucose M9 minimal medium (Figure 4-21). At 10 h the OD₆₀₀ of FleQS strains ranged from 0.14 – 0.32 with stationary phase maximum around 0.6 OD₆₀₀. Whereas by 10 h, *SBW5ΔfleQ* and *SBW25* had already reached an OD₆₀₀ = 0.65 and 0.69, respectively. Again FleQS4 exhibited a different pattern similar to that on ammonium, with a slow start, rapid exponential phase and reaching a stationary phase OD₆₀₀ of 0.92, close to that of growth on both M9-glucose with glutamine and LB (Figure 4-19).

Table 4-7 Growth in ammonium/glucose minimal medium M9 after 10 h and the motility phenotype of FleQS strains

Strain	Nitrogen Source when Isolated*	Mean Rate of colony expansion in 8 h (mm ² /h)	Motility Phenotype	Growth (Mean OD ₆₀₀)	<i>ntrB</i> Nucleotide Change	NtrB Amino Acid Change
FleQS1	ammonium	7.2	Fast	0.1017	A289C	T97P
FleQS2	ammonium	8.9	Fast	0.0956	A289C	T97P
FleQS3	ammonium	6.5	Fast	0.1260	A289C	T97P
FleQS4	ammonium	4.1	Slow	0.1189	A289C	T97P
FleQS5	ammonium	5.1	Medium	0.1068	Wild type	Wild type
FleQS6	ammonium	3.7	Slow	0.0577	A289C	T97P
FleQS7	glutamate	4.4	Slow	0.0347	Wild type	Wild type
FleQS8	glutamate	5.6	Medium	0.0872	A289C	T97P
FleQS9	glutamine	6.2	Fast	0.0472	A289C	T97P

Note: * Glucose was the carbon source.

Table 4-8 Strains SBW25Δ*fleQ* and SBW25 responded equally to rich and poor nitrogen sources

Strains	<i>N</i>	Medium	OD ₆₀₀ Mean (SD)	95% CI
SBW25	6	M9 + Glutamine	0.8171 (0.0790)	(0.7770, 0.8572)
SBW25	6	M9 +Glutamate	0.6886 (0.0784)	(0.6330, 0.7442)
SBW25	5	M9 +Ammonium	0.53280 (0.01377)	(0.42640, 0.63920)
SBW25	5	LB	1.5010 (0.1154)	(1.4457, 1.5564)
SBW25Δ <i>fleQ</i>	6	M9 +Glutamine	0.8701 (0.0286)	(0.8300, 0.9102)
SBW25Δ <i>fleQ</i>	6	M9 +Glutamate	0.6486 (0.0934)	(0.5930, 0.7043)
SBW25Δ <i>fleQ</i>	4	M9 + Ammonium	0.5777 (0.0255)	(0.4588, 0.6967)
SBW25Δ <i>fleQ</i>	5	LB	1.2748 (0.0477)	(1.2195, 1.3301)

Note: Average growth data (OD₆₀₀) at 10 h, *N*: biological replicates, CI: confidence interval. The carbon source for all treatments was glucose.

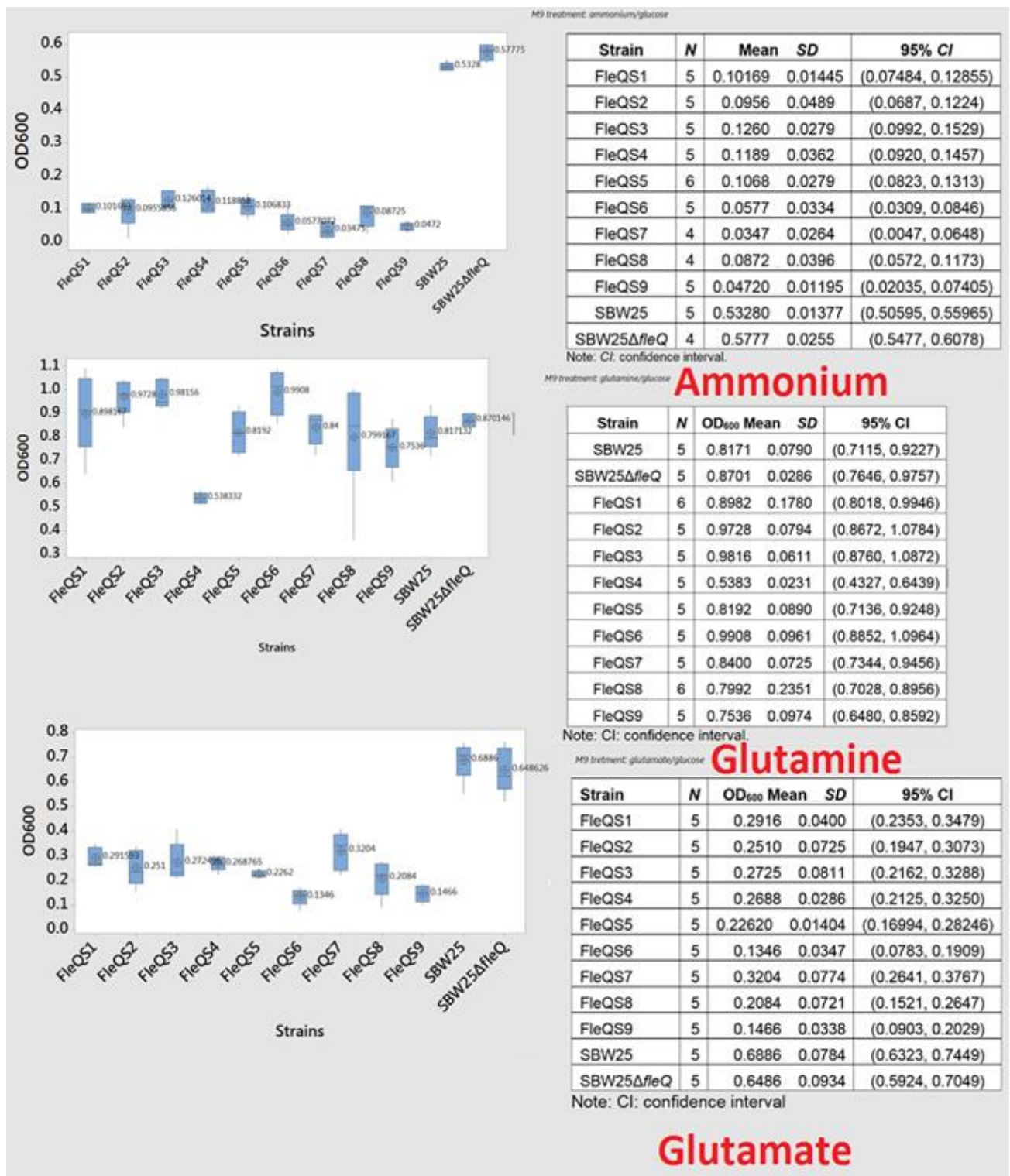


Figure 4-21 Box plot: Growth comparison between parent strain SBW25ΔfleQ and evolved FleQS strains in nitrogen/glucose minimal medium M9

The value shown inside each box plot is the average growth (OD₆₀₀) at 10 h. The mean is shown in each box plot (cross circle). All growth experiments were performed at the same time.

Data from Chapter 3 was used for comparison of growth properties of mutants with parent strain SBW25 Δ *fleQ* and SBW25. While direct comparison in the same experiment would confirm and highlight small differences, some important growth properties of the evolved FleQS mutants have been highlighted. Despite possession of the same *ntxB* mutation in seven of the nine FleQS isolates, six of these (FleQS1, 2, 3, 6, 8 and 9) grew as well as the parent strain SBW25 Δ *fleQ* on rich medium LB and on glutamine, but showed very poor growth on both ammonium and glutamate. This might be explained by overactivation of the nitrogen response and glutamine synthetase (GS) activity in the presence of the NtrB T97P mutation, which is assumed to decrease the phosphatase activity of NtrB^{149,309}. When grown on ammonium an inability to repress GS activity could lead to a N:C imbalance and poor growth. Interestingly FleQS4, with the same NtrB T97P mutation exhibited the opposite phenotype in relation to these N-sources. While it grew more poorly in rich medium and glutamine than the other mutants, after a lag FleQS4 grew well when either ammonium or glutamate was used as N-source. This points to an additional step in evolution of this strain which helps it survive and grow better on ammonium.

4.8 FleQS Strains Produce Flagella

Bacteria morphology was observed by staining the cells with Gram-stain and fluorescent NanoOrange dye as described in section 2.15. FleQS strains grew less in rich medium (LB) compared with wild type strain SBW25 (Figure 4-19; Figure 4-20), also the rod-shaped cells appeared to be smaller and wider than the wild type strain SBW25 (Figure 4-22). However, this apparent difference was not statistically significant (*P-value* 0.436 > 0.050) from the parent strain aflagellate SBW25 Δ *fleQ* (Appendix L: Table L-1 and Table L-2). TEM analysis revealed the production of flagellum by FleQS strains. In general, the flagellum did not differ in number and position compared to the wild type strain SBW25. Flagella localisation was lophotricus (1-2 flagella) (Figure 4-23), as shown for FleQS7. One FleQS5 cell appeared to have a polar flagellum and a lateral flagellum, this would suggest induction of a different motor (Figure 4-23). Reports of cryptic flagella operons in other *P. fluorescens* strains (F113 and et76)¹⁸¹ and lateral flagella in *Vibrio* sp involved additional genetic loci³⁰⁸. Thus, if lateral production of flagella proved to be the case in FleQS5 it would deserve further investigation.

It is notable that the cell size of the wild type strain SBW25 reported by Ping et al.²⁴ was found to be statistically significant different (P -value $0.000 < 0.050$) from the cell size determined in this research (Figure 4-24). This study used Gram-stain in order to stain the cells from an ON broth culture in rich medium LB. Ping et al.²⁴ harvested the cells grown in LB during the early exponential phase ($OD_{600} = 0.2$) and were incubated at 23 °C. However, in this study, they were incubated at 26 °C. The coefficient of variation of the data set was at 26.01 % and their mode was 2.586 μm (n for mode = 3); please refer to Appendix ZM: Table ZM-1. Both the parent strain SBW25 Δ *fleQ* and the wild type strain SBW25 were studied concomitantly and stained through the usage of Gram-stain. The evolved strains FleQS were then studied concomitantly and stained with the fluorescent NanoOrange dye. Notably, all studied strains were grown in rich medium LB and incubated in a rotary shaker at 220 rpm and incubated at 26 °C. The fluorescent dye was initially used to observe the flagella, but it was not possible to visualize this organelle using this method as the flagella are fragile. However, the stained cells were used for cell length measurements. Please refer to Appendix ZM: Table ZM-1 for descriptive statistics of all strains.

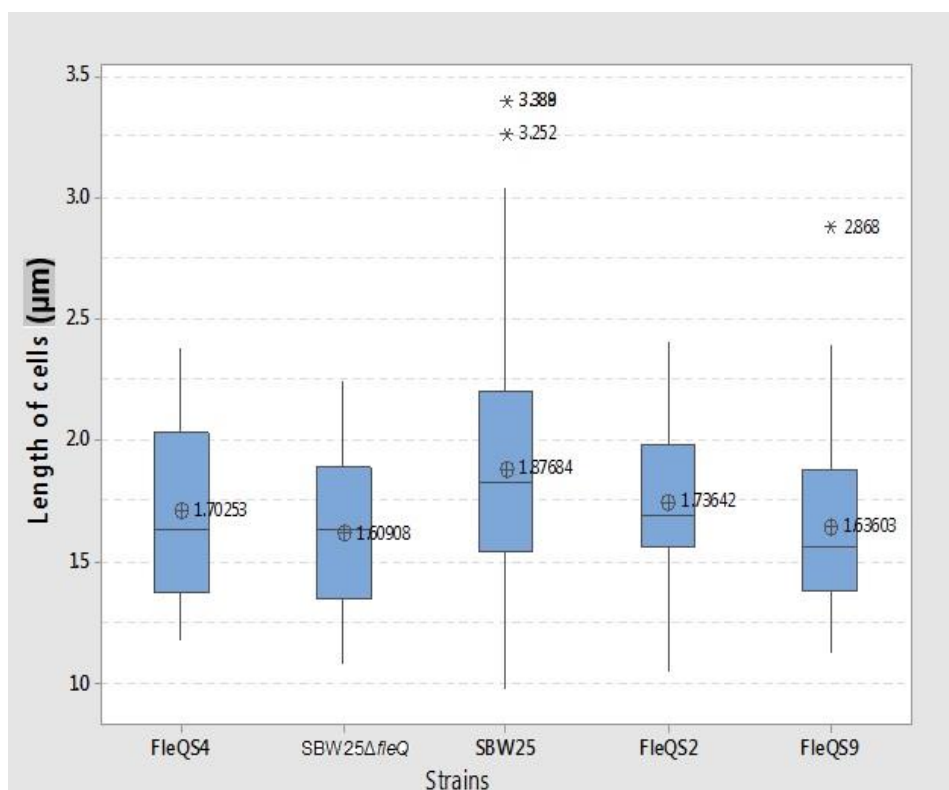


Figure 4-22 Box plot: Comparison of cell lengths (μm) among FleQS strains, parent (SBW25 Δ *fleQ*) and wild type strain SBW25

The cells were stained with NanoOrange dye or Gram-stain.

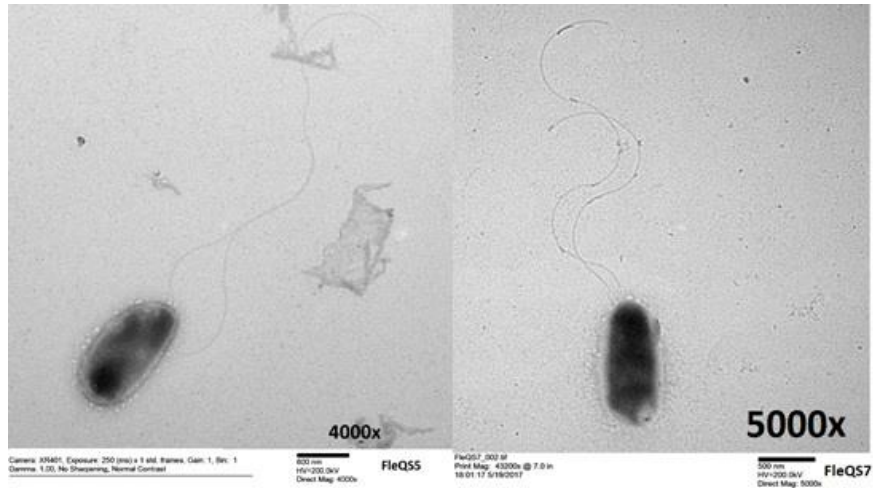
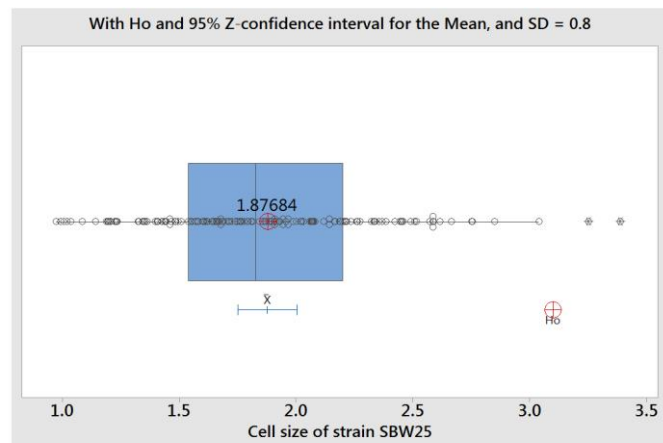


Figure 4-23 TEM of evolved strains FleQS7 and FleQS5

TEM of strain FleQS7 with flagella in the lophotrichous position and strain FleQS5 with a polar flagellum and a lateral flagellum. The cells were grown prior to EM in 3 mL LB (poured into 50 mL conical centrifuge tube) and incubated ON at 26 °C on a rotary shaker at 95 rpm (see section 2.14).



One-Sample Z: Strain SBW25
Descriptive Statistics

<i>N</i>	<i>Mean (μm)</i>	<i>SD</i>	<i>SE Mean</i>	<i>95% CI</i>
152	1.8768	0.4881	0.0649	(1.7497, 2.0040)

Known standard deviation = 0.8

Test

Null hypothesis	$H_0: \mu = 3.1$
Alternative hypothesis	$H_1: \mu \neq 3.1$

<i>Z-value</i>	<i>P-value</i>
-18.85	0.000

Figure 4-24 Box plot: Comparison of the cell size (μm) of strain SBW25 determined in this research with the reported value of Ping et al.²⁴

The strain SBW25 was grown in LB (ON) at 26 °C and constantly shaken, whereas Ping et al.²⁴ used a lower incubation temperature of 23 °C. The value shown inside each box plot denotes the average cell size (μm).

4.9 Multivariate Analysis: Discriminant

A multivariate analysis (discriminant) was used to determine the similarities and differences of the evolved strains (Table 4-9). This discriminant analysis did not distinguish strains FleQS1, FleQS2, and FleQS3 consistent with the highly similar phenotypes of these 3 isolates, each of which was from a different replica plate. These strains were categorized as Group I. Hence, these strains presented a high probability of being genotypically identical for selection. In order to confirm the identical characteristics of the carried mutations, it was necessary to conduct a whole genome sequencing of all the FleQS strains. Therefore, these strains were categorized in Group I. Although the strains FleQS5 and FleQS8 were slightly similar to the strains in Group I, they were not phenotypically identical despite showing certain similarities with Group I. Therefore, they were classified into Group II. The other strains, FleQS4, FleQS6, FleQS7, and FleQS9 were phenotypically different and were not similar to any FleQS strain. Hence, it was not possible to categorize these strains in a group. Based on the discriminant analysis and growth curves, all the evolved strains showed metabolic differences from the parent strain. For example, all the evolved FleQS strains grew less in ammonium and glutamate treatments compared to their parent strain SBW25 Δ *fleQ* and the wild type strain SBW25. However, FleQS strains (except FleQS4) showed no differences in growth in glutamine compared to their parent aflagellate strain SBW25 Δ *fleQ* and the wild type strain SBW25.

Table 4-9 Discriminant analysis**Summary of Classification**

Put into Group	True Group									
	SBW25Δ <i>fleQ</i>	FleQS1	FleQS2	FleQS3	FleQS4	FleQS5	FleQS6	FleQS7	FleQS8	FleQS9
SBW25Δ <i>fleQ</i>	4	0	0	0	0	0	0	0	0	0
FleQS1	0	3	0	0	0	0	0	0	0	0
FleQS2	0	1	2	1	0	0	0	0	1	0
FleQS3	0	0	2	3	0	1	0	0	0	0
FleQS4	0	0	0	0	5	0	0	0	0	0
FleQS5	0	1	1	0	0	4	0	0	0	0
FleQS6	0	0	0	0	0	0	4	0	0	0
FleQS7	0	0	0	0	0	0	0	2	0	0
FleQS8	0	0	0	1	0	0	0	0	3	0
FleQS9	0	0	0	0	0	0	0	0	0	2
SBW25	0	0	0	0	0	0	0	0	0	0
Total N	4	5	5	5	5	5	4	2	4	2
N correct	4	3	2	3	5	4	4	2	3	2
Proportion	1.000	0.600	0.400	0.600	1.000	0.800	1.000	1.000	0.750	1.000
Put into Group	SBW25									
SBW25Δ <i>fleQ</i>	0									
FleQS1	0									
FleQS2	0									
FleQS3	0									
FleQS4	0									
FleQS5	0									
FleQS6	0									
FleQS7	0									
FleQS8	0									
FleQS9	0									
SBW25	4									
Total N	4									
N correct	4									
Proportion	1.000									

Correct Classifications

N	Correct	Proportion
45	36	0.800

Note: phenotypes included were growth (OD₆₀₀) at 10 h under different nitrogen sources with glucose as carbon source, rich medium LB, and colony's spreading area (mm²) in swarming medium at different time points (2 h, 4 h, 6 h, 24 h).

Table 4-10 Summary of results

Strain	M9 Culture Medium ^B			LB (Mean OD ₆₀₀)	Swimming Motility Phenotype	Swarming	Mean Rate of Colony Expansion in 8 h (mm ² /h)	<i>ntrB</i> nt Change	NtrB AA Change	^a Area (mm ²) Mean (SD)
	NH ₄ ⁺ (Mean OD ₆₀₀)	Glutamine (Mean OD ₆₀₀)	Glutamate (Mean OD ₆₀₀)							
^c SBW25	0.5328	0.8171	0.6886	1.5010	WT	WT	26.3	WT	WT	12328.7 (6204.0)
^c SBW25Δ <i>fleQ</i>	0.5777	0.8701	0.6486	1.2748	None	None	1.3	WT	WT	11104.5 (6969.0)
FleQS1	0.10169	0.8982	0.2916	1.2600	Fast	Wild	7.2	A289C	T97P	948.6 (538.0)
FleQS2	0.0956	0.9728	0.2510	1.2734	Fast	Spidery	8.9	A289C	T97P	1863.8 (869.0)
FleQS3	0.1260	0.9816	0.2725	1.2284	Fast	Spidery	6.5	A289C	T97P	929.8 (408.0)
FleQS4	0.1189	0.5383	0.2688	0.4876	Slow	Spidery/Wild	4.1	A289C	T97P	763 (453.0)
FleQS5	0.1068	0.8192	0.2262	1.2634	Medium	Spidery	5.1	*WT	*WT	751.9 (559.0)
FleQS6	0.0577	0.9908	0.1346	1.2054	Slow	Wild	3.7	A289C	T97P	846.8 (362.0)
FleQS7	0.0347	0.8400	0.3204	1.2002	Slow	Spidery	4.4	WT	WT	652.8 (52.0)
FleQS8	0.0872	0.7992	0.2084	1.1270	Medium	Spidery	5.6	A289C	T97P	1172.4 (681.0)
FleQS9	0.0472	0.7536	0.1466	1.3428	Fast	Spidery	6.2	A289C	T97P	2307.3 (1670.0)

Note: ^aMean area (mm²) covered by different strains in 24 h when grown on swarming medium. ^bGlucose as the carbon source. ^cData for strains SBW25 and SBW25Δ*fleQ* came from Chapter 3 in 15 cm diameter plates.

WT wild type; AA amino acid; nt nucleotide.

The strains shaded red grew more or the area covered by them was greater than the strains shaded yellow. The strains shaded blue grew less or the area covered by them was less than the ones shaded yellow. All the evolved strains did not show any mutation in the target sequence for *ntrC*, and there were no mutations present in *glnK*.

*The results from WGS recognised that this strain was a mix population, which carried two non-identical single point mutations in *ntrB*: T97P/D228G. The mutation D228G was not situated in the region covered by the primers, hence initially it was regarded as *WT*.

5 Evolution of Swimming Motility in Sessile Strains AR1 and AR2 under different Nitrogen and Carbon sources

5.1 Introduction

The flagella re-wiring in sessile strain AR2 (*Fla* , *Visc*) was initially discovered and studied by Taylor et al.¹⁰⁸. They found out that these evolved mutant strains AR2S and AR2F evolved from the sessile strain AR2 grown in swarming medium (0.25 % agar LA) after 3-4 days. The whole genome sequencing data showed that the evolved mutant strains AR2S and AR2F mutated in two component system NtrBC for nitrogen regulation under starvation to restore flagella expression. These evolved strains mutate in a step manner, so the first point mutation occurred in NtrB leading to a slow swimming phenotype and the second single point mutation happened in NtrC, thus the double mutant *ntrB ntrC* showed a fastest swimming phenotype. However, it was not proved that nitrogen starvation was the evolutive force for these mutational event, as all evolved mutants obtained derived from sessile colonies inoculated into rich medium 0.25 % agar LA. Hence, the use of nitrogen sources (glutamate, glutamine and ammonium) that are key metabolites in nitrogen assimilation GS/GOGAT [glutamine synthetase (GS)/glutamate synthase (GOGAT)] pathway were employed, as it was necessary to evaluate the effect of nitrogen source in the flagella rewiring it was necessary to use glucose as carbon source to block the use of these amino acids as carbon sources and only evaluate the effect of nitrogen limitation under a rich energy environment. The rich energy environment means that there is plenty of carbon (glucose) available to provide all energy necessary to sustain metabolism, but when the nitrogen levels drop, the cells turn on the GS/GOGAT pathway to assimilate nitrogen. The use of this system under stress increases the probability of selection of any beneficial mutation in this system that improve the probability of survival of the population.

This chapter brings forth the evolution of swimming motility in sessile strains AR1 and AR2 under different nitrogen and carbon sources. This chapter describes the experiments to determine if nitrogen starvation is responsible for exerting pressure on the GS-pathway (GS: glutamine synthetase) based on the hypothesis that a bacterial population will evolve earlier when the chemical environment primes the GS-pathway

through the use of poor nitrogen sources, such as glutamine and glutamate. As such, based on the supplementary hypotheses described later, it first presents the summary of evolution of swimming motility in sessile strains AR1 and AR2, which presented no significant statistical differences in the evolution time of swimming motility under different nitrogen/carbon treatments for both sessile strains. Subsequently, the evolution of swimming motility in strains AR1 and AR2 with different nitrogen sources is studied, with a comparison of the percentage of non-evolved colonies for different nitrogen treatments. This is subsequently followed by studying the swimming colony expansion curves of evolved replicates under different nitrogen treatments using glucose as carbon source. Specifically followed by the study of evolution of swimming motility for different nitrogen sources and a poor carbon source. The hypothesis was further studied by experimenting the motility of evolved sessile strains AR1 and AR2 colonies for different nitrogen sources and a poor carbon source, wherein two colonies exhibited dramatically different motilities. This was followed by studying the stability of swimming phenotype of evolved isolates. The chapter also discusses study of single AR2S15 colonies, wherein no mutations were found within the region of the *ntrB* gene studied for strain AR2S15.

As in Chapter 4, experiments were conducted to determine if nitrogen starvation is responsible for exerting pressure on the GS-pathway which is regulated by the NtrBC system. It was hypothesized that a bacterial population will evolve earlier when the chemical environment primes the GS-pathway through the use of poor nitrogen sources, such as glutamine and glutamate. It was also hypothesized that there is a lower probability of sessile strains evolving when nitrogen rich sources, such as ammonium (NH_4^+), are available because it will take longer to prime the NtrBC system. It is also important to identify if the evolution of swimming motility is strain dependent and is due to the genotype of the sessile strains. This can be understood through experimental evolution using the sessile strains AR1 and AR2.

To determine whether the localisation of the IS- Ω -Km/hah transposon has any effect on the re-wiring of the nitrogen pathway to the flagella regulon and if nitrogen starvation is the main evolutionary force which acts independently of the strain, two sessile strains AR1 and AR2, which differ only in the position of the transposon within the viscosin operon were utilised. The physiological status under different nitrogen sources was investigated as the evolutionary force independent of the carbon source

which drives the development of swimming motility, and also whether the evolution of swimming occurs at a higher frequency and earlier when the NtrBC system is primed. In addition, it was hypothesized that bacterial populations randomly evolve swimming motility, and consequently evolve multiple swimming motility phenotypes.

5.2 Evolution of Swimming Motility in Strain AR1 with Different Nitrogen Sources in a Rich Energy Environment

Experimental evolution studies were conducted with a 0.25 % agar minimal medium M9 with different nitrogen sources to trigger upregulation of the NtrBC system and determine if there exists an association between the nitrogen source and the observation time of the evolved colonies derived from aflagellate strains as a result of the nitrogen limitation in their milieu, see research hypothesis (Figure 1-59). Additionally, it was recorded by the hand-drawn method the colony's area covered by the parents and the colonies evolved under the different nitrogen sources to determine the effect of nitrogen source on colony spreading (see section 2.4.3.1).

Evolution of swimming in AR1 as parent was also tested in minimal medium M9 with ammonium, glutamate or glutamine as nitrogen source and glucose as carbon source (as in section 2.6). The medium was supplemented with kanamycin to prevent loss of the transposon (IS- Ω -Km/hah) in *viscA* and *viscC*. The sessile parent, AR1 exhibited growth as a rounded dot and eventually evolved swimming motility as shown (Figure 5-1). Occasionally, a different form of motility assumed to be twitching was observed (Figure 5-1). Nine samples were taken from ammonium plates, 48 samples from glutamine plates and 10 samples from glutamate plates. Swimming was observed earlier at 3.2 days ($SD = 0.8$ days) and 3.55 ($SD = 2.06$ days) when glutamine or glutamate, respectively was the nitrogen source compared to ammonium 5.79 days ($SD = 0.54$ days), refer to Table 5-1. There was no significant statistical difference (P -value $0.633 > 0.050$; Appendix H: Table H-2 and Figure H-1) between the evolution time (days) of swimming motility when grown on glutamine or glutamate plus glucose. However, there was a significant statistical difference between the mean number of days it took for the evolution of swimming motility when grown on ammonium compared to glutamine as nitrogen source (P -value $0.000 < 0.050$; Appendix H: Table H-1). Therefore, the evolution of swimming motility was selected and observed earlier in the poor nitrogen sources, glutamine and glutamate and took longer when supplied

with rich nitrogen source ammonium. The higher probability of observing evolution of swimming motility in glutamine and glutamate was the expression of the GS pathway which is regulated by the NtrBC system in the presence of these amino acids, as shown in studies conducted in M9 minimal medium¹³³. This pathway is up-regulated under nitrogen limitation conditions (low levels of glutamine and ammonium) in a rich energy environment (glucose as the carbon source).



Figure 5-1 Cumulative growth and presumably twitching of sessile strain AR1

AR1 was grown on 0.25 % agar M9 medium with glutamine and glucose as the nitrogen and carbon sources, respectively, supplemented with kanamycin. The sessile colony expanded via cumulative growth and exhibited presumably twitching. It had also begun to evolve swimming motility. Plate: 9 cm diameter. Picture taken after 26 days.

Table 5-1 Mean number of days for the evolution of swimming motility for different nitrogen sources with glucose as carbon source

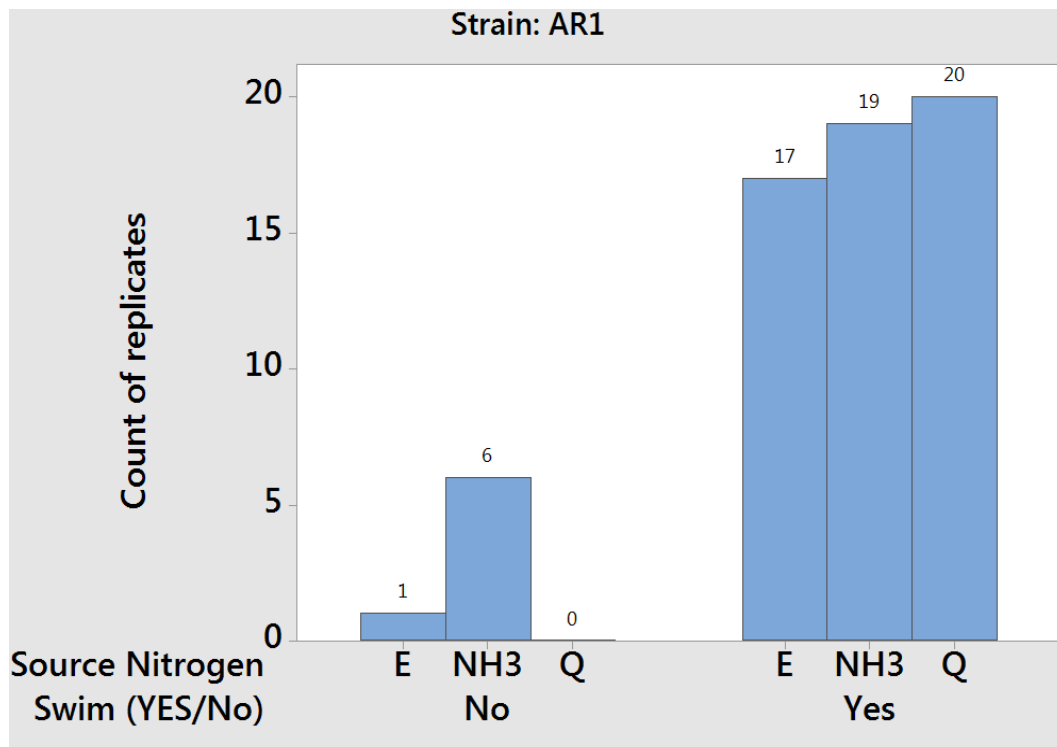
Nitrogen Source	<i>N</i>	Mean (days)	<i>SD</i> (days)	95% CI
glutamate	17	3.294	0.772	(2.641, 3.948)
ammonium	19	5.789	0.535	(5.171, 6.408)
glutamine	20	3.550	2.064	(2.948, 4.152)

Note: Pooled *SD* = 1.343, CI = confidence interval. Information for individual plates is shown in Appendix ZU: Table ZU-1.

It is important to note that not all replicates evolved swimming motility, and a chi-square test for association (Pearson chi-square) showed significant differences (*P-value* $0.026 < 0.050$; Figure 5-2) between nitrogen sources. There was a much higher number (six out of 25 replicates) of plates with no evolved swimming motility when ammonium was the nitrogen source compared to the two poor nitrogen sources (Figure 5-2). In addition, for plates showing swimming, the evolution of blebs appeared earlier at an increased number with poor nitrogen sources compared to ammonium (Table 5-2). Blebs are secondary populations which evolve from the main swimming

colony, and as there were more blebs for growth on poor nitrogen sources this suggested that these bacteria were evolving at a higher rate than when grown on a rich nitrogen source such as ammonium (Figure 5-3).

The phenotype of the evolved swimming colonies did not differ between different nitrogen sources (Figure 5-4 to Figure 5-6); a white colour initially appeared on one side of a sessile colony (dot shaped) and swimming then commenced in circles, with the colony turning yellow after approximately 4 days - 7 days.



Chi-Square Test for Association: Source Nitrogen, Swim (YES/No)

Swim=1 No Swim=0

Rows: Source Nitrogen Columns: Swim (YES/No)

	0	1	All
E	1 2.000	17 16.000	18
NH3	6 2.778	19 22.222	25
Q	0 2.222	20 17.778	20
All	7	56	63

Cell Contents
Count
Expected count

Chi-Square Test

	Chi-Square	DF	P-Value
Pearson	7.267	2	0.026
Likelihood Ratio	8.675	2	0.013

3 cell(s) with expected counts less than 5.

Figure 5-2 Chi-Square test for association

Chi-Square test for association between number of evolved and non-evolved replicates and different nitrogen sources/glucose. Q: glutamine. E: glutamate. NH₄⁺: ammonium.

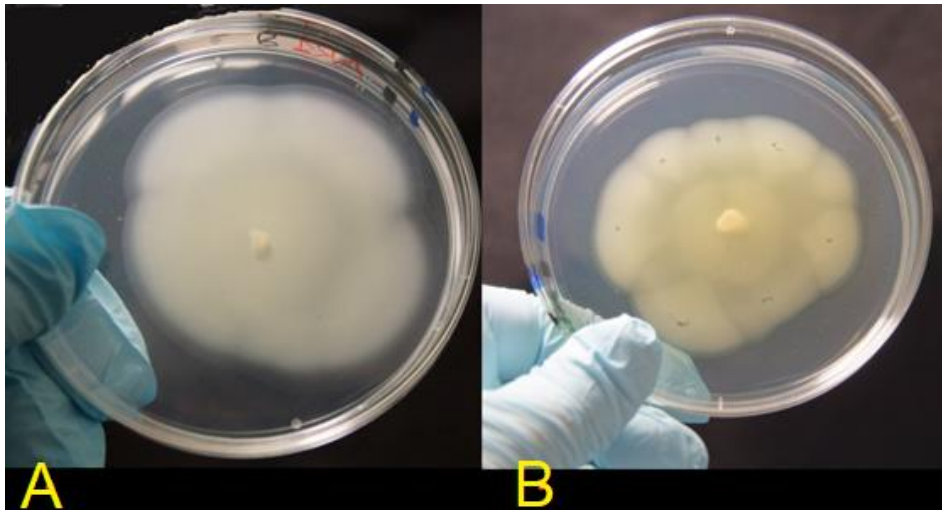


Figure 5-3 Blebbing of evolved colonies grown on poor nitrogen sources

Colonies were grown on 0.25 % agar M9 medium with glutamine and glucose as the nitrogen and carbon source, respectively. (A) Strain AR1 after 5 days of evolving swimming motility. (B) Strain AR2 after 4 days of evolving swimming motility. There was a tendency for blebs to appear earlier and in greater numbers for medium containing glutamine and glucose.

Table 5-2 Range of days and the number of blebs after the evolution of swimming motility for different nitrogen sources

Strain	Carbon Source	Nitrogen Source	Number of Blebs	Range of Days
AR1	glucose	ammonium	1 or 2	6-7
AR1	glucose	glutamate	3 or 5	2-5
AR1	glucose	glutamine	3 or 5 or 8	1-5



Figure 5-4 Evolution of swimming motility in sessile strain AR1 with ammonium as the nitrogen source

Colonies were grown on 0.25 % agar M9 medium with ammonium and glucose as the nitrogen and carbon sources, respectively. (A) No swimming movement after 24 h. (B) No swimming movement after 48 h. (C) Swimming motility observed after 6 days; picture taken 10 days after swimming motility commenced.

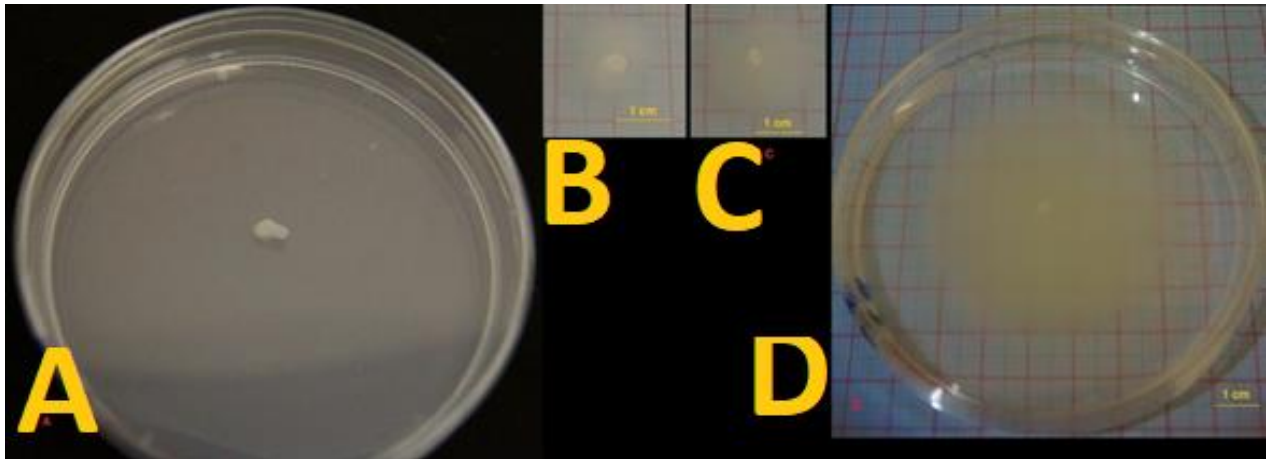


Figure 5-5 Evolution of swimming motility in sessile strain AR1 with glutamine as the nitrogen source

Colonies were grown on 0.25 % agar M9 medium with glutamine and glucose as the nitrogen and carbon sources, respectively. (A) No swimming movement after 24 h. (B) Swimming motility observed after 48 h. (C) Swimming motility after 3 days after swimming motility commenced. (D) Swimming at 7 days, this colony had turned yellow.

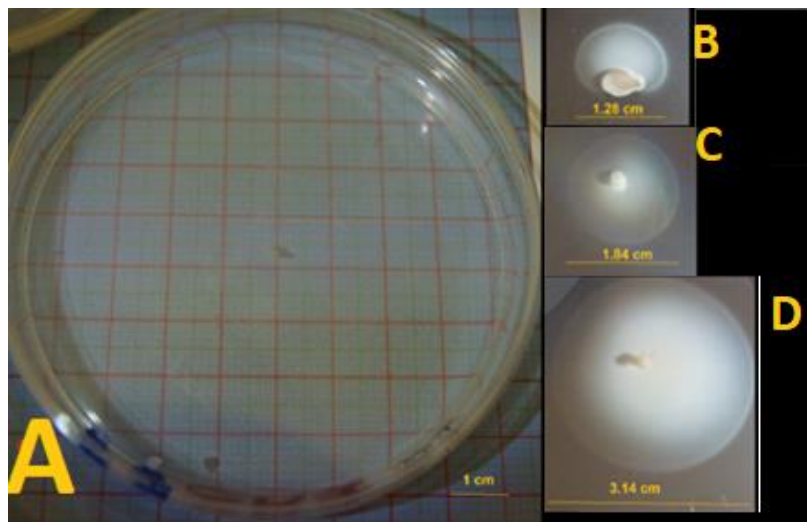


Figure 5-6 Evolution of swimming motility in sessile strain AR1 in with glutamate as the nitrogen source

Colonies were grown on 0.25 % agar M9 medium with glutamate and glucose as the nitrogen and carbon sources, respectively. (A) No swimming movement after 24 h. (B) Swimming observed after 48 h. (C) Swimming after 4 days. (D) Swimming colony after 5 days.

5.2.1 Colony expansion curves of evolved replicates under different nitrogen treatments using glucose as carbon source

The evolution of swimming motility in sessile strain AR1 (*Fla⁻*, *Visc⁻*) did not occur concomitantly for all replicates inoculated on the same day, so it was necessary to use a normalisation method to construct the colony expansion curves. There were

statistically significant differences (P -value $0.000 < 0.050$; Appendix ZX: Table ZX-1) between the colony's spreading area (mm^2) of the evolved swimming colonies from the sessile parent strain AR1 under different nitrogen sources in 0.25 % agar M9 medium reformed with kanamycin (Figure 5-7). Also, there were significant statistical differences (P -value $0.006 < 0.050$; Appendix ZX: Table ZX-2) between the spreading of the evolved colonies between the nitrogen sources glutamine and glutamate. The colony spreading area of the evolved swimming colonies was higher in ammonium compared with glutamine and glutamate as shown in Figure 5-8 (Appendix ZX: Figure ZX-1).

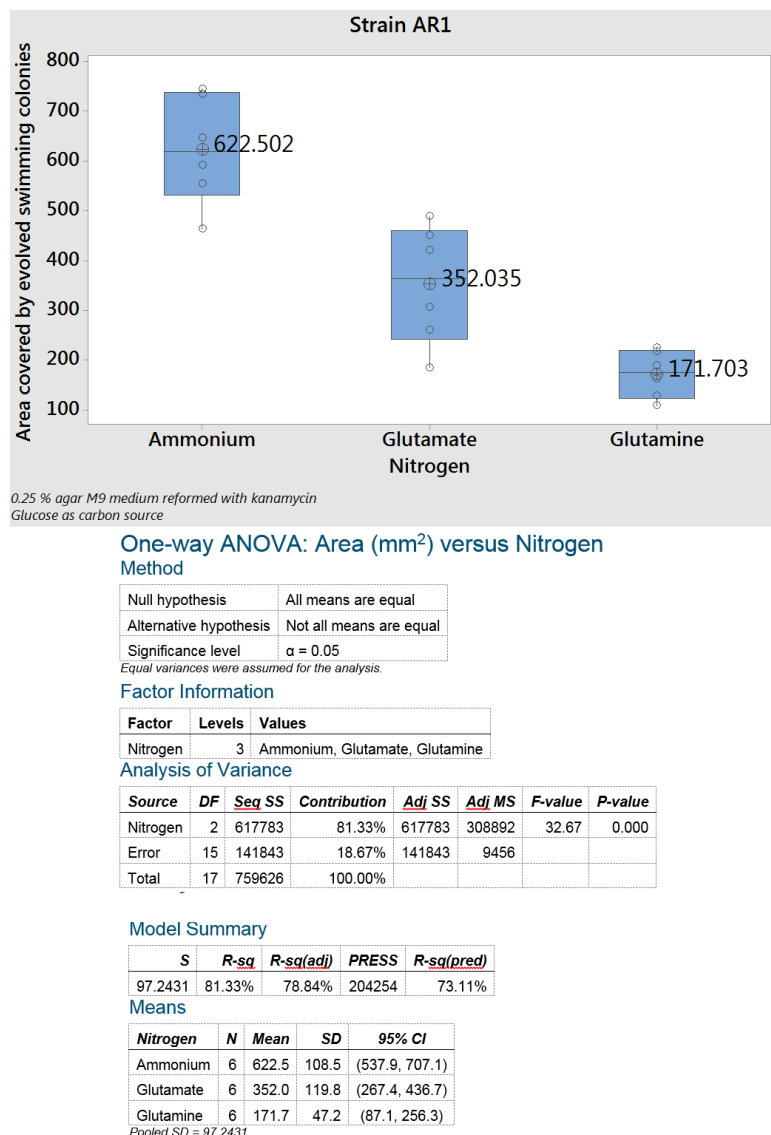


Figure 5-7 Box plot: Comparison of colony's spreading area of evolved colonies

The normalisation method was used to construct the colony's expansion curves of the evolved swimming colonies. The data analysed corresponds to the colony's spreading area at 10 h from Figure 5-8. The value shown inside each box plot denotes the average area (mm^2). Descriptive statistics is shown in Appendix ZN: Table ZN-1.

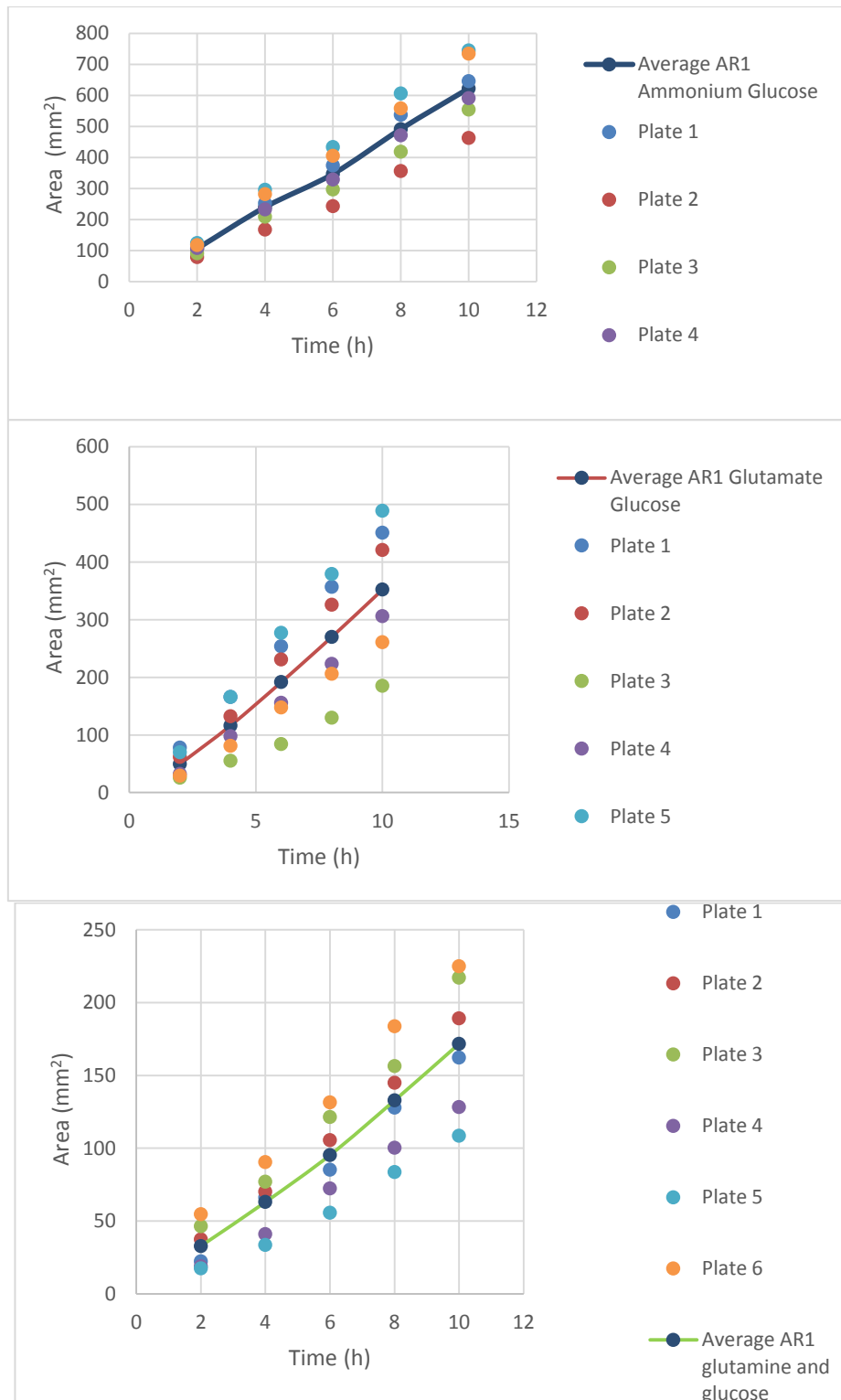


Figure 5-8 Colony expansion curves of evolved swimming AR1 colonies

Colonies were grown on 0.25 % agar M9 medium with a nitrogen source (ammonium, glutamate or glutamine) and glucose as carbon source; the medium was supplemented with kanamycin. The colony expansion curve was constructed using the normalisation method (see section 2.6), as colonies did not evolve swimming motility at the same time. The colony expansion curve is average of all replicates. The colony's area subtracted from all consecutive measurements (normalisation method) are shown in Appendix ZV: Table ZV-1.

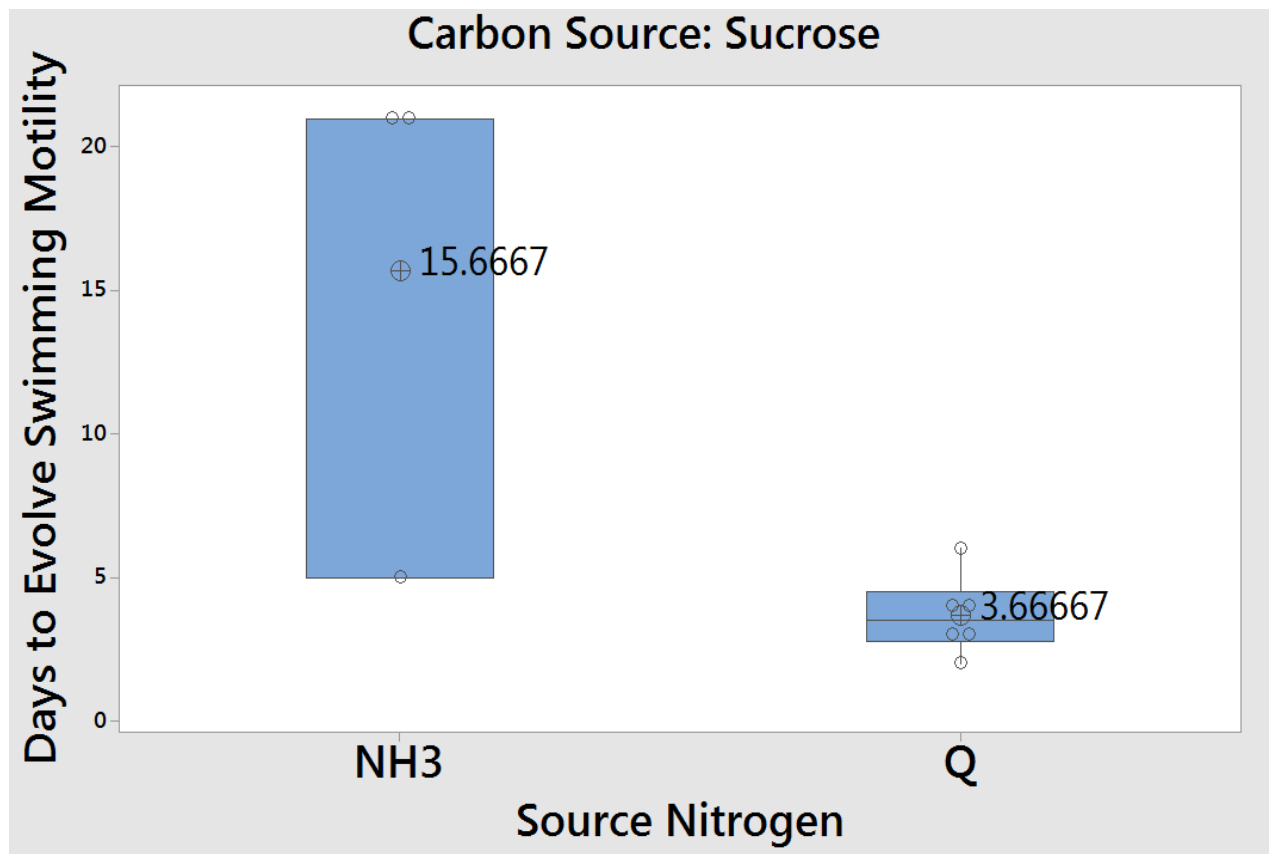
5.3 Evolution of Swimming Motility for Different Nitrogen Sources and a Poor Carbon Source

The evolution of swimming motility in glutamine did not demonstrate a significant statistical difference (*P-value* 0.898 > 0.050; Appendix H: Table H-3, Table H-4) when using glucose or sucrose as the carbon source. However, a higher number of replicates (6 out of 8) of evolved colonies was observed for glutamine/sucrose compared to ammonium/sucrose (3 out of 6) (Table 5-3; Figure 5-9) because glutamine was priming the NtrBC system, while the combination of ammonium/sucrose did not support growth because sucrose can not be actively transported by SBW25¹³¹. Notably, the Pearson chi-square test showed no statistically significant association (*P-value* 0.334 > 0.050) between the number of non-evolved replicates and nitrogen source when sucrose was the carbon source. Periplasmic glutaminase/asparaginase (PGA) is subject to catabolite repression by glucose¹⁴⁸. As only sucrose was present in the medium as a carbon source, together with glutamine as the nitrogen source, PGA was expressed enabling glutamine hydrolysis. GS-pathway is always expressed when glutamine is present in the minimal medium¹⁵⁰. In the absence of glucose, glutamine was used as both the nitrogen and carbon source. Expression of the GS-pathway is induced by glutamine and glutamate, and is up-regulated under nitrogen limitation conditions¹³³; therefore, the NtrBC system was primed, and this increased the probability of observing swimming evolution by putting pressure on this system to select any swimming mutant as result of the re-wiring of NtrC to presumably assume the role of FleQ in its absence. Evolved swimming colonies were observed earlier when colonies were grown on glutamine/sucrose or glutamine/glucose compared to ammonium/sucrose or ammonium/glucose (Figure 5-10).

Table 5-3 Average number of days for the evolution of swimming motility for different carbon sources when glutamine was the nitrogen source

Sugar	<i>N</i>	Days Mean (<i>SD</i>)	95% CI
glucose	20	3.550 (2.064)	(2.655, 4.445)
sucrose	6	3.667 (1.366)	(2.032, 5.301)

Note: Pooled *SD* = 1.940 CI = confidence interval.



Chi-Square Test for Association: Source Nitrogen, Swim (YES/No)

Swim= 1 No Swim= 0
 Rows: Source Nitrogen Columns: Swim (YES/No)

	0	1	All
NH3	3	3	6
Q	2	6	8
All	5	9	14

Cell Contents
 Count
 Expected count

Chi-Square Test

	Chi-Square	DF	P-Value
Pearson	0.933	1	0.334
Likelihood Ratio	0.934	1	0.334

3 cell(s) with expected counts less than 5.

Figure 5-9 Box plot: Evolved swimming motility when sucrose was the carbon source and different nitrogen sources

Q: glutamine. NH₃: ammonia.

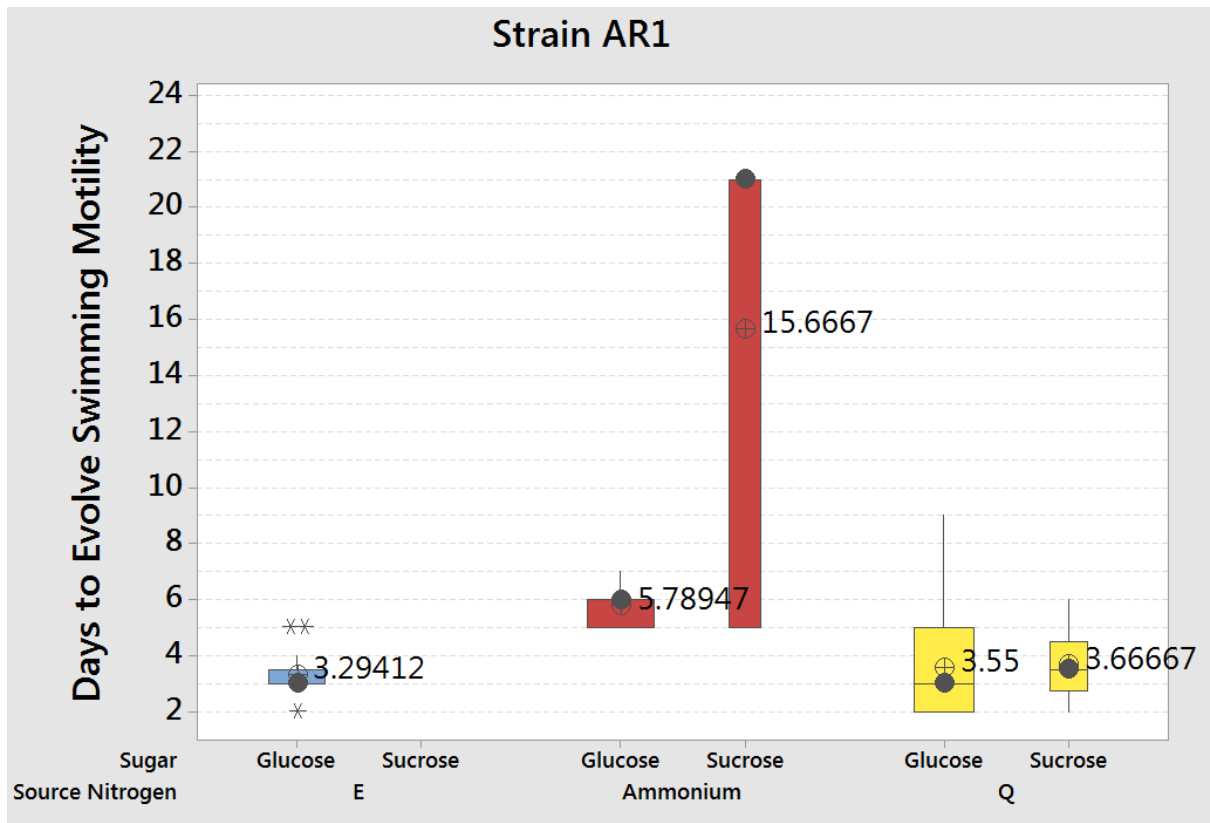


Figure 5-10 Box plot: Comparison of the evolution of swimming motility in sessile strain AR1 for different carbon and nitrogen sources

Growth on glutamate/sucrose was not assessed. E: glutamate; Q: glutamine. The value shown inside each box plot (cross dot) is the average time of evolution of swimming motility, and the shaded area represents the 25th to 75th percentiles. The median is shown as a line (grey dot) inside the box plot, and the whiskers denote the lower limit ($Q_1 - 1.5 \times IQR$) and upper limit ($Q_3 + 1.5 \times IQR$); stars indicate outliers in the observations that are outside these limits. Grey dot: median. $Q_1 = 25^{\text{th}}$ percentile, $Q_2 = 75^{\text{th}}$ percentile, IQR = Interquartile Range.

5.3.1 Colony spreading of evolved sessile strain AR1 for different nitrogen sources and a poor carbon source

Two colonies exhibited dramatically differences in spreading; plate 1 was the fastest and plate 2 the slowest, compared to plates 3 and 5; the motility of plates 3 and 5 were similar and closer to the fastest plate 1. These data showed that there was diversity in the evolved colonies and did not behave in the same manner despite their evolution within the same chemical environment (Figure 5-11). The evolved colonies were not observed earlier for ammonium and glucose as the nitrogen and carbon sources, respectively, compared to glutamine or glutamate as the nitrogen source and glucose as the carbon source. Ammonium is a rich source of nitrogen and does not require many metabolic steps to be assimilated (see sections 1.11.1 and 1.11.2). Glutamine and glutamate are poor nitrogen sources because they must be metabolized via

GS/GOGAT pathway in order to release ammonium for assimilation, which is an energy demanding metabolic pathway (see Figure 1-37). In addition, these amino acids always trigger the expression of the GS pathway, which demands energy in order to synthesise enzymes and produce glutamine for anabolic purposes. Sucrose is not a good carbon source (the cell must leaky or die to release levansucrase) and does not repress PGA (glutaminase/asparaginase), consequently a colony uses glutamine as both the carbon and nitrogen source. Glutamine is transported or degraded outside a cell by PGA to release ammonium for assimilation, the carbon skeleton is fed into the Krebs cycle to produce energy. However, there were no statistically significant differences (P -value $0.898 > 0.050$; Appendix H: Table H-3) in time (days) to evolve swimming motility in both carbon sources when glutamine was used as nitrogen source (Figure 5-12).

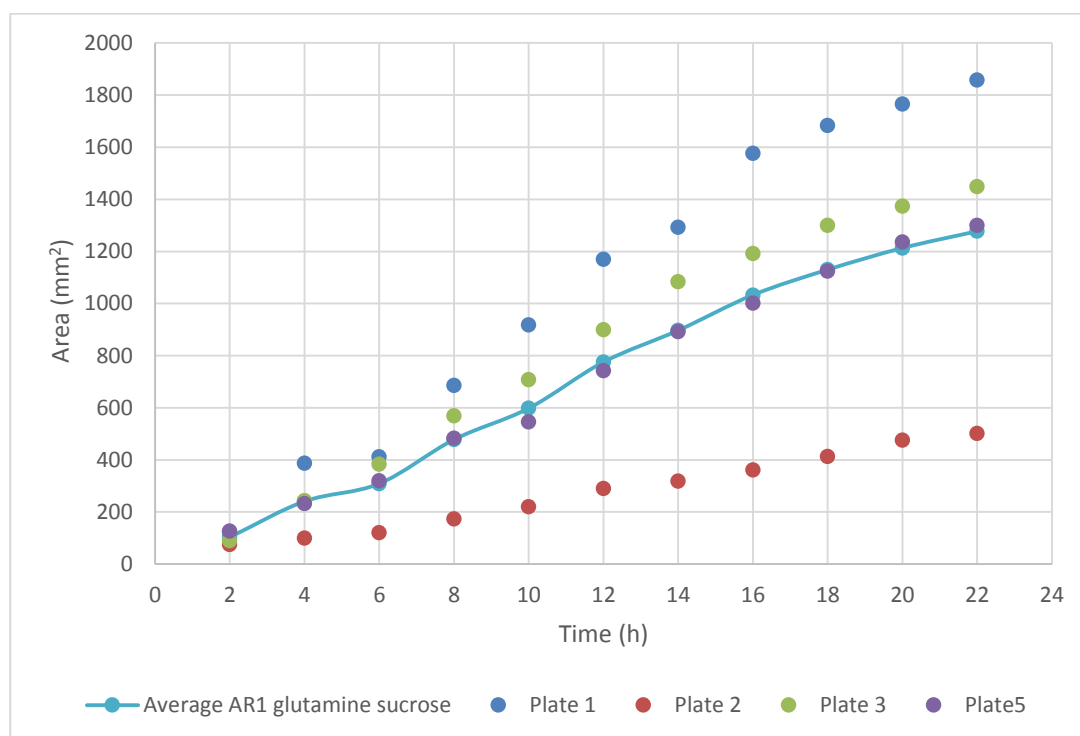
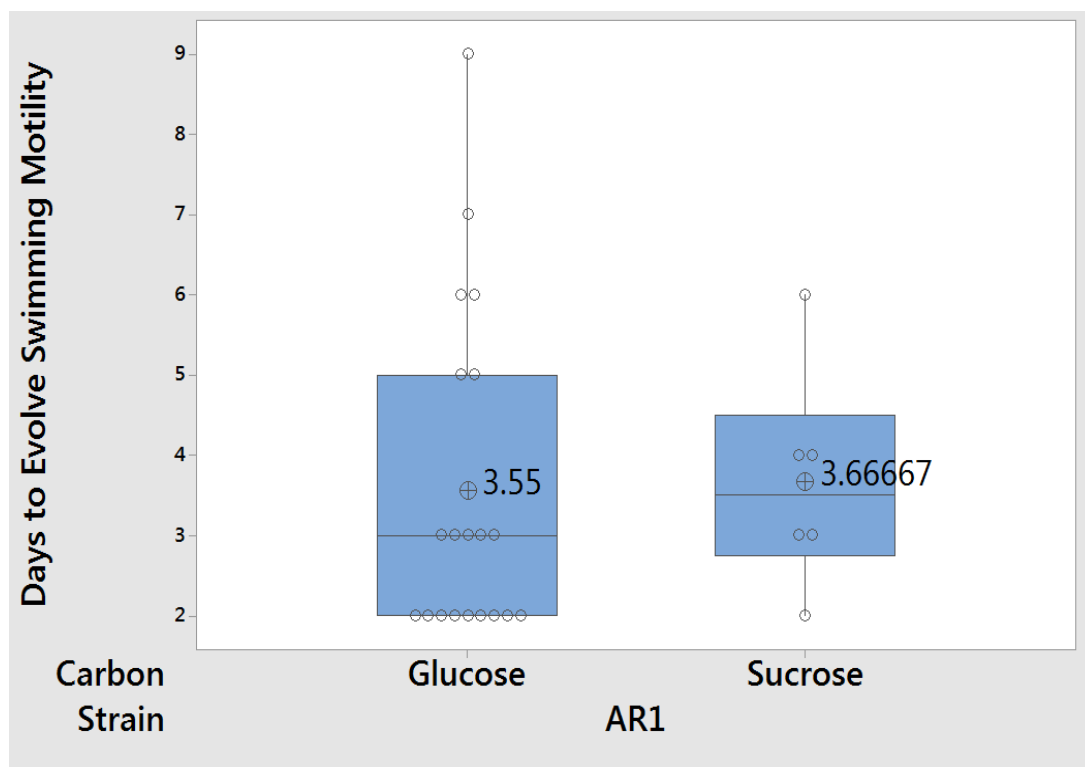


Figure 5-11 Colony expansion curve of evolved sessile strain AR1

Colonies were grown on 0.25 % agar M9 medium with glutamine as nitrogen source and sucrose as carbon source; the medium was supplemented with kanamycin. The colony's area subtracted from all consecutive measurements (normalisation method) are shown in Appendix ZV: Table ZV-1. The curve shown is the average of all plates.



One-way ANOVA: Days versus Carbon

Method

Null hypothesis All means are equal
 Alternative hypothesis Not all means are equal
 Significance level $\alpha = 0.05$

Equal variances were assumed for the analysis.

Factor Information

Factor	Levels	Values
Carbon	2	Glucose, Sucrose

Analysis of Variance

Source	DF	Seq SS	Contribution	Adj SS	Adj MS	F-Value	P-Value
Carbon	1	0.0628	0.07%	0.0628	0.06282	0.02	0.898
Error	24	90.2833	99.93%	90.2833	3.76181		
Total	25	90.3462	100.00%				

Model Summary

S	R-sq	R-sq(adj)	PRESS	R-sq(pred)
1.93954	0.07%	0.00%	103.135	0.00%

Means

Carbon	N	Mean	StDev	95% CI
Glucose	20	3.550	2.064	(2.655, 4.445)
Sucrose	6	3.667	1.366	(2.032, 5.301)

Pooled StDev = 1.93954

Figure 5-12 Box plot: Days to observe evolution of swimming motility under different carbon sources and glutamine as nitrogen source

The ANOVA table compares days to observe evolution of swimming motility under different carbon sources.

5.4 Testing Isolates Picked from Evolved AR1 Colonies for Swimming Motility

Many isolates were lost due to technical problems. When the isolates obtained from the evolved swimming colonies grown on different nitrogen and carbon sources in 0.25 % agar M9 medium were examined, it was found that most did not maintain their swimming phenotype (Table 5-4). Some strains were derived from blebs. From published data¹⁰⁸, these might be expected to have both *ntrB* and *ntrC* mutations and

show faster swimming. Unexpectedly, isolates from blebs apparently showed slow rate of colony expansion but it was not possible to directly compared isolates from blebs and swimming discs of the same replicates.

Table 5-4 Frequency of recovery of evolved AR1 isolates

		Nitrogen Source				Total Isolates
		Swimming	Ammonium	Glutamate	Glutamine	
Carbon Source	Glucose	Evolved	0	0	2	2
		Non Evolved	4	3	3	10
		Total Isolates	4	3	5	12
	Sucrose	Evolved	3	0	1	4
		Non Evolved	2	0	0	2
		Total Isolates	5	0	1	6

Note: A total of 18 samples were picked from evolved colonies and tested for swimming motility using the same medium in which they initially were isolated. Only 6 isolates showed swimming motility after testing.

5.5 Swimming Motility Phenotypes

5.5.1 Spurs and spur-swarming

The motility phenotype of the evolved strains was studied on 0.25 % agar LA plates not supplemented with kanamycin (Appendices B, C and F). There was high variability in the colony expansion curves for the evolved strains, and not all replicates spread in a comparable manner, as some replicates of the same isolate were very slow and others much faster (Appendix E: Figure E-32 and Figure E-33). In addition, some replicates formed a spur, that was raised from the central base of the colony towards the agar surface and then slid quicker over the surface than the swimming colony underneath. These spurs remained on top of agar and after reaching the outside of the swimming colony's border, they changed to a fast movement that spread through the agar (spur-swarming). This switching was not always immediate as some spurs remained without movement for a few hours (2 h or more) before switching to spur-swarming movements; and in other cases, the spur continued to slide on top of the agar for a few hours. The time taken for the formation of a spur among replicates was very variable in all the studied evolved strains; some initiated spur formation 2 h after inoculation, whereas in others it was after 14 h or 18 h. Therefore, spur appearance and spur-swarming time was highly variable between replicates and strains, with some never exhibiting swarming or spur formation, although they might have after more time spent swimming, and growth on larger plates (15 cm) would allow a swimming colony

to expand more without the border hindrance due to the use of small plates (9 cm), see Figure 5-13. The strains were classified as an earlier swarmer if spur-swarming occurred earlier than 18 h or at 18 h.

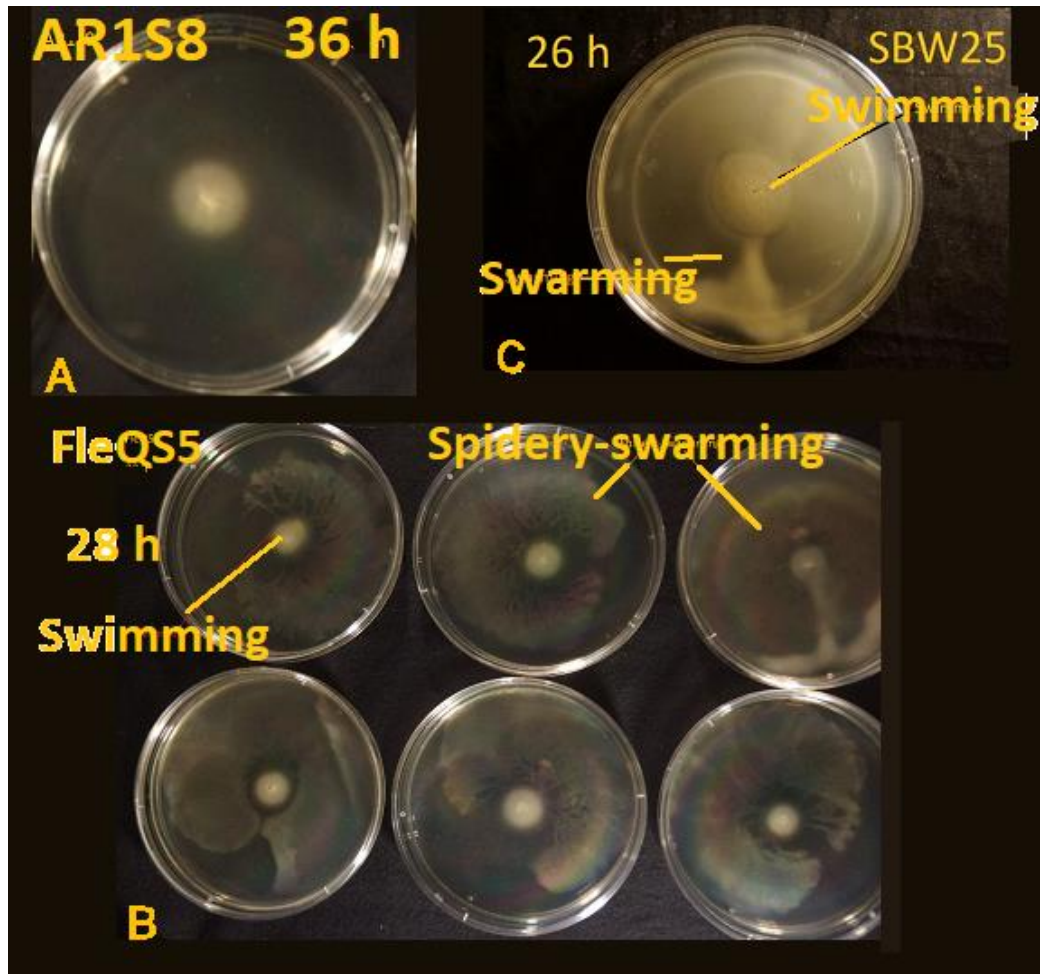


Figure 5-13 Phenotypic comparison of AR1S8, FleQS5 and SBW25

Swarming medium without antibiotic. (A) AR1S8 expanding colony was slow and had not covered the plate (9 cm) within 36 h. (B) FleQS5 swam and exhibited spidery swarming; replicates did not initiate swarming concomitantly, but after 28 h all colonies had demonstrated swarming and almost covered the plate (9 cm). (C) Wild type strain SBW25 swam and initiated swarming at 22 h, and had covered the plate (15 cm) in 26 h.

5.5.2 Differences in colony expansion rate

Swimming rate in all the evolved strains AR1S was as much slower compared to FleQS and SBW25 (Table 4-10; Table 5-5). The average rate of colony expansion changes over a period of 8 h enabled strains to be classified as fast, medium or slow swimmers (Table 5-5, Table 5-6 and Appendix E: Figure E-32 and Figure E-33). AR1S strains experimental populations were skewed and followed a Log-Normal distribution. AR1S5 was an example of this variability in colony expansion among the replicates,

as plate 1 and 3 exhibited swimming, albeit at remarkably different rate of expansion, whereas plates 4 and 5 showed similar rates as plate 3 until 10 h (Figure 5-14). In addition, plate 4 formed a spur at 14 h, and commenced to expand faster as compared to replicates 3 and 5.

Table 5-5 Origin of evolved isolates and motility phenotype

Strain Name	Isolated from Bleb	Average Rate of Colony Expansion (mm ² /h)	Motility Phenotype	Replicate	Treatment: Nitrogen/Carbon	Days Isolated after evolution of swimming motility
AR1S1	Yes	6.32	Slow	1	ammonium/sucrose	23
AR1S2	No	21.74	Fast	5	ammonium/sucrose	23
AR1S3	Yes	18.97	Fast	1	ammonium/sucrose	23
AR1S4	Yes	5.50	Slow	8	glutamine/glucose	16
AR1S5	Yes	3.73	Slow	5	glutamine/glucose	14
AR1S6	No	22.12	Fast	5	glutamine/sucrose	5

Note: Isolation of bacteria was not performed immediately after swimming evolution had occurred in the sessile parent strain AR1. Some isolates were obtained from main swimming disc and other from blebs.

Table 5-6 Time of spur appearance and motility phenotype

Strain	Mean Rate of colony expansion (mm ² /h)	Motility Phenotype	Spur Time [<i>N</i> , time (h)]	<i>N</i> total of replicates
AR1S1	6.32	Slow	<i>N</i> = 3, 14 h, 22 h and 72 h	5
AR1S2	21.74	Fast	<i>N</i> = 1, 4 h	5
AR1S3	18.97	Fast	<i>N</i> = 1, 4 h	5
AR1S4	5.50	Slow	<i>N</i> = 2, 18 h and 22 h	5
AR1S5	3.73	Slow	<i>N</i> = 2, 14 and 22 h	5
AR1S6	22.12	Fast	<i>N</i> = 2, 2 h and 6 h	5

Note: *N*: number of replicates in the colony expansion curve.

The formation of a spur was highly variable between replicates and strains, while swarming movement was very fast. Strain AR1S6 was classed as a fast swimmer. Its colony expansion curve showed that plate 4 initiated spur-swarming after 2 h (immediately after the appearance of a spur); whereas plates 1 and 5 switched to swarming 6 h after the formation of a spur. The remaining replicate, plate 3, did not form a spur and consequently did not swarm during the period of observation (Figure 5-15). Whenever a spur appeared it always emerged from the base of a colony at its centre and moved towards the surface, whereupon it slid on the agar surface and then switched to fast swimming movement (spur-swarming).

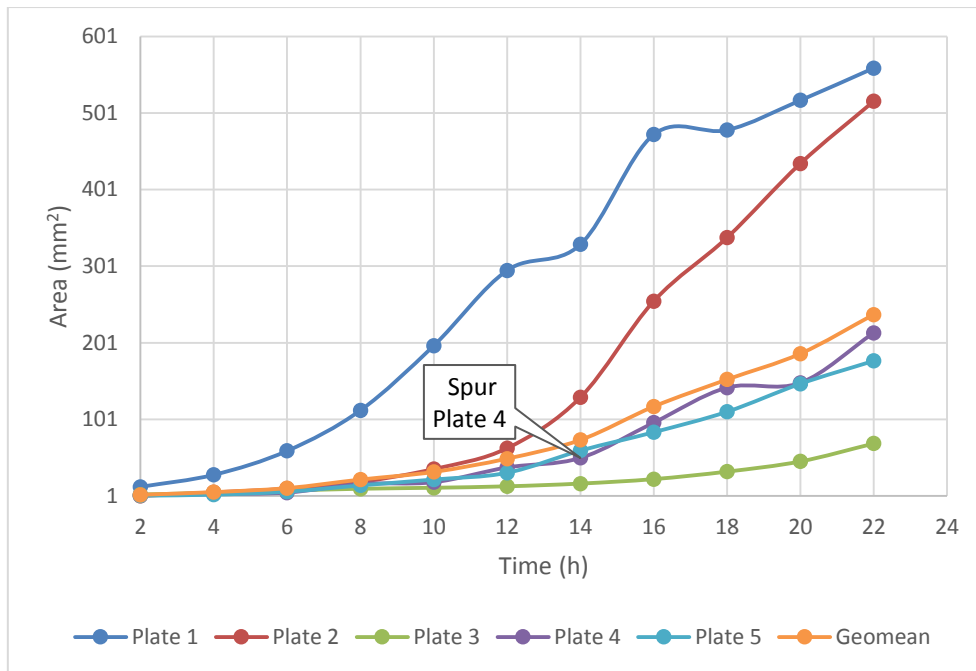


Figure 5-14 Colony expansion of the AR1S5

Colony expansion was observed at a remarkable rate in replicates 1 and 2. A spur appeared on plate 4 at 4 h and then spur-swarmed. Geomean of all replicates. Swarming medium non-reformed with antibiotic on 9 cm diameter plates.

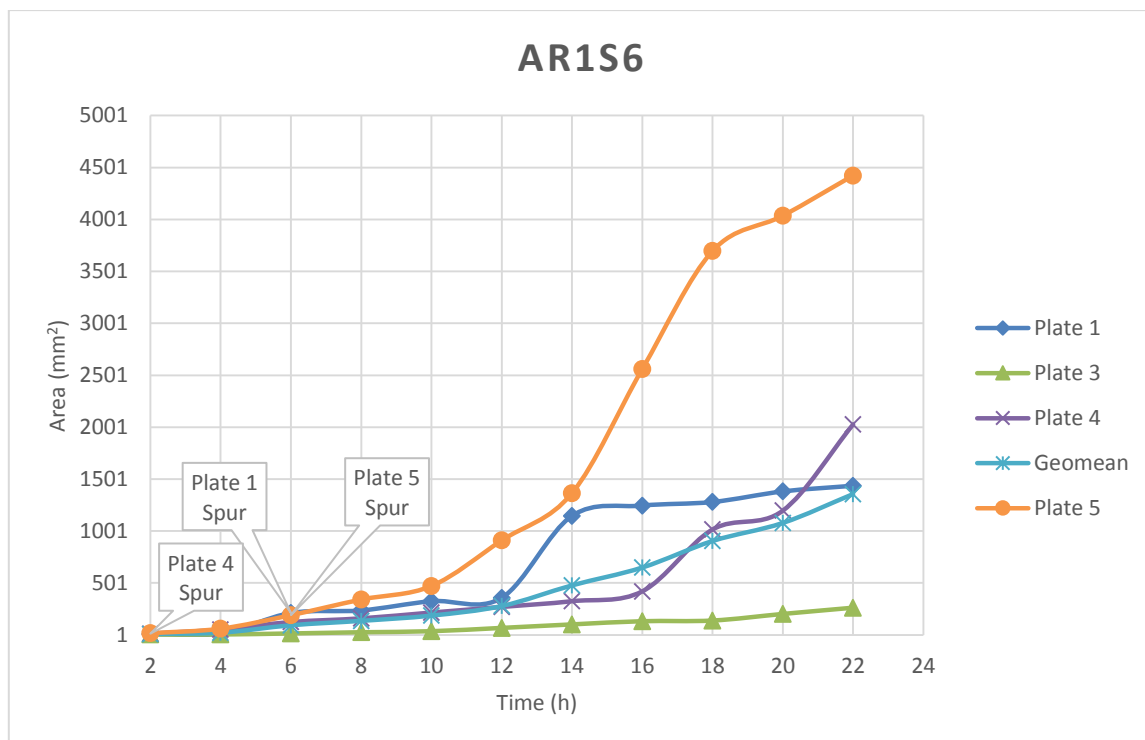


Figure 5-15 Colony expansion of the AR1S6

Curves for plates 1, 4 and 5 were constructed using time-lapse photography while that for plate 3 used the hand-drawn method. There were no noticeable differences in swimming rates before apparition of spurs, which were only appeared a few hours later in some plates (1 and 5). Geomean of all replicates. Motility plates: swarming medium without antibiotic. Plates 9 cm diameter.

The appearance of a spur and non-time dependent spur-swarming was probably due to a second mutation occurring within the swimming colony, making the spur-swarming region of the colony a double mutant (*ntrB ntrC*) and the swimming disc a single mutant (*ntrB*). As shown by Taylor et al.¹⁰⁸, the evolved strain AR2F is a double mutant (*ntrB ntrC*), which is faster than the initial evolved strain AR2S. The strain AR2S only mutated in *ntrB* and is much slower compared to its evolved bleb AR2F. In addition, in AR2F nitrogen metabolism is more fine-tuned than in the slower AR2S¹⁰⁸.

Slow and fast replicates were observed for the same strain, indicating variability and a skew experimental population (Log-Normal distribution), resulting in the dramatic change in rate of colony expansion at 17 h exhibited by AR1S4 (Appendix E: Figure E-33 and Figure E-34 and Appendix B: Figure B-4). As result of this biological variability, the geometric mean was used to calculate colony expansion curves and determine the rate of colony expansion changes over a 24 h period of time.

During the first 11 h it was possible to categorise the evolved strains AR1S1, AR1S4 and AR1S5 as slow (Appendix B: Figure B-1, Figure B-4, Figure B-5), as they showed little difference in their rate of colony expansion. However, after 12 h they began to differentiate dramatically, especially strain AR1S4 which began to spread very fast. The other group of strains, AR1S2, AR1S3 and AR1S6, were much faster during the first 11 h compared to the other three strains. However, after 11 h these marked differences began to disappear for the apparition of spurs. In general, colony expansion rate was constantly changing over the period of observation among replicates and strains as result of spur-swarming.

5.6 Mutations in the Nitrogen Metabolism Pathway in Strain AR1S

The NtrBC system and *glnK* genes (Appendix O: Figure O-1 and Figure O-5) were examined in all the evolved strains derived from AR1S. All were found to be wild type for *glnK* and *ntrC*, but all possessed the same SNP mutation at position A289C in *ntrB* (Table 5-7). This mutation was the most common in FleQS strains (Table 4-10), and must be the less lethal and more favourable for survival. The mutations in *ntrB* enabled the bacterial population to change niche. The swimming phenotype was found to be independent of the nitrogen/carbon source used, but the differences in motility indicated that there were probably other mutations within their genome. Therefore, the

evolved swimming phenotype was random, as multiple swimming phenotypes had evolved in the same environment (Table 5-7 and Figure 5-16).

Table 5-7 Genotype and phenotype of the evolved strains

Strain	Gene	Nucleotide Position	AA Position	Phenotype	Mean Rate of Colony Expansion (mm ² /h)	Treatment: Nitrogen/Carbon
AR1S1	<i>ntrB</i>	A289C	T97P	Slow	6.3	ammonium/sucrose
AR1S2				Fast	21.7	ammonium/sucrose
AR1S3				Fast	19.0	ammonium/sucrose
AR1S4				Slow	5.5	glutamine/glucose
AR1S5				Slow	3.7	glutamine/glucose
AR1S6				Fast	22.1	glutamine/sucrose

Note: All evolved strains did not show any mutation in the target sequence for *ntrC* and none of them mutated *glnK* gene.

AR1S Strains

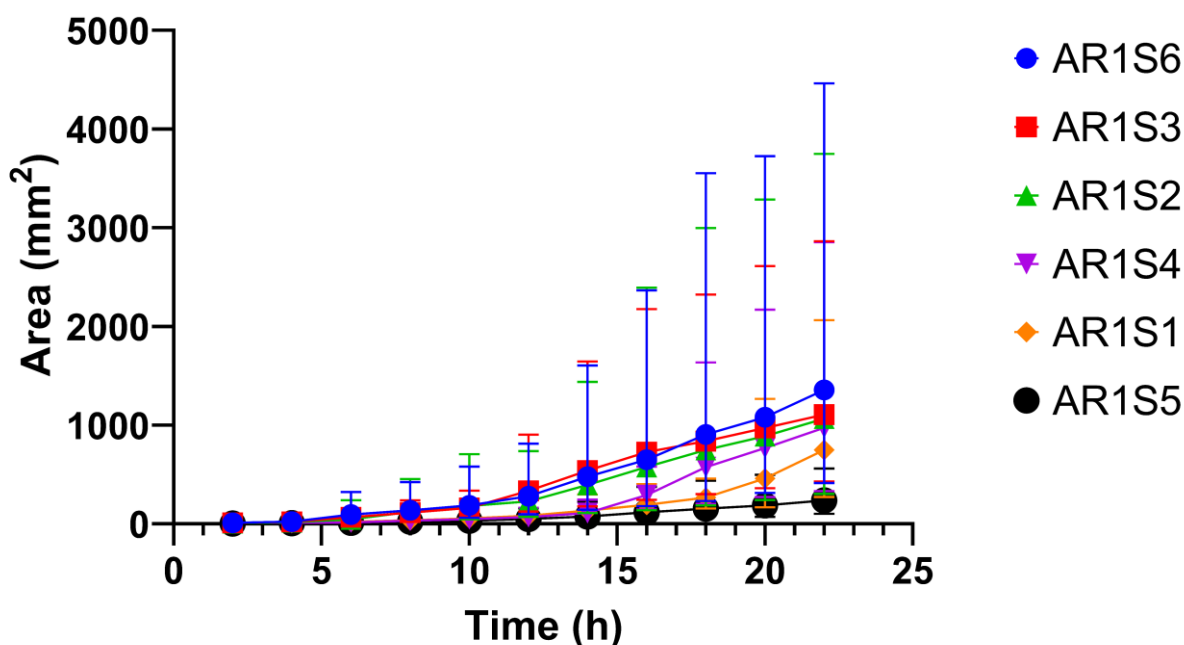


Figure 5-16 Colony expansion curves of all evolved strains AR1S

The expansion curve is the geomean of all replicates and the error bars represent the geometric standard deviation. Some error bars do not appear for certain points in the graph for being shorter than the size of the symbol (black dot). Swarming medium (no antibiotic).

5.7 Evolution of Swimming Motility in Strain AR2 for Different Nitrogen Sources in a Rich Energy Environment

There were significant statistical differences (P -value $0.023 < 0.050$; Appendix H: Table H-6 and Figure H-6) in the time to evolve swimming motility for different nitrogen sources. Sessile strain AR2 evolved swimming motility earlier in poor nitrogen sources (glutamine and glutamate) compared to a rich nitrogen source (ammonium) in a rich energy environment (Table 5-8). There were no statistical significant differences (P -value $0.370 > 0.050$; Appendix H: Table H-7) between poor nitrogen sources (glutamine and glutamate) and time to evolve swimming motility because both primed the NtrBC system, and so the probability of evolving in a poor nitrogen source in a rich energy environment is higher compared to an environment which is rich in energy and has a rich source of nitrogen (ammonium). There were no statistical significant differences (P -value $0.167 > 0.050$; Appendix H: Table H-8 and Table H-9) between the time to evolve swimming motility in a rich nitrogen source compared to strain AR1 (Table 5-8). It had been clearly shown that there were no statistically significant differences (P -value $0.370 > 0.050$; Appendix H: Table H-7) in time to evolve swimming motility between glutamate and glutamine as nitrogen sources using glucose as carbon source in strain AR2. The time (days) to observe evolution of swimming motility in poor nitrogen sources in sessile strains AR1 and AR2 did not show a statistical significant difference (P -value $0.702 > 0.050$; Appendix H: Table H-9). The phenotype of the swimming colony did not differ between nitrogen sources for strain AR2, and was the same as in strain AR1 (Figure 5-17, Figure 5-18 and Figure 5-19). However, blebs was observed to appear earlier and in higher numbers when a colony had evolved in glutamate or glutamine (Table 5-9). There was not a statistically significant association (P -value $0.095 > 0.050$; Figure 5-20) between priming the NtrBC system with different nitrogen sources and the number of non-evolved colonies (replicates) in which AR2 sessile colonies were inoculated.

Table 5-8 Days to evolve swimming motility in sessile strains in different nitrogen sources

Days to evolve swimming motility in sessile strain AR2 in different nitrogen sources				
Nitrogen Source	N	Mean	SD	95% CI
glutamate	17	2.94	0.80	(1.61, 4.28)
ammonium	19	5.53	0.61	(4.26, 6.79)
glutamine ^a	17	(4.00 ^a) 2.88 ^b	(4.72 ^a) 0.89 ^b	(2.66, 5.34)

Note: Pooled *SD* = 2.74 CI = confidence interval

^aThis average 4.00 days (*SD* = 4.72 days) for the evolution of swimming motility in glutamine treatment included the outlier plate that evolved swimming motility after 22 days. ^bWhereas the mean value 2.88 days (*SD* = 0.89 days) for the evolution of swimming phenotype in glutamate was calculated without the outlier, the statistical analysis presented no differences, irrespective of inclusion or exclusion of the outlier.

Days to evolve swimming motility in sessile strains AR1 and AR2 in ammonium

Strain	N	Mean	SD	95% CI
AR1	19	5.79	0.54	(5.52, 6.06)
AR2	19	5.53	0.61	(5.26, 5.79)

Note: Pooled *SD* = 0.58 CI = confidence interval

Days to evolve swimming motility in sessile strains AR1 and AR2 with glutamine as the nitrogen source

Strain	N	Mean	SD	95% CI
AR1	20	3.55	2.06	(1.95, 5.15)
AR2	17	4.00	4.72	(2.26, 5.74)

Note: Pooled *SD* = 3.53 CI = confidence interval

Note: Information for individual plates is shown in Appendix ZU: Table ZU-2.

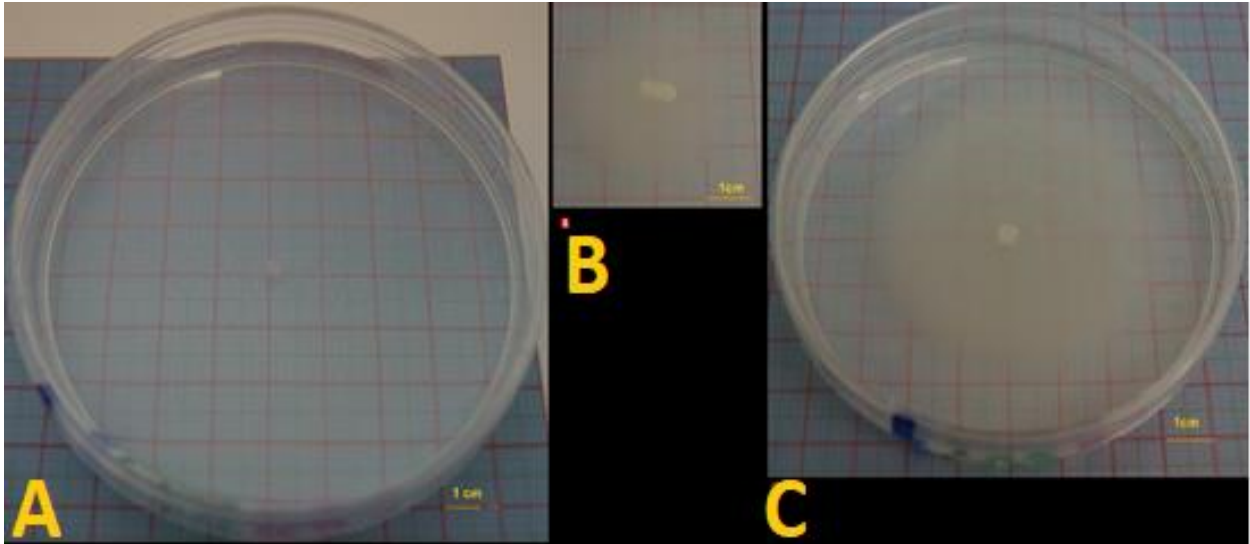


Figure 5-17 Evolution of swimming motility in sessile strain AR2 with ammonium as the nitrogen source and glucose as the carbon source

(A) No swimming movement after 3 days. (B) Swimming observed after 4 days, picture taken 2 days after swimming motility began. (C) Swimming 6 days after swimming motility began.

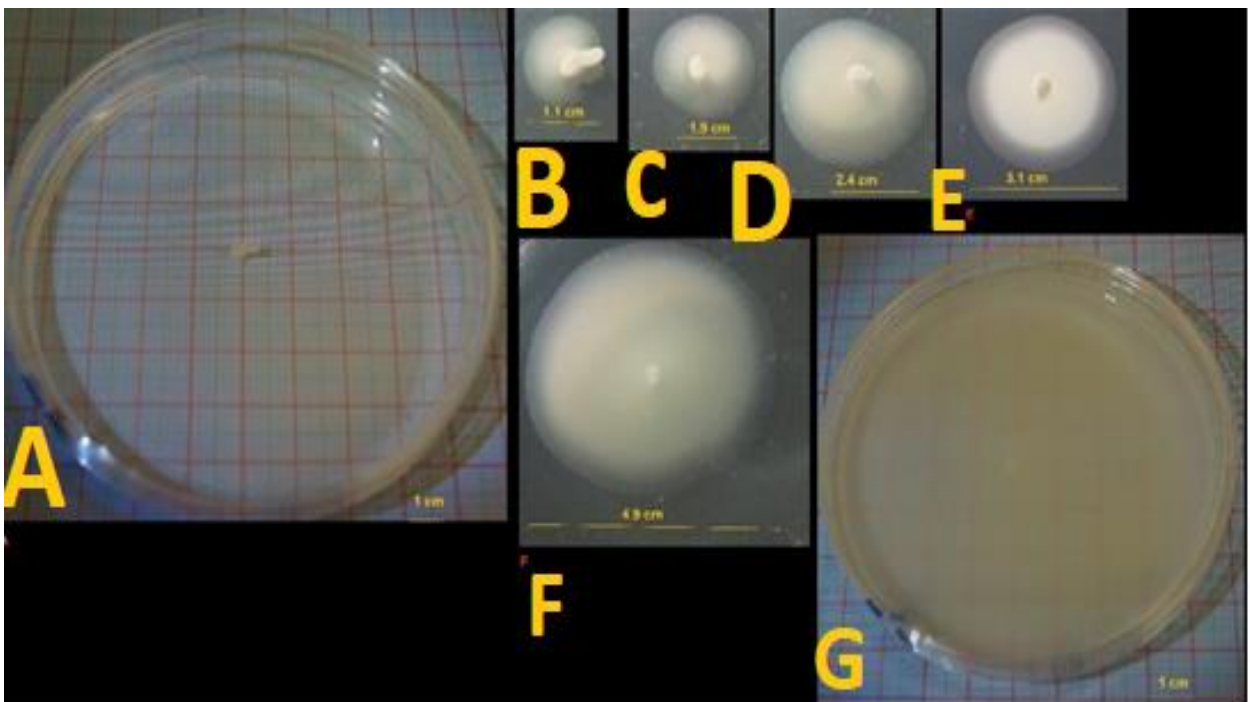


Figure 5-18 Evolution of swimming motility in sessile strain AR2 with glutamine as the nitrogen source and glucose as the carbon source

(A) No swimming movement for 2 days. (B) Swimming motility began after 48 h, picture taken 1 day after swimming began. (C) Swam for 3 days. (D) Swam for 5 days. (E) Swam for 6 days. (F) Swam for 7 days. (G) Completely covered plate after 9 days of swimming.

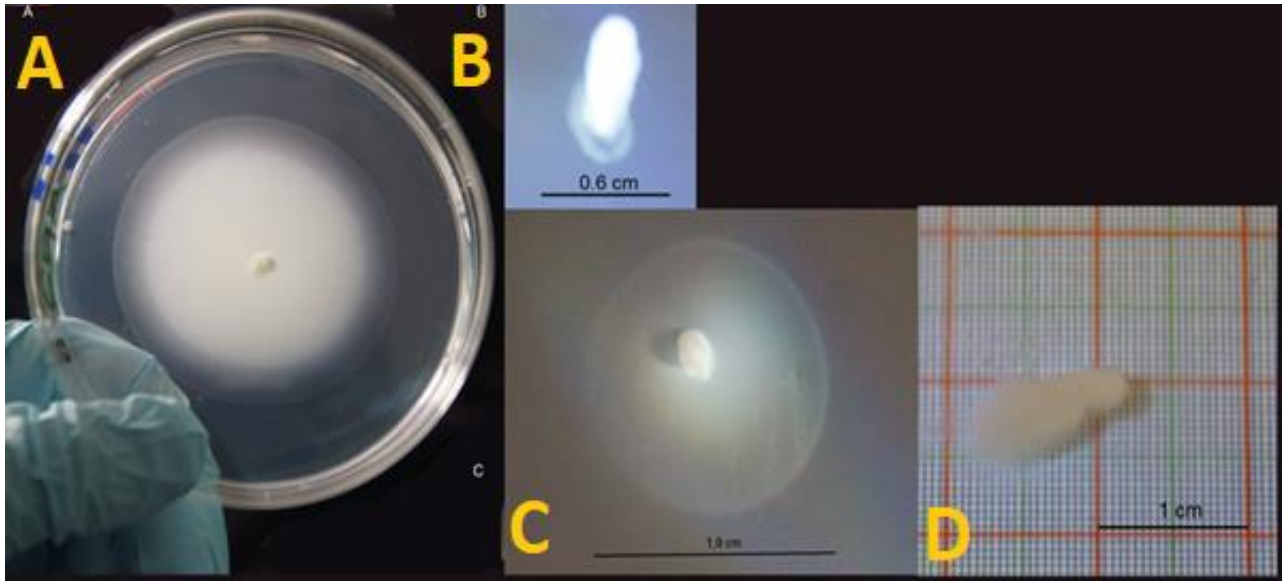
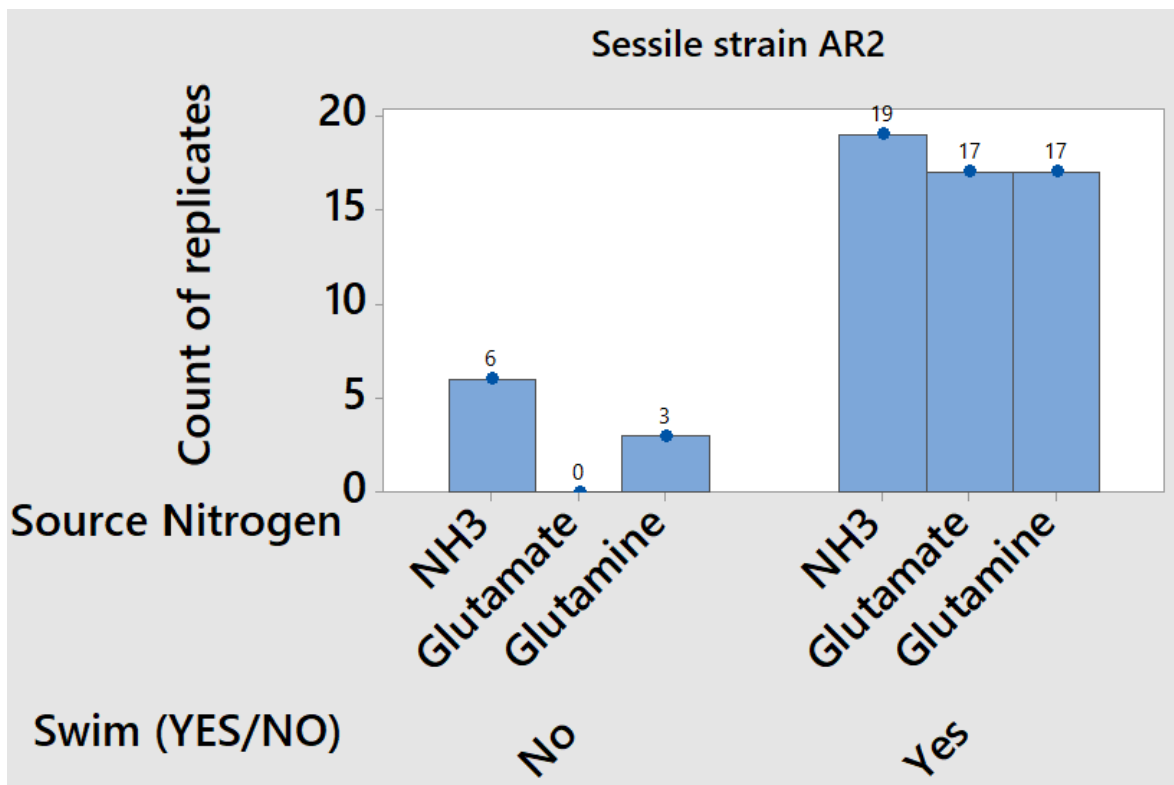


Figure 5-19 Evolution of swimming motility of sessile transposon mutants AR1 and AR2 with different nitrogen sources and glucose as the carbon source
 (A) Strain AR2 swam when grown on glutamate after 5 days. (B) Strain AR2 started to swim when grown on glutamate after 4 days. (C) Strain AR1 swam when grown on glutamate after 3 days. (D) Strain AR1 began to swim when grown on ammonium after 3 days. Pictures taken using a DSLR camera (model: Sony SLT-A65V).

Table 5-9 Range of days and number of blebs that appeared after swimming commenced for different nitrogen and carbon sources

Strain	Nitrogen Source/Glucose	Number of Blebs	Days to Appear Blebs
AR2	ammonium	1 or 2	6 or 7
AR2	glutamate	3 or 5	2 or 5
AR2	glutamine	3 or 5	1 or 6 ^a

^aFor colonies grown in medium containing glutamine and glucose it was possible to observe 8 blebs.



Chi-Square Test for Association: Source Nitrogen, Swim (YES/No)

Swim=1 No Swim= 0

Rows: Source Nitrogen Columns: Swim (YES/No)

	0	1	All
Ammonium	6	19	25
Glutamate	0	17	17
Glutamine	3	17	20
All	9	53	62

Cell Contents
Count

Chi-Square Test

	Chi-Square	DF	P-Value
Pearson	4.703	2	0.095
Likelihood Ratio	6.901	2	0.032

3 cell(s) with expected counts less than 5.

Figure 5-20 Chi-Square test for association

Chi-Square test for association between number of evolved and non-evolved replicates and different nitrogen sources/glucose.

5.7.1 Colony expansion of evolved AR2 colonies for different nitrogen sources in a rich energy environment

Different replicates for different nitrogen sources in a rich energy environment (glucose) were not found to evolve swimming motility at the same time. Therefore, normalisation method was applied to obtain colony expansion curves for the evolved colonies, see section 2.6. Based on the data obtained from the colony expansion

curves for different nitrogen sources (Figure 5-21) at 10 h, a statistical analysis was conducted on the colony's spreading area (mm^2). There was more variability in the data set from glutamate treatment (coefficient of variation = 67.12 %) as compared to glutamine (coefficient of variation = 22.67 %) and ammonium (coefficient of variation = 37.98%), see Appendix ZN: Table ZN-1. The colony's area was found to be 783.5 mm^2 ($SD = 526.0 \text{ mm}^2$, $n = 6$) in glutamate, and for glutamine 203.9 mm^2 ($SD = 46.2 \text{ mm}^2$, $n = 5$), and for ammonium 337.6 mm^2 ($SD = 128.2 \text{ mm}^2$, $n = 6$). No statistically significant differences were found between the strains AR2 and AR1 ($P\text{-value } 0.746 > 0.050$), however, there were statistically significant differences in spreading ($P\text{-value } 0.000 < 0.050$) under different nitrogen sources.

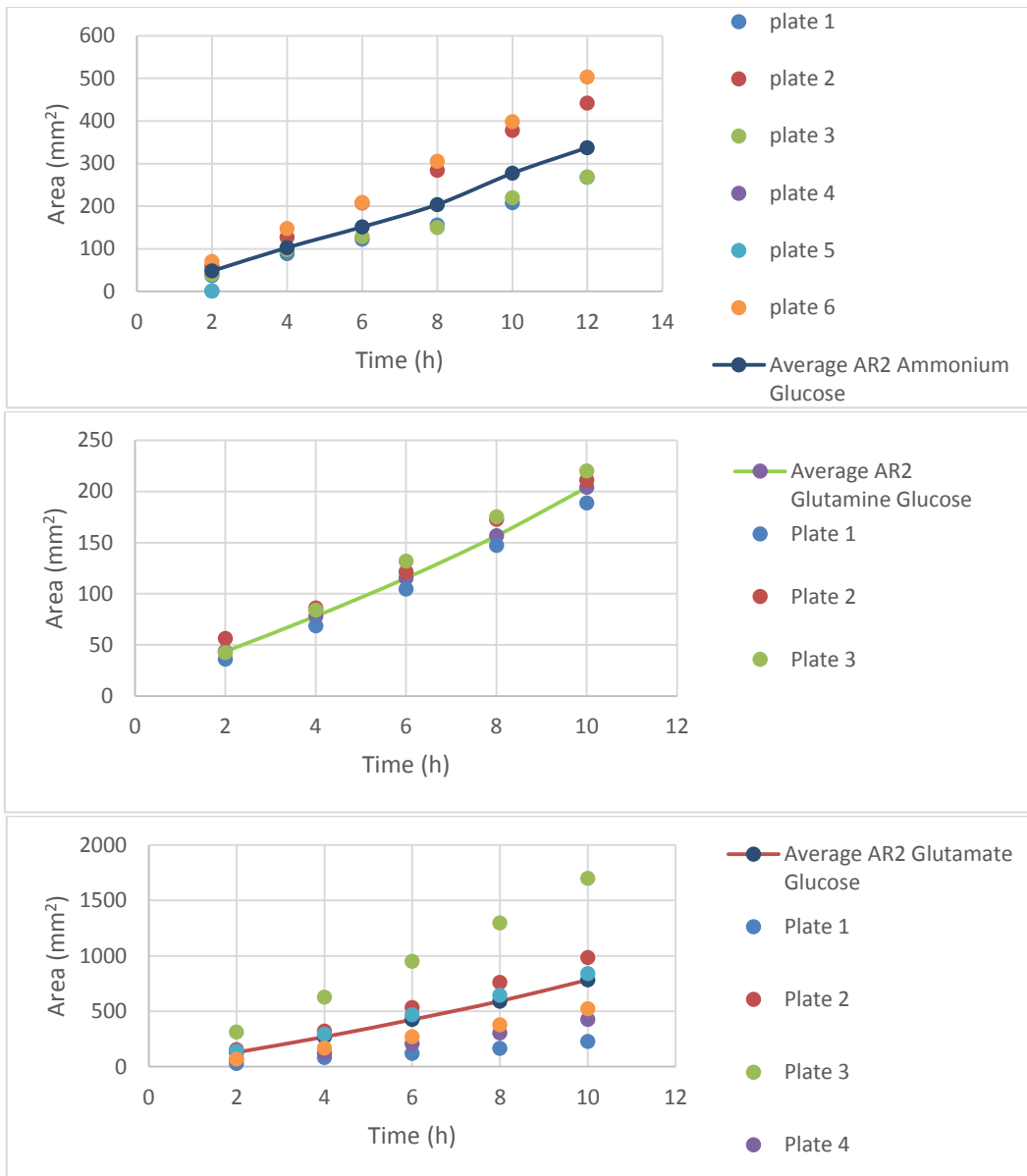
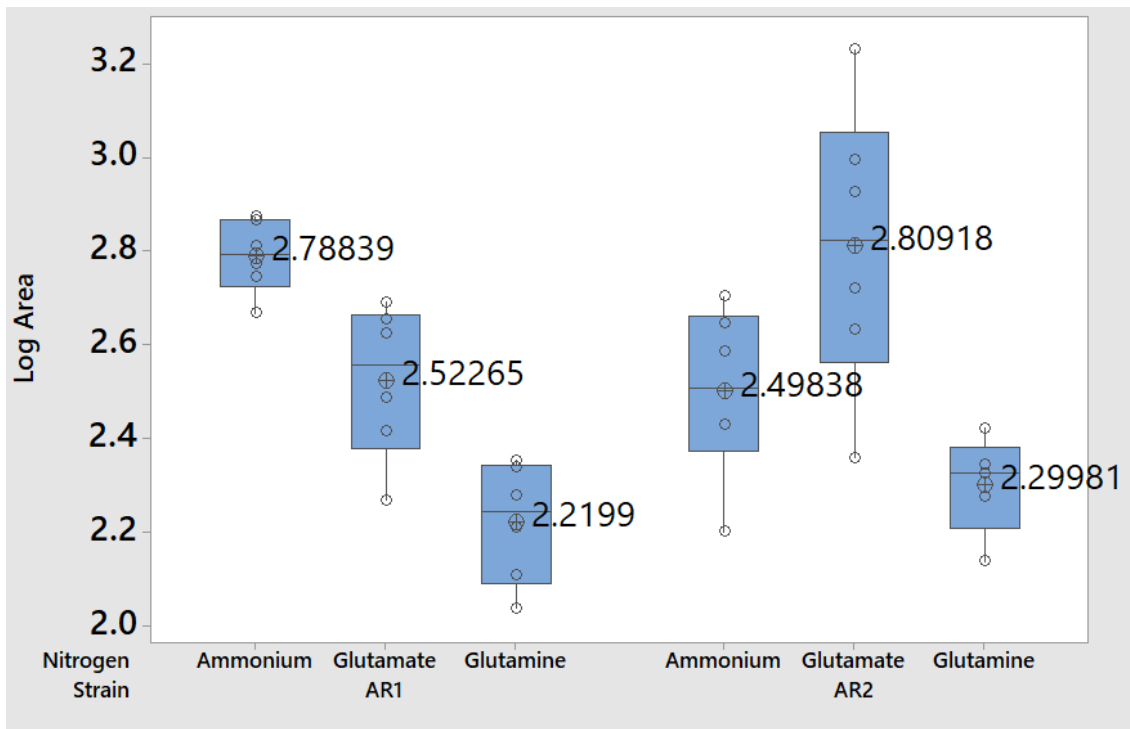


Figure 5-21 Colony expansion curves for evolved colonies from parent strain AR2

Colonies were grown on 0.25 % agar M9 medium with a nitrogen source (ammonium, glutamate or glutamine) and glucose as the nitrogen and carbon sources, respectively; the medium was supplemented with kanamycin. The colony expansion curve was constructed using the normalisation method (see section 2.6), as colonies did not evolve swimming motility at the same time. The colony expansion curve is average of all replicates. The colony's area subtracted from all consecutive measurements (normalisation method) are shown in Appendix ZV: Table ZV-1.



General Linear Model: Log Area versus Strain, Nitrogen

Factor Information

Factor	Type	Levels	Values
Strain	fixed	2	AR1, AR2
Nitrogen	fixed	3	Ammonium, Glutamate, Glutamine

Analysis of Variance for Log Area, using Adjusted SS for Tests

Source	DF	Seq SS	Adj SS	Adj MS	F	P
Strain	1	0.01355	0.00493	0.00493	0.11	0.746
Nitrogen	2	1.19183	1.19183	0.59592	12.86	0.000
Error	31	1.43696	1.43696	0.04635		
Total	34	2.64234				

Model Summary

S	R-sq	R-sq(adj)
0.215299	45.62%	40.36%

Figure 5-22 Box plot: Comparison of colony's spreading of evolved colonies
 Data analysed from Figure 5-8 and Figure 5-21. The logarithm of the colony's spreading area (mm²) was used to conduct the ANOVA.

5.8 Evolution of Swimming Motility in AR2 for Different Nitrogen sources in a Poor Energy Environment

Colonies did not evolve swimming motility when sucrose was the carbon source and ammonium the nitrogen source until much later (mean = 20.0 days, *SD* = 0.0 days) compared to when glutamine was the nitrogen source and sucrose the carbon source (mean = 3.3 days, *SD* = 0.6 days). Some plates did not evolve swimming motility in

sucrose/ammonium and did not show any visible growth (Table 5-10). The evolution of swimming motility was observed earlier when glutamine was the nitrogen/carbon source compared to ammonium regardless of the carbon source (Figure 5-23). It is important to note that there were no significant statistical difference (P -value $0.705 > 0.050$; Appendix H: Figure H-4) between the time to evolve swimming motility in strains AR1 and AR2 in sucrose and glutamine (Table 5-10). The colony expansion curve for the evolved AR2 colonies grown on glutamine and sucrose showed little variability (Figure 5-24), and the appearance of evolved swimming colonies did not differ between nitrogen sources (Figure 5-25 and Figure 5-26). It is important to mention that the appearance of blebs was not noted when sucrose was the carbon source. There were no statistically significant differences (P -value $0.362 > 0.050$) in the time to evolve swimming motility in strain AR2 between both carbon sources (glucose and sucrose) and glutamine as nitrogen source (Figure 5-27).

Table 5-10 Descriptive statistics

Descriptive statistics for the evolution of swimming motility in strain AR2 when ammonium was the nitrogen source and sucrose the carbon source					
Variable	N	N*	Mean	SE	SD
Days Start Swimming	2	4	20.000	0.000	0.000
*N is the number of plates with no evolved swimming motility and no visible growth SE= Standard Error					
Days to evolve swimming motility in strains AR1 and AR2 with glutamine as the nitrogen source and sucrose as the carbon source					
Strain	N	Mean	SD	95% CI	
AR1	6	3.667	1.366	(2.513, 4.820)	
AR2	3	3.333	0.577	(1.702, 4.965)	
Note: Pooled SD = 1.195 CI = confidence interval					

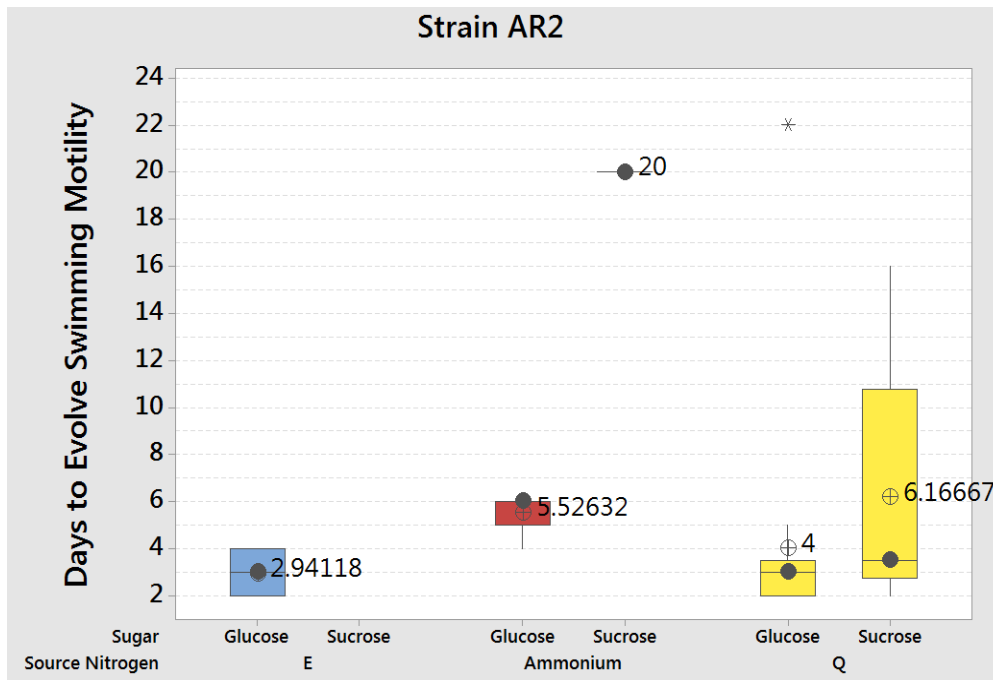


Figure 5-23 Box plot: Evolution of swimming motility in strain AR2 for different nitrogen and carbon sources

Growth on glutamate/sucrose was not assessed. E: glutamate; Q: glutamine. This average 4.00 days ($SD = 4.72$ days) for the evolution of swimming motility in glutamine/glucose treatment includes the outlier plate that evolved swimming motility after 22 days. Whereas the mean value 2.875 days ($SD = 0.885$ days) for the evolution of swimming phenotype in treatment glutamate/glucose was calculated without the outlier, the statistical analysis presented no differences, irrespective of inclusion or exclusion of the outlier. The median is shown as a line or grey dot inside the box plot.

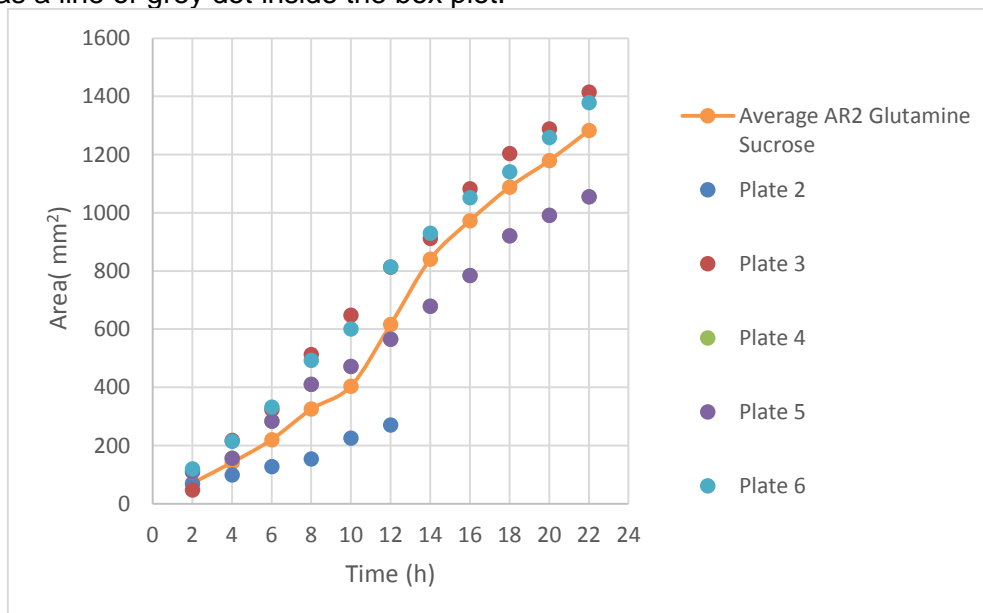


Figure 5-24 Colony expansion curve of evolved AR2 colonies

Colonies were grown on 0.25 % agar M9 medium with glutamine as the nitrogen source and sucrose as the carbon source, supplemented with kanamycin. Swimming motility did not evolve concurrently and so the normalisation method was utilised (see section 2.6). The curve shown is the average of all replicates. The colony's area subtracted from all consecutive measurements (normalisation method) are shown in Appendix ZV: Table ZV-1.

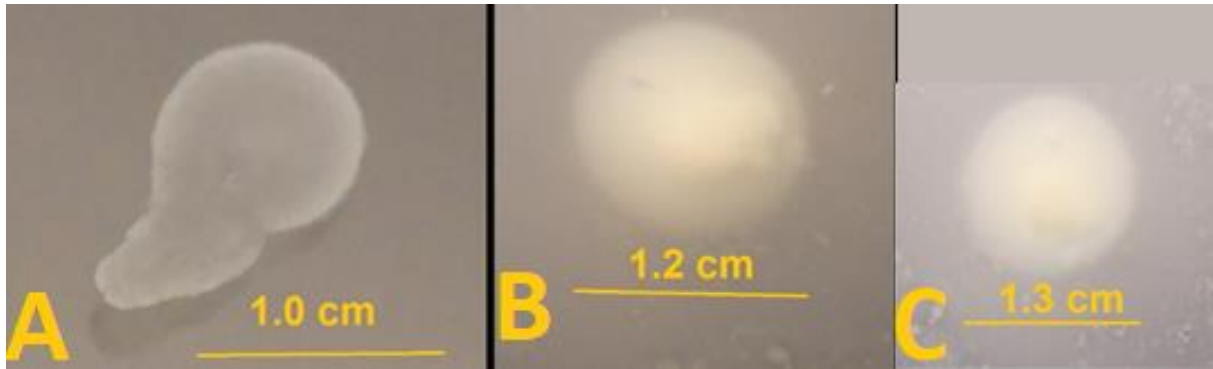


Figure 5-25 Swimming motility in evolved strain AR2

Colonies were grown on 0.25 % agar M9 medium with ammonium as the nitrogen source and sucrose as the carbon source, amended with antibiotic. (A) No swimming for 19 days. (B) Swimming was initiated after 20 days, picture taken 7 days after swimming motility began. (C) Swam for 10 days.

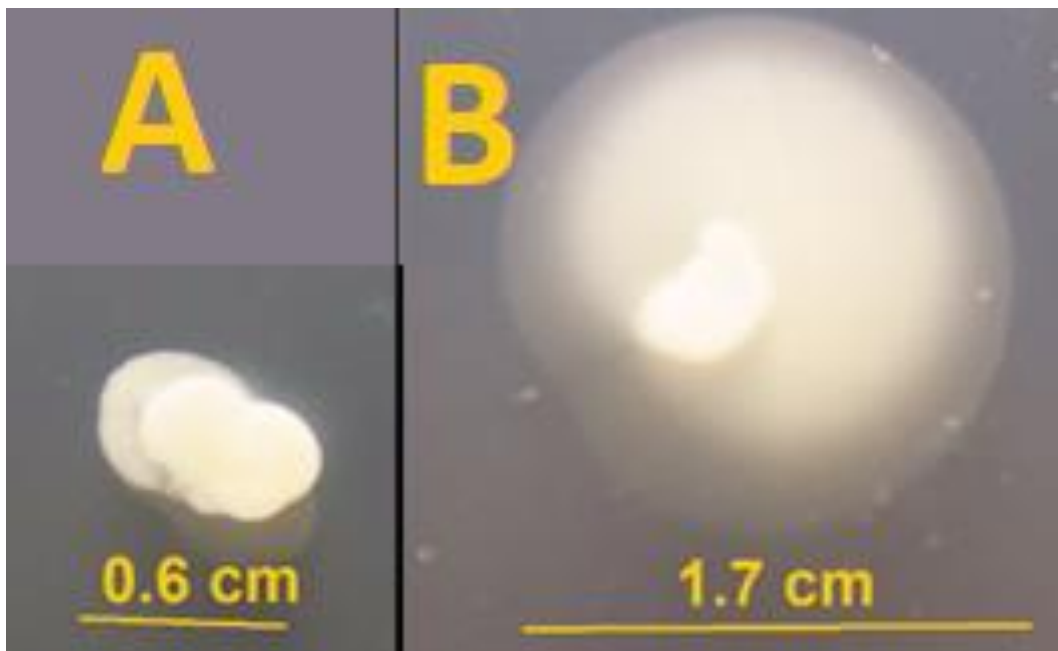
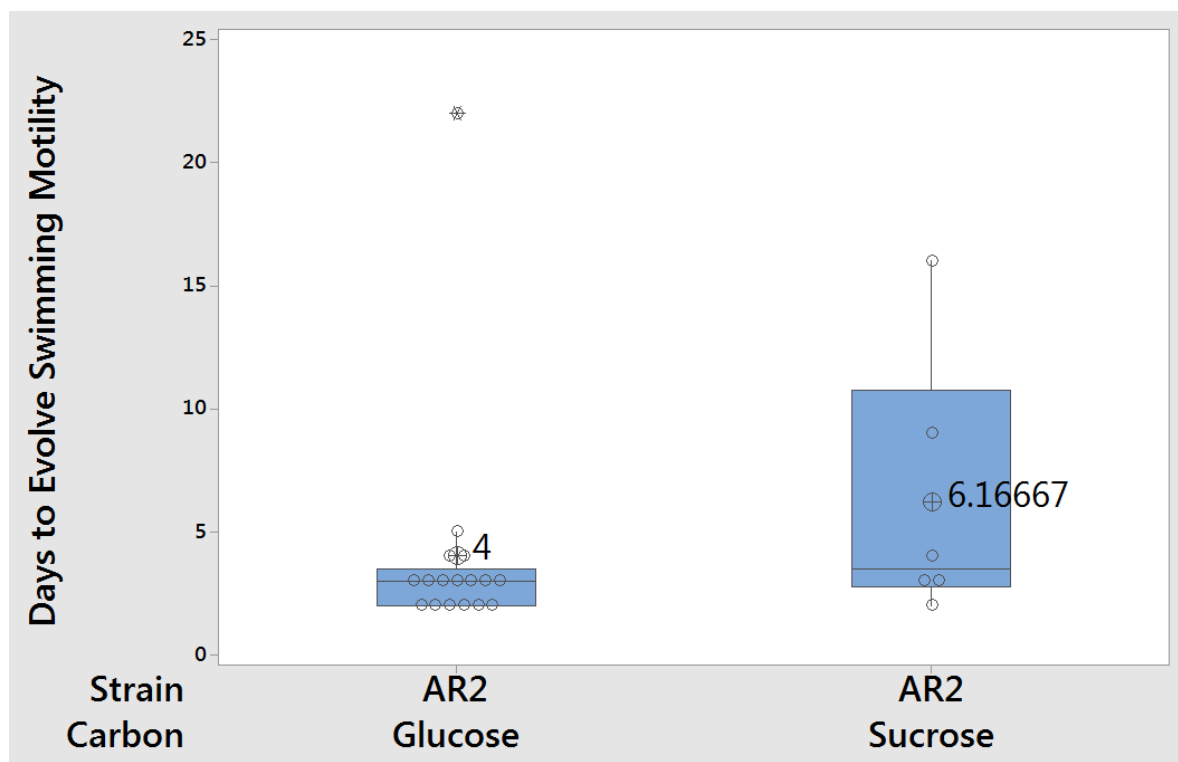


Figure 5-26 Swimming motility in evolved strain AR2

Colonies were grown on 0.25 % agar M9 medium with glutamine as the nitrogen source and sucrose as the carbon source, reformed with antibiotic. (A) Started to swim after 2 days. (B) Swam for 1 day.



One-way ANOVA: Days versus Carbon

Method

Null hypothesis All means are equal
 Alternative hypothesis Not all means are equal
 Significance level $\alpha = 0.05$

Equal variances were assumed for the analysis.

Factor Information

Factor	Levels	Values
Carbon	2	Glucose, Sucrose

Analysis of Variance

Source	DF	Seq SS	Contribution	Adj SS	Adj MS	F-Value	P-Value
Carbon	1	20.82	3.98%	20.82	20.82	0.87	0.362
Error	21	502.83	96.02%	502.83	23.94		
Total	22	523.65	100.00%				

Model Summary

S	R-sq	R-sq(adj)	PRESS	R-sq(pred)
4.89331	3.98%	0.00%	613.331	0.00%

Means

Carbon	N	Mean	StDev	95% CI
Glucose	17	4.00	4.72	(1.53, 6.47)
Sucrose	6	6.17	5.42	(2.01, 10.32)

Pooled StDev = 4.89331

Figure 5-27 Box plot: Comparison of evolution of swimming motility under different carbon sources and glutamine as nitrogen source

The one-way ANOVA table obtained to compare the time (days) to evolve swimming motility under different carbon sources is shown below the box plot.

5.9 Evolved AR2 Colonies from Different Nitrogen and Carbon Sources

Many isolates were lost due to technical problems. In total, 48 isolates were obtained from evolved swimming colonies of sessile strain AR2 grown on different nitrogen and carbon sources in 0.25 % agar M9 medium supplemented with kanamycin (Table 5-11). From these 48 isolates, 32 maintained their swimming phenotype, and were renamed evolved AR2S strains (Movie 1); the remaining 16 isolates were sessile upon re-testing (Table 5-11). All 32 AR2S strains obtained had evolved when glutamine or

ammonium was the nitrogen source, but only two of these when sucrose was the carbon source (Table 5-12). In addition, some were obtained from blebs that appeared on the evolved swimming colony. Ten to twelve days after evolving swimming motility a colony sometimes separated into sections, and this type of blebbing was named as cake blebbing. It was possible to obtain many blebs from the same swimming disc (same replicate number) for growth on glutamine/glucose. For example, strain AR2S18 was isolated from the evolved swimming disc for replicate number 10, and strain AR2S28 was isolated from a bleb that appeared on the same colony of replicate number 10.

Table 5-11 Testing isolates for swimming phenotype

Isolates obtained from evolved swimming AR2 colonies for different nitrogen and carbon sources								
Strain	Count	Percent	Nitrogen	Count	Percent	Carbon	Count	Percent
AR2	16	33.33	ammonium	10	20.83	glucose	41	85.42
AR2S	32	66.67	glutamate	3	6.25	sucrose	7	14.58
			glutamine	35	72.92			
Total Isolates	48		Total Isolates	48		Total Isolates	48	

Note: AR2 isolates from the agar plug of evolved swimming disc or bleb had not evolved and remained sessile upon re-testing; AR2S isolates had evolved swimming motility which was maintained upon re-testing.

Quantity of evolved and non-evolved isolates obtained from evolved swimming AR2 colonies for different nitrogen and carbon sources					
Carbon Source	Nitrogen Source	Non-evolved Isolates		Evolved Isolates	
		Count	Percent	Count	Percent
glucose	ammonium	2	16.67	2	6.90
	glutamate	3	25.00		
	glutamine	7	58.33	27	93.10
Total		12		29	
sucrose	ammonium	3	100	3	100
	glutamate				
	glutamine				
Total		3		3	

Note: There were 32 AR2S strains in total; 29 AR2S strains were obtained from nitrogen/glucose and 3 AR2S strains were isolated from nitrogen/sucrose treatment.

Table 5-12 List of evolved AR2S strains: phenotype and origin

Strain	Nitrogen/Carbon	Motility Phenotype	Mean Rate Colony Expansion (mm ² /h)	Bleb	Replicate	Days of Isolation
AR2S1	ammonium/glucose	Medium	8.93	Yes	5	17
AR2S10	glutamine/glucose	Fast	9.88	Yes/Cake	2	17
AR2S11	glutamine/glucose	Fast	11.63	No	7	3
AR2S12	glutamine/glucose	Slow	4.43	Yes	2	5
AR2S13	glutamine/glucose	Medium	8.59	Yes	4	8
AR2S14	glutamine/glucose	Medium	8.29	Yes	2	5
AR2S15	glutamine/glucose	Slow	7.49	No	6	3
AR2S16	glutamine/glucose	Fast	15.85	Yes	11	5
AR2S17	glutamine/glucose	Fast	9.57	Yes	2	17
AR2S18	glutamine/glucose	Medium	8.60	No	10	8
AR2S19^a	glutamine/glucose	Slow	0.76	Yes	11	5
AR2S20	glutamine/glucose	Fast	20.09	No	11	3
AR2S22	glutamine/glucose	Slow	7.50	No	2	3
AR2S23	glutamine/glucose	Fast	9.47	Yes	5	8
AR2S24	glutamine/glucose	Fast	9.44	Yes	1	22^b
AR2S25	glutamine/glucose	Fast	14.82	Yes	8	8
AR2S26	glutamine/glucose	Fast	14.54	Yes	5	8
AR2S27	glutamine/glucose	Slow	6.95	Yes	1	22^b
AR2S28	glutamine/glucose	Slow	5.79	Yes	10	10
AR2S29	glutamine/glucose	Fast	14.29	Yes	5	8
AR2S3	ammonium/glucose	Fast	9.18	Yes	9	17
AR2S30	glutamine/glucose	Fast	16.36	Yes	1	22^b
AR2S31	glutamine/glucose	Slow	5.24	Yes	8	8
AR2S32	glutamine/glucose	Slow	4.86	Yes	8	8
AR2S33	glutamine/glucose	Medium	8.61	Yes	4	8
AR2S34	glutamine/glucose	Fast	13.26	Yes	4	8
AR2S35	glutamine/glucose	Fast	20.07	Yes	4	8
AR2S4	ammonium/glucose	Slow	6.62	Yes	7	17
AR2S6	ammonium/sucrose	Slow	7.70	No	11	23^b
AR2S7	ammonium/sucrose	Fast	14.14	No	3	23^b
AR2S8	glutamine/glucose	Slow	6.57	Yes	2	5
AR2S9	glutamine/glucose	Slow	4.51	Yes	11	5

Note: Days of isolation after evolution of swimming motility in sessile strain AR2 is the time since a colony was inoculated onto the plate. Some isolates were obtained from blebs that evolved around the border of an evolved swimming colony. The motility phenotype classified as medium has an expansion rate of ~8 mm²/h. The values below it (from ~7 mm²/h and below) are classified as slow expansion rate, whereas those that above it (from ~9 mm²/h and above) are categorised as fast expansion rate. ^aAll evolved strains showed the same colony appearance (round), but only strain AR2S19 developed a star in the middle after 3 to 4 days. The treatment (nitrogen/carbon) from which they evolved is indicated.

^bThese strains evolved in a replicate that evolved swimming motility phenotype after 22 or 23 days.

Table 5-13 Blebs obtained from the same evolved swimming colony in treatment glutamine/glucose

Strain	Motility Phenotype	Mean Rate of Colony Expansion (mm ² /h)	Bleb	Replicate Unique Number
AR2S10	Fast	9.88	Yes/Cake	2
AR2S12	Slow	4.43	Yes	2
AR2S14	Medium	8.29	Yes	2
AR2S17	Fast	9.57	Yes	2
AR2S22	Slow	7.50	No	2
AR2S8	Slow	6.57	Yes	2
AR2S18	Medium	8.60	No	10
AR2S28	Slow	5.79	Yes	10
AR2S16	Fast	15.85	Yes	11
AR2S19	Slow	0.76	Yes	11
AR2S20	Fast	20.09	No	11
AR2S9	Slow	4.51	Yes	11

Note: 1) each replicate for every carbon/nitrogen combination had a unique number, and blebs that came from the same evolved swimming colony on the same plate had the same replicate number. 2) Isolates obtained from the same swimming disc colony and not from blebs but from the same plate number had the same replicate number as the strains derived from their corresponding blebs.

5.10 The Evolved AR2S Strains Possess Mutations in the NtrBC system

The three genes: *ntrB*, *ntrC* and *glnK* in all the evolved AR2S strains were examined. No mutations were identified in the *ntrC* or *glnK* genes (refer to Alignments in Supplementary Information). Most of the evolved strains had the same SNP in the region of the *ntrB* gene studied, which corresponded to the PAS domain. The same SNP was also found in the FleQS and AR1S strains studied (refer to Alignments in Supplementary Information). Therefore, the mutation A289C is the most common in the re-wiring of the NtrBC system for the restoration of swimming motility (Figure 1-59). Taylor et al.¹⁰⁸ also found this mutation in their evolved strains. It is important to note that the parent strain AR2 did not show any mutations in the regions of the *ntrB* and *ntrC* genes studied nor in the gene *glnK*. Only strain AR2S15 did not possess a mutation within the PAS domain. There were no *ntrC* mutants in the isolates obtained from blebs.

Table 5-14 Mutations in the genes studied for all evolved strains AR2S

Strain	<i>ntrB</i>		Mean Rate of Colony Expansion (mm ² /h)	Motility Phenotype
	Nucleotide Change	Amino Acid Change		
AR2S1	A289C	T97P	8.93	Medium
AR2S10	A289C	T97P	9.88	Fast
AR2S11	A289C	T97P	11.63	Fast
AR2S12	A289C	T97P	4.43	Slow
AR2S13	A289C	T97P	8.59	Medium
AR2S14	A289C	T97P	8.29	Medium
AR2S15	Wild	Wild	7.49	Slow
AR2S16	A289C	T97P	15.85	Fast
AR2S17	A289C	T97P	9.57	Fast
AR2S18	A289C	T97P	8.60	Medium
AR2S19*	A289C	T97P	0.76	Slow
AR2S20	A289C	T97P	20.09	Fast
AR2S22	A289C	T97P	7.50	Slow
AR2S23	A289C	T97P	9.47	Fast
AR2S24	A289C	T97P	9.44	Fast
AR2S25	A289C	T97P	14.82	Fast
AR2S26	A289C	T97P	14.54	Fast
AR2S27	A289C	T97P	6.95	Slow
AR2S28	A289C	T97P	5.79	Slow
AR2S29	A289C	T97P	14.29	Fast
AR2S3	A289C	T97P	9.18	Fast
AR2S30	A289C	T97P	16.36	Fast
AR2S31	A289C	T97P	5.24	Slow
AR2S32	A289C	T97P	4.86	Slow
AR2S33	A289C	T97P	8.61	Medium
AR2S34	A289C	T97P	13.26	Fast
AR2S35	A289C	T97P	20.07	Fast
AR2S4	A289C	T97P	6.62	Slow
AR2S6	A289C	T97P	7.70	Slow
AR2S7	A289C	T97P	14.14	Fast
AR2S8	A289C	T97P	6.57	Slow
AR2S9	A289C	T97P	4.51	Slow

Note: All strains did not mutate *glnK* gene, and none of them showed any mutation in the target sequence for gene *ntrC*. All swimming colonies were rounded, but only strain AR2S19 formed a star in the middle of the swimming colony after 3 days to 4 days. Wild: wild type.

5.11 Motility Phenotypes of Evolved Strains AR2S

The evolved strains studied followed a Log-Normal distribution due to a mixture of growth, mutational events, and different bacterial movements present in the plates. Consequently, the geometric mean was used to construct the colony expansion curves of the strains (Figure 5-28 and Figure 5-29; Appendix C). These curves showed a gradation of rate of colony expansion among the evolved strains, meaning that their evolution had led to diversity in motility phenotypes (Appendix E). Some strains were faster than AR2F (mean = 19.1 mm²/h) and slower than AR2S (mean = 2.25 mm²/h), which had been isolated by Taylor et al.¹⁰⁸, while the rate of colony expansion of other strains was in between and so these were classed as medium rate of colony expansion. It is important to note that the parent sessile strain AR2 exhibited a uniform rate of colony expansion with only slight changes because its movement was not active and depended only on colony expansion due to cumulative growth; whereas the swimming strains demonstrated dramatic changes in rate of colony expansion.

Spur-Swarming signifies a type of swarming initiated as a single spur that emerges from the centre and the base of a swimming colony (Figure 5-30). On reaching the agar surface, the spur begins to slide, almost always, faster than the underneath swimming colony. Then, this spur switches to a fast and diffused movement named as spur-swarming when it commences swimming through the agar after leaving the swimming colony border. In addition, a spur did not always switch immediately to spur-swarming (Figure 5-30). Spur-Swarming was observed in both groups of evolved strains AR2S and AR1S. It is interesting to note that the evolved strains isolated by Taylor et al.¹⁰⁸ were never observed to swarm or exhibit spur-swarming in this research. This type of spur-swarming was untimely and not always occurred in all replicates.

The geometric mean was used due to variability in motility of the replicates, and spur-swarming, which was variable in the time of its apparition; not all replicates formed spur and consequently, spur-swarmed (Figure 5-29). This skew experimental population also refers to some replicates of the same strain being remarkably slower than others owing to spur-swarming or differences in colony expansion rate, so they belong to a Log-Normal distribution (Figure 5-31). Spurs appeared randomly in replicates, although some replicates never formed spurs, but not at the same time (Table 5-15), with the earliest spur being observed at 2 h (AR2S7; Appendix C: Figure

C-17) at the latest at 90 h (AR2S14; Appendix C: Figure C-24). Some replicates had not spur-swarmed after 6 days and swam very slowly throughout this period (Figure 5-32). Strain AR2S32 was not observed to form a spur, and hence there was no spur-swarming movement in any replicate (Appendix C: Figure C-31); however, it would probably eventually spur-swarm if more replicates on larger diameter plates (15 cm) were observed. Some replicates of a strain spur-swarmed whilst others did not (AR2S19; Appendix C: Figure C-11), and it is likely that these replicates will eventually spur-swarm over a longer period of time and would be clearly seen on larger diameter plates (15 cm diameter). All the evolved AR2S swimming colonies had the same rounder shape and initially appeared white before gradually turning yellow. The only exception was strain AR2S19, which always formed a star in the middle of the colony and generally after 3 days - 4 days, and rarely earlier (50 h) (Figure 5-31 and Figure 5-32); this star was never observed to spur-swarm or reach out beyond the colony border.

It was hypothesized that this spur-swarming fast movement was the result of a second mutation, and the spur-swarming region was comprised of a double mutant population *ntrB ntrC*, while the initial slow swimming colony was a single mutant *ntrB* population. However, the whole genome sequencing results did not correlate with this hypothesis (Table 6-2). Taylor et al.¹⁰⁸ obtained the evolved faster mutant AR2F (genotype *ntrB ntrC*) from blebs that eventually appeared on the border of the evolved slower mutant AR2S (genotype *ntrB*) colony. Therefore, the evolution of a faster motility phenotype was the result of a double mutation which had occurred in the satellite population (bleb). However, AR2S, the slowest strain obtained by Taylor et al.¹⁰⁸ did not show spurs. The average rate of colony expansion (Equation 2-1) of the evolved strains in a period of 24 h was used to classify them as slow, medium and fast swimmers (Table 5-15; Appendix E).

Table 5-15 Motility phenotypes and spur formation time of the evolved AR2S strains

Strain	Mean Rate of Colony expansion (mm ² /h)	Motility Phenotype	Spur Formation [<i>N</i> plates, Time (h)]	<i>N</i> total
AR2S1	8.93	Medium	<i>N</i> = 2, 2 h and 18 h	5
AR2S10	9.88	Fast	<i>N</i> = 1, 2 h.	5
AR2S11	11.63	Fast	<i>N</i> = 2, 4 h and 10 h	6
AR2S12	4.43	Slow	<i>N</i> = 2, 12 h and 72 h	5
AR2S13	8.59	Medium	<i>N</i> = 2, 8 h and 10 h,	5
AR2S14	8.29	Medium	<i>N</i> = 2, 14 h and 90 h	6
AR2S15	7.49	Slow	<i>N</i> = 3, 6 h, 20 h and 72 h	5
AR2S16	15.85	Fast	<i>N</i> = 4, 10 h 14 h, 2 h and 8 h	7
AR2S17	9.57	Fast	<i>N</i> = 3, 16 h, 2 h, 18 h	5
AR2S18	8.60	Medium	<i>N</i> = 2, 2 h and 4 h	8
AR2S19*	0.76	Slow	<i>N</i> = 2, 18 h and 50 h	6
AR2S20	20.09	Fast	<i>N</i> = 2, 2 h and 2 h	5
AR2S22	7.50	Slow	<i>N</i> = 2, 6 h and 72 h	6
AR2S23	9.47	Fast	<i>N</i> = 2, 14 h and 72 h	5
AR2S24	9.44	Fast	<i>N</i> = 1, 4 h	5
AR2S25	14.82	Fast	<i>N</i> = 2, 6 h and 10 h	6
AR2S26	14.54	Fast	<i>N</i> = 3, 6 h, 2 h, and 12 h	5
AR2S27	6.95	Slow	<i>N</i> = 2, 2 h and 48 h	5
AR2S28	5.79	Slow	<i>N</i> = 3, 10 h, 16 h and 16 h,	5
AR2S29	14.29	Fast	<i>N</i> = 2, 2 h and 4 h	5
AR2S3	9.18	Fast	<i>N</i> = 3, 2 h, 10 h, and 12 h	6
AR2S30	16.36	Fast	<i>N</i> = 2, 4 h and 16 h	5
AR2S31	5.24	Slow	<i>N</i> = 2, 12 h and 48 h	5
AR2S32	4.86	Slow	No appeared	5
AR2S33	8.61	Medium	<i>N</i> = 3, 14 h, 22 h, and 72 h	6
AR2S34	13.26	Fast	<i>N</i> = 1, 4 h	5
AR2S35	20.07	Fast	<i>N</i> = 2, 30 h, and 50 h	5
AR2S4	6.62	Slow	<i>N</i> = 1, 82 h.	5
AR2S6	7.70	Slow	<i>N</i> = 1, 12 h	5
AR2S7	14.14	Fast	<i>N</i> = 1, 4 h	5
AR2S8	6.57	Slow	<i>N</i> = 2, 12 h and 14 h	7
AR2S9	4.51	Slow	<i>N</i> = 5, 2 h, 6 h, 8 h, 16 h, 3 days	7

Note: *N*: number of replicates in the colony expansion curve.

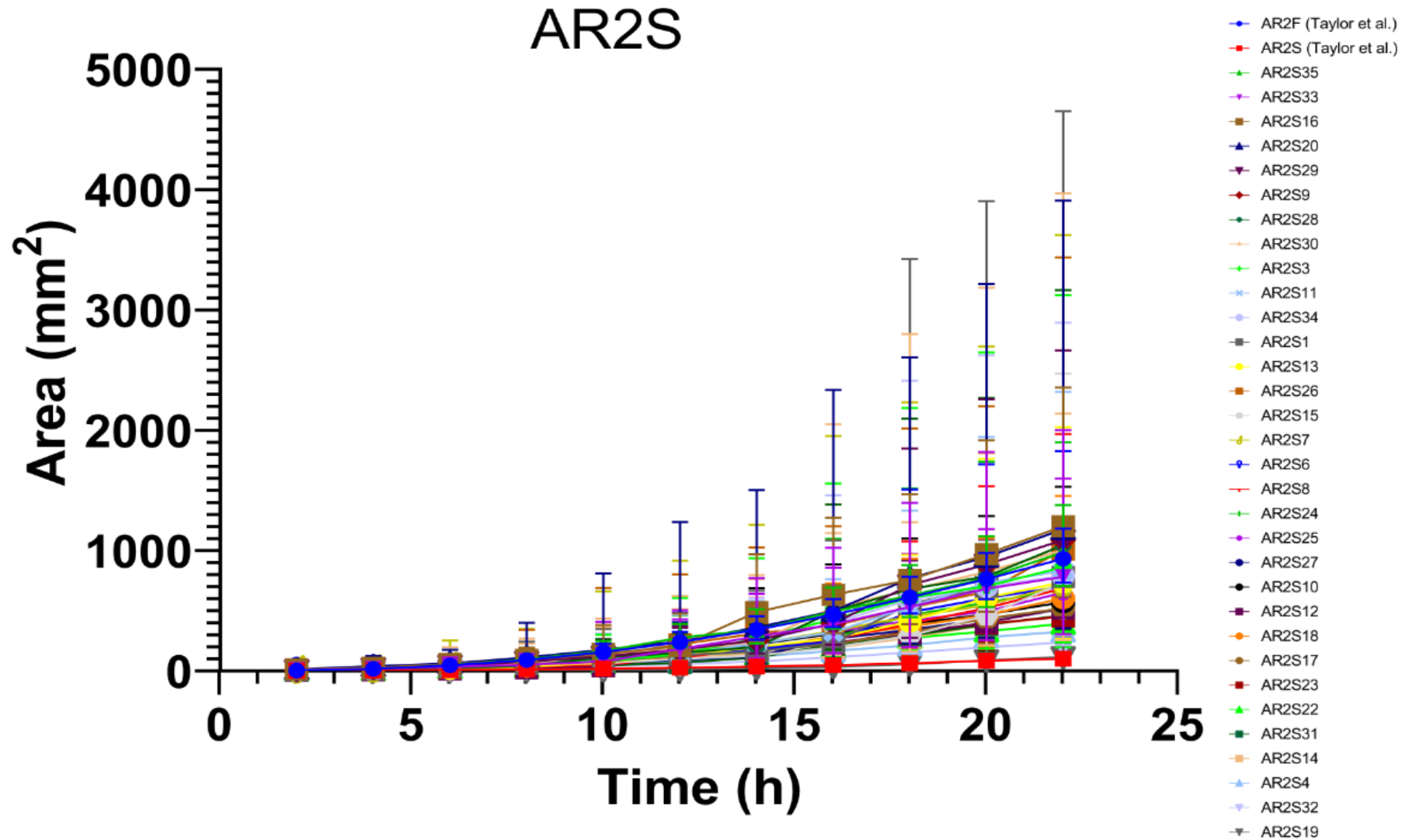


Figure 5-28 Colony expansion curves of all the evolved AR2S strains

The graph shows geomean of all replicates and the error bars represent geometric standard deviation. Swarming medium on 9 cm diameter plates. No antibiotic added.

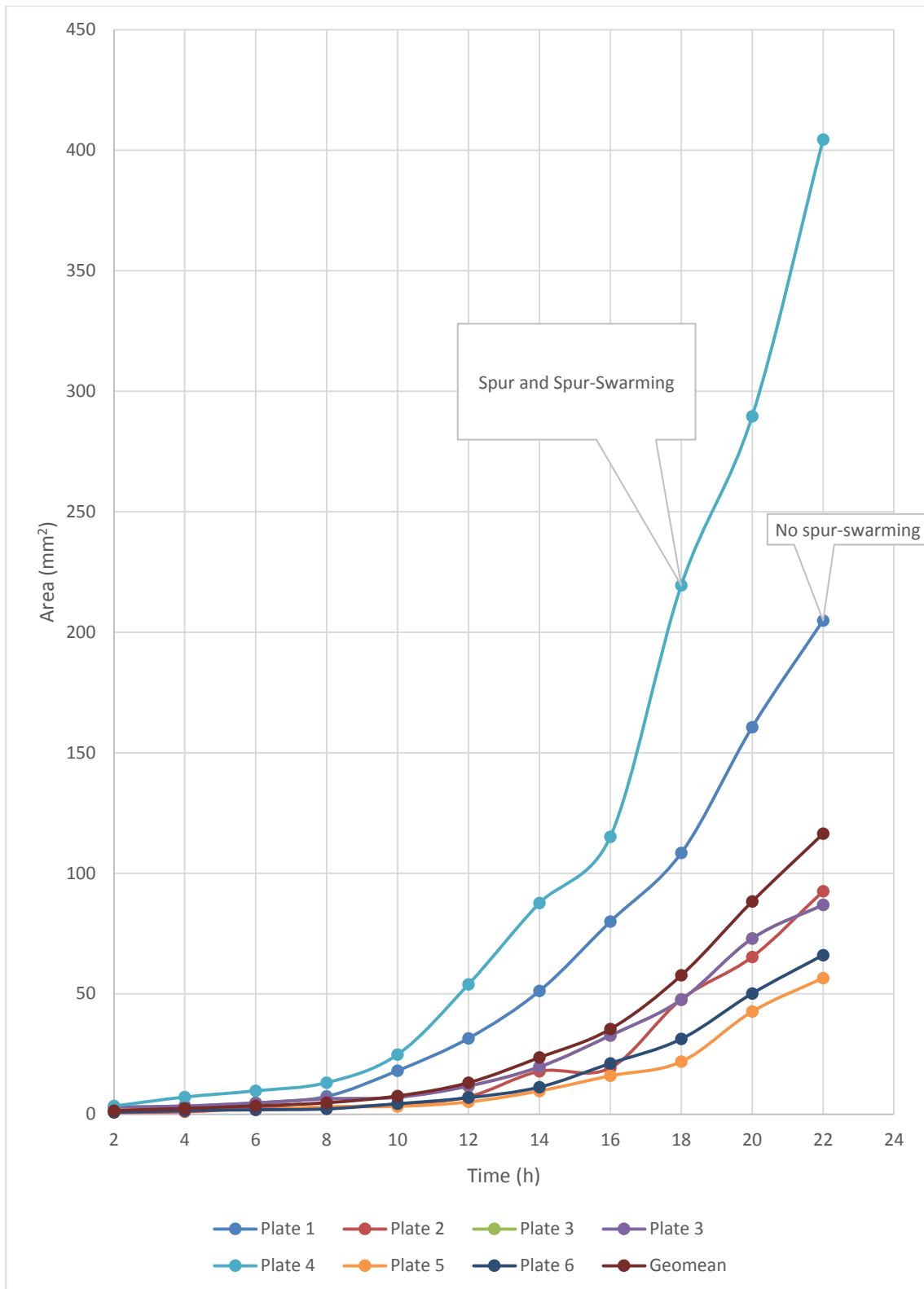


Figure 5-29 Colony expansion curves of all the replicates of strain AR2S19

This is a skew experimental population as some replicates swam faster than others. There was only one replicate which demonstrated spur-swarming, and this moved remarkably faster than the other replicates. Swarming medium without antibiotic on plates 9 cm diameter.

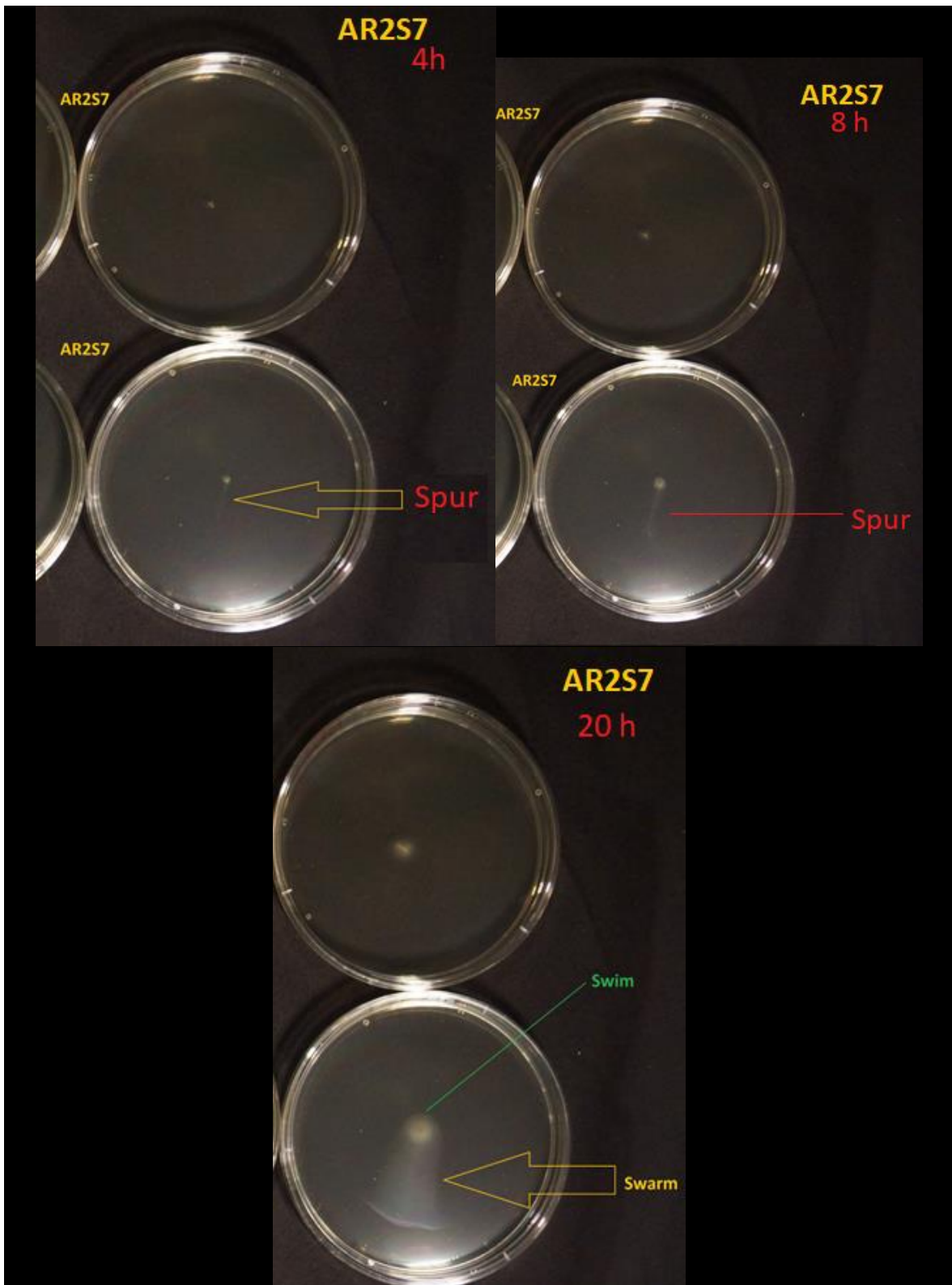


Figure 5-30 Spur and spur-swarming in strain AR2S7

Swarming medium (no antibiotic) on 9 cm diameter plates. The spur appeared at 4 h, slid on the top of agar until 8 h and then switched to swim through the agar and spread faster than the initial colony. As this fast spreading was derived from a spur it is named as spur-swarming. In the other replicate, no spur was formed and only swimming was observed.

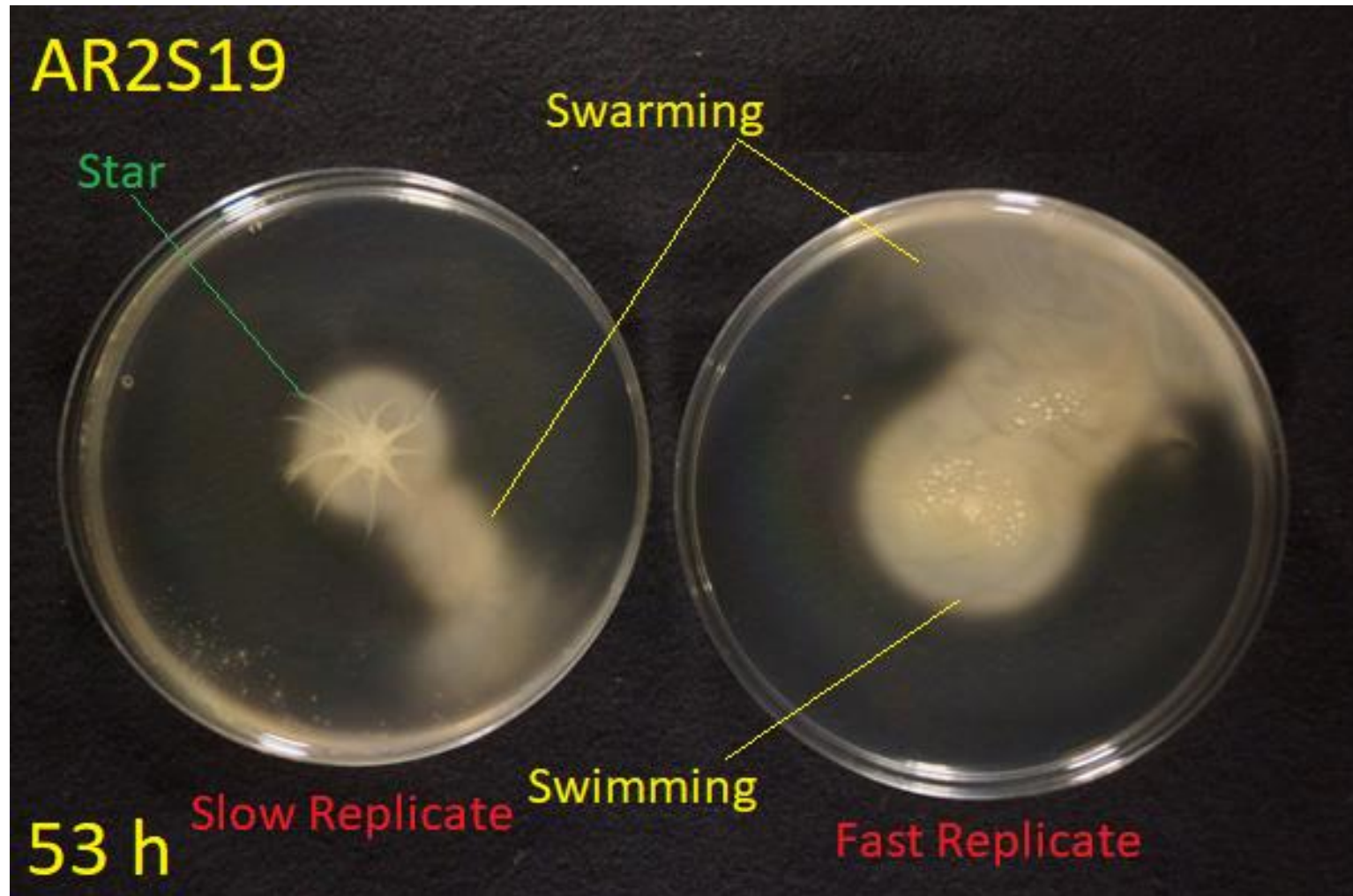


Figure 5-31 Example of a skew experimental population: evolved strain AR2S19

Some replicates were slower than others and demonstrated spur-swarming. The star tended to appear after 3 days, although it appeared earlier in one replicate. This strain was a *ntxB* mutant. Swarming medium (no antibiotic) on plates of 9 cm diameter.

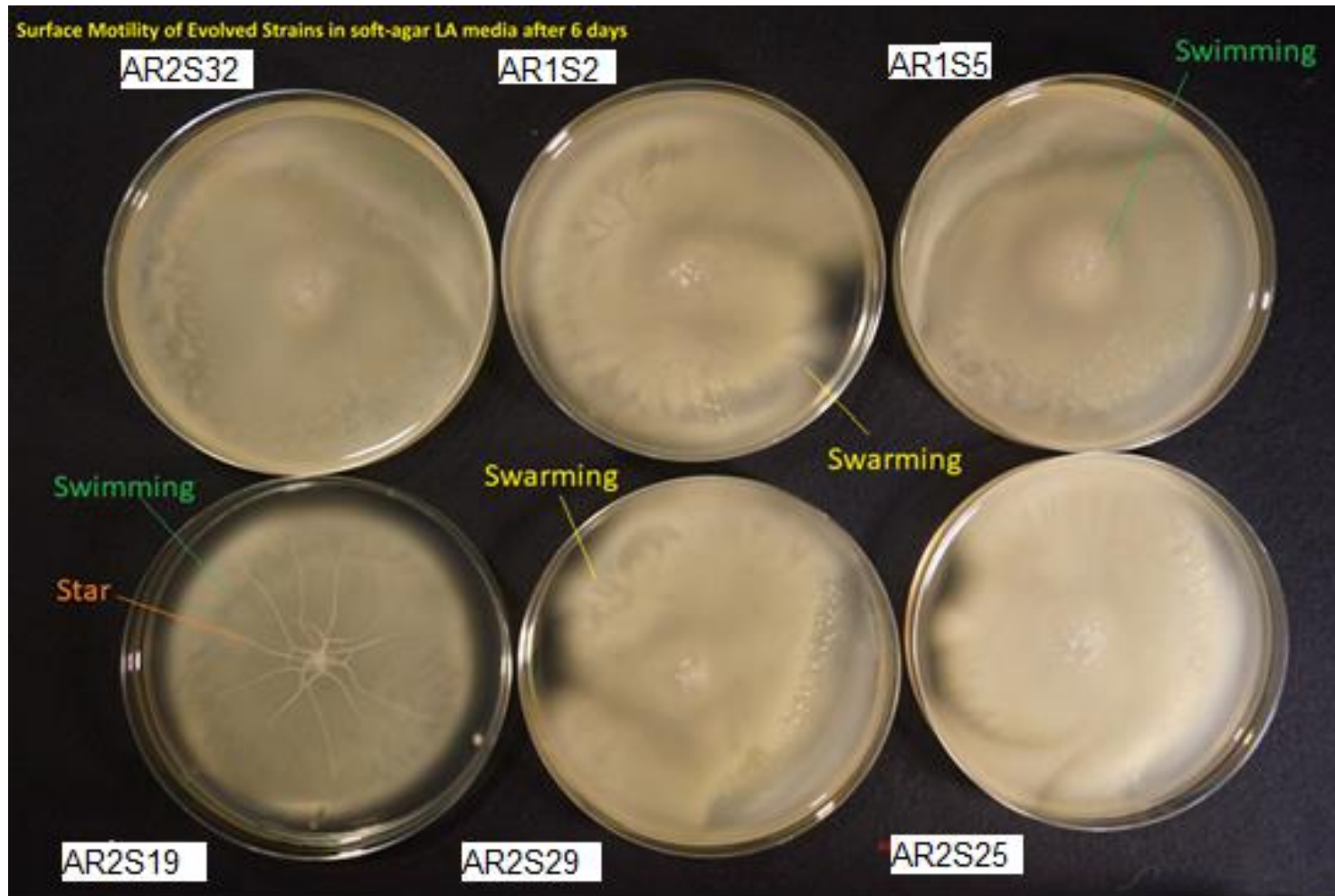


Figure 5-32 Comparison between swarming and non-swarming strains after 6 days

The only non-spur swarming strain was AR2S32 (upper plates and at left). All strains did eventually swarm, although some replicates of the same strain (AR2S19; lower plates at left) did not swarm and only showed swimming for 6 days. Strain AR2S19 was the only one that formed an star in the middle of the colony typically after 3 days.

5.11.1 Rate of colony expansion changes in evolved AR2S strains

Based on the geomean data, the AR2S strains generally showed a decrease in rate of colony expansion at 11 h and 17 h, whereas in AR1S strains it was after 13 h and 15 h, while the AR2S strains generally showed an increase in rate of colony expansion at 12 h, 17 h and 19 h, whereas in the AR1S strains it was at 18 h (Appendix G: Figure G-1 to Figure G-5). Therefore, both groups of evolved AR1S and AR2S strains tended to increase and decrease their rate of motilities at around similar times. It is interesting to note that AR1S and AR2S strains decreased rate of colony expansion at a similar time to FleQS strains (17 h and 28 h); however, they did not increase their rate of colony expansion at similar times to FleQS strains (22 h and 24 h).

It is important to highlight that both groups of evolved strains AR1S and AR2S do not produce viscosin. On the other hand, the group of FleQS strains are indeed viscosin producers. This represents a key element in their colony's rate expansion since biosurfactant production (viscosin) enhances colony spreading as well as swarming in wild type strain SBW25. It also facilitates sliding in the aflagellate parent strain SBW25 Δ *fleQ* (notably, this strain only slides and never swarms). Both groups of evolved AR2S and AR1S strains tended to increase rate of colony expansion (~18 h), whereas FleQS strains increased their rate of colony expansion at 22 h and 24 h; Appendix G: Figure G-6 and Figure G-7. In addition, these changes in rate of colony expansion were also related to changes in type of movement from swimming to any type of swarming (e.g. spur-swarming or spidery-swarming). In general, AR1S and AR2S strains tended to initiate spur-swarming around 12 h - 18 h, although not all replicates formed the spurs and then spur-swarmed concomitantly, some never formed spurs, and others spur-swarmed much earlier, whereas FleQS strains exhibited spidery-swarming around 12 h – 28 h, and all replicates showed spidery-swarming movement at 28 h. Spur-Swarming generally was observed in AR2S and AR1S strains between 12 h to 18 h. Spidery-Swarming in FleQS strains was appeared between 12 h to 28 h, and this type of swarming always occurred in all replicates of viscosin producer FleQS strains, as all replicates demonstrated spidery-swarming at 28 h, whereas in AR2S2 and AR1S1 strains spur-swarming sometimes occurred after 3 days and not in all

replicates. It is important to highlight that both groups of evolved strains AR1S and AR2S do not produce viscosin whereas FleQS strains are viscosin producers.

5.11.2 Types of swarming observed in evolved strains FleQS, AR1S and AR2S

There were 3 types of swarming (Figure 5-33):

- Wild-Swarming
- Spidery-Swarming
- Spur-Swarming

Wild-Swarming refers to any swarming that exhibits similar phenotype swarming of the wild type strain SBW25 that was always initiated at one side of the colony border and was fast and diffused; this was only observed in FleQS strains. Spidery-Swarming was a type of swarming observed only in FleQS strains that were initiated at different points of the swimming colony and had a dendritic appearance (Movies 5-7). This spidery-swarming was through the agar. Spur-Swarming was a class of swarming in non-viscosin producer strains (AR1S or AR2S). This commenced by initially emerging a spur from the middle bottom of the swimming colony and rising up the surface (Movies 14-16 and Movie 26). Here, it had the appearance of a sliding spur that slid slowly for hours or less until it started to spread very fast through the agar (spur-swarming).

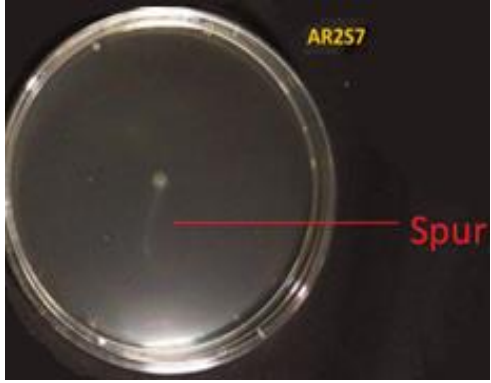
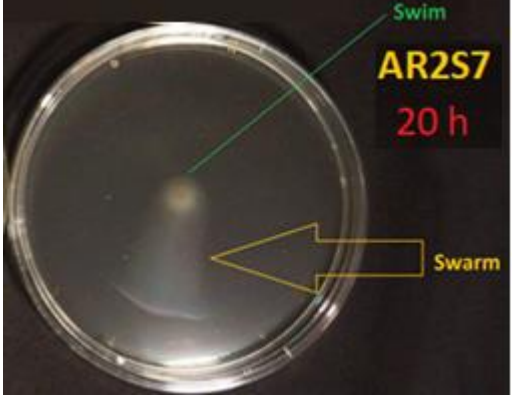
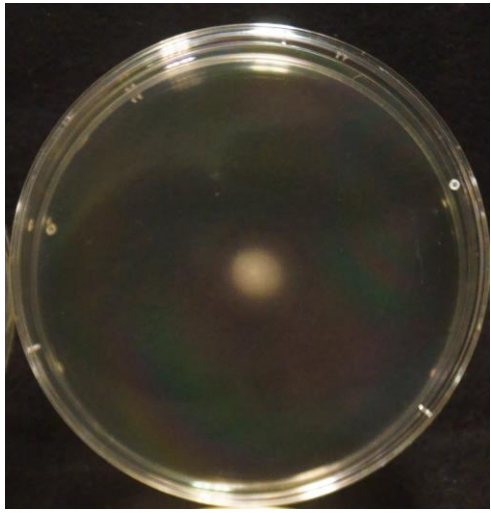
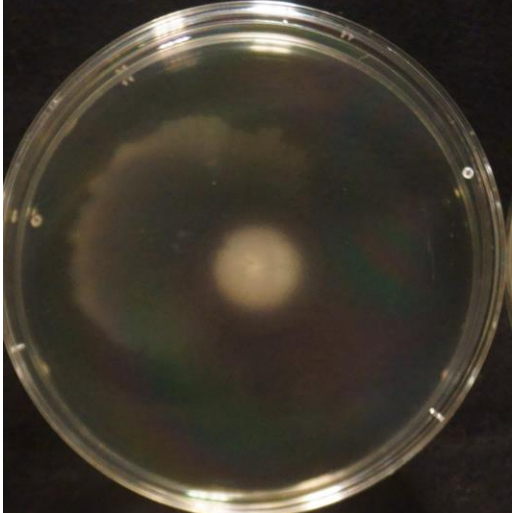
Spur-Swarming AR2S7		
	Swimming and spur at 8 h (plate 9 cm diameter)	Spur-Swarming at 20 h (plate 9 cm diameter)
Spidery-Swarming FleQS4		
	Swimming at 20 h (plate 15 cm diameter)	Spidery-Swarming at 30 h (plate 15 cm diameter)
Wild-Swarming FleQS6		
	Swimming, 30 h (plate 9 cm diameter)	Wild-Swarming, 38 h (plate 9 cm diameter)

Figure 5-33 Swarming types in evolved strains

Spur-Swarming: occurring in non-viscosin producer strains; spur rose to the surface where they slid for a while and then swam through the agar faster than the initial colony. It was only observed in AR1S and AR2S strains. Wild-Swarming originated at one side of the swimming colony and swam diffusely; it was only observed in FleQS strains. Spidery-Swarming was initiated at different points of the swimming colony and had a dendritic appearance. It was only observed in FleQS strains. Plates were taken from the colony expansion curves in swarming medium (0.25 % agar LA).

5.11.3 Strains isolated from blebs

The strains isolated from blebs of the evolved swimming colonies (Figure 5-34) did not correlate in terms of an increase in colony expansion rate as compared to the parent swimming colony (swimming disc) from which they evolved (Table 5-13). For example, strains AR2S8, AR2S10, AR2S12, AR2S14 and AR2S17 isolated from blebs were faster than their parent strain AR2S22, which was isolated from an evolved colony (from swimming disc) (Figure 5-35A). Strain AR2S28 (Appendix C: Figure C-29) which was isolated from a bleb turned out to be remarkably faster than its parent strain AR2S18 (Figure 5-35B; Appendix C: Figure C-32). Bleb isolate strain AR2S16 was not faster than its parent strain AR2S20 (Figure 5-35C; Appendix C: Figure C-25 and Figure C-23) but other bleb isolates from this parent strain, AR219 and AR2S9, were slower (Appendix C: Figure C-11 and Figure C-19). However, all this information was not sufficient enough in order to conclude that strains evolving from blebs necessarily swam faster than its parent as Taylor et al.¹⁰⁸ observed. It is also not possible to clearly establish the mutational events to explain their origin. In addition, the *ntrC* gene region studied did not show any mutation in the blebs. Hence, it is necessary to conduct a multivariate analysis (Discriminant), as described in section 2.16, to classify these strains and determine which strains are similar in order to conduct whole genome sequencing to clearly identify any mutational changes. Notably the strains isolated from blebs (Table 5-13 and Figure 5-35) were slower than strain AR2F (*ntrB ntrC*) isolated from Taylor et al.¹⁰⁸ which had mean colony expansion rate from 2 h - 8 h of 19.1 mm²/h when studied in swarming medium (Figure 3-16). However, the strains isolated from blebs (except for strain AR2S19 that had a mean colony expansion rate of 0.76 mm²/h) and their respective parents were faster than strain AR2F (19.1 mm²/h) isolated from Taylor et al.¹⁰⁸. The double mutant strain AR2F (*ntrB ntrC*) was isolated from a bleb appearing at the border of an evolved swimming colony from which the single mutant strain AR2S (*ntrB*) was initially obtained that had mean colony expansion rate from 2 h - 8 h of 2.25 mm²/h when studied in swarming medium (Figure 3-16).

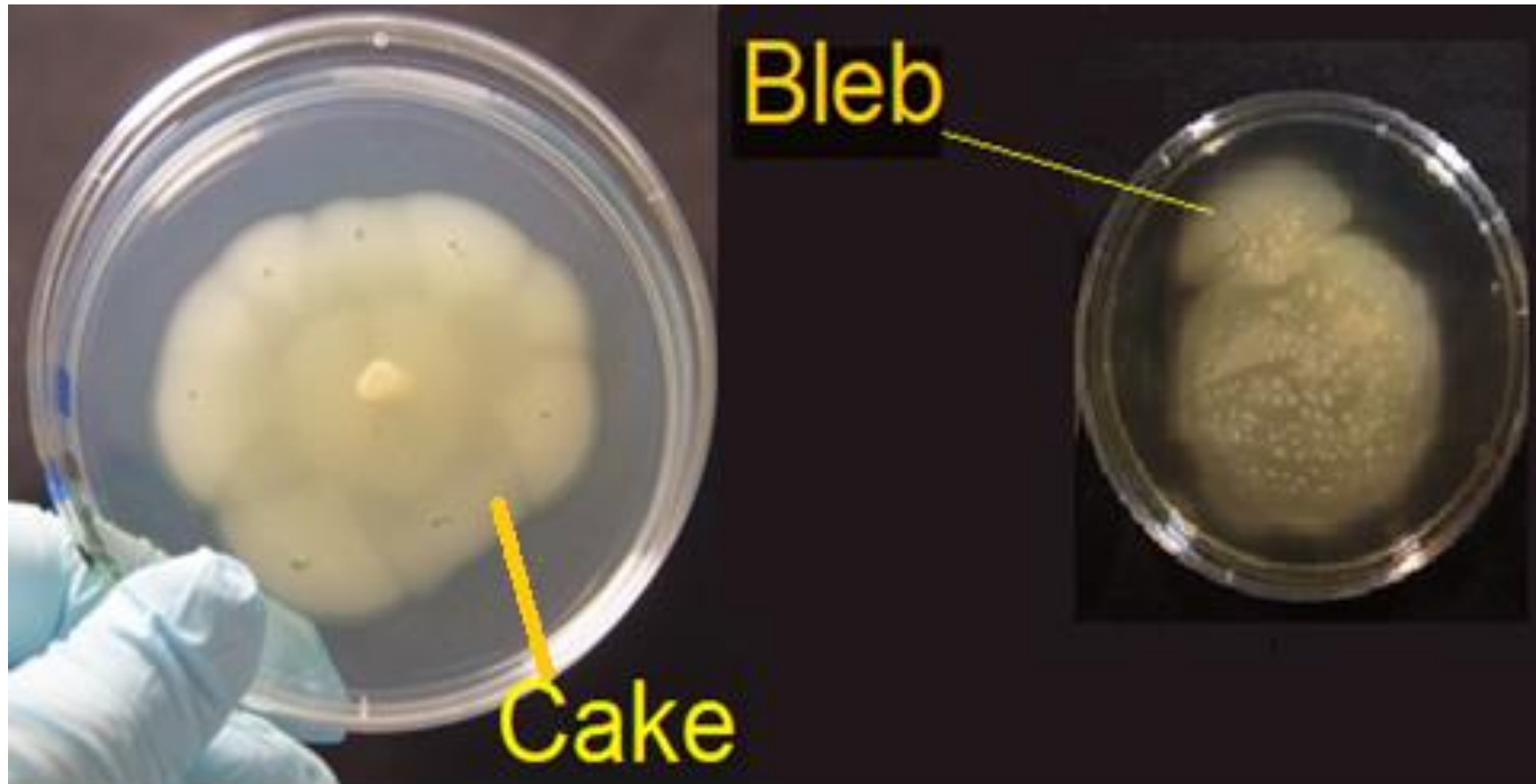


Figure 5-34 Types of blebs observed

Blebs (cake) were observed in the evolved swimming colonies and appeared as slices which were not separated from the swimming colonies. Blebs are evolved colonies that are clearly separated from the main population. The small punctures in the bleb (cake) are places where agar plugs were taken for isolation using a sterile tip.

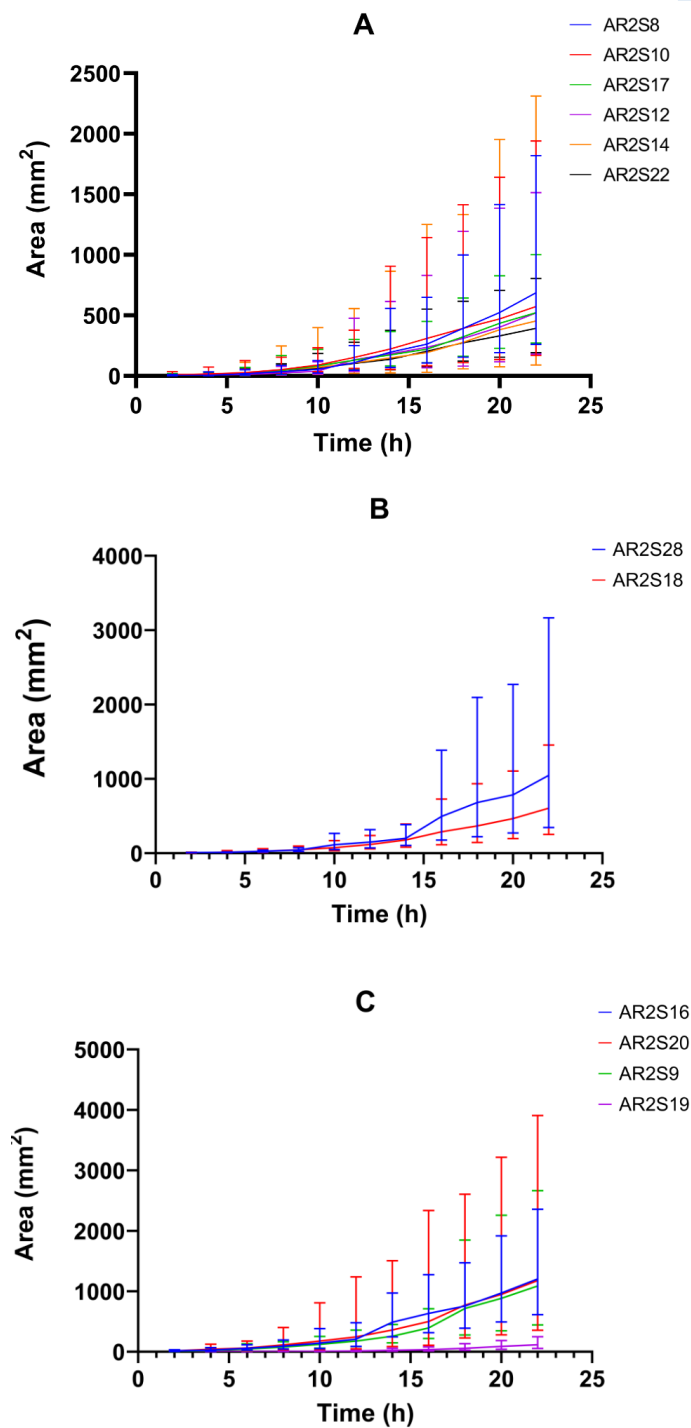


Figure 5-35 Comparison of colony spreading curves of strains isolated from blebs from an evolved parent colony

(A). Bleb isolates AR2S8, AR2S10, AR2S12, AR2S14 and AR2S17 were faster than the swimming colony parent strain AR2S22. (B) Bleb isolate AR2S18 was faster than its evolved swimming parent strain AR2S28. (C) Bleb isolates AR2S19 and AR2S9 were slower compared from the evolved swimming colony parent strain AR2S20. However, strain AR2S16 which was also obtained from a bleb from this parental strain was slightly faster than the parent AR2S20. The curves are the geomean of all replicates and the error bars represent geometric standard deviation.

5.12 Study of Single Colonies of Strain AR2S15

No mutations were found within the *nrB* gene's region studied for strain AR2S15 (Table 5-12; Table 5-14). This strain exhibited spur-swarming; however, not all replicates formed a spur simultaneously. In fact, some of them never really formed a spur so it followed a Log-Normal distribution and the geomean was necessary to construct the colony expansion curve of the strain (Figure 5-36; Figure 5-37; Appendix F: Figure F-3). The objective of studying a single colony (section 2.10) was to determine whether the spur development was genetically regulated or a consequence of a random mutational event within the swimming population. If it was an inherited trait, all the replicates derived from an initial colony would concomitantly form a spur.

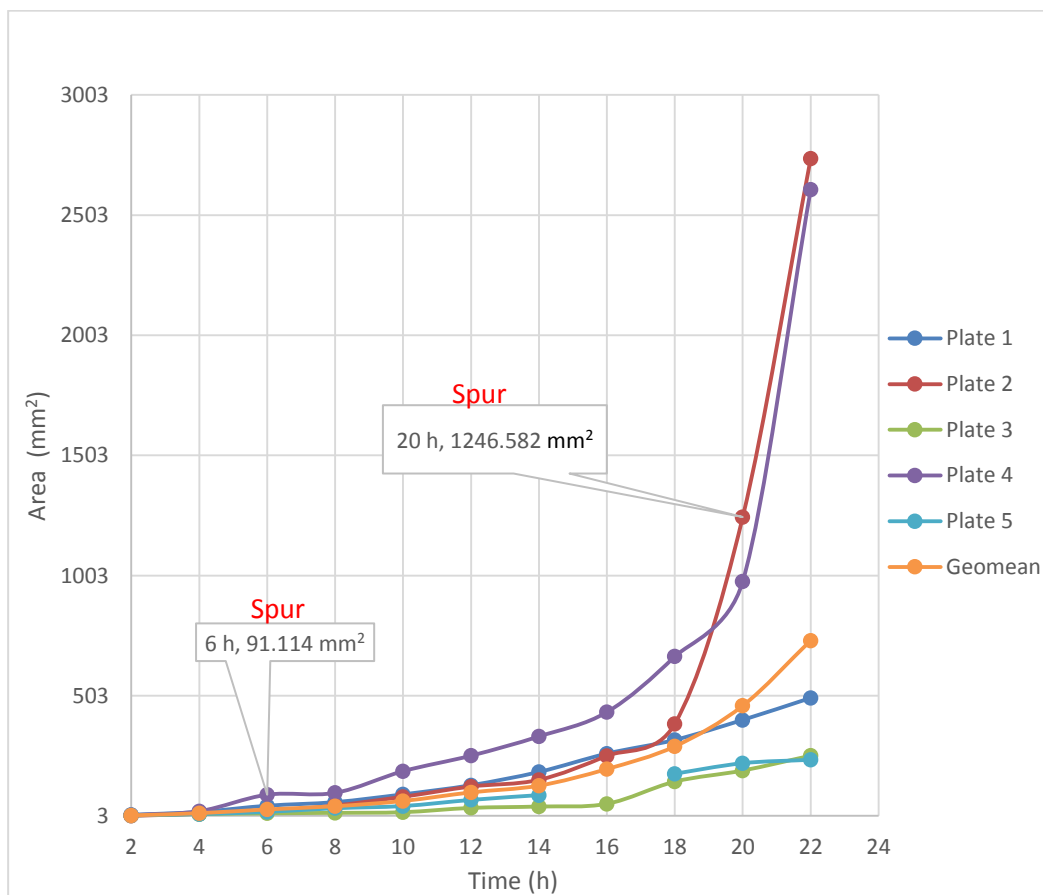


Figure 5-36 Colony expansion curve of strain AR2S15

The curves shown are for each replicate and were obtained using time-lapse photography and run concomitantly. The motility plates were done in plates of 9 cm diameter. The graph shows two populations: one faster (plates 4 and 2) than the other (plates 1, 3, and 5) due to apparition of spurs which are labeled in the curves. Geomean of all replicates is shown.

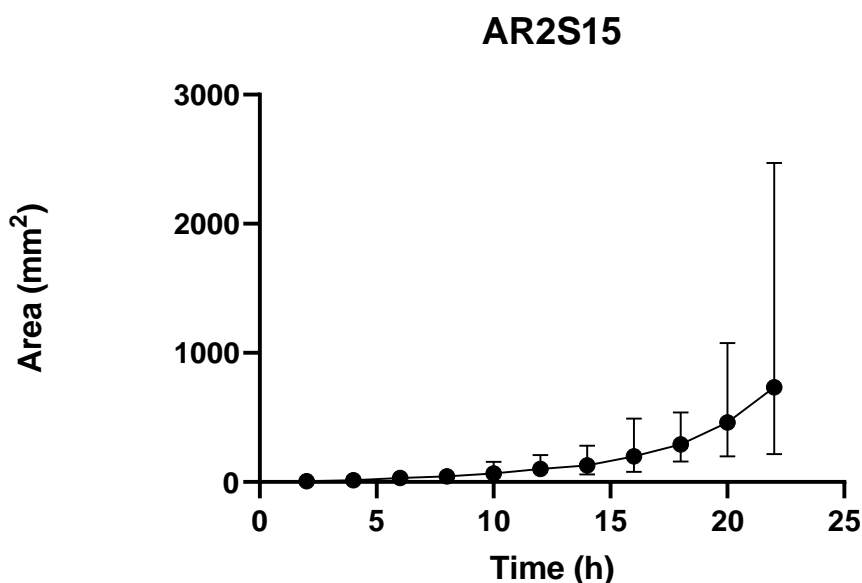


Figure 5-37 Colony expansion curve in swarming medium

The expansion curve is the geomean and the error bars represent the geometric standard deviation. Some error bars do not appear for certain points in the graph for being shorter than the size of the symbol (black dot). No antibiotic added.

Two different single colonies (A and B) were examined, using three replicates for each (Movie 26). According to the average and geomean curve constructed to represent each individual colony colony spreading (Figure 5-38A-B); the curves were not much different because of the absence of spur-swarming during the period of observation (Figure 5-38A-B). The single colonies' area at 32 h (Figure 5-38B) were not statistically significant different from each other (P -value $0.083 > 0.050$; Figure 5-39). The expansion rate for every single colony studied reflected changes between 11 h and 13 h (Figure 5-40; Figure 5-41); they also did not spur-swarm (Figure 5-42). As a result, no mixture of spur-swarmings plates with non-spur-swarming plates was observed when studying colony expansion area in motility plates (swarming medium). Then their rate of colony expansion and acceleration were also not different between both (Figure 5-40; Figure 5-41). The colony expansion curve can be constructed either using geomean or mean to represent every single colony of strain AR2S15. Notably, strain AR2S15 had a higher tendency to spur-swarm around 12 h when studying different colonies in the swarming medium. In addition, it was observed that only replicate of the single colony A formed a bleb after 76 h (Figure 5-42).

The gene *ntxB* was analysed for both single colonies A and B and was not found to reveal any mutation in the region studied (refer to Alignments in Supplementary Information). This, in turn, suggested that other mutations probably occurred in other regions of the genome altering their motility phenotype. Therefore, it would be interesting to choose samples from a swimming colony and compare their genome with the initial inoculum in order to determine whether the swimming disc was genetically identical to the initial inoculated population.

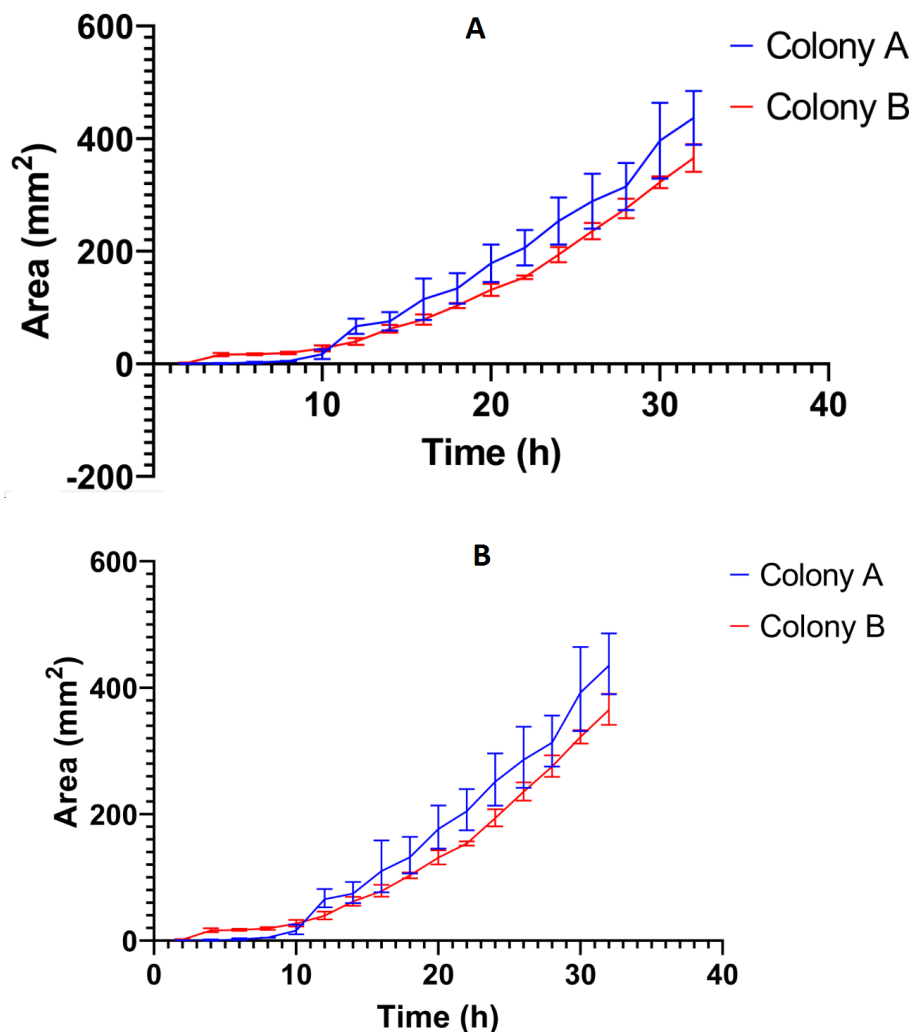
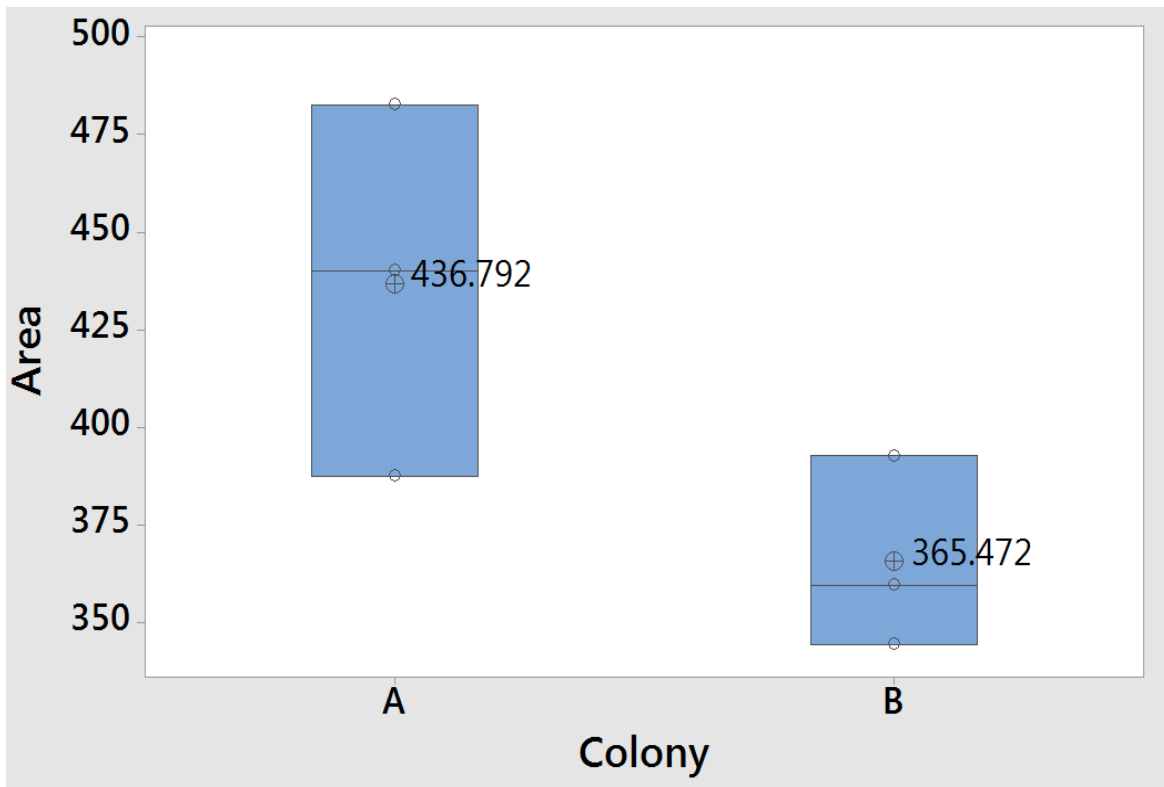


Figure 5-38 Colony expansion curves of two different single AR2S15 colonies: A and B

A single colony was picked and suspended in 9 μ l of sterile water, then 2 μ l was inoculated into the middle of an agar plate. Colony expansion curves were constructed using time-lapse photography. (A) The figure shows mean of all plates and the error bars represent the standard deviation. (B) The graph shows geomean of all replicates and the error bars represent the geometric standard deviation. No antibiotic added.



One-way ANOVA: Area versus Colony

Method

Null hypothesis All means are equal
 Alternative hypothesis Not all means are equal
 Significance level $\alpha = 0.05$

Equal variances were assumed for the analysis.

Factor Information

Factor	Levels	Values
Colony	2	A, B

Analysis of Variance

Source	DF	Seq SS	Contribution	Adj SS	Adj MS	F-Value	P-Value
Colony	1	7630	56.89%	7630	7630	5.28	0.083
Error	4	5782	43.11%	5782	1446		
Total	5	13412	100.00%				

Model Summary

S	R-sq	R-sq(adj)	PRESS	R-sq(pred)
38.0209	56.89%	46.11%	13010.3	3.00%

Means

Colony	N	Mean	StDev	95% CI
A	3	436.8	47.8	(375.8, 497.7)
B	3	365.5	24.7	(304.5, 426.4)

Pooled StDev = 38.0209

Figure 5-39 Box plot: Comparison of colony spreading area between single colonies A and B

The colony area (mm²) covered by both colonies at 32 h in the swarming medium (without antibiotic) was taken from its respective colony expansion curve (analysed data from Figure 5-38B). The one-way ANOVA is illustrated below the box plots. The replicates per colony were observed concomitantly. The time-lapse-photography method was used for evaluating the motility plates (9 cm diameter, swarming medium).

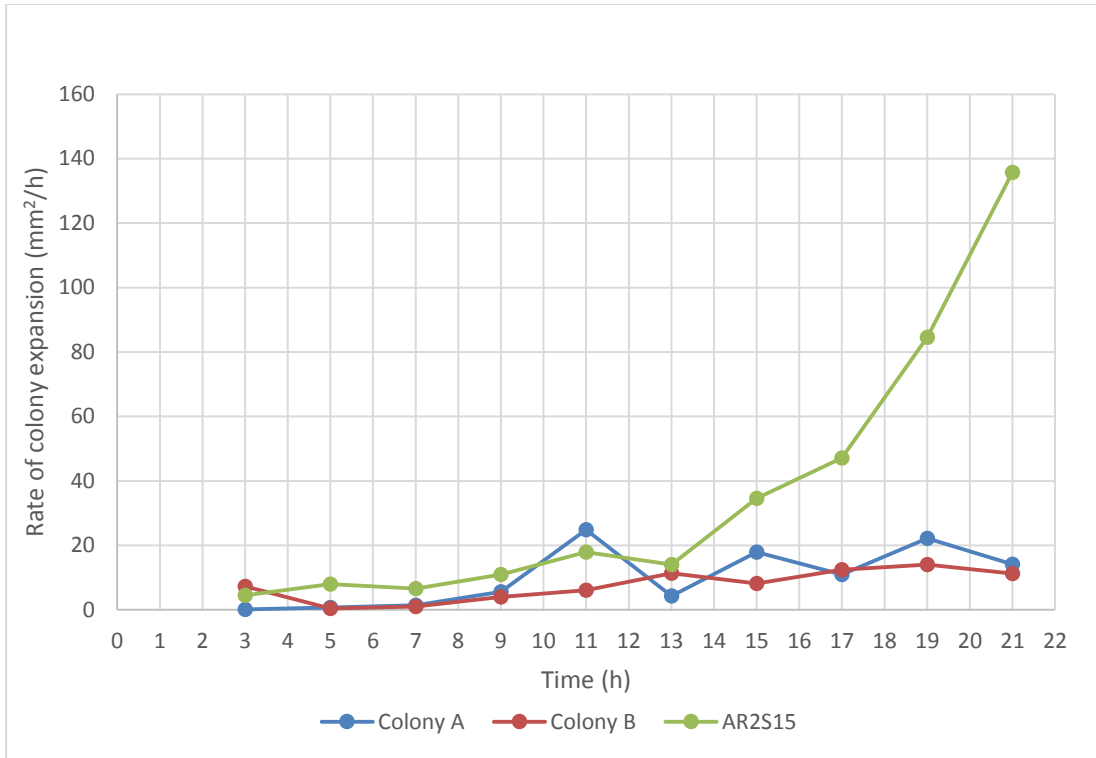


Figure 5-40 Comparison of rate of colony expansion changes in single colonies of AR2S15 with the rate of colony expansion changes of strain AR2S15

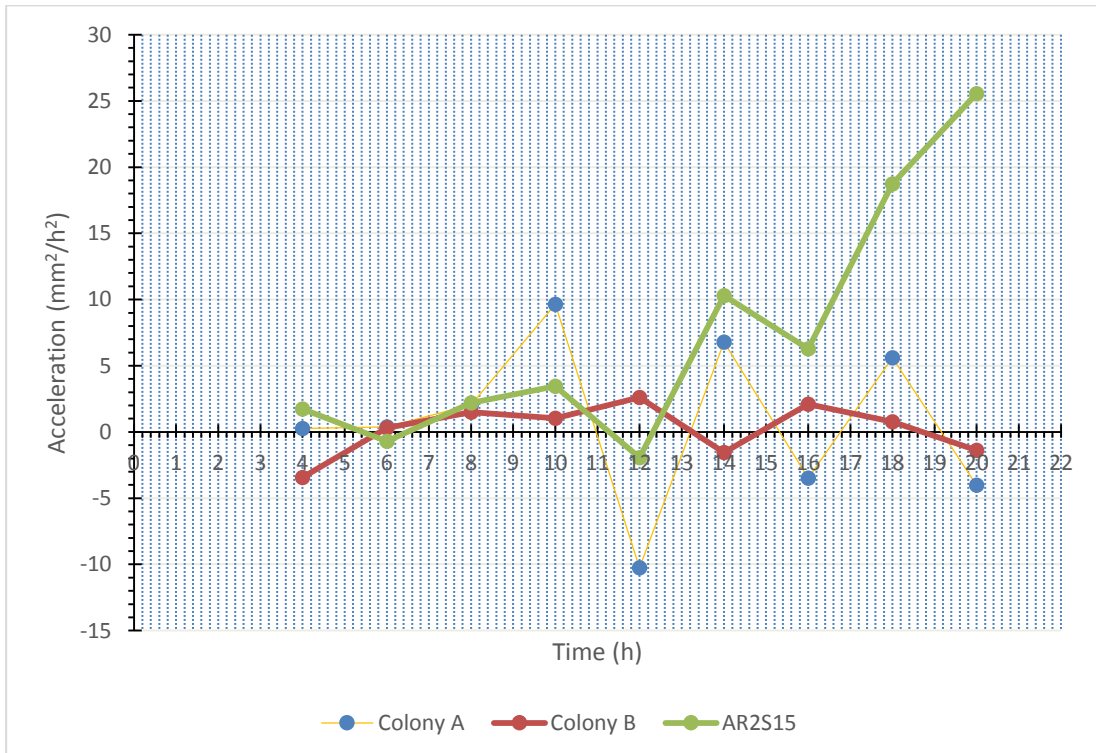


Figure 5-41 Comparison of acceleration changes in single colonies of AR2S15 with acceleration changes of strain AR2S15

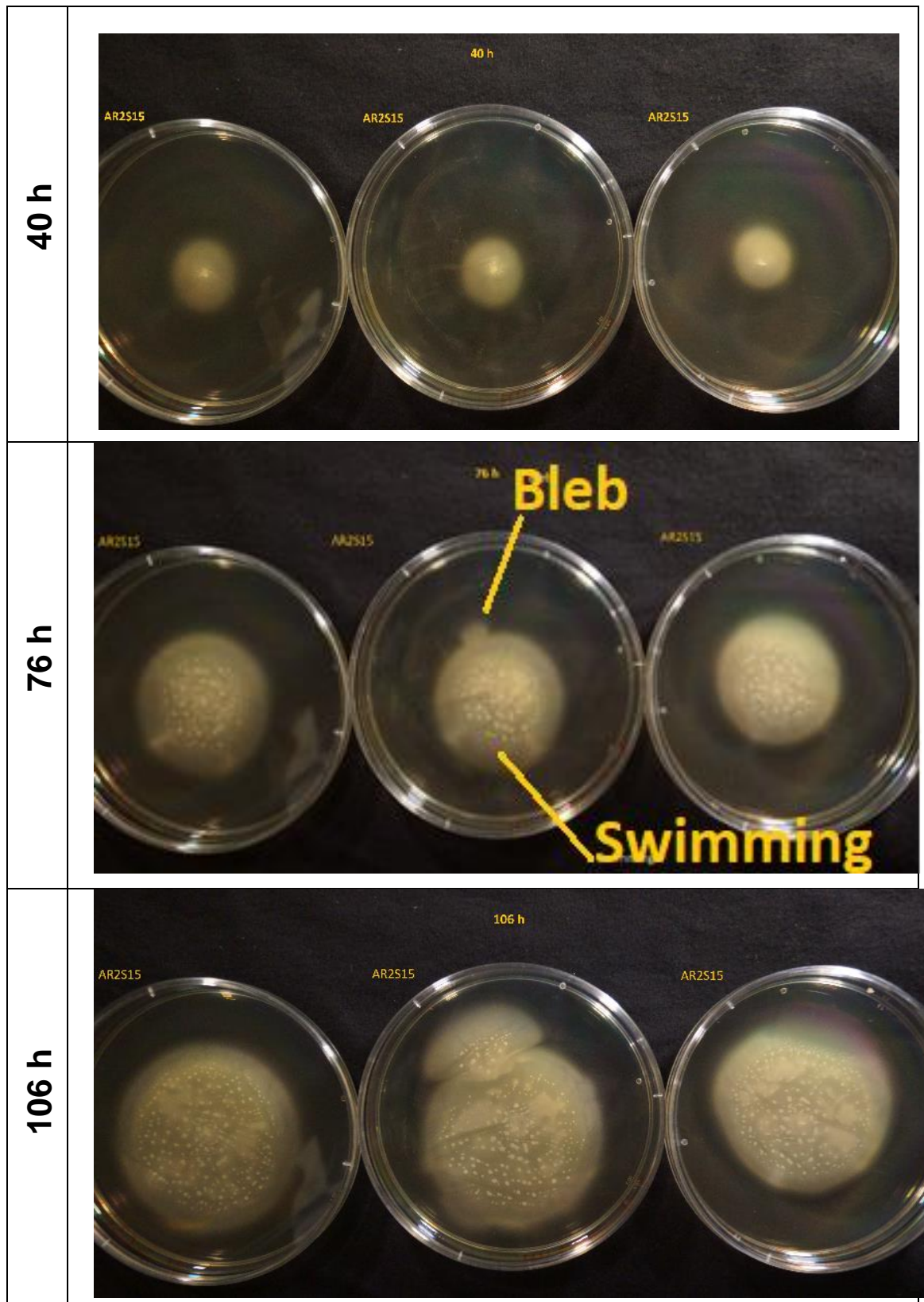


Figure 5-42 Single AR2S15 colony A at different time points

These replicates were used to obtain the colony expansion curve by time-lapse photography method. Plates 9 cm diameter.

5.13 Summary of Evolution of Swimming Motility in Sessile Strains AR1 and AR2

No significant statistical differences were observed (P -value $0.902 > 0.050$; Table 5-16) in the evolution time of swimming motility for the both sessile strains; however, statistical significant differences were found (P -value $0.000 < 0.050$; Table 5-16) among the evolution time under varying nitrogen sources. For this reason, the probability of selection and observing swimming motility evolution is strain independent, but it is nitrogen source dependent. Also, their swimming colony showed the same phenotype (rounded), with white gradually becoming yellow. They evolved the swimming motility later in rich nitrogen source (NH_4^+) (mean = 5.53 days, $SD = 0.61$ days; for AR2) than in poor nitrogen sources (glutamine or glutamate): mean = 2.94 days ($SD = 0.80$ days; for AR2) in glutamate, and in glutamine mean = 2.88 days ($SD = 0.89$ days; for AR2). Strain AR1 was selected and observed swimming motility evolution later in NH_4^+ mean = 5.79 days ($SD = 0.54$ days), and earlier both in glutamine mean = 3.55 days ($SD = 2.06$ days) and glutamate mean = 3.29 days ($SD = 0.77$ days). No significant statistical differences (P -value $0.304 > 0.050$; Table 5-17) were observed between the evolution time among poor nitrogen sources (glutamine or glutamate) with glucose as the carbon source in both these sessile strains. Six AR1S strains evolved from AR1, whereas 32 AR2S strains evolved from AR2. No significant statistical differences were found (P -value $0.362 > 0.050$; Table 5-18) over time to evolve the swimming motility in both the sessile strains AR1/AR2 with glutamine and sucrose being used as nitrogen and carbon sources, respectively. Furthermore, no significant statistical differences (P -value $0.356 > 0.050$; Table 5-18) were found over time to observe the evolved swimming colonies in glutamine as nitrogen source with either source of carbon (glucose or sucrose) in both these sessile strains. For this reason, the probability of selection and observing swimming motility is both nitrogen dependent and strain independent.

The observed evolved colonies under different nitrogen/carbon treatments in minimal medium M9 never formed a spur or swarmed. The evolved colonies eventually formed blebs. These blebs are satellite evolved populations from the main swimming colony; they are separated from the swimming disc (through the agar). However, there was a type of blebbling known as cake as the evolved

colonies split in the main swimming colony, akin to slices. It is important to mention that the evolved AR1S and AR2S strains only spur-swarm in rich medium 0.25 % agar LA (swarming medium), and rarely formed blebs. Also, it must be mentioned that not all replicates spur-swarmed; the timing of apparition of the spur was variable. Sometimes, the spur appeared at 4 h and slid slowly on the agar surface for 12 h before it swarmed. The colony expansion curves for the data set of AR1S/AR2S followed a Log-Normal distribution due to this variability.

Finally, the *ntrB* gene mutation was the primarily pathway for the evolution of swimming motility in KO *fleQ* background, irrespective of medium or strain. The second mutational event in *ntrC* gene was never observed in any of the evolved strains AR1S or AR2S, which are non-viscosin producers. However, this mutation was only observed in strain FleQS7W (*ntrB ntrC*; viscosin producer), which then evolved from strain FleQS7 (*ntrB*), which is going to be discussed in Chapter 6.

Table 5-16 ANOVA for Sessile Strains: Days to evolve swimming motility with different nitrogen/glucose sources

General Linear Model:						
Factor Information						
Factor	Type	Levels	Values			
Strain	fixed	2	AR1, AR2			
Source Nitrogen	fixed	3	E, NH ₄ ⁺ , Q			
Analysis of Variance for Days to Evolve Swimming Motility, using Adjusted SS for Test						
Source	Df	Seq SS	Adj SS	Adj MS	F-value	P-value
Strain	1	0.016	0.069	0.069	0.02	0.902
Source Nitrogen	2	127.875	127.875	63.937	14.14	0.000
Error	105	474.824	474.824	4.522		
Total	108	602.716				
Model Summary						
S	R-sq	R-sq(adj)				
2.12653	21.22%	18.97%				

Note: E: glutamate. Q: glutamine. NH₄⁺: ammonium.

Table 5-17 ANOVA for Sessile Strains: Days to evolve swimming motility with poor nitrogen sources and glucose as carbon source

General Linear Model						
Factor Information						
Factor	Type	Levels	Values			
Strain	fixed	2	AR1, AR2			
Source Nitrogen	fixed	2	E, Q			
Analysis of Variance for Days to Evolve Swimming Motility, using Adjusted SS for Tests						
Source	Df	Seq SS	Adj SS	Adj MS	F-value	P-value
Strain	1	0.026	0.073	0.073	0.01	0.918
Source Nitrogen	1	7.284	7.284	7.284	1.07	0.304
Error	68	462.267	462.267	6.798		
Total	70	469.577				
Model Summary						
S	R-sq	R-sq(adj)				
2.60731	1.56%	0.00%				

Note: E: glutamate. Q: glutamine.

Table 5-18 ANOVA for Sessile Strains: Days to evolve swimming motility with different carbon sources

General Linear Model						
Factor Information						
Factor	Type	Levels	Values			
Strain	fixed	2	AR1, AR2			
Sugar	fixed	2	Glucose, Sucrose			
Analysis of Variance for Days to Evolve Swimming Motility, using Adjusted SS for Tests						
Source	Df	Seq SS	Adj SS	Adj MS	F-value	P-value
Strain	1	11.92	11.11	11.11	0.85	0.362
Sugar	1	11.38	11.38	11.38	0.87	0.356
Error	46	602.62	602.62	13.10		
Total	48	625.92				
Model Summary						
S	R-sq	R-sq(adj)				
3.61946	3.72%	0.00%				

Note: glutamine was the nitrogen source.

6 Whole Genome Sequencing of Evolved Strains FleQS and AR2S

6.1 Introduction

In Chapters 4 and 5, the evolution of swimming motility was studied and swimming mutants selected following growth with either a poor N- source (glutamine or glutamate) or a rich N-source (ammonium). In all three parent strains, SBW25 Δ *fleQ*, AR1 and AR2, used in the evolution studies, the *fleQ* gene encoding the master regulator of flagella expression had been deleted resulting in an aflagellate phenotype and the absence of swimming motility. In accord with a previous study¹⁰⁸, it was predicted that evolved swimming mutants would be likely to have a mutation in a component of the Ntr system or possibly an alternate bEBP with homology to FleQ and NtrC. For this reason, initially for all evolved FleQS, AR1S and AR2S mutants, target segments of *ntrB* (encoding residues 35 -175) and *ntrC* (DNA binding segment, residues 350-455) and the entire *glnK* gene were amplified and sequenced by Sanger sequencing. A mutation in NtrB, T97P, was identified in most but not all strains. No other mutation was identified (see Table 6-1 for properties of mutants and summary of mutations identified by PCR). The purpose of whole genome sequencing was to identify if mutations were present in other segments of *ntrB*, *ntrC* or in any other genes relating to the Ntr system e.g. *glnA* (encoding glutamine synthetase), in a related bEBP or in any other gene that might explain differences in phenotype between isolated mutants.

It was predicted that the evolution of swimming motility in aflagellate cells within starving colonies occurred when the NtrBC system was expressed at high levels and hence subject to selection. Under conditions of nitrogen starvation nitrogen assimilation proceeds via the GS/GOGAT [glutamine synthetase (GS)/glutamate synthase (GOGAT)] pathway¹³³. NtrB phosphorylates and activates NtrC, in response to the C/N status of the cell, reflected in the 2-OG/glutamine ratio. NtrC-P in turn upregulates transcription of the *glnAntrBC* operon. Consequently mutations in *glnAntrBC* are expressed and subject to natural selection by environmental pressures. In this case, it is assumed that nutrient deprivation is the selecting pressure for evolved swimmers. It is also possible that other pressures

e.g. pH stress might also lead to selection of different genes. In addition, unrelated mutations are likely to happen and may be co-selected. In this Chapter, the genome of all nine of the FleQS mutants and two selected AR2S mutants, were sent for Illumina whole genome sequencing, in order to identify any additional mutations.

6.2 Whole Genome Sequencing Results

6.2.1 Parent strains AR2 and SBW25 Δ fleQ

Genome sequences of the two parent strains, SBW25 Δ fleQ and AR2, were used for comparison with the mutants. To ensure that the SBW25 Δ fleQ culture from which genomic DNA was prepared had not evolved swimming randomly during the 24 h incubation period in LB medium, multiple individual colonies isolated from the 24 h culture (used for genomic DNA isolation) were spotted on swarming agar and monitored for 24 h. Only spidery spreading was evident, there was no indication of swimming motility. The same was done for the 24 h culture of AR2 from which the genomic DNA was prepared. This time the typical AR2 growing colonies with no motility at all were noted (Figure 6-1). This screen of sample cells from the population used for WGS, confirmed the absence of evolution to swimming during growth for genomic DNA preparation. The WGS data (Table 6-1; Table 6-2 and also Variant Calling Data in Supplementary Information) was therefore valid to use for comparison with the mutant strain to identify any additional mutations that might influence the motility phenotype.

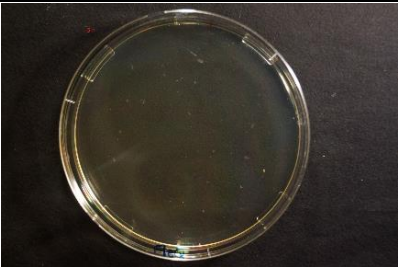
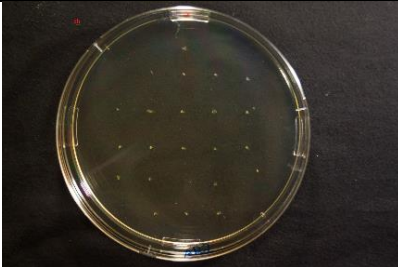
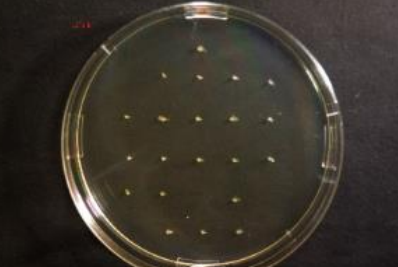
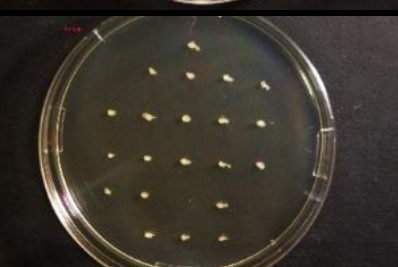
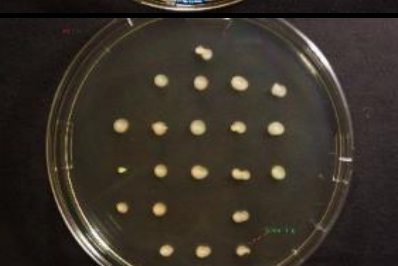
Time (h)	SBW25 Δ <i>fleQ</i>	AR2	Time (h)
5			5
13.26			12.3
19.46			24.8
22.66			45

Figure 6-1 Strain SBW25 Δ *fleQ* and AR2 grown on swarming medium

Broth growth used for whole genomic DNA sequencing was streaked onto LA medium with 1.5 % agar (propagation medium), and multiple colonies were individually inoculated onto a single 15 cm diameter motility plate (0.25 % agar LA medium without antibiotic) and incubated for 24 h. Strain SBW25 Δ *fleQ*: spidery-spreading phenotype (*Fla*⁻, *Visc*⁺). Spidery-Spreading colonies only, with no swarming or swimming were visible; (Movie 13). Strain AR2: Sessile phenotype (*Fla*⁻, *Visc*⁻). Colonies growth only was visible with no evolved swimming; (Movie 14).

6.2.2 Evolved strains FleQS and AR2S: nitrogen related mutations

Genomic DNA preparations of all FleQS mutants and two selected AR2 mutants were similarly prepared and sent for sequencing (see section 2.12 for details). Sequence data for each mutant was compared to sequences from each respective

parent. The data for the entire *ntrB* and *ntrC* genes is listed in Table 6-2. Complete comparison is available under 'Variant Calling Data' in Supplementary Information. The data shows that all of the evolved strains had mutated within the two component NtrBC system.

It is interesting to note that virtually all the evolved strains had a mutation in NtrB at T97P (7 of 9 FleQS and one of the two AR2S strains sequenced, AR2S15). Both strains for which no mutations were identified by Sanger sequencing were shown to have a missense mutation corresponding to NtrB D228, either D228N (FleQS7) or D228A (AR2S15). When the target region of the *ntrB* gene¹⁰⁸ was studied using PCR, strain FleQS5 (Chapter 5 and Appendix N: Figure N-4) appeared to be wild type with respect to this region of *ntrB*, however WGS identified a A289C (T97P) mutation within *ntrB*. Therefore it was hypothesized that this anomaly might be explained by a mixture of mutants present within the glycerol stock for FleQS5, despite this being made from a single colony. Alternately some bacteria might have evolved during broth growth (Movie 21). To address this, genomic DNA was also obtained from a loopful of plate growth culture (many different colonies) directly cultured from the -80 °C stock. The WGS data for FleQS5, obtained from the plate extracted DNA (Appendix Y: Table Y-1b), identified the presence of two different single point mutations: T97P and D228G. The T97P mutation is encoded in a region of the gene which was identified by the PCR primers, but the D228 codon was not. Therefore it was concluded that the glycerol stock for FleQS5 contains a mixed population of mutants, one with the T97P and another with only D228G mutation.

Hence, when WGS results of FleQS mutants are combined with the targeted sequencing of AR1 and 2 mutants (Chapter 5), it was identified that all recovered swimming mutants had a mutation in *ntrB* (9 FleQS mutants, 6 AR1S and 32 AR2S) and that 95.7 percent of these encoded T97P. Only three strains, FleQS7, AR2S15 and apparently also a strain within the FleQS5 glycerol stock encoded only an NtrB D228A/N/G mutation. Both of these mutations had been previously identified in evolved swimming mutants in the study of evolution in rich medium by Taylor et al.¹⁰⁸ T97 lies towards the end of PAS domain and D228 between the histidine kinase domain (HisKA) and ATPase domains (HATPase_c) (Figure 1-41). Both of these mutations are considered likely to enhance kinase activity or reduce phosphatase activity of NtrC and hence lead to higher levels of phosphorylated

NtrC^{108,312}. Transcriptome analysis has identified activation of expression of the flagellar regulon as well as overactivation of the Ntr regulon in the previously identified ARS T97P mutant¹⁰⁸.

Growth studies in LB, and M9 broth cultures, had identified a profound fitness cost of the NtrB mutation, particularly in M9-glucose with ammonium as N source (Chapter 4: Figure 4-19 and Figure 4-21). Taylor et al.¹⁰⁸ had also recorded this impact on growth of the AR2S mutant (see also Chapter 3, Figure 3-16) and hypothesized that subsequent appearance of the AR2F evolved mutant compensated for this with a mutation in the HTH DNA binding domain of NtrC. In this study, the *ntrC* sequence was wild-type ie identical to the parent SBW25 Δ *fleQ* strain for all FleQS mutants and both AR2 mutants subjected to WGS. All FleQS mutants had been picked from the swimming disc (Chapter 4). However, many of the AR1 and AR2 mutants had been picked from blebs of swimming growth on the M9-glucose agar with ammonium, glutamine or glutamate as N source (Chapter 5: Figure 5-35 and Table 5-12). Bleb formation on LB swarming medium had been assumed to correlate with faster swimming and was the source of the published AR2F mutants carrying NtrC mutations¹⁰⁸. None of the AR1 or AR2 mutants, isolated in this study carried a mutation in the HTH motif of NtrC (Chapter 5).

It was hypothesized that the unusual spur formation of AR2S mutants and the spidery-swarming phenotypes of FleQS mutants on rich swarming media, observed in this study, might be the result of a mutation in *ntrC*, and that the initial slow swimming colonies (*ntrB*) had acquired a second mutation to become double mutants (*ntrB ntrC*). To test this hypothesis, spur and spidery extension colonies, together with their respective swimming disc colonies of ARS20 and FleQS7, respectively, were isolated from swarming medium for WGS (see Figure 6-2). As anticipated, the initial *ntrB* mutation encoding T97P was identified in genomic DNA of cells isolated from the disc swimming area (FleQS7D) with no other mutation in the Ntr system. Isolates from the spidery swarming area (FleQS7W, Movie 22) possessed a mutation in *ntrC*, in addition to the *ntrB* mutation (Table 6-1, Table 6-2, Table 6-3). However, this mutation was not in the HTH motif but corresponded to position S171P NtrC, within the σ^{54} factor interaction domain. Thus, this mutation could also moderate the fitness cost of the NtrB mutation by decreasing the efficiency of σ^{54} interaction and hence initiation of NtrC activated transcription. Thus,

it may be that the spidery-swarming phenotype observed in the evolved FleQS strains on swarming media (Appendix N: Figures N-1 to N-6) required this or another mutation in *ntrC* to permit faster spidery-swarming spreading and access to more favorable environments. In this study there was no indication of this secondary mutation in isolates on M9 medium.

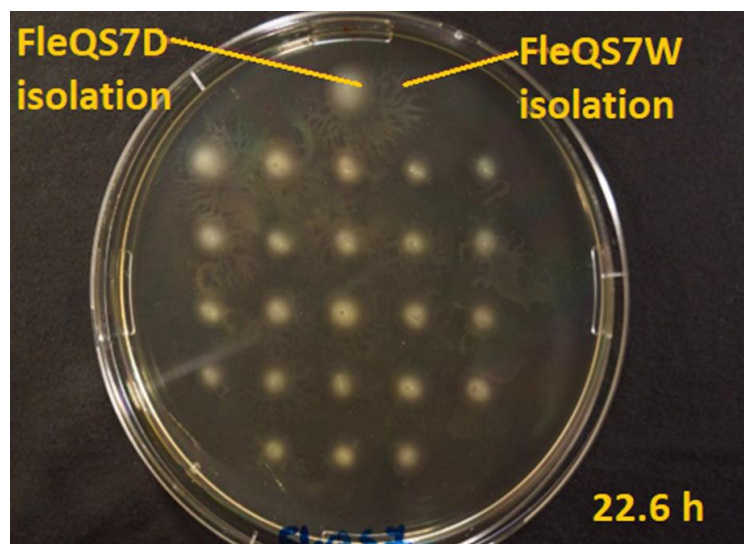


Figure 6-2 Origin of strains FleQSD and FleQS7W

Broth growth used for whole genomic DNA sequencing was streaked onto LA medium with 1.5 % agar (propagation medium), and multiple colonies were inoculated onto a single 15 cm diameter motility plate (0.25 % agar LA medium). A spidery-extension colony was isolated and named FleQS7W, and a sample from the swimming colony from which this spidery-extension had evolved was also isolated and named FleQSD.

Strain AR2S15 (Movie14 and Movie 15) was documented as a slow swimmer (7.5 mm²/h; mean) and was found to possess a mutation in the *ntrB* gene at position D228, close to the ATPase domain (HATPase_c). In contrast, strain AR2S20 was recorded as having faster swimming dependant colony expansion (mean = 20.1 mm²/h) and a mutation in the PAS domain of *ntrB* at T97P was identified (Movie 16). The difference in NtrB mutation cannot alone explain a difference in swimming expansion as many other isolates with the same NtrB T97P mutation migrated much more slowly. Interestingly, the mutant strain AR2S20 was recorded as having faster swimming dependant colony expansion than most other evolved AR2S strains, including isolates from blebs on the same replica plate (Table 5-13). For this reason, genomic sequences were also analysed from isolates obtained from the swimming disc (ARS20D) and the spur formation (AR20SW) of this strain. Surprisingly, no additional mutation of the Ntr system was identified in the genome of a spur isolate,

AR20SW (Table 6-2, see also Variant Calling in Supplementary Information and Appendix N: Figures N-7 to N-8). Only the original NtrB T97P mutation was present. However, the disc isolated strain (ARS20D) contained the deletion TRALR271 within NtrB, in addition to the T97P mutation present in this parent ARS20.

It is interesting to note that all the evolved strains mutated with a high frequency in NtrB at T97P, and rarely at D228N, D228A, or the deletion at TRALR271. There appeared to be no strict relationship between the nitrogen source and the evolved mutation in NtrB (Table 6-1, Table 6-2, Table 6-3), but there were too few isolates with the D228 mutation to establish if there was any trend.

The evolved strains FleQS1, FleQS2 and FleQS3 (Movies 18-20) were found to possess the same mutation in the *ntrB* gene (A289C; T97P) within the PAS domain region of the NtrB protein and no other identified difference (see also Variant Calling in Supplementary Information). These strains were isolated from different replica plates, but all had evolved during growth on the same nitrogen source (ammonium) with glucose as carbon source. Strains FleQS1, FleQS2 and FleQS3 did not demonstrate any remarkable differences in their colony or growth phenotype (Table 4-9 and Appendix N: Figures N-1 to N-3), and all exhibited either spidery-swarming or wild-type swarming around the same time (32 h), see Movies 18-20 in Supplementary Information. This is consistent with the NtrB T97P mutation being highly favourable, with a high probability of being selected during growth and recovery as an evolved swimming mutant.

Taylor et al.¹⁰⁸ did not investigate the evolutionary pressures that led to the observation of evolved swimmers derived from sessile parent strains. This research demonstrates that while poor nitrogen sources (glutamine and glutamate) lead to a more rapid identification of evolved swimmers via mutations in the NtrBC system, the same primary pathway of evolution, mutation in NtrB, is identified irrespective of the nitrogen source in M9 medium. No mutation in other components of the Ntr system e.g. in glutamine synthetase (*glnA*) or in PII (*glnK*) were identified from growth on M9 medium in this study. Interesting, no other bEBP was identified that might preferentially replace FleQ, despite the high fitness cost of mutation on NtrB.

Table 6-1 Phenotype and history of the strains

Strain	Isolated from	Phenotype on motility plates	Observation	*PCR results		Relevant Publication
				NtrB	NtrC	
SBW25	Leaf surface of sugar beet	WT (swimming, swarming)	Swarming at 12.3 h (<i>SE</i> = 1.3 h)			38,143
SBW25Δ<i>fleQ</i>	Genetically engineered	Spidery-Spreading (<i>Fla</i> ⁺ , <i>Visc</i> ⁺)	Spidery at 13.7 h (<i>SE</i> = 0.6 h)	WT	WT	107, 109
FleQS1	M9 NH ₄ ⁺ glucose	Fast swimmer	Wild-Swarming	T97P	WT	
FleQS2	M9 NH ₄ ⁺ glucose	Fast swimmer	Spidery-Swarming	T97P	WT	
FleQS3	M9 NH ₄ ⁺ glucose	Fast swimmer	Spidery-Swarming	T97P	WT	
FleQS4	M9 NH ₄ ⁺ glucose	Slow swimmer	Spidery/Wild swarming	T97P	WT	
FleQS5	M9 NH ₄ ⁺ glucose	Medium swimmer	Spidery-Swarming	WT	WT	
FleQS6	M9 NH ₄ ⁺ glucose	Slow swimmer	Wild-Swarming	T97P	WT	
FleQS7	M9 glutamate glucose	Slow swimmer; spidery-swarming	Spidery-Swarming	WT	WT	
FleQS7D	Isolated from swimming colony of FleQS7 in 0.25 % agar LA.	To be determined				
FleQS7W	Isolated from spidery-extension of swimming colony of FleQS7 in 0.25% agar LA	To be determined				
FleQS8	M9 glutamate glucose	Medium swimmer; spidery-swarming		T97P	WT	
FleQS9	M9 glutamine glucose	Fast swimmer; spidery-swarming	Switch between spidery-spreading and swimming	T97P	WT	
AR2	Transposon mutagenesis of SBW25Δ <i>fleQ</i>	Sessile (<i>Fla</i> ⁻ , <i>Visc</i> ⁻)		WT	WT	107,108
AR2S15	M9 glutamine glucose kanamycin	Slow swimmer	Spur-Swarming	WT	WT	
AR2S20	M9 glutamine glucose kanamycin	Fast swimmer	Spur-Swarming	T97P	WT	
AR2S20D	Isolated from swimming colony of AR2S20 in 0.25 % agar LA.	To be determined				
AR2S20W	Isolated from spur of AR2S20 in 0.25 % agar LA.	To be determined	Spur evolved after 8.3 h, but isolated after 131 h			

Note: *Amplicons for *ntrB* and *ntrC* cover only part of the gene. No mutation was found in *glnK* gene, where the amplicon covered the entire gene

Table 6-2 Whole genome sequencing results for evolved strains and their parent strains

Strain	WGS				Other unique mutations
	<i>fleQ</i>	<i>visc</i>	NtrB ^C	NtrC ^C	
SBW25	WT	WT	WT	WT	
SBW25Δ<i>fleQ</i>	Δ <i>fleQ</i>	WT	WT	WT	
FleQS1	Δ <i>fleQ</i>	WT	T97P	WT	
FleQS2	Δ <i>fleQ</i>	WT	T97P	WT	
FleQS3	Δ <i>fleQ</i>	WT	T97P	WT	
FleQS4	Δ <i>fleQ</i>	WT	T97P	WT	PFLU_RS08590 A128T PFLU_RS16245 A45V
FleQS5^a	Δ <i>fleQ</i>	WT	T97P	WT	A1754245G, <i>fusA</i> I61V,
FleQS5^b	Δ <i>fleQ</i>	WT	*T97P/D228G	WT	*PFLU_RS20605 S459A/R456K, <i>fusA</i> I61V, <i>algP1</i> V300A
FleQS6	Δ <i>fleQ</i>	WT	T97P	WT	<i>algP1</i> A282 (silent)
FleQS7	Δ <i>fleQ</i>	WT	D228N	WT	A3694384G
FleQS7D	Δ <i>fleQ</i>	WT	D228N	WT	A3694384G
FleQS7W	Δ <i>fleQ</i>	WT	D228N	S171P	
FleQS8	Δ <i>fleQ</i>	WT	T97P	WT	<i>algP1</i> S337T
FleQS9	Δ <i>fleQ</i>	WT	T97P	WT	G3311139A (PFLU_RS14795 A48 silent)
AR2	Δ <i>fleQ</i>	<i>viscB</i> ::Tn	WT	WT	
AR2S15^a	Δ <i>fleQ</i>	<i>viscB</i> ::Tn	D228A	WT	G3694159T, A3694384G
AR2S15^b	Δ <i>fleQ</i>	<i>viscB</i> ::Tn	D228A	WT	G3694159T, C3694186A, A3694384G, T5718018C
AR2S20	Δ <i>fleQ</i>	<i>viscB</i> ::Tn	T97P	WT	G3694159T, C3694186A, T5718018C
AR2S20D	Δ <i>fleQ</i>	<i>viscB</i> ::Tn	T97P, TRALR271 (deletion)	WT	
AR2S20W	Δ <i>fleQ</i>	<i>viscB</i> ::Tn	T97P	WT	G3694159T, G3694377T, A3694384G

Note: ^aGenomic DNA extracted from LB broth growth (no antibiotic). ^bGenomic DNA extracted from LA plate (no antibiotic) growth (many colonies). ^cAmino acid change position in the gene products.*Different SNPs within the same gene (Table Y-1b). Assembly quality visualisation for each strain is shown in Appendix W. FleQS7D and FleQS7W: 18.3 h on plate before isolation. AR2S20D and AR2S20W: 131 h (5.5 days) on plate before isolation. D: swimming disc. W: swarming/spur.

Table 6-3 Whole genome sequencing results for selected evolved strains

Other Unique Mutations	Strains
^d PFLU_RS08590 (A128T missense) ^e PFLU_RS16245 (A45V missense)	FleQS4
A1754245G	FleQS5 ^a
<i>fusA</i> * (I61V)	FleQS5 ^a
A3694384G	FleQS7 ^a , FleQS7D ^a , AR2S15 ^a , AR2S15^b AR2S20W _a
G3311139A (PFLU_RS14795 A48 silent)	FleQS9 ^a
G3694159T	AR2S15 ^a , AR2S15^b , AR2S20, AR2S20W,
C3694186A	AR2S15^b , ^a AR2S20,
T5718018C	AR2S15^b , ^a AR2S20
G3694377T	AR2S20WG
PFLU_RS20605 ^c (S459A missense)	FleQS5^b
PFLU_RS20605 ^c (R456K missense)	FleQS5^b
<i>algP1</i> (S337T missense)	FleQS8^b
<i>algP1^c</i> (V300A missense)	FleQS5^b
<i>algP1</i> (A282 silent)	FleQS6^b

Note: ^aGenomic DNA was extracted from LB broth growth. ^bGenomic DNA was extracted from LA plate growth. ^cThis mutation was only detected in genomic DNA extracted from LA plate growth. *This mutation was observed in genomic DNA extracted from both broth and plate growth. ^dAmmonium channel: old locus tag PFLU_1747. ^eOxidoreductase or short chain dehydrogenase: old locus tag PFLU_3332.

6.2.3 Other mutations, unrelated to nitrogen assimilation pathway

The WGS results provided a general idea of how a starving population supplied with different nitrogen sources responded, and the genetic variation that arose as result of this stress (Tables 6-1 and 6-2). Mutations are random and not directed, and so it is possible to observe mutations that are not directly related to nitrogen regulation, and may be selected as a consequence of other stresses or are simply random mutations that are co-selected with the sought phenotype of swimming motility. This section describes other mutations not directly related to the Ntr regulon that were identified in the genome of one or more of these mutants. The data is summarised in Table 6-2 and Table 6-3. The apparent intergenic mutations remain to be more fully analysed.

a) ***Putative ammonia channel (PFLU_RS08590, old locus tag PFLU_1747)***

PFLU_RS08590 is annotated as a putative ammonia transport-related membrane protein (Figure 6-3), distinct from the *amtB* locus (PFLU_RS29300, old locus tag PFLU_5952) that is genetically linked to *glnK* (PFLU_5953). The encoded protein shares only 29.49 % identity with SBW25 AmtB. It is interesting that the mutated codon A128T has been identified in the PFLU_RS08590 locus in FleQS4. The growth phenotype of FleQS strains for different nitrogen sources (Table 4-10) showed that all evolved mutants grew less in ammonium and glutamate compared to the wild type strain SBW25 and parent strain SBW25 Δ *fleQ*, but generally grew well in LB and M9-glucose with glutamine as N-source. FleQS4 was an exception. It grew more poorly than all the other FleQS mutants in rich medium LB and with glutamine as N-source, but following a lag during growth on ammonium grew much better than all the other FleQS mutants (Table 4-10). This putative ammonia transport related protein is widespread both within and outwith the genus *Pseudomonas* (Appendix ZW: Figure ZW-1; Figure ZW-2), but with no close homolog in *E. coli*. Swiss-Model identified the closest homologs with solved structures as the membrane domain of an ammonia sensor transducer from a plantomycete (36.7 % identity), (Figure 6-4) and an Archaeoglobus Amt homologue. When modelled on these proteins, the mutation A128T of the encoded PFLU_RS08590 protein is outward facing in a transmembrane helix (Appendix ZW: Figure ZW-3; Figure ZW-4; Table ZW-1; Table ZW-2). However, with no published characterisation of any close homolog of PFLU_RS08590, any role in ammonia sensing/ uptake of this protein and significance of the mutation remains to be established. Whether the A128T mutation somehow contributes to poorer growth on glutamine and improved growth on ammonium could be readily investigated by directed mutagenesis. It is possible that a combination of this mutation along with a mutation in the short-chain dehydrogenase improves fitness of this strain in ammonium as nitrogen source.

gene	transporter		
PFLU_RS08590	ammonium transporter		
<i>Pseudomonas fluorescens</i> SBW25			
Accession IDs	G1G1K-2614 (Pflu216595Cyc)	Length	1209 bp / 402 aa
	PFLU1747	Map Position	[1,914,696 -> 1,915,904] (28.48 centisomes, 103°)
	C3K7K8 (UniProt)	Location	membrane
Reaction	transport of ammonium		

Summary

Derived by automated computational analysis using gene prediction method: Protein Homology.

Molecular Weight of Polypeptide: 42.23 kD (from nucleotide sequence)

Gene-Reaction Schematic

Unification Links

NCBI-Protein: WP_012723022.1
String: 216595.PFLU1747
UniProt: C3K7K8

Relationship Links

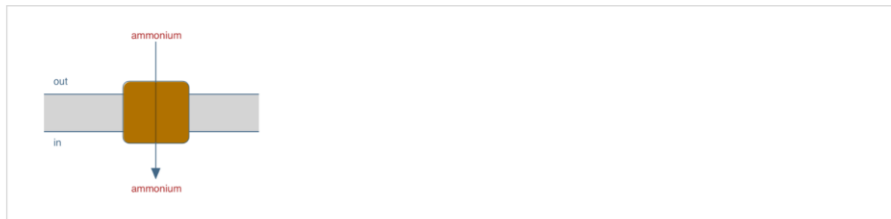
InterPro In-Family: IPR018047, IPR024041
Panther In-Family: PTHR11730
Pfam In-Family: PF00909
Prosite In-Family: PS01219

GO Terms:

Biological Process:	GO:0015696 - ammonium transport [GOA01a] GO:0072488 - ammonium transmembrane transport [GOA01a]
Molecular Function:	GO:0008519 - ammonium transmembrane transporter activity [GOA01a]
Cellular Component:	GO:0016020 - membrane [UniProtGOA11b, GOA01a] GO:0016021 - integral component of membrane [UniProtGOA11b]

Gene Class: UNCLASSIFIED

Enzymatic activity: ammonium transporter



Sequence Features

```

1  MENLQSAVDT LVHSSNTLFI LIGAVMVLAM HAGFAFLEVG TVRQKNQVNA LSKILSDFAI STLAYFFIGY WISYGVSPMQ PAAVISADHG YGLVKFFFL 100
101 TFAAAIPAI I SGGIAERARF APOLCATALI VAFIYPPFEG MVVWNGNFGLO VWLLARFGAS PHDFAGSVVV HAMGGWLALA AVLLGPRNG RYREGRLVAF 200
201 APSSIPFLAL GSWILIVGWF GFNVMSAQT L NGVSGLVAVN SLMAHVGGTV AALIIGRNDP GFLHNGPLAG LVAICAGSDL MHPVGLVTC AVAGGLFVWC 300
301 FIAAQDRWKI DDVLGVWPLH GLCGVWGGIA CGIFGQTALG GLGGVSLVSQ LIGTALGVIV ALVGGLLVYG VIKRVTGLRL SQEEEYAGD LSIHKI GAVS 400
401 Q D

```

Feature Class	Location	Citations	Comment
Pfam-PF00909	19->395	[Finn16]	Ammonium_transp : Ammonium Transporter Family [More...]

Gene Local Context (not to scale -- see Genome Browser for correct scale)



Figure 6-3 Ammonium channel PFLU_RS08590
 [Source: <https://biocyc.org>]

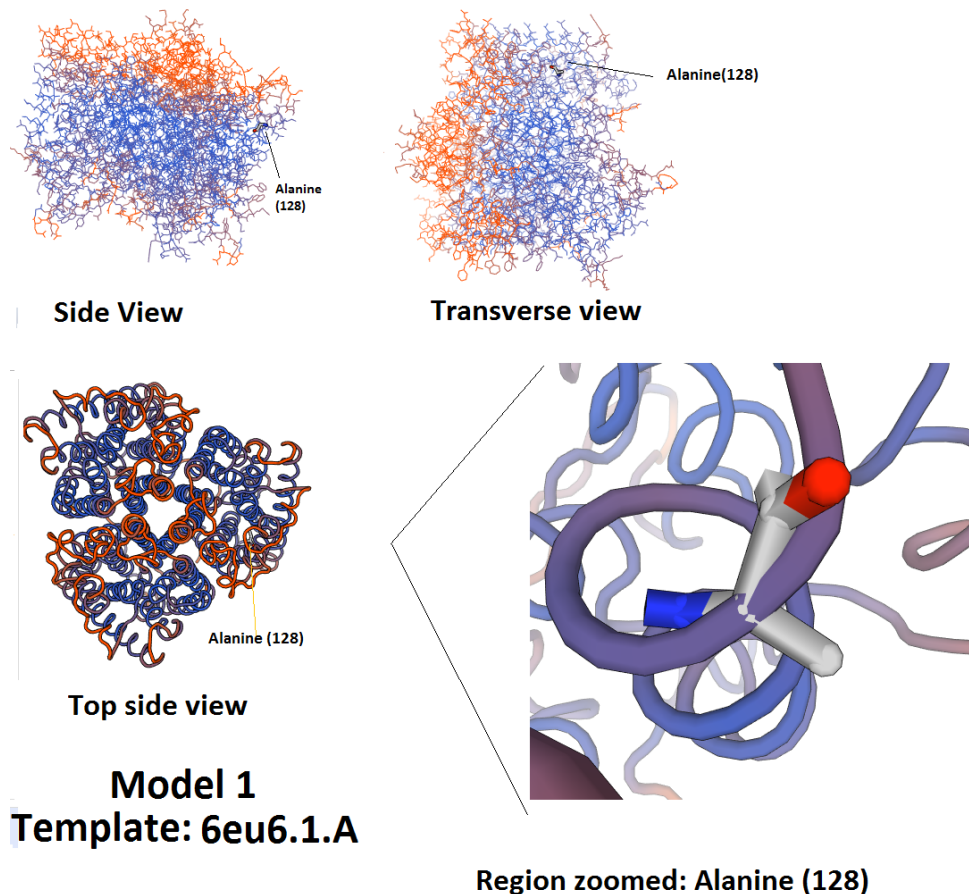


Figure 6-4 Model for ammonium channel

This model has 36.75% identity with the template and highlights the localization of alanine (128) in the ammonium channel. This residue is located in a transmembrane helix.

b) Oxidoreductase or short chain dehydrogenase (PFLU_RS16245; old locus tag PFLU_3332)

A missense mutation (encoding A45V) was identified in PFLU_RS16245 in strain FleQS4. This encodes a short-chain dehydrogenase that belongs to the Short-Chain NAD(P)(H)-dependent Dehydrogenases/Reductases (SDRs) superfamily. This enzyme contains 253 residues and is located in the cytoplasm. Enzymes of the SDR category play multiple roles in cell metabolism. They are involved in the metabolism of lipids, amino acids, carbohydrate and also are involved in redox sensor mechanisms. The enzyme (WP_012724493.1) converts glucose to D-glucono-1,5 lactone. The impact of this mutation on carbon metabolism and the carbon:nitrogen status of the cell is an avenue that could be investigated.

c) ***Fusidic acid resistance (PFLU_RS27180; old locus tag PFLU_5530)***

FleQS5 was found to have a mutation within the *fusA* gene (PFLU_RS27180) at position I61V and also within an intergenic region (A1754245G). This gene annotated as *fusA* encodes the multi-domain GTPase Elongation Factor G (EF-G) which is a target for antibiotics acting on protein translation. Hence mutations in this gene are also frequently identified as resistance markers to the antibiotic fusidic acid (see Appendix O: Figure O-7). FleQS5 was not exposed to any antibiotics, however, it is possible that this mutation somehow impacts the rate of protein translation. There was no marked difference of this mutant compared to others during growth in liquid medium (Figure 4-19), but a mutation in protein translation might compensate in some way for the dysregulation of the NtrB system.

d) ***Putative filamentous adhesin gene (PFLU_RS20605; old locus tag PFLU_4201)***

Adhesins are proteins which are present in T4P, fimbriae, filamentous hemagglutinin (FHA), and flagella. *P. fluorescens* strain TSS is a pathogen of shrimp and fish, including turbot. Sun et al.²⁰⁷ reported a mutant strain of *P. fluorescens*, strain TSS, that carries a defective *fha* gene encoding a filamentous haemagglutinin. This *fha* mutation caused low extracellular matrix production, decreased biofilm formation, did not trigger haemagglutination of red blood cells, and interestingly was reported to lead to a non-motile phenotype with no expression of flagella. FHA is an extracellular protein that is overproduced during iron starvation, and it was suggested that Fha may be somehow involved in flagella biosynthesis in *P. fluorescens* strain TSS, but this was not studied²⁰⁷. The genome of FleQS5, isolated from agar grown bacteria, but not bacteria grown in broth (Table 6-2) carried two closely linked mutations in this gene, S459A and R456K. It would be interesting to further investigate the significance of this gene product to colony spread, metabolism and root colonisation in *P. fluorescens*.

e) ***Transcriptional regulatory protein AlgP1 (PFLU_RS31200; old locus tag PFLU_5927)***

The genome of FleQS5, isolated from agar plates, also additionally contained a mutation in PFLU_RS31200 annotated as *algP1*. Interestingly, a mutation in the

same gene was also identified in the genomic DNA of FleQS6 and FleQS8, isolated from solid media, LA plates. AlgP1 (*P. fluorescens* SBW25: UniProtKB - C3K417; C3K417_PSEFS) is 408 residues long, has a molecular mass of 39419 Da and is predicted to have two coiled coil domains situated in positions 23 – 61 and 70 – 101. It is highly positive charged with an estimated isoelectric point of 11.42 (Figure 6-5 and Appendix Z: Figure Z-2). AlgP1, has the same repetitive motif Lys-Pro-Ala-Ala (KPAA) in the carboxy terminal region (Figure 6-5; Figure 6-6), as is present in AlgP from *P. aeruginosa*³¹⁴. This KPAA motif resembles the histone H1-like carboxy-terminal domain, hence the protein is also called H1³¹⁴. Studies conducted in *P. aeruginosa* have shown that AlgP and AlgQ act synergistically in order to activate *algD* gene that encodes the enzyme GDP mannose dehydrogenase³¹³. This enzyme is responsible for driving intermediate sugars towards the alginate biosynthesis pathway; hence, it is a regulatory step to trigger alginate production³¹³. AlgP and AlgQ are constitutively expressed³¹³. In *P. aeruginosa*, it is known that AlgR and AlgQ are necessary to commence AlgD expression³¹³. AlgR is homologous to NtrC, PhoB, OmpR and SpoOA. It also regulates the production of virulent determinants in plant pathogens³¹³. The *muc* loci are responsible for virulent mucoid phenotype, which overproduces alginate in *P. aeruginosa*³¹³. In addition, mutations in the *muc* loci of *P. aeruginosa* are known to upshift expression of genes *algD* and *algR*³¹³. Hence, this suggests that there probably exists a crosstalk between AlgR and other signal transduction signals³¹³.

In *Pseudomonas* spp, the transcriptional regulatory protein AlgP1 (locus tag PFLU_RS31200) is down-regulated by the ribosomal modification regulatory pathway which consists of ribosome proteins modified by the enzyme RimK. *P. fluorescens* SBW25 synthesises alginates before secreting them through the porin AlgE⁴⁴. Alginates are linear polysaccharides that comprise of two monomers: β -D-mannuronic acid (M) and α -L-guluronic acid (G) linked via 1,4-linkages. As these exopolysaccharides are not constructed out of a single monomer, and do not follow a unique sequence pattern of linked monomers, each polymer is unique and differs in the molar ratio of the constituent monomers as well as in the sequence order in which they are linked. Alginates consist of sequence blocks of α -L-guluronic acid (G block), β -D-mannuronic acid (M block), and α -L-guluronic acid bound to β -D-mannuronic acid (GM block). It has been reported that alginate production by *P.*

fluorescens grown in glucose causes acid stress owing to the production of gluconate and alginate³¹⁰. Although *P. fluorescens* SBW25 does not general produce alginate under standard laboratory conditions^{310,44}, it is possible that the *algP1* mutation in strains FleQS5, FleQS6 and FleQS8 arose as result of acid stress in the solid LA agar. However, this mutation might also possibly be linked to dysregulation of the C:N status of the bacterial cell and cross-talk between different regulators.

gene	polypeptide		
PFLU_RS31200	hypothetical protein		
<i>Pseudomonas fluorescens</i> SBW25			
Accession IDs	G1G1K-9257 (Pflu216595Cyc) PFLU_5927 C3K417 (UniProt)	Length	1227 bp / 408 aa
		Map Position	[6,485,555 <- 6,486,781] (96.47 centisomes, 347°)

Summary	Unification Links
Derived by automated computational analysis using gene prediction method: Protein Homology.	NCBI-Protein WP_015886485.1
Molecular Weight of Polypeptide 39.419 kD (from nucleotide sequence)	UniProt C3K417
	UniProt-via-RefSeq WP_015886485.1

Gene Local Context (not to scale -- see Genome Browser for correct scale) ?



Transcription Unit

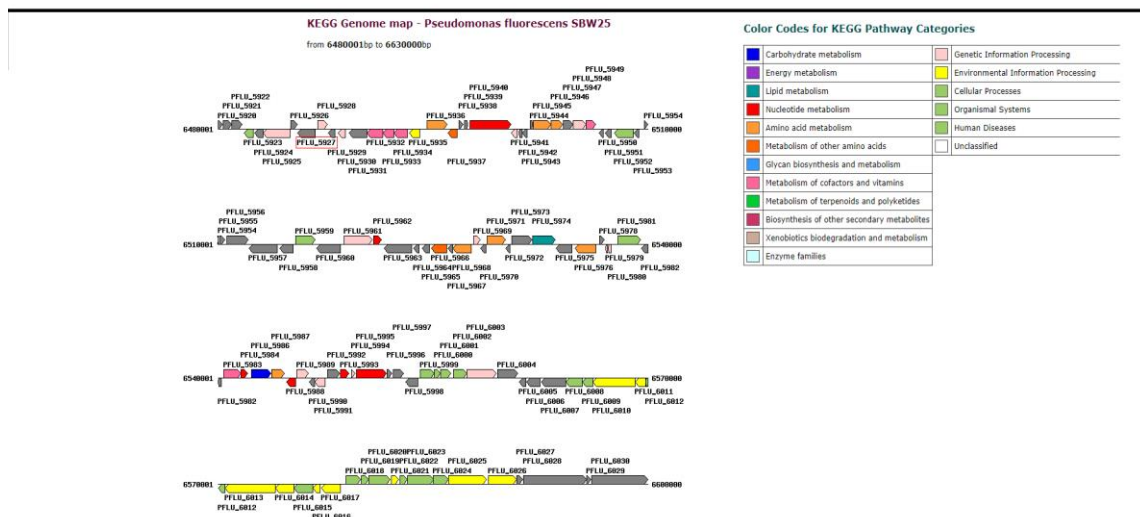


Figure 6-5 KEGG genome map: PFLU_RS31200 (gene *algP1*)

[Source: <https://www.genome.jp/kegg>; <https://biocyc.org>]

10	20	30	40	50
MSAKQKPVNT	PLHLLQQLSG	SLLEHLESAC	SQALADA EKL	LAKLEKQRGK
60	70	80	90	100
AQEKLHKSRT	KLQDAATAGK	AKAQAKAKDA	VKELEDLLDA	LKDRQAETRA
110	120	130	140	150
YISQLKKDAQ	ESLKLAQGVG	RVKEAVAKVL	GARTPAKAVA	ASAAKPKPASK
160	170	180	190	200
AVAAKAPAKA	AAKPAAKTAA	AKPAAKPAAK	TAAAKPAAKP	AAKTAAAKPA
210	220	230	240	250
AKPVAKTAAA	KPAAKPAAKT	AAAKPAAKPA	AKTAAAKPAA	KPAAKTAAAK
260	270	280	290	300
PAAKPAAKTA	AAKPAAKPAA	KTAAAKPAAK	PAAKTAAAKP	AAKPAAKTAV
310	320	330	340	350
AKPAAKPVAK	TAAAKPAAKP	AAKTAAAKPA	AKPVAKSAAA	KPAAKPAAKP
360	370	380	390	400
AAAKPAAKPA	VTKPAAKKPA	PAKPATPAAA	PTASTAPTAP	ASNTSAPVAP

STTPTSAS

Figure 6-6 AlgP1 is a regulatory transcription factor rich in proline

AlgP1 (length: 408 aa; molecular weight: 39,419 Da) resembles the H1- histone for having the repetitive motif Lys-Pro-Ala-Ala (KPAA) in its carboxy terminal domain (shaded in yellow/orange). This protein is highly positive as its isoelectric point is 11.42 and has two coiled coil domains positioned from residues 23 – 61 and 70 – 101 respectively. The mutations identified in this research are indicated with a red arrow: S337T (missense), V300A (missense), A282 (silent). NCBI-ProteinID: CAY53413. UniProt: C3K417. The protein has 75 residues of K (Lys), 156 residues of A (Ala) and 48 residues of P (Pro).

f) ***Hypothetical putative membrane protein (PFLU_RS14795; old locus tag PFLU_3035)***

It was found that FleQS9 (Movie 23) possessed a silent mutation within the PFLU_RS14795 gene (phospholipid carrier-dependent glycosyltransferase), which is a hypothetical putative membrane protein that had mannosyl-transferase activity (protein-O linked glycosylation). Glycosylation of flagella and T4P has been recognised¹⁵¹. However, as this is a silent mutation there would be no impact on the encoded protein sequence.

7 Concluding Remarks

7.1 Dominance of T97P NtrB Mutation in Evolutionary Pathway for Restoration of Swimming Motility

Swimming motility is an important trait for survival. It had previously been shown that mutants lacking the master regulator FleQ, readily evolve in rich media to a swimming phenotype, initially via mutation in the NtrB sensor and subsequently with an additional mutation in the DNA binding domain of the NtrC regulator¹⁰⁸. In this project it had been hypothesized that nitrogen limitation was a primary driving force for evolution of swimming mutants from the non-motile AR1 and AR2 strains. Based on this it was hypothesised that recovery of evolved mutants would depend on the N-source used and that with growth on high ammonium (replete nitrogen conditions) that an alternate evolution pathway might be identified. Interestingly, irrespective of timing of recovery of mutants, of N-source used in growth medium and whether the bacterial strain was non-motile (AR1 and AR2) or motile via viscosin dependent spidery-spreading (SBW25 Δ fleQ), all evolved mutants carried a mutation in NtrB. Thus, it can be concluded that mutation in NtrB is the primary *in vitro* evolutionary pathway for re-expression of flagella in aflagellate SBW25 mutants lacking the FleQ regulator.

It is interesting to note that 95.7 % of the 47 evolved swimming strains analysed showed the same single point mutation (A289C) encoding a T97P mutation within the PAS domain (transmitter domain) of NtrB (Table 4-6; Table 5-14; Table 5-7; Table 6-3). Previous studies have shown that mutations in the N-terminal PAS domain result in decreased phosphatase activity, despite the fact that this domain is not involved in PII interaction³¹⁶ (see Table 1-6). Studies in *Klebsiella pneumoniae* and *E. coli* have shown that a mutation, A129T in the central domain of NtrB also shows significantly decreased NtrB phosphatase activity acting on NtrC and consequently a substantial increase in the level of NtrC-P^{309,316}. It has been shown in *E. coli*¹⁴⁹ that the autophosphatase activity of NtrC-P is very slow with a half-life of bound phosphate groups of ~3.5 min to 5 min at 37°C and pH 7.5. Thus, despite the autophosphatase activity of NtrC, in the absence of NtrB phosphatase activity, levels of NtrC-P would increase. It is assumed that the T97P mutation in the PAS domain impacts conformational changes required for regulatory control of

phosphatase activity of NtrB³⁰⁹. The NtrB T97P mutation in AR2 and SBW25Δ*fleQ* led to flagella production and swimming motility (Figure 4-7; Figure 5-25) and as shown by Taylor et al.¹⁰⁸ with AR2S this mutation also leads to overstimulation of the Ntr regulon, as well as upregulation of flagellar genes. Thus, the assumption is that the NtrB T97P mutation results in over-phosphorylation of NtrC and that the overexpressed NtrC-P can replace FleQ regulator to activate flagella expression. The ability of NtrC-P to bind to the FleQ binding site and activate Fla genes has still to be demonstrated.

PII regulates the balance between the phosphatase and kinase activities of NtrB according to the carbon and nitrogen status in the cell³⁰⁹ (Figure 1-39; Figure 7-1). The level of nitrogen in the cell is sensed by the uridylyltransferase/uridylyl-removing enzyme (GlnD) that attaches or removes UMP groups from PII. PII is uridylylated and unable to interact with NtrB under nitrogen limitation conditions, and is deuridylylated permitting PII driven enhancement of NtrB phosphatase activity under nitrogen replete conditions (Figure 1-39; Figure 7-1). The only other NtrB mutation identified in this study was a D228A/N/G mutation. The D228N mutation was identified in FleQS7 and D228A in AR2S15, only by whole genome sequencing. No other mutation was identified elsewhere in NtrB or in any other ORF of these strains. FleQS5 appeared to originally be a mixed culture of a mutant with NtrB T97P and a second isolate with NtrB D228G. D228 is in a well characterised region of the C terminal ATP-binding domain that interacts with PII (Table 1-6). In *E.coli*³¹⁶ and *P. aeruginosa*¹⁷⁴ it has been shown that mutation of this region results in loss of interaction with PII and hence reduced phosphatase activity. This mutation was rarer than the NtrB T97P mutation and identified in only 3 of the 11 mutants subjected to WGS. Possession of an NtrB D228A mutation was common in evolved swimming mutants of the viscosin and *fleQ* deficient strain Pf0-2x when isolated on rich media¹⁰⁸. It would be interesting to further investigate this apparent preferred selection of the T97P mutation and much rarer recovery of D228A mutations during growth on minimal media.

During this study, the region of hypervariability for both *ntrB ntrC* genes, as determined by Taylor et al.¹⁰⁸ and the complete *glnK* (PII) gene were initially targeted for sequencing for all the evolved strains. In contrast to results with Pf0-2x, no mutation in *glnK* was identified for any of the evolved mutants and WGS did not identify any mutations in *glnA*. More surprisingly, no mutations were identified

in the targeted DNA binding HTH domain of NtrC, identified by Taylor et al.¹⁰⁸ as a standard second mutation to produce fast spreading colonies. This was despite the fact that during the evolution experiment, plates were routinely incubated up to 26 days and samples were taken from both the swimming disc and from 'blebs'. Indeed 78.13 % of AR2 swimming mutants were isolated from blebs (for example see Figure 5-3). Possible explanations for this include the following. (i) The NtrB T97P mutation alone is sufficient for swimming with the slower growth rate on minimal medium (ii) A second mutation in NtrC lies outside the DNA binding site (although this was not the case for any of the 9 FleQS or 2 AR2S mutants analysed by WGS) (iii) The blebs observed after around 5-20 days incubation were not due to faster swimming mutants, but a consequence of physical properties of the medium. Similar 'cake-like' colonies also called 'instability blebs' of *E. coli* have been observed on swarming medium and were attributed to bacteria growing and swarming deeper into the medium where moisture content was higher³¹⁹. One mutant FleQS7 (NtrB D228N) was tested for faster spreading on rich swarming medium. In this case, an NtrC S171P mutation, which is within the sigma 54 binding region, was identified in isolates from spidery-swarming growth. Irrespective of the reason, it is notable that during swimming evolution on minimal medium, no NtrC mutations were detected.

7.2 Reduced Recovery of Evolved Mutants with Ammonium As Nitrogen Source

One aim of this project was to expose the non-flagellate and viscosin producer strain SBW25 Δ *fleQ* (*Fla*⁻, *Visc*⁺), and the two aflagellate and non-viscosin strains, AR1 and AR2 to different environments that triggered nitrogen assimilation, regulated via the NtrBC system, and monitor the impact on evolution. This chemical environment is governed by ammonium and the amino acids, glutamine and glutamate. Based on information from *E. coli* and *Pseudomonas*, Figure 7-1 summarises the presumed physiological status of *P. fluorescens* during growth on each of these N-sources. Growth on ammonium (nitrogen replete conditions) utilizes the GDH pathway for nitrogen assimilation, using 2-oxoglutarate (2-OG) to fix the inorganic nitrogen. NtrC is primarily in the non-phosphorylated state, as NtrB is complexed with PII activating phosphatase activity. Hence, there is only a low level of transcription of *glnAntrBC* and other genes of the Ntr regulon. In addition, GS

becomes gradually inactivated through adenylation. Ammonia (NH_3) can diffuse freely through bacterial membranes and at low concentrations is transported via the AmtB transporter; thus uptake is cheap in terms of energy costs. Glutamine (Gln) is a signalling compound that regulates the expression of the NtrBC system; its intracellular pool is an indicator of nitrogen status in the cell. The compound 2-OG is carbon signalling. The ratio of glutamine/2-OG (N/C) is sensed by the signal transduction protein, PII which changes its conformation upon binding to 2-OG. The uridylyltransferase/uridylyl-removing enzyme (UTase/RT), when not covalently attached to glutamine, adds uridine 5'-monophosphate (UMP) groups to PII and blocks PII-NtrB interaction, but if glutamine (replete N-signal) is high and attached to UTase/RT the enzyme removes any uridine 5'-monophosphate (UMP) groups linked to PII, activating NtrB phosphatase activity.

When glutamate or glutamine is used as sole nitrogen source, the response is one of a nitrogen limiting environment with an increased 2-OG level and depletion of the intracellular glutamine pool, thus triggering nitrogen starvation responses^{285,306}. In this case, glutamate synthase (GOGAT) is expressed to produce glutamate and glutamine synthetase (GS) production and activation is triggered.

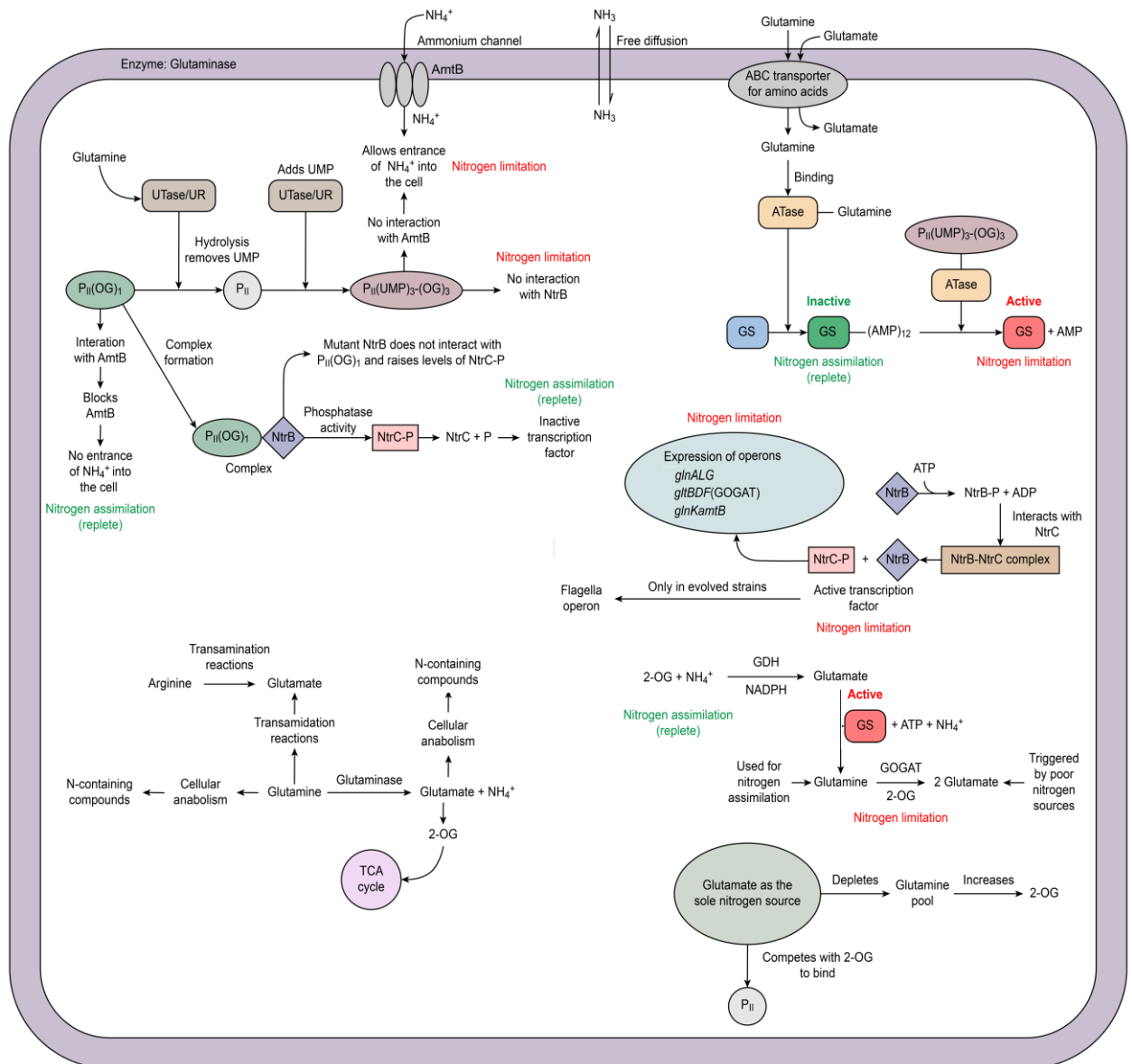


Figure 7-1 Summary of nitrogen regulation and evolution of swimming motility

Under nitrogen limitation conditions, the NtrBC system is upregulated and the glutamine synthetase (GS)/glutamate synthase GOGAT pathway is used for nitrogen assimilation. In an evolved mutant strain, the mutated NtrB (GlnL) is unable to interact with PII(OG)₁ complex in order to trigger its phosphatase activity for removing the phosphate groups from NtrC (GlnG), so the levels of active NtrC-P raises and upshifts the expression of *glnALG*, *glnKamtB* and *gltBDF* operons. As NtrC is paralogous to FleQ, it presumably takes FleQ's role in its absence triggering the expression of flagella regulon. GDH pathway is not used for nitrogen assimilation under nitrogen limitation conditions. Ammonium is assimilated via this pathway in a low energy environment with high levels of ammonium as nitrogen source. The full adenylylated form of glutamine synthetase [GS-(AMP)₁₂] is inactive, whereas the unadenylylated enzyme is active. NtrB only interacts with the non-uridylylated form of PII at high levels of nitrogen. Under nitrogen limitation conditions, the uridylylated PII stimulates ATase to remove the AMP groups bound to GS. 2-OG or OG: 2-oxoglutarate. AMP: adenosine 5'-monophosphate. AmtB: ammonium channel. ATase: adenylyltransferase. *glnALG*: *glnAntrBC* operon. GDH: glutamate dehydrogenase. GlnK: PII. GS: glutamine synthetase or GlnA. GS: glutamine synthetase. GOGAT: glutamate synthase, encoded by operon *gltBDF*. Ntr: nitrogen regulator. NtrB: GlnL or NII. NtrC: GlnG or NI. UMP: uridine 5'-monophosphate. UTase/UR: uridylyltransferase/uridylyl-removing enzyme. Refer to sections 1.11 and 1.11.2 for a detailed explanation and references cited therein.

The research hypothesis was based on the fact that under the carbon rich: nitrogen limitation conditions triggered during growth on the amino acids glutamine or glutamate the NtrBC system is upregulated, whereas under nitrogen replete conditions (growth on ammonium) the NtrBC system is down-regulated. Thus the probability of observing swimming mutants, that had evolved via mutations in NtrBC, would be higher under nitrogen limitation when these genes are maximally expressed. This effect was shown to be the case for the frequency of evolution of the sessile strain AR1. The Pearson chi-square test confirmed a statistically significant association (P -value $0.026 < 0.050$; Figure 5-2) between the nitrogen source and the number of evolved and non-evolved plates of strain AR1. There were a higher number of non-evolved plates with growth on ammonium/glucose compared to growth on glutamine or glutamate/glucose. However, this association did not hold for AR2. Analysis of a much larger number of test samples using multiple inoculum on each plate would resolve if the apparently lower frequency of recovery of mutants when growth on ammonium is statistically significant for both AR1 and AR2.

It was also anticipated that evolved mutants carrying *ntrB* mutations would appear more rapidly under nitrogen limiting conditions and this was proven to be the case. Evolution of swimming appeared earlier on plates with glutamine or glutamate as nitrogen source. There was no significant statistical difference in the time to evolution of swimming motility (P -value $0.633 > 0.050$) between glutamine or glutamate as N-source (mean = 2.9 days, $SD = 0.8$ days). The time to evolution was also strain independent, as there was no statistically significant difference in the time taken to evolve swimming motility between the two sessile strains, AR1 and AR2 (P -value $0.702 > 0.050$). However, when comparing both sessile strains, it was found that the time to evolve swimming motility with ammonium was significantly different (P -value $0.000 < 0.050$; Table 5-16) and longer (mean = 5.5 days, $SD = 0.6$ days) when compared to the time to evolution on the poor nitrogen sources (glutamine or glutamate). This is in accord with the fact that the NtrBC system would be only poorly expressed and stimulated (primed) under nitrogen replete conditions (10 mM NH_4^+).

Taylor et al.¹⁰⁸ observed upregulation of expression of a plethora of genes in AR2S NtrB T97P compared to the parent AR2, in particular genes involved in flagella

synthesis and chemotaxis, nitrogen regulation, ammonium transportation and loci encoding amino acid transport proteins. The latter group often showed an exceptionally high increase in expression. Increase in genes directly related to NtrBC function included: *amtB*, 84 fold; *glnK* (PIL, PFLU_RS29305), 7.9 fold; *glnA* (GS, PFLU_RS01710), 5.8 fold; *glnG* (NtrC, PFLU_RS01685), 38 fold *glnL* (NtrB, PFLU_RS01690), 28 fold. For *gdh* (PFLU_RS17095), there was no significant change.

These observations suggest that the biochemical impact in the evolved strains FleQS and AR1S/AR2S is constitutive expression of an Ntr system that is no longer responsive to the source or levels of nitrogen in the milieu. This is in accord with the earlier report that mutations in NtrB at position 228 such as D228A in *P. aeruginosa* trigger the NtrBC system to be constitutively expressed³²⁰. While this constitutively upregulated Ntr phenotype was selected in both a nitrogen limitation (glutamine or glutamate) and nitrogen replete (ammonium) environment this phenotype was clearly less effective in the nitrogen replete environment. All evolved mutants with the NtrB T97P or D228A mutation grew very poorly in M9 ammonium + glucose compared to the parent strain, but still grew well if glutamine or glutamate was the N-source. In the wild type, with sufficient inorganic nitrogen (NH₄⁺) assimilated, the NtrBC system is shut down, transport of amino acids slows down and levels of active glutamine synthetase (GS) decreases, as the inactive adenylated glutamine synthetase (GS-AMP) levels increase. In the mutant, over expression of the Ntr regulon will continue even when grown in ammonium. It is likely that uncontrolled assimilation of ammonium leads to a severe dysregulation of the crucially regulated N:C balance within the cell. To fully understand the physiological status of these mutant cells, it would be interesting to compare the extent of adenylation of GS in ammonium grown and glutamine grown cells. This very poor ability of the NtrB mutants to grow with ammonium as N-source, must surely also contribute to the delayed recovery of evolved swimming mutants on this rich N-source.

7.3 Mutation of the Sensor Might Be a More Effective Pathway to Replacement of FleQ

Although binding of NtrC-P to the FleQ binding site remains to be proven, the over expression of flagella genes in the NtrB mutant AR2S¹⁰⁸ is consistent with NtrC-P over expression permitting binding of native NtrC-P to an alternate sigma-54

dependent promoter region without a mutation in the NtrC DNA binding site. Hence, mutation of the sensor appears to be a more effective pathway to replacement of FleQ than direct mutation of the bEBP. Mutation of the DNA binding site of any essential bEBP would likely have a significant fitness cost. Perhaps the indirect effect of mutations in the sensor domain rather than direct mutation of a bEBP is less detrimental, as ultimately this leads to overexpression of a native phosphorylated regulator. While Taylor et al ¹⁰⁸ selected a faster swimming mutant with a mutation in the NtrC DNA binding domain and high expression of flagellar genes, this mutant followed a two step pathway also with an initial mutation in the NtrB sensor.

Cross-talk between sensing and regulator modules of two-component sensor-regulators, including NtrBC has been recognised *in vitro*^{197,321}. In this study with selection on minimal media, all evolved mutants carried a mutation in NtrB and second step mutation in NtrC was not identified. The possibility that the resulting overexpression of mutated NtrB might lead to cross-talk and overphosphorylation of another EBP in addition to NtrC was considered. *P. fluorescens* has a number of bEBPs that are phylogenetically related to FleQ and similar in terms of both structure and sequence (Figure 1-29). Analysis of the WGS data of selected evolved mutants for potential second step mutations, did not identify mutations in any of these bEBPs. This, however, does not exclude the possibility that mutated NtrB T97P does activate an alternate EBP. An indication of involvement of another bEBP might be the fact that mutations in the histone-like protein AlgP were identified in three different FleQS mutants. Whether these mutations were selected in relation to the swimming phenotype or were directed to an another co-incidental phenotype, for example in response to pH changes during amino acid catabolism, requires further investigation.

In addition to NtrBC mutations and AlgP mutations, other single point mutations occur in ORF of apparently unrelated genes, such as *fusA* (EF-G) (Appendix O: Figure O-7) and glycosyltransferase (PFLU_RS14795; old locus tag PFLU_3035) (Appendix Z: Figure Z-3), which is a hypothetical putative membrane protein with mannosyl-transferase activity (protein-O linked glycosylation). The appearance of the silent mutation in the glycosyltransferase gene appears to be aleatory with evolution not directed towards any specific phenotype. This may also be the case

of the *fusA* mutation. However, it may have become fixed in the population due to an indirect effect for example on protein translation. Growth on the minimal medium M9 with the limited nitrogen source and limited pH regulation is likely to have different selective pressures compared to growth on the rich medium LB. In addition to the mutations in the ORFs there were some differences in intergenic regions. These could be analysed in more detail for any possibility of impact on regulation of transcription of relevant genes. Ultimately, the evolution of favourable adaptations for a population under stress has both costs and benefits, the energy costs of adaptation is compensated, because it enables a population to respond to chemotaxis signals and reach a nutrient rich environment.

7.4 Poor Growth in Ammonia Is the Biochemical Impact of a Mutated NtrBC System

The growth curves conducted in minimal medium M9 (broth), using different nitrogen sources and glucose, for the wild type strain SBW25 and SBW25 Δ *fleQ* showed no differences between them, although both grew better in glutamine compared with glutamate and ammonium. The fact that glutamine can spontaneously hydrolyze at a low rate to pyroglutamate and ammonia providing both nitrogen sources¹³⁴, and glutamate which acts as a carbon skeleton for the TCA intermediate and C-sensing molecule 2-oxoglutarate (2-OG) may contribute to good growth on glutamine. According to Goss et al.²⁷⁹, periplasmic glutaminases which release ammonium and glutamate²⁷⁹, in addition to the glutamine ABC transporter, also contribute to glutamine uptake. Ammonia diffuses freely through the cell membrane and is transported by AmtB, ammonium (NH₄⁺) transporter only at low concentrations. Glutamate is also transported through an ABC transporters which is not highly expressed²⁷⁹. Ammonium (NH₄⁺) is a rich source of nitrogen because it does not require energy in order to be assimilated into 2-OG for the formation of glutamate when using the GDH pathway in a low energy environment¹²⁰. The enzyme glutamate dehydrogenase (GDH) has a K_m for ammonium of ~2 mM¹²⁰. The alternative pathway GS/GOGAT [glutamine synthetase (GS)/glutamate synthase (GOGAT)] is turned on under ammonium limiting conditions and is ATP-driven¹⁴⁷. However, the evolved FleQS strains grow very poorly on both ammonium and glutamate.

The data shown in Table 4-4 and Table 4-10 indicate that the metabolism of rich and poor nitrogen sources was impacted. All the evolved FleQS strains were able to grow in a rich medium LB (Figure 4-20), while the regulation of nitrogen was altered, as shown by their low growth in minimal medium M9 when glutamate and ammonium were the nitrogen source (Figure 4-21). In addition, it was observed that all FleQS strains (except strain FleQS4) assimilated glutamine as effectively as the wild type strain SBW25 (Figure 4-21). This showed that these strains can effectively utilise the glutamine present, although the metabolism of ammonium and glutamate was affected.

Taylor et al.¹⁰⁸ hypothesized that evolved strains, as result of NtrBC system re-wiring toward flagella regulon, over import ammonium (NH_4^+) poisoning the cell. Interestingly, the evolved mutant FleQS4 carried a mutation in a putative ammonium channel (PFLU_RS08590) in addition to the NtrB T97P mutation. This gene product is distinct from the AmtB ammonium transporter, indeed the BLAST results of both sequences showed no significant similarity in spite of increasing the EXPECT threshold to 50. Its function has not been studied in any bacteria. However, unlike all of the other FleQS mutants, FleQS4 grew well in ammonium following a lag, but grew more poorly in glutamine and LB. It is possible that glutamine compensates a metabolic deficiency in nitrogen metabolism derived from NtrBC system mutations in most mutants, or these strains use an unknown alternative assimilation pathway not regulated by the NtrBC system and ultimately with growth on glutamine there is a better N:C balance. However, this the evidence presented indicates that this is not the case with FleQS4, quite likely linked to the mutation in PFLU_RS08590. It would be interesting to compare FleQS4 in more detail to the other mutants, for example through microarray analysis. In conclusion, the biochemical impact of a mutant NtrBC system is a dysregulation of operons expressed in response to the intracellular nitrogen status.

7.5 Swarming Types of the Evolved Strains FleQS, AR1S/AR2S

Swarming was only observed on rich media and never in minimal media M9. Three types of swarming were observed in the evolved mutant strains isolated in this research:

- Wild-Swarming: similar swarming to the wild type strain, SBW25. Observed only in FleQS strains.
- Spur-Swarming: commenced as a single spur that appeared in the centre of the swimming colony, moved to the surface to become a spur that slid over the surface. Upon reaching the surface, swimming colony underneath for a few hours before starting to swarm diffusely (multiple directions) fast. As a result, it covered more area than the swimming population with a disc shape. Observed only in AR1S and AR2S strains.
- Spidery-Swarming: swarmed in a dendritic manner through the agar, and started at different points from the border of a swimming circle colony. Observed only in FleQS strains. This was opposed to spidery-spreading (sliding) of the parent strain SBW25 Δ *fleQ* which was only observed on the surface of the medium.

Furthermore, the swarming times of the wild type strain, SBW25, are not different from the spidery times in the aflagellate strain, SBW25 Δ *fleQ* (*Fla*⁻, *Visc*⁺).

7.6 FleQ is the Sole Master Regulator of Flagella Expression in *P. fluorescens* KO FleQ

The flagella operon is expressed in a hierarchical and timely manner in *P. fluorescens* SBW25. The biosynthesis of this energy-consuming organelle is regulated by the master flagella regulator, FleQ, which is a bEBP (bacterial enhancer binding protein), that does not require phosphorylation to actively interact with sigma factor 54 (σ^{54} or NtrA) to bind an enhancer and commence flagellar gene expression. The control for swimming motility was the aflagellate KO *fleQ* strain SBW25 Δ *fleQ*. To confirm that the aflagellate phenotype in the KO *fleQ* strain, SBW25 Δ *fleQ*, results from the absence of FleQ, a complementation experiment was performed using pBBRMCS-5 carrying full length *fleQ*. The aflagellate strain, SBW25 Δ *fleQ* remained sessile (colony appearance is a dot) for 24 h in the swimming medium, after which it gradually and slowly acquired a spidery phenotype and slid, whereas the SBW25Q(*pfleQ*) strain, carrying the full length *fleQ*, formed a swimming expanding colony through the agar after 2 h, suggesting that flagella expression is mediated by FleQ, therefore, *fleQ* was necessary for expression of the flagella operon.

7.7 Active and Passive Motilities

In this project, it was observed for active motility (swimming and swarming) and passive motility (viscosin dependent spidery-spreading), that colony spreading (changes in the total area in mm²) constantly exhibited acceleration changes and dramatic alterations in colony expansion rates (mm²/h). However, the sessile strains only expanded to a maximum colony size of 30 mm² after 24 h and <~1 cm², after even 30 days growth.

Passive movements were observed in aflagellate strains, as they slide on the top of the agar surface, and viscosin production aids in the colony's expansion¹⁰⁷. Thus, the sliding colony acquires a spidery shaped phenotype: spidery-spreading. However, the aflagellate and non-viscosin producing strains, such as AR1, AR2 and their colonies, have a dot-shaped appearance because the cells accumulate in the same place (cumulative growth). Sliding motility is not driven by chemotaxis or any energy requiring motor, but is the result of physical force expansion of the growing cells as they spread on the agar surface. If viscosin is present, these colonies expand more and cover a greater area, as observed in SBW25Δ*fleQ* (*Fla*⁻, *Visc*⁺) and AR9 (*Fla*⁻, *Visc*^{*}). Spidery-Spreading is faster at normal viscosin levels (SBW25Δ*fleQ*) because the cells are more compact, whereas in overproducer strains (AR9) the sliding is slower, as the colony is less compact.

There were no statistically significant differences (*P-value* 0.610 > 0.050) between the colony's area of strains SBW25Δ*fleQ* and SBW25 in rich LA medium (0.25 % agar, 15 diameter plates). The spidery-spreading colonies of the strain, SBW25Δ*fleQ* (*Fla*⁻, *Visc*⁺), reached an area of 11104.47 mm² over 24 h, in rich LA medium (0.25 % agar), and the swimming expanding colony of wild type strain SBW25, in the same medium and period of time (24 h), covered 12328.66 mm². However, the overproducing viscosin strain, AR9 (*Fla*⁻, *Visc*^{*}), covered less area (916.47 mm²) than SBW25Δ*fleQ* (*Fla*⁻, *Visc*⁺), because excess biosurfactant does not facilitate sliding, as the cells are looser. On the other hand, the expanding colony of the flagellate and non-viscosin strain SBW25C (*Fla*⁺, *Visc*⁻), covers less area (766.12 mm²) than the wild type strain, SBW25 (*Fla*⁺, *Visc*⁺). In conclusion, flagella and viscosin both facilitate the dispersion and expansion of the colony, when expanding through agar or on top of soft-agar medium.

As published¹⁰⁷, viscosin allows a non-swimming colony to move further to locate nutrients, as compared to a colony that can only utilise flagella driven movements, such as SBW25C (*Fla*⁺, *Visc*). Viscosin is necessary for swarming of *P. fluorescens*^{83,107}, and has been identified as a fast movement that permits bacteria to explore a new environment²⁴⁴.

The motility of the *P. fluorescens* strains in soft-medium (0.25 % agar) follows a Log-Normal distribution, owing to growth and the mixture of movements within the population, which arises from quorum sensing (swarming), pH changes, physicochemical properties in the medium or stochastic mutational events that subsequently lead to faster phenotypes on the motility plate.

Variability in the amount of inoculum, temperature changes in the walk-in incubator, differences in humidity among the motility plates, and biological diversity are all likely to contribute to variability in colony expansion area (mm²) among motility plates (swarming medium). When compared with plates made with swimming medium, there is greater variation, because swarming initiation depends on temperature and humidity content of the medium²⁹⁰. Thus there was a marked increase in variation of colony area around the time of the initiation of swarming, as the time of initiation of swarming varied greatly between plates. Tremblay & Diézel²⁹⁰, when studying the swarming motility of *P. aeruginosa*, also conducted experiments using large (15 cm diameter) and small (9 cm diameter) Petri dishes, with the same agar thickness in both. These authors found that dish size impacted on colony morphology due to the boundary effect of the plate, as the swarming colony did not have more space to expand onwards; it moved inwards to cover all available space. There were no significant statistical differences (mean = 12.33 h, *SE* = 1.41 h; *P-value* 0.087 > 0.050) between the swarming times of the SBW25 colonies, inoculated onto different plate sizes. However, there was not much difference in variability in the swarming time data from the plates of 9 cm diameter (coefficient of variation = 30.11 %) compared with the 15 cm diameter plates (coefficient of variation = 27.64 %). Additionally, there was no statistically significant difference (mean = 13.67 h, *SE* = 0.61 h; *P-value* 0.913 > 0.050) in the time taken to generate the spidery-shaped colony (among the distinct plate diameters used to study the strain SBW25 Δ *fleQ*). However, more variability was observed in spidery-time data for 9 cm diameter plates (coefficient of variation = 41.40 %) compared

with data from 15 cm diameter plates (coefficient of variation = 11.02 %). Therefore, we can see that the plate size does not affect the swarming and spidery times among replicates, but instead increases the variability among replicates caused by differences in plate humidity; as the 15 cm diameter plates are prepared individually and located in the same position inside the laminar flow, so their humidity content is more uniform among replicates. As the amount of humidity of the plates is affected by their position inside the laminar flow cabinet as shown by Tremblay and Déziel²⁹⁰, it would be advisable to work concomitantly with lesser number of replicates of 9 cm diameter (e.g. working concomitantly with 6 replicates of 9 cm diameter), in order to decrease the variability in humidity content as 6 plates can be located together in the centre of the laminar flow. Furthermore, the average swarming time among 15 cm replicate plates of the wild type strain SBW25 did not have a significant statistical difference (*P-value* 0.405 > 0.050) from the time of development of spidery shapes in the sliding colonies of SBW25 Δ *fleQ* in the swarming media (0.25 % agar LA).

7.8 Sources of Variation in Motility Plates

Swimming is a flagella-dependent movement of free cells in liquid media, or movement through a semi-solid medium like swarming medium. When swimming through a semi-solid medium, the bacterial population (colony) has the appearance of a circle²⁴⁶, the borders of which expand over time. The circular appearance of this relocating population is caused by nutrient gradients, whereby individual cells move in different directions in response to these gradients (chemotactic responses)²⁴⁶. Hence, the colony appears circular and its total area (mm²) increases over time.

7.8.1 Water content in the motility plates

Swimming motility requires a high content of water (e.g. liquid broth) and also occurs in semi-solid medium (e.g. swimming medium)¹⁰⁷. This type of motility does not require surfactants (e.g. viscosin) because it is flagella driven¹⁰⁷. The swarming medium was poured (about 50 °C) into the plates to control the water content¹⁹³ and allowed to dry in a laminar flow hood (without the lid) for 20 min to remove the surface water, and thus decreasing swimming motility contribution¹⁹³ for the expansion of the colony on the agar surface²⁸⁹. Studies conducted in *P. aeruginosa*

to determine the influence of drying time and agar content in swarming indicated that longer drying times and higher agar content (e.g. 1 %) decreased swarming motility²⁹⁰; whereas, shorter drying times and low agar content promoted swarming motility²⁹⁰. Hence, the swimming medium after being poured into the plates was allowed to dry under the laminar flow cabinet for 30 min to have less water on the agar surface to prevent swarming as surfactants require water for diffusing²⁹⁰. According to Tremblay and Déziel²⁹⁰, another factor contributing to the variability of the motility plates is their localisation in the laminar flow cabinet as the plates allowed to dry near at borders are subject to a higher airflow intensity compared to ones positioned in the middle, and this intensity also is different between different laminar flow models²⁹⁰.

7.8.2 Physical factors that affect swarming motility

Swarming motility is the phenomenon of swimming in a group^{193,243} and viscosin facilitates this movement⁵⁴. Swarming is a multicellular movement across semi-solid moist surfaces^{193,290} that generally occurs in rich medium (energy rich)¹⁹³ after reaching certain population density²⁴³ because it is triggered by high growth rates¹⁹³ and is not an individual movement¹⁹³ as in a swimming population^{193,243}. Additionally, swarming is faster than swimming²⁹⁰ and permits a rapid colonisation and dispersion²⁴³. In *P. fluorescens* SBW25, biosurfactants enhance swarming motility¹⁰⁷ as these compounds decrease the surface tension of the liquid through which the colony advances²⁴³. Chemotaxis is observed in individual swimming cells and in swarming bacteria²⁴³. There are physical factors, such as osmotic pressure (swarming bacteria secretes osmolytes), matrix permeability and medium viscosity, which affect swarming motility²⁴³. The osmolytes are compounds that extract water from the agar, and these substances are high-molecular weight lipopolysaccharides (LPS)²⁴³. Studies in swarming motility of *P. aeruginosa* showed that higher agar content impedes water flow and hence decreases swarming motility²⁴³. Other compounds (e.g. sugars and salt) also increase the osmotic pressure hindering swarming motility²⁴³.

7.8.3 Changes in pH and temperature affect bacterial growth

Physicochemical factors also affect bacterial growth²⁵¹; they can be intrinsic owing to culture medium, such as pH, or extrinsic, for example temperature and oxygen²⁵¹.

Culture media such as Luria-Bertani broth or the minimal medium M9, contain buffers such as glucose and phosphate salts²⁵¹ (refer to sections 2.3.1.2 and 2.3.1.3); however, they do not impede fluctuations in pH owing to microbial metabolism e.g. release of ammonium or acids²⁵¹ (Figure 1-53); also the medium is consumed^{251,254} given that it comprises amino acids (see section 1.12), phosphates and glucose, causing decrease in buffering capacities. *Pseudomonas* sp exert catabolite repression regulation (CCR), meaning they prefer using carbon sources in an orderly manner (Figure 1-52). For example, they use some amino acids first, then glucose when both carbon sources are present in the medium²³. Studies investigating pH changes in *E. coli* growing on M9 minimal medium (glucose as carbon source), are indicative of changes in ΔpH (pH/h) of 0.043 units between 8 h to 14 h²⁵³. However, it was reported that when *P. fluorescens* is grown on glucose, it does not secrete many metabolic by-products into the culture media²⁵⁵ and there is little change in pH.

The phospholipid fatty acid content of *P. fluorescens* membranes is altered in the presence of metabolites, released into the medium, and also changes with temperature and pH²⁵⁴. In turn, membrane viscosity is also altered, owing to changes in phospholipid fatty acid composition in these membranes²⁵⁴. These changes preserve membrane chemical and mechanical properties, which is necessary to maintain cellular function²⁵⁴. These compositional modifications in cell membranes trigger metabolism modifications because metabolite synthesis is regulated by two-component sensor: regulator systems (e.g. EnvZ/OmpR which is involved in osmoregulation)²⁵⁴ which transmit changes to alter the transcriptome²⁵⁴. Therefore, it is important to consider pH fluctuations as an additional stress factor in the bacterial population studied here either sitting on top of agar or swimming in through the agar. This might have been a contributing factor in the selection of mutants, for example the *algP* mutation. In addition, changes in pH during growth in broth cultures testing different different nitrogen treatments and in rich medium LB might have impacted growth. The rich medium (LB) contains oligopeptides (~650 Da), which can be transported by permeases (membrane transport proteins) into the cells, and then degraded in order to release amino acids²⁰⁰. However, the bacteria preferentially use the free available amino acids present in the broth²⁰⁰ (Appendix V: Table V-1) before degrading more complex carbon sources

(oligopeptides)²⁰⁰. Catabolism of amino acids can lead to an increase in pH as ammonia is released.

7.9 Experimental Evolution Shows that Nitrogen Limitation Is the Evolutive Force for NtrB Re-Wiring to Flagella Restoration in KO *fleQ* Strains

Experimental evolution research can be conducted in *P. fluorescens* SBW25 owing to its short generation times (~20 min) and small genome size (6.31529 Mb). The existence of genetic techniques for WGS, coupled with the study of individual genes, enables the identification of novel mutations that arise in bacterial populations when under stress. Since the evolution of a population is stochastic, it is not possible to predict how or when a favourable adaptation will appear. As mutations are random events and not directed, it is in theory possible to observe a range of morphological and metabolic phenotypes in the swimming populations since all mutations interact and contribute to this phenotype (epistasis).

There could in theory be many mutational paths that a stressed bacterial population may follow to reach a favourable adaptation. However, this study has shown a very dominant path. Despite the prediction that alternate pathways (mutations in different bEBPs) might be identified, all evolved mutants followed the *ntrB* mutation pathway. Thus, despite the detrimental effect on growth, particularly in ammonium, the benefit of this mutation must be higher than the impact on fitness, hence the mutational frequency and number of cells carrying this mutation would have increased until the genotype was fixed in the swimming population. The less detrimental the evolutionary path leading to a beneficial phenotype the more frequently it should occur. When the NtrBC system was primed (upregulated), e.g. grown under poor nitrogen conditions (glutamine or glutamate), the frequency of evolved swimmers was high because they resulted from a mutation in the system, which required only a single step to lead to a swimming motility phenotype. Such mutations are beneficial despite their metabolic costs, since they allow an aflagellate population to respond to chemotaxis cues (e.g. amino acids) and switch niches to reach fresh nutrients, whilst escaping from harsh environmental conditions.

Novel adaptations exert trade-offs because an evolved phenotype may be beneficial under specific environmental conditions, whilst being detrimental in others. This is the reason why FleQS strains become more efficient at utilising glutamine, and less effective at utilising ammonium and glutamate; notably, their evolved metabolism was selected in an environment that favoured this type of metabolic change.

7.9.1 Absolute and relative fitness of the evolved swimming phenotype

Evolutionary rescue is a heritable adaptation, selected by natural selection to avoid extinction of a population under deleterious environmental conditions¹⁹⁸. The aflagellate and viscosin producing strain SBW25 Δ fleQ was used as a control to corroborate that nitrogen limitation was indeed the main factor driving evolutionary rescue. The bacteria positioned in the centre of a dendritic colony after depleting the available nutrients are unable to switch to an alternative niche to obtain food, because they do not express flagella. Notably, this strain is not a chemotactic mutant and can respond to nutrient gradients in the medium, but the cells starve as they cannot swim. This can explain why evolution of SBW25 Δ fleQ swimming was generally observed from the centre of a dendritic colony. The FleQS strains, which evolved from SBW25 Δ fleQ under different nitrogen conditions, are well suited to the environment from where they evolved. It is important to note that not all evolved colonies, isolated under different nitrogen conditions, maintain the evolved swimming phenotype after isolation. This can be explained by relative fitness and absolute fitness¹⁹⁸:

- ❖ Absolute fitness is the increase in population in an environment.
- ❖ Relative fitness denotes the increase in the frequency of a specific phenotype, in a population, relative to the average phenotype of the population.

Relative fitness means that the frequency of a specific phenotype outweighs the frequency of another phenotype in the population, since this phenotype rescues the population from extinction; however, this phenotype may not be suitable for survival upon stress or when exposed to another stressful environment. This variation is heritable and eventually replaces the mean phenotype of a population, as long

as it has a positive impact on the abundance of the whole population in the environment. Hence, this adaptation (e.g. mutant gene) replaces the mean population phenotype and becomes fixed, consequently avoiding extinction¹⁹⁸.

This evolutionary selective process acts on mutations that are already present in the population, before being exposed to a specific stress and to those that may arise as a result of novel mutations which occur in the wake of harsh environments¹⁹⁸. Microbes generate diversity when faced with hostile environments; in addition, gene expression is regulated by their environment¹⁹⁹. Under deleterious conditions, there is a higher probability that a mutator phenotype will arise, which has long-term disadvantages despite being a source of variation. Hypermutators will eventually disappear from a population, or their frequency will drop dramatically in response to environmental conditions¹⁹⁹, because they generate lineages that contain mutated housekeeping genes, which are not under selective pressure and are non-lethal under the conditions they evolved¹⁹⁹. There is also the other possibility that an advantageous phenotype is only expressed when necessary, when it confers an advantage on a population; genetic buffering¹⁹⁹. Notably, in asexual populations, generating diversity via a high mutation rate due to stress produces lineages that compete against each other, as it is impossible for all favourable mutations to be present in the same lineage. This eventually leads to extinction or a dramatic decline in certain lineages.

Studying the re-wiring of systems under selective pressure assumes significance to understand the evolutionary rescue of populations, under stress. This knowledge can be applied to other systems, such as cancer cells which evolve in response to treatments, or similarly, pathogens evolving resistance to antibiotics, given that the same evolutionary strategies are used by all organisms.

7.10 Significance

P. fluorescens SBW25 is a PGPB, which is important for agriculture because of its biofertiliser and pesticidal properties⁹. Using this bacterium to diminish the use of chemical fertilisers and pesticides to protect the crops will have a positive economic and environmental impact. Firstly, the costs of crop production is reduced as use of chemical fertilisers diminishes and secondly, it will protect the environment caused by loss of N-P-K fertilisers to rivers decreases. Also, the application of chemical

pesticides should dramatically diminish and hence will protect the environment due to their use as these chemicals can eliminate beneficial insects, kill beneficial nematodes and beneficial microflora, and also decrease plant biodiversity. Hence, the crop yield will increase, with more food per hectare obtained. Hence, it will be possible to feed more people at lower costs and use all the available arable land in a better way. As motility and chemotaxis are important traits for *P. fluorescens* SBW25 to move towards its host, it is necessary to understand any metabolic pathway (nitrogen assimilation) that cross talk with motility. Therefore, it may be possible to exploit this cross talk and determine which type of soil is more favourable for *P. fluorescens* colonization. As *P. fluorescens* SBW25 survives on aerial plant surfaces and rhizosphere for long periods^{299,300} after being applied to seeds or sprayed on crop fields; however, this initial inoculum gradually decreases over the time^{300,301}. Amino acids are strong chemoattractants for *P. fluorescens*, and these are present in higher percentage in plant roots exudates^{70,72,133,239,298,302-305}. So, studying their impact in motility will assist to choose which crops will be more suitable to apply *P. fluorescens* SBW25. The study of evolution of pathways that involve two component systems like the NtrBC can be exploited to delve into process of evolution of resistance to antibiotics, virulence expression, and also can be exploited to develop therapies to target two component systems because these are exclusive for bacteria, and human pathogenic fungi (*Candida albicans*, *Aspergillus fumigatus*, and *Cryptococcus neoformans*). In addition, flagella expression is important for biofilm formation and swarming. Swarming permits the bacteria to explore and move faster towards other parts of the host, and biofilm formation is also important to protect microbes from desiccation and other environmental insults. Therefore, studying factors like nitrogen limitation in the expression of flagella is important because *P. fluorescens* can form biofilms and reach other tissues of the host after colonization according to their surrounding environment. Also this study demonstrates that evolution is random and gives more insight into the different evolution strategies and plasticity of the bacteria genome because the evolution of motility in aflagellate strains is an aleatory consequence of high homology between NtrC and FleQ. Thus, this study shows the existence of a relationship in the type of nitrogen source and the higher probability of rewiring, when the environment requires the expression of the NtrBC system; this suggest that flagellation is a trait that appears as a response due to the strong chemotaxis

of these amino acids in non-flagellate bacteria. Also, starving bacteria are subject to higher rate of mutation and there is more probability that natural selection chooses a mutant phenotype able to respond to the chemotaxis signal due to the nutrients available but non-reachable for the starving population.

7.11 Further Research

Mutations in NtrB are the consistent pathway in these evolved swimming mutants. The mechanism is assumed to be via an enhanced phosphorylation state of NtrC, which in turn leads to upregulation of the Ntr system, including NtrB and C. The unnaturally high level of NtrC-P then permits binding to the FleQ binding site and sigma54 dependent expression of the FleQ regulon. However an NtrC mutant with a deletion in the DNA binding domain was also reported to show the same evolved genotype. Hence, it is important to establish details of the mechanism by which these NtrB mutations promote transcription of the flagella operon. How well does NtrC-P recognise the FleQ consensus sequence and relative importance of sigma 54 binding to recognition of the DNA binding site. Promotion of transcription could involve cross-talk of NtrB with a different DNA binding regulator, perhaps one more closely related to FleQ, or an indirect effect on transcription of another regulator included in the *P. fluorescens* SBW25 genome.

It would also be interesting to compare the swimming rate of different mutants directly. Since *P. fluorescens* SBW25 is a PGPB, it would be interesting to investigate the behaviour of the evolved FleQS strains (Group I: FleQS1, FleQS2, and FleQS3) if they swim faster when inoculated into plant-roots. Field studies using these evolved microbes will be necessary to determine their interaction with the microbial community within the rhizosphere and phyllosphere, as this were effectively growing in poor nitrogen conditions (glutamine), although roots are generally rich in glutamine^{133,302}, and these microbes that did not carry an antibiotic resistance gene could be used as a biofertiliser for crops.

P. fluorescens SBW25 is a good model organism for the study of alginate metabolism, as the evolved strains from Group II (FleQS8, FleQS5; Table 6-3) and FleQS6 possessed a mutated *algP1* gene, and it would be interesting to determine the levels of alginate production and if the nitrogen status improved biosynthesis. As FleQS strains demonstrate mutations in the alginate pathway, which are

important biopolymers for the preparation of live microbes as biopesticides, it would be interesting to ascertain if these strains become alginate overproducers and resist desiccation more effectively than wild type strain.

In order to fully understand the impact of the NtrB mutations on nitrogen assimilation, it would also be interesting to determine levels of glutamate dehydrogenase (GDH) and glutamine synthetase (GS) for different nitrogen sources and the adenylation status of GS in response to different nitrogen sources. This approach could identify novel metabolites derived from glutamine that regulate these enzymes and are controlled by changes in cell permeability and/or glycosylation. It is important to understand the impact of the identified mutations related to glycosylation and flagella stability, as well as changes in the thermostability of flagella. As flagellin subunits are triggers for host responses, it is also important to determine if glycosylation patterns of FleQS strains affect their plant-host interactions, virulence, and adhesion and swimming motilities in a viscous medium. FleQS strains should be studied to examine how they colonise plant roots and interact with other plant microbes in the rhizosphere, with a view to their application as biopesticides.

8 Bibliography

1. Weyens N, van der Lelie D, Taghavi S, Vangronsveld J. Phytoremediation: plant–endophyte partnerships take the challenge. *Curr. Opin. Biotechnol.* (2009). **20** (2): 248–254.
2. Bulgarelli D, Schlaeppi K, Spaepen S, Ver Loren van T E, Schulze-Lefert P. Structure and functions of the bacterial microbiota of plants. *Annu. Rev. Plant Biol.* (2013). **64**: 807–838.
3. Yang J, Kloepper J W, Ryu C-M. Rhizosphere bacteria help plants tolerate abiotic stress. *Trends Plant Sci.* (2009). **14** (1): 1–4.
4. Glick B R. Bacteria with ACC deaminase can promote plant growth and help to feed the world. *Microbiol. Res.* (2014). **169** (1): 30–39.
5. Compant S, Clément C, Sessitsch A. Plant growth-promoting bacteria in the rhizo- and endosphere of plants: Their role, colonization, mechanisms involved and prospects for utilization. *Soil Biol. Biochem.* (2010). **42** (5): 669–678.
6. Nadeem S M, Ahmad M, Zahir Z A, Javaid A, Ashraf M. The role of mycorrhizae and plant growth promoting rhizobacteria (PGPR) in improving crop productivity under stressful environments. *Biotechnol. Adv.* (2013). **32** (2): 429-448.
7. Weyens N, van der Lelie D, Taghavi D, Newman L, Vangronsveld J. Exploiting plant-microbe partnerships to improve biomass production and remediation. *Trends Biotechnol.* (2009). **27** (10): 591–598.
8. Ma Y, Prasad M N V, Rajkumar M, Freitas H. Plant growth promoting rhizobacteria and endophytes accelerate phytoremediation of metalliferous soils. *Biotechnol. Adv.* (2011). **29** (2): 248–258.
9. Silby M W, Cerdeño-Tárraga A M, Vernikos G S, Giddens S R, Jackson R W, Preston G M, ...Thomson N R. Genomic and genetic analyses of diversity and plant interactions of *Pseudomonas fluorescens*. *Genome Biology.* (2009). **10** (5): 1-16.
10. Vessey J K. Plant growth promoting rhizobacteria as biofertilizers. *Plant Soil.* (2003). **255** (2): 571–586.
11. Ahemad M, Kibret M. Mechanisms and applications of plant growth promoting rhizobacteria: Current perspective. *J. King Saud Univ. Sci.* (2014). **26** (1): 1–20.
12. Compant S, Duffy B, Nowak J, Cle C, Barka E A. Minireview use of plant growth-promoting bacteria for biocontrol of plant diseases: Principles, mechanisms of action, and future prospects. *Appl. Environ. Microbiol.*(2005). **71** (9): 4951–4959. doi:10.1128/AEM.71.9.4951.
13. Grandlic C J, Mendez M O, Chorover J, Machado B, Maier R M. Plant growth-promoting bacteria for phytostabilization of mine tailings. *Environ. Sci. Technol.* (2008). **42** (6): 2079–2084.

14. Khan M R, Brien E O, Carney B F, Doohan F M. A fluorescent pseudomonad shows potential for the control of net blotch disease of barley. *Biological Control*. (2010). **54** (1): 41–45.
15. de-Bashan L E, Hernández J P, Bashan Y. The potential contribution of plant growth-promoting bacteria to reduce environmental degradation –A comprehensive evaluation. *Appl. Soil Ecol.* (2012). **61** (2012): 171–189.
16. Glick B R. Plant growth-promoting bacteria: Mechanisms and applications. *Scientifica*. (2012). **2012**: 1-15. doi: 10.6064/2012/963401.
17. Silby M W, Winstanley C, Godfrey S A C, Levy S B, Jackson R W. *Pseudomonas* genomes: Diverse and adaptable. *FEMS Microbiol. Rev.* (2011). **35** (4): 652–680.
18. Garrity G M, Bell J A, Lilburn. Order IX Pseudomonadales. (1984) In D J, Krieg, N R & Staley, J T (Eds.), *Bergey manual of systematic bacteriology, the proteobacteria, part B: The Gammaproteobacteria*. (Vol. 2, pp. 323-378). Berlin, Heidelberg: Springer.
19. Bossis E, Lemanceau P, Latour X, Gardan L. The taxonomy of *Pseudomonas fluorescens* and *Pseudomonas putida*: Current status and need for revision. *Agronomie*. (2000). **20** (1): 51-63.
20. Weller D. Biological control of soilborne plant pathogens in the rhizosphere with bacteria. *Ann. Rev. Phytopathol.* (1988). **26**: 379–407.
21. Kersters K, Ludwig W, Vancanneyt M, DE vos P, Gillis M, Schleifer K H. Recent changes in the classification of the *Pseudomonads*: An overview. *Syst. Appl. Microbiol.* (1996). **19** (4): 465–477.
22. Moorel E R B, Maul M, Arnscheidt A, Bottger E C, Hutson R A, Collins M D,... Timmis K N. The determination and comparison of the 16S rRNA gene sequences of species of the genus *Pseudomonas* (sensu stricto) and estimation of the natural intrageneric relationships. *Syst. Appl. Microbiol.* (1996). **19** (4): 478–492.
23. Goldman E, Green L H (Eds.). *Practical handbook of microbiology*. (2015). Boca Raton, FL: CRC Press.
24. Ping L, Birkenbeil J, Monajembashi S. Swimming behavior of the monotrichous bacterium *Pseudomonas fluorescens* SBW25. *FEMS Microbiol. Ecol.* (2013). **86** (1): 36–44.
25. Gross H, Loper J E. Genomics of secondary metabolite production by *Pseudomonas* spp. *Nat. Prod. Rep.* (2009). **26** (11): 1408-1446.
26. Liu Y, Gokhale C S, Rainey P B, Zhang X-X. Unravelling the complexity and redundancy of carbon catabolic repression in *Pseudomonas fluorescens* SBW25. *Mol. Microbiol.* (2017). **105** (4): 589-605.
27. Rojo F. Carbon catabolite repression in *Pseudomonas*: Optimizing metabolic versatility and interactions with the environment. *FEMS Microbiol. Rev.* (2010). **34** (5): 658–684.
28. Chakravarty S, Anderson G G. New Aspects of *Pseudomonas* Biology. (2015) In J L Ramos, J B Goldberg, A. Filloux (Eds.), *Pseudomonas* (Vol. 7), Berlin, Heidelberg: Springer.

29. Garrido-Sanz D, Meier-Kolthoff J P, Göker M, Martín M, Rivilla R, Redondo-Nieto M. Genomic and genetic diversity within the *Pseudomonas fluorescens* complex. PLoS One. (2016). **11** (2): e0150183. doi: 10.1371/journal.pone.0150183.
30. Scher F M, Kloepper J W. Colonization of soybean roots by *Pseudomonas* and *Serratia* species: Relationship to bacterial motility, chemotaxis, and generation time. Phytopathology. (1988). **78** (8): 1055–1059.
31. Peix A, Ramírez-Bahena M H, Velázquez E. Historical evolution and current status of the taxonomy of genus *Pseudomonas*. Infect. Genet. Evol. (2009). **9** (6): 1132–1147.
32. Palleroni N J. Prokaryote taxonomy of the 20th century and the impact of studies on the genus *Pseudomonas*: A personal view. Microbiology. (2003). **149**: 1–7.
33. Gomila M, Peña A, Mulet M, Lalucat J, García-Valdés E. Phylogenomics and systematics in *Pseudomonas*. Front. Microbiol. (2015). **6** (214): 1–13.
34. Yamamoto S, Kasai H, Arnold D L, Jackson R W, Vivian A, Harayama S. Phylogeny of the genus *Pseudomonas*: Intrageneric structure reconstructed from the nucleotide sequences of *gyrB* and *rpoD* genes. Microbiology. (2000). **146** (10): 2385–2394.
35. Palleroni N J. The *Pseudomonas* story. Environ. Microbiol. (2010). **12** (6): 1377–1383.
36. Scales B S, Dickson R P, Lipuma J J, Huffnagle G B. Microbiology, genomics, and clinical significance of the *Pseudomonas fluorescens* species complex, an unappreciated colonizer of humans. Clin. Microbiol. Rev. (2014). **27** (4): 927–948.
37. Loper J E, Hassan, K A, Mavrodi D V, Davis, E W, Lim, C K, Shaffer, B. T,... Paulsen T. Comparative genomics of plant-associated *Pseudomonas* spp: Insights into diversity and inheritance of traits involved in multitrophic interactions. PLoS Genet. (2012). **8** (7): 1-27.
38. Rainey P B, Bailey M J. Physical and genetic map of the *Pseudomonas fluorescens* SBW25 chromosome. Mol. Microbiol. (1996). **19** (3): 521–533.
39. Preston G M, Bertrand N, Rainey P B. Type III secretion in plant growth-promoting *Pseudomonas fluorescens* SBW25. Mol. Microbiol. (2001). **41**: 999–1014.
40. Weller D M, Raaijmakers J M, Gardener B B M, Thomashow L S. Microbial populations responsible for specific soil suppressiveness to plant pathogens. Annu. Rev. Phytopathol. (2002). **40**: 309–348.
41. Weller D M, Landa B B, Mavrodi O V, Schroeder K L, De La Fuente L, Blouin Bankhead S,... Thomashow L S. Role of 2,4-diacetylphloroglucinol-producing fluorescent *Pseudomonas* spp in the defense of plant roots. Plant Biol. (2007). **9** (1): 4–20.
42. Cheng X, de Bruijn I, van der Voort M, Loper J E, Raaijmakers J M. The *Gac* regulon of *Pseudomonas fluorescens* SBW25. Environ. Microbiol. Rep. (2013). **5** (4): 608–619.

43. Roongsawang N, Washio K, Morikawa M. Diversity of nonribosomal peptide synthetases involved in the biosynthesis of lipopeptide biosurfactants. *Int. J. Mol. Sci.* (2011). **12** (1): 141–172.
44. Maleki S, Almaas E, Zotchev S, Valla S, Ertesvåg H. Alginate biosynthesis factories in *Pseudomonas fluorescens*: Localization and correlation with alginate production level. *Appl. Environ. Microbiol.* (2016). **82** (4): 1227–1236.
45. Spiers A J, Bohannon J, Gehrig S M, Rainey P B. Biofilm formation at the air-liquid interface by the *Pseudomonas fluorescens* SBW25 wrinkly spreader requires an acetylated form of cellulose. *Mol. Microbiol.* (2003). **50** (1): 15–27.
46. Trippe K, McPhail K, Armstrong D, Azevedo M, Banowetz G. *Pseudomonas fluorescens* SBW25 produces furanomyacin, a non-proteinogenic amino acid with selective antimicrobial properties. *BMC Microbiol.* (2013). **13** (111): 1-10.
47. Gal M, Preston G M, Massey R C, Spiers A J, Rainey P B. Genes encoding a cellulosic polymer contribute toward the ecological success of *Pseudomonas fluorescens* SBW25 on plant surfaces. *Mol. Ecol.* (2003). **12** (11): 3109–3121.
48. Jackson R W, Preston G M, Rainey P B. Genetic characterization of *Pseudomonas fluorescens* SBW25 *rsp* gene expression in the phytosphere and in vitro. *J. Bacteriol.* (2005). **187** (24): 8477–8488.
49. Vinatzer B A, Jelenska J, Greenberg J T. Bioinformatics correctly identifies many type III secretion substrates in the plant pathogen *Pseudomonas syringae* and the biocontrol isolate *P. fluorescens* SBW25. *Mol. Plant-Microbe Interact.* (2005). **18** (8): 877–888.
50. Portaliou A G, Tsolis K C, Loos M S, Zorzini V, Economou A. Type III secretion: building and operating a remarkable nanomachine. *Trends Biochem. Sci.* (2016). **41** (2): 175-189.
51. Puhar A, Sansonetti P J. Type III secretion system. *Curr. Biol.* (2014). **24** (17): R784-R791.
52. Mazurier S, Merieau A, Bergeau D, Decoin V, Sperandio D, Crépin A, ...Latour X. Type III secretion system and virulence markers highlight similarities and differences between human- and plant-associated pseudomonads related to *Pseudomonas fluorescens* and *P. putida*. *Appl. Environ. Microbiol.* (2015). **81** (7): 2579–2590.
53. Lang S. Biological amphiphiles (microbial biosurfactants). *Curr. Opin. Colloid Interface Sci.* (2002). **7** (1-2): 12–20.
54. Bonnichsen L, Bygvraa Svenningsen N, Rybtke M, de Bruijn I, Raaijmakers J M, Tolker-Nielsen T, Nybroe O. Lipopeptide biosurfactant viscosin enhances dispersal of *Pseudomonas fluorescens* SBW25 biofilms. *Microbiol.* (2015). **161** (12): 2289–2297.
55. Elliott K T, Cuff L E, Neidle E L. Copy number change: evolving views on gene amplification. *Future Microbiol.* (2013). **8** (7): 887-899.

56. Laycock M V, Hildebrand P D, Thibault P, Walter J A, Wright J L C. Viscosin, a potent peptidolipid biosurfactant and phytopathogenic mediator produced by a pectolytic strain of *Pseudomonas fluorescens*. *J. Agric. Food Chem.* (1991). **39** (3): 483–489.
57. Fechtner J, Koza A, Sterpaio P Dello, Hapca S M, Spiers A J. Surfactants expressed by soil pseudomonads alter local soil-water distribution, suggesting a hydrological role for these compounds. *FEMS Microbiol. Ecol.* (2011). **78** (1): 50–58.
58. Mazzola M, De Bruijn I, Cohen M F, Raaijmakers, J M. Protozoan- induced regulation of cyclic lipopeptide biosynthesis is an effective predation defense mechanism for *Pseudomonas fluorescens*. *Appl. Environ. Microbiol.* (2009). **75** (21): 6804–6811.
59. de Bruijn I, Raaijmakers J M. Diversity and functional analysis of LuxR- type transcriptional regulators of cyclic lipopeptide biosynthesis in *Pseudomonas fluorescens*. *Appl. Environ. Microbiol.* (2009). **75** (14): 4753–4761.
60. de Bruijn I, de Kock M J, Yang M, de Waard P, van Beek T A, Raaijmakers J M. Genome-based discovery, structure prediction and functional analysis of cyclic lipopeptide antibiotics in *Pseudomonas* species. *Mol. Microbiol.* (2007). **63**: 417–428.
61. Motta S S, Cluzel P, Aldana M. Adaptive resistance in bacteria requires epigenetic inheritance, genetic noise, and cost of efflux pumps. *PLoS One.* (2015). **10** (3): 1-18.
62. Challis G L, Naismith J H. Structural aspects of non-ribosomal peptide biosynthesis. *Curr. Opin. Struct. Biol.* (2004). **14**: 748–756.
63. Smith T G, Hoover T R. Deciphering bacterial flagellar gene regulatory networks in the genomic era. *Adv. Appl. Microbiol.* (2009). **67**: 257-295.
64. Gerhardson B. Biological substitutes for pesticides. *Trends Biotechnol.* (2002). **20** (8): 338–343.
65. Lefèvre C T, Bennet M, Landau L, Vach P, Pignol D, Bazylnski D A, ...Faivre D. Diversity of magneto-aerotactic behaviors and oxygen sensing mechanisms in cultured magnetotactic bacteria. *Biophysical Journal.* (2014). **107** (2): 527–538.
66. Simons M, Permentier H P, De Weger L, Wijffelman, C, Ben J. J. Amino acid synthesis is necessary for tomato root colonization by *Pseudomonas fluorescens* strain. *Mol. Plant. Microbe. Interact.* (1997). **10** (1): 102–106.
67. Hol W H G, Bezemer T M, Biere A. Getting the ecology into interactions between plants and the plant growth-promoting bacterium *Pseudomonas fluorescens*. *Front. Plant Sci.* (2013). **4** (81): 1-9.
68. Turnbull G A, Morgan J A W, Whipps J M, Saunders J R. The role of motility in the in vitro attachment of *Pseudomonas putida* PaW8 to wheat roots. *FEMS Microbiol. Ecol.* (2001). **35**: 57–65.

69. de Weger L A, van der Vlugt C I, Wijffjes A H, Bakker P A, Schippers B, Lugtenberg B. Flagella of a plant-growth-stimulating *Pseudomonas fluorescens* strain are required for colonization of potato roots. *J. Bacteriol.* (1987). **169** (6): 2769–2773.
70. de Weert S, Vermeiren H, Mulders I H, Kuiper I, Hendrickx N, Bloemberg G V,...Lugtenberg B J. Flagella-driven chemotaxis towards exudate components is an important trait for tomato root colonization by *Pseudomonas fluorescens*. *Mol. Plant. Microbe. Interact.* (2002). **15** (11): 1173–1180.
71. Howie W J, Cook R J, Weller, D M. Effects of soil matric potential and cell motility on wheat root colonization by fluorescent pseudomonads suppressive to take-all. *Phytopathology.* (1987). **77**: 286–292.
72. Lugtenberg B J, Dekkers L, Bloemberg G V. Molecular determinants of rhizosphere colonization by *Pseudomonas*. *Annu. Rev. Phytopathol.* (2001). **39** (1): 461-490.
73. Rodríguez-Navarro D N, Dardanelli M S, Ruíz-Saínz J E. Attachment of bacteria to the roots of higher plants. *FEMS Microbiol. Lett.* (2007). **272** (2): 127–136.
74. Brennan C A, Hunt J R, Kremer N, Krasity B C, Apicella M A, McFall-Ngai M J,... Ruby E G. A model symbiosis reveals a role for sheathed-flagellum rotation in the release of immunogenic lipopolysaccharide. *eLife.* (2014). **3** (e01579): 1–11. doi:10.7554/eLife.01579.
75. Soutourina O A, Bertin P N. Regulation cascade of flagellar expression in Gram-negative bacteria. *FEMS Microbiol. Rev.* (2003). **27**: 505–523.
76. Sampedro I, Parales R E, Krell T, Hill J E. *Pseudomonas* chemotaxis. *FEMS Microbiol. Rev.* (2015). **39** (1):17-46. doi:10.1111/1574-6976.12081.
77. Jarrell K F, McBride M J. The surprisingly diverse ways that prokaryotes move. *Nat. Rev. Microbiol.* (2008). **6** (6): 466–476.
78. Nogales J, Vargas P, Farias G A, Olmedilla A. FleQ coordinates flagellum-dependent and independent motilities. *Appl. Environ. Microbiol.* (2015). **81** (21): 7533–7545.
79. Lu A, Cho K, Black W P, Duan X Y, Lux R, Yang Z,...Shi W. Exopolysaccharide biosynthesis genes required for social motility in *Myxococcus xanthus*. *Mol. Microbiol.* (2005). **55** (1): 206–220.
80. Miller M B, Bassler B L. Quorum sensing in bacteria. *Annu. Rev. Microbiol.* (2001). **55** (1): 165-199.
81. Schuster M, Sexton D J, Hense B A. Why quorum sensing controls private goods. *Front. Microbiol.* (2017). **8** (885): 1–16.
82. Szurmant H, Ordal G W. Diversity in chemotaxis mechanisms among the bacteria and Archaea. *Microbiol. Mol. Biol. Rev.*(2004). **68** (2): 301–319.
83. Daniels R, Vanderleyden J, Michiels J. Quorum sensing and swarming migration in bacteria. *FEMS Microbiol. Rev.* (2004). **28** (3): 261–289.
84. Turnbull G. The role of motility in the in vitro attachment of *Pseudomonas putida* PaW8 to wheat roots. *FEMS Microbiol. Ecol.* (2001). **35** (1): 57–65.

85. Harshey R M. Bacterial motility on a surface: many ways to a common goal. *Annu. Rev. Microbiol.* (2003). **57**: 249–73.
86. Yang P, Dirk van Elsas Jan. Mechanisms and ecological implications of the movement of bacteria in soil. *Applied Soil Ecology.* (2018). **129**: 112-120.
87. Zhao X, Norris S J, Liu J. Molecular architecture of bacterial flagellar motor in cells. *Biochemistry.* (2014). **53** (27): 4323–4333.
88. Altegoer F, Schuhmacher J, Pausch P, Bange G. From molecular evolution to biobricks and synthetic modules: A lesson by the bacterial flagellum. *Biotechnol. Genet. Eng. Rev.* (2014). **30** (1): 49–64.
89. Raaijmakers J M, de Bruijn I, de Kock M J D. Cyclic lipopeptide production by plant-associated *Pseudomonas* spp.: Diversity, activity, biosynthesis, and regulation. *Molecular Plant-Microbe Interactions.* (2006). **19** (7): 699–710
90. Ferrández A, Hawkins A C, Summerfield D T, Harwood C S. Cluster II *che* genes from *Pseudomonas aeruginosa* are required for an optimal chemotactic response. *J. Bacteriol.* (2002). **184** (16): 4374–4383.
91. Chanchal, Banerjee P, Jain D. ATP-induced structural remodeling in the antiactivator FleN enables formation of the functional dimeric form. *Structure.* (2017). **25** (2): 243–252.
92. Baraquet C, Murakami K, Parsek M R, Harwood C S. The FleQ protein from *Pseudomonas aeruginosa* functions as both a repressor and an activator to control gene expression from the *pel* operon promoter in response to c-di-GMP. *Nucleic Acids Res.* (2012). **40** (15): 7207–18.
93. Tart A H, Blanks M J, Wozniak D J. The AlgT-dependent transcriptional regulator AmrZ (AlgZ) inhibits flagellum biosynthesis in mucoid, nonmotile *Pseudomonas aeruginosa* cystic fibrosis isolates. *J. Bacteriol.* (2006). **188** (18): 6483–6489.
94. Burrows L L. *Pseudomonas aeruginosa* twitching motility: Type IV pili in action. *Annu. Rev. Microbiol.* (2012). **66**: 493–520.
95. Vesper S J. Production of pili (fimbriae) by *Pseudomonas fluorescens* and correlation with attachment to corn roots. *Appl. Environ. Microbiol.* (1987). **53** (7): 1397–1405.
96. Maier B, Wong G C L. How bacteria use type IV pili machinery on surfaces. *Trends Microbiol.* (2015). **23** (12): 775–788.
97. Dasgupta N, Ferrell E P, Kanack K J, West S E H, Ramphal R. FleQ, the gene encoding the major flagellar regulator of *Pseudomonas aeruginosa*, is 70 dependent and is downregulated by *vfr*, a homolog of *Escherichia coli* cyclic AMP receptor protein. *J. Bacteriol.* (2002). **184**: 5240–5250.
98. Baraquet C, Harwood C S. FleQ DNA binding consensus sequence revealed by studies of *fleQ*- dependent regulation of biofilm gene expression in *Pseudomonas aeruginosa*. *J. Bacteriol.* (2016). **198** (1): 178–186.
99. Baraquet C, Harwood C S. Cyclic diguanosine monophosphate represses bacterial flagella synthesis by interacting with the Walker A motif of the enhancer-binding protein FleQ. *PNAS. U. S. A.* (2013). **110** (46): 18478–18483.

100. Jyot J, Dasgupta N, Ramphal R. FleQ, the major flagellar gene regulator in *Pseudomonas aeruginosa*, binds to enhancer sites located either upstream or atypically downstream of the RpoN binding site. *J. Bacteriol.* (2002). **184**: 5251–5260.
101. Bush M, Dixon R. The role of bacterial enhancer binding proteins as specialized activators of σ^{54} -dependent transcription. *Microbiol. Mol. Biol. Rev.* (2012). **76**: 497–529.
102. Adam M, Murali B, Glenn N O, Potter S S. Epigenetic inheritance based evolution of antibiotic resistance in bacteria. *BMC Evol. Biol.* (2008). **8** (52): 1-12.
103. Fazli M, Almlad H, Rybtke M L, Givskov M, Eberl L, Tolker-Nielsen T. Regulation of biofilm formation in *Pseudomonas* and *Burkholderia* species. *Environ. Microbiol.* (2014). **16** (7): 1961–1981.
104. Kazmierczak, Barbara I, Hendrixson, David R. Spatial, numerical regulation of flagellar biosynthesis in polarly-flagellated bacteria. *Mol. Microbiol.* (2013). **88** (4): 655–663.
105. Studholme D J, Dixon R. Domain architectures of sigma54-dependent transcriptional activators. *J. Bacteriol.* (2003). **185** (6): 1757–1767.
106. Guttenplan S B, Kearns D B. Regulation of flagellar motility during biofilm formation. *FEMS Microbiol. Rev.* (2014). **37** (6): 849–871.
107. Alsohim A S, Taylor T B, Barrett G A, Gallie J, Zhang X X, Altamirano-Junqueira A E, Johnson L J,... Jackson R W. The biosurfactant viscosin produced by *Pseudomonas fluorescens* SBW25 aids spreading motility and plant growth promotion. *Environ. Microbiol.* (2014). **16** (7): 2267–2281.
108. Taylor T B, Mulley G, Dills A H, Alsohim A S, McGuffin L J, Studholme D J,... Jackson R W. Evolutionary resurrection of flagellar motility via rewiring of the nitrogen regulation system. *Science.* (2015). **344** (6225): 1014–1017.
109. Alsohim A. (2010). *Characterization of bacterial genes involved in motility, plant colonization and plant growth promotion* (Unpublished doctoral dissertation). University of Reading, Reading, United Kingdom.
110. Kussell E. Evolution in microbes. *Annu. Rev. Biophys.* (2013). **42**: 493–514.
111. Gabaldón T, Koonin E V. Functional and evolutionary implications of gene orthology. *Nat. Rev. Genet.* (2013). **14** (5): 360–366.
112. Dasgupta N, Arora S K, Ramphal R. *fleN*, a gene that regulates flagellar number in *Pseudomonas aeruginosa*. *J. Bacteriol.* (2000). **182** (2): 357–364.
113. Soutourina O A, Semenova E A, Parfenova V V, Danchin A, Bertin P. Control of bacterial motility by environmental factors in polarly flagellated and peritrichous bacteria isolated from lake Baikal. *Applied and Environmental Microbiology.* (2001). **67** (9): 3852-3859. doi:10.1128/AEM.67.9.3852.
114. Zapras A, Hoffmann T, Wünsche G, Flórez L A, Stülke J, Bremer E. Mutational activation of the RocR activator and of a cryptic *rocDEF* promoter bypass loss of the initial steps of proline biosynthesis in *Bacillus subtilis*. *Environ. Microbiol.* (2014). **16** (3): 701–717.

115. White D, Drummond J, Fuqua C. (2012). The physiology and biochemistry of prokaryotes. New York, NY: Oxford University Press.
116. Marijuán P C, Navarro J, del Moral R. On prokaryotic intelligence: strategies for sensing the environment. *Biosystems*. (2010). **99** (2): 94–103.
117. Khorchid A, Ikura M. Bacterial histidine kinase as signal sensor and transducer. *Int. J. Biochem. Cell Biol.* (2006). **38** (3): 307–312.
118. Rapoport G. Novel regulatory protein controlling arginine utilization in *Bacillus subtilis*, belongs to the NtrC/NifA family of transcriptional activators. *J. Bacteriol.* (1994). **176** (5): 1234–1241.
119. Gardan R, Rapoport G, Débarbouillé M. Role of the transcriptional activator RocR in the arginine-degradation pathway of *Bacillus subtilis*. *Mol. Microbiol.* (1997). **24** (4): 825–837.
120. Reitzer L. Amino acid synthesis. (2009) In *Encyclopedia of Microbiology* (3rd ed., pp. 1-17). New York, NY: Academic Press Books.
121. Pelton J G, Kustu S, Wemmer D E. Solution structure of the DNA-binding domain of NtrC with three alanine substitutions. *J. Mol. Biol.* (1999). **292** (5): 1095–1110.
122. Szurmant H, Ordal G W. Diversity in chemotaxis mechanisms among the Bacteria and Archaea. *Microbiol. Mol. Biol. Rev.* (2004). **68** (2): 301–319.
123. Bi S, Lai L. Bacterial chemoreceptors and chemoeffectors. *Cell. Mol. Life Sci.* (2015). **72** (4): 691–708.
124. Seshasayee A S, Bertone P, Fraser, G M, Luscombe N M. Transcriptional regulatory networks in bacteria: from input signals to output responses. *Curr. Opin. Microbiol.* (2006). **9** (5): 511–519.
125. Rojo F. Carbon catabolite repression in *Pseudomonas*: Optimizing metabolic versatility and interactions with the environment. *FEMS Microbiol. Rev.* (2010). **34** (5): 658–684.
126. Moreno R, Rojo F. The target for the *Pseudomonas putida* Crc global regulator in the benzoate degradation pathway is the BenR transcriptional regulator. *J. Bacteriol.* (2008). **190** (5): 1539–1545.
127. Amador C I, Canosa I, Govantes F, Santero E. Lack of CbrB in *Pseudomonas putida* affects not only amino acids metabolism but also different stress responses and biofilm development. *Environ. Microbiol.* (2010). **12** (6): 1748–1761.
128. Sonnleitner E, Abdou L, Haas D. Small RNA as global regulator of carbon catabolite repression in *Pseudomonas aeruginosa*. *PNAS*. (2009). **106** (51): 21866–21871.
129. Lessie T G, Phibbs P V. Alternative pathways of carbohydrate utilization in pseudomonads. *Annu. Rev. Microbiol.* (1984). **38**: 359–387.
130. Spiers A J, Rainey P B. The *Pseudomonas fluorescens* SBW25 wrinkly spreader biofilm requires attachment factor, cellulose fibre and LPS interactions to maintain strength and integrity. *Microbiology*. (2005). **151** (9): 2829–2839.

131. Hall J P, Harrison E, Lilley A K, Paterson S, Spiers A J, Brockhurst M A. Environmentally co-occurring mercury resistance plasmids are genetically and phenotypically diverse and confer variable context-dependent fitness effects. *Environ. Microbiol.* (2015). **17** (12): 5008–5022.
132. Hosie A H F, Poole P S. Bacterial ABC transporters of amino acids. *Res. Microbiol.* (2001). **152**: 259–270.
133. Sonawane A, Klöppner U, Derst C, Röhm K H. Utilization of acidic amino acids and their amides by pseudomonads: Role of periplasmic glutaminase-asparaginase. *Arch. Microbiol.* (2003). **179** (3): 151–159.
134. van Heeswijk W C, Westerhoff H V, Boogerd F C. Nitrogen assimilation in *Escherichia coli*: putting molecular data into a systems perspective. *Microbiol. Mol. Biol. Rev.* (2013). **77** (4): 628–95.
135. Ninfa A J, Atkinson M R. PII signal transduction proteins. *Trends Microbiol.* (2000). **8** (4): 172–179.
136. Arcondéguy T, Jack R, Merrick M, Arconde T. P II Signal transduction proteins, pivotal players in microbial nitrogen control. *Microbiol. Mol. Biol. Rev.* (2001). **65** (1): 80–105.
137. Jiang P, Pioszak A, Atkinson M R, Peliska J A, Ninfa A J. (2003). New Insights into the mechanism of the kinase and phosphatase activities of *Escherichia coli* NRII (NtrB) and their regulation by the PII protein. In *Histidine kinases in signal transduction* (pp. 143-164). New York, NY: Academic Press Books. doi:10.1016/B978-012372484-7/50008-4
138. Leigh J A, Dodsworth J A. Nitrogen regulation in bacteria and archaea. *Annu. Rev. Microbiol.* (2007). **61**: 349–77.
139. Keener J, Kustu S. Protein kinase and phosphoprotein phosphatase activities of nitrogen regulatory proteins NTRB and NTRC of enteric bacteria: Roles of the conserved amino-terminal domain of NTRC. *PNAS.* (1988). **85** (14): 4976–4980.
140. Magasanik B. PII: A remarkable regulatory protein. *Trends Microbiol.* (2000). **8** (10): 447–448.
141. Huergo L F, Chandra G, Merrick M. PII signal transduction proteins: Nitrogen regulation and beyond. *FEMS Microbiol. Rev.* (2013). **37** (2): 251–283.
142. Giddens S R, Jackson R W, Moon C D, Jacobs M A, Zhang X X, Gehrig S M, Rainey P B. Mutational activation of niche-specific genes provides insight into regulatory networks and bacterial function in a complex environment. *PNAS.* (2007). **104** (46): 18247–18252.
143. Bailey M J, Lilley A K, Thompson I P, Rainey P B, Ellis R J. Site directed chromosomal marking of a fluorescent pseudomonad isolated from the phytosphere of sugar beet; stability and potential for marker gene transfer. *Mol. Ecol.* (1995). **4** (6): 755–763.
144. Kovach M E, Elzer P H, Hill D S, Robertson G T, Farris M A, Roop II R M, Peterson K M. Four new derivatives of the broad-host-range cloning vector pBBR1MCS, carrying different antibiotic-resistance cassettes. *Gene.* (1995). **166** (1): 175–176.

145. Grossart H, Steward G F, Martinez J. A simple, rapid method for demonstrating bacterial flagella. *Appl. Environ Microbiol.* (2000). **66** (8): 3632–3636.
146. Murray T S, Kazmierczak B I. FlhF is required for swimming and swarming in *Pseudomonas aeruginosa*. *J. Bacteriol.* (2006). **188** (19): 6995–7004.
147. Tyler, B. Regulation of the assimilation of nitrogen compounds. *Annu. Rev. Biochem.* (1978). **47**: 1127-1162.
148. Sonawane A, Klöppner, U, Hövel, S, Völker, U, Röhm K.H. Identification of *Pseudomonas* proteins coordinately induced by acidic amino acids and their amides: A two-dimensional electrophoresis study. *Microbiology.* (2003). **149**: 2909–2918.
149. Pioszak A A, Ninfa A J. Mutations altering the N-terminal receiver domain of NRI (NtrC) that prevent dephosphorylation by the NRII-Pil complex in *Escherichia coli*. *J. Bacteriol.* (2004). **186** (17): 5730–5740.
150. Hüser A, Klöppner U, Röhm K H. Cloning, sequence analysis, and expression of *ansB* from *Pseudomonas fluorescens*, encoding periplasmic glutaminase/asparaginase. *FEMS Microbiol. Lett.* (1999). **178** (2): 327–335.
- 151 Taguchi F, Shibata S, Suzuki T, Ogawa Y, Aizawa S I, Takeuchi K, Ichinose Y. Effects of glycosylation on swimming ability and flagellar polymorphic transformation in *Pseudomonas syringae* pv. *tabaci* 6605. *J. Bacteriol.* (2008). **190** (2): 764-768.
- 152 Mayr E. *What Evolution is.* (2001). New York, NY: Basic Books.
- 153 Battista J R, Earl, A M. Mutagenesis and DNA repair: the consequences of error and mechanisms for remaining the same. (2004) In Robert V Miller, Martin J Day (Eds.), *Microbial evolution: Gene establishment, survival and exchange.* (2nd edition, pp. 3-20). Washington, WA: ASM Press.
- 154 Drake J. A constant rate of spontaneous mutation in DNA-based microbes. *PNAS.* (1991). **88** (16): 7160-7164.
- 155 Radman M. Fidelity and infidelity. *Nature.* (2001). **413** (6852): 115.
- 156 Luria S E, Delbrück M. Mutations of bacteria from virus sensitivity to virus resistance. *Genetics.* (1943). **28** (6): 491–511.
- 157 Swings T, Van den Bergh B, Wuyts S, Oeyen E, Voordeckers K, Verstrepen K J,... Michiels J. Adaptive tuning of mutation rates allows fast response to lethal stress in *Escherichia coli*. *eLife.* (2017). **6** (e22939): 1-24. doi: 10.7554/eLife.22939.
- 158 Celina J. A new look at adaptative mutations in bacteria. *Acta Biochimica Polonica.* (2000). **47** (2): 451-457.
- 159 Cairns J, Overbaugh J, Miller S. The origin of mutants. *Nature.* (1988). **335**: 142-145.
- 160 Hall, B G. Spontaneous point mutations that occur more often when advantageous than when neutral. *Genetics.* (1990). **126** (1): 5-16.
- 161 Poole A M, Phillips, M J, Penny, D. Prokaryote and eukaryote evolvability. *BioSystems.* (2003). **69**: 163–185.

- 162 Shapiro J. Adaptive mutation: Who's really in the garden? *Science*. (1995). **268**: 373-374.
- 163 Radicella J P, Park P U. Fox, M. S. Adaptive mutation in *Escherichia coli*: A role for conjugation. *Science*. (1995). **268** (5209): 418-420.
- 164 Benson S A. Is bacterial evolution random or selective? *Nature*. (1988). **336** (6194): 21-22.
- 165 Lenski R E. The direct mutation controversy and neo-darwinism. *Science*. (1993). **259** (5092): 188-194.
- 166 Anderson D I, Hughes D. Gene amplification and adaptative evolution in bacteria. *Annu. Rev. Genet.* (2009). **43**: 167-195.
- 167 Roth R J, Kugelberg E, Reams A B, Kofoed E. Origin of mutations under selection: The adaptive mutation controversy. *Annu. Rev. Microbiol.* (2006). **60**: 477–501.
- 168 Hervás A B, Canosa I, Santero E. Regulation of glutamate dehydrogenase expression in *Pseudomonas putida* results from its direct repression by NtrC under nitrogen-limiting conditions. *Mol. Microbiol.* (2010). **78** (2): 305–319.
- 169 Merrick M J, Edwards, R A. Nitrogen control in bacteria. *Microbiological Reviews*. (1995). **59** (4): 604-622.
- 170 Huergo L F, Dixon R. The emergence of 2-oxoglutarate as a master regulator metabolite. *Microbiol. Mol. Biol. Rev.* (2015). **79** (4):419-435.
- 171 Hervas A B, Canosa I, Little R, Dixon R, Santero, E. NtrC-Dependent regulatory network for nitrogen assimilation in *Pseudomonas putida*. *J. Bacteriol.* (2009). **191** (19): 6123-6135.
- 172 Ninfa A J, Jiang P, Atkinson M R, Peliska J A. Integration of antagonistic signals in the regulation of nitrogen assimilation in *Escherichia coli*. *Current Topics in Cellular Regulation*. (2000). **35**: 31-75.
- 173 Rombel I, North A, Hwang I, Wyman C, Kustu S. The bacterial enhancer-binding protein NtrC as a molecular machine. (1998) In *Cold Spring Harbor Symposia on Quantitative Biology* (Vol. 63, pp.157-166). Long Island, NY: Cold Spring Harbor Laboratory Press.
- 174 Wei L, Chung-Dar L. Regulation of carbon and nitrogen utilization by CbrAB and NtrBC two-component systems in *Pseudomonas aeruginosa*. *J. Bacteriol.* (2007). **189** (15): 5413–5420.
- 175 Zhang X-X, Rainey P B. Dual involvement of CbrAB and NtrBC in the regulation of histidine utilization in *Pseudomonas fluorescens* SBW25. *Genetics*. (2008). **178**: 185–195.
- 176 Ferro-Luzzi G, Nikaido K. Nitrogen regulation in *Salmonella typhimurium*: Identification of an *ntrC* protein-binding site and definition of a consensus binding sequence. *EMBO Journal*. (1985). **4** (2): 539-547.
- 177 Meye, J M, Stadtman E. R. Glutamine synthetase of pseudomonads: Some biochemical and physicochemical properties. *J. Bacteriol.* (1981). **146** (2): 705-712.

- 178 Nelson D L, Cox, M M. (2013). *Lehninger principles of*. (6th edition). New York, NY: W.H. Freeman.
- 179 Su T, Liu S, Wang K, Chi K, Zhu D, Wei T,... Gu L. The REC domain mediated dimerization is critical for FleQ from *Pseudomonas aeruginosa* to function as a c-di-GMP receptor and flagella gene regulator. *Journal of Structural Biology*. (2015). **192**: 1-13.
- 180 Jenal U, Reinders A, Lori C. Cyclic di-GMP: Second messenger extraordinaire. *Nat. Rev. Microbiol.* (2017). **15**: 271-284.
- 181 Barahona E, Navazo A, Garrido-Sanz D, Muriel C, Martínez-Granero F, Redondo-Nieto M,... Rivilla R. *Pseudomonas fluorescens* F113 can produce a second flagellar apparatus, which is important for plant root colonization. *Frontiers in Microbiology*. (2016). **7** (1471): 1-12.
- 182 Evans L D B, Hughes C, Fraser, G M. Building a flagellum outside the bacterial cell. *Trends Microbiol.* (2014). **22** (10): 566-572.
- 183 Ryan M. (2014). *Calculus for dummies*. (2nd editon). New Jersey, NY:John Willey & Sons.
- 184 Harris D C. (2016). *Quantitative chemical analysis*. (9th edition). New York, NY: W. H. Freeman & Company.
- 185 Berg H C. Chemotaxis in bacteria. *Annu. Rev. Biophys.* (1975). **4**: 119-136.
- 186 Kato J. (2008). *Pseudomonas* motility and chemotaxis. In Bernd H A Rehm (Ed.) *Pseudomonas* model organism, pathogen, cell factory (pp. 109-128). Weinheim, Germany: Wiley-VCH.
- 187 Harshey R M, Partridge J D. Shelter in a swarm. *J. Mol. Biol.* (2015). **427** (23): 3683–3694.
- 188 Sambrook J, Green, M R. (2012). *Molecular cloning: A laboratory manual*. (4th edition). Long Island, NY: Cold Spring Harbor Laboratory Press.
- 189 Macnab R. Examination of bacterial flagellation by dark-field microscopy. *Journal of Clinical Microbiology*.(1976). **4** (3): 258-265.
- 190 Adler J A. Method for measuring chemotaxis and use of the method to determine optimum conditions for chemotaxis by *Escherichia coli*. *Journal of General Microbiology*. (1973). **74**: 77-91.
- 191 Henrichsen J, Bacterial surface translocation: A survey and a classification. *Bacteriological Reviews*. (1972). **36** (4): 478-503.
- 192 Swiecicki J M, Sliusarenko O, Weibel D B. From swimming to swarming: *Escherichia coli* cell motility in two-dimensions. *Integr. Biol. (Camb)*. (2013). **5** (12): 1490–1494.
- 193 Kearns D B. A field guide to bacterial swarming motility. *Nat. Rev. Microbiol.* (2010). **8** (9): 634–644.
- 194 Masduki A, Nakamura J, Ohga T, Umezaki R, Kato J, Ohtake H. Isolation and characterization of chemotaxis mutants and genes of *Pseudomonas aeruginosa*. *J. Bacteriol.* (1995). **177** (4): 948–952.

- 195 Hong C S, Kuroda A, Takiguchi N, Ohtake H, Kato J. Expression of *Pseudomonas aeruginosa aer-2*, one of two aerotaxis transducer genes, is controlled by RpoS. *J. Bacteriol.* (2005). **187** (4): 1533–1535.
- 196 Higa A I, R, De Forchetti Milrad S R, Cazzulo J. J. CO₂-fixing enzymes in *Pseudomonas fluorescens*. *Journal of General Microbiology.* (1976). **93**: 69-74.
- 197 Taylor T B, Mulley G, McGuffin L J, Johnson L J, Brockhurst M A, Arseneault T, Silby M W, Jackson R W. Evolutionary rewiring of bacterial regulatory networks. *Microbial. Cell.* (2015). **2** (7): 256-258.
- 198 Bell G. Evolutionary rescue. *Annu. Rev. Ecol. Evol.* (2017). **48**: 605-627.
- 199 Aertsen A, Michiels C W. Diversity or die: Generation of diversity in response to stress. *Critical Reviews in Microbiology.* (2004). **31**: 69-78.
- 200 Sezonov G, Joseleau-Petit D, D'Ari R. *Escherichia coli* physiology in Luria-Bertani broth. *J. Bacteriol.* (2007). **189** (23): 8746–8749.
- 201 Garneau-Tsodikova S, Labby J K. Mechanisms of resistance to aminoglycoside antibiotics: Overview and perspectives. *MedChemComm.* (2016). **7** (1): 11–27.
- 202 Taguchi F, Suzuki T, Takeuchi K, Inagaki Y, Toyoda K ,... Yuki Ichinose. Glycosylation of flagellin from *Pseudomonas syringae* pv. *tabaci* 6605 contributes to evasion of host tobacco plant surveillance system. *Physiological and Molecular Plant Pathology.* (2009). **74** : 11-17.
- 203 Hitchen P G, Dell A. Bacterial glycoproteomics. *Microbiology.* (2006). **152**: 1575–1580.
- 204 Tan R M, Kuang Z, Hao Y, Lee F, Lee T,...Lau Gee. Type IV pilus glycosylation mediates resistance of *Pseudomonas aeruginosa* to opsonic activities of the pulmonary surfactant protein A. *Infection and Immunity.* (2015). **83** (4): 1339-1346.
- 205 Giddens S R, Jackson RW, Moon CD, Jacobs M A, Zhang X-X, Gehrig S M, Rainey P B. Mutational activation of niche-specific genes provides insight into regulatory networks and bacterial function in a complex environment. *PNAS.* (2007). **104** (46): 18247-18252.
- 206 Winsor G L, Griffiths E J, Lo R, Dhillon B K, Shay J A, Brinkman F S L. Enhanced annotations and features for comparing thousands of *Pseudomonas* genomes in the *Pseudomonas* genome database. *Nucleic Acids Res.* (2016). **44**: D646-D653.
- 207 Sun Y-Y, Chi H, Sun Li. *Pseudomonas fluorescens* filamentous hemagglutinin, an iron-regulated protein, is an important virulence factor that modulates bacterial pathogenicity. *Frontiers in Microbiology.* (2016). **7** (1320): 1-11.
- 208 Janssen D B, Joosten H M L J, Herst P M, Van Der Drift C. Characterization of glutamine-requiring mutants of *Pseudomonas aeruginosa*. *J. Bacteriol.* (1982). **151** (3): 1176-1183.

- 209 Meyer J M. Glutamine synthetase from *Pseudomonas fluorescens*: A tool for studying changes in cell permeability and enzyme regulation. (1985) In Rodney Levine, Ann Ginsburg (Eds.), Current Topics in Cellular Regulation (Vol. 26, pp.150- 161). London, United Kingdom: Academic Press Inc.
- 210 Dasgupta N, Wolfgang M C, Goodman A L, Arora S K, Jyot J, Lory S, Ramphal R. A four-tiered transcriptional regulatory circuit controls flagellar biogenesis in *Pseudomonas aeruginosa*. Mol. Microbiol. (2003). **50** (3): 809–824.
- 211 Spiers, J. A mechanistic explanation linking adaptive mutation, niche change, and fitness advantage for the wrinkly spreader. International Journal of Evolutionary Biology. (2014). **2014** (675432): 1-10.
- 212 Redondo-Nieto M, Barret M, Morrissey J, Germaine K, Martínez-Granero F, Barahona E, Navazo A, Sánchez-Contreras M, Moynihan J A, Muriel C, Dowling D, O’Gara F, Martín M, Rivilla R. Genome sequence reveals that *Pseudomonas fluorescens* F113 possesses a large and diverse array of systems for rhizosphere function and host interaction. BMC Genomics. (2013). **14** (54): 1-17.
- 213 Schmidt J, Müsken M, Becker T, Magnowska Z, Bertinetti D, Möller S, Zimmermann B, Herberg F W, Jänsch L, Häussler S. The *Pseudomonas aeruginosa* chemotaxis methyltransferase CheR1 impacts on bacterial surface sampling. PLoS ONE. (2011). **6** (3): 1-11.
- 214 Baraquet C, Murakami K, Parsek M R, Harwood C S. The FleQ protein from *Pseudomonas aeruginosa* functions as both a repressor and an activator to control gene expression from the *pel* operon promoter in response to c-di-GMP. Nucleic Acids Res. (2012). **40** (15): 7207–7218.
- 215 Robleto E A, López-Hernández I, Silby M W, Levy S B. Genetic analysis of the AdnA regulon in *Pseudomonas fluorescens*: Nonessential role of flagella in adhesion to sand and biofilm formation. J. Bacteriol. (2003). **185** (2): 453-460.
- 216 Arora S K, Ritchings B W, Almira E C, Lory S, Ramphal R. A transcriptional activator, FleQ, regulates mucin adhesion and flagellar gene expression in *Pseudomonas aeruginosa* in a cascade manner. J. Bacteriol. (1997). **179** (17): 5574–5581.
- 217 Baraquet C, Harwood C. Cyclic diguanosine monophosphate represses bacterial flagella synthesis by interacting with the Walker A motif of the enhancer-binding protein FleQ. PNAS. (2013). **110** (46): 18478-18483.
- 218 Jyot J, Dasgupta N, Ramphal R. FleQ, the major flagellar gene regulator in *Pseudomonas aeruginosa*, binds to enhancer sites located either upstream or atypically downstream of the RpoN binding site. J. Bacteriol. (2002). **184** (19): 5251–5260.
- 219 Muriel C, Arrebola E, Redondo-Nieto M, Martínez-Granero F, Jalvo B, Pfeilmeier S, Blanco-Romero E, Baena I, Malone J G, Rivilla R, Martín M. AmrZ is a major determinant of c-di-GMP levels in *Pseudomonas fluorescens* F113. Sci. Rep. (2018). **8** (1): 1-10.

- 220 Matsuyama B Y, Krasteva P V, Baraquet C, Harwood C S, Sondermann H, Navarro M V A S. Mechanistic insights into c-di-GMP– dependent control of the biofilm regulator FleQ from *Pseudomonas aeruginosa*. PNAS. (2016). **113** (2): E209-E2018.
- 221 Valentini M, Filloux A. Biofilms and cyclic di-GMP (c-di-GMP) Signaling: Lessons from *Pseudomonas aeruginosa* and other bacteria. J. Biol. Chem. (2016). **291** (24): 12547–12555.
- 222 Boyd C, O’Toole G A. Second messenger regulation of biofilm formation: Breakthroughs in understanding c-di-GMP effector systems. Annu. Rev. Cell Dev. Biol. (2012). **28**: 439-462.
- 223 Navarro M V A S, Newell P V, Krasteva P V, Chatterjee D, Madden D R, O’Toole G A, Sondermann H. Structural basis for c-di-GMP-mediated inside-out signaling controlling periplasmic proteolysis. PLoS Biol. (2011). **9** (2): e1000588.
- 224 Newell P D, Monds R D, O’Toole G A. LapD is a bis-(3’,5’)-cyclic dimeric GMP-binding protein that regulates surface attachment by *Pseudomonas fluorescens* Pf0–1. PNAS. (2009). **106** (9): 3461-3466.
- 225 Hall B G, Yokoyama S, Calhoun D H. Role of cryptic genes in microbial evolution. Mol. Biol. Evol. (1983). **1** (1): 109-124.
- 226 Tamburini E, Mastromei G. Do bacterial cryptic genes really exist? Res. Microbiol. (2000). **151** (3): 179-182.
- 227 Darmon E, Leach D R F. Bacterial genome instability. Microbiol. Mol. Biol. Rev. (2014). **78** (1): 1-39.
- 228 Barton M D, Petronio M, Giarrizzo J G, . Bowling B V, Barton H A. The genome of *Pseudomonas fluorescens* strain R124 demonstrates phenotypic adaptation to the mineral environment. J. Bacteriol. (2013). **195** (21): 4793-4803.
- 229 Martins M L, Pinto U M, Riedel K, Vanetti M C D, Mantovani H C, Araújo E F. Lack of AHL-based quorum sensing in *Pseudomonas fluorescens* isolated from milk. Braz. J. Microbiol. (2014). **45** (3): 1039–1046.
- 230 Raaijmakers J M, de Bruijn I, de Kock M J D. Cyclic lipopeptide production by plant-associated *Pseudomonas* spp: Diversity, activity, biosynthesis, and regulation. Molecular Plant-Microbe Interactions. (2006). **19** (7): 699–710.
- 231 Raaijmakers J M, Mazzola M. Diversity and natural functions of antibiotics produced by beneficial and plant pathogenic bacteria. Annu. Rev. Phytopathol. (2012). **50**: 403-424.
- 232 Romero D, Palacios R. Gene amplification and genomic plasticity in prokaryotes. Annu. Rev. Genet. (1997). **31**: 91–111.
- 233 Hölscher T, Kovács A T. Sliding on the surface: bacterial spreading without an active motor. Environ. Microbiol. (2017). **19** (7): 2537–2545.
- 234 Schikora A, Schenk S T, Hartmann A. Beneficial effects of bacteria-plant communication based on quorum sensing molecules of the N-acyl homoserine lactone group. Plant Mol. Biol. (2016). **90**: 605-612.

- 235 El-Sayed A K, Hothersall J, Thomas C M. Quorum-sensing-dependent regulation of biosynthesis of the polyketide antibiotic mupirocin in *Pseudomonas fluorescens* NCIMB10586. *Microbiology*. (2001). **147**: 2127-2139.
- 236 Khan S R, Mavrodi D V, Jog G J, Suga H, Thomashow L S, Farrand S K. Activation of the *phz* operon of *Pseudomonas fluorescens* 2-79 requires the LuxR homolog PhzR, N-(3-OH-hexanoyl)-L-homoserine lactone produced by the LuxI homolog PhzI, and a cis-acting *phz* Box. *J. Bacteriol.* (2005). **187** (18): 6517-6527.
- 237 Körstgens V, Flemming HC, Wingender J, Borchard W. Influence of calcium ions on the mechanical properties of a model biofilm of mucoid *Pseudomonas aeruginosa*. *Water Sci. Technol.* (2001). **43** (6): 49-57.
- 238 Cui X, Harling R, Mutch P, Darling D. Identification of N-3-hydroxyoctanoyl-homoserine lactone production in *Pseudomonas fluorescens* 5064, pathogenic to broccoli, and controlling biosurfactant production by quorum sensing. *European Journal of Plant Pathology*. (2005). **111**: 297-308.
- 239 Moe L A. Amino acids in the rhizosphere: From plants to microbes. *American Journal of Botany*. (2013). **100** (9): 1692-1705.
- 240 Maleki S, Hrudikova, R, Zotchev S B, Ertesvag H. Identification of a new phosphatase enzyme potentially involved in the sugar phosphate stress response in *Pseudomonas fluorescens*. *Appl. Environ. Microbiol.* (2017). **83** (2): 1-12.
- 241 Nelson E B. Microbial dynamics and interactions in the spermosphere. *Annu. Rev. Phytopathol.* (2004). **42**: 271–309.
- 242 Merino S, Shaw J G, Tomás J M. Bacterial lateral flagella: An inducible flagella system. *FEMS Microbiol. Lett.* (2006). **263** (2): 127-135.
- 243 Yang A, Tang W S, Si Tieyan, Tang J X. Influence of physical effects on the swarming motility of *Pseudomonas aeruginosa*. *Biophysical Journal*. (2017). **112** (7): 1462-1471.
- 244 Verstraeten N, Braeken K, Debkumari B, Fransaer J, Vermant J, Michiels J. Living on a surface: swarming and biofilm formation. *Trends Microbiol.* (2008). **16** (10): 496-506.
- 244 Singh T, Arora D K. Motility and chemotactic response of *Pseudomonas fluorescens* toward chemoattractants present in the exudate of *Macrophomina phaseolina*. *Microbiol. Res.* (2001). **156** (4): 343-351.
- 245 Singh T, Srivastava A K, Arora D K. Horizontal and vertical movement of *Pseudomonas fluorescens* toward exudate of *Macrophomina phaseolina* in soil: influence of motility and soil properties. *Microbiol. Res.* (2002). **157** (2): 139-148.
- 246 Navazo E, Barahona E, Redondo-Nieto M, Martínez-Granero F, Rivilla R, Martín M. Three independent signalling pathways repress motility in *Pseudomonas fluorescens* F113. *Microb. Biotechnol.* (2009). **2** (4): 489-498.
- 247 Bi S, Sourjik V. Stimulus sensing and signal processing in bacterial chemotaxis. *Curr. Opin. Microbiol.* (2018). **45**: 22-29.

- 248 Gosztolai A, Schumacher J, Behrends V, Bundy J, Heydenreich F, Bennett M, Buck M, Barahona M. GlnK facilitates the dynamic regulation of bacterial nitrogen assimilation. *Biophys J.* (2017). **112** (10): 2219-2230.
- 249 Lassalle F, Muller D, Nesme X. Ecological speciation in bacteria: Reverse ecology approaches reveal the adaptive part of bacterial cladogenesis. *Research in Microbiology.*(2015). **166**: 729-741.
- 250 Barker K. (2005). *At the bench: A laboratory navigator.* (Updated edition). Long Island, NY: Cold Spring Harbor Laboratory Press.
- 251 Breznak J A, Costilow R N. Physicochemical factors in growth. (2007) In C. A. Reddy, T J Beveridge, J A Breznak, G A Marzluf, T M Schmidt, & L R Snyder (Eds.), *Methods for general and molecular microbiology.* (3rd ed., pp. 309-329). Washington, DC: ASM Press.
- 252 Beveridge T J, Moyles D, Harris B. Electron Microscopy. (2007) In C. A. Reddy, T J Beveridge, J A Breznak, G A Marzluf, T M Schmidt, & L R Snyder (Eds.), *Methods for general and molecular microbiology.* (3rd ed., pp. 56-81). Washington, DC: ASM Press.
- 253 Azatian S, Kaur N, Latham M P. Increasing the buffering capacity of minimal media leads to higher protein yield. *Journal of Biomolecular NMR.* (2018). **73** (11): 11-17. doi: org/10.1007/s10858-018-00222-4.
- 254 Fouchard S, Abdellaoui-Maane Z, Boulanger A, Llopiz P, Neunlist S. Influence of growth conditions on *Pseudomonas fluorescens* strains: A link between metabolite production and the PLFA profile. *FEMS Microbiol. Lett.* (2005). **251** (2): 211-218.
- 255 Fuhrer T, Fischer E, Sauer U. Experimental identification and quantification of glucose metabolism in seven bacterial species. *J. Bacteriol.* (2005). **187** (5): 1581–1590.
- 256 Wang J, Yan D, Dixon R, Wang Y-P. Deciphering the principles of bacterial nitrogen dietary preferences: a strategy for nutrient containment. *mBIO.* (2016). **7** (4): e00792- 16.
- 257 Betlach M R, Tiedje J M, Firestone R B. Assimilatory nitrate uptake in *Pseudomonas fluorescens* studied using Nitrogen-13. *Arch. Microbiol.* (1981). **129** (2): 135-140.
- 258 Ikeda T P, Shauger A E, Kustu S. *Salmonella typhimurium* apparently perceives external nitrogen limitation as internal glutamine limitation. *J. Mol Biol.* (1996). **259** (4): 589-607.
- 259 McCully A L, Behringer M G, Gliessman J R, Pilipenko E V, Mazny J L, Lynch M, Drummond D A, McKinlay J B. An *Escherichia coli* nitrogen starvation response is important for mutualistic coexistence with *Rhodopseudomonas palustris*. *Appl. Environ. Microbiol.* (2018). **84** (14): e00404-18.
- 260 Walker M C, van der Donk WA. The many roles of glutamate in metabolism. *J. Ind. Microbiol. Biotechnol.* (2016). **43** (2-3): 419-430.
- 261 McDonald T R, Ward J M. Evolution of electrogenic ammonium transporters (AMTs). *Front. Plant. Sci.* (2016). **7** (352). doi: 10.3389/fpls.2016.00352.

- 262 Soupene E, He L, Yan D, Kustu S. Ammonia acquisition in enteric bacteria: Physiological role of the ammonium/methylammonium transport B (AmtB) protein. PNAS. (1998). **95** (12): 7030–7034.
- 264 Hoshino T. Transport systems for branched-chain amino acids in *Pseudomonas aeruginosa*. J. Bacteriol. (1979). **139** (3): 705–712.
- 265 Phillips A T. Biosynthetic and catabolic features of amino acid metabolism in *Pseudomonas*. (1986) In Sokatch J R, L Nicholas Ornston & I C Gunsalus (Eds.), The Bacteria: A treatise on structure and function, the biology of *Pseudomonas*. (Vol. 10, pp. 385-438). Orlando, FL: Academic Press.
- 266 Hechtman P, Scriver C R. Neutral amino acid transport in *Pseudomonas fluorescens*. J. Bacteriol. (1970). **104** (2): 857–863.
- 267 Davidson A L, Dassa E, Orelle C, Chen J. Structure, function, and evolution of bacterial ATP-Binding cassette systems. Microbiol. Mol. Biol. Rev. (2008). **72** (2): 317-364.
- 268 Fellay R, Krisch H M, Prentki P, Frey J. Omegon-Km: A transposable element designed for in vivo insertional mutagenesis and cloning of genes in Gram-negative bacteria. Gene. (1989). **76** (2): 215-216.
- 269 Hainrichson M, Yaniv O, Cherniavsky M, Nudelman I, Shallom-Shezifi D, Yaron S, Baasov T. Overexpression and initial characterization of the chromosomal aminoglycoside 3-O-Phosphotransferase APH(3)-IIb from *Pseudomonas aeruginosa*. Antimicrob. Agents Chemother. (2007). **51** (2): 774-776.
- 270 Forchhammer K. Glutamine signalling in bacteria. Front. Biosci. (2007). **1** (12): 358-370.
- 271 Tian Z X, Li Q S, Buck M, Kolb A, Wang Y P. The CRP-cAMP complex and downregulation of the *glnAp2* promoter provides a novel regulatory linkage between carbon metabolism and nitrogen assimilation in *Escherichia coli*. Mol. Microbiol. (2001). **41**: 911-924.
- 272 Commichau F M, Forchhammer K, Stülke J. Regulatory links between carbon and nitrogen metabolism. Curr. Opin. Microbiol. (2006). **9** (2): 167-172.
- 273 Belitsky B R, Sonenshein A L. Modulation of activity of *Bacillus subtilis* regulatory proteins Gltc and Tnra by glutamate dehydrogenase. J. Bacteriol. (2004). **186** (11): 3399-3407.
- 274 Hashim S, Kwon D H, Abdelal A, Lu C D. The arginine regulatory protein mediates repression by arginine of the operons encoding glutamate synthase and anabolic glutamate dehydrogenase in *Pseudomonas aeruginosa*. J. Bacteriol. (2004). **186** (12): 3848-3854.
- 275 Reitzer L. Biosynthesis of glutamate, aspartate, asparagine, L-alanine, and D-alanine. EcoSal Plus. (2004). doi:10.1128/ecosalplus.3.6.1.3.
- 276 Park S, Chung-Dar L, Abdelal A. Cloning and characterization of *argR*, a gene that participates in regulation of arginine biosynthesis and catabolism in *Pseudomonas aeruginosa* PAO1. J. Bacteriol. (1997). **179** (17): 5300–5308.

- 277 Lu C D, Abdelal A T. The *gdhB* gene of *Pseudomonas aeruginosa* encodes an arginine inducible NAD(+)-dependent glutamate dehydrogenase which is subject to allosteric regulation. *J. Bacteriol.* (2001). **183** (2):490-499.
- 278 Tokushige M, Miyamoto K, Katsuki H. Occurrence of thermolabile and regulatory NAD-linked glutamate dehydrogenase in *Pseudomonas fluorescens*. *J. Biochem.* (1979). **85**: 1415-1420.
- 279 Goss T J, Perez-Matos A, Bender R A. Roles of glutamate synthase, *gltBD*, and *gltF* in nitrogen metabolism of *Escherichia coli* and *Klebsiella aerogenes*. *J. Bacteriol.* (2001). **183** (22): 6607-6619.
- 280 McKinlay J B. Systems biology of photobiological hydrogen production by purple non-sulfur bacteria. (2014) In Zannoni D, De Philippis R (Eds.), *Microbial BioEnergy: Hydrogen production, part I: Advances in Photosynthesis and Respiration (Including Bioenergy and Related Processes)* (Vol. 38, pp. 155 -176). Dordrecht: Springer.
- 281 Hervás A B, Canosa I, Little R, Dixon R, Santero E. NtrC-Dependent regulatory network for nitrogen assimilation in *Pseudomonas putida*. *J. Bacteriol.* (2009). **191** (19): 6123–6135.
- 282 Dennis J J, Zylstra G J. Plasposons: Modular self-cloning minitransposon derivatives for rapid genetic analysis of Gram-negative bacterial genomes. *Appl. Environ. Microbiol.* (1998). **64** (7): 2710-2715.
- 283 de Bruijn I, de Kock M J, Yang M, de Waard P, van Beek T A, Raaijmakers JM. Genome-based discovery, structure prediction and functional analysis of cyclic lipopeptide antibiotics in *Pseudomonas* species. *Mol. Microbiol.* (2007). **63** (2): 417-428.
- 284 Kumada Y, Benson D R, Hillemann D, Hosted T J, Rochefort D A, Thompson C J, Wohlleben W, Tateno Y. Evolution of the glutamine synthetase gene, one of the oldest existing and functioning genes. *PNAS.* (1993). **90** (7): 3009-3013.
- 285 Jensen L E, Nybroe O. Nitrogen availability to *Pseudomonas fluorescens* DF57 is limited during decomposition of barley straw in bulk soil and in the barley rhizosphere. *Appl. Environ. Microbiol.* (1999). **65** (10): 4320–4328.
- 286 Betlach M R, Tiedje J M, Firestone R B. Assimilatory nitrate uptake in *Pseudomonas fluorescens* studied using nitrogen-13. *Arch. Microbiol.* (1981). **129** (2): 135–140.
- 287 Brown C M, Macdonald-Brown D S, Stanley S O. The mechanisms of nitrogen assimilation in pseudomonads. *Antonie Leeuwenhoek.* (1973). **39** (1): 89–98.
- 288 Jahns T. Regulation of urea uptake in *Pseudomonas aeruginosa*. *Antonie Leeuwenhoek.* (1992). **62** (3): 173–179.
- 289 Patrick J E, Kearns D B. Laboratory strains of *Bacillus subtilis* do not exhibit swarming motility. *J. Bacteriol.* (2009). **191** (22): 7129–7133.
- 290 Tremblay J, Déziel E. Improving the reproducibility of *Pseudomonas aeruginosa* swarming motility assays. *Journal of Basic Microbiology.* (2008). **48**: 509-515.
- 291 Greenwood N N, Earnshaw A. (1997). *Chemistry of the Elements.* (2nd edition). Oxford: Elsevier.

- 292 Wylie J, Worobec E. The OprB porin plays a central role in carbohydrate uptake in *Pseudomonas aeruginosa*. *J. Bacteriol.* (1995). **177** (11): 3021–3026.
- 293 Pahel G, Rothstein D M, Magasanik B. Complex *glnA-glnL-glnG* operon of *Escherichia coli*. *J. Bacteriol.* (1982). **150** (1): 202-213.
- 294 Alvarez-Morales A, Dixon R, Merrick M. Positive and negative control of the *glnA ntrBC* regulon in *Klebsiella pneumoniae*. *The EMBO Journal.* (1984). **3** (3): 501-507.
- 295 He L, Soupene E, Kustu S. NtrC is required for control of *Klebsiella pneumoniae* NifL activity. *J. Bacteriol.* (1997). **179** (23): 7446–7455.
- 296 Ninfa A J, Jiang P. PII signal transduction proteins: sensors of α -ketoglutarate that regulate nitrogen metabolism. *Curr. Opin. Microbiol.* (2005). **8** (2): 168-173.
- 297 Finkel O M, Castrillo G, Herrera Paredes S, Salas González I, Dangl J L. Understanding and exploiting plant beneficial microbes. *Curr. Opin. Plant Biol.* (2017). **38**: 155–163.
- 298 Futamata H, Sakai M, Ozawa H, Urashima Y, Sueguchi T, Matsuguch T. Chemotactic response to amino acids of fluorescent pseudomonads isolated from spinach roots grown in soils with different salinity levels. *Soil Science and Plant Nutrition.* (1998). **44** (1): 1-7.
- 299 Rainey P B. Adaptation of *Pseudomonas fluorescens* to the plant rhizosphere. *Environ. Microbiol.* (1999). **1** (3): 243-257.
- 300 De Leij F A A M, Sutton E J, Whipps J M, Fenlon J S, Lynch J M. Field release of a genetically modified *Pseudomonas fluorescens* on wheat: establishment, survival and dissemination. *Bio/Technology.* (1995). **13**: 1488–1492.
- 301 Thompson I P, Lilley A K, Ellis R J, Bramwell P A, Bailey M J. Survival, colonization and dispersal of genetically modified *Pseudomonas fluorescens* SBW25 in the phytosphere of field grown sugar beet. *Nature Biotechnology.* (1995). **13** (12): 1493-1497.
- 302 Barber D A, Gunn K B. The effect of mechanical forces on the exudation of organic substances by the roots of cereal plants grown under sterile conditions. *New Phytol.* (1974). **73**: 39–45.
- 303 Boulter D, Jeremy J J, Wilding M. Amino acids liberated into the culture medium by pea seedling roots. *Plant Soil.* (1966). **24**: 121–127.
- 304 Shepherd D, Davies H V. Patterns of short term amino acid accumulation and loss in the root zone of liquid-cultured forage rape. *Plant Soil.* (1994). **158**: 99–109.
- 305 Jones D L, Darrah P R. Influx and efflux of amino acids from *Zea mays* L. roots and their implications for N-nutrition and the rhizosphere. *Plant Soil.* (1993). **155**: 87–90.
- 306 Reitzer L. Nitrogen assimilation and global regulation in *Escherichia coli*. *Annu. Rev. Microbiol.* (2003). **57**: 155-176.

- 307 Valentini M, García-Mauriño S M, Pérez-Martínez I, Santero E, Canosa I, Lapouge K. Hierarchical management of carbon sources is regulated similarly by the CbrA/B systems in *Pseudomonas aeruginosa* and *Pseudomonas putida*. *Microbiology*. (2014). **160**: 2243–2252.
- 308 Dasgupta N, Arora S K, Ramphal R. The flagellar system of *Pseudomonas aeruginosa*. (2004) In J L Ramos, J B Goldberg, A. Filloux (Eds.), *Pseudomonas* (Vol. 1), Boston, MA: Springer.
- 309 Martínez-Argudo I, Salinas P, Maldonado R, Contreras A. Domain interactions on the *ntr* signal transduction pathway: two-hybrid analysis of mutant and truncated derivatives of histidine kinase NtrB. *J. Bacteriol.* (2002). **184** (1): 200-206.
- 310 Maleki S, Mærk M, Hrudikova R, Valla S, Ertesvåg H. New insights into *Pseudomonas fluorescens* alginate biosynthesis relevant for the establishment of an efficient production process for microbial alginates. *New Biotechnology*. (2017). **37**: 2-8.
- 311 Bijtenhoorn P, Mayerhofer H, Müller-Dieckmann J, Utpatel C, Schipper C, Hornung C,...Streit W R. A novel metagenomic Short-Chain Dehydrogenase/Reductase attenuates *Pseudomonas aeruginosa* biofilm formation and virulence on *Caenorhabditis elegans*. *PLoS ONE*. (2011). **6** (10): e26278. doi:10.1371/journal.pone.0026278.
- 312 Kamberov E S, Atkinson M R, Chandran P, Ninfa A J. Effect of mutations in *Escherichia coli glnL* (*ntrB*), encoding nitrogen regulator II (NRII or NtrB), on the phosphatase activity involved in bacterial nitrogen regulation. *The Journal Biochemical Chemistry*. (1994). **269** (45): 28294-28299.
- 313 Konyecsni W M, Deretic V. DNA sequence and expression analysis of *algP* and *algQ*, components of the multigene system transcriptionally regulating mucoidy in *Pseudomonas aeruginosa*: *algP* contains multiple direct repeats. *J. Bacteriol.* (1990). **172** (5): 2511-2520.
- 314 Konyecsni W M, Deretic V. A procaryotic regulatory factor with a histone HI-like carboxy-terminal domain: clonal variation of repeats within *algP*, a gene involved in regulation of mucoidy in *Pseudomonas aeruginosa*. *J. Bacteriol.* (1990). **172** (5): 2511-2520.
- 315 Khademi S, O'Connell J, Remis J, Robles-Colmenares Y, Miercke W L J, Stroud R M. Mechanism of ammonia transport by Amt/MEP/Rh: Structure of AmtB at 1.35 Å. *Science*. (2004). **305** (5690): 1587-1594.
- 316 Pioszak A A, Ninfa A J. Genetic and biochemical analysis of phosphatase activity of *Escherichia coli* NRII (NtrB) and its regulation by the PII signal transduction protein. *J. Bacteriol.* (2003). **185** (4): 1299-1315.
- 317 Karp P D, Billington R, Caspi R, Fulcher C A, Latendresse M, Kothari A, Keseler I M,...Subhraveti P. The BioCyc collection of microbial genomes and metabolic pathways. *Briefings in Bioinformatics*. (2017). 1-9. doi: org/10.1093/bib/bbx085.

- 318 Martínez-Argudo I, Martín Nieto J, Salinas P, Maldonado R, Drummond M, Contreras A. Two-hybrid analysis of domain interactions involving NtrB and NtrC two-component regulators. *Molecular Microbiology*. (2001). **40** (1): 169-178.
- 319 Croze O A, Ferguson G P, Cates M E, Poon W C K. Migration of chemotactic bacteria in soft agar: Role of gel concentration. *Biophys. J.* (2011).**101** (3): 525–534.
- 320 Wei L, Chung-Dar L. Regulation of carbon and nitrogen utilization by CbrAB and NtrBC two-component systems in *Pseudomonas aeruginosa*. *J. Bacteriol.* (2007).**189** (15): 5413–5420.
- 321 Wei C-F, Tsai Y-H, Tsai S-H, Lin C-S, Chang C-J, Chen C, Huang H-C, Lai H-C. Cross-talk between bacterial two-component systems drives stepwise regulation of flagellar biosynthesis in swarming development. *Biochemical and Biophysical Research Communications*. (2017). **489** (1): 70-75.